



Potter, Sarah Jane (2001) *Molecular analysis of human CD23 (Fc[epsilon]RII) protein isoform function*. PhD thesis.

<http://theses.gla.ac.uk/2107/>

Copyright and moral rights for this thesis are retained by the author

A copy can be downloaded for personal non-commercial research or study, without prior permission or charge

This thesis cannot be reproduced or quoted extensively from without first obtaining permission in writing from the Author

The content must not be changed in any way or sold commercially in any format or medium without the formal permission of the Author

When referring to this work, full bibliographic details including the author, title, awarding institution and date of the thesis must be given

**MOLECULAR ANALYSIS OF HUMAN CD23 (FcεRII)  
PROTEIN ISOFORM FUNCTION**

**Sarah Jane Potter**

Division of Biochemistry and Molecular Biology,  
Institute of Biomedical and Life Sciences,  
University of Glasgow,  
Glasgow G12 8QQ.

**This thesis is submitted in part fulfilment of the degree of Doctor of Philosophy**

**Dec 2001**

**© S. J. Potter. Dec 2001**



## ABSTRACT

CD23 (Fc $\epsilon$ RII), the low affinity receptor for IgE, is a single chain, 45kDa, type II transmembrane glycoprotein and member of the C-type lectin superfamily. CD23 is a multifunctional receptor/ligand and cytokine, playing a role in antigen presentation, macrophage activation and cell adhesion. Human CD23 exists as two distinct isoforms, CD23a and CD23b, that differ only by a 6 or 7 amino acid region located at their extreme cytoplasmic N-termini. CD23a is constitutively and cell type-specifically expressed on B cells, whereas CD23b can be expressed on B cells, monocytes and other cells of the haematopoietic lineage when activated by stimuli including IL-4 and IL-13. The two CD23 isoforms appear to be linked to both different intracellular trafficking pathways and to distinct intracellular signalling pathways. It is the issues of isoform-specific trafficking and signalling that are the focus of the research discussed in this thesis.

Early evidence suggests two distinct roles for CD23, one being a stage-dependent involvement in B-cell growth and differentiation, the second involving the effector phase(s) of IgE-mediated immunity, including allergy and response to parasitic infection. The patterns of CD23 gene expression and functional diversity has led to the assumption that CD23a and CD23b are involved in B cell function and IgE-mediated immunity, respectively. More recently studies by Yokota *et al*, suggest that the two isoforms are internalised via distinct pathways, with CD23a having been shown to enter the cell via a receptor-mediated endocytic pathway in  $\psi$ 2 cells, and CD23b showing a more phagocytic route of cellular entry in a macrophage-like cell line (J774).

In the research described in this thesis, the trafficking of each CD23 isoform was studied in detail, in both wild-type and mutant CD23 proteins, using an identical cell system and the same method of CD23 ligation for both isoforms. Confocal microscopic analysis demonstrated intracellular sorting differences to exist between the two isoforms, with CD23a utilising the endocytic pathway, and CD23b following both the endocytic and phagocytic pathways in a B-cell line. Site-directed mutagenesis was used to investigate a number of potentially key residues present in the unique N-terminal tail of each isoform. The serine groups at positions 7 and 5 in the CD23a and b isoforms,

respectively, and the NNP tri-peptide motif in the b isoform were found to be necessary for accurate trafficking of these proteins. The discovery that the CD23 isoforms utilise different trafficking pathways corroborates the hypothesis that CD23a and CD23b may have functionally different roles.

Current models of human CD23 signalling link the CD23a isoform to a cAMP-generating pathway and the CD23b isoform to stimulation of inositol-1,4,5-trisphosphate production and calcium mobilisation. The ability of CD23 to transmit a signal within various cells and the fact it has a very short cytoplasmic tail, of only 23 amino acids and bereft of catalytic motifs, strongly suggests that CD23 may associate with other molecules involved in signal transduction. The divergence in the signalling pathways associated with each CD23 isoform has been attributed to the unique amino acids at the N-terminal cytoplasmic tails, as the remainder of the proteins are identical. However, there is no definitive evidence to link directly CD23 to any of these individual signalling pathways. The research presented in this thesis utilises the yeast two-hybrid assay to investigate binding partners for the N-terminal tail of CD23. Filamin A was identified as a potential interacting protein, and was found to interact with both the CD23a and CD23b isoforms. It is hypothesised that CD23 interacts with filamin A, which functions as an adaptor protein, to enable downstream responses to CD23 through connections to the appropriate signalling pathways in an isoform-specific manner.

**Dedicated to the loving and everlasting memory  
of my Grannies, two very special ladies  
who will never be forgotten.....**



## ACKNOWLEDGEMENTS

I would firstly like to express my heartfelt thanks and gratitude to Dr William Cushley for his supervision, encouragement and expertise throughout the course of this research. I would also like to express my appreciation to both Professor Gwyn Gould and Dr Gerhard May for their expertise, patience and time and Professor Graeme Milligan and Professor John Coggins for making the facilities of the Division of Biochemistry and Molecular Biology, IBLS available to me to undertake this research. This research was funded by the Medical Research Council (MRC), and much gratitude is also expressed to them.

Special thanks to the members of laboratory 232 (both past and present) for their continual support, encouragement and advice; Dr Andy Allan for his amazing cheeriness and willingness to help at all times, even if the art of 'tequila slamming' passed you by the first time! Dr Gillian Borland, the lady with an amazing knowledge of all things science and for being patient with all my persistent questions. Mr Tom Carr for his support, fantastic sense of humour and unbelievable general knowledge. Dr John Curran for his fantastic friendship, continual support and valued advice. Dr Marie-Ann Ewart, a fellow PhD student, who shared with me the highs and lows of postgraduate research and introduced me to the joys of ice-hockey. Dr Johanne Matheson for her technical expertise, organizational skills and much valued friendship.

A special extended thank you to my colleague Dr. Johanne Matheson and her husband Keith for their cherished friendship, valued advice, encouragement and seemingly endless supply of red wine! And to Andrew, their wonderful son, the wee star that loves to giggle and can't help but spread happiness to all those around him.

Love to my family. To Rachel, my 'big-little' sister, who has grown to become one of my best friends and confidants. Your dedication is inspirational. To Mum and Dad, without whom this would not have been possible. Thank you both for your enduring love, encouragement, support and continual belief in me. At last, your eternal student has moved on and got, to quote your words, a 'proper' job! Love always.

And finally, to my Fiancé Brian, my best-friend for longer than I care to remember, and true believer in me. Isn't it strange how far we've come! Thank you for your steadfast love, patience and dedication. My life would be empty without you.

## **INDEX**

CHAPTER 1	INTRODUCTION	PAGE 1
CHAPTER 2	MATERIALS & METHODS	PAGE 60
CHAPTER 3	GENERATION AND ANALYSIS OF WILD TYPE CD23 OR GFP CD23 FUSION PROTEINS IN STABLY-TRANSFECTED HEK 293 CELL LINES	PAGE 96
CHAPTER 4	GENERATION AND ANALYSIS OF CD23A AND CD23B N-TERMINAL MUTANT PROTEINS	PAGE 118
CHAPTER 5	IDENTIFICATION OF CD23 N-TERMINAL TAIL BINDING PARTNERS USING THE YEAST TWO-HYBRID SYSTEM	PAGE 170
CHAPTER 6	GENERAL CONCLUSIONS & DISCUSSION	PAGE 208
	REFERENCES	PAGE 223
	APPENDIX	PAGE 246

## **TABLE OF CONTENTS**

<b>1</b>	<b>INTRODUCTION</b>	<b>PAGE 1</b>
<b>1.1</b>	<b>THE IMMUNE SYSTEM</b>	<b>PAGE 2</b>
<b>1.1.1</b>	<b>INNATE IMMUNITY</b>	<b>PAGE 2</b>
<b>1.1.2</b>	<b>ADAPTIVE IMMUNITY</b>	<b>PAGE 3</b>
<b>1.2</b>	<b>B LYMPHOPOIESIS</b>	<b>PAGE 6</b>
<b>1.2.1</b>	<b>EXPRESSION AND REARRANGEMENT OF IG GENES</b>	<b>PAGE 8</b>
<b>1.2.2</b>	<b>ROLES OF TRANSCRIPTIONAL PROTEINS</b>	<b>PAGE 9</b>
<b>1.2.3</b>	<b>STAGES OF ANTIGEN-DEPENDENT DEVELOPMENT</b>	<b>PAGE 13</b>
<b>1.2.3A</b>	<b>B LYMPHOCYTE ACTIVATION BY CONTACT-MEDIATED INTERACTION WITH T-LYMPHOCYTES</b>	<b>PAGE 14</b>
<b>1.2.3B</b>	<b>REGULATION OF GERMINAL CENTER B CELL DIFFERENTIATION</b>	<b>PAGE 20</b>
<b>1.3</b>	<b>MOLECULAR SORTING</b>	<b>PAGE 22</b>
<b>1.3.1</b>	<b>GENERAL MODELS OF INTRACELLULAR SORTING</b>	<b>PAGE 23</b>
<b>1.3.2</b>	<b>SECRETORY PATHWAYS</b>	<b>PAGE 25</b>
<b>1.3.3</b>	<b>ENDOCYTIC PATHWAYS</b>	<b>PAGE 25</b>
<b>1.3.3A</b>	<b>ENDOCYTOSIS</b>	<b>PAGE 26</b>
<b>1.3.3B</b>	<b>PHAGOCYTOSIS</b>	<b>PAGE 28</b>
<b>1.3.4</b>	<b>ANTIGEN PRESENTATION BY MHC CLASS II MOLECULES</b>	<b>PAGE 28</b>
<b>1.3.5</b>	<b>INTRACELLULAR SORTING SIGNALS</b>	<b>PAGE 29</b>
<b>1.4</b>	<b>CD23 (FcεRII)</b>	<b>PAGE 31</b>
<b>1.4.1</b>	<b>DISCOVERY OF CD23</b>	<b>PAGE 31</b>
<b>1.4.2</b>	<b>CELLULAR DISTRIBUTION AND REGULATION OF CD23 EXPRESSION</b>	<b>PAGE 32</b>
<b>1.4.3</b>	<b>STRUCTURE OF CD23</b>	<b>PAGE 35</b>
<b>1.4.3A</b>	<b>CD23 IS A MEMBER OF THE C-TYPE LECTIN SUPERFAMILY</b>	<b>PAGE 35</b>
<b>1.4.3B</b>	<b>STRUCTURAL DOMAINS OF HUMAN CD23</b>	<b>PAGE 36</b>
<b>1.4.4</b>	<b>SOLUBLE CD23</b>	<b>PAGE 37</b>
<b>1.4.5</b>	<b>CYTOKINE EFFECTS OF sCD23</b>	<b>PAGE 38</b>
<b>1.4.6</b>	<b>CD23 ISOFORMS</b>	<b>PAGE 38</b>
<b>1.4.7</b>	<b>LIGANDS FOR CD23</b>	<b>PAGE 41</b>
<b>1.4.7A</b>	<b>CD21</b>	<b>PAGE 41</b>
<b>1.4.7B</b>	<b>β2 INTEGRINS</b>	<b>PAGE 42</b>



1.4.7C	VITRONECTIN RECEPTORS	PAGE 43
1.4.8	DISEASE ASSOCIATION	PAGE 44
1.4.9	MURINE CD23	PAGE 47
1.4.10	CD23 TRANSGENIC MOUSE STUDIES	PAGE 47
1.5	AREAS OF RESEARCH INTEREST	PAGE 50
2	MATERIALS AND METHODS	PAGE 60
2.1	MATERIALS	PAGE 61
2.1.1	GENERAL CHEMICALS AND MATERIALS	PAGE 61
2.1.2	CELL AND TISSUE CULTURE REAGENTS & MATERIALS	PAGE 62
2.1.3	CELL LINES	PAGE 62
2.1.4	PLASMIDS & TRANSFECTION REAGENTS	PAGE 62
2.1.5	ANTIBODIES	PAGE 63
2.1.6	FLUORESCENT PROBES	PAGE 64
2.1.7	COMMERCIAL KITS	PAGE 64
2.1.8	OLIGONUCLEOTIDES	PAGE 64
2.2	METHODS	PAGE 65
2.21	CELL CULTURE	PAGE 65
2.2.1A	CULTURE OF NON-B CELL LINES	PAGE 65
2.2.1B	CULTURE OF HUMAN B CELL LINES	PAGE 65
2.2.1.C	DETERMINATION OF CELL VIABILITY	PAGE 65
2.2.1D	FROZEN CELL STOCKS	PAGE 66
2.2.2	FLOW CYTOMETRIC ANALYSIS	PAGE 66
2.2.2A	ANALYSIS OF CELL SURFACE PROTEINS	PAGE 67
2.2.2B	FLOW CYTOMETRIC CELL SORTING	PAGE 67
2.2.3	NUCLEIC ACIDS	PAGE 68
2.2.3A	SMALL SCALE PREPARATION OF DNA (MINI-PREPS)	PAGE 68
2.2.3B	LARGE SCALE PREPARATION OF DNA	PAGE 68
2.2.3C	DNA CONCENTRATION AND PURITY	PAGE 69
2.2.3D	RESTRICTION ENDONUCLEASE DIGESTION OF DNA	PAGE 70
2.2.3E	LIGATION OF DNA VECTOR AND INSERT FRAGMENTS	PAGE 70
2.2.3F	AGAROSE GEL ELECTROPHORESIS	PAGE 70

2.2.3G	PURIFICATION OF DNA RESTRICTION FRAGMENTS FROM LOW MELTING POINT AGAROSE GELS	PAGE 70
2.2.3H	“BIG DYE” TERMINATOR SEQUENCING (ABI 373A)	PAGE 71
2.2.4	POLYMERASE CHAIN REACTION (PCR)	PAGE 72
2.2.4A	RNA ISOLATION WITH TRIZOL	PAGE 73
2.2.4B	REVERSE TRANSCRIPTASE POLMERASE CHAIN REACTION (RT-PCR)	PAGE 73
2.2.5	CD23 N-TERMINAL TAIL MUTAGENESIS	PAGE 74
2.2.5A	PRIMER DESIGN	PAGE 75
2.2.5.B	STRATAGENE QUICKCHANGE MUTAGENESIS PCR REACTION	PAGE 75
2.2.5C	TRANSFORMATION OF EPICURIAN COLI XL-1 BLUE SUPERCOMPETENT CELLS	PAGE 76
2.2.6	TRANSFECTION & TRANSFORMATION OF CELLS	PAGE 77
2.2.6A	DOTAP TRANSFECTION OF HUMAN CELL LINES	PAGE 77
2.2.6B	ELECTROPORATION OF RAJI-A CELLS	PAGE 77
2.2.6C	RUBIDIUM CHLORIDE METHOD FOR MANUFACTURE OF TRANSFORMATION COMPETENT E.COLI	PAGE 78
2.2.6D	TRANSFORMATION OF COMPETENT CELLS	PAGE 78
2.2.7	PROTEIN ANALYSIS	PAGE 78
2.2.7A	PREPARATION OF WHOLE CELL “RIPA” LYSATES	PAGE 78
2.2.7B	BIO RAD PROTEIN CONCENTRATION ASSAY	PAGE 79
2.2.7C	PREPARATION OF IMMUNOPRECIPITATES	PAGE 79
2.2.7D	SDS-PAGE GEL ELECTROPHORESIS	PAGE 80
2.2.7E	IMMUNOBLOTTING	PAGE 80
2.2.7F	ECL DETECTION SYSTEM	PAGE 80
2.2.7G	SILVER STAIN	PAGE 81
2.2.7H	sCD23 ELISA	PAGE 81
2.2.8	CONFOCAL ANALYSIS	PAGE 82
2.2.8A	DIALYSIS OF FITC CONJUGATED ANTI-CD23 ANTIBODY, REMOVAL OF SODIUM AZIDE CONTAMINATION	PAGE 82
2.2.8B	PREPARATION OF NIP-CONJUGATED BSA/INSULIN	PAGE 82
2.2.8C	PREPARATION OF CELL SAMPLES	PAGE 83
2.2.8D	LIVE CELL CONFOCAL ANALYSIS OF WT CD23 AND GFP-CD23 FUSION PROTEINS	PAGE 83
2.2.8E	LIVE CELL ANALYSIS OF CD23 CO-LOCALISATION WITH TRANSFERRIN-MODIFIED TEXAS RED OR LYSOTracker DYES	PAGE 84



2.2.8F	ANALYSIS OF WT CD23 AND GFP-CD23 FUSION PROTEINS UNDER FIXED CONDITIONS	PAGE 84
2.2.9	PREPARATION OF THE MATCHMAKER cDNA LIBRARY	PAGE 85
2.2.9A	TITRATION OF MATCHMAKER cDNA LIBRARY	PAGE 85
2.2.9B	AMPLIFICATION OF THE MATCHMAKER LEUKOCYTE cDNA LIBRARY	PAGE 85
2.2.10	YEAST TWO-HYBRID STUDIES	PAGE 86
2.2.10A	DNA EXTRACTION FROM YEAST	PAGE 86
2.2.10B	TCA YEAST PROTEIN EXTRACTS	PAGE 86
2.2.10C	PREPARATION OF ELECTROCOMPETENT KC8 E.COLI CELLS	PAGE 87
2.2.10D	TRANSFORMATION OF ELECTROCOMPETENT KC8 E.COLI CELLS	PAGE 88
2.2.10E	LITHIUM ACETATE HIGH EFFICIENCY TRANSFORMATION	PAGE 88
2.2.10F	CALCULATION OF TRANSFORMATION EFFICIENCY & THE NUMBER OF ACTUAL CLONES SCREENED	PAGE 89
2.2.10G	DETECTION OF $\alpha$ -GALACTOSIDASE ACTIVITY	PAGE 90
2.2.10H	AMPLIFICATION AND ANALYSIS OF PLASMID INSERTS BY PCR	PAGE 90
2.2.10I	SEQUENCE ANALYSIS OF LIBRARY CLONES FOUND TO INTERACT WITH CD23	PAGE 91
<b>3</b>	<b>GENERATION AND ANALYSIS OF WILD TYPE CD23 OR GFP CD23 FUSION PROTEINS IN STABLY-TRANSFECTED HEK 293 CELL LINES</b>	<b>PAGE 96</b>
3.1	INTRODUCTION	PAGE 97
3.2	RESULTS	PAGE 98
3.2.1	GENERATION OF cDNAs AND PLASMIDS EXPRESSING EACH OF THE CD23 CONSTRUCTS	PAGE 98
3.2.2	WILD TYPE CD23 AND GFP-CD23 FUSION PROTEINS ARE EXPRESSED AT THE PLASMA MEMBRANE OF STABLY-TRANSFECTED HEK 292 CELLS	PAGE 99
3.2.3	VISUALISATION OF CD23 ISOFORM RE-DISTRIBUTION IN HEK 293 CELLS.	PAGE 99
3.2.4	GFP-FUSION PROTEINS FACILITATE THE STUDY OF CD23 ISOFORM TRAFFICKING IN “BASAL”, “LIGATED” AND “CROSS-LINKED” CONDITIONS	PAGE 100
3.2.5	CD23A BUT NOT CD23B PROTEINS ARE INTERNALISED VIA THE EARLY ENDOCYTIC PATHWAY	PAGE 101
3.2.6	NEITHER CD23 ISOFORM ENTERS A PHAGOCYTIC PATHWAY IN HEK 293 CELLS	PAGE 102

3.2.7	HEK 293 CELLS DO NOT UTILISE CLASSICAL PHAGOCYTOSIS	PAGE 102
3.2.8	HEK 293 CELLS DO NOT EXPRESS MHC CLASS II MOLECULES	PAGE 103
3.3	DISCUSSION	PAGE 104
4	<b>GENERATION AND ANALYSIS OF CD23A AND CD23B N-TERMINAL MUTANT PROTEINS</b>	<b>PAGE 118</b>
4.1	INTRODUCTION	PAGE 119
4.2	RESULTS	PAGE 120
4.2.1	GENERATION OF CDNAS AND PLASMIDS EXPRESSING EACH OF THE CD23 N-TERMINAL MUTANT PROTEINS	PAGE 120
4.2.2	EXPRESSION OF GFP-CD23A AND GFP-CD23B MUTANT PROTEINS IN HEK 293 CELLS	PAGE 121
4.2.3	REAL TIME VISUALISATION OF EACH GFP-CD23 MUTANT PROTEIN IN HEK 293 CELLS; THE GFP-CD23 BP3R MUTANT PROTEIN IS NOT TARGETED TO THE PLASMA MEMBRANE	PAGE 122
4.2.3A	INTERNALISATION AND INTRACELLULAR TRAFFICKING OF GFP-CD23A MUTANTS; ROLE FOR SERINE 7	PAGE 123
4.2.3B	INTERNALISATION AND INTRACELLULAR TRAFFICKING OF THE GFP-CD23B MUTANTS; A ROLE FOR SERINE 5	PAGE 125
4.2.3C	A ROLE FOR THE NPP TRI-PEPTIDE MOTIF	PAGE 126
4.2.4	MUTATION OF THE N-TERMINUS OF CD23 AFFECTS PROTEOLYTIC CLEAVAGE FROM THE CELL SURFACE	PAGE 128
4.2.5	EXPRESSION OF GFP-CD23 FUSION PROTEINS IN B LYMPHOCYTES	PAGE 129
4.2.5A	GENERATION OF G418-RESISTANT RAJI A CELLS EXPRESSING EACH OF THE WILD-TYPE GFP-CD23 FUSION PROTEIN ISOFORMS	PAGE 129
4.2.5B	REAL TIME VISUALISATION OF THE WILD-TYPE GFP-CD23 PROTEINS IN RAJI A CELLS	PAGE 130
4.2.5C	GFP-CD23B UTILISES THE ENDOCYTIC PATHWAY IN RAJI A CELLS WHEN LOADED WITH IGE AND WHEN LOADED AND SUBSEQUENTLY CROSS-LINKED WITH NIP-BSA	PAGE 131
4.2.5D	GFP-CD23B UTILISES THE PHAGOCYTIC PATHWAY IN RAJI A CELLS WHEN LOADED WITH IGE AND WHEN LOADED WITH IGE AND SUBSEQUENTLY CROSS-LINKED WITH NIP10-BSA	PAGE 132
4.2.6	ANALYSIS OF GFP-CD23 MUTANTS IN RAJI A CELLS	PAGE 133
4.2.6A	GENERATION OF G418-RESISTANT RAJI A CELLS EXPRESSING EACH OF THE GFP-CD23 MUTANT FUSION PROTEINS	PAGE 133
4.2.6B	REAL TIME VISUALISATION OF EACH GFP-CD23 MUTANT PROTEIN IN RAJI A CELLS	PAGE 134
4.3	DISCUSSION	PAGE 135



<b>5</b>	<b>IDENTIFICATION OF CD23 N-TERMINAL TAIL BINDING PARTNERS USING THE YEAST TWO-HYBRID SYSTEM</b>	<b>PAGE 170</b>
5.1	INTRODUCTION	PAGE 171
5.2	RESULTS	PAGE 175
5.2.1	GENERATION OF THE GAL4 DNA-BD-CD23 FUSION CONSTRUCTS	PAGE 175
5.2.2	EXPRESSION OF THE GAL4 DNA-BD-CD23 FUSION BAIT PROTEINS IN AH109 YEAST CELLS.	PAGE 175
5.2.3	SUCCESSFUL AMPLIFICATION OF THE MATCHMAKER HUMAN LEUKOCYTE cDNA LIBRARY.	PAGE 177
5.2.4	OPTIMISATION OF TRANSFORMATION EFFICIENCY & FIRST PILOT-SCALE SCREEN	PAGE 178
5.2.5	FIRST SMALL-SCALE SCREEN USING THE HUMAN LEUKOCYTE cDNA LIBRARY	PAGE 179
5.2.6	LARGE SCALE SCREEN WITH INCREASED SELECTION STRINGENCY	PAGE 180
5.2.6A	IDENTIFICATION OF EIGHT POTENTIALLY POSITIVE INTERACTORS	PAGE 180
5.2.6B	SEQUENCE ANALYSIS OF THE INTERACTING LIBRARY PROTEINS	PAGE 181
5.2.6C	CONFIRMATION OF THE INTERACTIONS IN YEAST	PAGE 182
5.2.6D	ANALYSIS OF HA-TAGGED PROTEIN EXPRESSION FROM EACH OF THE ISOLATED AD CONSTRUCTS	PAGE 183
5.2.7	THE CD23-FILAMIN INTERACTION	PAGE 184
5.2.7A	FILAMIN A	PAGE 184
5.2.7B	HUMAN FILAMIN MAY IMMUNO-PRECIPITATE WITH CD23 FROM THE RMPI 8866 B CELL LINE	PAGE 185
5.3	DISCUSSION	PAGE 186
5.3.1	THE STRUCTURE OF HUMAN FILAMIN A (FLNA)	PAGE 188
<b>6</b>	<b>GENERAL CONCLUSIONS &amp; DISCUSSION</b>	<b>PAGE 208</b>
6.1	CURRENT UNDERSTANDING OF THE HUMAN CD23 ISOFORMS	PAGE 209
6.1.1	MAIN CONCLUSIONS	PAGE 210
6.2	INTRACELLULAR TRAFFICKING OF CD23	PAGE 210
6.2.1	FUTURE WORK	PAGE 216
6.3	BINDING PARTNERS FOR THE N-TERMINAL TAIL OF CD23	PAGE 217
6.3.1	FUTURE WORK	PAGE 219

## **LIST OF FIGURES**

1.1	SCHEMATIC DIAGRAM ILLUSTRATING THE ANTIGEN-INDEPENDENT STAGES OF B CELL DEVELOPMENT	PAGE 53
1.2	SCHEMATIC DIAGRAM DETAILING THE ANTIGEN-DEPENDENT STAGES OF B CELL DEVELOPMENT	PAGE 54
1.3	SCHEMATIC DIAGRAM ILLUSTRATING THE COMMON MOLECULAR SORTING PATHWAYS PRESENT IN EUKARYOTIC CELLS	PAGE 55
1.4	COAT PROTEINS REGULATE PROTEIN TRANSPORT BETWEEN SPECIFIC COMPARTMENTS WITHIN THE CELL	PAGE 56
1.5	STRUCTURAL COMPARISON OF THE HIGH AND LOW AFFINITY RECEPTORS FOR IGE, FcεRI AND FcεRII	PAGE 57
1.6	STRUCTURE OF CD23	PAGE 58
1.7	CD23A AND CD23B ISOFORMS ARE GENERATED FROM ALTERNATIVE SPLICING OF THE SAME GENE	PAGE 59
2.1	THE BEAM PATH OF A TYPICAL FLOW CYTOMETER	PAGE 92
2.2	OVERVIEW OF THE STRATAGENE QUIKCHANGE™ SITE- DIRECTED MUTAGENESIS PROTOCOL	PAGE 93
2.3	BEAM PATH OF THE ZEISS LSM 410 INVERT CONFOCAL MICROSCOPE	PAGE 94
2.4	YEAST TWO-HYBRID SCREENING STRINGENCY OPTIONS	PAGE 95
3.1	GENERATION OF WILD-TYPE CD23 AND GFP-CD23 FUSION PROTEINS	PAGE 106
3.2	HEK 293 CELLS STABLY EXPRESS CD23 AND GFP-CD23 FUSION PROTEINS	PAGE 107
3.3	HEK 293 CELLS STABLY EXPRESS CD23 AND GFP-CD23 FUSION PROTEINS AT THE PLASMA MEMBRANE	PAGE 108
3.4	MEMBRANE LOCALISATION OF CD23 AND GFP-CD23 FUSION PROTEINS IN HEK 293 CELLS	PAGE 109
3.5	SCHEMATIC DIAGRAM ILLUSTRATING THE NIP SYSTEM	PAGE 110
3.6	TYPICAL PATTERNS OF RECEPTOR INTERNALISATION	PAGE 111
3.7	THE CD23A ISOFORM DOES CO-LOCALISE WITH TRANSFERRIN-MODIFIED TEXAS RED (Tf-TxR) IN HEK 293 CELLS	PAGE 112
3.8	THE CD23B ISOFORM DOES NOT CO-LOCALISE WITH TRANSFERRIN-MODIFIED TEXAS RED (Tf-TxR) IN HEK 293 CELLS	PAGE 113
3.9	THE CD23A ISOFORM DOES NOT CO-LOCALISE WITH LYSOTRACKER DYE IN HEK 293 CELLS	PAGE 114
3.10	THE CD23B ISOFORM DOES NOT CO-LOCALISE WITH LYSOTRACKER DYE IN HEK 293 CELLS	PAGE 115
3.11	HEK 293 CELLS DO NOT UTILISE THE CLASSICAL PHAGOCYTOTIC PATHWAY	PAGE 116



3.12	HEK 293 CELLS DO NOT EXPRESS MHC CLASS II MOLECULES	PAGE 117
4.1	GENERATION OF MUTANT GFP-CD23A FUSION PROTEINS	PAGE 140
4.2	GENERATION OF MUTANT GFP-CD23B FUSION PROTEINS	PAGE 141
4.3	AMINO ACID SIDE CHAINS - THE RELEVANCE OF EACH OF THE MUTATIONS GENERATED	PAGE 142
4.4	HEK 293 CELLS STABLY EXPRESS ALL OF THE GFP-CD23 MUTANT FUSION PROTEINS AT THE PLASMA MEMBRANE - CD23BP3R APPEARS TO BE THE EXCEPTION TO THE RULE	PAGE 143
4.5	CELLULAR LOCALISATION OF EACH OF THE GFP-CD23 MUTANT FUSION PROTEINS IN HEK 293 – GFP-CD23BP3R DOES NOT REACH THE PLASMA MEMBRANE	PAGE 144
4.6	GFP-CD23AS7A PROTEIN CO-LOCALISES WITH TRANSFERRIN-MODIFIED TEXAS RED (Tf-TxR) IN HEK 293 CELLS	PAGE 145
4.7	GFP-CD23AS7D PROTEIN CO-LOCALISES WITH TRANSFERRIN-MODIFIED TEXAS RED (Tf-TxR) IN HEK 293 CELLS	PAGE 146
4.8	GFP-CD23AY6F PROTEIN CO-LOCALISES WITH TRANSFERRIN-MODIFIED TEXAS RED (Tf-TxR) IN HEK 293 CELLS	PAGE 147
4.9	GFP-CD23AYS67FA PROTEIN CO-LOCALISES WITH TRANSFERRIN-MODIFIED TEXAS RED (Tf-TxR) IN HEK 293 CELLS	PAGE 148
4.10	THE GFP-CD23BS5A PROTEIN CO-LOCALISES WITH TRANSFERRIN-MODIFIED TEXAS RED (Tf-TxR) IN HEK 293 CELLS AFTER CROSS-LINKING WITH NIP-BSA	PAGE 149
4.11	THE GFP-CD23BS5D PROTEIN CO-LOCALISES WITH TRANSFERRIN-MODIFIED TEXAS RED (Tf-TxR) IN HEK 293 CELLS UNDER ALL THREE BASAL, LOADED AND CROSS-LINKED CONDITIONS	PAGE 150
4.12	THE GFP-CD23BS5F PROTEIN CO-LOCALISES WITH TRANSFERRIN-MODIFIED TEXAS RED (Tf-TxR) IN HEK 293 CELLS UNDER ALL THREE BASAL, LOADED AND CROSS-LINKED CONDITIONS	PAGE 151
4.13	THE GFP-CD23BP3R PROTEIN DOES NOT TARGET TO THE PLASMA MEMBRANE IN HEK 293 CELLS	PAGE 152
4.14	THE GFP-CD23BP4R PROTEIN CO-LOCALISES WITH TRANSFERRIN-MODIFIED TEXAS RED (Tf-TxR) IN HEK 293 CELLS UNDER ALL THREE BASAL, LOADED AND CROSS-LINKED CONDITIONS	PAGE 153
4.15	THE GFP-CD23BN2K PROTEIN CO-LOCALISES WITH TRANSFERRIN-MODIFIED TEXAS RED (Tf-TxR) IN HEK 293 CELLS UNDER ALL THREE BASAL, LOADED AND CROSS-LINKED CONDITIONS	PAGE 154
4.16	MUTATION OF THE CYTOPLASMIC N-TERMINUS OF CD23 AFFECTS PROTEOLYTIC CLEAVAGE FROM THE CELL SURFACE	PAGE 155
4.17	RAJI A CELLS STABLY EXPRESS BOTH OF THE GFP-CD23 ISOFORM FUSION PROTEINS AT THE PLASMA MEMBRANE	PAGE 156
4.18	CONFOCAL ANALYSIS CONFIRMS CELL SURFACE EXPRESSION OF BOTH OF THE GFP-CD23 ISOFORM FUSION PROTEINS IN RAJI A CELLS	PAGE 157



4.19	SCHEMATIC DIAGRAM ILLUSTRATES THE ENHANCED NIP SYSTEM USING AN ADDITIONAL PROTEIN CONJUGATE – NIP-INSULN	PAGE 158
4.20	GFP-CD23B ENTERS THE ENDOCYTIC PATHWAY IN RAJI A CELLS	PAGE 159
4.21	GFP-CD23B ENTERS THE PHAGOCYTIC PATHWAY IN RAJI A CELLS	PAGE 160
4.22	RAJI A CELLS STABLY EXPRESS EACH OF THE GFP-CD23A MUTANT FUSION PROTEINS	PAGE 161
4.23	RAJI A CELLS STABLY EXPRESS EACH OF THE GFP-CD23B MUTANT FUSION PROTEINS	PAGE 162
4.24	CELLULAR LOCALISATION OF EACH OF THE GFP-CD23A MUTANT FUSION PROTEINS IN RAJI A CELLS	PAGE 163
4.25	CELLULAR LOCALISATION OF EACH OF THE GFP-CD23B MUTANT FUSION PROTEINS IN RAJI A CELLS	PAGE 164
4.26	THE GFP-CD23BP3R MUTANT DEMONSTRATED TWO DISTINCT PATTERNS OF EXPRESSION	PAGE 165
4.27	BOTH GFP-CD23A S7A AND S7D MUTANTS APPEAR TO CO-LOCALISE WITH TEXAS RED-MODIFIED TRANSFERRIN (Tf-TxR) IN THE BASAL STATE IN RAJI A CELLS	PAGE 166
4.28	BASAL LOCALISATION IN RAJI A - GFP-CD23AY6F AND AYS67FA MUTANTS	PAGE 167
4.29	BASAL LOCALISATION IN RAJI A -GFP-CD23BS5A, S5D AND S5F MUTANTS	PAGE 168
4.30	BASAL LOCALISATION IN RAJI A - GFP-CD23BN2K AND P4R MUTANTS	PAGE 169
5.1A	SCHEMATIC REPRESENTATION OF THE PRINCIPLE BEHIND THE YEAST TWO-HYBRID SYSTEM	PAGE 191
5.1B	SCHEMATIC REPRESENTATION OF THE PRINCIPLE BEHIND THE MATCHMAKER 3 YEAST TWO-HYBRID SYSTEM	PAGE 192
5.2	THE AH109 YEAST STRAIN	PAGE 193
5.3	GENERATION OF THE CD23 BAIT CONSTRUCTS	PAGE 194
5.4	ALL FOUR OF THE CD23 N-TERMINAL BAIT CONSTRUCTS ARE NON-TOXIC IN YEAST AH109 CELLS	PAGE 195
5.5	EXPRESSION OF THE CD23 N-TERMINAL TAIL AS A C-MYC FUSION PROTEIN IN AH109 YEAST	PAGE 196
5.6	SUCCESSFUL AMPLIFICATION OF THE HUMAN LEUKOCYTE CDNA LIBRARY	PAGE 197
5.7	X- $\alpha$ -GAL TEST FOR MEL1 ACTIVATION	PAGE 198
5.8	THE RECURRING CDNA CLONE - IDENTIFIED TO ENCODE METALLOTHIONEIN II (MT-II) IN OPEN READING FRAME (ORF) 3	PAGE 199
5.9	FIGURE RESTRICTION ANALYSIS OF THE 8 'POSITIVES' IDENTIFIED IN THE HIGHER STRINGENCY YEAST TWO-HYBRID SCREEN	PAGE 200
5.10	SUMMARY OF THE SEQUENCE DATA OBTAINED FOR THE EIGHT POSITIVE CLONES IDENTIFIED IN THE FINAL YEAST TWO-HYBRID SCREEN	PAGE 201

5.11	CLONES 2, 3, 5, 8 AND 9 ARE ABLE TO ACTIVATE HIS3 EXPRESSION IN THE PRESENCE OF THE EMPTY BAIT VECTOR	PAGE 202
5.12	CLONES 4 AND 7 ARE ABLE TO ACTIVATE HIS3 EXPRESSION ONLY IN THE PRESENCE OF THE CD23 BAIT VECTORS	PAGE 203
5.13	PROTEIN EXPRESSION FROM THE ISOLATED AD VECTORS	PAGE 204
5.14	CD23 MAY INTERACT WITH FLNA IN RPMI 8866 CELLS	PAGE 205
5.15	CD23 MAY INTERACT WITH FLNA IN RPMI 8866 CELLS (2)	PAGE 206
5.16	SCHEMATIC DIAGRAM ILLUSTRATING THE PROPOSED STRUCTURE OF HUMAN FLNA	PAGE 207
6.1	PROPOSED MODEL FOR THE CD23-FILAMIN A INTERACTION	PAGE 222

## **LIST OF TABLES**

TABLE 2.1	CONVERSION TABLE - NG OF OLIGONUCLEOTIDES EQUIVALENT TO 3.2PMOLES	PAGE 71
TABLE 2.2	TYPICAL PCR REACTION COMPONENTS	PAGE 72
TABLE 2.3	PCR CYCLE PARAMETERS	PAGE 72
TABLE 2.4	RT-PCR SAMPLE COMPONENTS	PAGE 73
TABLE 2.5	REVERSE TRANSCRIPTASE (RT) AND PCR CYCLING PROFILE	PAGE 74
TABLE 2.6	PCR PARAMETERS FOR THE GENERATION OF THE TEN CYTOPLASMIC N-TERMINAL CD23 MUTANTS	PAGE 76
TABLE 3.1	OLIGONUCLEOTIDE SEQUENCES USED TO GENERATE THE PCD23 AND PGFP-CD23 PLASMIDS	PAGE 98
TABLE 5.1	OPTIMISATION OF TRANSFORMATION EFFICIENCY, RECORDED AS NUMBER OF CFU PER SD/-TRP/-LEU AGAR PLATE	PAGE 178
TABLE 5.2	CONFIRMATION OF INTERACTION IN AH109 CELLS RE-TRANSFORMATION OF ISOLATED AD CONSTRUCTS	PAGE 182
TABLE 5.3	PROPOSED NOMENCLATURE FOR THE HUMAN FILAMIN PROTEINS.	PAGE 185
TABLE 5.4	SOME OF THE BINDING PARTNERS IDENTIFIED FOR THE HUMAN FILAMINS	PAGE 189



## **ABBREVIATIONS**

ADCC	Antibody-dependent cell-mediated cytotoxicity
AD	Activation domain
AFC	Antibody forming cell
ALL	Acute Lymphocytic Leukaemia
AP	Adaptor protein
APRIL	A proliferation-inducing ligand
ATP	Adenosine triphosphate
BB	Binding buffer
B-CLL	B-cell chronic lymphocytic leukaemia
BCMA	B cell maturation antigen
BCR	B-cell receptor
bHLH	Basic helix-loop-helix
BM	Bone marrow
BSA	Bovine serum albumin
BSAP	B cell specific activator protein
BTK	Bruton's tyrosine kinase
cAMP	Cyclic adenosine monophosphate
CD	Cluster of differentiation
COP	Coat protein
CR	Complement receptor
DMSO	Dimethyl sulphoxide
DNA	Deoxyribonucleic acid
DNA-BD	DNA Binding Domain
dNTP	Deoxyribonucleotide triphosphate
DTT	Dithiothreitol
EBF	Early B cell factor
EBV	Epstein-Barr virus
EBVCS	Epstein-Barr virus cell surface
EGF	Epidermal growth factor
ELISA	Enzyme-linked immunosorbant assay
ER	Endoplasmic reticulum
FACS	Fluorescence activated cell sorter
FCS	Foetal calf serum
FDC	Follicular dendritic cells



<b>FITC</b>	<b>Fluorocein isothiocyanate</b>
<b>Fn</b>	<b>Fibronectin</b>
<b>GC</b>	<b>Germinal centre</b>
<b>GDP</b>	<b>Guanosine diphosphate</b>
<b>GFP</b>	<b>Green fluorescent protein</b>
<b>GRE</b>	<b>Glucocorticoid response element</b>
<b>GTP</b>	<b>Guanosine triphosphate</b>
<b>HA</b>	<b>Hemagglutinin tag</b>
<b>HRP</b>	<b>Horseradish peroxidase</b>
<b>Id</b>	<b>Inhibitor of development</b>
<b>IFN</b>	<b>Interferon</b>
<b>Ig</b>	<b>Immunoglobulin</b>
<b>IL</b>	<b>Interleukin</b>
<b>IP3</b>	<b>Inositol trisphosphate</b>
<b>IRS</b>	<b>Insulin receptor substrate</b>
<b>LEF</b>	<b>Lymphoid enhancer binding protein</b>
<b>Mab</b>	<b>Monoclonal antibody</b>
<b>MCS</b>	<b>Multiple cloning site</b>
<b>MHC</b>	<b>Major histocompatibility complex</b>
<b>mRNA</b>	<b>Messenger ribonucleic acid</b>
<b>NF-AT</b>	<b>Nuclear factor-AT</b>
<b>NFκB</b>	<b>Nuclear factor kappa B</b>
<b>NIP</b>	<b>4-hydroxy-3-iodo-5-nitrophenylacetic acid</b>
<b>NIP-Osu</b>	<b>Nitro-iodophenacetyl-O-succinimide</b>
<b>NRE</b>	<b>Negative response element</b>
<b>NRE-BP</b>	<b>Negative response element-binding protein</b>
<b>NRR</b>	<b>Negative regulatory region</b>
<b>PAGE</b>	<b>Polyacrylamide gel electrophoresis</b>
<b>pBCR</b>	<b>Pre B cell receptor</b>
<b>PCR</b>	<b>Polymerase chain reaction</b>
<b>PBL</b>	<b>Peripheral blood lymphocytes</b>
<b>PBS</b>	<b>Phosphate buffered saline</b>
<b>PE</b>	<b>Phycoerythrin</b>
<b>PEG</b>	<b>Polyethyleneglycol</b>
<b>PI-3-K</b>	<b>Phosphoinositide-3-kinase</b>
<b>PKC</b>	<b>Protein kinase C</b>

<b>PMA</b>	<b>Phorbol myristoyl acetate</b>
<b>PMNs</b>	<b>Polymorphonuclear cells</b>
<b>PTPase</b>	<b>Protein tyrosine phosphatase</b>
<b>RA</b>	<b>Rheumatoid arthritis</b>
<b>RAG</b>	<b>Recombinase activating gene</b>
<b>RE</b>	<b>Response element</b>
<b>RNA</b>	<b>Ribonucleic acid</b>
<b>RT</b>	<b>Reverse transcription</b>
<b>SA-QR</b>	<b>Streptavidin quantum red</b>
<b>SCID</b>	<b>Severe combined immunodeficiency</b>
<b>SCR</b>	<b>Short consensus repeat</b>
<b>SDS</b>	<b>Sodium dodecyl sulphate</b>
<b>SHP</b>	<b>SH2-containing phosphatase</b>
<b>SLE</b>	<b>Systemic lupus erythematosus</b>
<b>SRP</b>	<b>Signal recognition peptide</b>
<b>SRBC</b>	<b>Sheep red blood cells</b>
<b>STAT</b>	<b>Signal transducer and activator of transcription</b>
<b>SV-40</b>	<b>Simian virus-40</b>
<b>TCAI</b>	<b>Transmembrane activator and CAML interactor</b>
<b>TCA</b>	<b>Tricarboxylic acid</b>
<b>TCF</b>	<b>T cell specific transcription factor</b>
<b>TCR</b>	<b>T cell receptor</b>
<b>TD</b>	<b>Thymus dependent</b>
<b>TdT</b>	<b>Terminal deoxynucleotidyltransferase</b>
<b>TGN</b>	<b>Trans golgi network</b>
<b>Tf-TxR</b>	<b>Transferrin-modified Texas Red</b>
<b>T<sub>H</sub></b>	<b>Helper T cell</b>
<b>TNF</b>	<b>Tumour necrosis factor</b>
<b>TRAF</b>	<b>TNF-receptor associated factor</b>
<b>Vn</b>	<b>Vitronectin</b>

# **CHAPTER 1**

## **INTRODUCTION**

## **1.1 THE IMMUNE SYSTEM**

The environment contains a huge variety of infectious microbes, such as viruses, fungi, protozoa and multicellular parasites. These agents can cause disease and if left uncontrolled can multiply and pose a serious threat to the survival of their host. The body's natural defence against such attacks is the immune system, consisting of a highly complex network of cells, collectively known as leukocytes (white blood cells) and a variety of soluble factors. The immune response involves two phases; firstly 'recognising' the pathogen or foreign material and then secondly, mounting an effector phase reaction to eliminate it from the body. The different types of immune response fall broadly into two categories; innate (or non-adaptive) and acquired (or adaptive).

### **1.1.1 INNATE IMMUNITY**

Innate immunity is the body's first line of defence and is present prior to the arrival of the infectious agent(s). The innate immune system relies on a set of germ-line encoded receptors that recognise conserved molecular patterns found only in micro-organisms. Innate immunity is mediated by phagocytic cells such as mononuclear phagocytes and polymorphonuclear leukocytes. These cells utilise primitive, non-specific recognition systems, enabling the internalisation and subsequent destruction of foreign particles. Granulocytes make up 60-70% of the total normal blood leukocytes and play an important role in acute inflammation providing protection against micro-organisms. The importance of these cells is clear from individuals with reduced cell numbers as they show dramatically increased susceptibility to infection. Granulocytes can be divided into neutrophils, eosinophils and basophils, on the basis of how the cytoplasmic granules respond to different types of staining agent when prepared for microscopy [Janeway & Travers, 1997]. The three types of cell have distinct effector functions.

Neutrophils are the most numerous (>90% of circulating granulocytes) and constitute the majority of leukocytes in the bloodstream. Polymorphonuclear cells (PMNs) migrate in response to chemotactic agents such as protein fragments released when complement is activated (C5a), and the products of other leukocytes, platelets and certain bacterial products, facilitating localisation at the site of infection. These cells ingest micro-



organisms within phagosomes, which can then fuse with lysosomes initiating the neutralisation and breakdown of the infectious agent.

Eosinophils comprise 2-5% of blood leukocytes in healthy, non-allergic individuals and although not their primary function, are also capable of phagocytosing and killing ingested micro-organisms. Eosinophils are thought to be primarily involved in the defence against parasitic infections, and are attracted by the products released by T cells, mast cells and basophils. Certain stimuli can cause degranulation, enabling these cells to use their granule armament against large targets that cannot be phagocytosed. The stimulus for eosinophil or mast-cell degranulation is often an allergen, and to be effective the allergen must cross-link IgE molecules bound to the surface of the cell via the cells high affinity receptors for IgE (FcεRI). CD23 is also expressed on certain populations of eosinophils and monocytes, and in this capacity is thought to be an important mediator in allergic reactions and in the immune response to parasitic infection [Capron & Dessaint, 1986].

Basophils are found in very small numbers in the circulatory system, and make up less than 0.2% of leukocytes. The function of basophils is thought to be similar to that of mast cells, and they are believed to play a part in protecting the mucosal surfaces of the body with degranulation releasing substances affecting vascular permeability.

### **1.1.2 ADAPTIVE IMMUNITY**

Acquired or adaptive immunity is induced or stimulated after exposure to the foreign antigen, is highly specific for a particular pathogen [Male *et al.*, 1993] and illustrates immunological memory whereby responses significantly improve upon subsequent encounters with the same antigen [Zinkernagel *et al.*, 1996]. Lymphocytes, making up 20% of the leukocyte population in adult circulation, are responsible for adaptive immune responses and the specific recognition of antigens. Two basic categories of lymphocytes exist: B cells and T cells. Both B and T lymphocytes develop and differentiate from pluripotent, self-renewable stem cells in the primary lymphoid organs, the adult bone marrow (or foetal liver) and thymus respectively, acquiring the ability to recognise antigen through the development of specific cell surface antigen

receptors. The cells then migrate to the secondary lymphoid tissues, where they can respond to antigen. The functioning of the adaptive immune system is based upon its ability to generate a vast array of antigen receptor specificities by somatic mechanisms of gene rearrangement and several additional processes of receptor diversification.

B lymphocytes represent approximately 5-15% of the circulating lymphoid pool, and are classically defined by the presence of particular surface immunoglobulins (Ig) that act as specific antigen receptors [Mellman & Kotch, 1988]. The majority of circulating human B cells express two Ig isotypes on their surface, IgM and IgD. Very few B cells in circulation express IgG, IgA or IgE, although these are present in large numbers in specific locations, for example, IgA-bearing cells in the intestinal mucosa. The transmembrane segments of surface IgM is associated with disulphide bonded heterodimers of Ig $\alpha$  (CD79a) and Ig $\beta$  (CD79b) on the B cell surface forming the B cell antigen receptor complex (BCR). Most B cells display MHC class II antigens, important for co-operative interactions with T cells, and complement receptors CR1 (CD35) and CR2 (CD21) are also commonly expressed.

T cells also play an important role, not only in the activation of B cells, as highlighted in section 1.2.3A, but also in their own right as immunologically reactive cells. As mentioned previously T cells are derived from bone marrow stem cells that differentiate as they pass through the mature thymus [Shortman & Wu, 1996; van Ewijk, 1991]. T lymphocytes recognise antigen and MHC molecules via the definitive T-cell lineage marker, the T-cell antigen receptor (TCR), a receptor molecule distinct from, but related to the BCR and indeed all immunoglobulin molecules. This receptor consists of an antigen-binding portion formed by two different disulphide linked polypeptide chains ( $\gamma, \delta$  or  $\alpha, \beta$ ) associated with a set of five polypeptides known as the CD3 complex, giving the T-cell receptor complex (TCR-CD3 complex) [Clevers *et al.*, 1988]. T cells can be further divided into subpopulations, distinguished by their expression of either CD4 or CD8, which determines whether they 'see' antigen in association with major histocompatibility complex (MHC) class I or class II molecules. CD4<sup>+</sup> T cells act primarily as helper T cells (T<sub>H</sub>) and can be subdivided into T<sub>H</sub>1 and T<sub>H</sub>2 cells based on the cytokines they secrete (either IL-2 & IFN- $\gamma$  or IL-4, IL-5 IL-6 & IL-10, respectively). T<sub>H</sub>1 cells are important for combating intracellular pathogens whereas



T<sub>H</sub>2 cells are more effective at stimulating B cells to proliferate and produce antibody, functioning primarily to protect against free-living micro-organisms (humoral immunity). CD8<sup>+</sup> (cytotoxic) T cells are mainly associated with the cytotoxic destruction of virally-infected cells.

Both T and B cells are activated on binding their specific antigens. T cells need to recognise antigens in the context of MHC molecules on antigen presenting cells (APCs), whereas B cells can bind to free antigen, but generally require T cell help to become activated. Antigen-induced activation and proliferation generally occurs in the lymphoid tissues and leads to the production of cytokines and cytokine receptors which together drive proliferation of the selected clones to maturation and the production of effector or memory cells. Memory cells re-circulate and ultimately lodge in areas of the lymphoid tissues where they remain, ready to respond if the same antigen is encountered again. Many B cell blasts mature into antibody forming cells (AFC's), exclusively devoted to the production of secreted antibody. Circulating antibodies are structurally identical to the primary B cell antigen receptors, lacking the transmembrane and intracytoplasmic sections, with huge diversity associated with the antigen-binding region. Antibodies are mediators of the humoral immune response, binding to specific antigens and aiding in their elimination. These target antigens can either be a molecule on the surface of a pathogen particle, or a toxin that it produces. The basic structure of all immunoglobulin molecules is a unit consisting of two identical light polypeptide chains and two identical heavy polypeptide chains, linked together by disulphide bonds. The class and subclass of each immunoglobulin is determined by its heavy chains. Each immunoglobulin molecule is bi-functional: the variable region is primarily concerned with antigen binding and mediates the neutralisation of soluble antigen and opsonisation of particulate matter. The constant (Fc) region mediates the so-called effector functions enhancing phagocytosis and antibody-dependent-cell-mediated cytotoxicity (ADCC) as well as activation of the classical complement pathway through interactions with receptors on the host tissues. AFCs can progress *in vivo* into terminally differentiated plasma cells, (comprising less than 0.1% of the total lymphocyte population), and tend to be restricted to the secondary lymphoid organs, producing antibodies of one specificity and immunoglobulin class.

## 1.2 B LYMPHOPOIESIS

The B cell clearly plays a central role in the immune system. B lymphocyte development, also known as B lymphopoiesis, the process by which B cells differentiate from haematopoietic stem cells, proliferate and mature into functional cells, is a highly regulated and complex process. Briefly, in the primary lymphoid organs the lymphocytes attain their repertoire of specific antigen receptors to deal with the antigenic challenges they will receive during their lifespan before migrating to the peripheral secondary lymphoid tissues. The majority of B cells (over 75%) maturing in the bone marrow do not reach the circulation but undergo apoptosis and are phagocytosed by bone marrow macrophages. Many B cells die at the pre-B cell stage, due to non-productive rearrangements of antibody receptors. The B cells are also stringently selected for tolerance to auto-antigens, minimising the production of cells with reactivity to self when in the periphery. The secondary lymphoid tissues (comprising of the spleen, lymph nodes and mucosa-associated tissues) provide an environment in which lymphocytes can interact with each other, with accessory cells and with antigen and disseminate the immune response.

The stages of primary B cell development are defined by cell size, the expression pattern of a variety of B-cell-restricted markers, growth properties and the rearrangement status of the immunoglobulin (Ig) genes [Melchers & Rolink, 1998]. Figure 1.1 illustrates the general features of antigen-independent B cell development. The progenitor B (pro-B) cells, the first identifiable stage of B cell development, express B220 (CD45) a marker expressed by all cells committed to B lymphopoiesis, as well as CD43 [Hardy *et al.*, 1991; Melchers *et al.*, 1995; Li & Wasserman *et al.*, 1996]. As progenitors progress through the pro-B stage they express terminal deoxytransferase (TdT), RAG-1, RAG-2, surrogate light-chain genes,  $\lambda 5$  and Vpre-B, CD19, Ig $\alpha$  and Ig $\beta$ , and rearrange their heavy chain *Igh* genes.

The following pre-B cell stage is identified by a decrease in surface expression of CD43, a lack of TdT expression, the successful rearrangement of the *Igh* locus, and the appearance of the pre-B cell receptor complex (pBCR) [Karasuyama *et al.*, 1994]. Early stage cycling or dividing pre-B cells show a decrease in RAG-1 and RAG-2 expression



[Grawunder *et al.*, 1995; Li & Dordai *et al.*, 1996]. As differentiation continues the RAG gene expression is induced and Ig light chain rearrangements begin, the completion of antigen independent B cell development is marked by successful rearrangement of the light chain genes and expression of surface IgM. The cells then exit the bone marrow and migrate to the periphery as immature B cells.

The B220 (CD45) molecule is a phosphotyrosine phosphatase (PTPase) which appears to regulate B cell receptor signalling by dephosphorylation of the src family tyrosine kinases such as lyn, Ig $\alpha$  and Ig $\beta$  [Satterthwaite & Witte, 1996]. It has been assumed that CD45 integrates signals during development although it is not actually required for B lymphopoiesis [Kishihara *et al.*, 1993]. CD19 is also thought to be important for B cell signalling and has been shown to interact with a number of tyrosine kinases [Satterthwaite & Witte, 1996]. It should be noted however that the role of this protein in B cell development is unclear as CD19<sup>-/-</sup> mice are still able to generate B cells. Appropriate expression of the surrogate light chain proteins  $\mu$ , Ig $\alpha$ , and Ig $\beta$  is essential for B cell development as it is these molecules that form the pBCR on the cell surface during pro-B cell stage development [Karasuyama *et al.*, 1994; Melchers *et al.*, 1994; Rajewsky, 1996]. The pBCR has been shown to associate with non-receptor kinases and provide critical signals for both progression to the pro-B cell stage and establishing *Igh* allelic exclusion [Loffert *et al.*, 1996]. Indeed, gene targeting experiments have confirmed that individual components of the pBCR are required for normal B cell differentiation. Mice lacking Ig $\beta$  are blocked at the pro-B cell stage of development [Gong & Nussenzweig, 1996], while  $\lambda 5^{-/-}$  and  $\mu^{-/-}$  mice have been shown to be restricted at the early pre-B cell stage [Kitamura *et al.*, 1991; Kitamura *et al.*, 1992] and mice with non-functional Ig $\alpha$  have significantly lower numbers of peripheral B cells. The finding that *bcl-2* and *bcl-x* genes, involved in protecting cells against apoptosis, are differentially expressed during B cell development [Grillot *et al.*, 1996] is consistent with the hypothesis that the role of pBCR signalling in lymphopoiesis may reflect cell fate decisions at the pro/pre-B transition.

Additional molecules involved in signalling and having a role in B cell development include JAK3, with knockout mice lacking B220<sup>+</sup>/CD45<sup>+</sup> progenitors [Grillot *et al.*, 1996] this mimics  $\gamma_c^{-/-}$  mice giving an X-SCID phenotype; *flk2*, a receptor tyrosine

kinase that appears to influence progenitor B cell development [Mackarechtschian *et al.*, 1995]; syk, a tyrosine kinase that appears to be essential for the generation of pre-B cells [Cheng *et al.*, 1995; Turner *et al.*, 1995]; lyn, a kinase related to src, seems to affect the maturation of immature B cells [Hibbs *et al.*, 1995; Nishizumi *et al.*, 1995] and Bruton's tyrosine kinase [BTK], as mutations of this gene are shown to be associated with X-linked immunodeficiency in mice and X-linked  $\alpha$ -gammaglobulinemia in humans [Satterthwaite & Witte, 1996].

Additional proteins that display B cell-restricted functions include integrin proteins, necessary for mediating both cell-cell and cell-extracellular matrix interactions and the IL-7 receptor, required for pro/pre B-cell generation [Li *et al.*, 1993; Arroyo *et al.*, 1996; Candeias *et al.*, 1997].

### **1.2.1 EXPRESSION AND REARRANGEMENT OF Ig GENES**

Correct expression of both the Ig heavy and light chains is essential for B cell development, and the transcriptional regulation and recombination events involved have been extensively characterised [Tonegawa, 1983; Ernst & Smale, 1995; Henderson & Calme, 1995; Sleckman *et al.*, 1996]. In general, Ig genes are regulated by an array of tissue-specific *cis*-acting promoters and enhancers, these elements being regulated by a combinatorial mechanism that involves both tissue-specific and ubiquitous transcription factors.

V(D)J recombination is known to occur at specific times during B lymphopoiesis [Tonegawa, 1983], with recombination beginning in the pro-B cell stage when cells undergo DJ<sub>H</sub> recombination [Reth & Alt, 1984]. Expression of cytoplasmic  $\mu$ , characteristic of the pre-B cell, occurs after successful rearrangement of a V<sub>H</sub> segment to the previously joined DJ<sub>H</sub>. Successful rearrangement of V and J elements at one light chain locus in the pre-B cell signifies the final stage of primary B cell development.

V(D)J recombination is regulated by at least two mechanisms; expression of the RAG genes and accessibility of the Ig genes to recombinase activity, both of which are transcription dependent [Sleckman *et al.*, 1996]. Components of the V(D)J



recombination machinery include ubiquitously expressed DNA repair proteins such as DNA-dependent protein kinase complex and lymphoid-specific components consisting of RAG-1 and RAG-2, which together are sufficient for recognition of recombination signal sequences and mediation of cleavage [McBlane *et al.*, 1995; Difilippantonio *et al.*, 1996; Sleckman *et al.*, 1996; Van Gent *et al.*, 1996, Ramsden *et al.*, 1997; Eastman *et al.*, 1996]. Deficiencies in V(D)J recombination will result from defects in either of these components [Shinkai *et al.*, 1992; Mombaerts *et al.*, 1992]. Expression of RAG genes is primarily restricted to developing lymphocytes undergoing rearrangement of their antigen receptor genes, and is highly regulated during B lymphopoiesis. RAG-1 and RAG-2 mRNA can be detected in pro-B cells, but both are down-regulated in large pre-B cells upon completion of IgH gene rearrangements [Grawunder *et al.*, 1995; Lin & Desiderio, 1998]. The RAG genes are then transcribed again in small pre-B cells, enabling light chain gene rearrangement [Grawunder *et al.*, 1995].

Receptor editing is the process by which immature bone marrow B cells become tolerant to self [Gay *et al.*, 1993; Radic *et al.*, 1993; Tiegs *et al.*, 1993]. These rearrangements are induced by encounter with autoantigens, and receptor editing that is stimulated by an autoreactive receptor is geared to promote continued secondary Ig L gene rearrangements until the offending receptor is either eliminated or altered for specificity to non-self. Receptor editing has been shown to occur frequently in normal B cell development [Retter & Nemazee, 1998].

### **1.2.2 ROLES OF TRANSCRIPTIONAL PROTEINS**

The development of committed B lineage cells from multipotent progenitors requires the co-ordinated activity of many transcriptional factors. Recent findings regarding the function and target genes for seven transcription factors necessary for proper development of early B lineage cells shall be detailed briefly.

Transcriptional factors that are essential for B cell development appear to block differentiation primarily at two stages; prior to commitment to B lymphopoiesis and at the pro-B/pre-B cell transition when V<sub>H</sub>DJ<sub>H</sub> recombination is beginning. PU.1 seems to be required prior to the first developmental checkpoint, whereas E2A, EBF and BSAP

appear to act at the second developmental checkpoint [Urbanek *et al.*, 1994; Dorshkind, 1994; Singh, 1996].

## PU.1

PU.1 is a member of the *ets* family of transcription factors, that is expressed exclusively in haematopoietic cells, with expression being highest in macrophages, but is also detected in neutrophils, B and early T lymphocytes [Klemsz *et al.*, 1990, Anderson *et al.*, 1999]. The importance of PU.1 in the development of these lineages was confirmed by generating mutant PU.1 mice [Scott *et al.*, 1994; McKercher *et al.*, 1996]. Scott *et al.*, report a mutation resulting in mice that die at embryonic day 18, lacking macrophages, neutrophils and lymphocytes but containing normal erythrocytes and megakaryocytes. The PU.1 mutation produced by McKercher *et al.*, results in mice surviving for 48 hours after birth, but that subsequently die from bacterial infection. These mice lack macrophages, neutrophils and lymphoid cells at birth. These findings suggest that PU.1 is required for the development of multipotential progenitor cells common to both the lymphoid and myeloid lineages. DeKoter and Singh suggest PU.1 expression levels to be important in determining whether multi-potent progenitors commit to differentiation down the B lymphocyte or macrophage lineage [DeKoter & Singh, 2000].

## IKAROS

The Ikaros gene encodes a set of proteins, generated by alternative splicing, that contain kruppel-like zinc fingers organised in two functional domains; one for DNA binding and a second for dimerisation [Molnar & Georgopoulos, 1994, Hahm, *et al.*, 1994,]. Ikaros gene expression appears to be present throughout B cell development [Georgopoulos, *et al.*, 1992, Georgopoulos, *et al.*, 1997, Morgan *et al.*, 1997], and while it appears to increase as B cells mature, the relevance of absolute versus relative levels of Ikaros proteins is not understood [Georgopoulos, *et al.*, 1997]. Gene targeting experiments introducing an Ikaros null-mutation in mice [Wang, *et al.*, 1996] illustrate its role in lymphopoiesis with these animals lacking fetal lymphocytes and adult B cells, with B cell development block being very early, prior to the pro-B cell stage.

## E2A

The E2A gene encodes two proteins, E12 and E47, members of the basic helix-loop-helix (bHLH) family of transcription factors [Murre *et al.*, 1994]. The E2A<sup>-/-</sup> homozygous mice die shortly after birth [Bain *et al.*, 1994; Zhuang *et al.*, 1996], whilst in the heterozygotes B lymphocytes fail to develop and T cell development is significantly perturbed [Bain *et al.*, 1994; Zhuang *et al.*, 1996; Bain *et al.*, 1997]. The bone marrow and fetal liver of E2A-deficient mice lack CD19<sup>+</sup> cells, and rearrangement of the IgH loci cannot be detected. In addition few B-lineage-associated genes are expressed, with the exception of germline IgH transcripts and B29/Igβ [Bain *et al.*, 1994; Bain *et al.*, 1997]. The E2A proteins have been shown to be involved in the expression and re-arrangement of the *Igh* and *Igκ* gene loci, and are thought to be required for the correct expression of the recombinase activating genes [RAGs] [Schlissel *et al.*, 1991; Bain *et al.*, 1997]. E2A and early B cell factor (EBF) are necessary and function together to promote the development of B lineage cells at subsequent stages [O’Riordan & Grosschedl, 1999].

Mice lacking E12 alone have defects at later developmental stages, suggesting E12 and E47 have an overlapping, yet distinct influence on B cell development [Bain *et al.*, 1997]. There is also a noted gene dose effect with E47 proteins, with E47<sup>+/-</sup> heterozygotes showing exactly half the number of mature B cells relative to control mice [Zhuang *et al.*, 1994].

E2A may also play a role in later B cell differentiation as it is upregulated in germinal centre cells with class switching to some isotypes inhibited in B cell lines that over-express Id (inhibitor of development), implying a role for bHLH family factors in terminal differentiation [Goldfarb *et al.*, 1996].

## EBF

Early B cell factor (EBF), as the name suggests, has been shown to regulate early events in B cell differentiation. EBF is expressed throughout B cell differentiation, with the exception of terminally differentiated plasma cells [Hagman *et al.*, 1993]. In mice ablation of EBF results in a block in the B cell differentiation at the early pro-B cell



stage. Pro-B cells from these animals lack DJ<sub>H</sub> rearrangements, Ig $\alpha$ , Ig $\beta$ , surrogate light chain, RAG-1 and -2, although they do express Ig $\mu$  and IL-7R, leading to the proposal that developmental arrest occurs after commitment to the B lineage [Lin & Grosschedl, 1995]. EBF and E2A-deficient mice present with defects at similar stages in B cell development, suggesting these proteins may act co-operatively to regulate a common set of genes. Indeed ectopic expression of EBF, together with E47 dimers, was shown to induce expression of VpreB and  $\lambda$ 5 B cell-specific genes suggesting functional synergy between the EBF and E47 proteins [Sigvardsson *et al.*, 1997].

### **BSAP/PAX-5**

B cell specific activating protein (BSAP), the product of the Pax-5 gene, is expressed in all B lineage cells with the exception of plasma cells [Barberis *et al.*, 1990]. Mice that carry a targeted deletion of the Pax-5 gene lack pre-B, B and plasma cells [Urbanek *et al.*, 1994]. These mice lack CD19<sup>+</sup> cells and V<sub>H</sub>DJ<sub>H</sub> recombination is significantly reduced [Urbanek *et al.*, 1994; Nutt *et al.*, 1997]. In addition, most B-lineage associated genes are expressed normally with the exception of CD19, N-*myc*, mb-1/Ig $\alpha$  and LEF-1, which have all been shown to be Pax-5-responsive target genes [Nutt *et al.*, 1999]. In the absence of Pax-5, progenitors do not become committed to the B lineage, even although they have the phenotype of committed B lineage progenitors [Nutt *et al.*, 1999; Rolink *et al.*, 1999]. In the absence of Pax-5 the cells continue to express a number of genes associated with non-B lineage cells, indicating an ability of Pax-5 to repress the expression of genes that function in the differentiation of alternative cell lineages.

### **LEF-1**

Lymphoid enhancer-binding factor (LEF-1) is a member of the T-cell-specific transcription factor (TCF)/LEF family. LEF-1 is expressed in both pro-B and pre-B cells, but not immature or mature B cells [Reya *et al.*, 2000]. In the absence of LEF-1 B lymphocyte differentiation appears to be normal, although fewer pro-B and pre-B cells develop, as a result of a decrease in proliferation and survival of early B lineage progenitors. Recently LEF-1 has been shown to be the target of the Wnt signalling pathway. Signal transduction in response to Wnt binding to its receptor, Frizzled, leads to the stabilisation of cytosolic  $\beta$ -catenin, which then accumulates in the nucleus and

functions as a co-activator for LEF-1 transcriptional responses [Behrens *et al.*, 1996]. This signal transduction pathway is very important in a number of developmental processes and in many forms of cancer [Polakis, 2000]. Wnt signalling may also be involved in the development of some forms of pre-B-acute lymphoblastic leukaemia (ALL), as Wnt16 was identified as a target of the E2A-Pbx1 oncoprotein which is associated with a subset of pre-B ALL [McWhirter *et al.*, 1999].

## **NF- $\kappa$ B**

The NF- $\kappa$ B/rel family of transcriptional factors illustrate a high degree of homology in a shared 300 amino acid rel domain. This region is essential for DNA binding, dimerisation between rel proteins and interactions with other transcriptional factors. There are at least five rel family members which may be involved in B cell development, these include RelA (p65), Rel-c, RelB, NF- $\kappa$ B1 (p105) and NF- $\kappa$ B2 (p100). p105 and p100 generate precursor proteins processed by proteolytic cleavage to generate p50 and p52 subunits. These subunits can generate hetero- and homodimers that bind DNA. NF- $\kappa$ B, whose activity is regulated by interaction with I $\kappa$ B inhibitory proteins is proposed to regulate several genes important in B cell differentiation, including the Ig light chains [Baeuerle & Henkel, 1994]. Studies have suggested a hierarchy of NF- $\kappa$ B dimers during B cell development; pre-B cells primarily have p50/p65 dimers, mature B cells have Rel-c/p50 dimers and plasma cells have p52/RelB dimers [Liou *et al.*, 1994; Miyamoto *et al.*, 1994].

### **1.2.3 STAGES OF ANTIGEN-DEPENDENT DEVELOPMENT**

Developmental events and altered patterns of gene expression that occur after the B cell encounters antigen are summarized in Fig 1.2. The naïve B cell is initially activated following the first encounter of the BCR with cognate antigen, inducing proliferation and stimulating uptake, processing, and presentation of thymus-dependent (TD) antigens and altered patterns of gene expression.



### **1.2.3A B LYMPHOCYTE ACTIVATION BY CONTACT-MEDIATED INTERACTIONS WITH T LYMPHOCYTES**

B lymphocytes can bind many biologically active soluble molecules such as lymphokines and chemokines, however the development of affinity maturation and a highly effective humoral memory response requires the receipt of contact-mediated signals from an activated T lymphocyte. Bystander polyclonal activation of B cells by activated T cells does occur, but is not widespread in the normal immune response. This fact suggests that the cognate interactions between B cells that can present specific antigen, and activated T cells that are specific for that antigen-MHC complex, increase the efficiency of the delivery of non-cognate signals between the two cell types [Bishop *et al.*, 1995; Macaulay *et al.*, 1997; Kalberer *et al.*, 1997]. Three mechanisms are thought to contribute to this increased efficiency; first, signalling through the BCR primes the B cell to become more responsive to T cell activation signals and also stimulates enhanced expression of surface molecules contributing to antigen presentation, e.g. MHC class II molecules. Second, the ability of the cells to interact directly through MHC-TCR binding enhances physical proximity, assisting in the delivery of contact-mediated signals as well as soluble molecules. Third, signals delivered to the B cell via engagement of the MHC class II molecules have been shown to enhance both antigen presentation and B cell activation, and are thought to co-operate with both BCR signals and other contact-dependent signals.

The requirement for contact-mediated signals in antigen-specific B cell activation appears to serve two important roles; to enhance the effectiveness of the adaptive humoral response and to decrease the potential for activation of auto-reactive B cells, with recent reports highlighting the importance of contact-mediated signals in the development of autoimmunity [Korganow *et al.*, 1999; Kyburz *et al.*, 1999]. Through use of a TCR transgenic mouse strain that develops a disease resembling human rheumatoid arthritis (RA), Korganow and colleagues showed that autoreactive T cells and B lymphocytes secreting auto-antibody are both necessary for disease development, suggesting the close co-operation of cellular and humoral immune responses in the development of certain autoimmune diseases. Kyburz and colleagues demonstrate the potentially important role for CD40-CD154 interactions in the pathogenesis of RA. This



interaction is discussed in more detail in the section devoted to the TNF and TNF-receptor family members.

It was originally believed that T cell cytokine production was both necessary and sufficient to mediate the full activation of antigen specific B cells. However when more stringent cell separation procedures were employed it was shown that contact-mediated signals from T cells were also required. Historically, purified B cell samples would have still contained contaminating T cells, facilitating the generation of these essential signals, unbeknown to the investigator. A variety of receptor-ligand pairs are now thought to contribute to T cell contact-mediated B cell activation, these interactions are discussed briefly below.

## **MHC CLASS II MOLECULES**

The first such signal to be identified was that from MHC class II molecules [Palacios *et al.*, 1983; Bishop & Haughton, 1986a]. This interaction has been well characterised now, with engagement of class II molecules on B cells reported to stimulate early biochemical signalling events as well as later effector functions, such as B cell proliferation and differentiation [Scholl & Geha, 1994]. Indeed many of these interactions have been investigated and it is reported that both the cytoplasmic and transmembrane domains of the molecule contribute to these signalling events [Wade *et al.*, 1989; Harton *et al.*, 1995]. Work with class II deficient mice has shown that B cell activation can occur in the absence of class II expression [Markowitz *et al.*, 1993]. However, class II engagement has been shown to enhance both BCR and CD40 signalling [Bishop *et al.*, 1995], and is thought to contribute to the activation of CD40-deficient B cells [Schrader *et al.*, 1996]. These data suggest that class II signalling may promote the preferential activation of cognate antigen-presenting B cells by T cells through enhancing the effectiveness of other B cell activation signals. Class II signalling has recently been shown to be partly regulated by two BCR co-receptors, CD19 and CD22 [Bobbitt & Justement, 2000], a finding consistent with this suggested role.

## ADHESION MOLECULES

Both B and T lymphocytes express a variety of transmembrane intercellular adhesion molecules. Both cell types express CD54 (ICAM-1) and CD11a-CD18 (LFA-1), which can bind to each other and mediate both homotypic and heterotypic adhesion interactions. Signalling to the B cell via these molecules is not well understood, however enhanced adhesiveness between B and T cells can amplify the activation signals from one cell type to the other. Preliminary studies indicated that both CD11a-CD18 and CD54 may directly transmit activation signals to B cells [Bishop & Haughton, 1986b; Owens, 1991], and it was later shown that such signals are able to contribute to enhanced B cell antigen-presentation [Moy & Brian, 1992] and work together with CD40-mediated signalling [Poudrier & Owens, 1994]. More recently, CD54-mediated upregulation of class II expression on a B cell line has been shown to correlate with the activation of the Src family kinase, Lyn, and the mitogen-activated protein kinases [Holland & Owens, 1997]. Further investigation is needed to elucidate the physiological circumstances in which CD11a-CD18 and CD54 signal to B cells and how these signals co-ordinate with other T cell mediated signals.

CD22, an immunoglobulin family member that modulates BCR signalling [Cornall *et al.*, 2000], is another adhesion molecule capable of signalling to B cells. A vast number of potential binding partners exist for CD22, including a variety of cell-surface glycoproteins and glycolipids demonstrating its natural ligand of N-linked oligosaccharides containing  $\alpha$ 2,6-linked sialic acids, many of which are expressed on T lymphocytes. The physiologically important ligands *in vivo* remain unclear. CD22 has been shown to be a receptor for CD45/B220 [Sgroi *et al.*, 1995].

CD81, a tetraspanin family member, has also been implicated in adhesion and T cell dependent B cell activation [Maecker & Levy, 1997; Maecker *et al.*, 1998], but as yet no natural ligand has been isolated so its effect on T and B cell interactions is not yet known.

## CD72

Antibody-mediated engagement of CD72 on B cells has been shown to stimulate proliferation, enhance B cell survival and upregulation of MHC class II expression [Amakawa *et al.*, 1996]. However until recently the ligand for CD72 had remained elusive. CD100, a class IV semaphorin expressed on both B and activated T cells, was identified as the natural ligand for CD72 [Kumanogoh *et al.*, 2000] an interaction shown to enhance B cell activation mediated by CD40. Results also indicate that CD100-mediated CD72 signals are important for antigen presentation and may be responsible for inducing the dissociation of SHP-1 phosphatase from CD72 [Kumanogoh, *et al.*, 2000, Shi *et al.*, 2000].

## TNF AND TNF-RECEPTOR FAMILY PROTEINS

Signals delivered through membrane-bound members of the TNF and TNF receptor (TNF-R) family of proteins are some of the most biologically important signals that B cells receive from the cognate activated T cell.

### CD40

CD40 was one of the first TNF family members shown to be of major importance in T cell-dependent B cell-activation. CD40 is a 45-50kDa glycoprotein [Paulie *et al.*, 1989] expressed on B cells as well as T cells and follicular dendritic cells (FDCs) [Banchereau, *et al.*, 1994]. CD154 or CD40L, the ligand for CD40, is a 39kDa member of the TNF family and is expressed as a membrane-bound trimer on activated T lymphocytes, as well as mast cells and basophils. T cell CD40L expression levels have been shown to increase as the cells mature [Nonoyama, *et al.*, 1995].

Briefly, CD40 engagement on B lymphocytes is well characterised, resulting in B cell proliferation, antibody secretion, cytokine production, upregulation of various surface molecules involved in antigen presentation, isotype switching, development of germinal centers and a humoral memory response, recently reviewed in [van Kooten & Banchereau, 2000; Calderhead *et al.*, 2000]. Dendritic cells have been shown to be superior to B cells with respect to antigen presentation in many situations, however recent studies have shown that B cells can be important antigen-presenting cells for T



cell activation and that CD40 signalling to the B cell plays a critical role in this function [reviewed by Korganow *et al.*, 1999; Constant, 1999].

B cell CD40-T cell CD40L interaction is also involved in the rescue of B cells from apoptosis [Holder, *et al.*, 1993], and the promotion of IgE synthesis and CD23 expression on uncommitted naïve B cells requires a minimum of two signals, the first from IL-4 (or IL-13) and the second through the CD40-CD40L interaction [Bonney, *et al.*, 1995]. Enhanced CD23 expression is noted when B cells are co-induced with both sCD40L and IL-4 [Burlinson, *et al.*, 1996]. This increase in CD23 is thought to be due to the ability of IL-4 to elevate CD40 levels in B cells, thus increasing the number of receptors available for engaging sCD40L.

The molecular mechanism by which CD40 signals to B cells has not been established. The carboxy-terminal domain of CD40 has been shown to bind to a cytoplasmic family of adapter molecules, called 'TNF-R-associated factors' (TRAFs) [Arch *et al.*, 1998]. TRAFs play important roles in CD40 signalling, however it is not yet clear how they regulate CD40 function.

## CD27

CD27 is a TNF-R family member expressed by a subpopulation of B lymphocytes, its ligand, CD70, is expressed by T lymphocytes relatively late in their activation [Hintzen *et al.*, 1993]. CD27 signals have been shown to be important in the terminal differentiation of B cells into antibody-secreting plasma cells [Agematsu *et al.*, 1998; Jacquot *et al.*, 1997; Nagumo *et al.*, 1998] and like other TNF-R family members, signalling by CD27 is mediated, at least in part, by TRAF molecules (TRAF-2, -3 and -5) [Arch *et al.*, 1998]. CD27 does mediate the activation of NF- $\kappa$ B and c-Jun kinase, in common with CD40 signalling [Akiba *et al.*, 1998; Gravestien *et al.*, 1998], but additional unidentified signals and the timing of CD27 expression are thought to contribute to its unique activities in B cell differentiation [Bishop & Hostager, 2001].

## **CD30 AND CD153**

CD30 and its ligand CD153 have been proposed as negative regulators of the humoral immune response, as signalling through either molecule on B lymphocytes has been shown to inhibit isotype switching and limit the magnitude of the immune response and the activation of low affinity B cells [Cerutti *et al.*, 1998; Cerutti *et al.*, 2000]. Like many of its relatives, CD30 mediates its signalling through TRAF proteins [Arch *et al.*, 1998] and can stimulate NF- $\kappa$ B activation [Ansieau *et al.*, 1996], presumably delivering other unique 'negative' signals that are yet to be identified. Signal transduction through CD153 is even less well understood, with its engagement resulting in the loss of Blimp-1 (B-lymphocyte-induced maturation protein 1) mRNA expression and enhancement of BSAP (B-cell-specific-activator protein) repressor binding to the immunoglobulin 3' enhancer [Cerutti *et al.*, 2000] although the proximal signalling events leading to these phenomena have not been elucidated.

## **CD134 LIGAND AND CD137 LIGAND**

Early studies demonstrated that CD134 ligand (CD134L), expressed on activated B cells, may send signals to B cells to promote proliferation and differentiation [Stüber *et al.*, 1995; Stüber & Strober, 1996]. CD134L-deficient mice have been shown to have a reduced number of switched immunoglobulin isotypes [Murata *et al.*, 2000] but germinal centre formation is not affected [Stüber & Strober, 1996], suggesting these signals are more important for normal production of a strong secondary antibody response, rather than for the development of memory B cells. More recently, CD134 stimulation of B cells has been shown to enhance the rate of IgG production stimulated through CD40, IL-4 and IL-10 [Morimoto *et al.*, 2000].

CD137, expressed on activated T cells, interacts with CD137L expressed on B cells and this interaction has been shown to provide important co-stimulatory signals to the T cell [as reviewed by Vinay & Kwon, 1994], however a clear role in B cell signalling has not been demonstrated *in vivo*. Early *in vitro* studies observed stimulation with CD137 to enhance the B cell proliferative response to anti- $\mu$  antibody [Pollock *et al.*, 1994]. A more recent study suggests that CD137L serves primarily to stimulate CD137 signalling in T cells, rather than to deliver critical signals to the B cell [DeBenedette *et al.*, 1999].



## **BCMA AND TACI**

B-cell maturation antigen (BCMA) is a member of the tumour necrosis factor (TNF) receptor family and is expressed on B lymphocytes. Two recently identified TNF-related proteins, BAFF [Schneider *et al.*, 1999] (also known as BlyS [Moore *et al.*, 1999] or TALL-1 [Shu *et al.*, 1999]), and APRIL ('a proliferation-inducing ligand') [Hahne *et al.*, 1998], have been shown to be able to augment B cell growth and differentiation by signalling through either BCMA or transmembrane activator and CAML-interactor (TACI). BCMA and TCAI are both expressed on resting B cells [Schneider *et al.*, 1999]. Both BAFF and APRIL compete for receptor binding, binding BCMA and TACI with equivalent affinity [Yu *et al.*, 2000]. BAFF is known to stimulate B cell proliferation and immunoglobulin secretion [Schneider *et al.*, 1999], as well as modulating the survival of peripheral B cells [Batten *et al.*, 2000; Laâbi & Strasser, 2000]. APRIL has also been shown to stimulate B-cell proliferation [Yu *et al.*, 2000]. Recent studies in mice have suggested a functional redundancy of BCMA in B-cell physiology, probably due to the presence of TACI [Xu & Lam, 2001]. The role of APRIL and BAFF in T cell contact dependent B cell activation is yet to be confirmed. Both molecules, primarily sourced from myeloid cells, are type-II transmembrane proteins and may have the potential to be proteolytically cleaved from the cell surface; therefore, they may be more important as soluble molecules.

### **1.2.3B REGULATION OF GERMINAL CENTER B CELL DIFFERENTIATION**

The complex developmental events that occur in the germinal centre (GC) depend upon intimate associations between the B cells and T helper cells ( $T_H$ ) and follicular dendritic cells (FDC's), initiating proliferation, somatic hypermutation, selection for cells expressing high-affinity antibodies, isotype switch recombination and negative selection [MacLennan, 1994; Kelsoe, 1995; Kelsoe, 1996; Tsiagbe, *et al.*, 1996; Ferguson, *et al.*, 1996]. Predictably a number of gene products involved in B cell-T cell interactions are required for GC formation; CD28, CD40, CD40L, CD19 and B7-2.

Centroblasts that form the dark zone proliferate rapidly and express high levels of c-Myc, required for rapid cell division [Cutrona *et al.*, 1997]. Somatic hypermutation takes place in GC [Kuppers *et al.*, 1996] in centroblasts prior to isotype switch recombination [Liu *et al.*, 1996 a, b & c] although GC formation has been shown not to



be strictly required for somatic hypermutation [Stall *et al.*, 1996, Matsumoto *et al.*, 1996]. Receptor editing of immunoglobulin light chains and re-expression of RAG-1 and -2 also occur in GC centroblasts [Han *et al.*, 1996].

Signalling via CD40/CD40L induces expression of B7, CD23 and other surface molecules in GC cells [Barrett *et al.*, 1991; Ranheim & Kipps, 1993; Kennedy *et al.*, 1994]. If GC cells fail to receive signals from FDC or T cells they undergo spontaneous Fas-dependent cell death [Laman *et al.*, 1996; Choe *et al.*, 1996; Koopman *et al.*, 1997]. If the BCR is engaged by soluble antigen or in the presence of T cell help, the cells also undergo apoptosis independent of Fas and CD40L [Pulendran *et al.*, 1995; Shokat & Goodnow, 1995; Galibert *et al.*, 1996; Han *et al.*, 1995], which presumably deletes auto-reactive B cells [Han *et al.*, 1995; Billian *et al.*, 1997] thus eliminating the possibility of generating high affinity auto-reactive mutants.

B cell antigen receptors that fail to bind adequately to low levels of antigen presented by FDCs within the GC can trigger yet another mechanism for optimising the B cell immune response – receptor revision [Wilson *et al.*, 2000; Nemazee & Weigert, 2000]. Receptor revision refers to a process similar to receptor editing (yet differently triggered) as it occurs in the peripheral lymphoid organs, such as the spleen, lymph node and gut. Whilst editing minimises autoreactivity in immature, preimmune cells by specifically replacing auto-reactive receptors, revision occurs during antigen-driven immune responses and is suppressed, rather than induced, by sIg cross-linking. Successful antigen receptor revision in peripheral B cells results in the expression of a surface Ig molecule that binds antigen with an affinity higher than that of the parent Ig molecule, and therefore contributes to selection of an Ig repertoire of the best fit [Nemazee, 2000].

Following successive rounds of somatic hypermutation, receptor editing, isotype switch recombination and selection, GC B cells are signalled to proliferate, exit the germinal center and differentiate into either memory (able to make a robust secondary immune response) or plasma B cells (secreting high affinity antibody). These cells lose their ‘apoptotic’ phenotype by downregulating Fas [Choe *et al.*, 1996] and increasing expression of bcl-2, bcl-xL, and cyclin-dependent kinases 4 and 6 [Ishida *et al.*, 1995].

They switch from an autocrine to a paracrine dependence on IL-6 by downregulating IL-6 expression and upregulating IL-6R expression [Koopman *et al.*, 1997].

CD40 signalling also induces expression of a number of transcription factors, including jun via JNK [Berberich *et al.*, 1996; Li & Baccam *et al.*, 1996], NF- $\kappa$ B [Berberich *et al.*, 1994], and NF-AT [Choi *et al.*, 1994]. CD40 signalling is probably required for the generation of both memory and plasma cells [Lagresle *et al.*, 1995; Holder *et al.*, 1993]. The timing, strength, and interplay of signals from BCR, CD40, B7-1/2, and cytokines appears to determine cell fate [Grouard *et al.*, 1995; Arpin *et al.*, 1995; Malisan *et al.*, 1996; Maliszewski *et al.*, 1993; Urashima *et al.*, 1996]. Little is known about gene expression in memory cells, although human memory cells are CD38<sup>-</sup>CD20<sup>+</sup>CD39<sup>+</sup> and can be re-stimulated to proliferate in response to CD40L [Arpin *et al.*, 1995].

Plasmablasts exiting the GC are still proliferating, but outside the GC they become non-dividing plasma cells with a life span of approximately 1 month. IL-6 protects plasma cells from apoptosis [Kawano *et al.*, 1995], induces immunoglobulin and Oct-2 expression [Natkunam *et al.*, 1994], and leads to activation of cyclin-dependent kinase inhibitor p18, which blocks cell division [Morse *et al.*, 1997]. Plasma cells have immense levels of Ig and J chain mRNA, and transcription factor Blimp-1 is induced when B cells differentiate into plasma cells [Turner *et al.*, 1994]. Expression of many genes is decreased in plasma cells, including CD23, CD22, possibly CD19, class II MHC, c-Myc, BSAP, early B cell factor (EBF), and CIITA [Henderson & Calame, 1998].

### 1.3 MOLECULAR SORTING

All eukaryotic cells exhibit protein transport both out from and into the cell. Pathways that transport material out of the cell are termed exocytic or secretory pathways, whereas pathways that bring material into the cell are termed endocytic pathways. One of the areas addressed by the research presented and discussed within this thesis is CD23 intracellular trafficking from the plasma membrane into the cell, the endocytic molecular sorting pathways are therefore of particular importance in this work. Figure



1.3 illustrates an overview of the common intracellular compartments and transport pathways which exist in eukaryotic cells.

### **1.3.1 GENERAL MODELS OF INTRACELLULAR SORTING**

For the most part transport of materials between intracellular compartments, and indeed between the plasma membrane and intracellular compartments, occurs via vesicles and requires several steps, namely vesicle formation, targeting, docking and fusion. A general model of vesicular transport exists that has been found to be conserved in all eukaryotic organisms from yeast to man. Briefly, transport is initiated from one membrane compartment by the recruitment of cytosolic coat proteins resulting in the formation of coated pits that can then deform the membrane into coated bud structures. These buds then undergo scission to form mature coated transport vesicles. The membrane-bound coat proteins must then be released into the cytosol before the vesicle can then fuse with its target compartment. Fusion is directed by protein complexes, derived from components that reside in both the cytosol and membranes of the vesicle and target compartment, serving to bridge the interaction between the membranes of the vesicle and those of the target compartment/membrane [Rothman & Wieland, 1996; Schekman & Orci, 1996].

Transport vesicles, whether or not they are selective in the way they pick up cargo from the donor compartment, must be highly selective with respect to their target in order to fuse with the correct membrane, enabling transport to the correct compartment within the cell. The SNARE hypothesis, suggests fusion is mediated by specific v-SNAREs on the vesicle membrane that recognise and dock with t-SNAREs on the target membrane, and is an attractive hypothesis describing how membrane specificity may be achieved [Sollner *et al.*, 1993]. The v-SNAREs are thought to be co-packaged with coat proteins during budding of the transport vesicle, and remain associated with the vesicle as it moves to the target membrane. It is interesting to note that the v-SNAREs are also transported back, from the target compartment to their original compartment, in an inactivated form, after the fusion event [Rothman & Warren, 1994; Pfeffer, 1996]. It has been demonstrated that SNAREs are regulated by the Rab family of GTPases [Brennwald *et al.*, 1994]. The cognate pairs of v- and t-SNAREs were originally thought to be sufficient for both vesicle targeting and fusion, however it has recently



become clear that the SNAREs mediate the fusion event, whilst Rab proteins mediate the SNARE-mediated fusion indirectly by modulating a more upstream process that docks the vesicle to its proper target compartment [Barlowe, 1997; Lupashin *et al.*, 1996].

Three types of coated vesicles exist, and figure 1.4 summarises these proteins and the pathways they serve in. Two groups of coatamer proteins termed COPI and COPII (COP for Coat Protein) are involved in the ER-to-Golgi, intra-Golgi and Golgi-to-ER pathways [Rothman & Wieland, 1996; Schekman & Orci, 1996], whilst clathrin coated vesicles are involved in plasma membrane-to-early endosome, TGN-to-late endosome and TGN-to-lysosome transport. The clathrin coat complex consists of six subunits. Two of them are termed clathrin heavy and light chains. These molecules are known to assemble in trimeric pairs forming the clathrin triskelions (Figure 1.4, section 2). Triskelions assemble into a cage-like hexagonal lattice which attaches to membranes through the four other members of the clathrin coat, the adaptor proteins (AP) or adaptins [Brodsky, 1997; Schmid, 1997]. The adaptins demonstrate specificity for different membranes, and thus enable clathrin coat proteins to form coated vesicles for more than one transport pathway. For example, clathrin with AP-1 adaptins form vesicles that transport from the TGN to the late endosome whilst clathrin with AP-2 adaptins form vesicles that transport from the plasma membrane to the early endosome [Kirchhausen *et al.*, 1997; Trowbridge *et al.*, 1993]. A third adaptin complex has been identified, AP-3 [Dell'Angelica *et al.*, 1997; Simpson *et al.*, 1997] and has been shown to mediate transport from the TGN to the lysosome [Cowles *et al.*, 1997; Simpson *et al.*, 1997].

It should be noted that endocytosis can also occur via non-clathrin coated vesicles, however this is less understood and poorly characterised. One class of non-clathrin coated endocytosis can be defined pharmacologically as its action is unaffected by cytosolic acidification and potassium depletion, two factors which characteristically affect clathrin-mediated transport [Sandvig & van Deurs, 1994]. Another class is identified by the involvement of morphologically distinct structures termed caveolae [Parton, 1996]. Reconstitution studies suggest that a predicted multi-spanning membrane protein termed caveolin is essential for the organisation of the membrane

into the structures characteristic of caveolae [Fra *et al.*, 1995]. Isoforms of caveolin that have tissue specific distribution have been identified [Scherer *et al.*, 1996; Tang *et al.*, 1996] but this protein is absent in lymphocytes accounting for the lack of caveolae in these cells [Fra *et al.*, 1994; Gorodinsky & Harris, 1995].

### 1.3.2 SECRETORY PATHWAYS

Briefly, the endoplasmic reticulum (ER) is the port of entry for all proteins transported through the secretory pathways. Nascent proteins targeted to the ER contain an amino-terminal stretch of hydrophobic residues known as the signal peptide [Blobel & Dobberstein, 1975]. A protein complex termed the signal recognition particle (SRP) binds to the signal peptide and targets the nascent protein to another complex on the ER membrane. The target complex on the ER contains the binding site for the SRP, the SRP receptor and a channel that translocates the nascent protein across the ER membrane. Proteins proceed from the ER to the Golgi complex where they can be sorted into several different routes [Mellman & Simons, 1992]; some are retained in the Golgi, others are sorted for retrograde transport back to the ER, whilst others continue in the anterograde direction, through the Golgi stacks to reach the *trans*-Golgi network (TGN), from where they can be transported directly to the cell surface or diverted towards the endosomal/lysosomal system [Griffiths & Simons, 1986]. Depending on the cell type, secretion can either be a constitutive process or it may be regulated, as occurs in specialised cells, where by proteins are concentrated and stored until an extracellular signal stimulates their release.

### 1.3.3 ENDOCYTIC PATHWAYS

Endocytosis has been defined traditionally as the transport processes that brings materials into the cell, and is characterised by the continuous and regulated formation of large numbers of membrane vesicles at the plasma membrane. Endocytotic vesicles exist in several different varieties, ranging from actin-dependent formation of phagosomes involved in larger particle uptake or phagocytosis, to smaller clathrin-coated vesicles often responsible for the internalisation of extracellular fluid and receptor-bound ligands via endocytosis.



There are characteristic differences between endocytosis and phagocytosis, with the main one being that phagocytosis can bring much larger material into the cell. The initial step of each pathway is also different, with vesicular transport involving a localised inward curvature of the membrane, forming buds, whereas the initial step of phagocytosis involves local reorganisation of the submembranous actin-based cytoskeleton, enabling the cell surface to envelope the structure that is to be internalised [Swanson & Baer, 1995]. It should be noted that although endocytosis was originally used to include both these types of transport, the usage of the term endocytosis now often implies only to transport other than phagocytosis, and this is the case herein.

### 1.3.3A ENDOCYTOSIS

Proteins at the cell surface are internalised into endosomes by a process termed endocytosis [Goldstein *et al.*, 1985; Helenius *et al.*, 1983; Pastan & Willingham, 1983]. Endosomes can be divided into functionally distinct compartments; internalised proteins are first transported to the early endosome, which can be further divided into the sorting endosome, where membrane-associated proteins can be sorted for either further transport into the cell or return to the cell surface via the recycling endosome [Geuze *et al.*, 1983; Griffiths *et al.*, 1989]. Proteins that are taken further into the cell reach the late endosome [Salzman & Maxfield, 1988; Schmid *et al.*, 1988], where they can be either transported to the lysosome and degraded or transported to the TGN to join the exocytic pathway [Geuze *et al.*, 1988]. The endosomal system involves a pH gradient that becomes progressively more acidic from early endosomes (pH 5.5-6.0) to lysosomal compartments (pH 4.5-5.0) [Mellman *et al.*, 1986]. The acidic pH is known to serve at least two major purposes; firstly, playing a critical role in the dissociation of ligands from their receptors and secondly activating hydrolases that reside within lysosomes. Collectively this enables receptor recycling via endosomes, as well as the degradation of proteins within the lysosomal compartments. In many cases the unbound receptor is then free to be recycled back to the cell surface and perform further rounds of ligand uptake [Dautry-Varsat *et al.*, 1983; Klausner *et al.*, 1983]. There are four general fates for ligand receptor complexes and these are detailed below, with examples of each case;

- 1) Both receptor and ligand are recycled, e.g. the transferrin receptor,



- 2) Both receptor and ligand are degraded e.g. the epidermal growth factor (EGF) receptor,
- 3) Receptor is recycled whilst the ligand is degraded e.g. the low density lipoprotein (LDL) receptor
- 4) Both receptor and ligand are transported elsewhere, e.g. the immunoglobulin Fc $\gamma$  receptor family.

A good, extensively understood example is the transferrin receptor and its ligand ferrotransferrin. In this case the low pH causes the release of Fe<sup>3+</sup> from the ligand, which remains bound to the transferrin receptor and together they recycle back to the plasma membrane, where the apotransferrin dissociates from the receptor at the neutral pH, leaving the transferrin receptor free to bind another ferrotransferrin molecule and repeat the process again. Each cycle is thought to take about 15-20 minutes to complete and an individual receptor may complete the process up to 100 times.

Most of the known membrane receptors are internalised from the cell surface through specialised structures of the plasma membrane termed coated pits, characterised by the presence of a coat on the cytosolic side of the plasma membrane. The receptors undergoing endocytosis are first recruited and concentrated into coated pits and then internalised as a result of progressive invagination of the coated pits that pinch off from the membrane giving coated vesicles [Smythe & Warren, 1991].

Endocytosis has been studied most extensively for transport by clathrin-coated vesicles. Activation of many cell surface receptors induces their association with clathrin AP-2 adaptins and results in the endocytosis of the activated receptors at distinct areas along the plane of the cell membrane [Pearse & Robinson, 1990; Schmid, 1997]. The AP-2 adaptin complex plays a central role in both the organisation and function of plasma membrane coated pits [Kirchhausen, 1993]. AP-2 is composed of two large chains, the  $\gamma$  and  $\beta_2$  adaptins, a medium sized  $\mu_2$  chain and a small  $\sigma_2$  chain.  $\gamma$  adaptin is necessary for targeting to the plasma membrane and seems to modulate AP-2 function through interactions with phosphoinositides [Beck & Keen, 1991], whilst the  $\beta_2$  adaptin binds to clathrin [Gallusser & Kirchhausen, 1993; Shih *et al.*, 1995].  $\mu_2$  has been demonstrated to

bind to tyrosine-based sorting signals present in the cytoplasmic tail of many endocytosed receptors [Boll *et al.*, 1996; Ohno *et al.*, 1995 & 1996]. There is evidence to suggest that other proteins can act as functional homologues of AP-2, for example  $\beta$ -arrestin can cause the endocytosis of adrenergic receptors by physically coupling the receptors to clathrin triskelions [Goodman *et al.*, 1996].

### **1.3.3B PHAGOCYTOSIS**

Within the immune system, the ability to internalise large particles is most often associated with phagocytic leukocytes, e.g. macrophages and neutrophils. Phagocytic uptake is generally triggered by the binding of opsonised particles to cell surface receptors capable of transducing a phagocytic stimulus to the cytoplasm, resulting in the localised polymerisation of actin at the site of particle attachment. The completion of phagocytosis results in a compartment termed the phagosome that can then evolve into a phagolysosome after the incorporation of lysosomal proteases as a result of the phagosome fusing with a lysosomal compartment [Desjardins *et al.*, 1994].

In mammals phagocytosis serves as the first line of defence against microorganisms, as well as providing an important component of the humoral immune response by allowing the processing and presentation of pathogen-derived peptides to antigen-specific T-lymphocytes via MHC class II molecules [Harding & Geuze, 1992]. Receptors that mediate phagocytosis in leukocytes include members of the IgG Fc $\gamma$  receptor family as well as some integrins (e.g. complement receptor 3, CR3) and lectins (e.g. mannose receptor) [Kielian & Cohn, 1980; Mellman *et al.*, 1983; Wright & Silverstein, 1983; Ezekowitz *et al.*, 1991; Isberg *et al.*, 1994].

### **1.3.4 ANTIGEN PRESENTATION BY MHC CLASS II MOLECULES**

Antigen presentation by MHC class II molecules represents one of the most complex examples of co-ordinated protein assembly and transport [reviewed by Cresswell, 1994]. Mature MHC class II molecules on the cell surface consist of  $\alpha$  and  $\beta$  heterodimers with bound peptide in the peptide-binding groove. Briefly, upon their synthesis in the ER, class II heterodimers assemble with a third subunit, termed the invariant chain (I $\iota$ ). The I $\iota$  molecule covers the peptide-binding cleft of the class II



heterodimers and prevents them from acquiring peptide antigens in the ER. During transport through the secretory pathway, the cytoplasmic tail of Ii possesses a dileucine-based motif that diverts the nonameric complexes from the TGN to the endosomal pathway. Hydrolases that are activated by the acidic environment of the endosomal pathway degrade Ii, except for a peptide portion, termed CLIP that remains in the peptide-binding groove of the  $\alpha/\beta$  heterodimer. At the same time, protein antigens from the extracellular environment are endocytosed into the endocytic pathways, where they are degraded into peptides. An MHC-like molecule, termed HLA-DM in humans, catalyses the release of the CLIP peptide from the peptide-binding groove so that exogenously-derived peptides can be transferred into the cleft. The assembled class II molecules are then transported to the cell surface, where they present their bound peptides to T cells [Cresswell, 1994]. Both MHC class II molecules and phagocytosed antigens are present in phagosomes [Harding & Geuze, 1992]. The phagosomes may receive the MHC class II molecules following fusion with vesicles from the trans-golgi network that contain newly synthesised MHC class II molecules or by fusion with endocytic organelles [Rabinowitz, 1992]. Binding of antigen to the MHC may take place in the phagosome [Lang *et al.*, 1994] or alternatively, partially or fully processed antigens from the phagosome may be transported to the endocytic pathway for further processing, and transportation to the cell surface [Pitt *et al.*, 1992; Tjelle *et al.*, 1998].

### 1.3.5 INTRACELLULAR SORTING SIGNALS

A variety of intracellular sorting signals have been identified within the cytoplasmic domain of a number of transmembrane proteins and collectively these have led to the elucidation of a variety of consensus motifs found to be involved in several of the intracellular transport pathways. The first class of endocytic sorting signals are characterised by an essential tyrosine residue which is either part of the motif NPXY (X representing any amino acid) as initially described for the LDL receptors signal (NPVY), or in the context of YXX $\phi$  (where  $\phi$  is an amino acid with a bulky hydrophobic side chain such as leucine/isoleucine or phenylalanine), as exemplified by the internalisation signal of the transferrin receptor (YTRF). Interestingly, in some cases the internalisation signal is also functional with phenylalanine replacing tyrosine, e.g. the LDL receptor [Chen *et al.*, 1990]. The second class of internalisation motifs typically contains a di-leucine sequence LL; in some cases one of the leucines may be



replaced by isoleucine, valine, alanine or methionine. Both tyrosine-based [Glickman *et al.*, 1989; Ohno *et al.*, 1995] and di-leucine-based [Heilker *et al.*, 1996] motifs are recognised by clathrin with AP-2 adaptins, enabling proteins with these motifs to be transported from the cell surface to the early endosome [Letourneur & Klausner, 1992; Lobel *et al.*, 1989]. A dilysine motif KKKXX has also been associated with the transport of proteins from the plasma membrane to early endosomes, although the adaptin molecule involved has not been identified. The determinants for lysosomal sorting also generally involve typical tyrosine or dileucine motifs [Hunziker & Geuze, 1996], although the precise sequence requirements are not exactly the same. The lysosomal tyrosine motifs, for example, are immediately preceded by a glycine (e.g. lamp-1, GYQTI), which is important for direct lysosomal traffic but not necessary for endocytosis [Harter & Mellman, 1992].

Fc receptor-mediated phagocytosis of IgG-coated particles by macrophages is associated with localised tyrosine phosphorylation of a variety of cytoplasmic proteins [Greenberg *et al.*, 1993; Greenberg, 1995]. Two cytoplasmic tyrosine residues of FcγRs that undergo phosphorylation are arranged into a short domain, YxxL(x)<sub>7</sub>YxxL or YxxL(x)<sub>12</sub>YxxL, termed ITAM (immunoreceptor tyrosine-based activation motif) [Samelson & Klausner, 1992]. The phagocytic abilities of FcγRs depend on ITAM, as indicated by studies of COS cells transfected with wild-type or mutant FcγRs [Mitchel *et al.*, 1994; Indik *et al.*, 1994]. This reflects the recruitment of cytosolic src-family kinases to the Fc receptor cytoplasmic domain via its consensus tyrosine-containing ITAM motif [Greenberg *et al.*, 1994; Greenberg *et al.*, 1996]. Transfection of Fc receptor cDNAs into normally non-phagocytic cells can also result in phagocytosis, as long as the appropriate src-family kinases are co-expressed [Greenberg *et al.*, 1996]. ITAMs are also present in other receptors of the Ig gene superfamily, such as the BCR and TCR, which share common signalling motifs with the FcγRs.

The cytoplasmic domain of CD23, shown in figure 1.6, does not contain any of these characteristic tyrosine or di-leucine-based motifs. However, CD23a does contain a cryptic tyrosine motif (YSEI), utilising both “unique” and “common” elements of the CD23a cytoplasmic tail sequence that is similar to the tyrosine motif found in lamp-1 (GYQTI). The lack of the important preceding glycine residue however, suggests that

this motif may favour endocytic rather than lysosomal uptake of CD23a. Recently, an acidic dipeptide motif (EE) has been demonstrated to be important for intracellular sorting of HIV-1 Nef protein [Piguet *et al.*, 1999]. Mutation of the EE diacidic motif of HIV-1 Nef abrogates its ability both to target CD4 from the early to the late endosomal compartment and to interact with  $\beta$ -COP, yet it does not affect AP binding or indeed Nef-induced CD4 endocytosis. Both CD23 isoforms contain an EE acidic dipeptide motif in their N-terminal cytoplasmic tails. There is also a dileucine motif present within the transmembrane region of CD23, however, this is unlikely to be available for sorting purposes when it is retained within the lipid-bilayer.

## **1.4 CD23 (Fc $\epsilon$ RII)**

Human CD23 is a 45kDa leukocyte cell surface antigen that is expressed on a variety of cells of haematopoietic lineage [Capron *et al.*, 1986, Sarfati *et al.*, 1986, Bieber *et al.*, 1989 and Billaud *et al.*, 1989]. CD23 is known to exist in two membrane bound isoforms, each of which can be proteolytically cleaved from the cell surface to generate soluble CD23. The principal function of CD23, in its membrane-associated form, is to act as the low affinity receptor for IgE (Fc $\epsilon$ RII) [Bonney *et al.*, 1987; Yukawa *et al.*, 1987] and the majority of the immunological functions of CD23, such as IgE-dependent cellular toxicity, antigen focusing, processing and presentation of IgE-containing immune complexes, are a reflection of this property.

### **1.4.1 DISCOVERY OF CD23**

The CD23 molecule was initially identified in human B lymphocytes as Fc $\epsilon$ RII, a low affinity receptor for IgE [Gonzalez-Molina *et al.*, 1976] and was shown to be distinct from Fc $\epsilon$ RI, the high affinity IgE receptor which had previously been identified on mast cells and basophils [Carson *et al.*, 1975; Conrad *et al.*, 1976]. A panel of monoclonal antibodies able to precipitate a 45kDa glycoprotein from the surface of Epstein-Barr virus-transformed B cells was described, so the molecule was named EBV cell surface antigen, or EBVCS [Kintner & Sugden, 1981]. The same molecule was later shown to be expressed on the surface of both normal and activated B cells, and was now referred to as a B cell activation antigen (Blast-2), and was demonstrated to have a rapid turnover from the cell surface of transformed B cells as a result of proteolysis [Thorley-



Lawson *et al.*, 1985]. It was eventually demonstrated that antibodies within the CD23 cluster (including Blast-2) reacted with, and specifically precipitated, the 45kDa protein product of cDNA encoding the low affinity IgE receptor, demonstrating that CD23, EBVCS, Blast-2 and FcεRII were in fact the same molecule [Yukawa *et al.*, 1987; Bonnefoy *et al.*, 1987].

#### **1.4.2 CELLULAR DISTRIBUTION AND REGULATION OF CD23 EXPRESSION**

CD23 is expressed on numerous human cell types including B and T lymphocytes, natural killer cells, macrophages, eosinophils, a subset of platelets, follicular dendritic cells, epidermal Langerhans cells and some epithelial cells [Capron *et al.*, 1986; Sarfati *et al.*, 1986; Bieber *et al.*, 1989; Billaud *et al.*, 1989]. Expression of CD23 is tightly regulated in a tissue specific manner with the two CD23 isotypes having different cellular distribution patterns. CD23a illustrates constitutive, but cell-type specific, low level expression on B cell lineage cells, whereas CD23b is detectable on B cells and a variety of other cell types, usually after stimulation by cytokines such as IL-4 [DeFrance *et al.*, 1987; Bonnefoy *et al.*, 1988].

##### **B LYMPHOCYTES**

CD23 is a differentiation antigen for B cells, being restricted to certain stages of B cell development. CD23 is selectively expressed on sIgM/sIgD double-positive mature B cells, but not immature bone marrow cells, and is thought to be involved in the regulation of growth and differentiation of B cells. CD23 is generally lost after the Ig isotype switch [Kitutani *et al.*, 1986] and during B cell differentiation into Ig secreting cells, regardless of isotype switch [Snapper *et al.*, 1991].

CD23 has also been shown to be spatially associated with HLA-DR molecules on the B cell surface [Bonnefoy *et al.*, 1988]. This interaction facilitates a well characterised function of membrane bound CD23 in B cells, the enhancement of the IgE-dependent antigen presentation to T cells [Kehry *et al.*, 1989; Pirron *et al.*, 1990; van der Heijden *et al.*, 1993; Santamaria *et al.*, 1993; Squire *et al.*, 1994; Gustavsson *et al.*, 1994; Fujiwara *et al.*, 1994; Mudde *et al.*, 1995; Westman *et al.*, 1997; Oshiba *et al.*, 1997; Karagiannis *et al.*, 2001]. This requires the binding of antigen-IgE antibody complexes



to CD23, internalisation of the complexes and transport to compartments of the endosomal network containing proteolytic enzymes and major histocompatibility (MHC) class II antigens. After digestion of the antigen, restricted peptides are loaded onto MHC class II antigens and returned to the cell surface for presentation to T cells. Antigen presentation also requires interaction between CD23 and CD21 at points of contact on the B- and T-cell surfaces [Flores-Romo *et al.*, 1990; Grosjean *et al.*, 1994]. Recent data have also suggested that CD23a and MHC class II molecules can be co-internalised and co-localised to endocytic compartments in a human B cell line [Karagiannis *et al.*, 2001].

Another function of membrane-associated CD23, the negative feedback regulation of IgE receptors [Sarfati *et al.*, 1988; Sherr *et al.*, 1989; Saxon *et al.*, 1991; Yu *et al.*, 1994], may well be related to the endocytosis of antigen-IgE complexes and the degradation of IgE within B cells.

Conflicting data exist as to the effect of engagement of CD23 on B cells, some publications reporting enhancement [Gordon *et al.*, 1986], others inhibition [Luo *et al.*, 1991] of B cell progression from G<sub>1</sub> to S phase in the cell cycle. However, the definite involvement of CD23 in the regulation of B cell growth is underlined by its abnormal expression and dysregulation in two malignant diseases resulting from the clonal expansion of sIgM/sIgD mature B cells; namely chronic lymphocytic leukaemia (CLL) and small lymphocytic lymphoma [Sarfati *et al.*, 1988]. CD23 disease association is discussed in more depth in section 1.3.9.

## T LYMPHOCYTES

*In situ* hybridisation reveals that CD23 mRNA is expressed in the subcapsular region (outer cortex) of the thymus, a region known to contain very early thymocytes. Both membrane associated and soluble CD23 were suggested to play an accessory role in T cell response to mitogens and allogenic or autologous B cells [Armitage *et al.*, 1989]. More recent observations demonstrated that mitogen-induced proliferation of CD4<sup>+</sup> T cells, known to require interactions with HLA-DR<sup>+</sup> accessory cells, could be inhibited by the binding of anti-CD23 monoclonal antibodies [Bertho *et al.*, 1991], these data suggesting a role for CD23 in T cell activation.

## OTHER LEUKOCYTIC CELLS

CD23 on macrophages, eosinophils and platelets has been found to mediate IgE-dependent cytotoxicity and to promote phagocytosis of IgE-coated particles on monocytes [Spiegelberg, 1984; Capron *et al.*, 1986]. As monocytes and eosinophils have been shown to express only CD23b these effects must be mediated by this isoform. CD23b has thus been concluded to have a role in protective immunity against parasites and in IgE-mediated inflammatory responses.

Follicular dendritic cells (FDC) are crucial in the generation and maintenance of adaptive immune responses via their ability to retain immune complexes for long periods of time, thus contributing to the generation of memory B cells. FDCs, located exclusively in the germinal centres of secondary lymphoid tissues, have been shown to exhibit CD23 protein (although CD23 mRNA appears to be absent). The function of this high level of CD23 expression on FDCs is still unknown. Theories include the possibility of these cells being involved in the generation of IgE-memory B cells, with them also being a potential source of signals which may rescue germinal centre B cells from apoptosis [Liu *et al.*, 1991].

## REGULATION OF CD23 EXPRESSION

IL-4, a 15-19kDa cytokine is amongst the most potent inducers of CD23 expression, (particularly CD23b) and can act on all cell types capable of expressing CD23. IL-4 is a highly pleiotropic cytokine involved in the regulation of B cell growth and differentiation as well as playing a pivotal role in the control of IgE responses via induction of IgE isotype switching [Lebman & Coffman, 1988]. The enhancing effects of IL-4 on B cells has been found to be inhibited by interferon- $\gamma$  (IFN- $\gamma$ ), IFN- $\alpha$ , TGF- $\beta$  and glucocorticoids via a protein kinase-C (PKC) independent pathway [Delespesse *et al.*, 1991; Delespesse *et al.*, 1992, Lee *et al.*, 1993]. Regulation of CD23 expression on monocytes is different to that on B cells, with IFN- $\gamma$  enhancing CD23 expression, while the effects of glucocorticoids and TGF- $\beta$  are the same. Engagement of CD40 may override the suppressive effects of IFNs and TGF- $\beta$  on IL-4-induced CD23 expression [Gordon *et al.*, 1991].



### 1.4.3 STRUCTURE OF CD23

Human CD23 is a single chain, 45kDa type II transmembrane glycoprotein containing 1 chain of N-linked complex carbohydrates, several O-linked carbohydrates and sialic acids residues [Letellier *et al.*, 1988]. No similarities have been shown to exist between the amino acid sequence of human CD23 and any of the subunits of the high affinity IgE receptor. Figure 1.5 illustrates a schematic representation of the structural features of these two molecules. CD23 has also been found to be both structurally and functionally unique in comparison to other immunoglobulin (Ig) receptors. CD23 has since been shown to be a type II transmembrane glycoprotein, such that the amino terminus lies within the cell and the carboxy terminus outside, effectively the opposite orientation to other Ig receptors.

#### 1.4.3A CD23 IS A MEMBER OF THE C-TYPE LECTIN SUPERFAMILY

Extensive homology was discovered to exist between CD23 and the super-family of animal C-type lectins [Kikutani *et al.*, 1986; Suter *et al.*, 1987; Ludin *et al.*, 1987] a family of proteins found to bind carbohydrates in a calcium-dependent manner [Drickamer, 1988]. This region of homology lies between Cys 163 and Cys 282 in the CD23 molecule and contains four highly and two partially conserved cysteine residues, at positions 191, 259, 273, 282 and positions 163 and 174, respectively [Kikutani *et al.*, 1986; Ludin *et al.*, 1987]. These data illustrate that CD23, unlike all the other Fc receptors that belong to the Ig super-family, actually belongs to the C-type lectin super-family.

Two subgroups within the C-type lectin superfamily with different domain organisations, soluble collectins [Epstein *et al.*, 1996], and the macrophage mannose receptor [Ikeda *et al.*, 1987; Tenner *et al.*, 1995], are believed to be involved in the innate immune response. Selectins serve in the adaptive immune response and have been shown to mediate transient interactions between leucocytes and endothelium [Lasky, 1995; Rosen & Bertozzi, 1996]. NK cells display a set of cell surface receptors containing the C-type lectin-like domains that may be involved in protein-protein interactions rather than the protein-carbohydrate interactions classical of the C-type



lectin superfamily members. The C-type carbohydrate recognition domain (C-type CRD) is identified as a common feature of several different calcium-dependent animal lectins and illustrates the sequence motif characteristic of the sugar-binding domain from these proteins [Drickamer, 1993]. The module has been used to identify structurally related regions in other proteins [Taylor, 1997]. One of the largest groups of proteins containing C-type CRD's are the type II transmembrane proteins [Nakayama *et al.*, 1996], including CD23, that have C-terminal CRD-like sequences linked by neck regions of various lengths to signal-anchor sequences and N terminal cytoplasmic tails. These molecules are thought to have distinct functional mechanisms to the classical C-type lectin superfamily members.

#### **1.4.3B STRUCTURAL DOMAINS OF HUMAN CD23**

Human CD23 has been shown to contain several domains [Beavil *et al.*, 1992], these are summarized in the schematic diagram in Figure 1.6. The extracellular portion of CD23 contains two domains, namely a stalk region and a C-type lectin-like domain. The stalk region is thought to be involved in oligomerisation of CD23 molecules at the cell surface. CD23 also contains a leucine zipper motif, located between the transmembrane domain and the lectin-like domain. This region consists of 3 short consensus repeats of 21 amino acids, including 5 heptadic repeats of leucines or isoleucines. The heptad repeats illustrate an  $\alpha$ -helical coiled-coil secondary structure [Beavil *et al.*, 1992] separating the lectin heads from the cell membrane, with the tertiary conformation being a common motif present in other members of the C-type lectin family. This stalk region has been suggested to provide a possible mechanism for oligomerisation of CD23 on the cell surface [Beavil *et al.*, 1995], a structural feature important for IgE binding [Dierks, *et al.*, 1993]. This theory has been verified by protein chemical cross-linking studies where human CD23 has been shown to exist in both dimer and trimer surface complexes [Beavil *et al.*, 1995].

The so-called lectin-like domain has been further characterised by mutational analysis and demonstrated to contain the IgE-binding site [Bettler *et al.*, 1989]. IgE has been shown to bind CD23 via protein-protein interactions [Vercelli *et al.*, 1989], as deglycosylation of IgE does not eradicate binding. This interaction has also been shown to be calcium dependent [Richards & Katz, 1990] and it can be inhibited by fucose-1-

phosphate [Delespesse *et al.*, 1992]. Further investigation has shown the cytokine activity of CD23 to be mediated by an epitope overlapping, yet distinct from the IgE binding domain [Mossalayi *et al.*, 1992], these cytokine effects are discussed more fully in section 1.4.5.

CD23 has an extended C-terminal tail containing a DGR (inverse RGD) sequence (a common recognition triad in receptors/ligands for integrin molecules) which seems to be involved in binding class II MHC molecules [Kijimoto-Ochiai & Noguchi, 2000]. CD23 contains a single, transmembrane hydrophobic domain (residues 24-44) and a short, largely hydrophilic cytoplasmic domain thought to be involved in signal transduction (residues 1-23). The two membrane-associated CD23 isoforms differ only in this region, and these differences are discussed further in section 1.4.6.

#### **1.4.4 SOLUBLE CD23**

Similar to other Fc receptors, full length CD23 can be cleaved to produce a number of soluble (sCD23) fragments, with all cleavage sites located in the stalk region of full length CD23. Intact/45kDa CD23 is initially cleaved to release the 37kDa species, containing the lectin-like domain and a large portion of the stalk region [Lettelier *et al.*, 1989; Marolewski *et al.*, 1998]. This species can be, and frequently is, sequentially cleaved into smaller fragments of 33, 29, 25 and 16kDa, each of which has been demonstrated to have cytokine activity *in vitro* [Liu *et al.*, 1991]. The 25kDa species, conventionally known as sCD23, has been identified as the most stable of all the soluble products [Lettelier *et al.*, 1989] and the one most readily available for use. All the soluble fragments retain the lectin-like domain and studies with anti-IgE antibodies have demonstrated that they also all retain their ability to bind IgE [Delespesse *et al.*, 1992]. The 16kDa species binds IgE with much lower affinity, a property believed to be due to the monomeric nature of this form [Bettler, *et al.*, 1989], as the avidity of CD23 for IgE is determined by oligomerisation [Dierks, *et al.*, 1993]. The 25kDa and larger fragments enhance IgE synthesis, while the 16kDa fragment has been found to inhibit the synthesis of IgE by B cells.



The binding of IgE has been shown to protect CD23 from cleavage [Lee *et al.*, 1987] with the amount of cleavage also significantly reduced in the presence of anti-CD23 antibodies. However, in contrast to this, cleavage is increased after the use of agents that prevent CD23 glycosylation [Delespesse, *et al.*, 1989] indicating that the carbohydrate chain exerts a stabilising effect on CD23. Studies with highly-purified 37kDa and 29kDa soluble CD23 proteins have shown these products to be able to cleave the full length, membrane-bound CD23 into the soluble 25kDa fragment [Lettelier *et al.*, 1990]. These data have been used as evidence to suggest CD23 can be cleaved in an autocatalytic manner, although CD23 does not show homology to any known proteolytic enzymes [reviewed by Bonnefoy *et al.*, 1997]. A recent publication refutes this however, reporting that CD23 release from human RPMI 8866 cell membranes is mediated by a metalloprotease distinct from substrate CD23 and that the cleavage process can be repressed by specific protease inhibitors [Marolewski *et al.*, 1998]. The same group subsequently suggested that the proposal of auto-proteolysis was a result of the co-purification of the metalloprotease with CD23, and speculate that there may be a whole family of metalloproteases that mediate the cleavage of CD23. Clearly the details of this cleavage process have still to be elucidated.

#### **1.4.5 CYTOKINE EFFECTS OF sCD23**

Human CD23 and its soluble products display a variety of biological functions in addition to their ability to bind IgE. Soluble CD23 may exert several regulatory effects, either alone or in synergy with other cytokines, on a variety of hematopoietic cells, including the differentiation of prothymocyte and myeloid precursors [Mossalayi *et al.*, 1990a & 1990b], inhibition of monocyte migration [Flores-Romo *et al.*, 1989], induction of CD3 positive thymocytes [Mossalayi *et al.*, 1990] and stimulus of antigen presentation by both B cells and monocytes to T cells [Bertho *et al.*, 1991]. Signal transduction of sCD23 is closely dependent upon the cell subset and ligands involved as well as the functional co-factors required.

#### **1.4.6 CD23 ISOFORMS**

Early evidence suggested two distinct roles for CD23, one being a stage-dependent involvement in B cell growth and differentiation [Gordon, *et al.*, 1987; Kolb, *et al.*,



1990], the second involving the effector phase(s) of IgE-mediated immunity, including allergy and the response to parasitic infections [Kehry & Yamashita, 1989; Luo, *et al.*, 1991]. Two species of human CD23 were originally hypothesised by Yokota and colleagues and then later identified and termed CD23a and CD23b [Yokota *et al.*, 1988]. These isoforms have been demonstrated to differ only in a short amino acid stretch in the cytoplasmic tail region where the N-terminal 7 amino acids of CD23a (MEEGQYS) are distinct from the alternative 6 amino acids of CD23b (MNPPSQ), Figure 1.6.

The human CD23 gene (EMBL accession number: M30447) spans approximately 13kb and has been specifically mapped to an 11 exon gene located on chromosome 19, encoding both the CD23 isoforms [Ludin, *et al.*, 1987; Suter *et al.*, 1987; Wendel-Hansen *et al.*, 1990]. Southern and Northern blot analysis of the CD23 genomic gene and the receptor-specific mRNA was carried out using fragments of CD23 cDNA as probes. A novel exon, specific for CD23b was found to be located between exons 2 and 3 of the CD23a mRNA. Primer extension studies then revealed it was in fact the initiation site for CD23b transcription. Three species of CD23 mRNA have been identified which differ only within their 5' regions. Two mRNAs code for CD23a and their sequences differ by only four nucleotides in the 5' untranslated region [Kikutani, *et al.*, 1986], which is thought to be due to differential splicing. The third mRNA codes for CD23b and is completely different from the other two in the 5' upstream region, in a position that corresponds to the exon 2-3 boundary of CD23a mRNA. It was concluded that these two transcripts are generated from different initiation sites and thus alternative splicing patterns of the same gene [Yokota *et al.*, 1988]. These data are summarized in Figure 1.7.

The promoter regions of each CD23 isoform have been shown to possess distinct response elements. The CD23a promoter region contains two IL-4 response elements (IL-4RE), an NFκB site, a glucocorticoid response element (GRE) and a B cell activator protein (BSAP) or Pax-5 binding site. In contrast, the CD23b promoter region comprises two IL-4RE sites surrounding an NFκB site, and two activated protein 1 (AP-1) binding sites. CD23a is expressed constitutively and cell type-specifically in B cells, whereas CD23b is expressed on several cell types of haematopoietic lineage following

activation with various stimulants (IL-4, IL-13, anti-CD40, anti- $\mu$  chain, PMA). Reporter vector construct studies of the CD23a and CD23b promoters revealed that the CD23a promoter was activated by IL-4 alone, but that the CD23b promoter was initiated with IL-4, anti-CD40, anti- $\mu$  and PMA [Ewart *et al.*, in press]. The presence of both cell type-specific and stimulus-specific expression of the two CD23 variants suggests that each isoform has a different cellular function, despite having identical extracellular domains.

The highly regulated manner of CD23 gene expression suggests that CD23a and CD23b are involved in B cell function and IgE mediated immunity, respectively. Further investigations illustrated the slight amino acid differences of the two isoforms to be responsible for their separate functions [Yokota *et al.*, 1992]. Early studies of CD23a and CD23b indicated that the two isoforms were internalised via distinct pathways, with CD23a entering the cell via receptor-mediated endocytosis and CD23b showing a more phagocytic route of cellular entry. CD23-mediated endocytosis was observed only in the CD23a-expressing cells. Site-directed mutagenesis revealed that the aromatic tyrosine residue at position 6 in CD23a was important for this process. It should be noted that these data are in good agreement with many other studies where cytoplasmic aromatic amino acids have been illustrated to be particularly important for endocytotic functions in many different receptor molecules; namely the low density lipoprotein receptor [Davis, *et al.*, 1987], mannose-6-phosphate receptor [Lobel, *et al.*, 1989] and transferrin receptor [Jing, *et al.*, 1990]. IgE-dependent phagocytosis was observed only in the CD23b-expressing cells with the Asn-Pro residues at positions 2-4 found to be necessary. These findings suggest endocytosis and phagocytosis to be separate functions that appear to be attributable to distinct amino acid residues.

Divergence in the signalling pathways coupled to the two membrane-bound CD23 isoforms must be related to the first 6/7 amino acids of the cytoplasmic N-terminal tail, as the remainder of each protein is identical. Current understanding generally links the CD23a isoform to a cAMP pathway with the CD23b isoform thought to function generally via inositol-1,4,5-trisphosphate and  $\text{Ca}^{++}$  mobilisation [as reviewed by Mossalayi *et al.*, 1997]. The ability of CD23 to transmit a signal to various cells and the fact it has a very short cytoplasmic tail strongly suggest that CD23 may be associated



with other molecules involved in signal transduction. Further research is obviously required to gain a comprehensive understanding of the signalling pathways employed by each isoform and this was one of the general aims of the work presented herein.

#### **1.4.7 LIGANDS FOR CD23**

##### **1.4.7A CD21**

CD21 was identified as a ligand for CD23 after CD23 liposomes were shown to bind specifically to cells transfected with recombinant CD21 [Aubry *et al.*, 1992]. CD21 is a 145kDa membrane glycoprotein expressed on a variety of cell types, including B cells, T cells and FDCs, and is also known as the complement receptor-2 (CR2) [Weis *et al.*, 1984]. CD21 has also been identified as a receptor for the gp350/220 envelope protein of EBV (EBV-R) [Tanner *et al.*, 1987] and a receptor for IFN- $\alpha$  [Declayre *et al.*, 1991]. CD21 exists within a molecular complex on B cells, in association with CD12, Leu 13 and TAPA-1 [Bradbury *et al.*, 1992]. The extracellular domain of CD21 contains 16 short consensus repeats (SCRs) [Weis *et al.*, 1988].

Characterisation of the CD21-CD23 interaction has showed that it is a calcium-dependent interaction, [Pochon *et al.*, 1992] involving two sites on the CD21 molecule [Aubry *et al.*, 1994]. A lectin type interaction occurs at SCRs 5-8, as tunicamycin treatment inhibits this binding [Aubry *et al.*, 1994]. Tunicamycin served to inhibit N-glycosylation during protein biosynthesis [Sarfati *et al.*, 1992]. SCRs 1-2 were also found to be involved in CD21-CD23 binding, but via a protein-protein interaction [Aubry *et al.*, 1994]. Soluble forms of CD21 shed from B and T cells have also recently been shown to interact with recombinant oligomeric soluble CD23 [Fremeaux-Bacchi *et al.*, 1996]. Collectively the data on this interaction indicate that the IgE promoting effects of CD23 are most probably exerted through CD21.

CD23 is known to be highly pleiotropic with many studies describing non-IgE-mediated effects and others demonstrating that CD23 expression is increased in several diseases not linked to IgE. It was quite correctly hypothesised that not all of these activities could be attributed to the interaction of CD23 with IgE and/or CD21. This has fuelled further research into discovering other novel ligands for CD23.



### 1.4.7B $\beta_2$ Integrins

CD23 was found to interact with the  $\alpha$  chain of two of the  $\beta_2$  integrins, CD11b (17kDa) and CD11c (15kDa) on monocytic cells [Lecoanet-Henchoz *et al.*, 1995]. These integrins are adhesion molecules which participate in many cell-cell and cell-matrix interactions [Springer, 1990]. The  $\alpha$  chains exist as heterodimer with a common  $\beta$  subunit known as CD18, forming the CD11b-CD18 (Mac-1) and CD11c-CD18 (p150, 95) glycoprotein receptors [Corbi *et al.*, 1988; Kurzinger & Springer, 1982]. The functional significance of CD23 binding to CD11b/c was demonstrated by triggering CD11b and CD11c on monocytes with either recombinant CD23 bound to liposomes or anti-CD11b and anti-CD11c MAbs. CD23 binding caused a marked increase in production of nitrite, oxidative products and pro-inflammatory cytokines [Lecoanet-Henchoz *et al.*, 1995], suggesting a physiological role for CD23 in the activation of monocytic cells. Furthermore, CD23 engagement has been demonstrated to elicit an increase in the production of interleukin 1 $\alpha$  (IL-1 $\alpha$ ), IL-1 $\beta$ , interferon- $\gamma$  (IFN- $\gamma$ ), IL-6 and tumour necrosis factor  $\alpha$  (TNF- $\alpha$ ). Collectively these data support the theory that CD11b and CD11c are functional receptors for CD23, and that CD23 is clearly a pro-inflammatory mediator [Lecoanet-Henchoz *et al.*, 1995].

IgE binding to CD23 was shown to inhibit CD23 binding to monocytes and the presence of EDTA was also found to decrease binding of CD23 to CD11b/c [Lecoanet-Henchoz *et al.*, 1995], indicating that CD23 may be acting as a C-type lectin with the CD23-CD11b/c interaction being  $\text{Ca}^{2+}$ -dependent and involving both lectin and protein-protein interactions. These findings are similar to those associated with the interaction of CD23 and CD21, where CD23 acts as a C-type lectin recognising structures that have both sugar and protein components [Pochon *et al.*, 1992; Aubry *et al.*, 1994]. As discussed previously the CD23 molecule contains a DGR motif, which in the reverse orientation is known to be a common recognition site for integrin receptors. This sequence was found not to be involved in the CD11b and CD11c interactions [Lecoanet-Henchoz *et al.*, 1995].

### 1.4.7C VITRONECTIN RECEPTORS

#### $\alpha_v\beta_3$

A recent publication suggests the vitronectin receptor,  $\alpha_v\beta_3$ , to be a novel receptor component for CD23 in monocytes [Hermann *et al.*, 1999]. This study has demonstrated that the trimolecular complex (VnR/ $\alpha_v\beta_3$  & CD47) mediates pro-inflammatory cytokine synthesis via interaction with CD23. The  $\alpha_v\beta_3$  integrin is a ubiquitous receptor known to interact with a number of ligands, including vitronectin (Vn), fibronectin (Fn), osteopontin and the matrix metalloproteinase MMP-2 [Felding-Habermann & Cheresch, 1993].  $\alpha_v\beta_3$  plays an important role in the phagocytosis of apoptotic cells, tumour cell invasion and angiogenesis [Glasdson & Cheresch, 1994] and is usually found physically associated with CD47, a multi-spanning transmembrane receptor molecule.

#### $\alpha_v\beta_5$

On B cells, the most likely receptor for CD23 is the CD21 molecule [Pochon *et al.*, 1992; Aubry *et al.*, 1992], although CD21 is only expressed from the late pre-B cell stage. White and colleagues initially suggested the possibility of a novel, or previously undefined, receptor for CD23 to exist on SMS-SB cells [White *et al.*, 1997], a human pre-B cell line derived from a female patient presenting with acute lymphocytic leukaemia (ALL) [Smith, 1984]. This receptor was demonstrated to be involved in the rescue of these cells from apoptosis, possibly by influencing the expression of Bcl-2 [White *et al.*, 1997]. BIAcore studies have demonstrated SMS-SB cell extracts to bind immobilised sCD23 and analysis by flow cytometry has demonstrated that these cells do not express any of the common CD23 receptors, namely CD21, CD11b-CD18 or CD11c-CD18 [White *et al.*, 1997]. Data have also shown that SMS-SB cells do not express membranous CD23 protein nor do they contain any RNA message for this receptor, strong evidence that sCD23 cannot function in an autocrine fashion in this model.

The CD23 binding entity expressed on the model pre-B cell line (SMS-SB) has recently been identified as  $\alpha_v\beta_5$  [Matheson *et al.*, 2001] and it has been reported that a number of pre-B cell lines also bind CD23 via this receptor.  $\alpha_v\beta_5$  has indeed been shown to be present on all ALL samples analysed [Matheson & Borland, *et al.*, paper in press] but is

not expressed by B chronic lymphocytic leukaemia cells (B-CLL). *In vitro* studies using purified proteins demonstrate that soluble CD23 interacts specifically with the  $\alpha_v\beta_5$  vitronectin receptor isoform, both by ELISA and by surface plasmon resonance studies [Matheson & Borland *et al.*, in press].

#### 1.4.8 DISEASE ASSOCIATION

CD23 has been implicated in a variety of pathological conditions, with data from many laboratories suggesting elevated soluble CD23 serum levels are a useful prognostic indicator in a range of allergic [Yanagihara *et al.*, 1990], inflammatory [Bansal *et al.*, 1992], autoimmune [Hellen *et al.*, 1991] and neoplastic conditions [Sarfati *et al.*, 1996; Mossalayi *et al.*, 1997].

##### ATOPIC DISEASES

Atopic disease usually describes the clinical presentation of type I hypersensitivity reactions, and includes conditions such as asthma, hay fever, atopic eczema and anaphylaxis. These allergic conditions can be defined as an inappropriate response of the immune system to an otherwise harmless environmental allergen, for example pollen [Robinson, *et al.*, 1997]. These conditions are dependent upon the specific triggering of IgE-sensitised mast cells by (generally low levels of) environmental allergen. The initial contact of an allergen with the mucosa is followed by a complex series of events leading to the production of IgE. This is a local event, occurring at the site of allergen entry into the body. The locally produced IgE first sensitises local mast cells before excess IgE can then enter the circulation and bind to specific receptors on both circulating basophils and tissue fixed mast cells throughout the body. IgE, when cross-linked with allergen, binds to both basophils and mast cells via the Fc $\epsilon$ RI receptor, stimulating the release of pharmacological mediators, producing the inflammatory responses leading to the allergic symptoms [Mudde *et al.*, 1990]. Several cytokines are also released as a result of IgE-mediated mast-cell activation [Dugas *et al.*, 1992]. It should be noted that Th2-type cytokines play an important role in atopic disease, particularly in atopic asthma. Development of atopic disease is linked to increased circulating levels of IgE [Burrows *et al.*, 1989; Sears *et al.*, 1991; Naclerio *et al.*, 1993].



Serum CD23 levels tend to be significantly higher in atopic compared to normal individuals, with these levels thought to be weakly but significantly correlated with IgE levels. It is thought that both membrane-bound and soluble forms of CD23 contribute to the pathogenesis of atopic disease by; (i), regulating IgE production [Sarfati *et al.*, 1984 & 1988]; (ii), direct interaction with CD21 to induce histamine release from basophils [Bacon *et al.*, 1993]; (iii), IgE-dependent release of inflammatory mediators by monocytes and eosinophils etc and (iv), activation of monocytes and macrophages via CD11b/c-CD18 integrins [Lecoanet-Henchoz *et al.*, 1995]. In late allergic reactions, IL-4 also induces CD23b expression on various cells, thus enabling the release of more inflammatory cytokines. The CD23-triggered histamine release from basophils clearly suggests CD23 may have a direct role in mediator release.

### INFLAMMATORY DISEASES

Increased levels of CD23 have been reported in various chronic inflammatory diseases including rheumatoid arthritis (RA) [Hellen, *et al.*, 1991], systemic lupus erythematosus (SLE) [Bansal, *et al.*, 1992] and inflammatory bowel disease [Kaiserlian, *et al.*, 1993]. RA is a long-term inflammatory disease resulting in swelling and joint pain. Patients with RA have been found to have elevated levels of circulating CD23-positive B cells [Kumagais *et al.*, 1989], as well as increased levels of circulating sCD23 in both their serum and synovial fluid [Ikizawa *et al.*, 1993]. Furthermore, CD5<sup>+</sup> B cells are specifically activated in these individuals, leading to the constitutive expression of CD23a mRNA and accelerated release of sCD23 [Ikizawa *et al.*, 1993]. The levels of serum sCD23 in RA patients are related to disease status, as demonstrated by a large study on identical twins discordant for RA [Bansal *et al.*, 1994]. Pro-inflammatory cytokines, such as TNF- $\alpha$  and IL-1 $\beta$  have also been found to be present in the synovial fluid of these patients [Brennan *et al.*, 1989] and subsequent studies have shown a marked reduction in disease severity and tissue destruction after the neutralisation of these cytokines [Williams *et al.*, 1992]. Pro-inflammatory cytokines have thus been postulated to play a role in the destruction of tissues within the arthritic joints [Elliot *et al.*, 1993]. IgE is not implicated in RA therefore it has been proposed that CD23 must bind other ligands in order to induce the production of these pro-inflammatory cytokines. As has been previously described in section 1.4.7, CD23 is capable of binding to either CD11b or CD11c, with the result of increased nitric oxide and

inflammatory mediators [Lecoanet-Henchoz *et al.*, 1995]. Recent evidence also links the binding of CD23 to  $\alpha_v\beta_3$  to pro-inflammatory immune responses [Hermann *et al.*, 1999].

## LEUKAEMIC DISORDERS

Chronic lymphocytic leukaemia (CLL) is characterised by the accumulation of long-lived and slowly dividing malignant CD5<sup>+</sup> B cells co-expressing sIgM, sIgD and CD23 antigens, which have escaped programmed cell death and are arrested in the G<sub>0</sub>/G<sub>1</sub> stage of the cell cycle [Fournier *et al.*, 1992; O'Brien *et al.*, 1995]. B-CLL accounts for ~30-40% of all the reported cases of leukaemia in Western Europe and North America [Sarfati *et al.*, 1988]. The CD23 protein is over-expressed and abnormally regulated in B-CLL [Fournier *et al.*, 1992], with a selective increase in CD23 (mainly CD23b) in B-CLL lymphocytes provoking entry of these cells into S phase of the cell cycle [Fournier *et al.*, 1994]. B-CLL sera have been reported to have between 3 to 500 fold more sCD23 than control sera [Sarfati *et al.*, 1988] and a level of >575U/ml sCD23 has been shown to be correlated with disease progression and a poor prognosis [Sarfati *et al.*, 1996]. sCD23 levels have also been shown to reliably reflect disease activity [Reinisch *et al.*, 1994] and correlate significantly with tumour load [Beguin *et al.*, 1993].

Acute lymphocytic leukaemia (ALL) is the most common pediatric malignancy and also accounts for a significant proportion of adult lymphoid neoplasms [Greaves, 1999; Chessells, 2000]. B-ALL is successfully treated in the great majority of pediatric cases by combination chemotherapy leading to complete remission and disease-free survival [Chessells, 2000]. The prognosis in adult B-ALL is less encouraging with blast crisis, an overwhelming number of neoplastic cells in the bloodstream, being a frequent and life-threatening event in the disease progression. In the leukaemic phase, sCD23 in the blood may be able to provide a signal to the neoplastic cell, but there are no reports of elevated sCD23 in the plasma of ALL patients with any form of the malignancy. This may be due to the fact that B-ALL neoplastic cells are derived from B cell precursors, where the CD23 gene is silent.  $\alpha_v\beta_5$ , a receptor for CD23, is expressed on all B-ALL cell samples analysed in our laboratory [Matheson *et al.*, in Pres.]. CD23 is expressed on bone marrow stromal cells [Fourcade *et al.*, 1992], and may serve to provide transient anti-apoptotic signals to B cell precursors at a particular window in antigen-independent



differentiation. This does not explain the overt proliferation of leukaemic cells, a function thought to be dependent upon a chromosomal translocation or other event that takes place within the transformed cell. The precise function of CD23 in the regulation of normal and neoplastic B lymphoid differentiation remains to be defined.

#### **1.4.9 MURINE CD23**

Murine CD23 has been shown to be very similar to its human counterpart. It is a 49kDa glycoprotein, has two (instead of one) N-linked glycosylation sites, no DGR motif [Bettler *et al.*, 1989], and four (instead of three) consensus repeats. Controversial data have in the past suggested that murine CD23, like its human equivalent, existed as two isoforms, however the majority of groups now believe there to be only one murine CD23 form (likened to the human CD23a isoform) at the protein level. Evidence suggests that murine CD23 can also form oligomers at the cell membrane [Dierks *et al.*, 1993], and there is evidence to support the hypothesis that IgE requires at least dimers of the murine CD23 to bind to cells and, further, that this binding stabilises the oligomerisation.

#### **1.4.10 CD23 TRANSGENIC MOUSE STUDIES**

Numerous groups have generated a wide variety of mouse models, utilising gene knockout and transgenic technology in an attempt to determine the *in vivo* function of CD23 in relation to IgE synthesis. The resultant phenotypes and observations obtained have been deemed by most to be more controversial than informative.

Mice genetically deficient for CD23 were generated using homologous recombination in embryonic stem (ES) cells, targeting the exons encoding the transmembrane domain of CD23 thus ensuring the eradication of all forms of this protein, whether they be the a or b isoform or the membrane-associated or soluble form [Yu *et al.*, 1994]. Except for the lack of CD23 proteins the rest of the immune system was shown to be the same as that of the control mice with regards to cell number, distribution and surface marker expression. The knockout mice were reported to have a single abnormal phenotype; they were found to make more IgE than control animals [Yu *et al.*, 1994]. These animals were shown to have two-fold higher serum IgE levels than their littermate



controls, and mount a 10-100-fold higher specific IgE response upon challenge with thymus-dependent antigens. Immune response to helminths was unaffected. This phenotype indicates that CD23 negatively regulates IgE production *in vivo* [Yu *et al.*, 1994].

Two other CD23-deficient mouse strains were made using the gene targeting technique, [Stief *et al.*, 1994; Fujiwara *et al.*, 1994] and these confirmed the lack of major disturbances to the normal immune system. However neither strain was found to corroborate the enhanced IgE responses found by Yu and colleagues. Heyman and colleagues [Heyman *et al.*, 1993] reported that IgE-antigen complexes could augment immune responses by interacting with CD23, supported by the findings that this augmentation was not present in the CD23<sup>-/-</sup> animals [Fujiwara *et al.*, 1994]. The general conclusion from these data was that CD23 acts as a negative regulator for IgE production, however it was also noted that the absence of CD23 resulted in only a modest phenotype.

Texido and colleagues produced a transgenic strain whereby CD23 transgenic expression was controlled by the Thy1.1 promoter [Texido *et al.*, 1994]. Mice transgenic for the membrane-associated form of CD23, but not those for the soluble form, were found to have about a 50% suppression of IgE production, thus demonstrating an impaired IgE immune response. Expression of the transgene was mainly restricted to T lymphocytes, however backcrossing onto the CD23<sup>-/-</sup> phenotype did demonstrate some expression on B cells [Texido *et al.*, 1994]. These studies indicate CD23 expression on T cells has a modest effect on IgE production, however they do not address its role on B cells, where CD23 is more typically expressed at high levels.

More recently a new transgenic model in which CD23 was over-expressed using the murine MHC class I promoter, H-2Kb, in conjunction with an IgH enhancer was reported [Payet *et al.*, 1999]. This strain resulted in the clearly enhanced expression of CD23 on both resting and stimulated B lymphocytes, (an advantage over the Texido report), and T lymphocytes. Expression of the transgene was not observed on non-lymphoid tissue. The serum IgE half-life was found to be similar in control and transgenic animals. The transgenics were also tested for *in vitro* and *in vivo* regulation

of IgE, demonstrating a consistently strong suppression of IgE synthesis in both primary and secondary responses against antigen/alum immunisation, *Nippostrongylus brasiliensis* (Nb) infections and anti-IgD injection models. Furthermore, enzyme-linked immunospot analysis of activated B lymphocytes revealed a reduced number of IgE antibody-forming cells. The humoral Ig levels were mildly dampened after immunisation, suggesting that the transgene affected production of all isotypes, potentially through interactions of CD23 with an alternate ligand, possibly CD21 [Payet *et al.*, 1999]. The dramatic suppression of IgE responses further supports the concept that CD23 can regulate IgE levels.

It was hypothesised that the high levels of CD23 expression on B cells was responsible for the suppression of the IgE response in these transgenic mice. However, *in vitro* culture of the transgenic B cells revealed IgE production to be normal. Furthermore, adoptive transfer of transgenic lymphocytes into normal mice further confirmed that B lymphocytes alone were not sufficient to cause suppression. No functional abnormalities were observed in the transgenic T cells either. Suppression of the IgE response was therefore concluded to be most likely dependent on a cell type other than B or T cells and follicular dendritic cells (FDCs) were thought to be the most likely candidates. The adoptive transfer experiments detailed in this report highlight the importance of the host environment and the high levels of CD23 expression in the germinal center, where FDC reside and the recall responses are initiated, suggest CD23 expression on FDCs is playing a role in the phenotype observed [Payet-Jamroz *et al.*, 2001]. This concept was supported by the demonstration that IgE synthesis was significantly reduced by culturing B cells in the presence of transgenic FDC, in comparison to culture with normal FDC.

Because both membrane and soluble CD23 levels are enhanced in the transgenic mice, the observed phenotype could be attributable to either membrane or soluble CD23 (or both). Soluble CD23 transgenic mice had no observable phenotype [Texido *et al.*, 1994] therefore membrane-associated CD23 is favoured as being responsible [Payet-Jamroz *et al.*, 2001]. The current model for CD23 predicts that three monomers interact with each other to form a functional trimer on the cell surface. This model is based on the noted heptad repeat pattern found in the stalk region of the molecule [Beavil *et al.*, 1992] and



chemical cross-linking studies [Dierks *et al.*, 1993]. CD23 is cleaved by an as yet unknown metalloprotease [Marolewski *et al.*, 1998] and the cleaved monomeric product interacts with only a single IgE with low affinity. Development of anti-CD23 antibodies raised against the stalk region, having the potential to inhibit CD23 oligomerisation, may have more potential to investigate this further, however these antibodies are not available yet.

Transgenic and knockout mouse models have provided new insights into the immunological functions of CD23, however there are a number of limitations. There are marked differences between CD23 in mouse and CD23 in humans. At the molecular level, there is only 57% homology between the CD23 proteins. Furthermore, human CD23 exists in two distinct isoforms (1.4.6), each protein displaying different cellular expression patterns and hypothesised to have differential functions, whereas mice are generally believed to have only a single CD23 protein, likened to human CD23a, expressed on mature B cells, T cells and FDCs. In humans most of the regulatory effects of CD23 are ascribed to its IgE binding capacity, with the mouse CD23 having been shown to not retain the same extent of IgE binding [Bartlett *et al.*, 1995]. The relevance of the observations discussed in this section to the human system is therefore ambiguous. However as *in vivo* experimentation in humans is not an option, the mouse model is still the most practical experimental tool for studying CD23 function *in vivo*. In summary, a certain amount of care must be used when extrapolating results from one system to the other.

## 1.5 AREAS OF RESEARCH INTEREST

As previously discussed there are two distinct CD23 isoforms, CD23a and CD23b [Yokota *et al.*, 1992], with both species derived from a single, 11 exon gene [Suter *et al.*, 1987; Wendel-Hansen *et al.*, 1990] and differing only by 6/7 amino acids at the very N-terminus of their short intracytoplasmic tails. Early studies employing radioiodinated anti-CD23 MAb to probe endocytic function and IgE-coated erythrocytes for assay of phagocytosis, indicated that the two CD23 isoforms were internalised via distinct pathways, with CD23a entering the cell via receptor-mediated endocytosis and CD23b showing a more phagocytic route of cellular entry [Yokota *et al.*, 1988]. Individual amino acids residues, a tyrosine at position 6 in CD23a and the asparagine-proline-



proline residues at positions 2-4 in CD23b, were also identified as being responsible for these differences. Two separate cell types were used to analyse the trafficking pathways of each isoform using two sets of separate experimental conditions. Unoccupied CD23 trafficking could not be studied due to the nature of the assays utilised.

The research presented herein employs identical systems for ligating both CD23a and CD23b, namely chimaeric, hapten-specific IgE and a haptenated protein antigen for cross-linking purposes. The wild-type proteins were analysed initially before being used to generate GFP-CD23 fusion proteins to enable direct analysis of each isoform in a basal, ligated and crosslinked state in HEK 293 cells. A small panel of specifically designed GFP-tagged mutant CD23 proteins were then generated in an attempt to identify the essential amino acids involved in CD23 isoform receptor trafficking in the same system. CD23 is expressed primarily in haematopoietic tissues, and it is in these cells that many of the biologically important functions of CD23 take place. One of the aims of this research was to utilise the GFP-CD23 fusion proteins and the NIP system discussed above to visualise the intracellular trafficking of CD23 in a natural host cell.

Present knowledge of the downstream signalling pathways employed by the CD23 isoforms is somewhat preliminary and incomplete to say the least. However, it is generally believed that these isoforms utilise unique trafficking and signalling pathways. CD23a has been linked to a cAMP pathway whilst CD23b is thought to function via inositol-1,4,5-trisphosphate and calcium mobilisation. However no studies have been performed to address the question of what actually binds to CD23 in order to initiate either of these pathways, or indeed any other signalling pathways which may be involved in CD23 function. The cytoplasmic tail of CD23 is small, in comparison to other cell surface receptors, and does not contain any of the more commonly recognised protein binding motifs, such as NPXY or YXX $\phi$  [Heilker *et al.*, 1999]. It therefore seems likely that CD23 may bind to an adaptor-like protein in order to facilitate the recruitment of the necessary signalling component(s) required for its function. This hypothesis was addressed in the final section of research, where the cytoplasmic N-terminal tail of CD23 was used as bait to screen for potential binding partners in a human leukocyte cDNA library, using the yeast two-hybrid technique. The aim of this

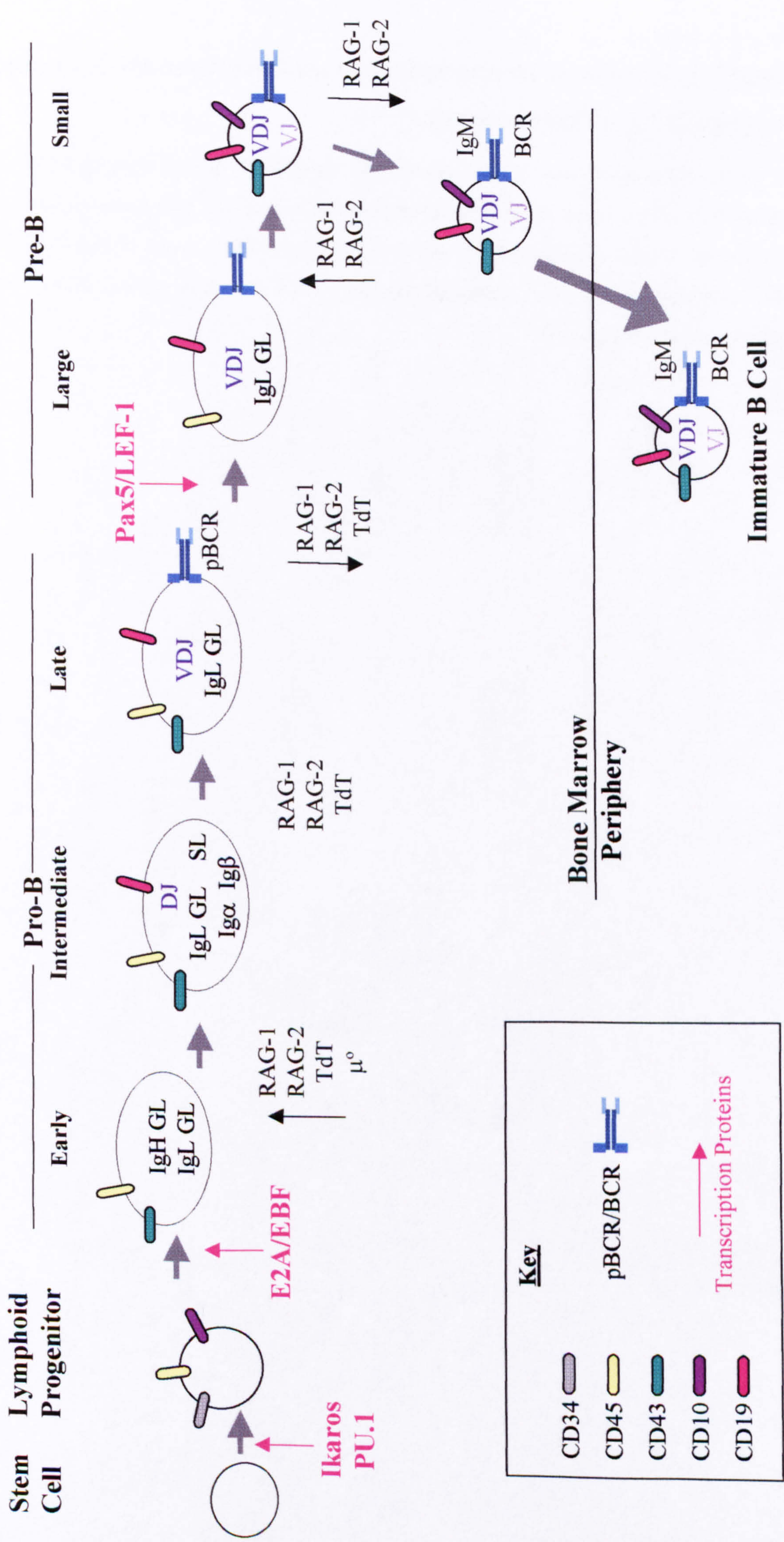
study was to identify interacting protein species with the goal of elucidating the first step in the signalling cascade employed by CD23.

## **FIGURE 1.1 SCHEMATIC DIAGRAM ILLUSTRATING THE ANTIGEN-INDEPENDENT STAGES OF B CELL DEVELOPMENT**

This diagram illustrates the characteristic cell surface markers and gene expression patterns present at each stage of antigen-independent B cell development. The transcription proteins important at each stage are shown in pink. The black 'up' arrows indicate induction of gene expression, whereas the black 'down' arrows represent repression of gene expression. No arrow indicates gene expression occurs but is not altered from the previous stage. Components of the pBCR include surrogate light chains,  $\mu$ , and Ig $\alpha/\beta$ , the components of the BCR are identical except that the light chain genes are associated with  $\mu$ .

Abbreviations: GL - Germ line, SL - Surrogate light chain,  $\mu^0$  - Sterile  $\mu$  transcript.





Key	
CD34	
CD45	
CD43	
CD10	
CD19	
pBCR/BCR	
Transcription Proteins	



**FIGURE 1.2 SCHEMATIC DIAGRAM DETAILING THE ANTIGEN-DEPENDENT STAGES OF B CELL DEVELOPMENT**

The diagram illustrates the stages of antigen dependent B cell development. The anatomical location, types of B cell, developmental events and expression patterns for genes known to increase (up arrows) or decrease (down arrows) are all indicated. Cell status is colour coded, **blue** indicates resting, **green** indicates cycling whilst **pink** indicates quiescent stage cells.







## **FIGURE 1.3 SCHEMATIC DIAGRAM ILLUSTRATING THE COMMON MOLECULAR SORTING PATHWAYS PRESENT IN EUKARYOTIC CELLS**

This diagram illustrates the main compartments present in most eukaryotic cells and the common sorting pathways that facilitate protein trafficking between these compartments. The pathways of particular interest to the work presented in this thesis are the endocytic pathways (blue arrows) and phagocytosis (purple arrow).



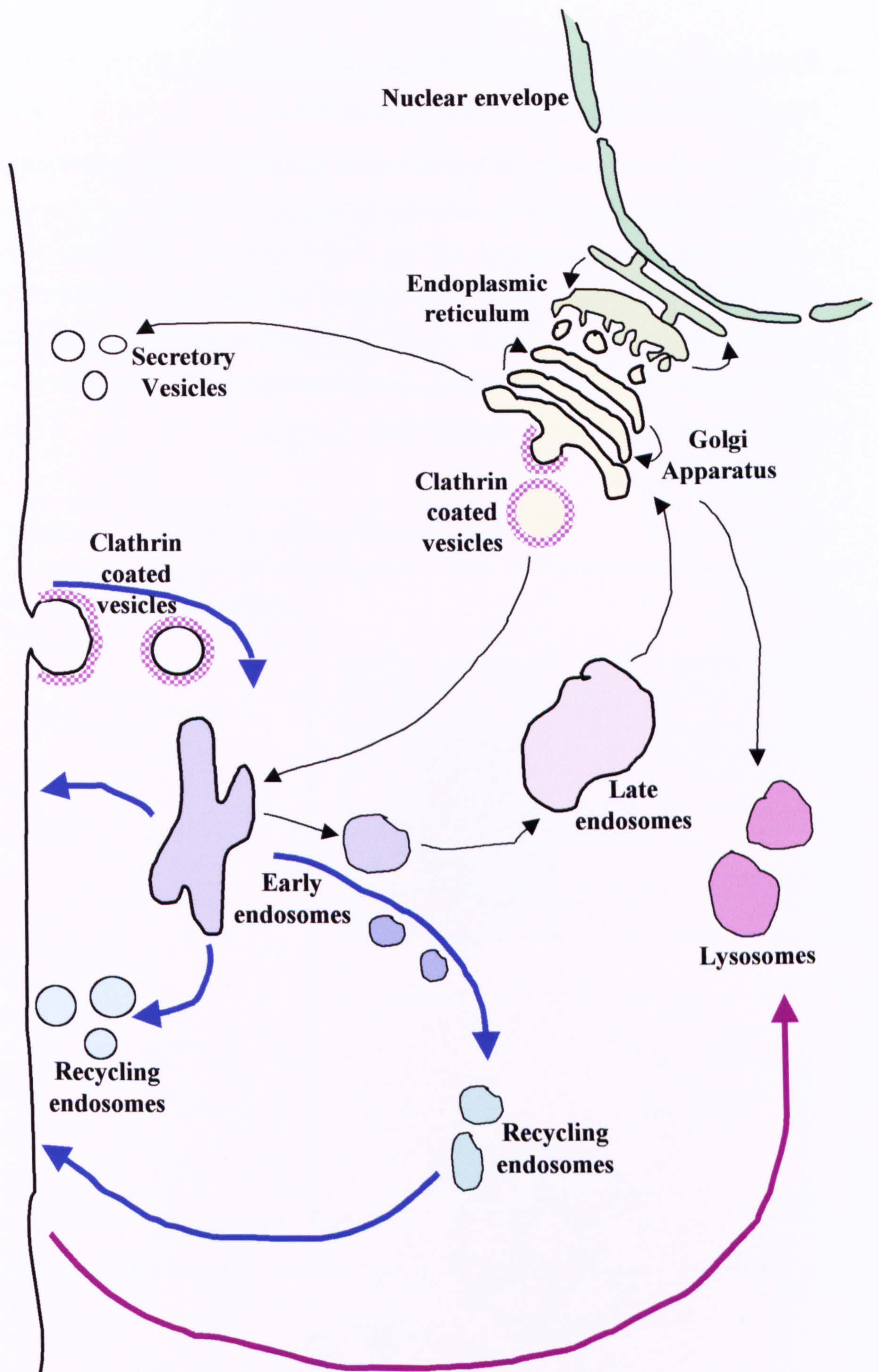




## **FIGURE 1.4 COAT PROTEINS REGULATE PROTEIN TRANSPORT BETWEEN SPECIFIC COMPARTMENTS WITHIN THE CELL**

Three types of coat proteins are known to exist in eukaryotic cells and these are detailed in table 1. Clathrin is the best characterised and figure 2 illustrates how the clathrin heavy and light chains assemble into the clathrin triskelion. The triskelions assemble into a cage-like hexagonal lattice which attached specifically to membranes through the coat proteins. Three coat proteins have been identified and the subunits of each are shown in figure 3. Figure 4 illustrates receptor-mediated uptake from clathrin coated pit with a membrane into clathrin coated buds.



1	Name	Subunits	Transport Pathway
	<b>Clathrin Triskelion</b>	Heavy chain, Light chain	
	AP-1 adaptins	$\gamma, \beta 1, \mu 1, \sigma 1$	TGN-to-late endosomes
	AP-2 adaptins	$\alpha, \beta 2, \mu 2, \sigma 2$	PM-to-early endosomes
	AP-3 adaptins	$\delta, \beta 3, \mu 3, \sigma 3$	TGN-to-lysosomes Early endosome-to-?
	<b>COPI</b>	$\alpha, \beta', \beta, \gamma, \delta, \epsilon, \zeta$	ER-to-Golgi intra-Golgi Golgi-to-ER
	<b>COPII</b>	Sec31p, Sec24p, Sec23p, Sec13p	ER-to-Golgi

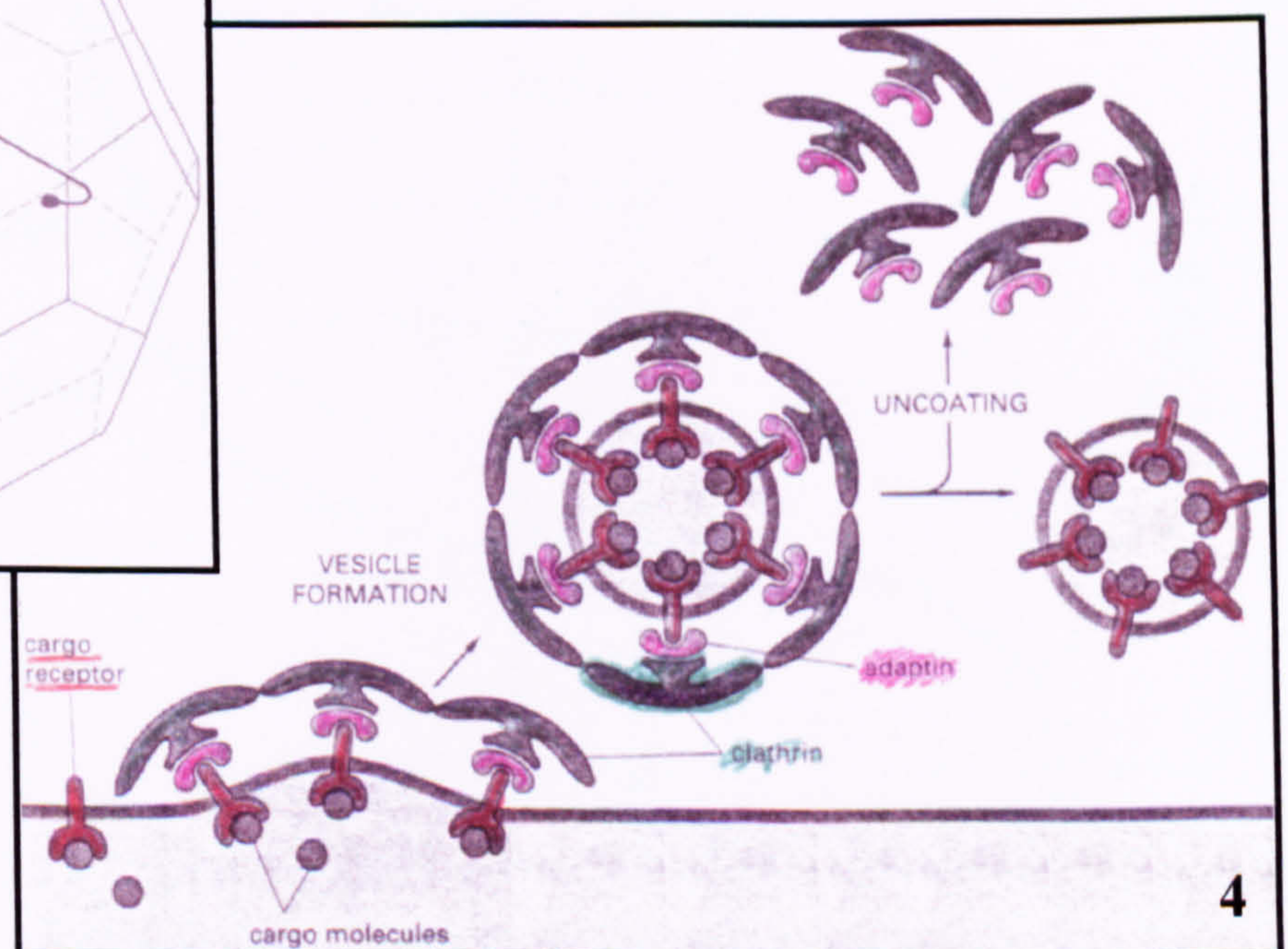
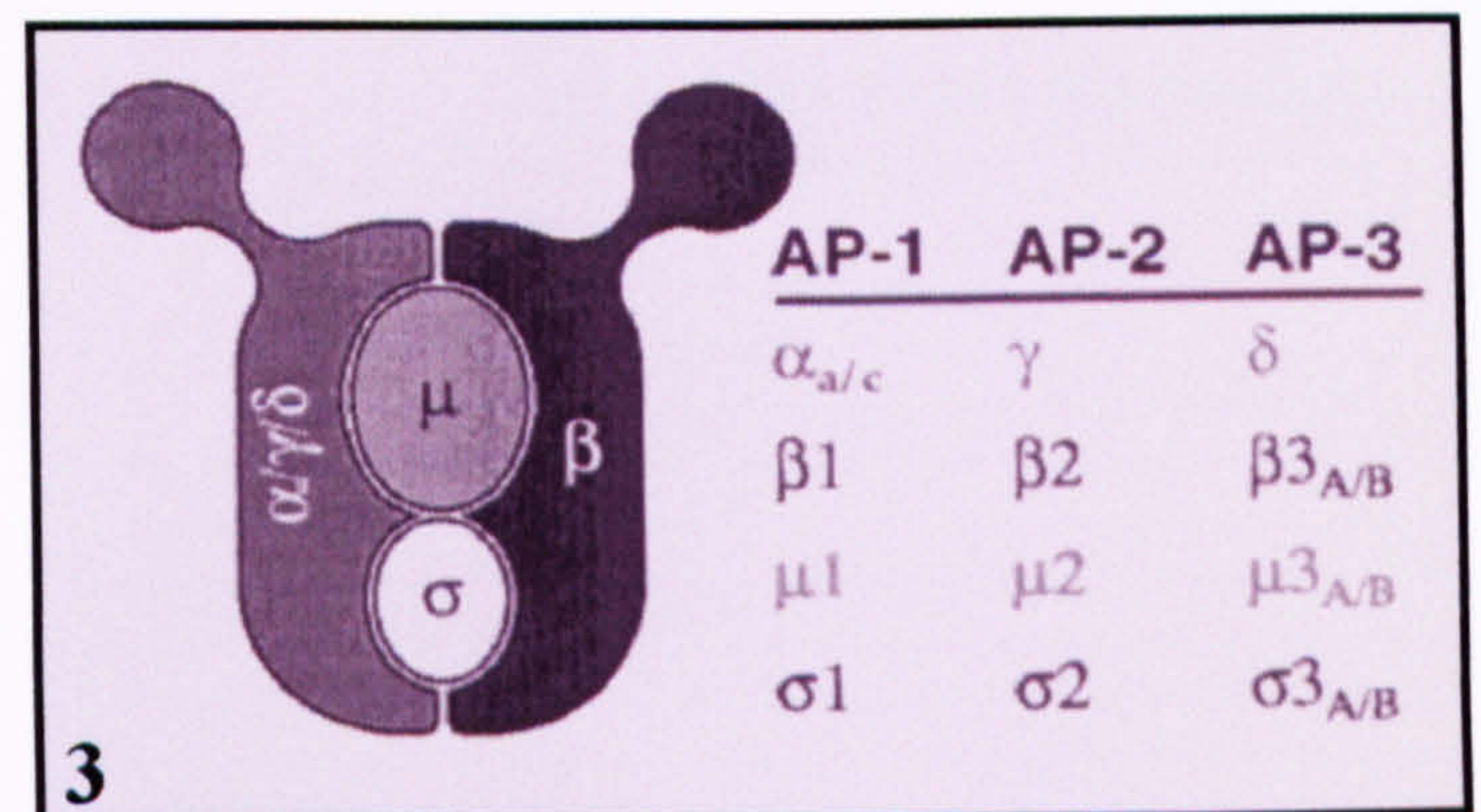
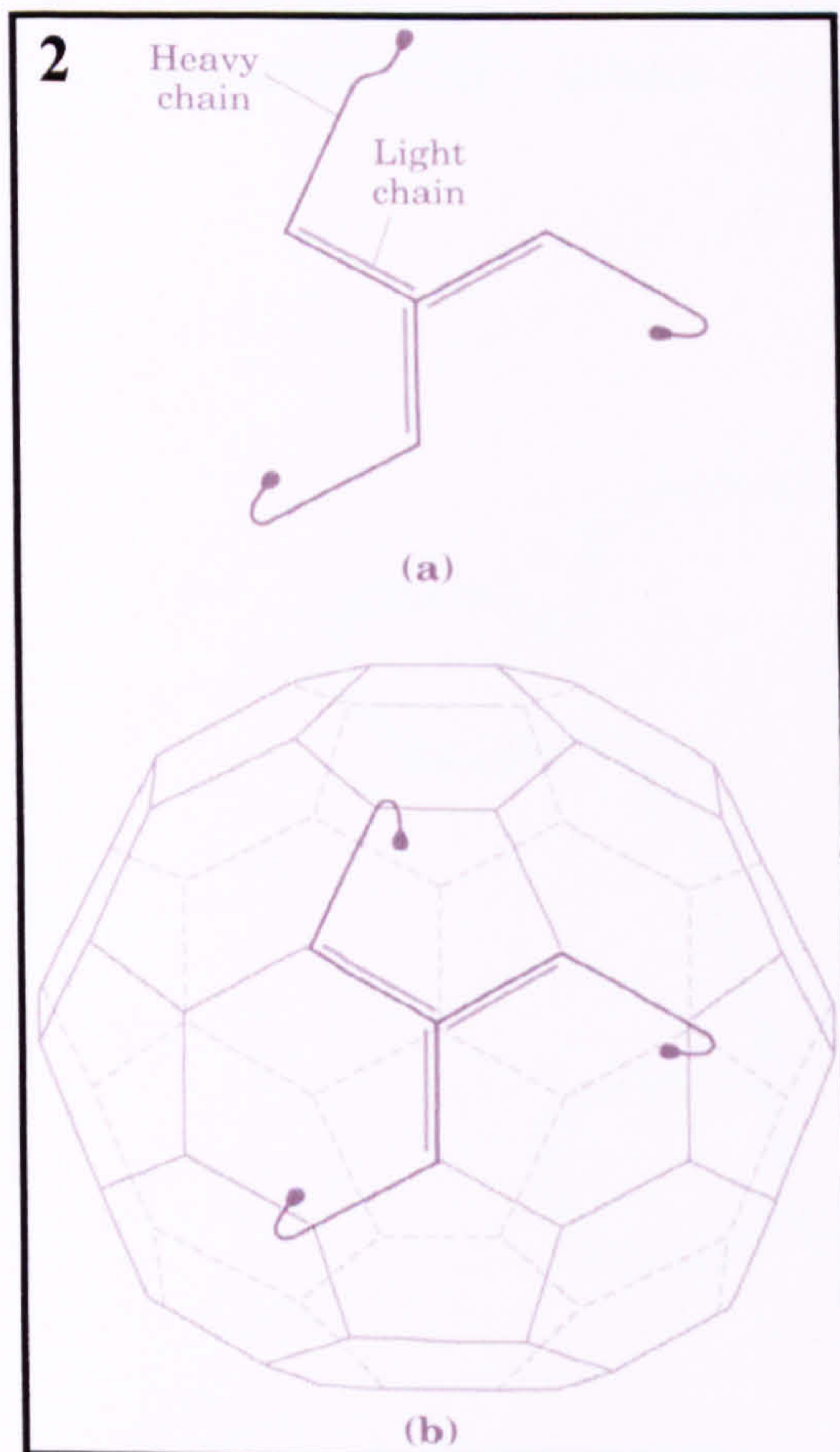


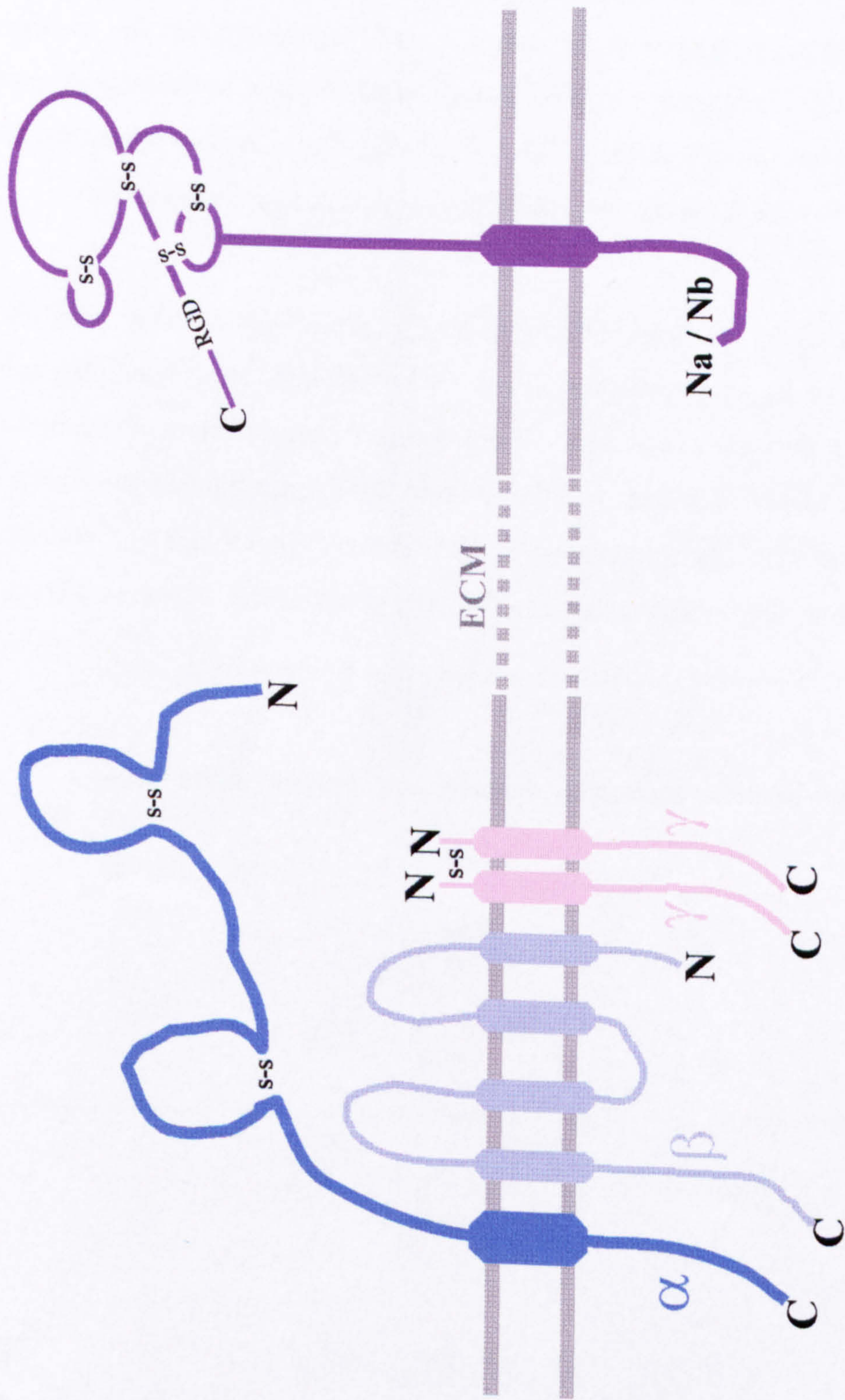


## **FIGURE 1.5 STRUCTURAL COMPARISON OF THE HIGH AND LOW AFFINITY RECEPTORS FOR IgE, FcεRI AND FcεRII**

The high affinity receptor for IgE (FcεRI) is a tetramer consisting of one  $\alpha$  chain with two disulphide-linked immunoglobulin-like loops, a  $\beta$  chain and two  $\gamma$  chains. The  $\beta$  chain has two extracellular and one intracellular loop and is located close to the two  $\gamma$  chains, which are linked by a single disulphide bond. The  $\alpha$  chain contains the IgE binding site.

The diagram of the low affinity receptor for IgE (FcεRII or CD23) is a proposed model based upon sequence data and similarity with animal lectins. CD23 is a single chain, type II transmembrane glycoprotein, lying in the opposite orientation to the other Fc receptors. The IgE binding site is located within the lectin-like domain. Proteolytic cleavage of the full-length form can release several soluble CD23 fragments, each retaining the ability to bind IgE.





FcεRI

FcεRII



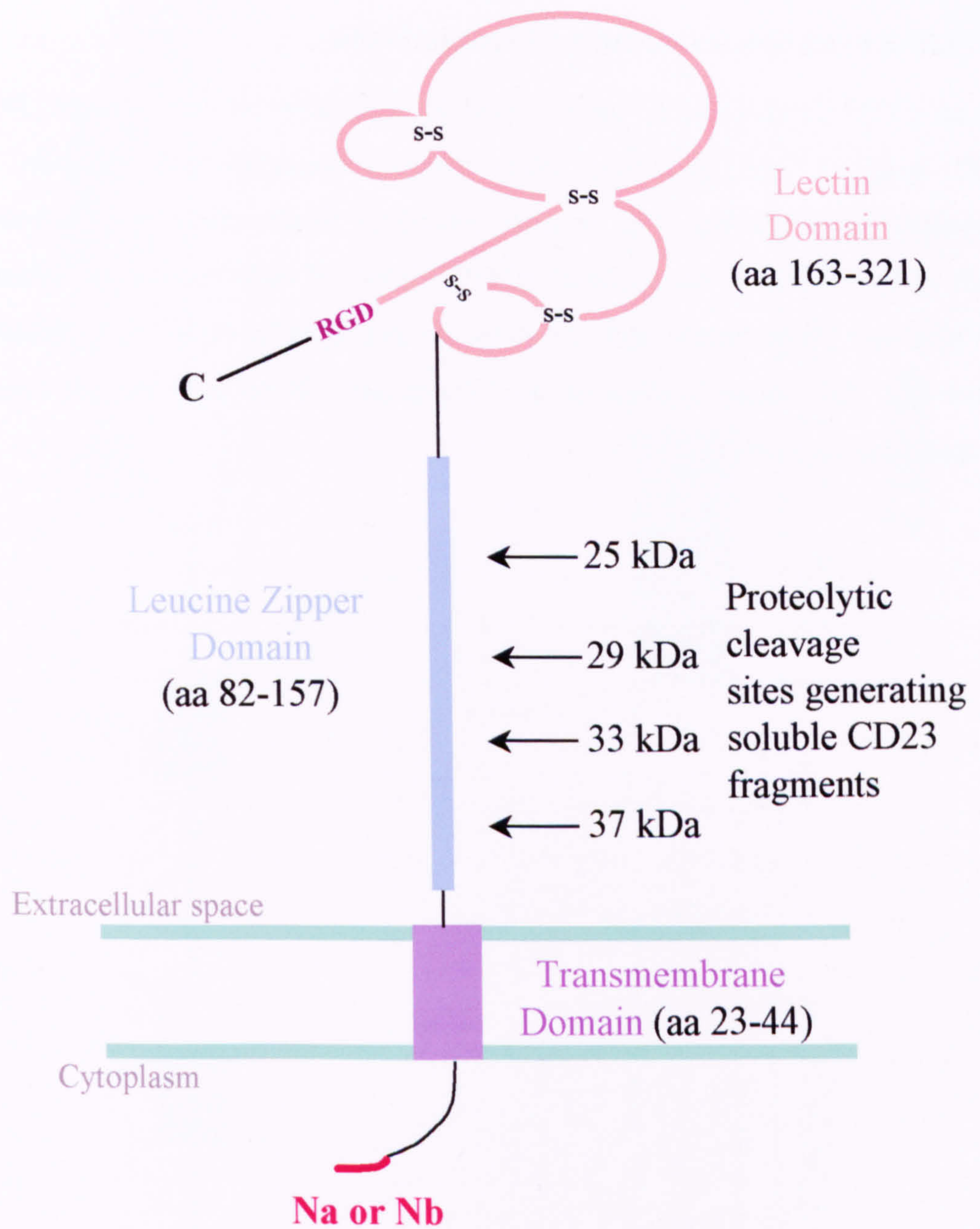
## FIGURE 1.6 STRUCTURE OF CD23

This diagram illustrates the proposed structure of the human CD23 molecule, detailing the location of each of the domain regions referred to within the text of the introduction chapter. CD23 is a 45kDa type-II transmembrane glycoprotein. CD23 has a short cytoplasmic tail and a single hydrophobic transmembrane domain with the remainder of the protein located outwith the cell. The stalk region contains the leucine zipper motif and a number of heptad repeats, thought to be involved in the oligomerisation of these molecules on the cell surface. The IgE binding site is located within the lectin domain. DGR represents the amino acid sequence Aspartate, Glycine, Arginine.

The two CD23 isoforms differ only by the six or seven amino acids at the very N-terminus of the short cytoplasmic tail, with these differences being highlighted in **red** in the box at the base of this figure. The **black** and **purple** letters represent the amino acids common to each isoform, with the **purple** letters representing the amino acids located within the transmembrane domain. The coloured boxes highlight the location of two potential sorting motifs within the CD23 N-terminal tail. These motifs are discussed in section 1.3.5.

This figure has been adapted from Marolewski *et al.*, (1998).





**CD23a** MEEGQ YSEI EE LPRRRCCRRGTQI VLL-----

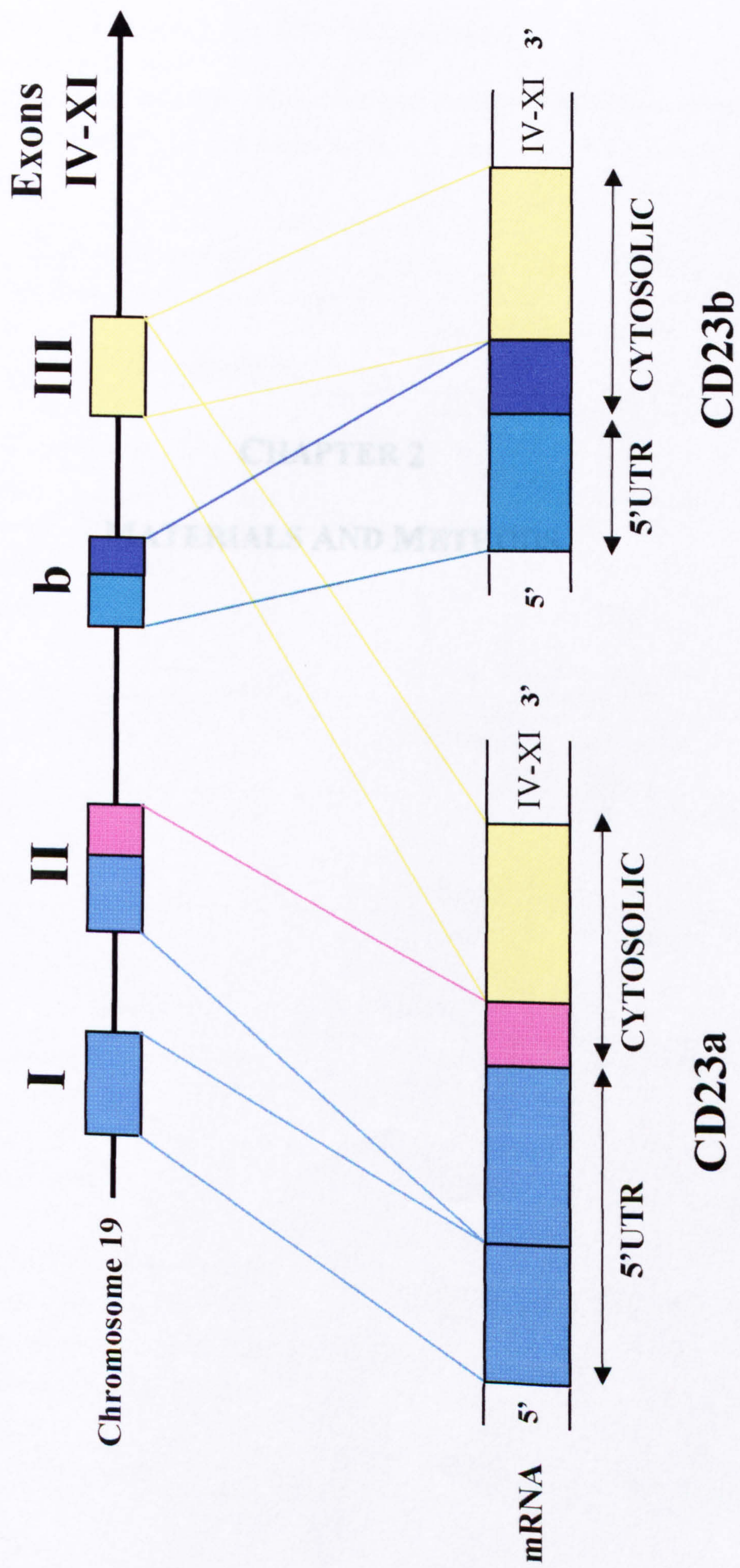
**CD23b** MNPPSQEI EE LPRRRCCRRGTQI VLL-----



## **FIGURE 1.7 CD23A AND CD23B ISOFORMS ARE GENERATED FROM ALTERNATIVE SPLICING OF THE SAME GENE.**

Human CD23 is encoded by an 11 exon gene located on chromosome 19. The two CD23 isoforms are generated using distinct transcriptional initiation sites and differential RNA splicing. The diagram illustrates which exons are incorporated into which isoform. The 5' untranslated (UTR) region of each isoform is indicated by the pale blue and green boxes, and the sequence provided by exon III is indicated by the yellow box. The unique regions of the CD23a and CD23b isoforms are shown in pink and dark blue respectively.







## **CHAPTER 2**

### **MATERIALS AND METHODS**



## 2.1 MATERIALS

### 2.1.1 GENERAL CHEMICALS AND MATERIALS

All general chemicals and reagents, unless otherwise stated below, were purchased from Sigma-Aldrich or BDH Chemicals, both Poole, Dorset, UK. All reagents were of 'AnalaR' grade.

Chemical/Reagent	Supplier
Kaleidoscope and Broad-range protein molecular weight markers. Hybond™ ECL nitrocellulose membrane	Amersham Life Science Ltd. Buckinghamshire, UK.
Bio-Rad™ Protein Assay 40% Acrylamide/Bis solution, 29:1	Bio-Rad Laboratories Ltd. Hertfordshire, UK.
X-α-Gal (5-Bromo-4-chloro-3-indoly-a-D-galactopyranoside) Chromogenic substrate KC8 Electrocompetent E.coli Drop Out Supplement Peptone	Clontech Laboratories UK Ltd. Hampshire, UK
Mowiol® used for mounting coverslips onto slides	CN Biosciences, UK.
Sheep Red Blood Cells	Diagnostics Scotland. Lanarkshire, UK.
TRIzol® Reagent	Gibco BRL, Life Technologies Ltd. Paisley, UK.
Bacto-agar Bacto-tryptone Yeast Extract	Oxoid Ltd. Hampshire, UK.
Restriction Endonucleases and Buffers Taq DNA polymerase T4 DNA ligase T4 Polynucleotide kinase JM109 E.coli Epicurian Coli XL1-Blue Supercompetent Cells	Promega UK Ltd. Southampton, UK.
Agarose MP (multi-purpose) DNA molecular weight marker X (0.07-12.2 kbp) Restriction Endonucleases and Buffers dNTP's (PCR grade)	Roche Diagnostics, UK.
Cloned Pfu DNA Polymerase	Stratagene Ltd, Cambridge, UK.



## 2.1.2 CELL AND TISSUE CULTURE REAGENTS & MATERIALS

Reagent/Material	Supplier
Disposable plastic graduated pipettes	Bibby Sterlin Ltd. Staffordshire, UK.
Tissue culture Flasks 50 ml centrifuge tubes 6 well plates	Corning Costar. Buckinghamshire, UK.
Gene Pulser Electroporation Cuvettes	Bio-Rad Laboratories Ltd. Hertfordshire, UK.
Dulbecco's Modified Eagles Medium RPMI-1640 Medium Foetal Calf Serum Penicillin/Streptomycin/Glutamine Cryovials	Gibco BRL, Life Technologies Ltd. Paisley, UK.
Haemocytometer	Phillip Harris Scientific. Lanarkshire, UK.
G418 antibiotic	Promega UK Ltd. Southampton, UK.
Cell Dissociation Media Trypan Blue	Sigma-Aldrich. Dorset, UK.

## 2.1.3 CELL LINES

Cell Line	Supplier
COS 7 - SV40 Transformed, African Green Monkey Kidney Cells.	Gift from Prof. G Milligan, Department of Biochemistry & Molecular Biology, University of Glasgow, UK.
EDR - EBV Transformed Mature Human B Lymphoblastoid Cell Line	Gift from Prof. C Watts, University of Dundee, UK.
HEK 293 - Human Embryonic Kidney Cells	Laboratory Stocks
Raji & Raji A – Human EBV-negative Burkitt's lymphoma Cell Line	European Collection of Animal Cell Cultures, CAMR, Wiltshire, UK.
SMS-SB – Human Pre-BII Acute Lymphoblastic Leukaemia Cell Line	Gift from Prof. Brad Ozanne, CRC Beatson Laboratories, Glasgow, UK.
P3HR1 – Mature Human Burkitt's Lymphoma B Cell Line	Laboratory Stocks

## 2.1.4 PLASMIDS & TRANSFECTION REAGENTS

Plasmid/Reagent	Supplier
Gene Pulser Electroporation Cuvettes	Bio-Rad Laboratories Ltd. Herts, UK.



DOTAP™	Boehringer Mannheim Ltd. Herts, UK.
Human Leukocyte MATCHMAKER cDNA Library, GAL 4 AD vector, pACT2 GAL 4 DNA-BD vector, pGBKT7	Clontech Laboratories UK Ltd. Hampshire, UK.
pcDNA3.1 <sup>+</sup>	Invitrogen, Netherlands.
Full length enhanced green fluorescent protein, pEGFP-N1	Gift from Brad Ozanne, CRC Beatson Laboratories, Glasgow, UK.

### 2.1.5 ANTIBODIES

Antibody	Supplier
p-Tyr (phosphotyrosine) mouse monoclonal IgG anti-human CD23-R-phycoerythrin (RPE) conjugate (B-G6) IgG1 anti-HA mouse monoclonal IgGa2	Autogen Bioclear. Wiltshire, UK.
Protein-A, with horseradish peroxidase (HRP) conjugate	Amersham Life Science Ltd. Bucks., UK.
Anti-Human CD23 (Bu38) IgG1	ImmunoKontakt, AMS Biotechnology (Europe) Ltd., Oxon, UK.
CD19 R-phycoerythrin (RPE) (HD37) Isotype IgG1 CD19-FITC (HD37) Isotype IgG1 CD23-FITC (MHM6) Isotype IgG1 CD21-FITC (IF8) Isotype IgG1 CD3-FITC (UCHT1) Isotype IgG1	DAKO Ltd. Cambridgeshire, UK.
Rabbit-anti-human CD23 (Rb55)	Gift from Dr J-Y Bonnefoy, Geneva Biomedical Research Institute, Switzerland
Mouse-anti-human CD23	Gift from Prof. J Gordon, University of Birmingham, UK.
Mouse-anti-GFP	Gift from Prof. Brad Ozanne, CRC Beatson, Glasgow, UK.
Anti-HLA DR (Class II)	Gift from Dr H Jorgenson, Academic Transfusion Medicine Unit, Glasgow Royal Infirmary, Glasgow, UK.
Chimeric Human IgE anti-NIP Mouse-anti-human CD23	Serotec, UK.
Anti-Rabbit IgG, with HRP conjugate Anti-Mouse IgG, with HRP conjugate	Scottish Antibody Production Unit (SAPU). Lanarkshire, UK.



2.1.6 FLUORECENT PROBES

Reagent	Supplier
Transferrin-modified Texas Red (Tf-TxR) LysoTracker Red	Molecular Probes, USA.
Phalloidin-modified Texas Red (P-TxR)	Gift from Brad Ozanne, CRC Beatson Laboratories, Glasgow, UK.

2.1.7 COMMERCIAL KITS

Kit	Supplier
ECL Western Blotting Detection System	Amersham Life Sciences Ltd. Buckinghamshire, UK.
GAL 4 Yeast-2-Hybrid MATCHMAKER 3 System	Clontech Laboratories UK Ltd. Hampshire, UK.
OptEIA™ Human sCD23 ELISA	Pharmingen. San Diego, CA, USA.
Wizard Plus SV™ DNA Mini Preps RT-PCR System	Promega UK Ltd. Southampton, UK.
Qiagen Plasmid Giga, Mega & Maxi DNA Purification Kits Qiagen QIAquick™ Gel Extraction Kit	Qiagen Ltd. West Sussex, UK.
QuikChange™ Site-Directed Mutagenesis	Stratagene Ltd. Cambridge, UK.
QuickStep™ PCR Purification Kit	Vh Bio Ltd. UK.

2.1.8 OLIGONUCLEOTIDES

All oligonucleotides were synthesized and purified by MWG Biotech, to PSF purity. The lyophilised oligonucleotides were resuspended in nuclease free water at a concentration of 100pmol/μl and stored at -20°C. The sequences of each of the oligonucleotides used are detailed in the appropriate figures.



## **2.2 METHODS**

The composition of all the solutions and buffers referred to in the following sections are detailed in the appendix.

### **2.2.1 CELL CULTURE**

#### **2.2.1A CULTURE OF NON-B CELL LINES**

COS7 and HEK 293 cells were routinely cultured in Dulbecco's Modified Eagles Medium (DMEM), supplemented with 0.05mg/ml penicillin, 2mM L-glutamine and 10% (v/v) foetal calf serum ("complete medium"). Cells were generally cultured in 75cm<sup>2</sup> flasks at 37°C in a humidified 5% CO<sub>2</sub> incubator and manipulated aseptically in Laminar flow hoods. Cells were split 1/3 every 2-3 days. HEK 293's were bashed from the flask whilst cell dissociation fluid (Sigma) was used to detach the COS7 cells.

#### **2.2.1B CULTURE OF HUMAN B CELL LINES**

RAJI, RAJI A, SMS-SB, EDR and P3HR1 cells were routinely cultured in RPMI-1640 medium supplemented with 2mM L-glutamine, 0.05mg/ml penicillin and 10% (v/v) heated inactivated fetal calf serum. Cells were propagated in 75cm<sup>2</sup> flasks at 37°C in a humidified 5% CO<sub>2</sub> incubator and sub-cultured aseptically in laminar flow hoods every 2-3 days as necessary.

#### **2.2.1C DETERMINATION OF CELL VIABILITY**

Cell viability was determined using trypan blue dye. Dead cells, after losing the integrity of their plasma membrane, become stained as a result of the trypan blue entering into the cell. Numbers of live and dead cells were counted using a Neubauer haemocytometer. The total number of cells in the twenty-five grid squares was multiplied by 10<sup>4</sup> and also the dilution factor in order to estimate the number of cells per ml of culture.

$$\% \text{ viability} = \frac{\text{number of live cells}}{\text{total number of cells}} \times 100$$

### **2.2.1D FROZEN CELL STOCKS**

Frozen sample stocks of each cell line were maintained in liquid nitrogen. Cells were removed from logarithmically growing cultures, centrifuged and resuspended in ice-cold freezing media, 90% (v/v) heat-inactivated FCS and 10% (v/v) dimethyl sulphoxide (DMSO) at approximately  $1 \times 10^6$  cells/ml. Cells were transferred to pre-chilled Nunc cryovials, each sample was then frozen at  $-70^{\circ}\text{C}$  overnight before being placed into liquid nitrogen for long term storage.

Cell samples removed from liquid nitrogen storage were rapidly thawed in lukewarm water and immediately washed in 9ml of the appropriate incomplete medium in order to remove residual traces of DMSO. The cells were harvested at 1000rpm, re-suspended in 5ml of complete medium, transferred to a  $25\text{cm}^2$  flask and incubated in a  $37^{\circ}\text{C}$  incubator with 5%  $\text{CO}_2$  allowing recovery before further manipulation.

### **2.2.2 FLOW CYTOMETRIC ANALYSIS**

A Becton-Dickinson FACScan Flow Cytometer fitted with an argon laser was utilised for the analysis of all cell samples, and each sample was prepared in a 6ml Falcon tube. Samples were analysed using CellQuest<sup>TM</sup> software.

Flow cytometers measure and analyse the optical properties of single cells passing through a focused laser beam and can analyse hundreds of cells per second, providing a statistically significant picture of the samples, physical and biochemical make up. When cells pass through the laser beam they disrupt and scatter the laser light (detected as forward and side scatter). Forward scatter (FSC) relates to the size of the cell, whilst side scatter (SSC) is an indicator of the cells internal complexity. In addition to scatter the cytometer also measures fluorescence (FL) parameters (FL1-FL3). Cells can therefore be stained with fluorescent dyes or fluorochromes. The fluorochromes absorb the laser light and emit a portion of this absorbed light in different regions of the spectrum. With fluorochromes coupled to MAbs directed against cell surface antigens, the relative amount of each dye on an individual cell can be determined, generating information about the molecular properties of these cells. The flow cytometer then



processes the electronic signals resulting from each cell, creating numeric values for each parameter. It assigns each value a channel number and passes these values to the computer system for display and analysis. Cell size, shape, internal complexity and in this case any cell component or surface molecule that can be detected by a fluorescent compound can therefore be examined and analysed by flow cytometric techniques. Figure 2.1 shows a schematic representation of the beam path of a typical flow cytometer and a brief explanation of its operation.

### **2.2.2A ANALYSIS OF CELL SURFACE PROTEINS**

Flow cytometry was used to analyse the surface expression of a variety of proteins on a number of cell lines as well as transiently and stably-transfected HEK 293 and RAJI-A cells. Cells to be analysed were harvested from culture and washed twice in ice-cold PBS. Approximately  $5 \times 10^5$  cells were incubated with  $1\mu\text{g}$  of the appropriate fluorescein isothiocyanate (FITC) or R-phycoerythrin (RPE) conjugated antibody for 45 minutes on ice protected from light. After incubation the cells were washed twice, resuspended in 0.5ml ice-cold PBS and analysed. Indirect staining was used initially to detect cells expressing green fluorescent protein-CD23 fusion proteins (GFP-CD23).  $1\mu\text{g}$  of biotinyl-anti-CD23 was added, excess washed off as described previously and any MAb binding was then detected using streptavidin-Quantum Red (SA-QR). Cells were washed and resuspended in ice-cold PBS as before. FL-1/525nm was used to detect green fluorescence emitted from either FITC or (GFP). FL2/575nm was used to detect red fluorescence from RPE. Unstained cells were also analysed, and used as a control, testing for auto-fluorescence. In all cases a minimum of  $10^4$  events were collected. Propidium iodide (PI) was added to certain samples, at a final concentration of  $\sim 5\mu\text{g/ml}$ , in order to highlight the dead cell population within any given cell sample.

### **2.2.2B FLOW CYTOMETRIC CELL SORTING**

GFP-CD23b expressing HEK293 cells were sorted using a Becton-Dickinson FACStar Flow Cytometer fitted with an argon laser. Cells were analysed in the FL1/530nm cytometer channel, detecting fluorescence from expression of the GFP protein itself. Cells registering fluorescence above a certain level were selected from the remainder of the population and subsequently returned to cell culture, thus selecting cells expressing a

minimum level of GFP-CD23 fusion proteins. This process was used to generate a stock of HEK 293 cells expressing a useful level of GFP-CD23b proteins, since the signal was initially very low and the original sample was not comparable to the GFP-CD23a sample.

## **2.2.3 NUCLEIC ACIDS**

### **2.2.3A SMALL SCALE PREPARATION OF DNA (MINI-PREPS)**

The Promega Wizard SV Mini plasmid purification kit was used according to the manufacturer's instructions. Briefly, a 5ml overnight *Escherichia coli* (*E.coli*) bacterial culture expressing the required plasmid DNA was harvested by centrifugation at 13,500 x g for 1 minute. The cell pellet was fully resuspended in 250µl of Resuspension solution. 250µl of Lysis solution was added, samples mixed by inversion and incubated at room temperature for 5 minutes. 10µl of protease solution was then added, samples were incubated again for 5 minutes at room temperature. 350µl of Neutralization solution was added, samples were mixed by inversion and immediately spun at 13,500 x g in a desktop microfuge for 10 minutes. The supernatants were transferred to a Wizard SV mini prep resin column, and spun at 13,500 x g for 1 minute permitting the DNA to bind the resin. The columns were then washed with Wash buffer and the DNA was collected in an eluate of approximately 100µl of nuclease free dH<sub>2</sub>O. Samples were assayed for concentration and purity, as per section 2.2.3C, and stored at -20°C.

### **2.2.3B LARGE SCALE PREPARATION OF DNA**

Modification of the alkali lysis method proposed by Sambrook *et al.*, 1989, was used to extract plasmid DNA from bacterial cultures. Cells from a 200ml overnight culture of *E.coli* expressing the desired plasmid were harvested by centrifugation at 5,500 x g for 15 minutes at 4°C. The supernatant was removed and the pellet fully resuspended in 10ml of Solution 1. 10ml of Solution 2 was added, the sample inverted four times to facilitate mixing, and incubated on ice for 5 minutes. 7.5ml of Solution 3 was added, the sample mixed as before and incubated on ice for 10 minutes. The samples were then centrifuged at 15,000 x g for 15 minutes at 4°C to collect the cellular debris. The supernatant, containing the nucleic acids, was filtered using Whatman 3MM filter paper and incubated with 0.6 volumes of isopropanol for 15 minutes at room temperature. The



samples were centrifuged at 350 x g for 15 minutes at 4°C and the supernatant discarded. The pellet was resuspended in 2ml of TE buffer and incubated with 2ml 5M LiCl/50mM Tris-HCl, pH 8.0, for 10 minutes on ice, serving to precipitate the RNA. The RNA was then separated from the sample by centrifugation at 350 x g for 5 minutes at 4°C. The DNA content was precipitated from the sample supernatant using two volumes of ethanol and a 15 minute incubation on ice. The resultant DNA pellet was collected by centrifugation at 1200 x g for 15 minutes at 4°C in a Beckman bench-top centrifuge. The pellet was dissolved in 500µl of TE buffer and 300µg of RNase added. The sample was incubated at 37°C for 1 hour, serving to remove any contaminating RNA. The nucleic acid content was then purified using two phenol/chloroform and chloroform extractions. The aqueous phase, containing the DNA was incubated with 50% volume of ammonium acetate and two volumes of ethanol for 10 minutes at -70°C serving to precipitate the final DNA preparation. The supernatant was removed and the DNA pellet resuspended in 500µl of TE or dH<sub>2</sub>O. Concentration and purity were assayed as per section 2.2.3C, and the samples stored at -20°C. The pellet was resuspended in a small volume of sterile dH<sub>2</sub>O and stored at -20°C.

The Qiagen Maxi and Giga plasmid purification kits were also occasionally used for large scale DNA purification in accordance with the manufacturers instructions.

### **2.2.3C DNA CONCENTRATION AND PURITY**

DNA concentration and purity was measured using a Helios γ spectrophotometer. The DNA sample to be measured was diluted 1/100 and 1/500 in dH<sub>2</sub>O and the absorbance at 260nm and 280nm recorded. The concentration of DNA was calculated by manipulating the A<sub>260</sub> reading as shown in the equation below, where 50 is the multiplication factor for DNA (40 for RNA).

$$\text{DNA Concentration} = \frac{A_{260} \times 50 \times \text{Dilution Factor}}{1000} = \text{x mg/ml}$$

The A<sub>260</sub>:A<sub>280</sub> ratio provided an estimation of the purity of the DNA sample, with values between 1.8 and 2.0 indicating a quality DNA preparation containing minimal impurities.

### **2.2.3D RESTRICTION ENDONUCLEASE DIGESTION OF DNA**

1 unit of the appropriate restriction enzyme was used per  $\mu\text{g}$  of plasmid DNA, each sample reaction being carried out in the appropriate reaction buffer, supplied by the enzyme manufacturer. Samples were incubated for at least 1 hour at an appropriate temperature, the reaction was terminated by the addition of loading buffer and the samples were separated on a 0.8% agarose gel, section 2.2.3F.

### **2.2.3E LIGATION OF DNA VECTOR AND INSERT FRAGMENTS**

5 $\mu\text{l}$  of each of the vector and insert samples to be ligated were run out on a 0.8% agarose gel along with a known amount of DNA markers, facilitating an estimation of the amount of DNA in each preparation. The ligation reaction was assembled as follows; 50ng vector DNA, 200ng insert DNA, 1 $\mu\text{l}$  T4 DNA ligase, 2 $\mu\text{l}$  10 x Ligase buffer and dH<sub>2</sub>O to a final reaction volume of 20 $\mu\text{l}$ . The mixture was incubated at 16°C overnight, and then used to transform competent cells, see section 2.2.6.

### **2.2.3F AGAROSE GEL ELECTROPHORESIS**

Non-denaturing 0.8% (w/v) agarose gels were used to visualize DNA fragments of >100bp. Higher percentage gels (2%) were used to visualise small fragments, i.e. PCR products. Agarose was dissolved in 60ml (mini-gel) or 100ml (maxi-gel) of 1x TAE buffer for fragment resolution or DNA purification respectively. Ethidium bromide was added to a final concentration of 0.4mg/ml, and the gels were set at room temperature. Prior to loading, the DNA samples were mixed with 2 $\mu\text{l}$  of 10x DNA loading buffer and electrophoresed along with the appropriately sized DNA markers at 100V in 1x TAE buffer. The DNA fragments were visualized on a UV transilluminator and the results recorded as a photographic image of the gel.

### **2.2.3G PURIFICATION OF DNA RESTRICTION FRAGMENTS FROM LOW MELTING POINT AGAROSE GELS.**

The Qiagen QIAquick Gel Extraction kit was used to purify DNA fragments from low melting point TAE agarose gels. The appropriate DNA fragment was excised from the



gel using a sterile scalpel and transferred to an eppendorf tube. The gel slice was weighed, 3 volumes of QA added (i.e. 100µl/100µg) and incubated at 50°C for 10 minutes to melt the gel. 1 volume of isopropanol was added to each sample and the mix loaded onto the resin purification column. After microcentrifugation at high speed for 1 minute, the resin bound with DNA was washed twice with QF or wash solution, the second spin serving to remove all residual wash solution. The bound DNA was then eluted from the column with the addition of 30µl of dH<sub>2</sub>O at room temperature for 1 minute and the eluate was collected by microcentrifugation for 1 minute. Purified fragments were analysed by gel electrophoresis and stored at -20°C.

### 2.2.3H “BIG DYE” TERMINATOR SEQUENCING (ABI 373A)

The DNA to be sequenced (200-500ng for double stranded DNA) was mixed with 3.2 pmoles of primer to a final volume of 12µl with dH<sub>2</sub>O. Table 2.1 lists the ng amount of a variety of oligonucleotide lengths equivalent to 3.2pmoles. 8µl of kit reaction premix was added and PCR amplification was carried out in a Perkin Elmer Cetus DNA Thermal Cycler as follows; 2 minutes at 96°C for 1 cycle to denature the dsDNA, 10 seconds at 96°C, 5 seconds at 50°C and 4 minutes at 60°C for 25 cycles.

**Table 2.1 Conversion table -  
ng of Oligonucleotides equivalent to 3.2pmoles**

Oligonucleotide Size (No. bases)	ng equivalent to 3.2 pmoles
15	15.85
16	16.90
18	19.00
20	21.12
22	23.23
24	25.34

2µl of 3M sodium acetate (pH 4.5) and 50µl of ethanol were then added and each sample incubated at 70°C for 15 minutes. Samples were centrifuged on high in a microfuge and the supernatants removed. Pellets were washed in 100µl 70% ethanol and then air-dried. Samples were resuspended in loading dye/formamide and denatured in a hotplate at 90°C for 2 minutes prior loading on the sequencing gel. The samples were



run, generally overnight and the resultant sequence data analysed using the ABI Prism software.

2.2.4 POLYMERASE CHAIN REACTION (PCR)

All PCR reactions were carried out in accordance with the method of Saiki *et al* (1985) in 0.5ml microcentrifuge tubes and performed in a Techne Genius PCR machine. Optimal conditions and components were determined for each primer set, and the PCR annealing temperature was set at least 5°C below the melting temperature ( $T_m$ ) of the primer with the lowest  $T_m$ . Typical reaction mixtures and example PCR cycle parameters are shown in the table 2.2 and 2.3, respectively.

Table 2.2 Typical PCR Reaction Components

Component	Final concentration
Template DNA	10ng/μl
Upstream Primer	50pmol
Downstream Primer	50pmol
dNTP mix	0.2mM
10 x Taq Reaction Buffer	1x
25mM magnesium	1.25mM
Taq DNA Polymerase	0.025u/μl

Table 2.3 PCR Cycle Parameters

Temperature	Time (minutes)	No. of Cycles
95°C	2	1
95°C ( $T_m$ -5°C) 72°C	1 1.5 1.5	35
72°C	7	1
4°C	Hold	-

Following the PCR reaction, 2x loading buffer was added and the samples were analysed by agarose gel electrophoresis, gel-purified, digested and cloned into the appropriate vector.



**2.2.4A RNA ISOLATION WITH TRIZOL**

Suspension cells of interest were pelleted, by centrifugation at 1200 x g for 5 minutes, transferred to disposable polypropylene tubes and lysed in TRIzol® reagent (1ml per 5-10 x 10<sup>6</sup> cells). Cells grown in monolayers were harvested by adding the TRIzol® directly into the culture dish (1ml/10cm<sup>2</sup>) and passing the cell lysate through a pipette several times. The homogenized sample was incubated at room temperature for 5 minutes. 0.2ml of chloroform was added per 1ml of TRIzol® reagent. The sample tubes were capped and shaken vigorously by hand for 15 seconds and incubated at room temperature for 2-3 minutes. The samples were centrifuged at 12,000 x g for 15 minutes at 4°C, separating the mixture into a lower red phenol-chloroform phase, an interphase and a colourless upper aqueous phase. The RNA sample, remaining exclusively in the upper aqueous phase, was transferred to a fresh polypropylene tube. The RNA was precipitated by the addition of iso-propanol (1ml/1ml TRIzol®) and incubated at room temperature for 10 minutes. Samples were centrifuged at 12,000 x g for 10 minutes at 4°C. The supernatant was removed and the RNA pellet washed once with 70% ethanol (again, at least 1ml for every 1ml of TRIzol® added initially). The samples were vortexed and centrifuged at 7,500 x g for 5 minutes at 4°C. The pellet was briefly air-dried at room temperature for 5 minutes before being resuspended in DEPC-treated water. Each sample was incubated at 55°C for 10 minutes to aid complete dissolution of the RNA. The concentration and purity of the samples were assayed as per section 2.2.3C and the RNA stored at -20°C.

**2.2.4B REVERSE TRANSCRIPTASE POLMERASE CHAIN REACTION (RT-PCR)**

The reaction mix was prepared by combining all the reagents listed in Table 2.4 below in a thin-walled 0.5ml reaction tube on ice, with the enzymes being added last.

**Table 2.4 RT-PCR Sample Components**

Reagent	Volume	Final Concentration
RNA sample/control	1-5µl	500ng
Tfl DNA Polymerase (5u/µl)	1µl	0.1u/µl
AMV Reverse Transcriptase (5u/µl)	1µl	0.1u/µl
25mM MgSO <sub>4</sub>	2µl	1mM



Upstream Primer (15µM)	50pmol	1µM
Downstream Primer (15µM)	50pmol	1µM
dNTP Mix (10mM each dNTP)	1µl	0.2mM
AMV/Tfl 5x Reaction Buffer	10µl	1x

The sample tubes were gently vortexed for 10 seconds to mix the components. All additions were carried out using RNase-free pipette tips and separate tips were used for every addition. The tubes were placed in a controlled temperature heat block equilibrated to 48°C and incubated for 45 minutes. Thermal cycling was performed in a Techne Genius PCR machine, see Table 2.5, to facilitate second strand cDNA synthesis and amplification. The resultant PCR products were analysed by agarose gel electrophoresis on a 2% gel. Reaction products were stored at -20°C.

**Table 2.5 Reverse Transcriptase (RT) and PCR Cycling Profile**

	Temperature	Time (minutes)	No. of Cycles
Synthesis of first strand of cDNA (Reverse transcription)	48°C	45	1
AMV RT inactivation RNA/cDNA/primer denaturation	94°C	2	1
Synthesis of second strand of cDNA	72°C	7	1
PCR amplification, denaturation	94°C	0.5	40
Annealing	T <sub>m</sub> - 5°C	1	
Extension	68°C	2	
Final extension	68°C	7	1

### 2.2.5 CD23 N-TERMINAL TAIL MUTAGENESIS

*In vitro* site directed mutagenesis is an invaluable technique for studying protein structure-function relationships and for identifying amino acids that may mediate these functions. Several methods for performing this technique have appeared in the literature, but these protocols generally require single stranded DNA templates [Kunkel, 1985; Vandeyar *et al.*, 1988; Sugimoto *et al.*, 1989; Taylor *et al.*, 1985] and can often be labour intensive. The QuikChange site-directed mutagenesis kit was used to make



specific point mutations in the cytoplasmic N-terminal tail section of both CD23 isoforms, using a typical dsDNA cloning vector.

Briefly, the oligonucleotide primers, each complementary to opposite strands of the vector, extend during temperature cycling by means of *PfuTurbo* DNA polymerase generating mutagenised, nicked circular strands. The methylated, non-mutated parental DNA template was then digested with *Dpn I* and the circular nicked dsDNA transformed into XL1-Blue supercompetent cells. Figure 2.2 illustrates an overview of this process.

### 2.2.5A PRIMER DESIGN

Both mutagenic primers contained the desired mutation and were designed to anneal to corresponding sequences on opposite strands of the plasmid DNA. Primers were between 25 and 45 bases in length, with a melting temperature ( $T_m$ ) of 78°C or more. The following formula was used to estimate the  $T_m$  of each primer. Where, N = the length of each primer, measured in base pairs.

$$T_m = 81.5 + 0.41(\%GC) - \frac{675}{N} - \% \text{ mismatch}$$

The desired mutation (deletion or insertion) was designed to be in the center of the primer, with 10-15 bases of correct sequence present on either side. Each of the primers were designed to have a minimum GC content of 40% and terminated in one or more single G or C bases.

### 2.2.5.B STRATAGENE QUICKCHANGE MUTAGENESIS PCR REACTION

Each set of sample reactions were set up using both 10ng and 25ng of dsDNA template concentrations, whilst the primer concentration was kept constant (125ng of each). The control reaction contained 10ng of pWhitescript™ 4.5kb control plasmid and 125ng of each of the control primers. 2.5 units of *PfuTurbo* DNA polymerase was added to each reaction.



specific point mutations in the cytoplasmic N-terminal tail section of both CD23 isoforms, using a typical dsDNA cloning vector.

Briefly, the oligonucleotide primers, each complimentary to opposite strands of the vector, extend during temperature cycling by means of *PfuTurbo* DNA polymerase generating mutagenised, nicked circular strands. The methylated, non-mutated parental DNA template was then digested with *Dpn I* and the circular nicked dsDNA transformed into XL1-Blue supercompetent cells. Figure 2.2 illustrates an overview of this process.

#### **2.2.5A PRIMER DESIGN**

Both mutagenic primers contained the desired mutation and were designed to anneal to corresponding sequences on opposite strands of the plasmid DNA. Primers were between 25 and 45 bases in length, with a melting temperature ( $T_m$ ) of 78°C or more. The following formula was used to estimate the  $T_m$  of each primer. Where, N = the length of each primer, measured in base pairs.

$$T_m = 81.5 + 0.41(\%GC) - \frac{675}{N} - \% \text{ mismatch}$$

The desired mutation (deletion or insertion) was designed to be in the center of the primer, with 10-15 bases of correct sequence present on either side. Each of the primers were designed to have a minimum GC content of 40% and terminated in one or more single G or C bases.

#### **2.2.5.B STRATAGENE QUICKCHANGE MUTAGENESIS PCR REACTION**

Each set of sample reactions were set up using both 10ng and 25ng of dsDNA template concentrations, whilst the primer concentration was kept constant (125ng of each). The control reaction contained 10ng of pWhitescript™ 4.5kb control plasmid and 125ng of each of the control primers. 2.5 units of *PfuTurbo* DNA polymerase was added to each reaction.



The cycling parameters detailed in Table 2.6 were used for the generation of all ten of the CD23 N-terminal point mutations (The N-terminal tail deletion mutant was generated independently from the Stratagene mutagenesis kit, using a simple cloning strategy).

**Table 2.6 PCR Parameters for the Generation of the Ten Cytoplasmic N-Terminal CD23 Mutants**

Purpose	Temperature	Time (minutes)	No. of Cycles
Denaturation of dsDNA	95°C	0.5	1
Denaturation	95°C	0.5	16
Annealing	T <sub>m</sub> - 5 °C	1	
Elongation	68 °C	14	

The amplification process was checked by running 10µl of each sample on a 0.8% agarose electrophoresis gel. The remaining sample was digested with 10 units of *Dpn I* at 37°C for one hour to digest the parental, i.e. non-mutated, super coiled dsDNA.

#### **2.2.5C TRANSFORMATION OF EPICURIAN COLI XL-1 BLUE SUPERCOMPETENT CELLS**

Epicurian Coli XL-1 Blue Supercompetent cells were thawed on ice and 50µl aliquots transferred into pre-chilled labeled microfuge tubes. 1µl of the *Dpn I* treated PCR reaction/control sample was added to each tube, the cell suspension mixed by flicking, and the samples incubated on ice for 30 minutes. The samples were then heat-shocked at 42°C for 45 seconds and allowed to recover on ice for 2 minutes. 500µl of pre-warmed NZY<sup>+</sup> broth was then added to each sample and the tubes transferred to an orbital shaker and incubated at 37°C for more than 1 hour. At the end of the 60 minute incubation the entire volume of each sample was spread onto individual LB amp agar plates. 250µl of the control transformation reaction and 5µl of the pUC18 control reaction was spread onto an LB Amp X-gal IPTG plate. All plates were incubated at 37°C overnight to allow colonies to develop. Random colonies were chosen, grown up and the plasmid DNA extracted and analysed using endonuclease restriction digestion. Clones found to contain an appropriately sized insert were sequenced (section 2.2.3H) in order to confirm that



mutagenesis had occurred correctly without incorporating any unwanted changes into the remainder of the CD23 or vector sequence. Once the sequences had been confirmed to be correct, large-scale DNA preparations were made for each mutant construct and the DNA was stored at -20°C.

## **2.2.6 TRANSFECTION & TRANSFORMATION OF CELLS**

### **2.2.6A DOTAP TRANSFECTION OF HUMAN CELL LINES**

Cells were harvested and seeded onto 6-well plates. 5µg plasmid DNA was added to 30µl DOTAP and 100µl filter-sterilized 20mM Hepes, pH 7.2 and incubated at room temperature for 15 minutes in a sterile universal. The DNA-DOTAP suspension was then added to the cell mono-layer in 2ml of fresh complete DMEM and the cells were incubated over night as normal. Next day the medium was replaced with complete DMEM supplemented with 700µg/ml G418. Cells were gently sub-cultured for 4-6 weeks before a stable population of G418-resistant cells emerged.

### **2.2.6B ELECTROPORATION OF RAJI-A CELLS**

RAJI-A cells were grown in cell culture in complete RPMI medium and sub-cultured the day prior to use. The cells were harvested in serum free RPMI medium and centrifuged at 350 x g for 5 minutes. The cell pellet was resuspended in a known volume of serum-free RPMI medium and cell viability measurements (section 2.2.1C) were made. The cells were resuspended in RPMI medium to a final concentration of  $6.25 \times 10^6$  cell/ml. 0.8ml of this mix was transferred to a pre-chilled, 0.4cm gap electroporation cuvette and the 40µg of the appropriate DNA plasmid added. The cells were electroporated using a Biorad Gene Pulser. The capacitance was set to 960µF and the voltage set to 0.25kV. Cells were allowed to recover on ice for 5 minutes before being transferred to pre-warmed complete RPMI medium and returned to the 37°C incubator with 5% CO<sub>2</sub>. Stable cells lines were selected by culturing the cells in complete RPMI medium with the addition of 700µg/ml G418 after the first 24 hours recovery period. Stable G418-resistant cell lines were usually obtained after around 6-10 weeks in selection.



## **2.2.6C RUBIDIUM CHLORIDE METHOD FOR MANUFACTURE OF TRANSFORMATION COMPETENT *E. COLI***

250ml of Psi broth was inoculated using 1ml of overnight culture and incubated at 37°C with aeration to  $A_{550} = 0.48$ . Cells were chilled on ice for 15 minutes and centrifuged at 3-5000g for 5 minutes. The supernatant was discarded and the cell pellet resuspended in 100ml of TfbI and incubated on ice for a further 15 minutes. Cells were pelleted as before, resuspended in 10ml of TfbII and incubated on ice for 15 minutes. The cells were either used immediately or quick-frozen in ethanol-dry ice prior to storage at -70°C.

### **2.2.6.D TRANSFORMATION OF COMPETENT CELLS**

Competent *E. coli* cells (either DH5 $\alpha$  or JM109) were thawed on ice and 25 $\mu$ l volumes aliquoted into pre-chilled eppendorf tubes. 1 $\mu$ l of the appropriate DNA plasmid was added and the cell samples were incubated on ice for a further 20 minutes. The cells were then heat-shocked at 42°C for 45 seconds, incubated for a further 2 minutes on ice and resuspended in 500 $\mu$ l of pre-warmed SOC medium and incubated at 37°C for 30 minutes. An appropriate dilution, or indeed the entire sample, was then plated onto antibiotic selection agar and incubated overnight at 37°C. Representative colonies were selected, used to inoculate 5ml of LBroth (containing the appropriate antibiotic selection), and amplified by overnight incubation in an orbital shaker at 37°C.

## **2.2.7 PROTEIN ANALYSIS**

### **2.2.7A PREPARATION OF WHOLE CELL “RIPA” LYSATES**

Cells were isolated from culture, washed twice with serum-free medium, re-suspended in ice-cold PBS at approximately  $5 \times 10^6$  cells per ml and washed by centrifugation at 350 x g for 5 minutes. Cells were resuspended in 300 $\mu$ l of RIPA buffer (50mM Tris-HCl (pH 7.4), 1% (v/v) NP40, 1mM Na Deoxycholate, 150mM NaCl, 1mM EGTA, 1mM Na<sub>3</sub>VO<sub>4</sub>, 1mM NaF, 1mM PMSF, 2 $\mu$ g/mL Leupeptin, 0.5mM DTT) and lysed by pipetting. Cells were further lysed by incubation on ice for 30 min. Cellular debris was removed by centrifugation at 13,500 x g for 15 min at 4°C. The supernatant was retained and the protein concentration of each sample determined by Biorad protein assay, followed by storage of aliquoted samples at -70°C.



### **2.2.7B BIORAD PROTEIN CONCENTRATION ASSAY**

BSA standards were made at concentrations of 0.2, 0.4, 0.6, 0.8, 1.0, 1.2, 1.4, 1.6, 1.8 and 2.0 mg/ml. BioRad assay buffer was diluted 1:5 in dH<sub>2</sub>O, filtered through Whatmann filter paper and 1ml aliquots transferred to labelled eppendorf tubes. Samples were routinely measured at dilutions of 1:10 and 1:20. 20µl of the appropriate standard/sample was added to each designated tube containing the 1ml sample of BioRad assay buffer, mixed and left for 5 minutes at room temperature. The absorbance of each sample at 595nm was analysed on a Helios  $\gamma$  spectrophotometer. The results obtained for the standards were used to plot a calibration curve, from which the unknown protein concentrations of the samples could be determined.

### **2.2.7C PREPARATION OF IMMUNOPRECIPITATES**

Cells were isolated from culture, washed twice in incomplete medium and resuspended at  $1 \times 10^7$  cells/ml in complete medium. The cells were then treated as described in the appropriate results section, and recovered by centrifugation for 5 minutes at 350 x g. Cells were subsequently lysed by the addition of 400µl of OGP buffer (50mM HEPES-KOH, pH 7.4, 5mM CaCl<sub>2</sub>, 140mM NaCl, 1% octyl- $\beta$ -D-glucopyranoside, 1mM PMSF, 1mM Aprotinin, 1mM Leupeptin) and incubated on ice for 30 minutes, after which cell membranes were disrupted by repeated aspiration through a 21-gauge needle. Cellular debris was pelleted by centrifugation at 1000 x g at 4°C for 5 minutes, and the supernatant transferred into fresh tubes. In accordance with the method described by Harlow and Lane [Harlow & Lane, 1988], the protein solution was then pre-cleared for 2 hours by rotation with 10µl of 50% slurry of Protein-G agarose in OGP buffer and the pre-clearing Protein-G removed, prior to the addition of 1µg of appropriate antibody and subsequent incubation at 4°C for 4 hours on a rotating table. Samples were finally rotated overnight with 25µl of Protein-G agarose at 4°C, in order to allow the immunoprecipitates to be captured. Immunoprecipitates were then collected by centrifugation at 350 x g for 5 minutes, washed twice with OGP buffer and re-suspended in 50µl of Laemmli/protein loading buffer. Each sample was denatured by boiling for 3 minutes, centrifuged gently to pellet the Protein-G agarose and loaded on to an appropriate percentage SDS-PAGE gel.



### **2.2.7D SDS-PAGE GEL ELECTROPHORESIS**

Acrylamide separating gels were prepared as described by Laemmli [Laemmli *et al.*, 1970] using a Biorad mini-gel rig. The gels were set at 30°C with an isopropanol overlay, before the 5% (w/v) acrylamide stacking gel was poured. Gel compositions are detailed in the appendix. Appropriate sample volumes were added to the gel and electrophoresed at 15mA in 1 x running buffer through the stacking gel. The current was increased to 25mA after the samples had entered the separating gel, and run until the dye front reached the bottom of the separating gel layer. If two gels were run simultaneously using the same gel rig the gels were run at 35-40mA.

Following SDS-PAGE, separated proteins were often transferred onto nitrocellulose membrane to facilitate immuno-detection of particular proteins of interest. Following electrophoresis the glass gel plates were separated facilitating removal of the separating gel. The gel was transferred to a Scotlab wet blotting apparatus in a sandwich of nitrocellulose membrane and filter paper. The protein samples were then transferred to the nitrocellulose membrane in protein transfer buffer at 250mA for 45 minutes.

### **2.2.7E IMMUNOBLOTTING**

After transfer, the nitrocellulose membrane was incubated in blocking buffer for either 30 minutes at room temperature or overnight at 4°C, serving to prevent any non-specific antibody binding. The membrane was then rinsed in phosphate buffered saline (PBS)/0.05% (v/v) Tween-20 and subsequently incubated with primary antibody prepared at 1/1000 in "Blotto" for 1 hour at room temperature. The nitrocellulose membrane was washed 3 x 15 minutes in Blotto and incubated with the secondary antibody (1/1000 in Blotto) for 45 minutes at room temperature. Finally the nitrocellulose was washed 3 x 15 minutes in PBS/0.05% (v/v) Tween-20.

### **2.2.7F ECL DETECTION SYSTEM**

The Amersham Enhanced Chemiluminescence (ECL) kit was used in accordance to the manufacturer's instructions to develop all immunoblots. Briefly, 2ml volumes of the two ECL solutions were mixed, poured over the nitrocellulose and incubated for 1 minute.



Excess ECL reagent was removed with a tissue and the nitrocellulose membrane wrapped in saran wrap. The nitrocellulose membrane was exposed to Fuji RX film for an appropriate time interval (from 1 second to 20 minutes, depending on signal strength) and developed using an X-omat developer.

#### **2.2.7G SILVER STAIN**

Protein gels were initially fixed in 40% methanol/10% acetic acid (v/v) for 30 minutes with shaking before being transferred into fresh 10% ethanol/5% acetic acid (v/v) fixer for two 15 minutes incubations. The gels were subjected to oxidizer (0.02g sodium-thio-sulphate in 100ml dH<sub>2</sub>O), for 5 minutes and then washed in dH<sub>2</sub>O. The silver stain (0.2g AgNO<sub>3</sub>, 75µl formaldehyde in 100ml dH<sub>2</sub>O), was then added and the gels incubated for 20 minutes. The gels were washed in dH<sub>2</sub>O for 1 minute to remove any excess silver reagent before being placed into developer (6g sodium carbonate, 4mg sodium-thio-sulphate, 50µl formaldehyde in 100ml dH<sub>2</sub>O). The reaction was stopped at an appropriate time point by submerging the gel in 5% acetic acid stop solution. Stained gels were dried onto Whatman 3MM filter paper for storage.

#### **2.2.7H SCD23 ELISA**

Each of the wells on the 96 well ELISA plate to be used were coated with 100µl of capture antibody and incubated overnight. Each well was aspirated and washed 3 times with wash buffer and then blocked with 200µl of assay diluent for 1 hour. The wells were aspirated and washed 3 times with wash buffer. 100µl of sample or standard was then added to each well and incubated for 2 hours. Each well was aspirated and washed 5 times before 100µl of Detector Solution was added and incubated for 1 hour. The wells were aspirated and washed 7 times with wash buffer before 100µl of Substrate was added to each well and incubated for 30 minutes in the dark. 50µl of Stop Solution was added to each well and the plate was read at 450nm, within 30 minutes. All incubations were carried out at room temperature. Standards used were 50, 25, 12.5, 6.3, 3.1, 1.6, and 0.8ng/ml. All antibody and buffer details are listed in the appendix.



## **2.2.8 CONFOCAL ANALYSIS**

### **2.2.8A DIALYSIS OF FITC CONJUGATED ANTI-CD23 ANTIBODY, REMOVAL OF SODIUM AZIDE CONTAMINATION**

Dialysis tubing was boiled in 1mM EDTA for 5 minutes and allowed to cool. Two knots were tied in one end of the tubing and the antibody sample was carefully added to the tube. The open end was then tied with two knots and the tubing was submerged in dialysis buffer, exactly the same as the buffer the antibody was stored in minus sodium azide. In this case, 0.05M Tris-HCl, pH 7.2 with 1% (w/v) BSA. The sample was dialysed against a total of 3 litres of buffer in a conical flask at 4°C with continual stirring, protected from any light source. The buffer was replaced three times, every 10-14 hours. The antibody sample was collected from the dialysis tubing and stored at 4°C protected from light.

### **2.2.8B PREPARATION OF NIP-CONJUGATED BSA/INSULIN**

BSA was derivatised with 4-hydroxy-3-iodo-5-nitrophenylacetic acid (NIP) using established procedures. Briefly, 5-10mg NIP-OSu was dissolved in 200µl of dichloromethane and added to 15-20mg of BSA protein in sodium carbonate buffer, pH 9.5 (1ml volume). The mixture was incubated at room temperature, with occasional mixing for 16 hours, and then dialysed against several litres of PBS, pH 7.2.

NIP-Insulin was generated using a slightly modified protocol as the amino terminus had to be blocked in order to enable only a single NIP molecule to bind to each insulin molecule [Roth *et al.*, 1981]. Briefly, insulin was dissolved in carbonate buffer to generate a 0.7mM solution. 5µl of citraconic anhydride was added and the sample was incubated for 30 minutes at room temperature. The sample was dialysed against 2 litres of carbonate buffer at 4°C for 24 hours each. 5-10mg NIP-OSu was dissolved in 200µl of dichloromethane, added to the dialysed insulin sample and incubated for 1 hour at room temperature with occasional mixing. The sample was then dialysed against PBS (pH 7.2) overnight at 4°C. The blocked amino group was then unblocked by sequential dialysis against dH<sub>2</sub>O for 2 hours at room temperature, 10mM HCl for 6 hours at room temperature and then PBS (pH 7.2), for 18 hours at 4°C. A small sample of the end



products were run on an SDS-PAGE gel, transferred to nitrocellulose and immunoblotted with NIP-specific IgE antibody to check conjugation had taken place successfully. The derivatisation ratio was worked out by measuring the  $A_{280}$  for the NIP-conjugated protein, calculating the molar concentration of BSA and then relating this to the molar extinction co-efficient for NIP thus calculating the number of NIP molecules per molecule of BSA. The derivatisation ratio was calculated to be approximately 10 NIP molecules per molecule of BSA or a 1:1 ratio for NIP-insulin. Protein-hapten conjugates were filter-sterilised and stored at  $-20^{\circ}\text{C}$ .

#### **2.2.8C PREPARATION OF CELL SAMPLES**

Glass cover slips were submerged in concentrated hydrochloric acid for 1 hour, washed in copious amounts of  $\text{dH}_2\text{O}$ , transferred to metal cover slip racks, wrapped in tin foil and sterilized by autoclaving at  $126^{\circ}\text{C}$  for 11 minutes. Stably-transfected HEK 293 cells were harvested from culture and seeded onto glass cover slips coated with 0.01% Poly-D-Lysine (PDL) and incubated at  $37^{\circ}\text{C}$  in a humidified 5%  $\text{CO}_2$  incubator for 36-48 hours. Stably-transfected Raji A cells were harvested from culture and seeded directly onto glass cover slips with no need for the addition of the PDL coating.

All cell samples were washed in KRH buffer prior to analysis on a Zeiss LSM 410 confocal microscope. GFP and FITC fluorescence were excited using a 488nm argon/krypton laser and emission fluorescence was detected with a 515-540 band pass filter. Co-localisation studies utilized Transferrin-modified Texas Red, LysoTracker and Phalloidin-modified Texas Red dyes, each of which was excited at 543nm and emission fluorescence detected with a 570nm long band pass filter. Figure 2.3 shows a schematic representation of the beam path of the LSM 410 microscope and the table lists each of the abbreviations used in the diagram.

#### **2.2.8D LIVE CELL CONFOCAL ANALYSIS OF WT CD23 AND GFP-CD23 FUSION PROTEINS**

Analysis of CD23 movement in transfected cells was performed using a Zeiss confocal microscope. Individual cover slips were transferred to the live cell chamber, kept at  $37^{\circ}\text{C}$



using a heated stage facility and imaged in KRH buffer. Images were collected using the 63 x magnification lens, at the time points indicated in the individual figure legends. Each data set is representative of at least three separate experiments. Experiments examining unmodified WT CD23a/b proteins were monitored by the addition of 1µg of FITC-conjugated anti-CD23 monoclonal antibody. Movement of GFP-CD23a/b fusion protein was directly monitored via the GFP tag, and evaluated in several contexts (see Figure 3.5). Images were collected from untreated cells (basal), from cells exposed to 1 µg of NIP-specific Chimeric IgE (loaded) and finally, cells treated with NIP-specific IgE and then cross-linked with 1µg of NIP-BSA.

#### **2.2.8E LIVE CELL ANALYSIS OF CD23 CO-LOCALISATION WITH TRANSFERRIN-MODIFIED TEXAS RED OR LYSOTRACKER DYES.**

In live cell co-localisation experiments, cells were exposed to Transferrin-modified Texas Red (Tf-TxR) or LysoTracker<sup>TM</sup> for 20 minutes at 37°C, at a final concentration of 10µg/ml and 50nM respectively. Any further additions (FITC anti-Human CD23 antibody or NIP-specific IgE and/or NIP-BSA) were subsequently added prior to a final wash in KRH buffer before the cells were analysed on the confocal microscope using a heated stage facility, as described in 2.2.8D.

#### **2.2.8F ANALYSIS OF WT CD23 AND GFP-CD23 FUSION PROTEINS UNDER FIXED CONDITIONS**

Cells were harvested and seeded onto glass cover slips, as described above. WT CD23 samples were bathed in 250µl of KRH buffer and treated with 1µg FITC-conjugated anti-CD23 MAb for 5 minutes at room temperature before being washed in KRH buffer. Each sample was incubated at 37°C in a humidified 5% CO<sub>2</sub> incubator for the appropriate time period. All samples were washed in KRH buffer, transferred into 4% formaldehyde in ice cold PBS and fixed for 15 minutes. The cover slips were then washed in ice cold PBS and mounted onto glass microscope slides, using 15µl of Mowiol. The slides were stored at 4°C and visualized on the Zeiss Confocal microscope within 5 days of preparation.



## **2.2.9 PREPARATION OF THE MATCHMAKER CDNA LIBRARY**

### **2.2.9A TITRATION OF MATCHMAKER CDNA LIBRARY**

A 10µl aliquot of the Clontech leukocyte cDNA library sample was added to 10µl of LBroth. 2µl of this solution was transferred into 1ml of LBroth in a 1.5ml eppendorff and the tube vortexed to mix (Dilution A,  $1/10^3$ ). A 1µl aliquot was removed from Dilution A and added to 1ml of LBroth in a 1.5ml eppendorff and the tube vortexed (Dilution B,  $1/10^6$ ). 1µl of Dilution A was added to 50µl of LBroth, mixed and the entire sample spread onto a pre-warmed LB/ampicillin agar plate. 50µl and 100µl of Dilution B were spread onto 2 separate LB/ampicillin agar plates. All plates were incubated at 37°C for 30-48 hours to allow colonies to grow. The number of colonies on each plate were counted, and the titre determined using the following formulae, as per the manufacturers instructions;

$$\text{Dilution A, cfu/ml} = \text{number of colonies} \times 10^3 \times 10^3$$

$$\text{Dilution B, cfu/ml} = \text{number of colonies/plating volume} \times 10^3 \times 10^3 \times 10^3$$

### **2.2.9B AMPLIFICATION OF THE MATCHMAKER LEUKOCYTE CDNA LIBRARY.**

The Clontech cDNA library sample had to be amplified in order to ensure enough DNA was available for screening purposes. This process was carried out exactly as per the manufacturers instruction to minimise any loss of clone representation. Due to the fact that the library was cloned into the pACT2 vector, lower incubation temperatures were used (30-31°C), again to aid maintenance of clone representation. The library was plated directly onto LBroth agar plates, containing 50µg/ml ampicillin, at a high enough density to ensure the resulting colonies would be nearly confluent ( $2 \times 10^4$  cfu/150mm plate) in order to obtain 2-3 times the number of independent clones present within the library. The number of plates required is dependent upon the size of the library to be amplified, with  $1 \times 10^6$  independent clones requiring 50 x 150mm agar plates. In this case the library contained  $3.5 \times 10^6$  independent clones, therefore  $10.5 \times 10^6$  colonies had to be plated, requiring 550 x 150mm LBroth/ampicillin agar plates. Since the library titre was calculated to be  $4 \times 10^8$  cfu/ml, 26.25µl of library stock was required. 26.25µl of the library stock was diluted in 82.5ml of dH<sub>2</sub>O, the sample was thoroughly mixed and 150µl spread onto each of the 550 agar plates. The plates were incubated at 30°C until



colonies appeared, usually 24-48 hours later. 5ml of LBroth was added to each plate and the colonies were left to soak for a few minutes before being scraped from the plate. Any residual cells were washed off in a further 2ml of LBroth. Every colony was collected and the entire sample was pooled into a sterile 3 litre conical flask and placed at 30°C for a 4 hour incubation to maximize DNA yield. A 25% volume of glycerol was added and the stocks stored in the fridge overnight. The DNA was isolated using five Qiagen Giga plasmid purification columns, and the concentration and purity of the collective sample was assayed as per section 2.2.3C and stored at -20°C.

## **2.2.10 YEAST TWO-HYBRID STUDIES**

### **2.2.10A DNA EXTRACTION FROM YEAST**

Fresh colonies were used to inoculate 5ml of SD/-Trp/-Leu, media and incubated at 30°C for a minimum of 20 hours. 4.5ml of each culture was centrifuged at 13,500 x g in a microcentrifuge, the supernatant removed and the cell pellet resuspended in 0.5ml of S Buffer and vortexed to facilitate complete resuspension. The samples were incubated at 37°C for 30 minutes, 100µl of Lysis solution (25mM Tris-HCl, 25mM EDTA, 25% (w/v) SDS) was then added to each tube and the samples were then vortexed and incubated at 65°C for 30 minutes. 166µl of 3M potassium acetate was added, the samples were incubated on ice for 10 minutes, centrifuged at 13,500 x g in a benchtop microcentrifuge for 10 minutes and the supernatant transferred to a fresh tube. The DNA was precipitated by the addition of 800µl of ice-cold ethanol, a 10 minute incubation on ice and a 10 minute spin in the microfuge at 13,500 x g. The pellet was then washed in 500µl of 70% ethanol and air dried for 15 minutes. The final pellet was resuspended in 40µl of nuclease-free dH<sub>2</sub>O. The isolated DNA extracted from double transfection will contain both the DNA-AD and DNA-BD vectors (and in some cases more than a single DNA-AD vector may be present). This DNA must be used to transform KC8 *E.coli* cells should the aim be to purify the AD vector alone, see section 2.2.10D.

### **2.2.10B TCA YEAST PROTEIN EXTRACTS**

A 2-3 OD<sub>600</sub> quantity of freshly pelleted cells, or a match head sized ball of yeast cells from a fresh agar plate, were resuspended in 1ml of dH<sub>2</sub>O. 150µl of 1.85M sodium



hydroxide containing 7.5% (v/v)  $\beta$ -mercaptoethanol was added, the sample mixed and incubated on ice for 10 minutes. 150ml of 55% (w/v) TCA mix was then added, and the sample incubated for a further 10 minutes on ice. The sample was then centrifuged at 13,500 x g in a desktop microfuge for 15 minutes at 4°C. The supernatant was removed and the sample briefly spun again. The remaining supernatant was removed and the precipitated proteins resuspended in 150 $\mu$ l of high urea buffer (HU-Buffer). The sample was heated at 65°C for 15 minutes to aid complete resuspension of the pellet. If necessary, a few microlitres of 1M Tris was added neutralizing the sample (returning buffer back to blue from yellow). The samples were centrifuged for 5 minutes at 13,500 x g in a microcentrifuge and 10-15  $\mu$ l analysed by SDS-PAGE gel electrophoresis and western blotting.

#### **2.2.10C PREPARATION OF ELECTROCOMPETENT KC8 *E. COLI* CELLS**

400ml of LBroth was inoculated to a cell density of  $5 \times 10^6$  cells/ml or an OD<sub>600</sub> of 0.1 with a stationary phase overnight culture of KC8 cells and grown at 37°C with 250rpm shaking to an OD<sub>600</sub> of 0.4-0.6. The culture mix was chilled on ice for 20-30 minutes and the cells were pelleted by centrifugation at 4,300 x g at 4°C for 30 minutes. The supernatant was removed and the cell pellet resuspended in a small volume of ice-cold dH<sub>2</sub>O. 500ml of ice-cold water was added and the cells were recentrifuged as above. The supernatant was removed and the cells washed again in ice-cold dH<sub>2</sub>O. The supernatant was removed and the cells were then resuspended in the remaining liquid. The cell suspension was transferred into a narrow bottomed 50ml polypropylene tube and centrifuged at 4,300 x g at 4°C for 10 minutes. The pellet volume was estimated and resuspended in an equal volume of ice-cold dH<sub>2</sub>O. 50 $\mu$ l volumes of the cell suspension were aliquoted into pre-chilled microcentrifuge tubes. Frozen stocks were made by resuspending the cell pellet in an equal volume of sterile 10% glycerol, transferred to pre-chilled cryovials and frozen on dry ice. The electrocompetent cells were stored at -80°C.



#### **2.2.10D TRANSFORMATION OF ELECTROCOMPETENT KC8 *E. coli* CELLS**

The yeast DNA extractions detailed in section 2.2.10A were used to transform KC8 *E. coli* cells to facilitate selection of the GAL4 AD plasmids containing library cDNA of interest. 40µl aliquots of electrocompetent KC8 cells were transferred into pre-chilled, labeled 0.1cm gap electroporation cuvettes. 2µl of each DNA preparation was added and the cuvettes tapped to mix the sample. 1µl of pUC19 DNA was added to the control sample. Each electroporation was carried out using the following conditions, 2.4kV voltage, 25µF constant capacitance and 200 Ohms resistance. 1ml of pre-warmed SOC medium was added to each sample immediately after the electroporation step and the samples were then transferred to universals and incubated at 37°C with shaking for 1 hour. Each cell sample was harvested by centrifugation at 1200 x g for 5 minutes, resuspended in 100µl of M9 media and spread onto M9 agar. The control sample was not centrifuged but 10µl of the SOC culture was diluted 1/10 in LBroth and spread onto LBroth agar containing ampicillin. The plates were incubated at 37°C for 36-48 hours until colonies appeared and the DNA was rescued using the Promega SV Wizard plasmid purification columns, as per the manufacturers instructions, 2.2.3A.

#### **2.2.10E LITHIUM ACETATE HIGH EFFICIENCY TRANSFORMATION**

All reactions were performed in accordance with the method described by Agatep and colleagues, [Agatep *et al.*, 1998; Gietz *et al.*, 1997]. 2-5ml of the appropriate media was inoculated with the yeast sample (YPDA for untransformed yeast or SD/-Trp for yeast already containing the bait plasmid) and incubated with shaking overnight at 30°C. 50ml of pre-warmed YPDA was inoculated to a cell density of  $5 \times 10^6$  cells/ml or OD<sub>600</sub> 0.1. The culture was incubated at 30°C on an orbital shaker at 200rpm for 3-5 hours until an OD<sub>600</sub> of 0.4-0.6 had been reached. Producing enough cells for 10 transformations, this method was scaled up or down as required. The culture was harvested in a sterile 50ml centrifuge tube at 1200 x g for 5 minutes. The medium was removed and the cell pellet resuspended in 25ml of sterile dH<sub>2</sub>O and centrifuged again. The water was removed and the cells resuspended in 1ml of 100mM of lithium acetate (LiAc) and transferred to a 1.5ml eppendorf tube. The cells were pelleted at 13,500 x g in a benchtop microcentrifuge for 1 minute and the LiAc removed with a micro-pipette. The cells were resuspended to a final volume of 500µl in 100mM LiAc. A 1ml sample of 2mg/ml single-



stranded carrier DNA (ssDNA) was boiled for 5 minutes and chilled quickly on ice. The cell suspension was vortexed and 50µl aliquots were transferred into labeled eppendorff tubes. The cells were pelleted and the LiAc removed. The transformation mix was then added in the following order, 240µl polyethyleneglycol (PEG) (50% w/v), 36µl 1M LiAc, 50µl SS-DNA (2mg/ml), Xµl Plasmid DNA (0.1-10mg), 34-Xµl Sterile dH<sub>2</sub>O, enabling the PEG to shield the cells from the detrimental effects of the concentrated lithium acetate solution. Each tube was vortexed vigorously, until the cell pellet was completely mixed, and incubated at 30°C for 30 minutes. The samples were then heat shocked at 42°C for 30 minutes and centrifuged at 6-8000 rpm for 15 seconds and the transformation mix removed. The cells were resuspended in 1ml of sterile water and an appropriate volume plated onto appropriate selection SD-minus agar plates in a final volume of 200µl. The plates were incubated at 30°C for 2-15 days to recover transformants. Figure 2.4 illustrates the screening stringency options.

It should be noted that two sequential transformation steps were used to introduce the bait plasmid and then cDNA library plasmids separately. This maximized transformation efficiency for each plasmid and thus enabled the largest number of double transformants to be screened in each experiment. For library scale transformations the co-transformation efficiency was tested by spreading 100µl of a 1/1000, 1/100 and 1/10 dilution onto SD/-Trp/-Leu agar. In order to test the transformation efficiency of each plasmid. 1µl of the transformation mixture was diluted 1/100 with dH<sub>2</sub>O, and 1µl of this dilution was spread onto 90mm SD/-Leu and SD/-Trp plates in 100µl of the appropriate media.

#### **2.2.10F CALCULATION OF TRANSFORMATION EFFICIENCY & THE NUMBER OF CLONES SCREENED**

Transformation efficiency was calculated by counting the number of clones (cfu) growing on SD/-Trp/-Leu plates with 30-300 cfu.

$$\frac{\text{cfu} \times \text{total suspension volume } (\mu\text{l})}{\text{Volume plated } (\mu\text{l}) \times \text{dilution factor} \times \text{amount of DNA used } (\mu\text{g})^*} = \text{cfu}/\mu\text{g DNA}$$

\*In co-transformations this value relates to the amount of the limiting plasmid.



The total number of colonies screened was estimated by multiplying the number of cfu present by the amount of DNA used in the transformation.

$$\text{Total number of screened clones} = \text{cfu} \times \text{amount of DNA used } (\mu\text{g})$$

#### **2.2.10G DETECTION OF $\alpha$ -GALACTOSIDASE ACTIVITY**

Yeast colonies to be assayed for  $\alpha$ -galactosidase activity were incubated on the appropriate SD media agar plates containing 20mg/L of the X- $\alpha$ -Gal substrate. Plates were incubated at 30°C until colony growth appeared. Blue colonies indicated the ability to activate the MEL1 reporter gene, usually via the interaction of bait and prey proteins, thus inducing  $\alpha$ -galactosidase activity and metabolism of the X- $\alpha$ -Gal substrate from colourless to blue [Aho *et al*, 1997].

#### **2.2.10H AMPLIFICATION AND ANALYSIS OF PLASMID INSERTS BY PCR**

DNA extracts were made from yeast cells expressing the plasmids of interest (see section 2.2.10A). PCR was then used to amplify the cDNA inserts encoding proteins initially found to interact with the N-terminal tail of CD23. These fragments were then subjected to endonuclease restriction analysis to eliminate colonies expressing the same cDNA inserts. Oligonucleotides specific for the AD vector (sequence details listed in Table 2.1.8C) were used to amplify the insert fragments from these plasmids. PCR amplification was carried out using 30 cycles of the following conditions; 90°C for 30 seconds, 62°C for 2 minutes and 74°C for 1 minute. The samples were incubated for 5 minutes at 72°C to ensure full extension of any incomplete DNA.

The PCR products were then analysed by agarose gel electrophoresis (2.2.3F) to identify any clones containing multiple AD plasmids. 10 $\mu$ l of the PCR product was also subjected to endonuclease restriction analysis (2.2.3D) with *Hae III* and *Alu I* for 2 hours at 37°C. The samples were again analysed by agarose gel electrophoresis to identify clones with similarly sized fragments.



### **2.2.10I SEQUENCE ANALYSIS OF LIBRARY CLONES FOUND TO INTERACT WITH CD23**

The primers used to sequence the library clones were as follows;

Forward Primer 5'-ctattcgatgatgaagataccccaccaaacc-3'

Reverse Primer 5'-aagtgaacttgcgggggttttcagtatctacg-3'.

Sequence analysis was performed as per section 2.2.3H. Sequences were checked and manipulated using the Macintosh-based Edit View and Gene Jockey programs respectively. Library sequence homology searches were performed by comparison with sequences listed in the GenBank, EMBL and other databases using BLAST searches on the world wide web (<http://www.ncbi.nlm.nih.gov/BLAST>) to identify interacting library cDNAs.



## **FIGURE 2.1 THE BEAM PATH OF A TYPICAL FLOW CYTOMETER**

The diagram illustrates the beam path of the Becton-Dickinson FACScan Flow Cytometer. Every flow cytometer consists of a laser light source, collection optics, electronics and a computer, facilitating the respective generation, collection and translation of the signals into data. The cell suspension enters the system at the interrogation point shown at the base of the diagram and passes through the beam of the laser, which emits coherent light at a specified wavelength. The cells cause the laser light to scatter, and the resultant pattern is collected by two lenses, one set directly in front of the light source (forward scatter, FSC) and one set at right angles to it (side scatter, SSC).

FITC/GFP and PE fluorochromes absorb blue laser light (488nm) enabling their excitation and thus emission of signals around 530nm and 585nm, respectively. Specified wavelengths of fluorescence are measured by a series of optics, beam splitters and filters. The FL1 and FL2 detectors receive emissions of around 530nm and 585nm, detecting FITC or GFP and PE, respectively. The dichroic mirror allows light of less than 560nm to pass straight through to the FL1 detector whilst it reflects light above this frequency towards the FL2 detector. This enables the cytometer to separate and distinguish between the fluorescence emitted from green (FITC or GFP) and red (PE) fluorochromes, enabling accurate collection of data from dual staining experiments.



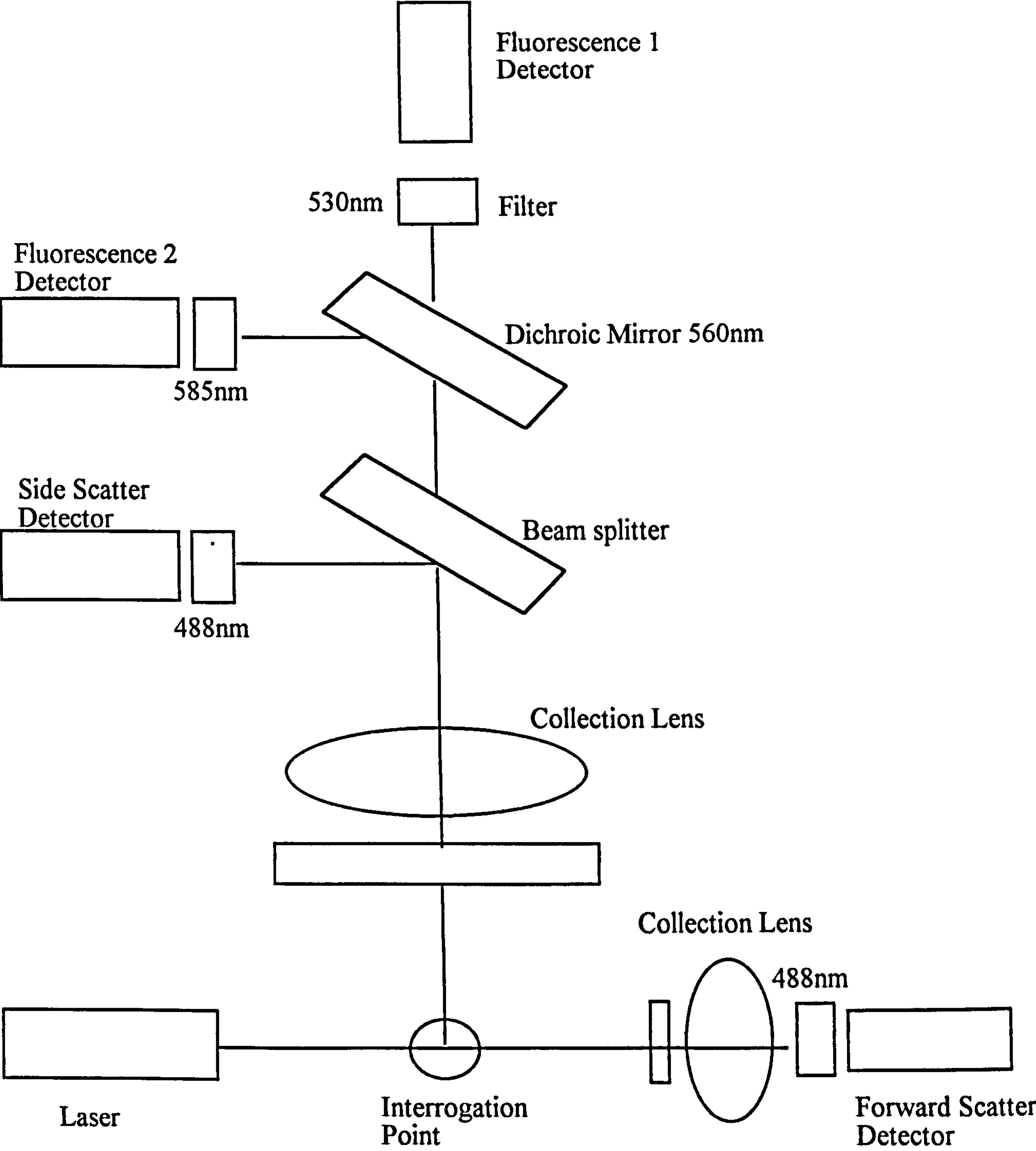




## **FIGURE 2.2 OVERVIEW OF THE STRATAGENE QUIKCHANGE™ SITE-DIRECTED MUTAGENESIS PROTOCOL**

The basic procedure utilises a supercoiled, double-stranded DNA (dsDNA) vector containing the insert of interest and two synthetic oligonucleotide primers. The primers are complimentary to opposite strands of the vector with each containing the desired mutation. Primer extension and amplification occurs during temperature cycling, generating nicked plasmids encoding the desired mutation(s). The parental, non-mutated dsDNA is digested with DpnI (specific for methylated and hemi-methylated DNA) allowing transformation of the nicked vectors into E.coli cells. Mutated plasmids are detected as blue colonies on LB/ampicillin selection agar containing IPTG and X-gal.



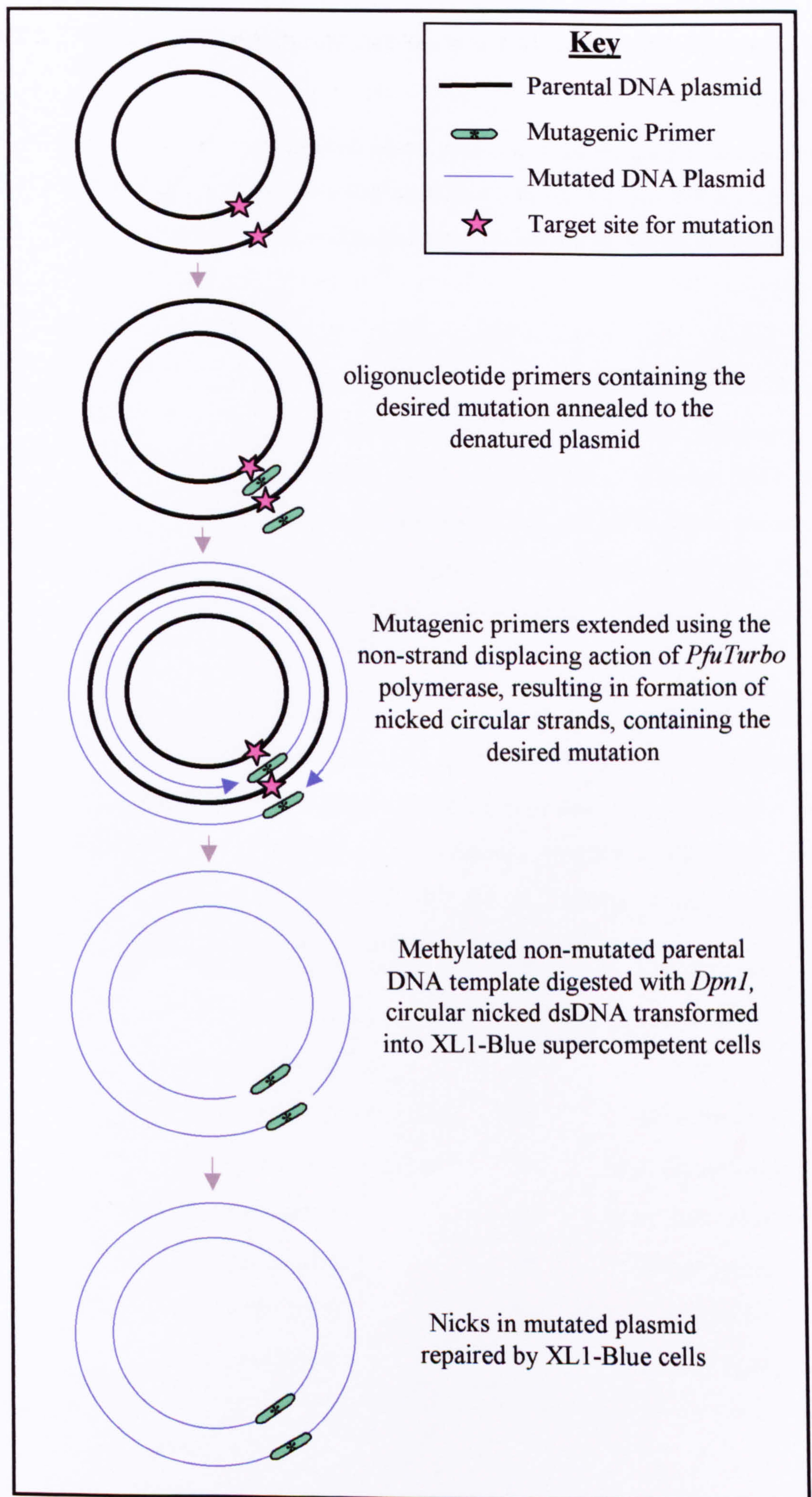




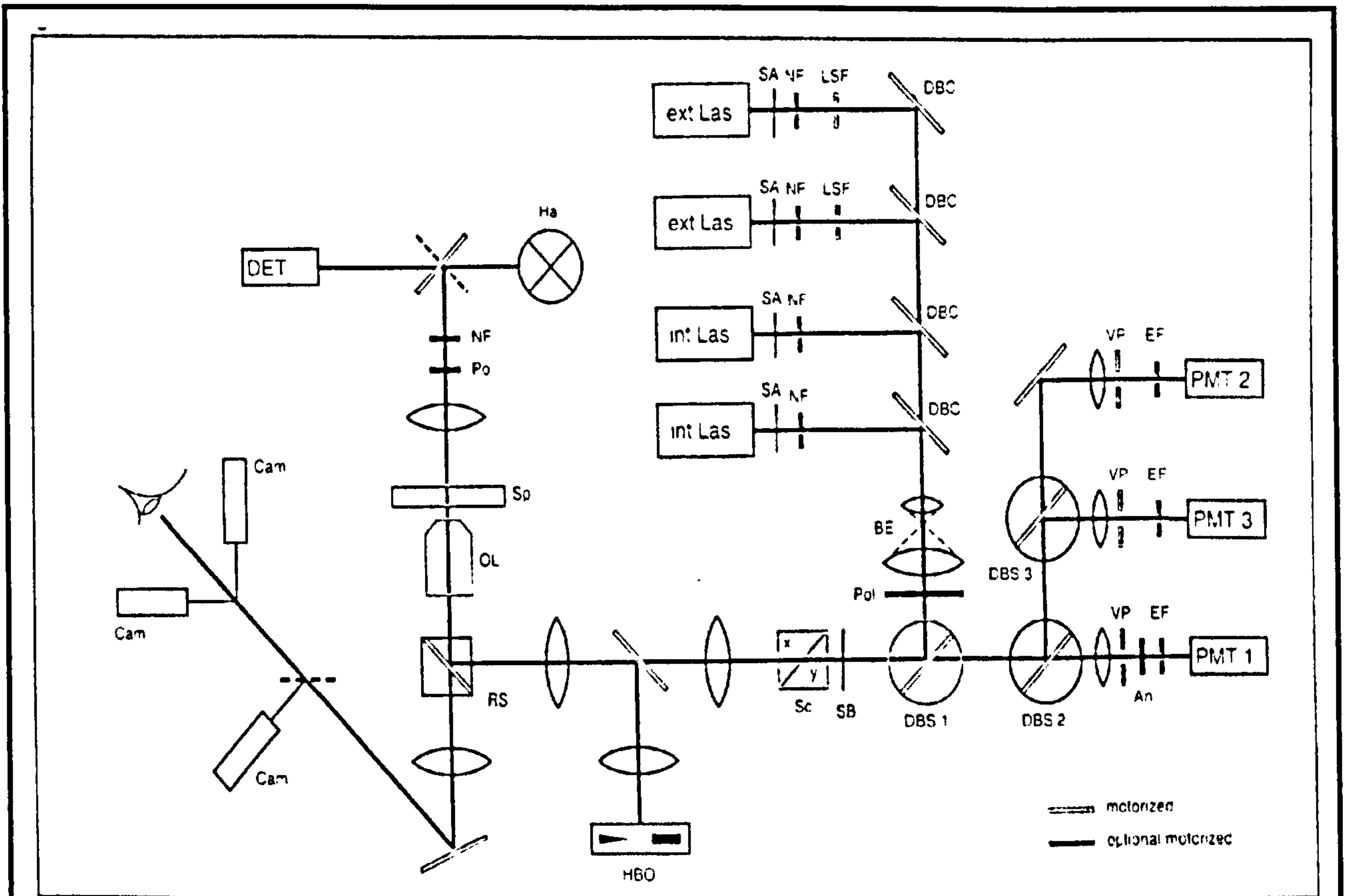
## **FIGURE 2.3 BEAM PATH OF THE ZEISS LSM 410 INVERT CONFOCAL MICROSCOPE**

This diagram illustrates the beam path of the Zeiss LSM 410 Confocal Microscope, the machine used to analyse all live and fixed cell samples discussed in chapters 3 and 4. The table lists the definition for all the abbreviations used within the diagram.

The internal laser was a HeNe 543nm laser enabling the excitation of red fluorochromes, in this case either Tf-TxR or LysoTracker Red. The external laser was an Argon/Krypton 488nm laser used for the excitation of green fluorochromes, in this case GFP or FITC. The dichroic beam splitters used were the FT510 for single excitation of the Ar/Kr line, the FT560 for the single excitation of the NeHe line and the DBSP 488/543 or double-banded beam splitter for the simultaneous excitation of both 488 and 543 stimulated fluorochromes.

The emission filters used were a BP 515-525, a special bandpass filter for blue-488 fluorescence, detecting emission after excitation with the Ar/Kr 488nm laser. An LP 570, a long-pass filter was used to detect emission after excitation with the HeNe 543 laser. These filters allowed simultaneous detection of both green (488nm) and red (543nm) emission signals. The LP 590 filter was also available for use if the green emission was found to bleed-through in double fluorescence experiments using the LP 570 filter.





### Key

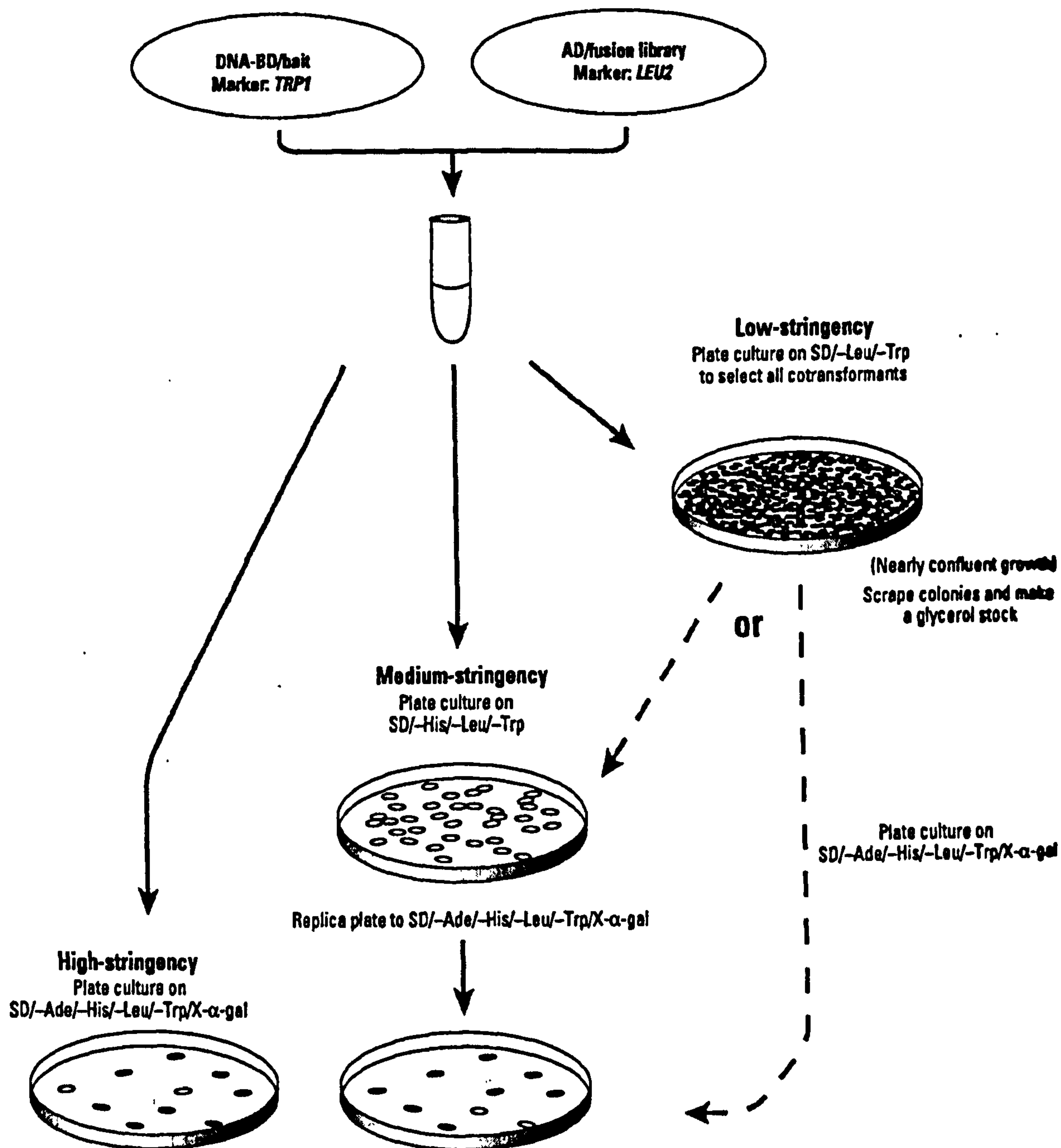
An	Analyser	LSF	Line Filter
BE	Beam Expander	NF	Neutral Density Filter
Cam	Port for microscope or TV camera	OL	Objective Lens
DBC	Dichroitic Beam Combiner	PMT	Photomultiplier
DBS	Dichroic Beam Splitter	Pol	Polarizer
Det	Transmitted Light Detector for LSM	RS	Reflector Slider
EF	Emission Filter	SA	Laser Safety Shutter A
Ext Las	External Laser	SB	Laser Safety Shutter B
Hal	Halogen Lamp	Sc	Mirror Scanner
HBO	Mercury Lamp	Sp	Specimen
Int Las	Internal Laser	VP	Variable Pinhole



## **FIGURE 2.4 YEAST TWO-HYBRID SCREENING STRINGENCY OPTIONS**

The schematic diagram (adapted from the MATCHMAKER GAL4 Two-Hybrid System 3 & Libraries User Manual) illustrates the options for altering the stringency at which a yeast two-hybrid screen is performed. This is primarily controlled through growth on nutritional selection media with additional stringency also being incorporated by the addition of the X- $\alpha$ -Gal substrate to the agar plates. Obviously lower stringency methods increase the number of false positives but may aid in the identification of weak or transient interactors, whilst high stringency can result in false negatives, (loss of real interactors due to the interaction being too weak or transient and thus going undetected).







## **CHAPTER 3**

### **GENERATION AND ANALYSIS OF WILD TYPE CD23 OR GFP CD23 FUSION PROTEINS IN STABLY-TRANSFECTED HEK 293 CELL LINES.**



### 3.1 INTRODUCTION

Two species of the low affinity human Fc receptor for IgE exist, FcεRIIa (CD23a) and FcεRIIb (CD23b) [Kikutani, *et al.*, 1986; Yokota, *et al.*, 1988]. As previously discussed these two isoforms have been found to differ only by a short stretch of amino acids at the N-terminal cytoplasmic tail, and result from different transcription initiation sites, leading to the incorporation of distinct 5' exons in the CD23a and CD23b mRNAs (see Figures 1.6 & 1.7) [Yokota *et al.*, 1988].

CD23 is expressed on numerous cell types with the two isoforms having been observed to have distinct cellular expression patterns; CD23a shows constitutive, but cell specific expression on B cells [Yokota, *et al.*, 1988], whereas CD23b is inducible in a range of haematopoietic cell types, usually following stimulation by cytokines such as IL-4 [DeFrance *et al.*, 1987; Bonnefoy *et al.*, 1998]. CD23 has also been shown to have a variety of different functions including those as an adhesion molecule and involvement in IgE-mediated allergic responses and protective immunity against parasites. The two isoforms appear to be linked to both separate intracellular signalling pathways [as reviewed by Mossalayi *et al.*, 1997] and to distinct intracellular trafficking pathways [Yokota *et al.*, 1992] and it has been suggested that the slight amino acid differences between the two isoforms may be responsible for these distinct differences, although the molecular evidence for this is incomplete.

A potential complication for studying the cellular trafficking of CD23 in native cells is the simultaneous presence of both endogenous CD23 isoforms, making it difficult to follow accurately the independent molecular movement of the two CD23 isoforms. Green fluorescent protein (GFP) obtained from the jellyfish *Aequorea victoria* [Prasher *et al.*, 1992; Tsien, 1998] has been utilised in many systems as a means to generate fusion proteins whose fates can be followed by immunohistochemistry, flow cytometry or in real time by laser-scanning confocal microscopy [Milligan, 1999; Tsien, 1998]. In this study fusion proteins of GFP and each of the CD23 isoforms were generated, with a view to visualising the movement of these molecules in real time in living cells.



3.2 RESULTS

3.2.1 GENERATION OF cDNAs AND PLASMIDS EXPRESSING EACH OF THE CD23 CONSTRUCTS.

Prior to the initiation of this project, plasmids encoding each of the human CD23 isoforms were generated by Dr. Clare Bradshaw. CD23 coding sequences were vectorially cloned into the *Bam* *H1*/*Not* *I* site of pcDNA3.1<sup>+</sup> using the oligonucleotides detailed in Table 3.1, to generate the pCD23a and pCD23b plasmids. Constructs encoding GFP-CD23 fusion proteins were generated using a similar cloning strategy and the synthetic oligonucleotides (see Table 3.1) corresponding to the distinct 5' and 3' ends of the enhanced green fluorescent protein (eGFP) coding sequence, and containing an additional flanking restriction site, were used to introduce *Kpn* *I* and *Bam* *H1* sites at the ends of the eGFP coding sequence by PCR. The resultant DNA fragments were directionally sub-cloned, in-frame, into the pcDNA3.1<sup>+</sup> plasmids already containing the appropriate CD23 isoform (pCD23a or pCD23b, respectively), generating cDNAs encoding a fusion protein comprising GFP fused via a tetra-peptide linker sequence to the extreme N-terminus of CD23a or CD23b. The schematic diagram in Figure 3.1 illustrates these pGFP-CD23a or pGFP-CD23b constructs, and automated DNA sequencing was used to confirm the correct cloning of each isoform (data not shown). Table 3.1 illustrates the sequence of each oligonucleotide, with the additional restriction sites shown in red.

Table 3.1 Oligonucleotide sequences used to generate the pCD23 and pGFP-CD23 plasmids.

Primer	Oligonucleotide Sequence
CD23a Forward	5' – gtaggatccaccgccatggaggaaggtc –3'
CD23b Forward	5' – gtaggatccagcataatgaatcctccaagccaggagatcgaggagcttcccagg – 3'
CD23 Reverse	5' – gtagcggccgctcaagagtggagaggggcag – 3'
GFP Forward	5' – cgggggtaccgccaccatgagtaaaggagaagaac – 3'
GFP Reverse	5' – cgcggatcctgatttgtatagttcatccatgg – 3'



### **3.2.2 WILD TYPE CD23 AND GFP-CD23 FUSION PROTEINS ARE EXPRESSED AT THE PLASMA MEMBRANE OF STABLY-TRANSFECTED HEK 292 CELLS.**

The principal function of CD23 as a membrane protein is as the low affinity receptor for IgE. In order for the GFP-CD23 fusion system to be of practical value in probing CD23 function, the fusion proteins must be accurately targeted to the plasma membrane, correctly folded and displayed in a manner analogous to the endogenous CD23 proteins.

The ability of transfected cells to express CD23 and GFP-CD23 fusion proteins at the cell membrane was tested by transfection of plasmids containing the appropriate cDNAs into HEK 293 cells. After 5-6 weeks in selection G418-resistant cell lines eventually emerged and these were characterised, firstly by Western Blotting (Figure 3.2) and then by flow cytometric (FACS) analysis (Figure 3.3). Collectively these results indicate that both the wild type CD23 and GFP-CD23 fusion proteins are firstly being properly synthesised and secondly being correctly targeted to and expressed on the plasma membrane in HEK 293 cells. The flow cytometric data also demonstrates that the addition of the GFP tag does not prevent the expression and targeting of these fusion proteins. The extracellular domain of the fusion proteins must also be correctly folded at the plasma membrane, as once on the cell surface, they are readily recognised by the anti-CD23 antibodies.

### **3.2.3 VISUALISATION OF CD23 ISOFORM RE-DISTRIBUTION IN HEK 293 CELLS.**

Stably-transfected HEK 293 cells expressing individual wild type CD23 isoforms were assessed by laser scanning confocal microscopy. In each case live cells were studied and CD23 receptor protein trafficking was monitored over a fixed time interval. Figure 3.4A illustrates two representative stills, detailing the typical initial staining pattern observed for CD23a and CD23b respectively, after the addition of FITC anti-CD23 antibody. In agreement with flow cytometric data in Figure 3.3, these pictures illustrate that at an initial time point (i.e. relatively soon after the addition of the anti-CD23 antibody) the majority of CD23a or CD23b is localised to the plasma membrane. In order to probe



movement of the CD23 protein isoforms appropriate cell samples were monitored on a heated stage facility for a further 30-45 minute period. Specific fields of view were chosen and data were collected from these at defined time intervals. When the data pictures were then run together as a 'movie' it was evident that re-distribution of fluorescence was occurring, both along the plane of the membrane and within the cell, indicating that both isoforms show a certain level of re-cycling after the addition of FITC anti-CD23 antibody. It is impossible in this experimental configuration to tell whether or not this re-cycling would still occur if the receptor were unoccupied/cross-linked by antibody.

Figure 3.4B illustrates representative confocal microscopic images of HEK 293 cells expressing either GFP-CD23a or GFP-CD23b proteins and, as per the wild type protein data (Figure 3.4A), a distinct plasma membrane localisation is evident. These data are consistent with the flow cytometric, cell surface expression data illustrated in Figure 3.3, and again confirm that the GFP-CD23 fusion proteins are correctly targeted to and expressed upon the cell membrane. Movement along the membrane and a low level of "re-cycling" of these proteins was observed when time-lapse images were collated as a 'movie', indicating that GFP-CD23a and GFP-CD23b proteins, and presumably wild-type CD23 proteins do indeed illustrate basal re-cycling movement.

#### **3.2.4 GFP-FUSION PROTEINS FACILITATE THE STUDY OF CD23 ISOFORM TRAFFICKING IN "BASAL", "LIGATED" AND "CROSS-LINKED" CONDITIONS.**

Figure 3.4A and the associated time-lapse movies (data not shown) illustrate that CD23a and CD23b proteins can be driven to internalise upon antibody-mediated cross-linking. This system does not however facilitate the analysis of CD23 isoform re-distribution in the unligated state as the addition of fluorophore-conjugated and intact anti-CD23 antibodies, by definition, move the system from resting to cross-linked. Philosophically, therefore, the addition of the probe has in itself perturbed the experiment. These and previous studies of CD23 trafficking [Yokota *et al.*, 1992] have been unable to address the issues of movement in the unoccupied, basal state or in the state where CD23 molecules are occupied by IgE but are not cross-linked by antigen. GFP-CD23 fusion



proteins allow these questions to be addressed directly. Figure 3.5 illustrates GFP-CD23 fusion proteins and NIP-specific chimaeric human IgE antibody being utilised to investigate the potential trafficking differences between CD23 in an unligated or “basal” state, CD23 “loaded” with its natural ligand IgE (NIP-specific) and following the addition of NIP-BSA to cells pre-loaded with IgE, to evaluate “cross-linked” CD23.

Initial time-lapse studies in the basal state show that both GFP-CD23a and GFP-CD23b proteins move within the plane of the plasma membrane and illustrate modest uptake into the cell to a peri-nuclear compartment and movement back out to the plasma membrane (data not shown). Figure 3.4B shows two representative ‘snapshot’ time point pictures illustrating this for both GFP-CD23 isoforms. The rate of this re-cycling movement appeared to be slightly increased when the CD23 molecules were loaded with IgE, as demonstrated by comparison of the time-lapse movies (Data not shown). Pre-loading the cells with NIP-specific IgE, followed by the addition of NIP-BSA stimulates distinct receptor internalisation, initially demonstrated by punctate fluorescence on the plasma membrane, followed by the appearance of multiple discrete foci of fluorescence within the cell. Figure 3.6 shows a diagrammatic representation of this process and illustrative confocal images demonstrating the consequent localisation of receptor staining at each stage.

### **3.2.5 CD23A BUT NOT CD23B PROTEINS ARE INTERNALISED VIA THE EARLY ENDOCYTIC PATHWAY.**

Co-localisation studies were carried out using live HEK 293 cells expressing either CD23a or GFP-CD23a proteins. The cells were exposed to Transferrin-modified-Texas Red dye (Tf-TxR) for 20 minutes at 37°C, (wild type proteins were then labelled with FITC anti-CD23 antibody for 5 minutes at room temperature) and then analysed on the confocal microscope using the heated stage. Images were recorded over a 45-minute period (unless otherwise stated).

Figure 3.7 illustrates a single data set representative of the many CD23a experiments recorded. The results indicate that MAb cross-linked CD23a isoform appears to move



into endosomal compartments, denoted by the yellow signal, resulting from the co-localisation of CD23a (green) and Tf-TxR (red). GFP-CD23a was also found to co-localise with Tf-TxR, but only under “cross-linked” conditions where the CD23 proteins were loaded with IgE and then cross-linked with ‘antigen’. The results of the wild type CD23a study support these findings for the GFP-CD23a proteins, and reconfirms that the addition of anti-CD23 antibody moves the system from a basal to cross-linked state.

The same experiments were also carried out for HEK 293 cells expressing either CD23b or GFP-CD23b proteins. Figure 3.8 shows a single data set representative of the many CD23b experiments recorded. Co-localisation of Tf-TxR with either the wild type CD23b or GFP-CD23b fusion proteins was not observed under any of these experimental conditions. This indicates that CD23b, unlike CD23a, does not move into the early endosomal pathway within this HEK 293 cell system. Again the results from both the wild type and GFP fusion proteins are similar, illustrating the utility of the system. A difference between the two isoforms has already been observed, reconfirming the usefulness of this cell system for studying CD23 isoform trafficking issues.

### **3.2.6 NEITHER CD23 ISOFORM ENTERS A PHAGOCYTOTIC PATHWAY IN HEK 293 CELLS.**

Co-localisation studies with LysoTracker Red dye were routinely carried out over a 45-minute time period (and occasionally over 75 minutes). Figures 3.9 and 3.10 illustrate single data sets representative of many experiments recorded for CD23a/GFP-CD23a and CD23b/GFP-CD23b proteins, respectively. Co-localisation was never observed in any of these experiments indicating that neither CD23 isoform was found to enter the lysosomal pathway in HEK 293 cells.

### **3.2.7 HEK 293 CELLS DO NOT UTILISE CLASSICAL PHAGOCYTOSIS.**

The data of Figures 3.9 and 3.10 indicate that neither of the CD23 protein isoforms were found to co-localise with LysoTracker dye, suggesting that neither protein appeared to undergo classical phagocytosis. Before drawing too many conclusions about the



trafficking patterns of each of the CD23 proteins it was important to establish the phagocytic capability of HEK 293 cells. A phagocytic assay was carried out utilising opsonised sheep red blood cells (SRBC).

A 1ml suspension of sheep red blood cells (SRBC) was spun down and exposed to 5mg of FITC dissolved in 10µl of DMSO and then resuspended in 500µl of 1M carbonate buffer, pH 7.2. The mixture was incubated in the dark at room temperature for several hours with occasional gentle mixing. Finally anti-SRBC stromal antibodies were added to the mixture, generating opsonised SRBC. The antibody-coated cell suspension was then presented to HEK 293 cells at 37°C for 30 minutes and the results analysed under a fluorescent microscope. Engulfed SRBC could be located either by their FITC fluorescence or by simple bright field analysis. No SRBC were found within any HEK 293 cells (Figure 3.11), indicating that HEK 293 cells cannot be used to study the trafficking of proteins via the classical phagocytic pathway, as these cells do not in fact use this method of uptake. Figure 3.11 also illustrates a control test indicating that U937s, a macrophage-like cell line, can take up the opsonised SRBC probably mediated through FcγRI and FcγRII. Neither cell was observed to engulf non-opsonised SRBC. HEK 293 cells may not have Fc receptors therefore the use of a non-opsonised target may have been a better positive control in this case.

### **3.2.8 HEK 293 CELLS DO NOT EXPRESS MHC CLASS II MOLECULES**

Recent data suggests that CD23a and MHC class II molecules can be co-internalised and co-localised into endocytic compartments in a human RPMI-8866 B cell line [Karagiannis *et al.*, 2001], as demonstrated by the endosomal uptake of any anti-CD23, anti-HLA-DR or IgE/antigen complexes. These experiments raise the question as to which of the molecules present within the ternary complex provides the sorting signals for movement of the complex into the cell. It is a distinct possibility that the HLA-DR molecules may provide the necessary sorting signals for uptake and that these experiments may report more on HLA-DR trafficking rather than CD23 trafficking.

Flow cytometric analysis of HEK 293 cells was performed to investigate whether or not this cell line expressed endogenous HLA-DR molecules. The results demonstrate that



HEK 293 cells do not express HLA-DR molecules, but that the Raji A immature B cell line, used as a positive control, did express MHC class II molecules (Figure 3.12). The absence of MHC class II antigen expression in HEK 293 cells enables investigation of CD23 trafficking independently of any contribution which the HLA-DR molecules may have provided. The protein motifs responsible for CD23 trafficking in the experiments described in this chapter, are therefore most likely to be intrinsic to the CD23 isoforms themselves, since the HEK 293 cell line does not express MHC class II antigens.

### 3.3 DISCUSSION

The studies presented herein employed identical cell systems and methods for assessment of the trafficking of both CD23a and CD23b molecules; namely HEK 293 cells and chimaeric, hapten-specific IgE and a haptenated protein antigen for cross-linking purposes. The use of GFP-tagged proteins has enabled visualisation of CD23 in both the unoccupied or “basal” state and in the state where CD23 molecules are occupied by IgE but not cross-linked by antigen, two scenarios never previously visualised. Another strong advantage of this system is the ability to study live cells and collect real-time images as each individual experiment progresses.

The data presented in this chapter demonstrate that CD23a and CD23b molecules show a degree of re-cycling in the basal, unligated state. CD23a cross-linked with FITC anti-CD23 MAb and GFP-CD23a fusion proteins loaded with IgE and then cross-linked with ‘antigen’ were both found to show rapid co-localisation with Tf-TxR in the early endosomal pathway. GFP-CD23a fusion proteins in the basal or loaded state were never observed to co-localise with Tf-TxR. Neither CD23b nor GFP-CD23b fusion proteins in any of the three states were found to co-localise into the endosomal pathway. Neither isoform was found to traffic to the lysosomal pathway under any of the experimental conditions tested.

In contrast to these results, earlier studies [Yokota *et al.*, 1992] employed radio-iodinated anti-CD23 MAb to probe endocytic function, and IgE-coated erythrocytes to probe phagocytosis, using separate cell types to analyse each protein trafficking



pathway. J774 macrophage cells, a cell line with extremely high phagocytic capability, were used to probe the possible uptake of CD23 into the lysosomal pathway.  $\psi$ 2 cells were used to analyse endocytic uptake of CD23. At this point it is necessary to say that the Yokota studies indicated that the CD23 isoforms were internalised via distinct routes; CD23a was observed to enter  $\psi$ 2 cells via receptor-mediated endocytosis whereas CD23b was shown to illustrate phagocytic uptake into J774 cells. The findings from these studies will be discussed at greater length in the general discussion chapter. The results presented within this chapter support these previous findings for CD23a and CD23b trafficking in the context of endocytic pathways, but are unable to provide any information on the trafficking methods employed by CD23b with respect to phagocytosis, other than to suggest that receptor-mediated endocytosis is not the internalisation route of choice for this isoform.

In summary, these studies clearly demonstrate that GFP-CD23 fusion proteins are a viable and informative means of probing the cell biological properties and intracellular trafficking of the CD23 isoforms. The limitations of this system lie with the cell line chosen since HEK 293 cells have subsequently been shown to be unsuitable for the analysis of phagocytic routes of trafficking. HEK 293 cells are a typical choice for this type of expression work as they benefit from ease of transfection with a plasmid of choice, and generation of stable cell lines producing the required protein at a reasonable expression level. Their adhesion properties are also an important benefit, facilitating analysis of cells attached to glass cover slips by confocal microscopy. HEK 293 cells are routinely used as a model system to study receptor-mediated endocytic trafficking by many research groups and no doubt will continue to be used for this type of work in the future. HEK 293 cells have also been used to analyse the endocytic trafficking capacity of a small library of GFP-CD23 N-terminal mutant fusion proteins. This work is presented and discussed in chapter 4 of this thesis.



### **FIGURE 3.1 GENERATION OF WILD-TYPE CD23 AND GFP-CD23 FUSION PROTEINS**

Human CD23 was amplified by RT-PCR from a B lymphoblastoid cell line and directionally cloned into the *Bam* *H*1 - *Not* 1 sites in the multiple cloning region of pcDNA3.1+, generating pCD23a and pCD23b plasmids. Enhanced green fluorescent protein (eGFP) was then subcloned into the *Kpn* 1 – *Bam* *H*1 sites, generating cDNAs encoding a fusion protein comprising eGFP fused via a tetra-peptide linker sequence to the extreme N-terminus of CD23a and CD23b, generating pGFP-CD23a and pGFP-CD23b plasmids.



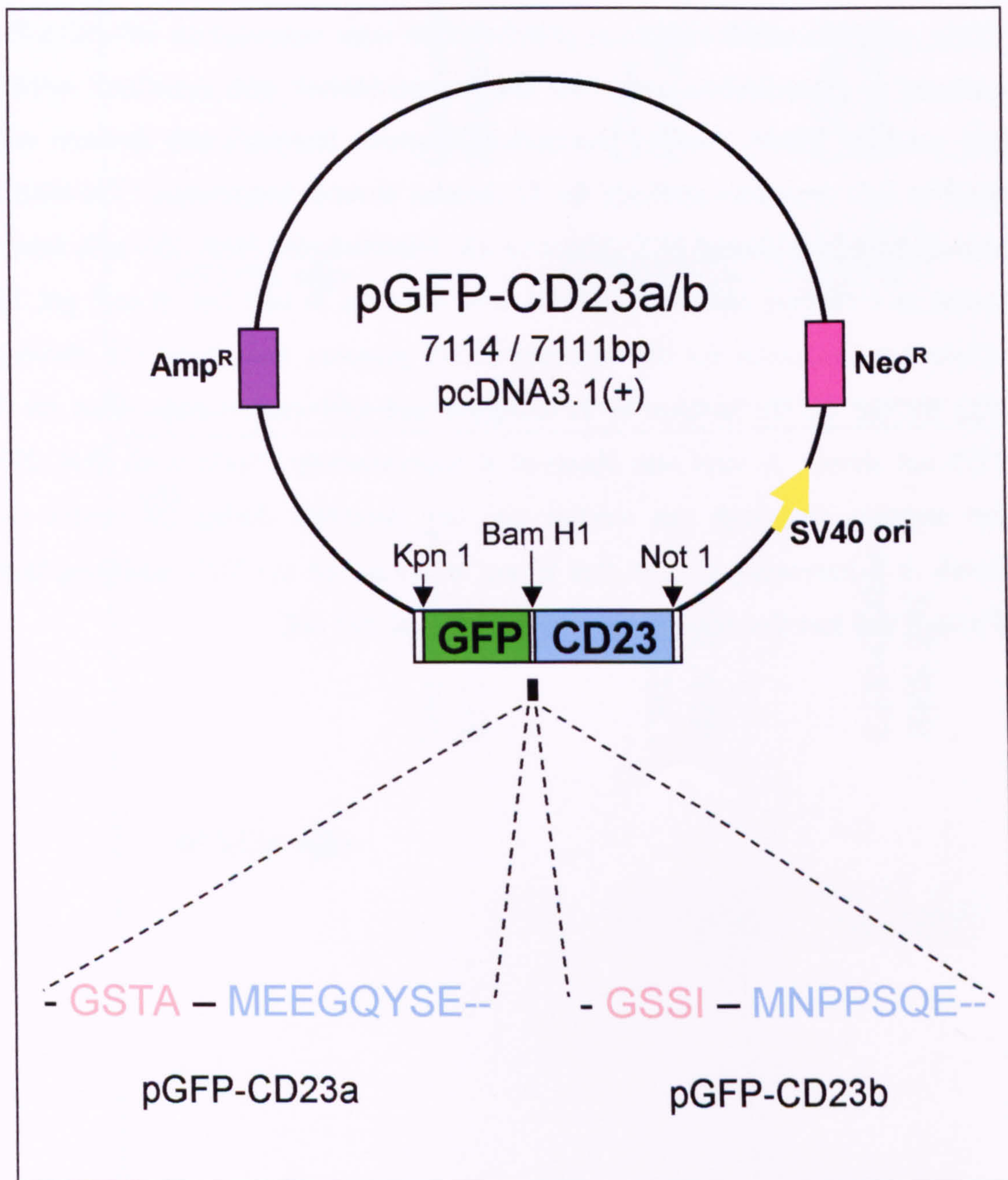




### **FIGURE 3.2 HEK 293 CELLS STABLY EXPRESS CD23 AND GFP-CD23 FUSION PROTEINS**

30µg of total RIPA cell lysate protein from HEK 293 cells stably transfected with pCD23a, pCD23b, pGFP-CD23a or pGFP-CD23b were separated on 10% SDS-PAGE, transferred to nitrocellulose membrane and immunoblotted with polyclonal rabbit anti-CD23 antibody (Rb55, Geneva Biomedical Research Institute) and detected with an anti-rabbit IgG secondary antibody for 45 minutes at room temperature. The blots were visualised using the Biorad ECL detection kit. Untransfected HEK 293 cells have been included as a control, and these samples have been run in lane one of each gel. Figure (i) illustrates the results for the wild-type CD23 proteins, with figure (ii) showing the results for the CD23a isoform in its untagged and GFP-tagged state. Data for GFP-CD23b not shown. A band was observed at approximately 75kDa in all HEK 293 cell lysate samples. Although this species was not identified during the course of this research, it is interesting to note that it was not observed in CD23 producing-bacterial cell lysates and may therefore be specific to the HEK 293 cell.



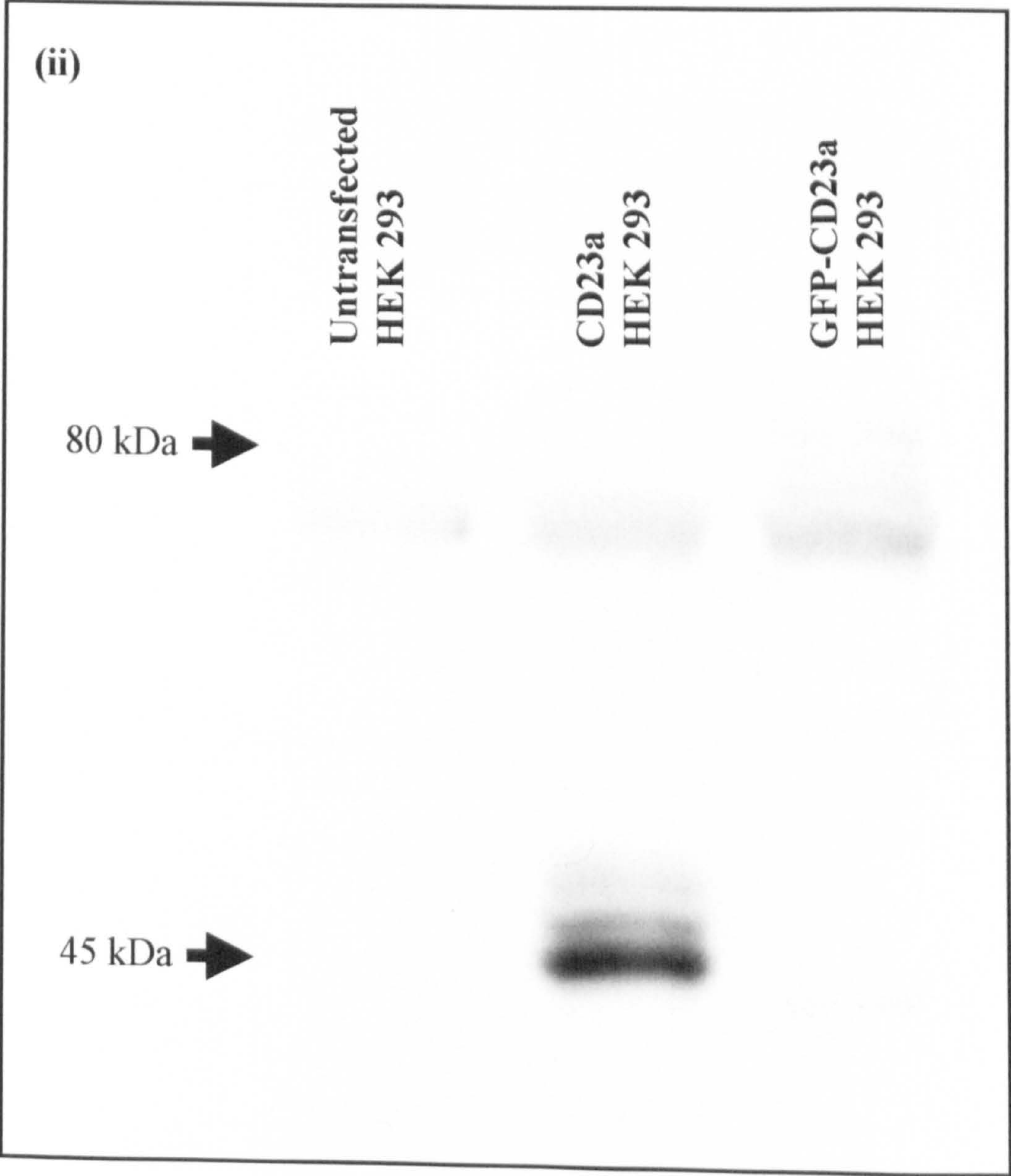
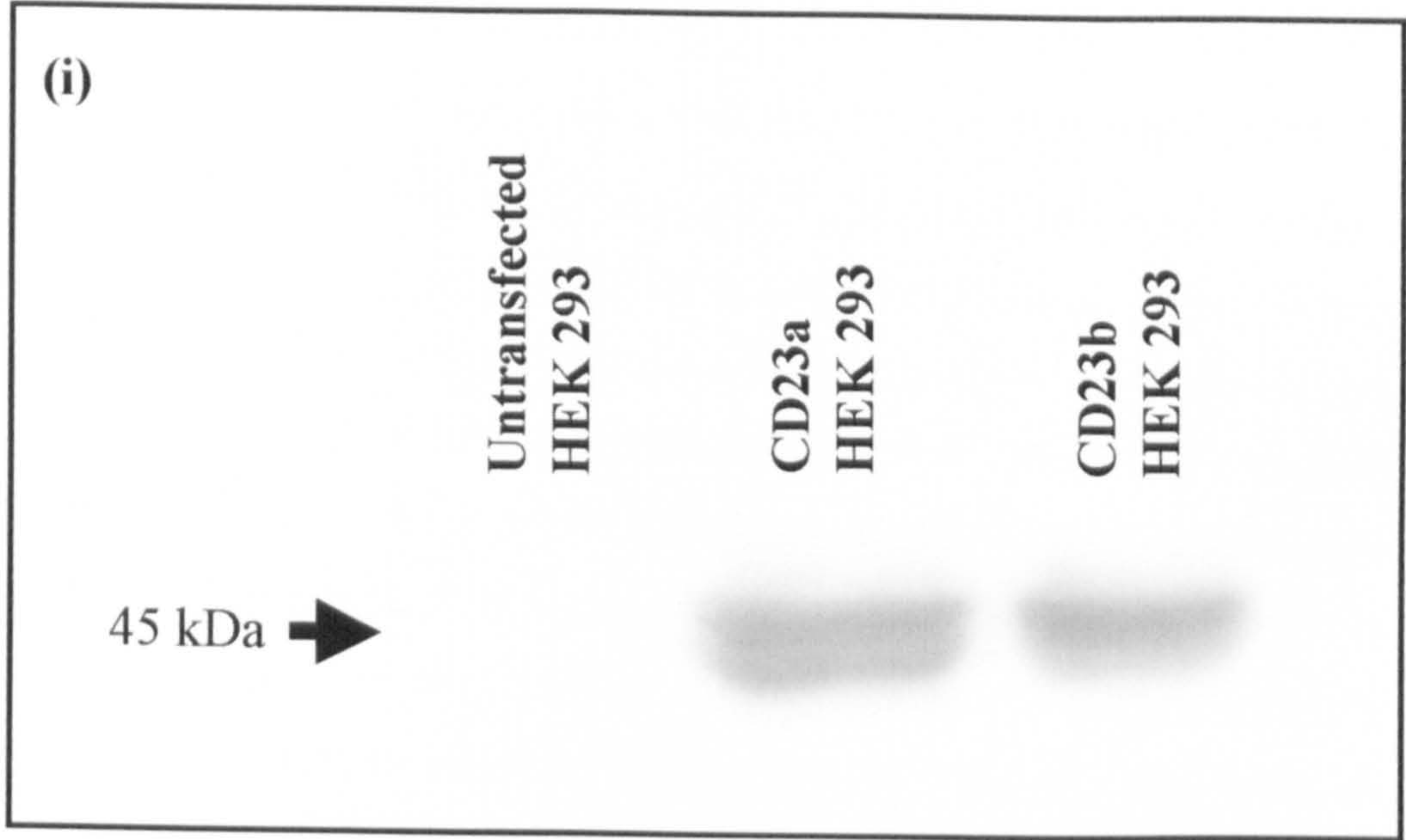




### **FIGURE 3.3 HEK 293 CELLS STABLY EXPRESS CD23 AND GFP-CD23 FUSION PROTEINS AT THE PLASMA MEMBRANE**

G418-resistant HEK 293 cells stably transfected with pCD23a, pCD23b (**Panel A**) or pGFP-CD23a, pGFP-CD23b (**Panel B**) were subjected to flow cytometry. **Panel A** - The green line represents the presence of CD23, as detected by a FITC anti-CD23 antibody. The black line represents the negative control illustrating the results for untransfected HEK 293 cells with the addition of the anti-CD23 antibody. **Panel B** - The presence of CD23 was detected by an anti-CD23 PE antibody (FL-2), whilst the presence of the GFP tag was directly detected from its green fluorescence (FL-1). The data has been presented as a number of dot-plots enabling the percentage of double positive cells to be calculated.



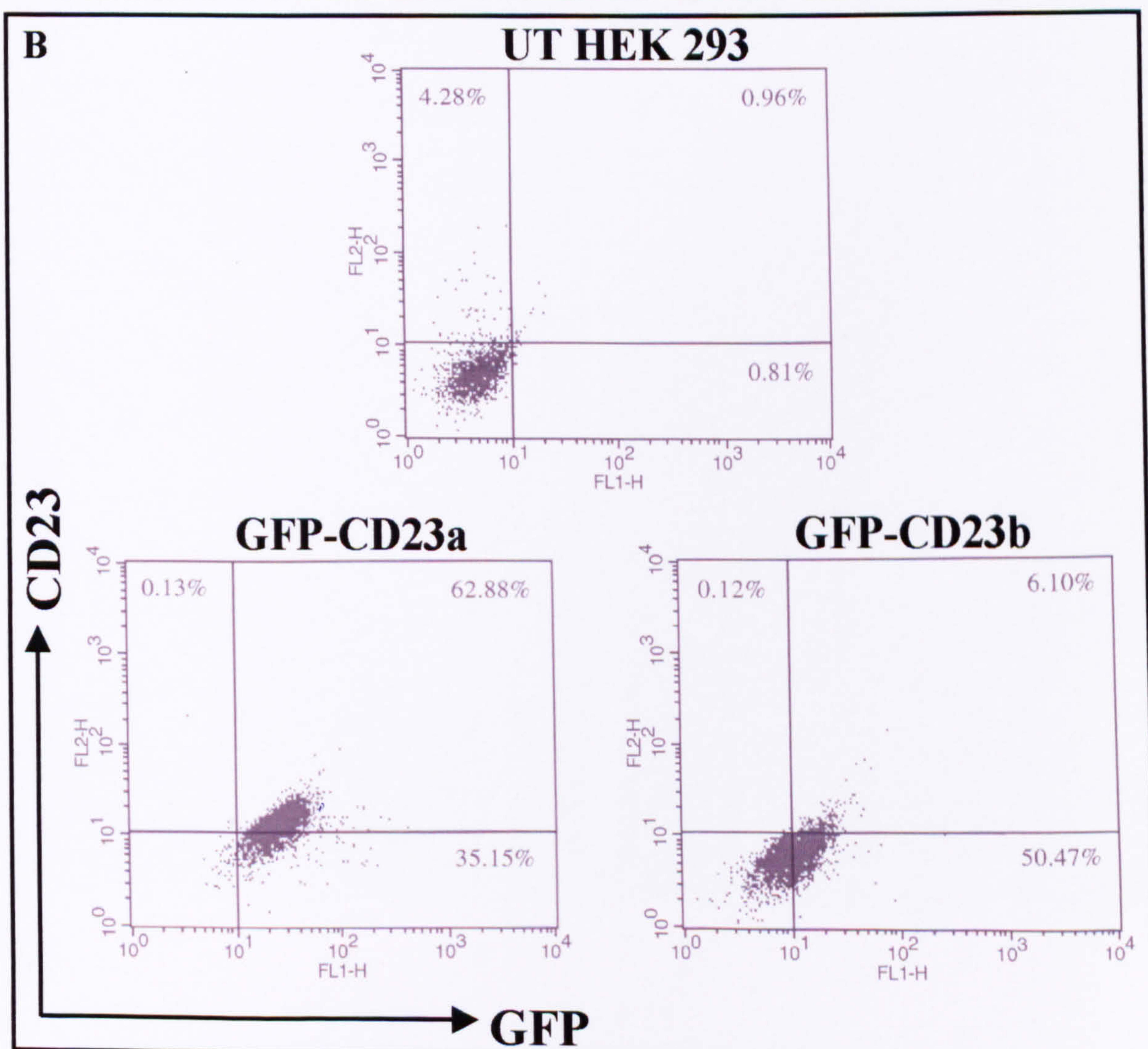
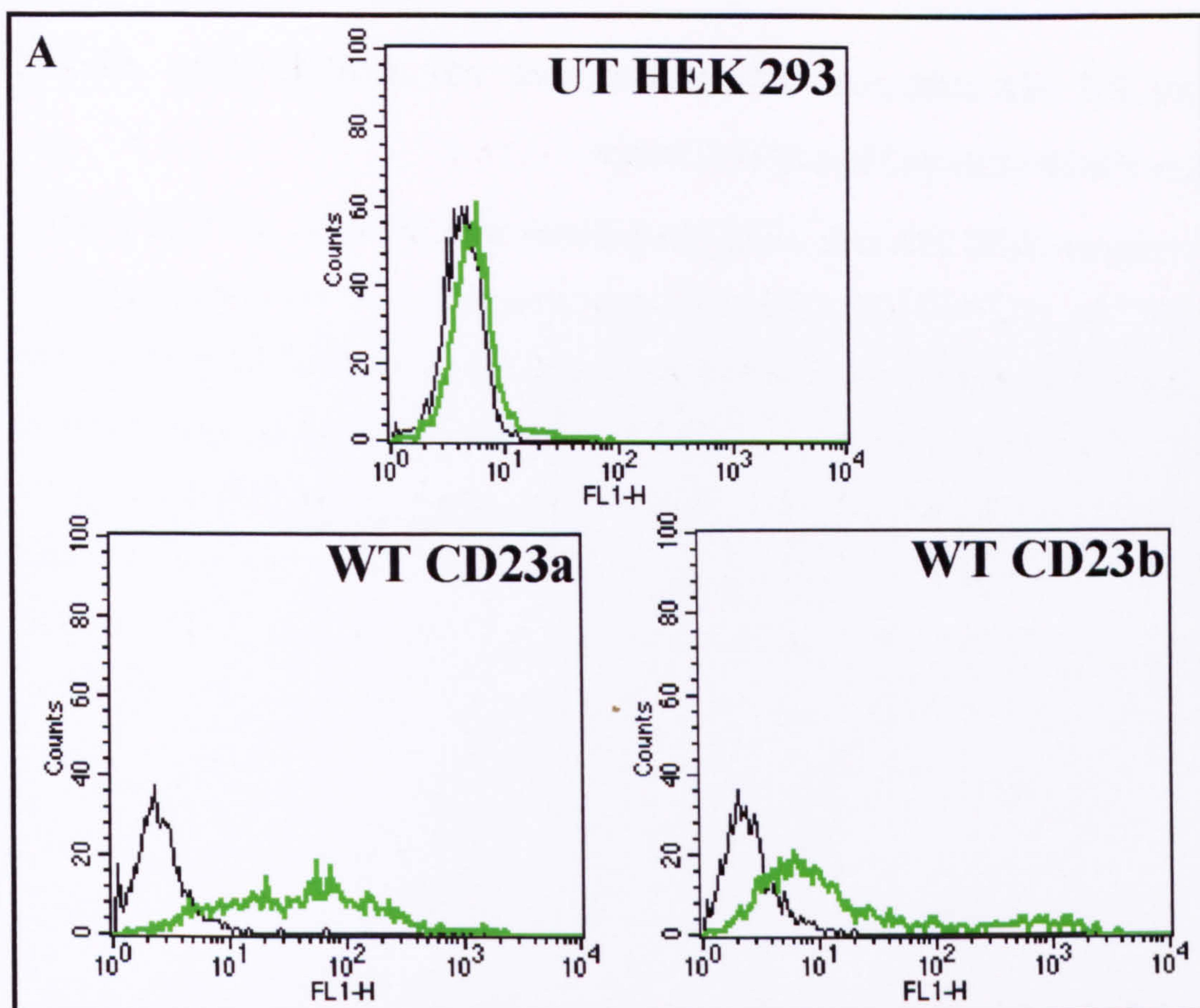




### **FIGURE 3.4 MEMBRANE LOCALISATION OF CD23 AND GFP-CD23 FUSION PROTEINS IN HEK 293 CELLS**

G418-resistant HEK 293 cells stably transfected with pCD23a, pCD23b (**Panel A**) or pGFP-CD23a, pGFP-CD23b (**Panel B**) were propagated for 48 hours on poly-D-lysine (PDL) coated coverslips before being harvested, washed in KRH buffer and subjected to Confocal analysis. Wild-type CD23 was visualised by the addition of FITC-anti-CD23 antibody for 5 minutes, prior to rinsing and then subjected to confocal analysis.



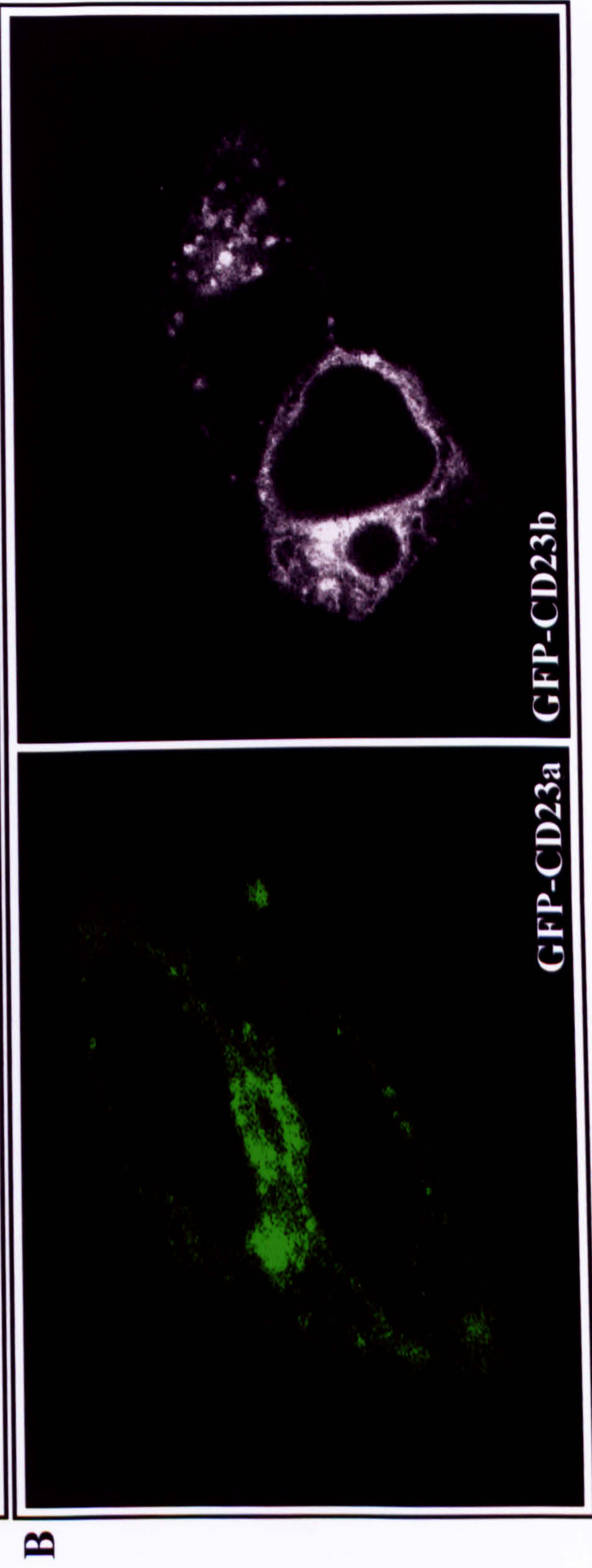
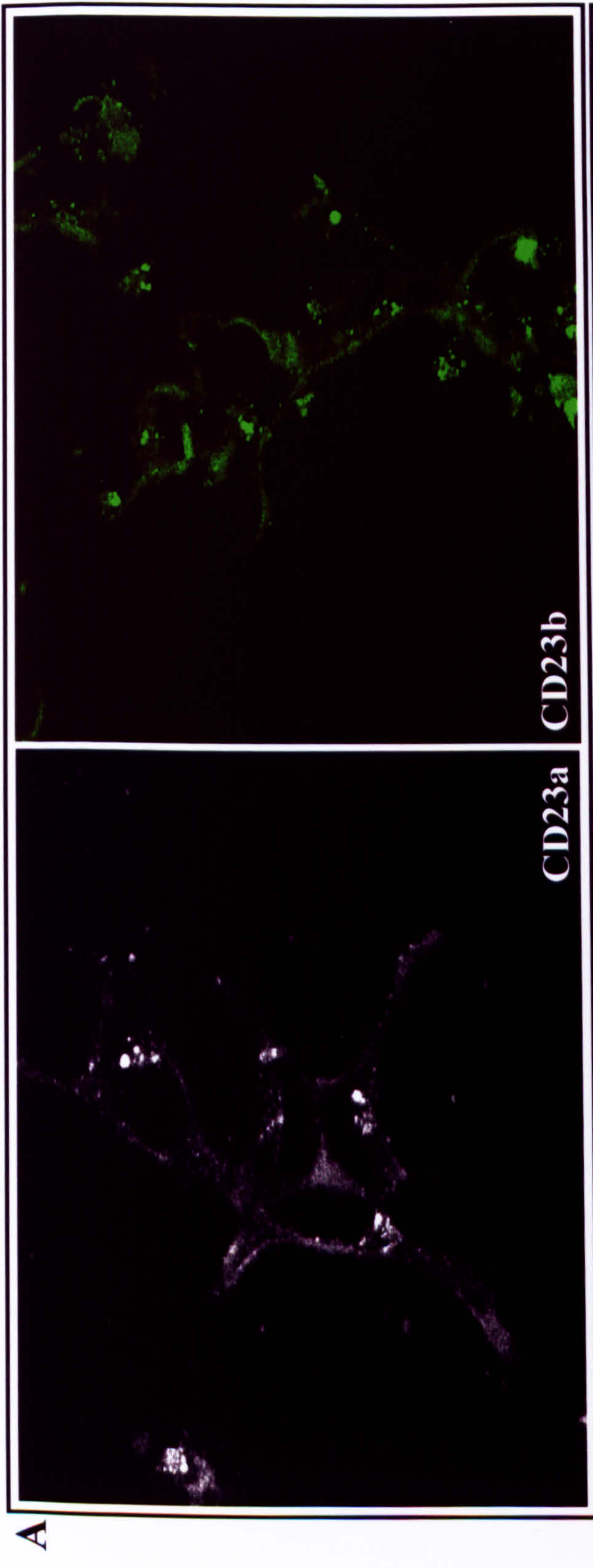




### **FIGURE 3.5 SCHEMATIC DIAGRAM ILLUSTRATING THE NIP SYSTEM**

BSA was conjugated with 4-hydroxy-3-iodo-5-nitrophenylacetic acid (NIP) and used in conjunction with NIP-specific IgE antibody. The NIP-BSA preparation had an average derivatisation ratio of approximately 10 NIP molecules per each BSA molecule. GFP-CD23 fusion proteins were stably expressed in HEK 293 cells and their trafficking patterns assessed in an unoccupied or “Basal” state, a “Loaded” state following the addition of NIP-specific chimaeric IgE antibody and a “Cross-linked” state following the addition of NIP-BSA to cell pre-loaded with NIP-specific IgE. The green star in each instance represents the GFP tag at the N-terminus of each CD23 fusion protein.



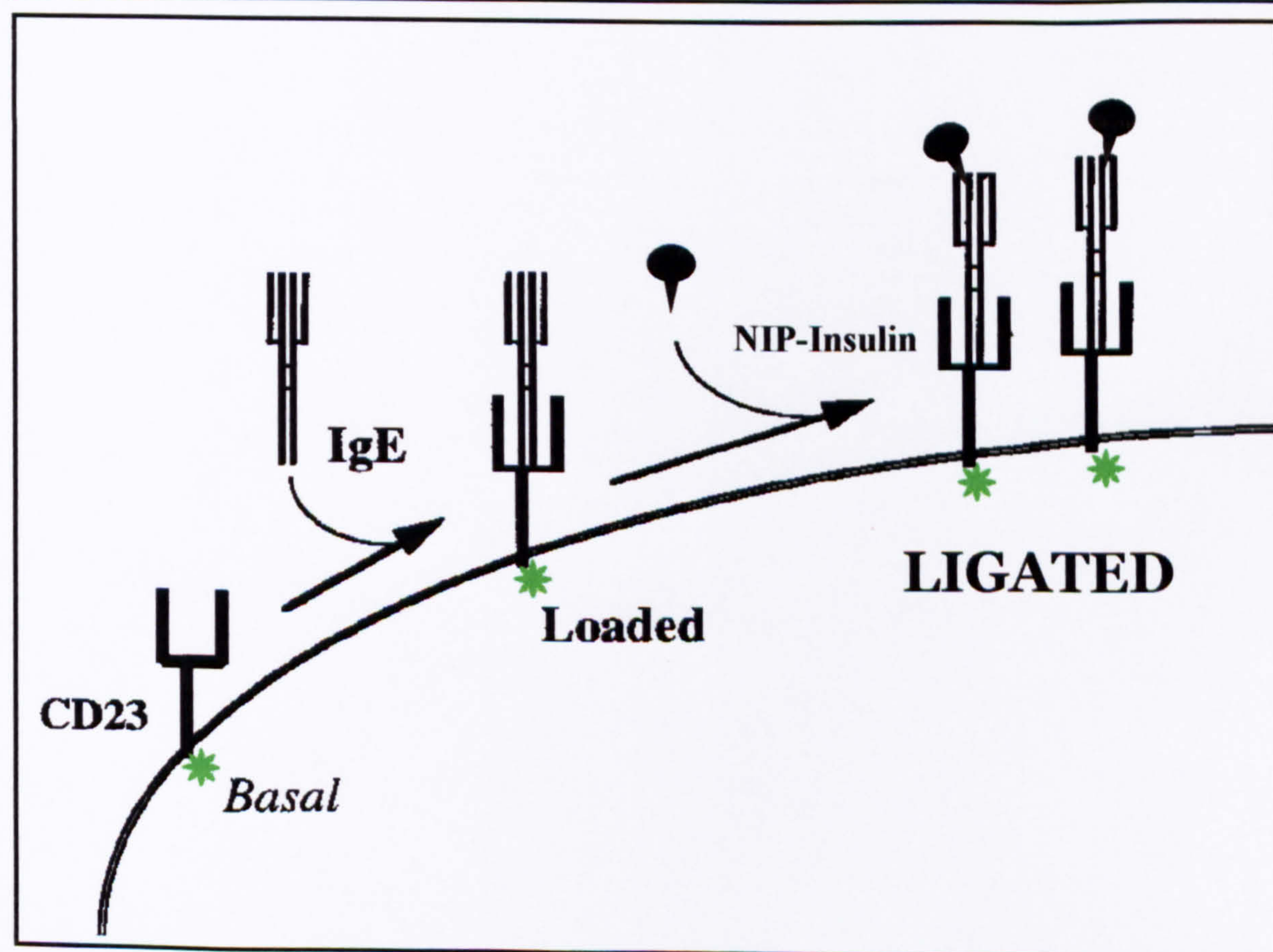
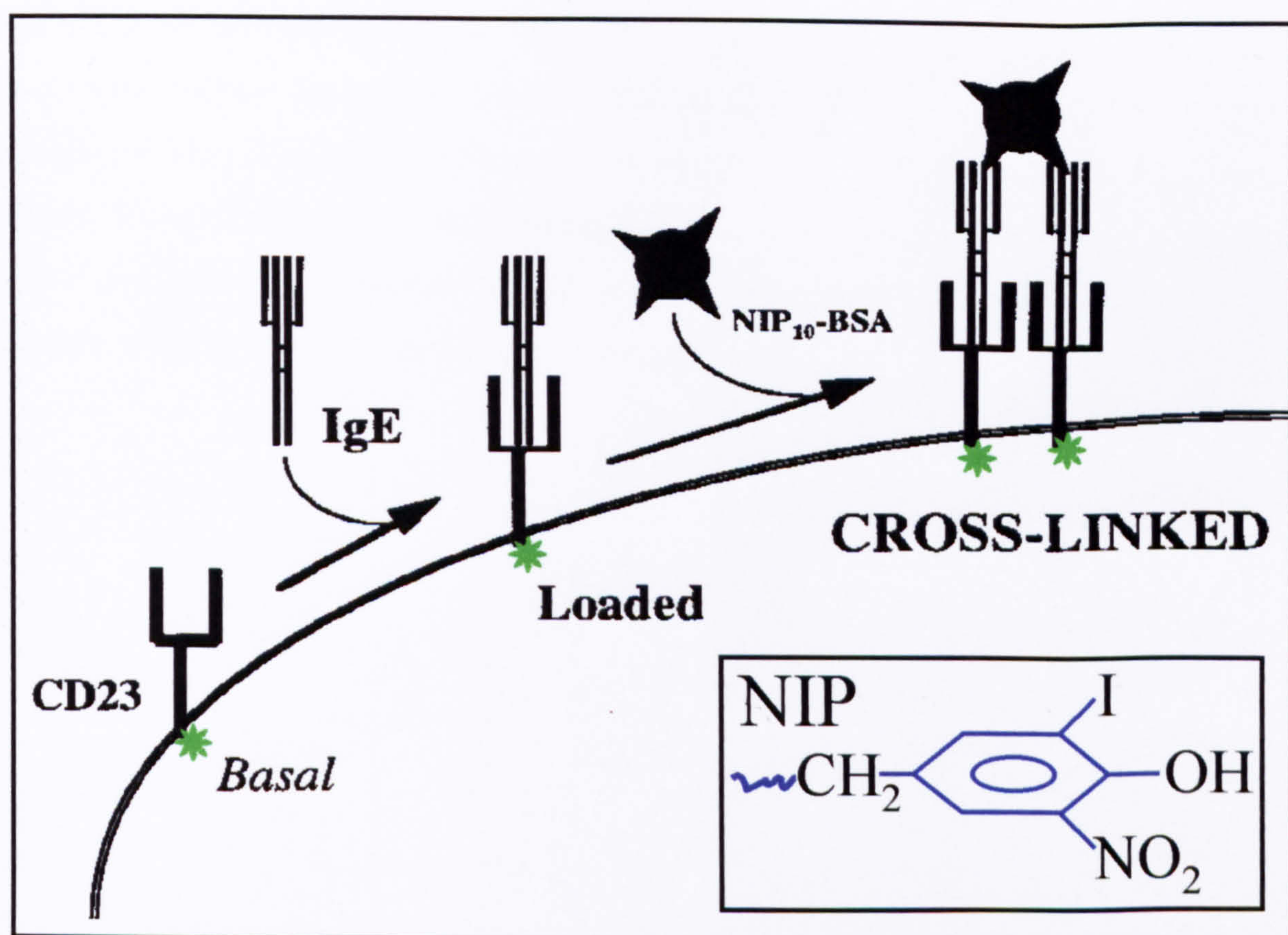




### **FIGURE 3.6 TYPICAL PATTERNS OF RECEPTOR INTERNALISATION**

Many cell surface receptors are ubiquitously expressed on the plasma membrane until a stimulus causes them to cluster at particular points on the cell surface prior to their internalisation or entry into the cell. Panel (i) shows a schematic diagram illustrating the steps of receptor internalisation. Panel (ii) shows three confocal microscope images of GFP-tagged CD23 illustrating the main stages of receptor internalisation, with the images demonstrating the classical punctate morphology referred to when discussing the confocal results herein.



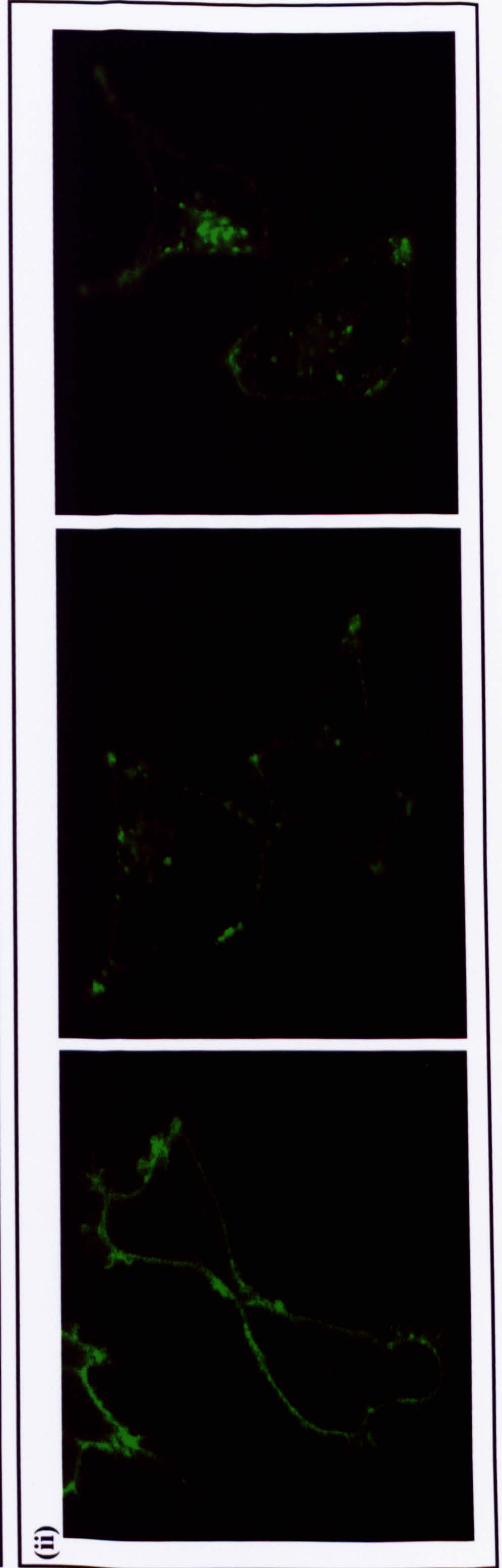
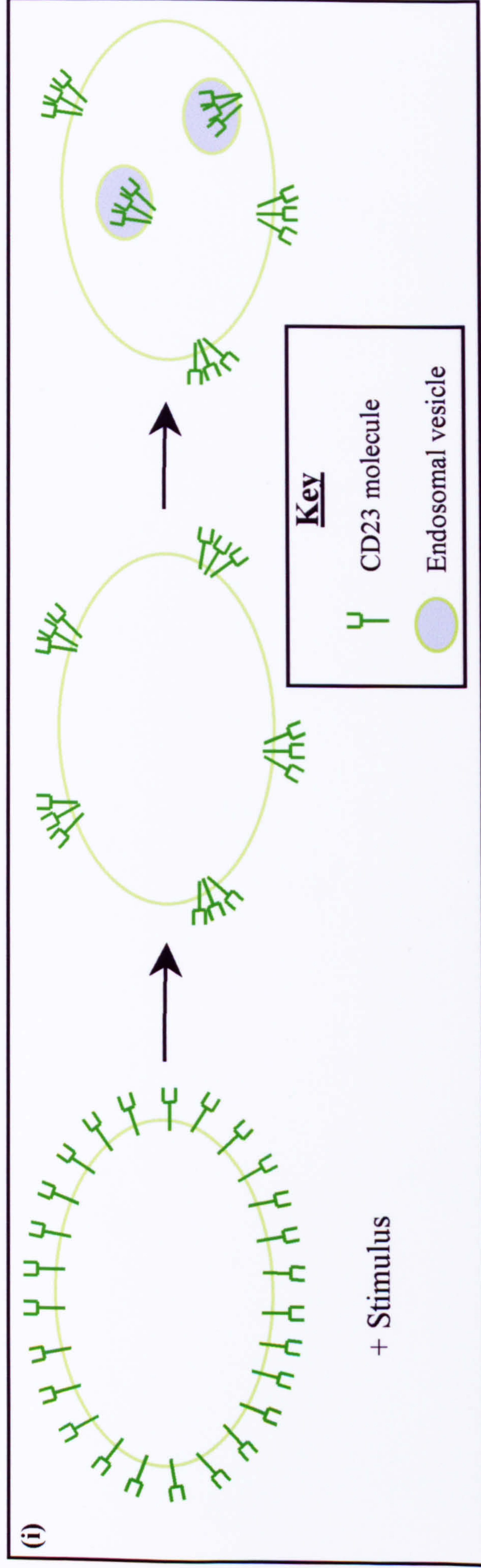
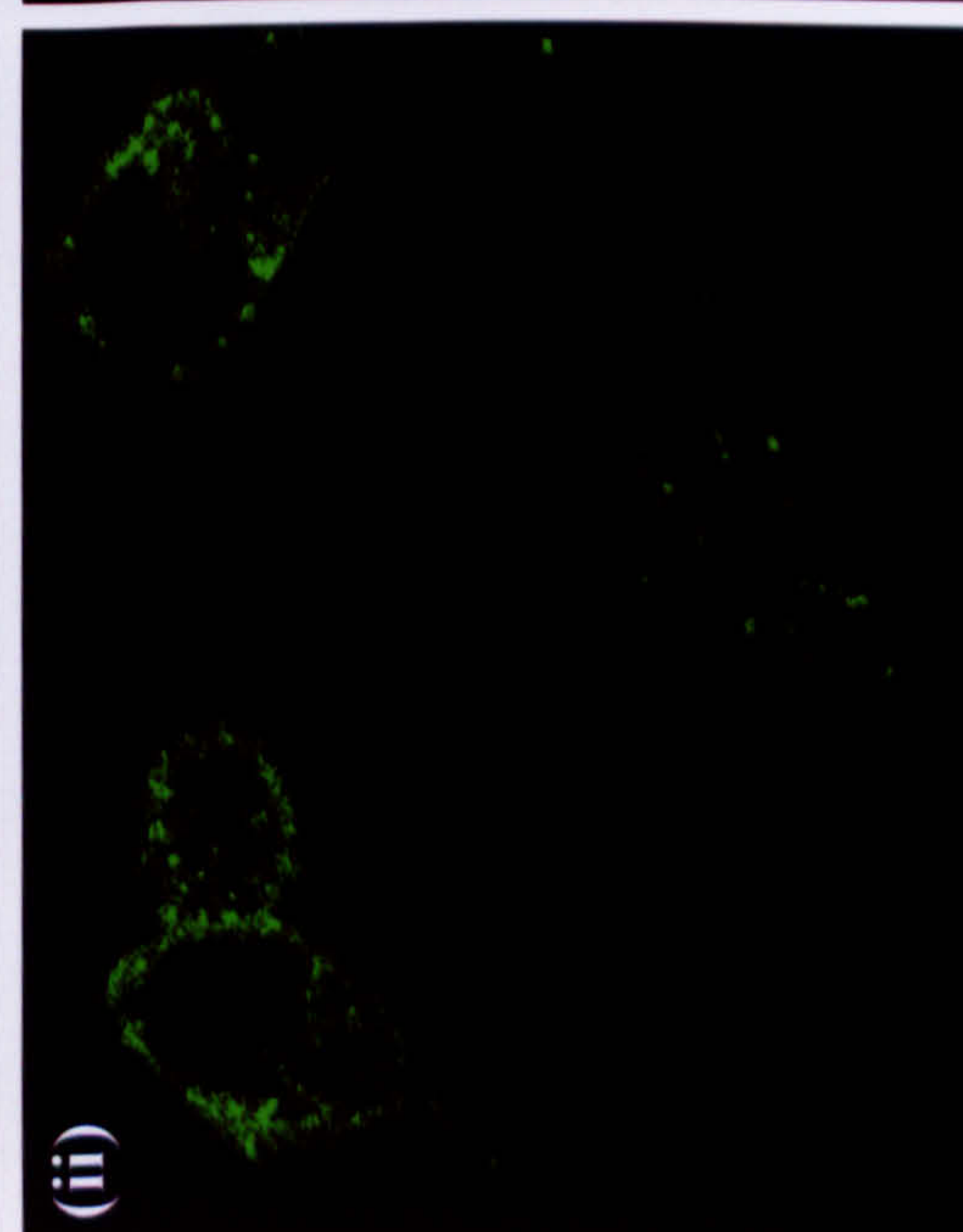
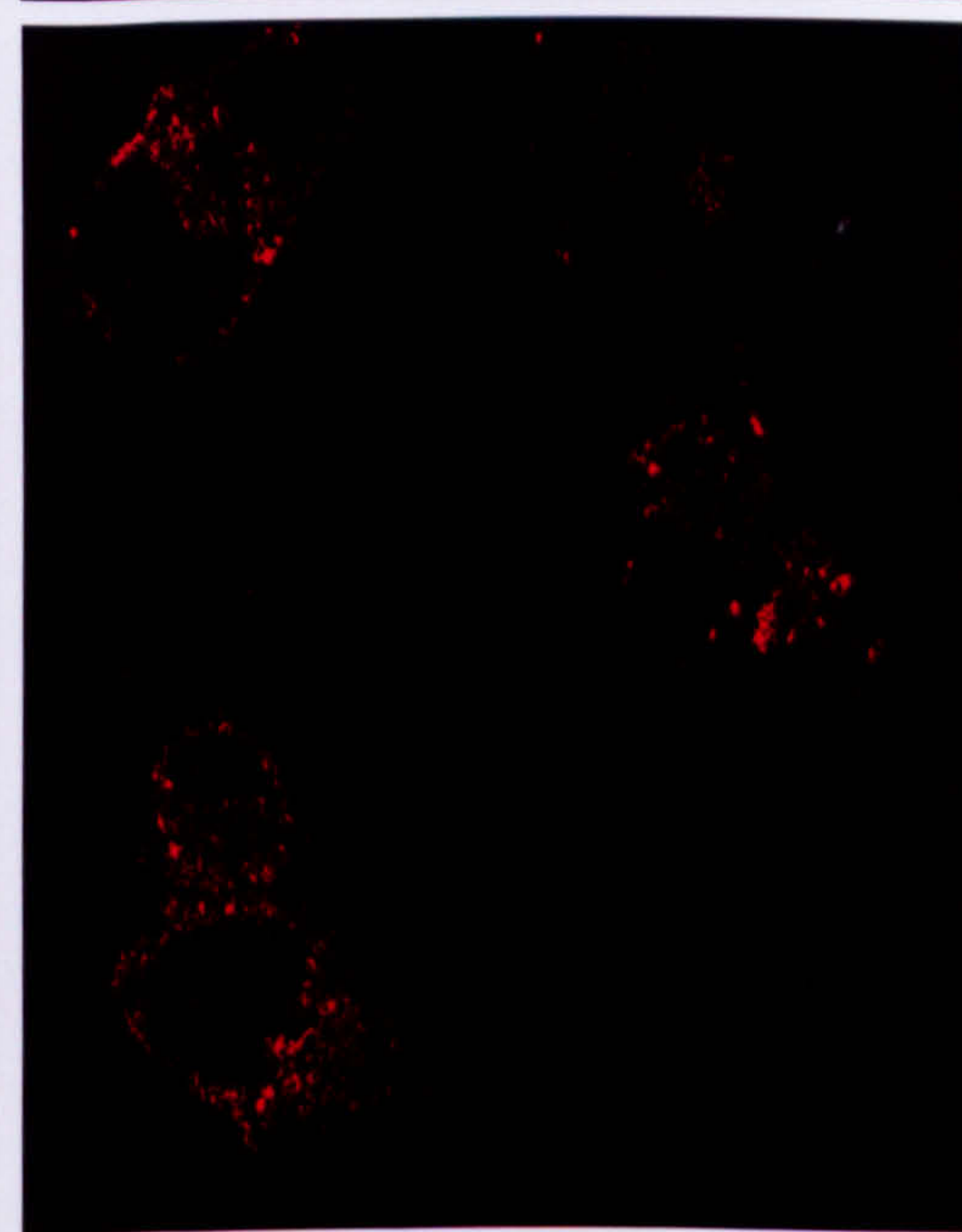
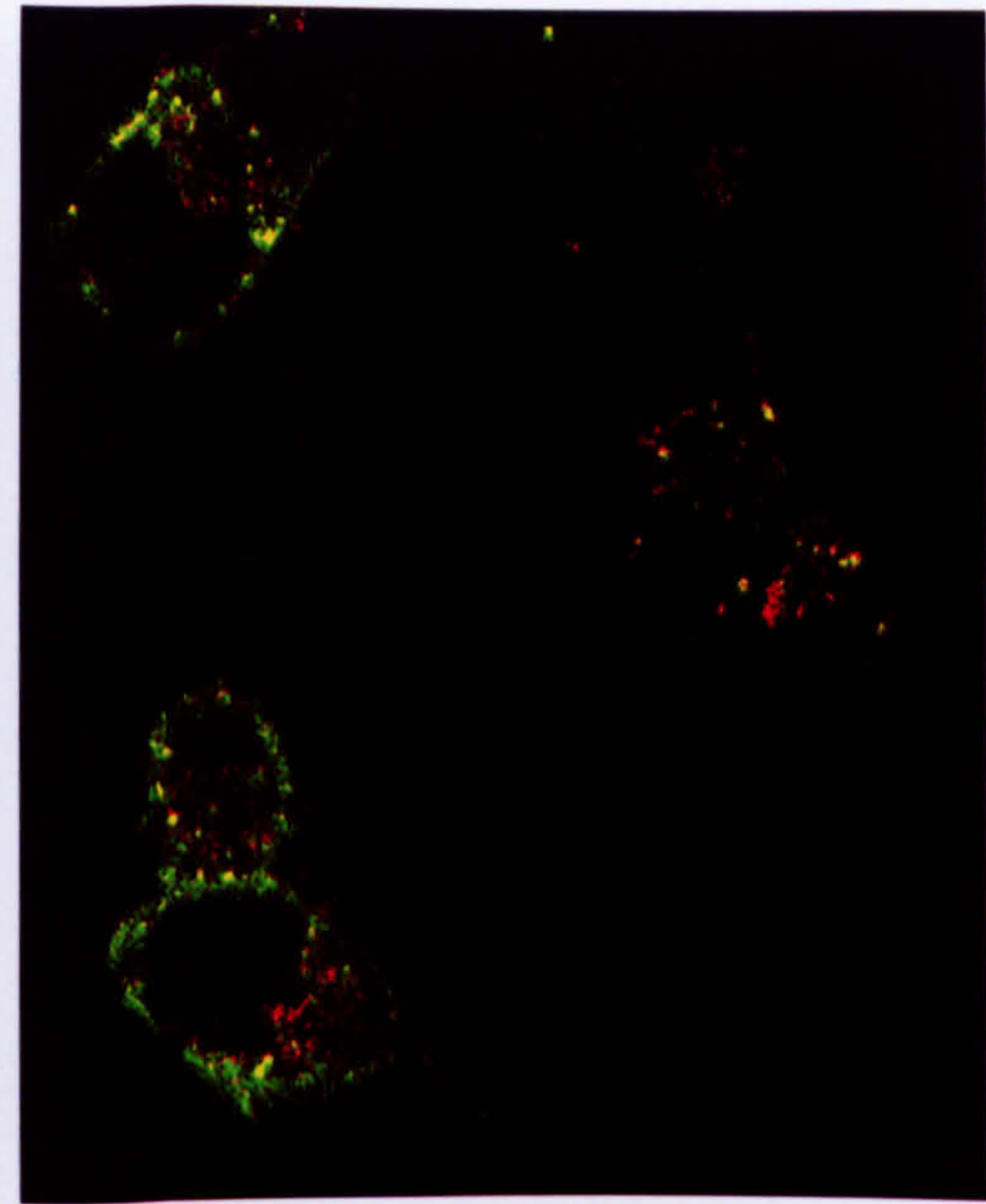
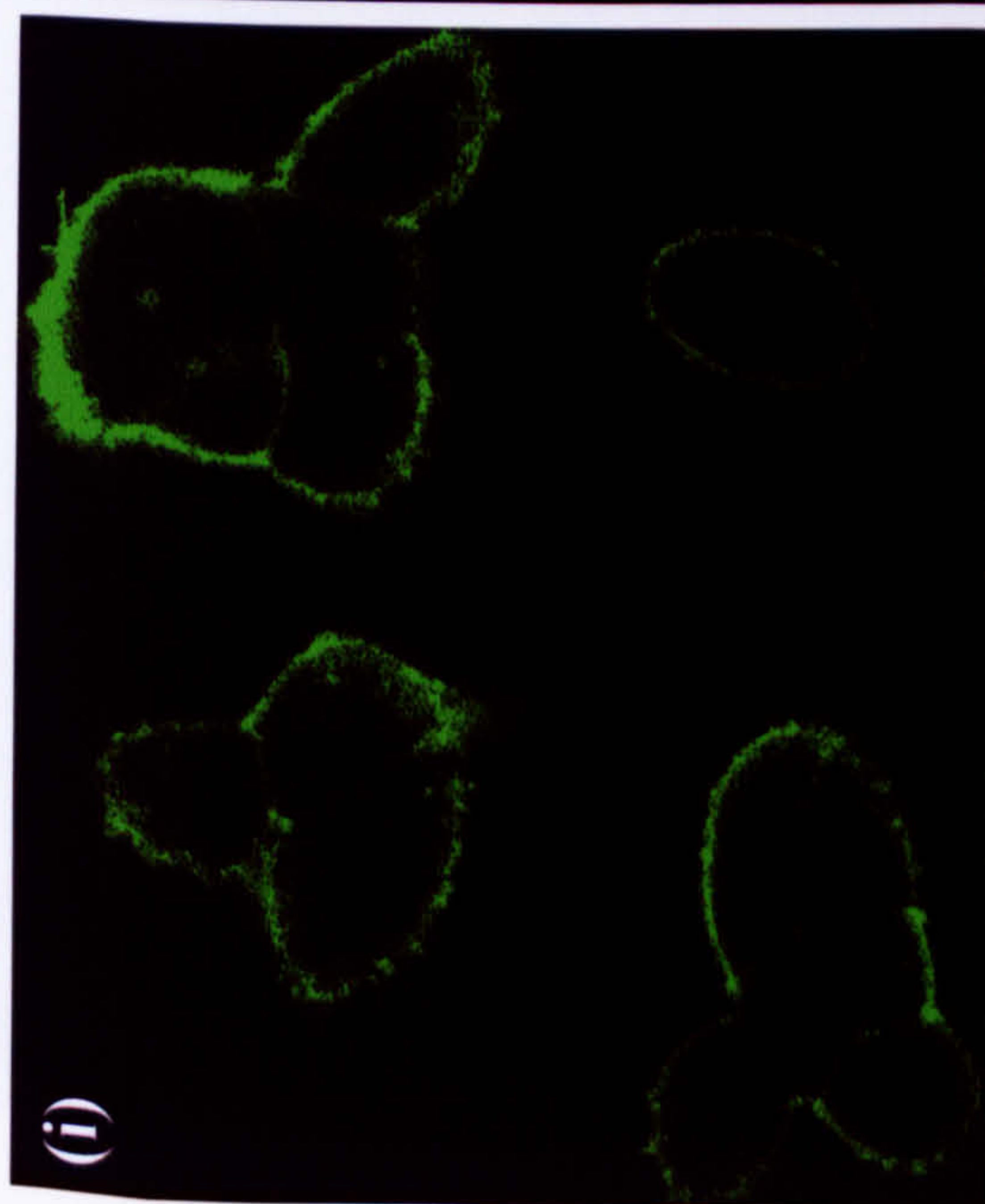
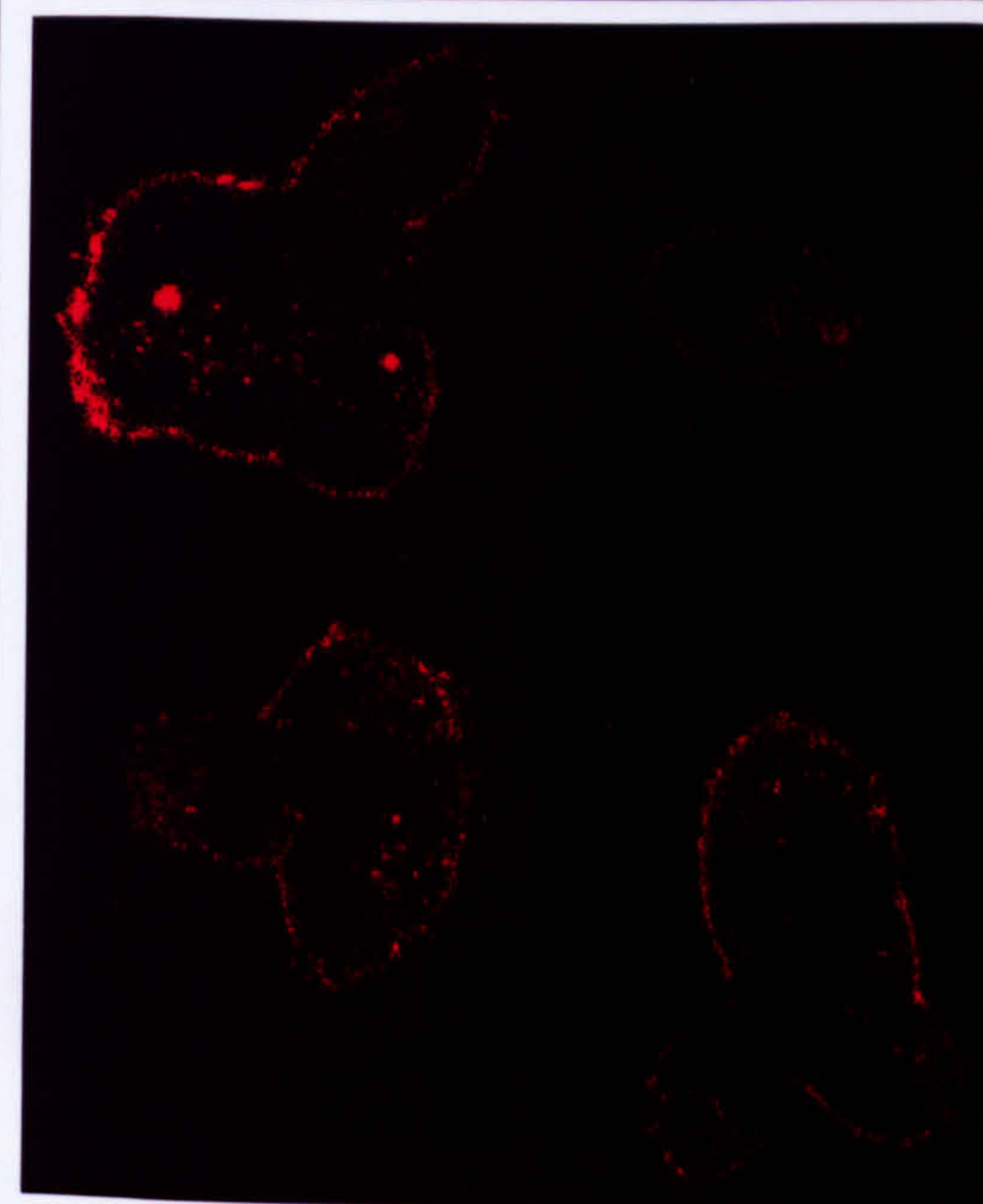
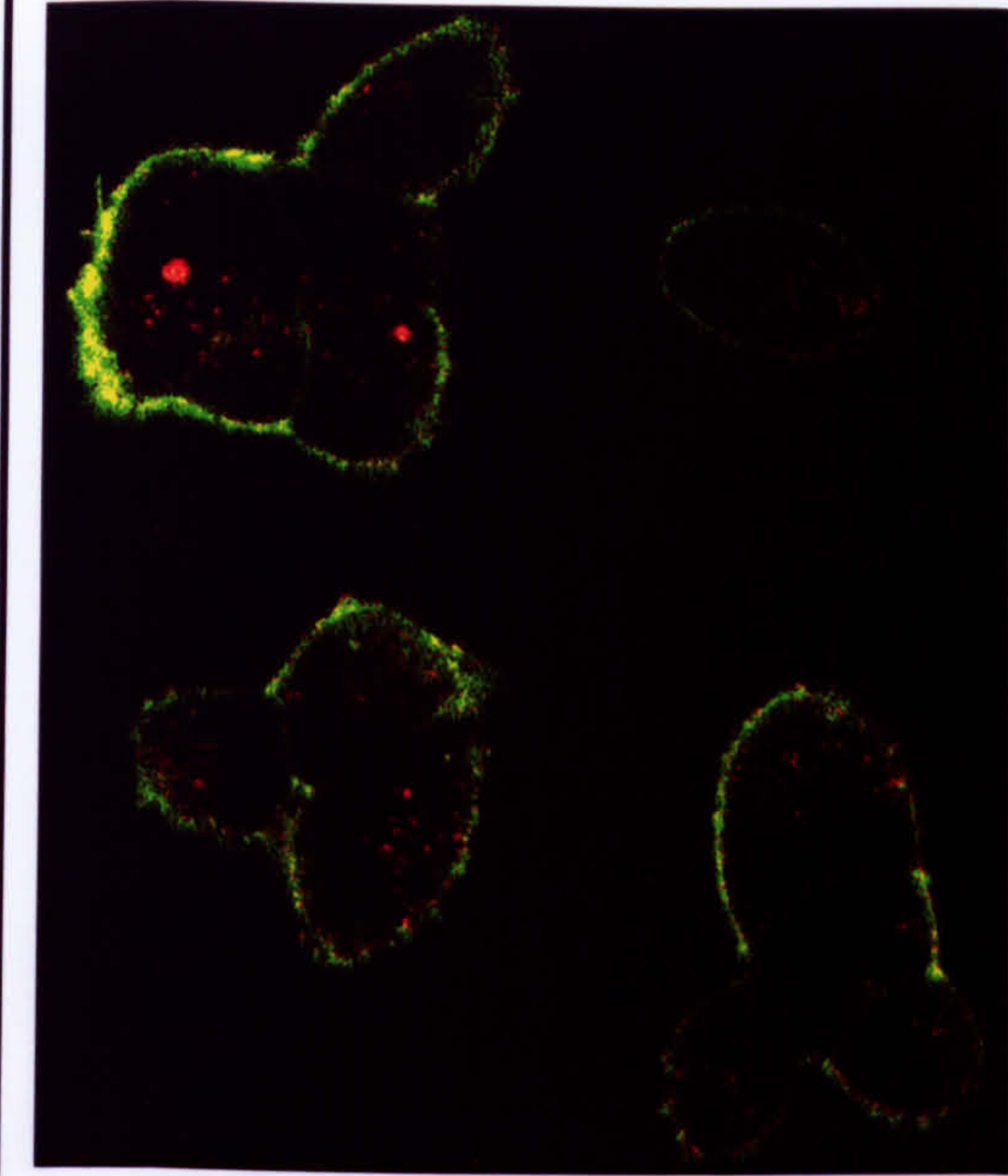




### **FIGURE 3.7 THE CD23A ISOFORM CO-LOCALISES WITH TRANSFERRIN-MODIFIED TEXAS RED (Tf-TxR) IN HEK 293 CELLS**

Coverslips bearing G418-resistant HEK 293 cells expressing CD23a or GFP-CD23a were pre-incubated with 20µg Tf-TxR prior to confocal analysis. The wild type CD23a proteins were visualised after the addition of FITC-anti-CD23 antibody. The GFP-CD23a fusion proteins were exposed to no stimulus, 1µg NIP-specific IgE or to 1µg NIP-specific IgE followed by the addition of 1µg NIP<sub>10</sub>-BSA and examined by confocal microscopy over a 45 minute period. The pictures illustrate the results for wild type CD23a at a (i) zero and (ii) 20 minute time point and GFP-CD23a in the (iii) basal, (iv) loaded and (v) cross-linked states respectively. Co-localisation was observed in the wild type situation after the addition of FITC-anti-CD23 antibody. GFP-CD23 fusion proteins were also found to co-localise with Tf-TxR, but only after being “cross-linked” with antigen.





Merged

Tf-TxR

FITC

(i)

(ii)



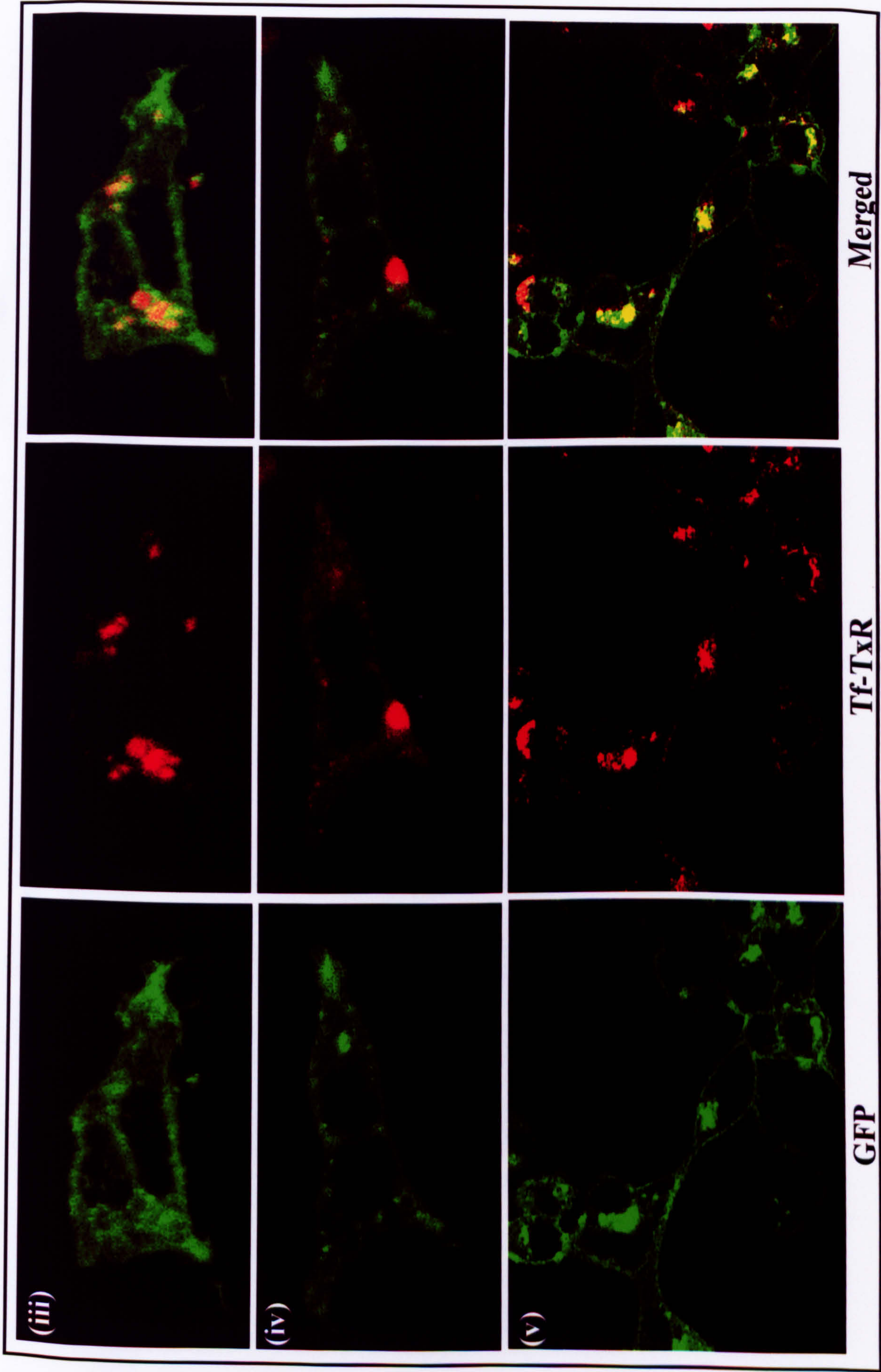
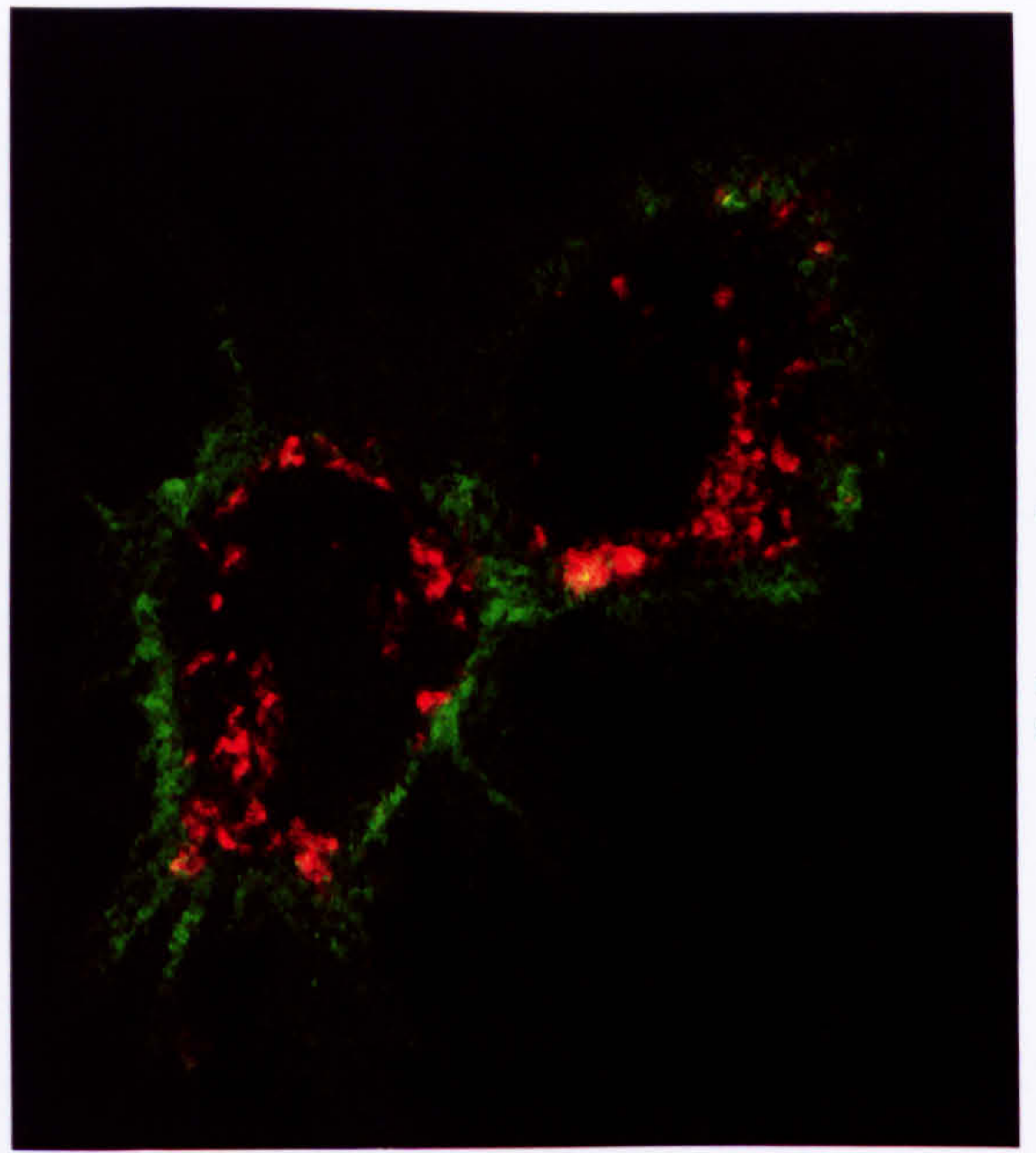
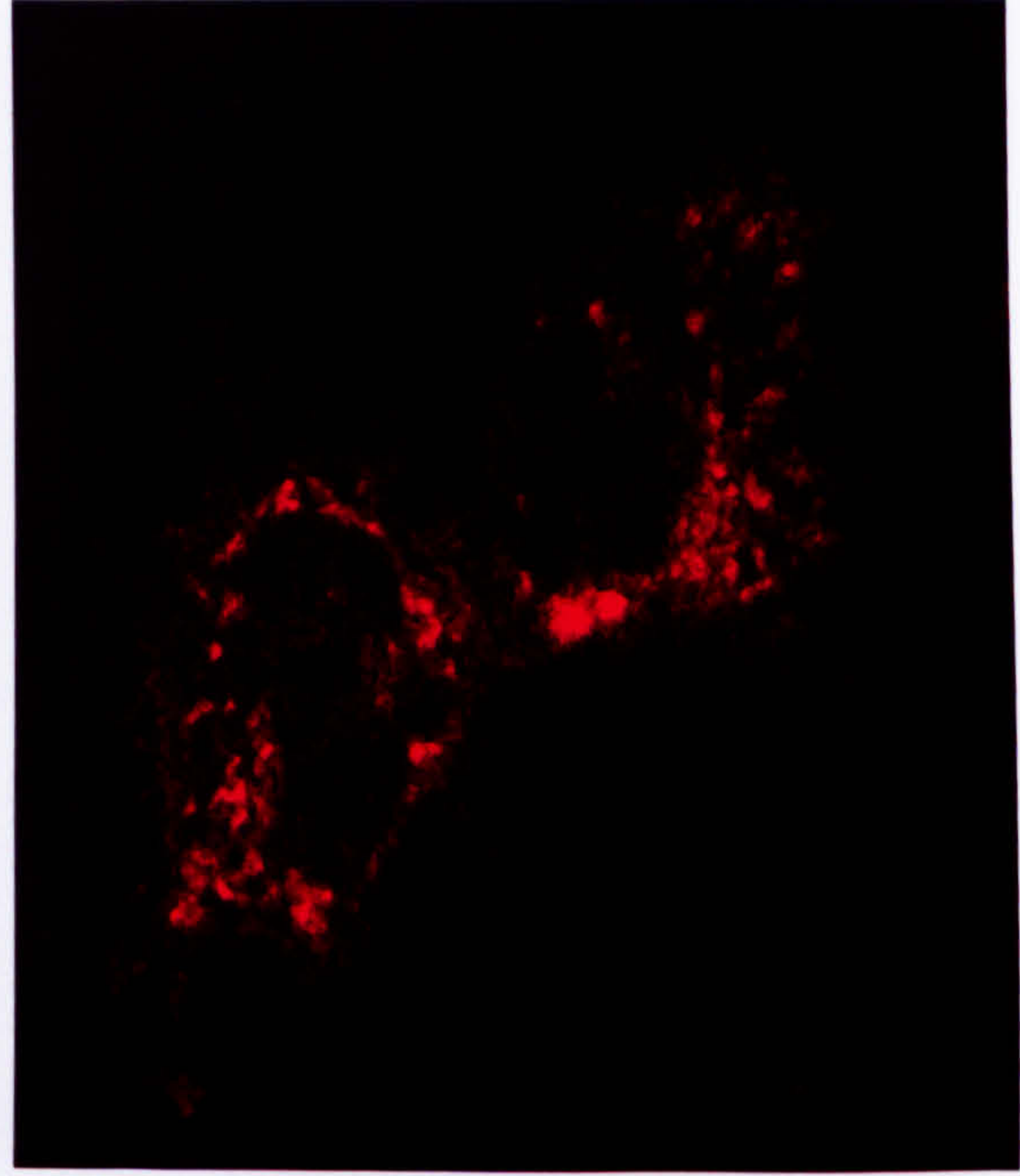
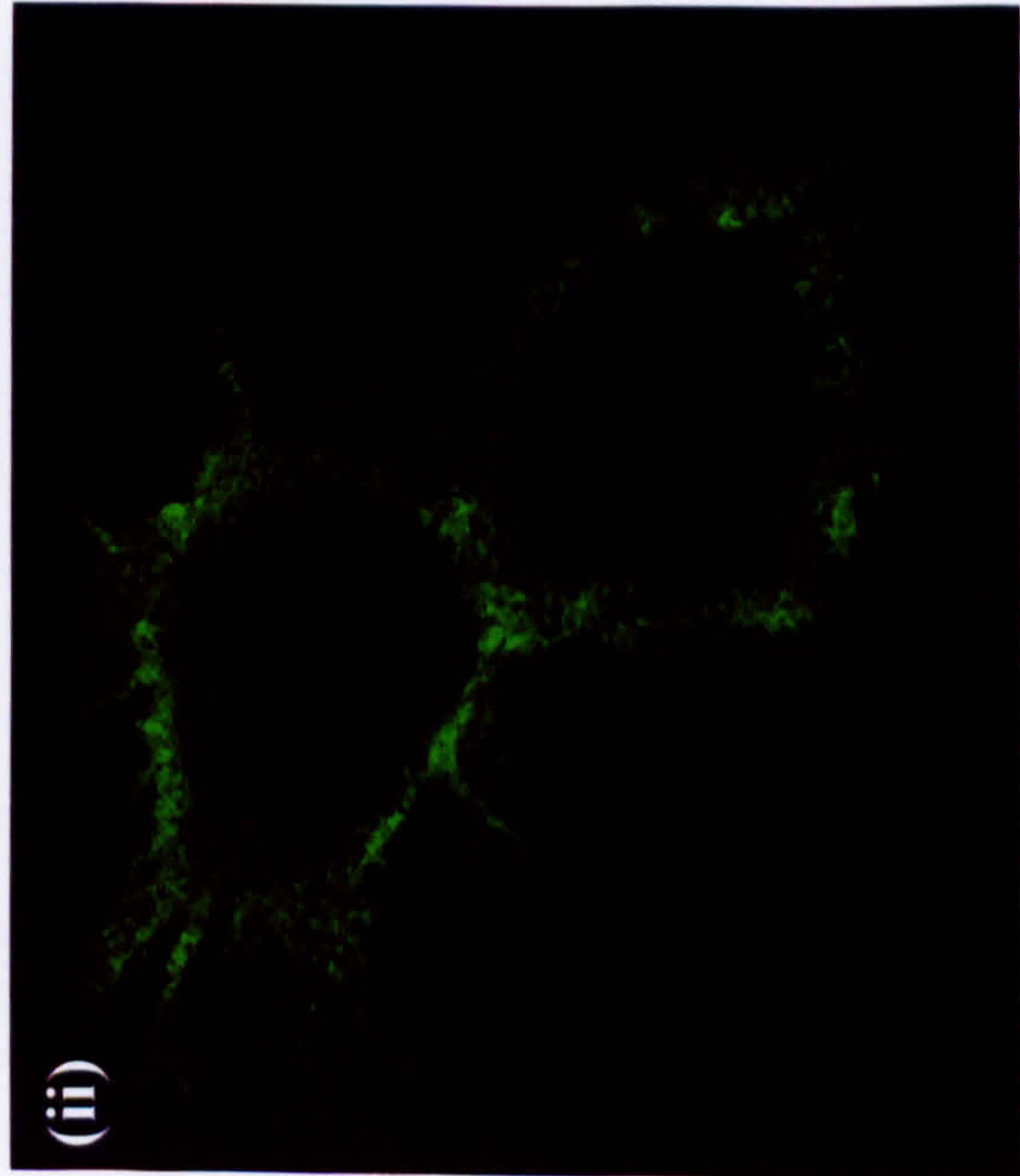
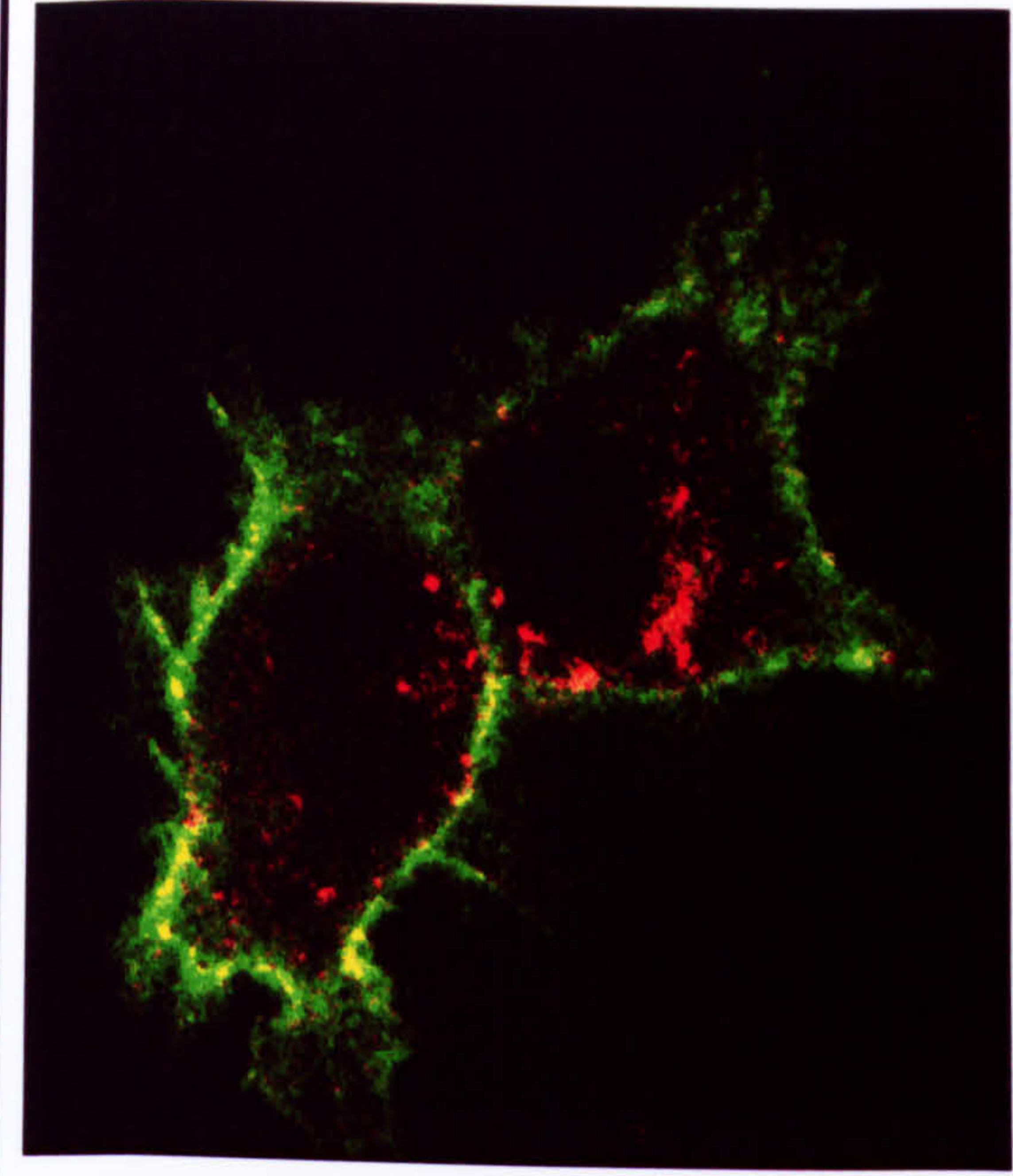
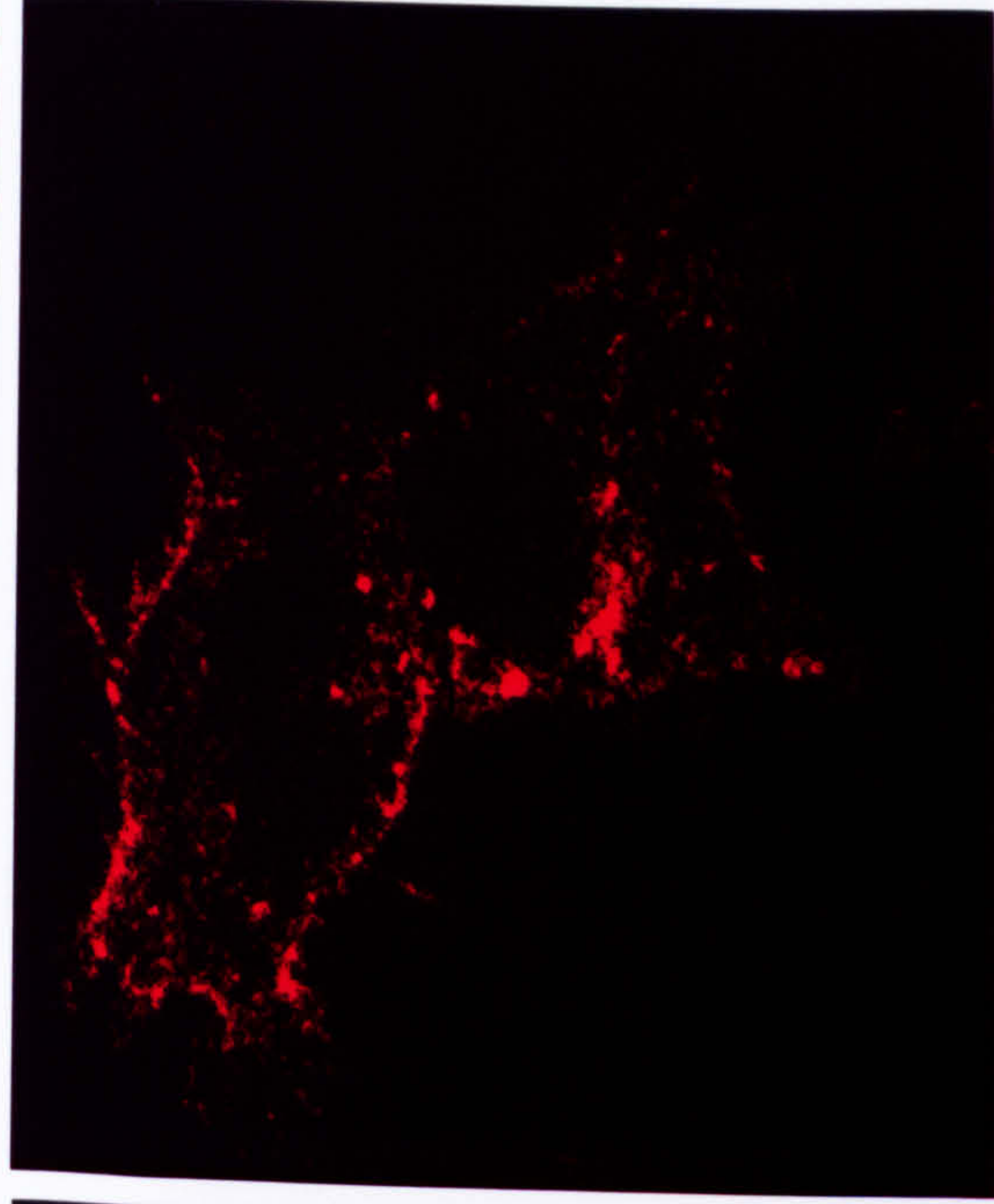
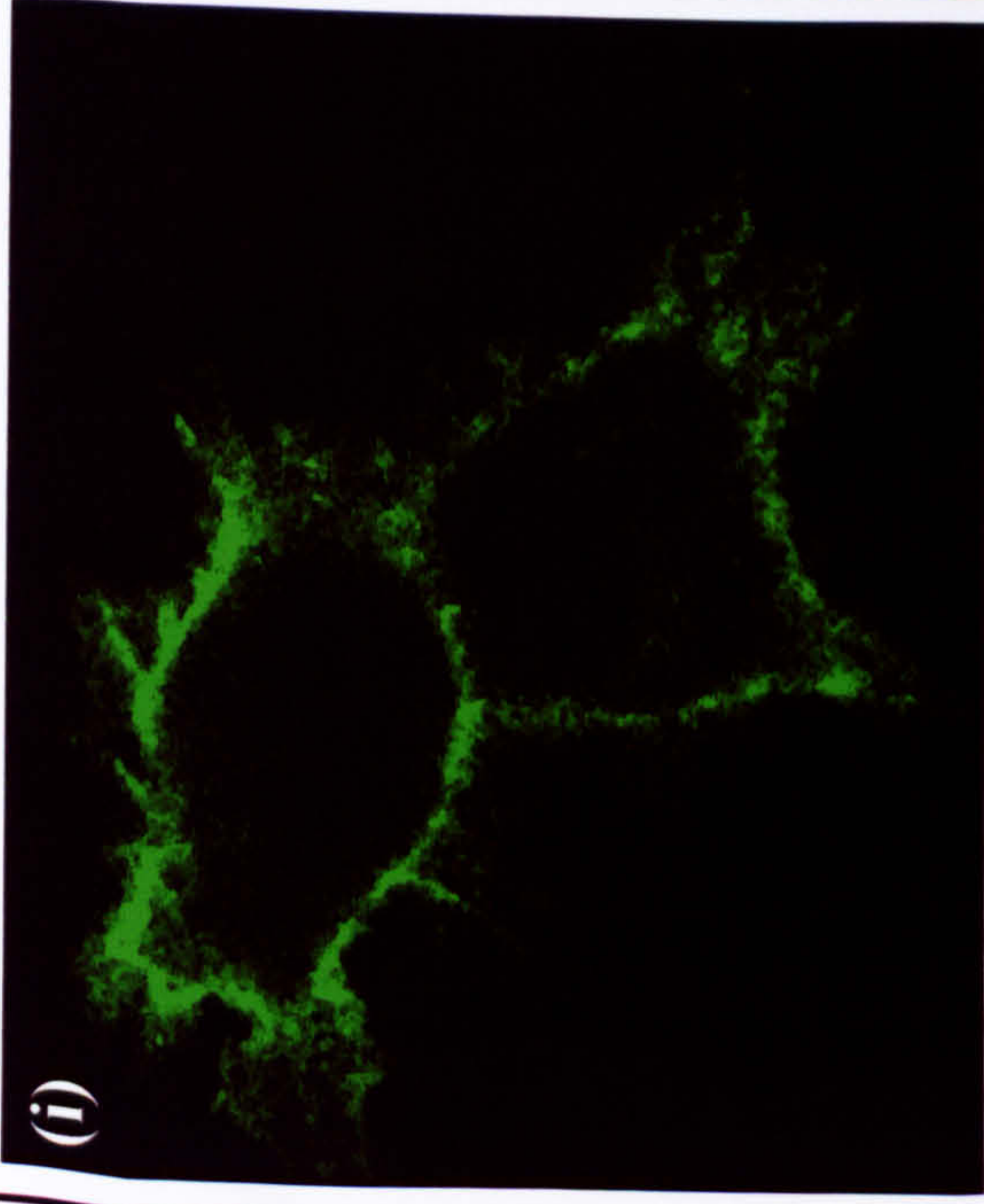




### **FIGURE 3.8 THE CD23B ISOFORM DOES NOT CO-LOCALISE WITH TRANSFERRIN-MODIFIED TEXAS RED (Tf-TxR) IN HEK 293 CELLS**

Coverslips bearing G418-resistant HEK 293 cells expressing CD23b or GFP-CD23b were pre-incubated with 20µg Tf-TxR prior to confocal analysis. The wild type CD23b proteins were visualised after the addition of FITC-anti-CD23 antibody. The GFP-CD23b fusion proteins were exposed to no stimulus, 1µg NIP-specific IgE or to 1µg NIP-specific IgE followed by the addition of 1µg NIP<sub>10</sub>-BSA and examined by confocal microscopy over a 45 minute period. The pictures illustrate the results for wild type CD23b at a (i) zero and (ii) 20 minute time point and GFP-CD23b in the (iii) basal, (iv) loaded and (v) cross-linked states respectively. Co-localisation was not observed under any of these experimental conditions.





FITC

Tf-TxR

Merged



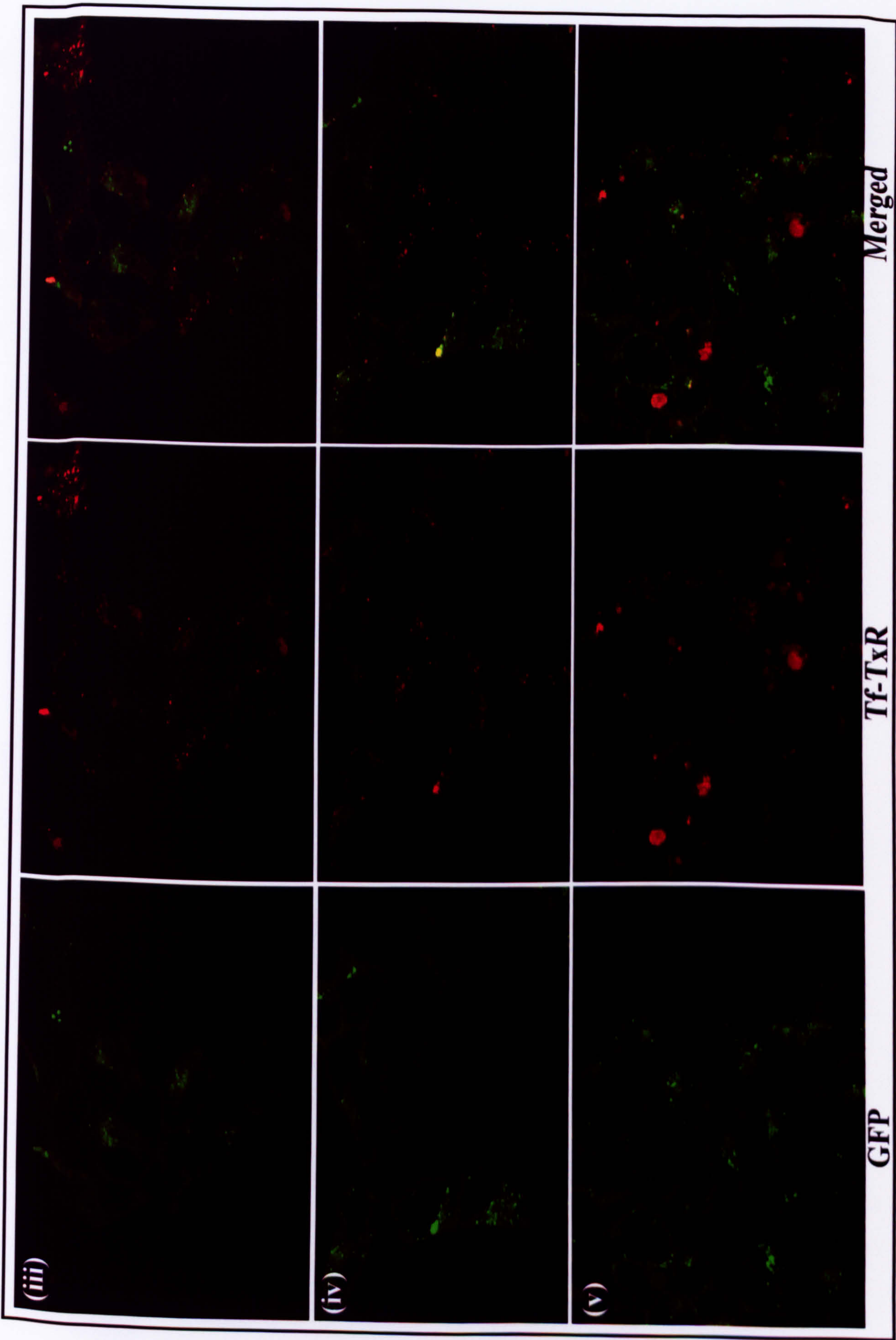
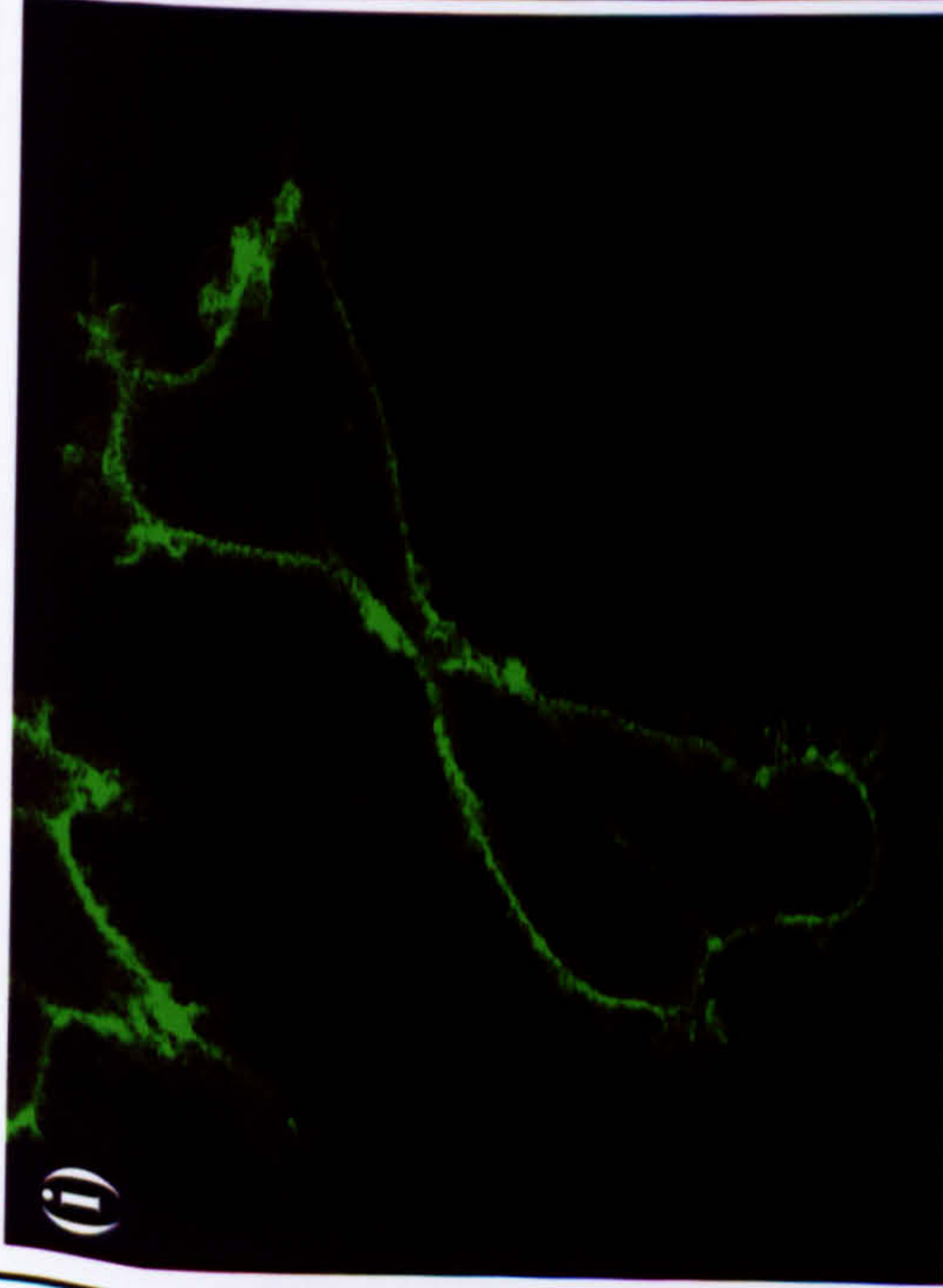




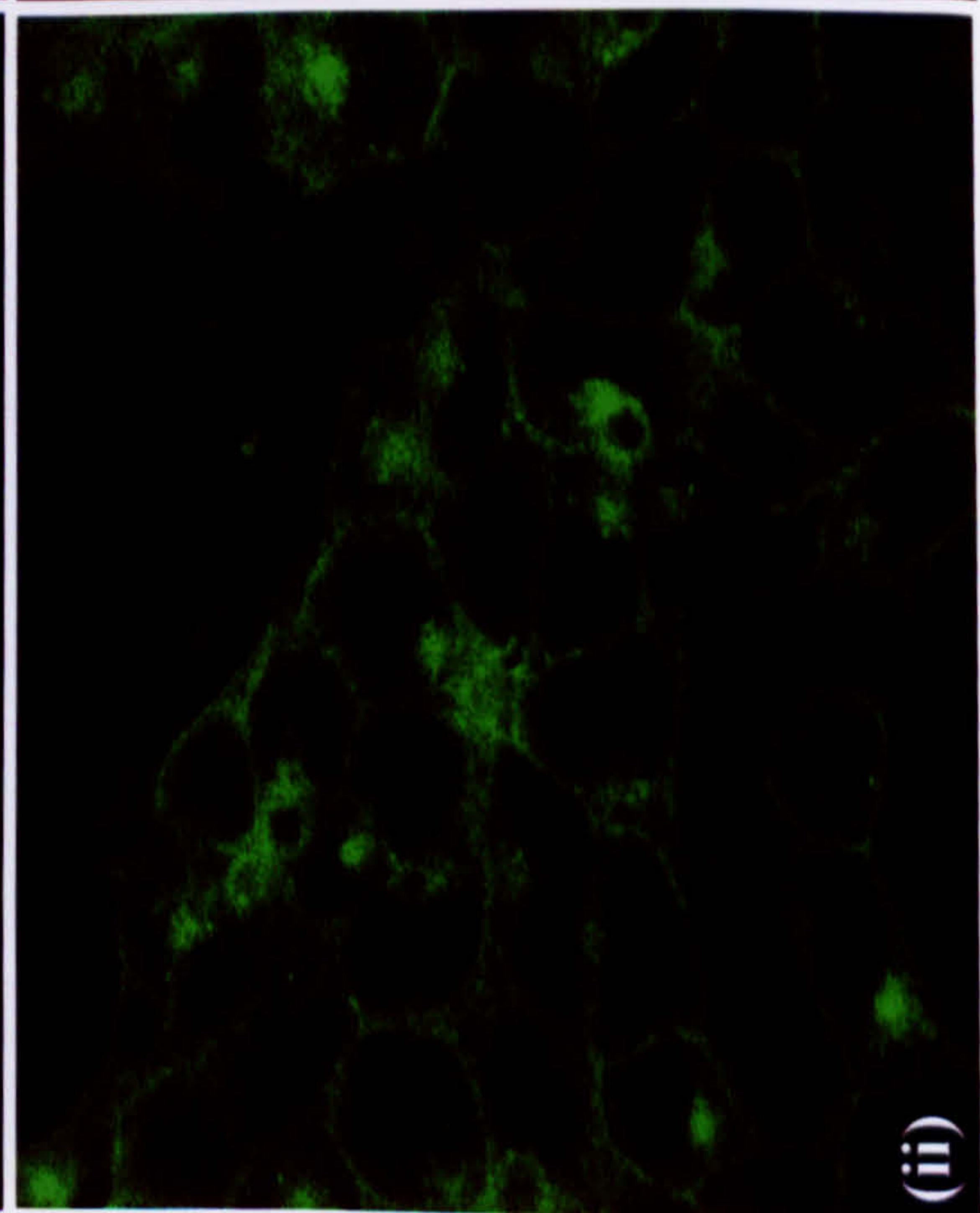
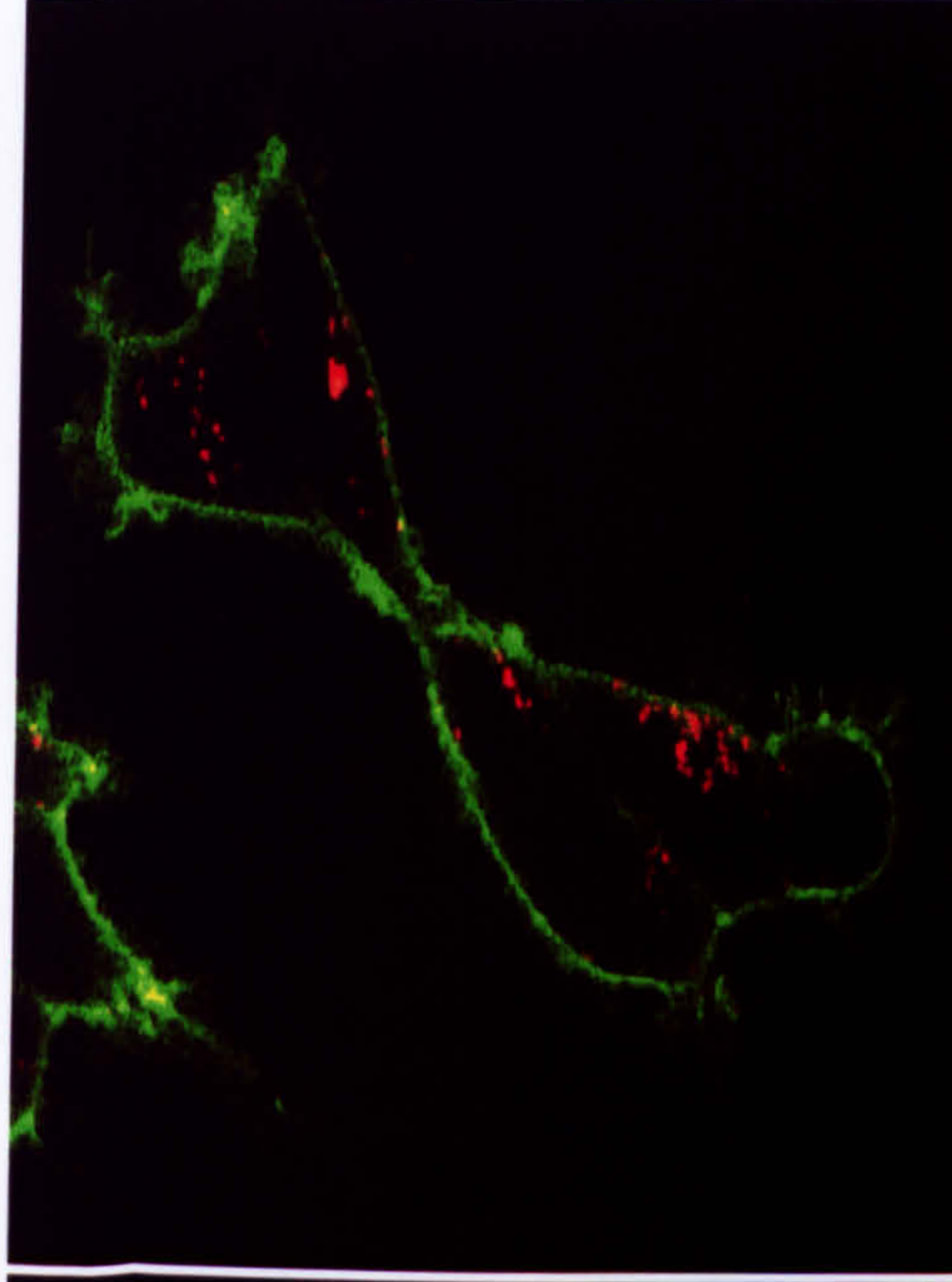
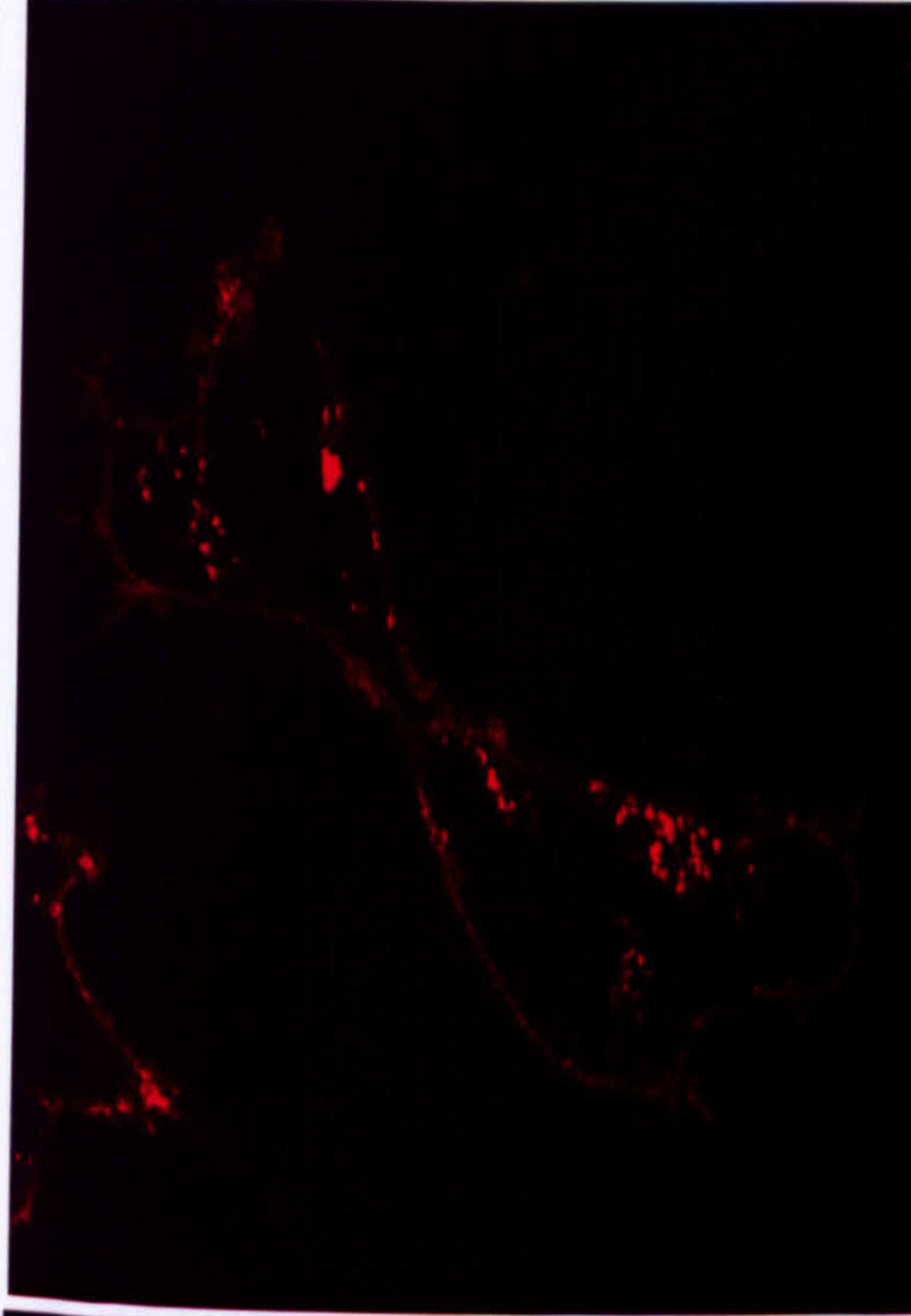
### **FIGURE 3.9 THE CD23A ISOFORM DOES NOT CO-LOCALISE WITH LYSOTracker DYE IN HEK 293 CELLS**

Coverslips bearing G418-resistant HEK 293 cells expressing CD23a or GFP-CD23a were pre-incubated with 50nM LysoTracker dye prior to confocal analysis. The wild type CD23a proteins were visualised after the addition of FITC-anti-CD23 antibody. The GFP-CD23a fusion proteins were exposed to no stimulus, 1µg NIP-specific IgE or to 1µg NIP-specific IgE followed by the addition of 1µg NIP<sub>10</sub>-BSA and examined by confocal microscopy over a 45 minute period. The pictures illustrate the results for (i) wild type CD23a and GFP-CD23a in the (ii) basal, (iii) loaded and (iv) cross-linked states respectively. Co-localisation was not observed under any of these experimental conditions.

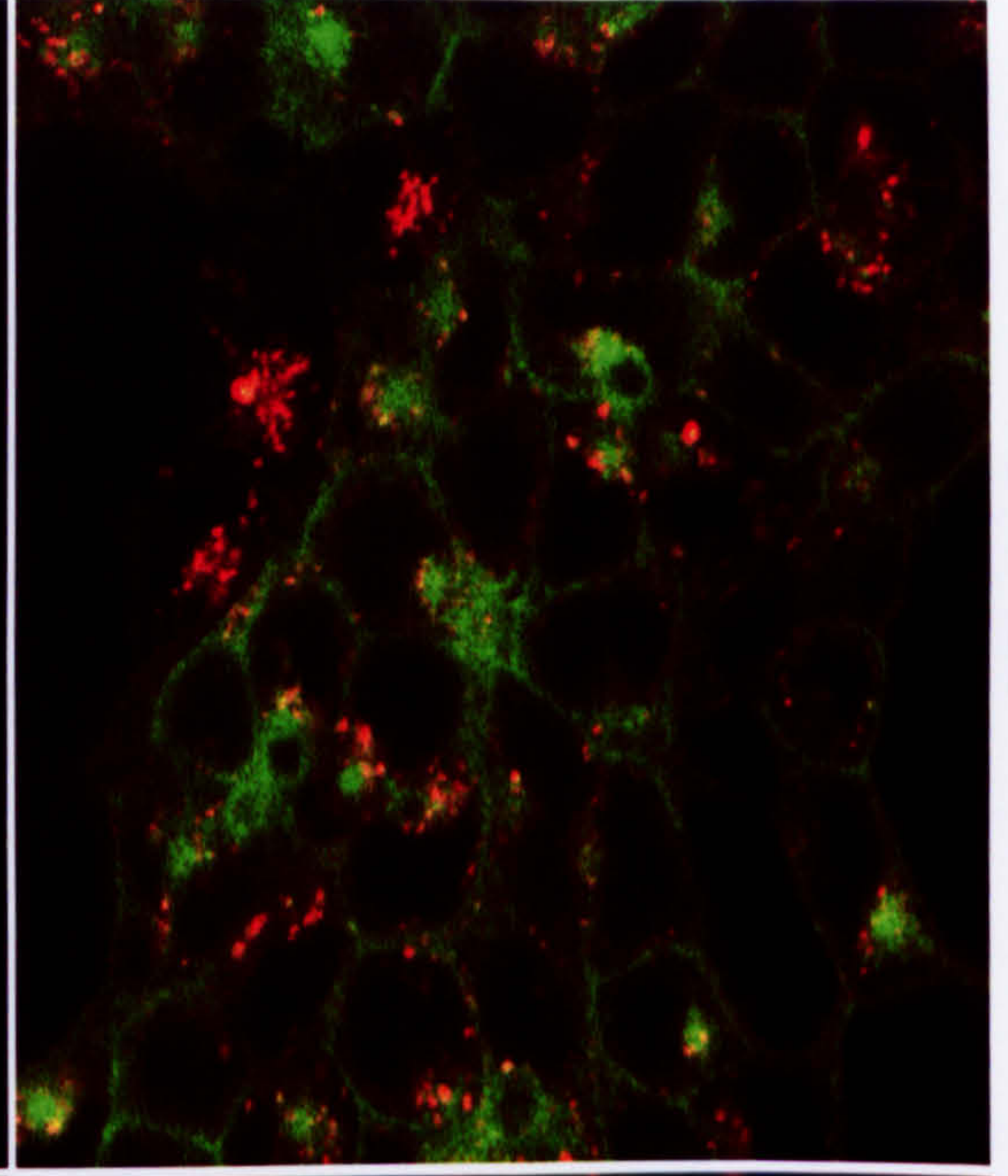
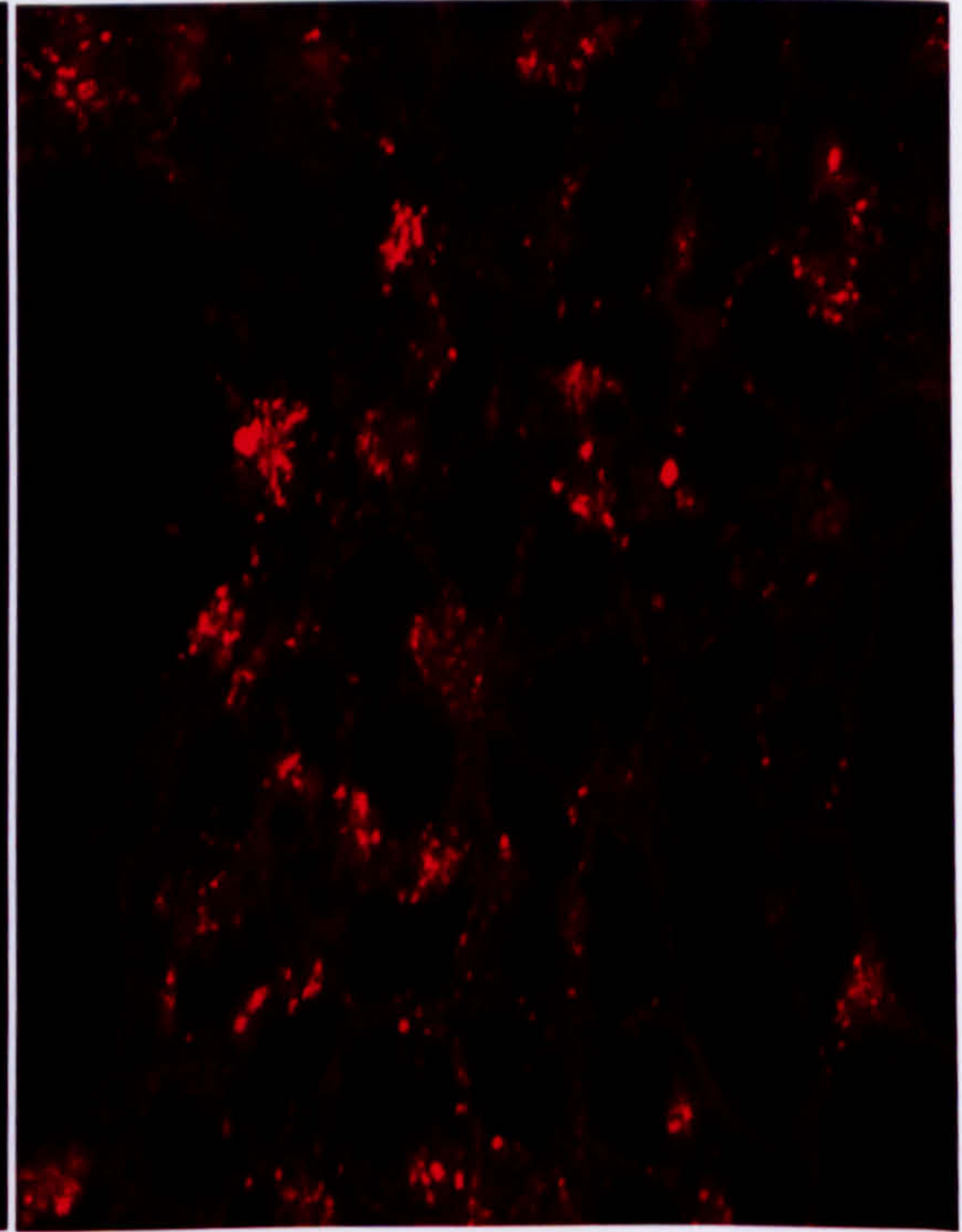




(i)



(ii)

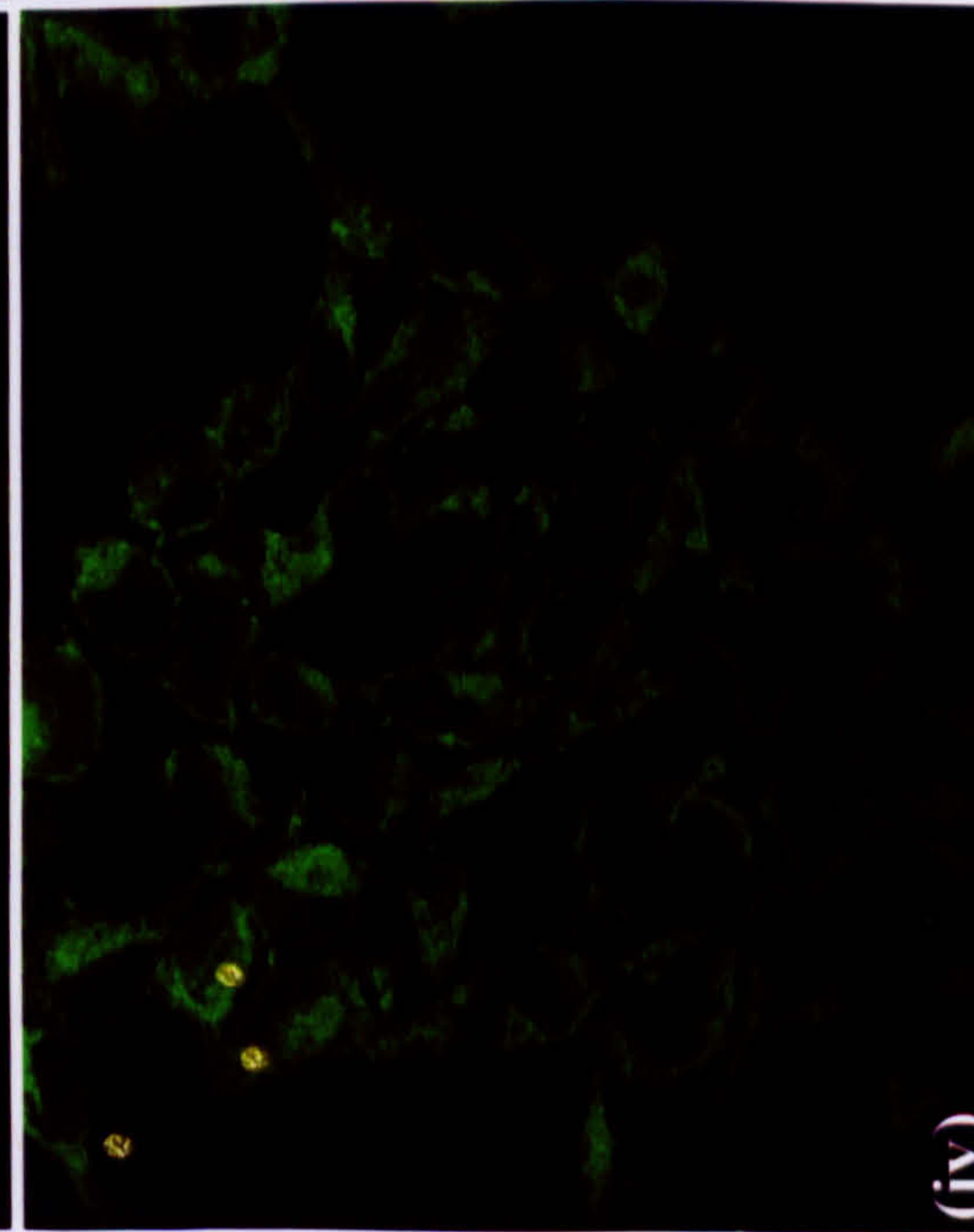
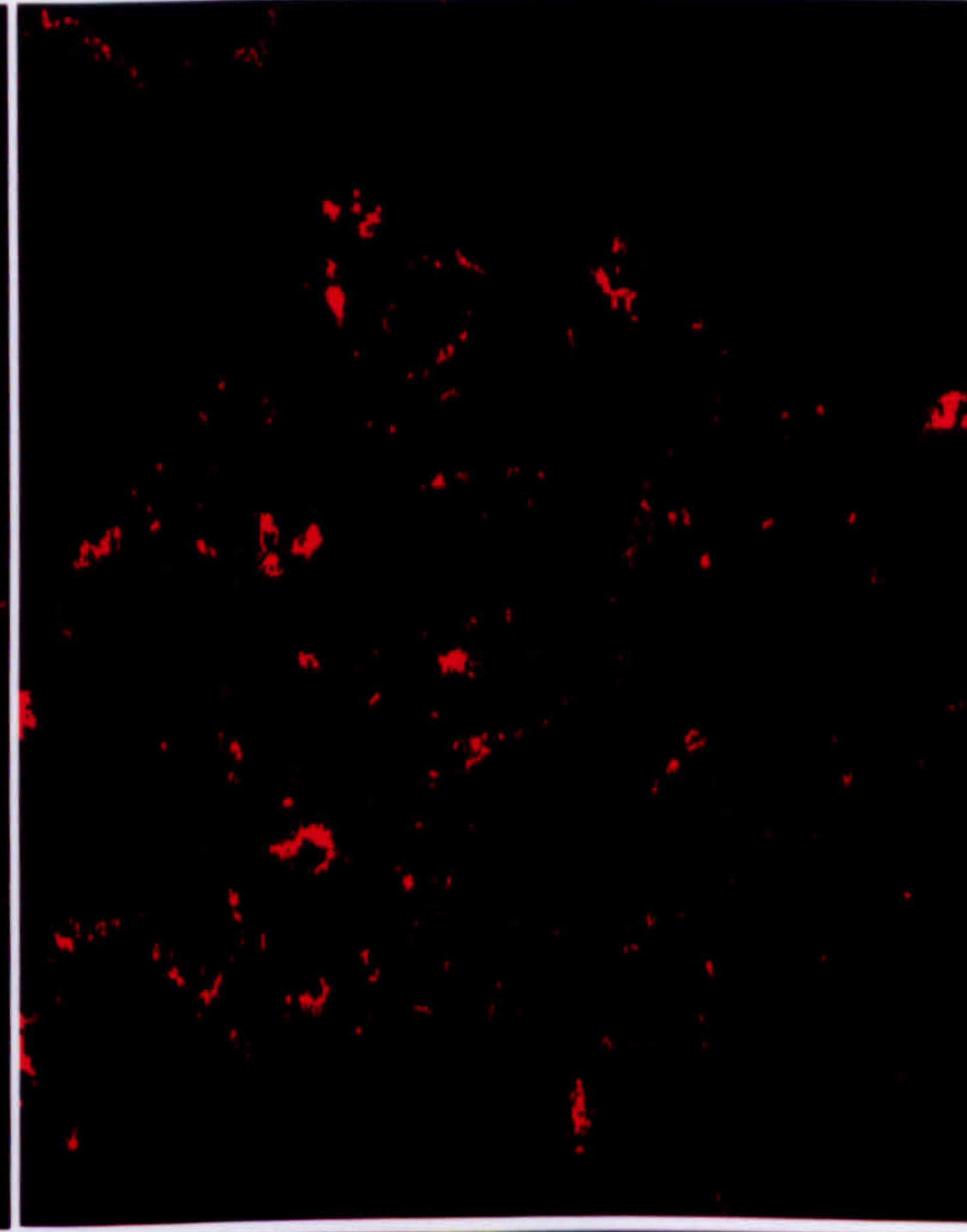
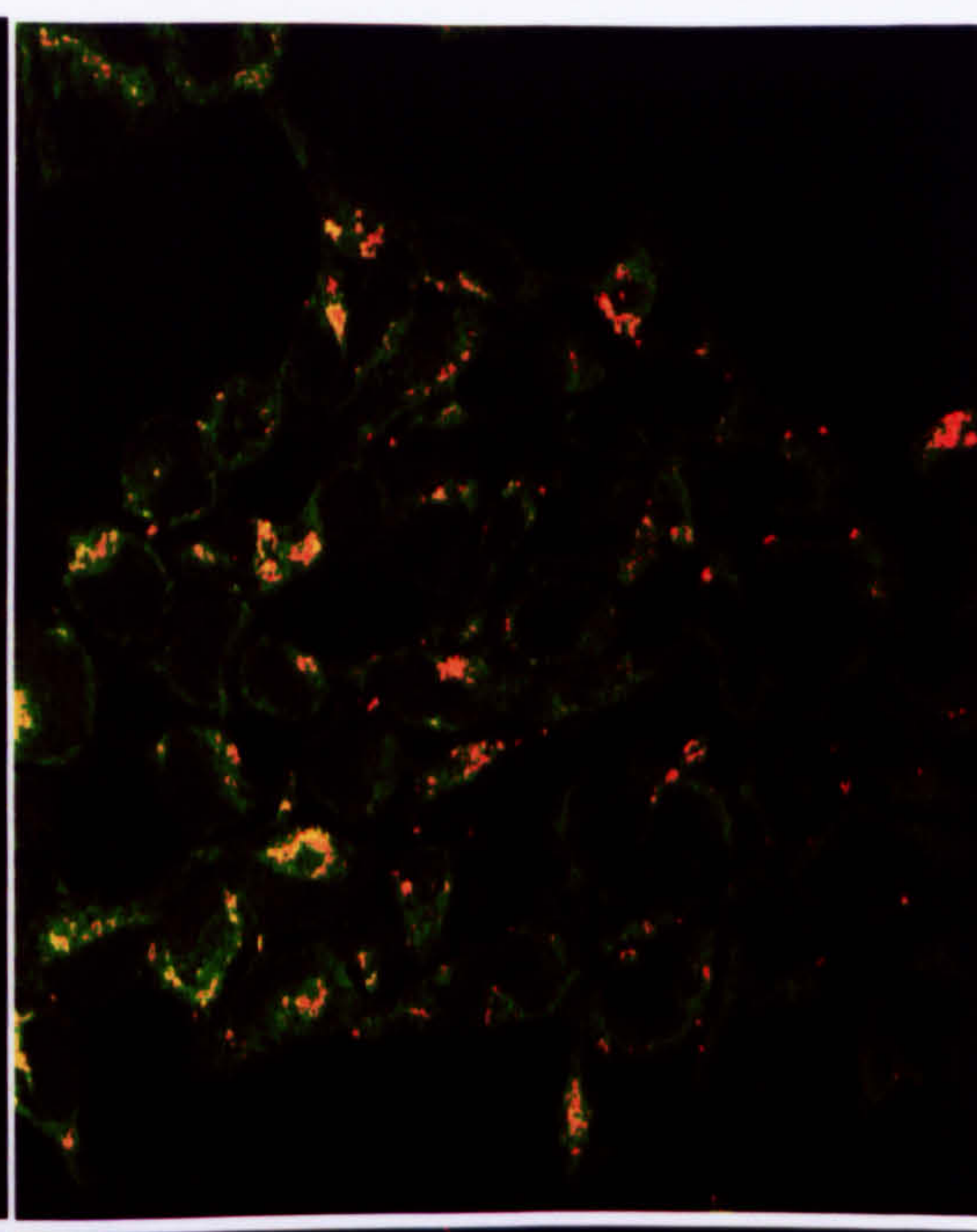
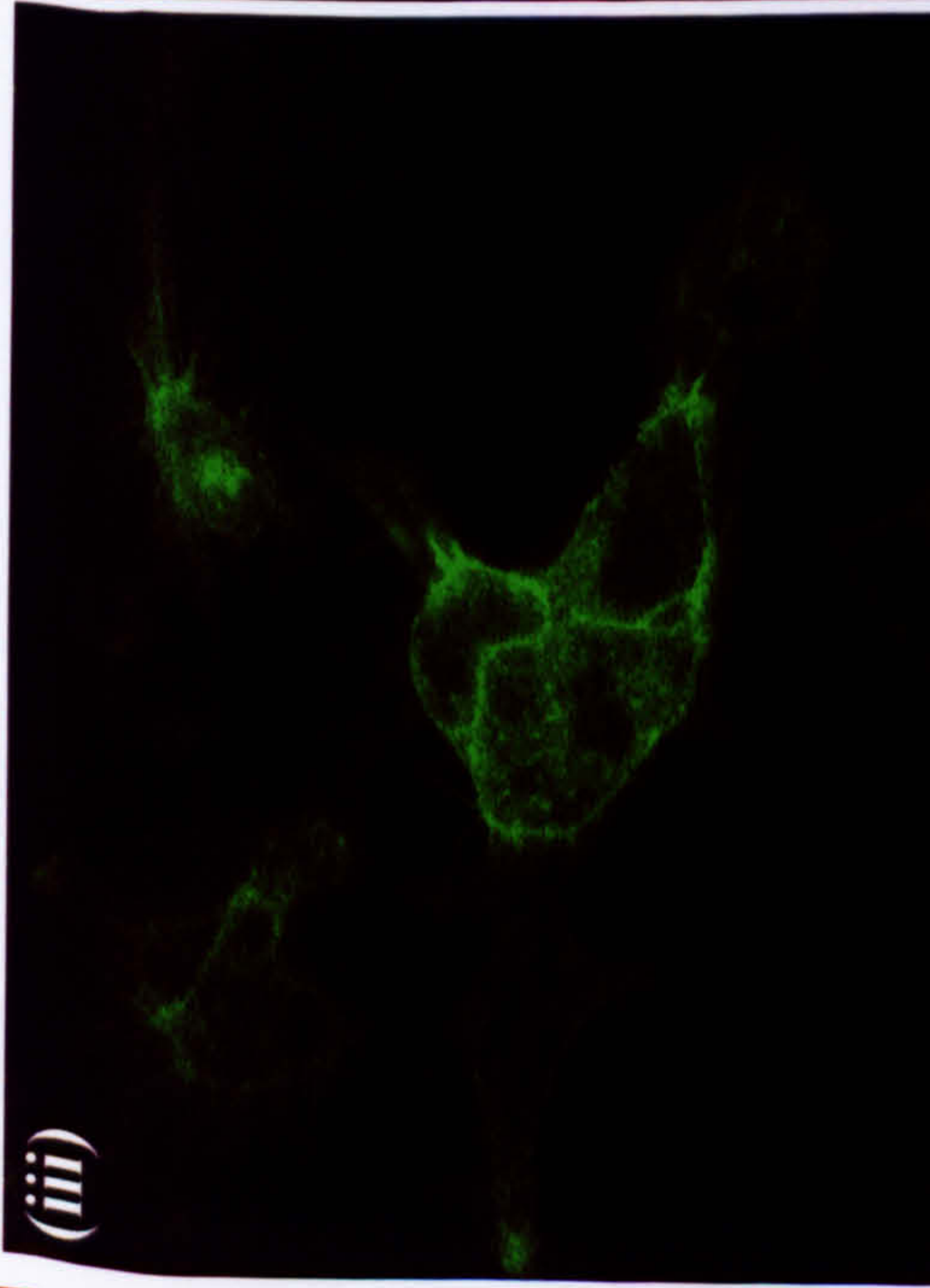
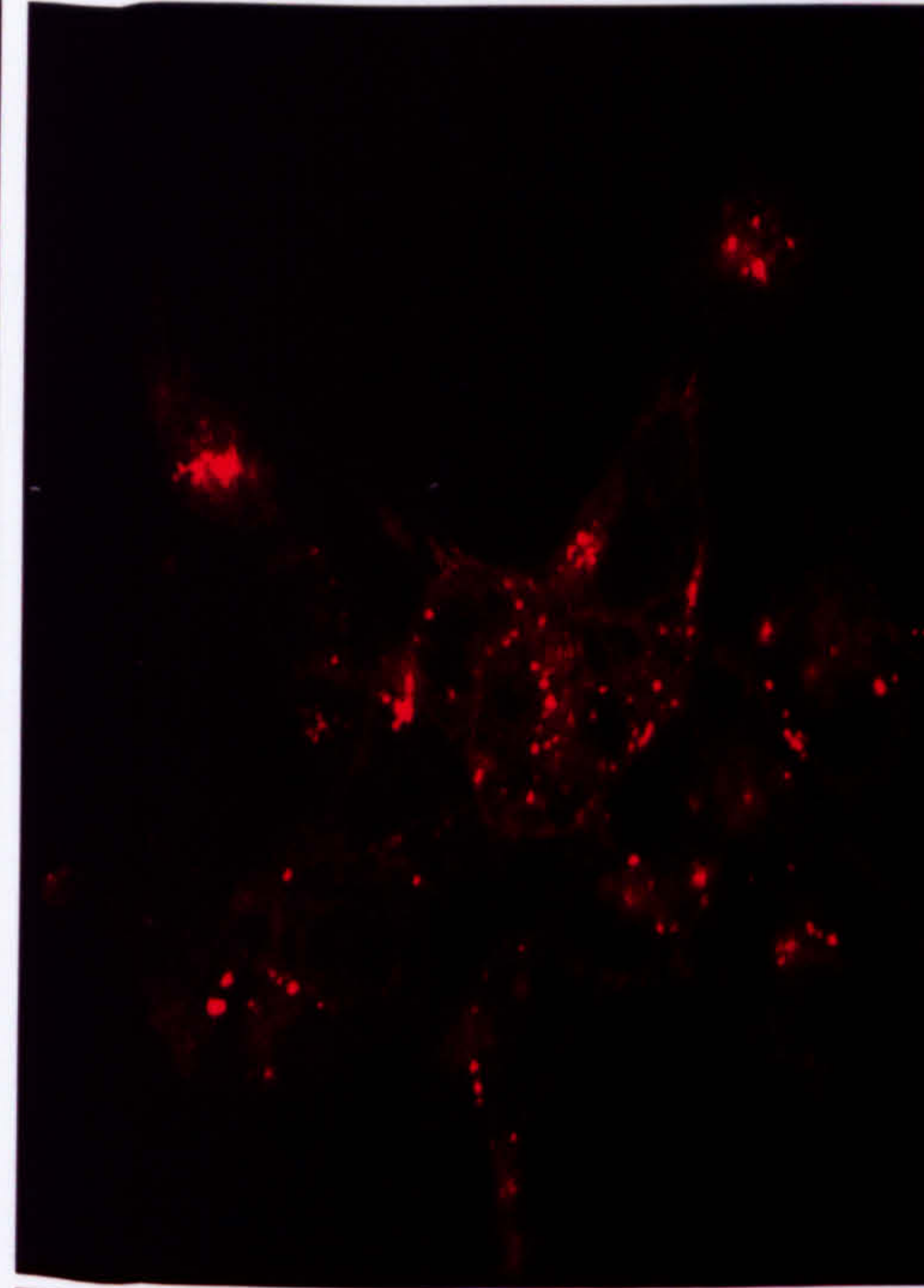
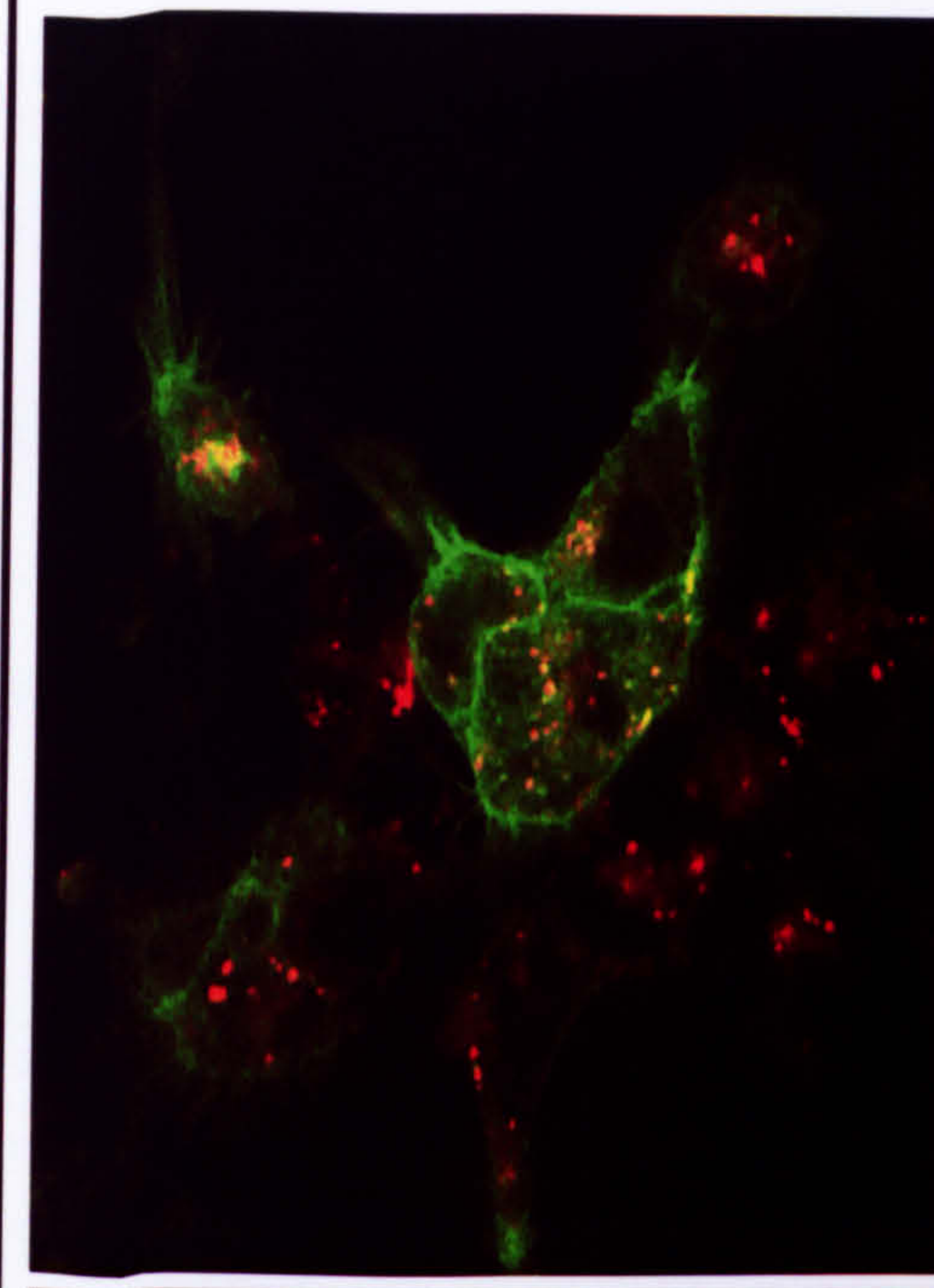


**FITC/GFP**

**LysoTracker**

**Merged**





**Merged**

**LysoTracker**

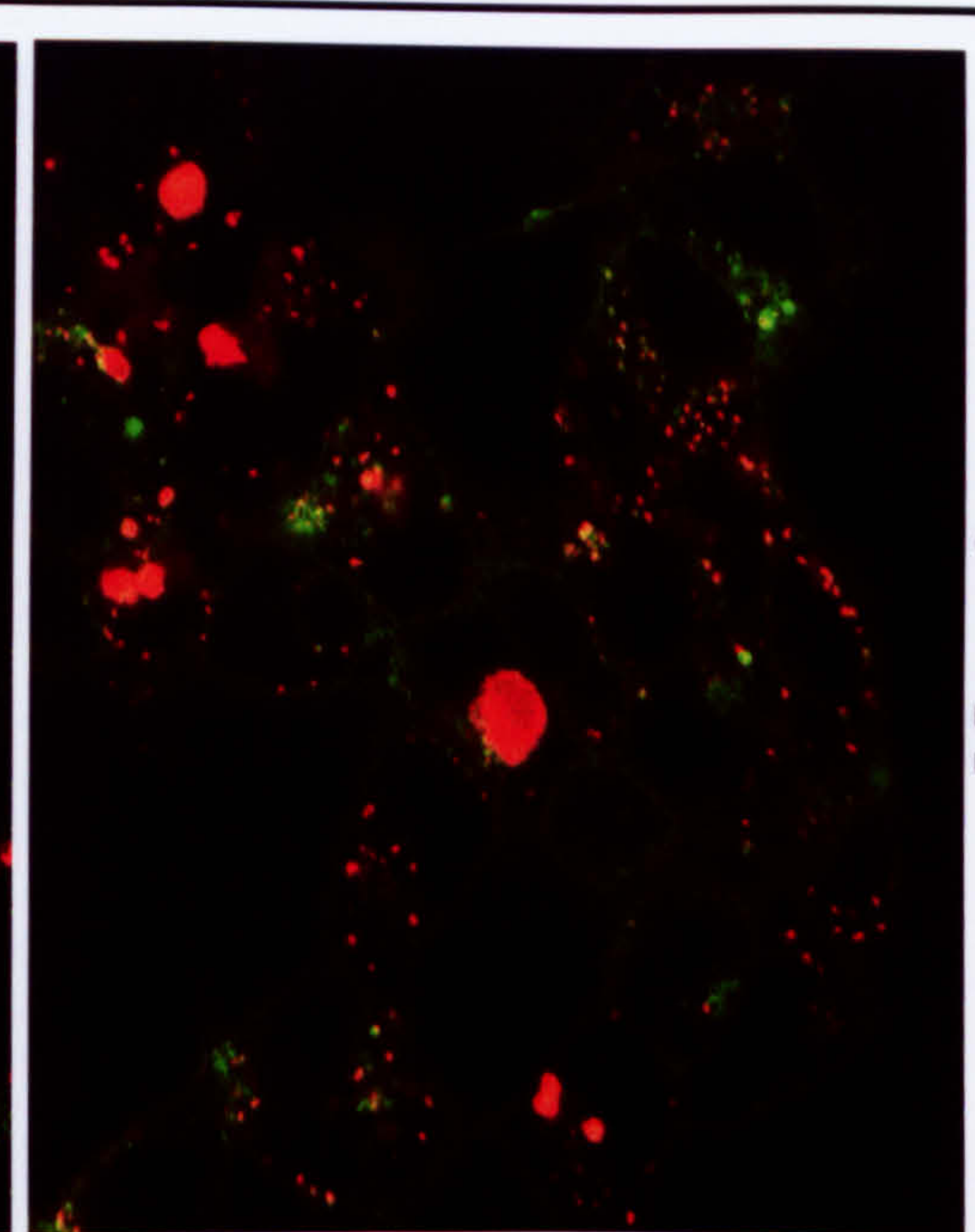
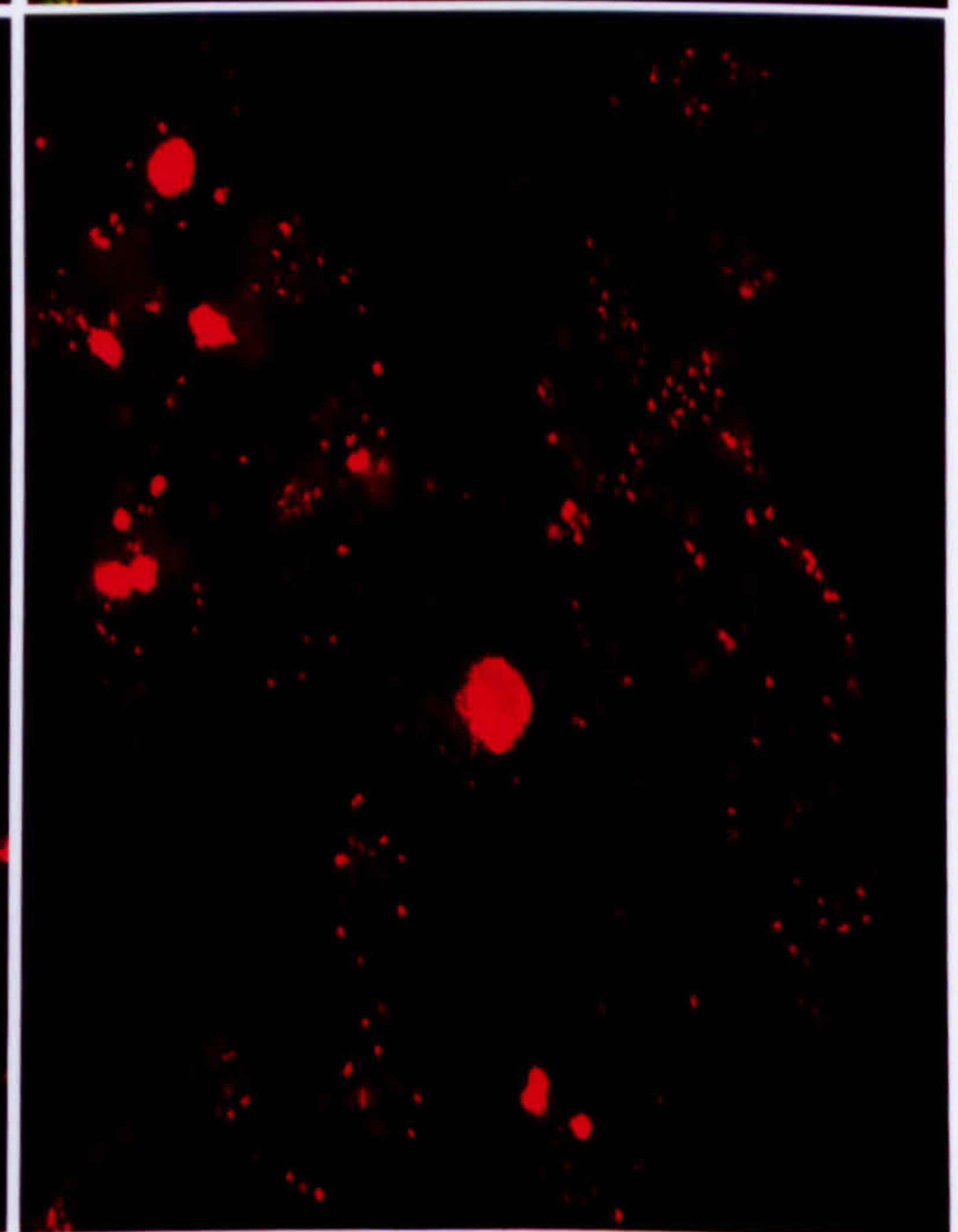
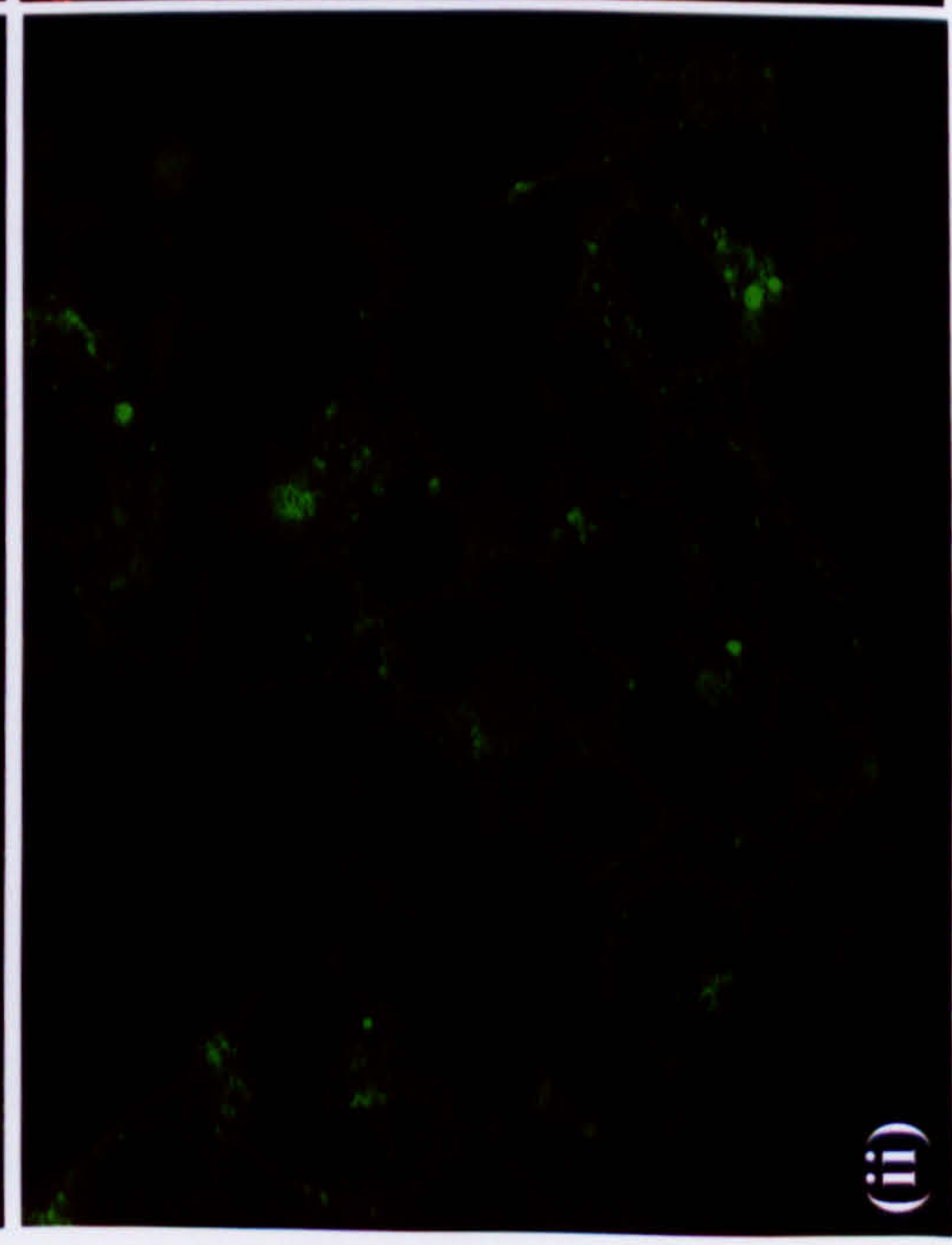
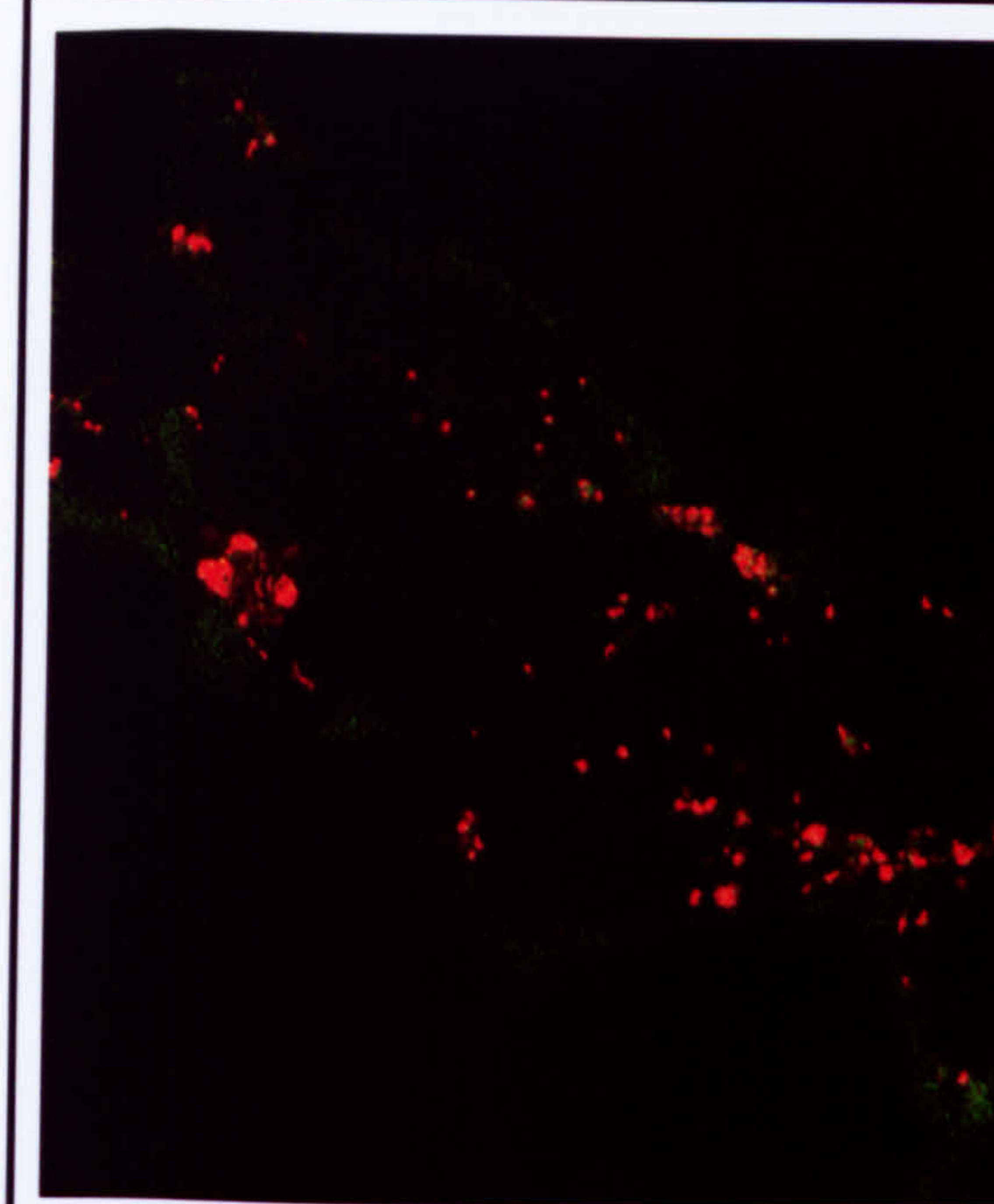
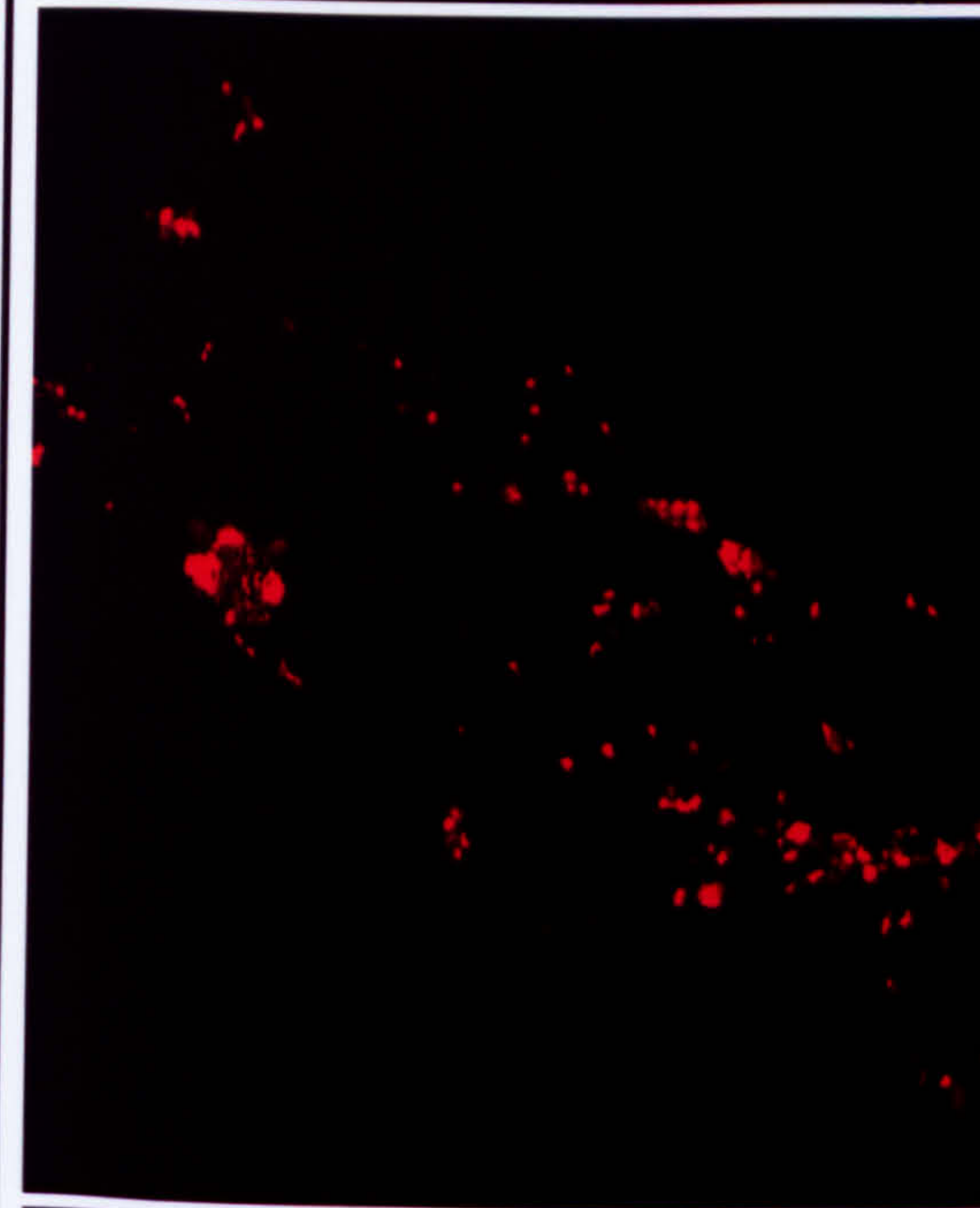
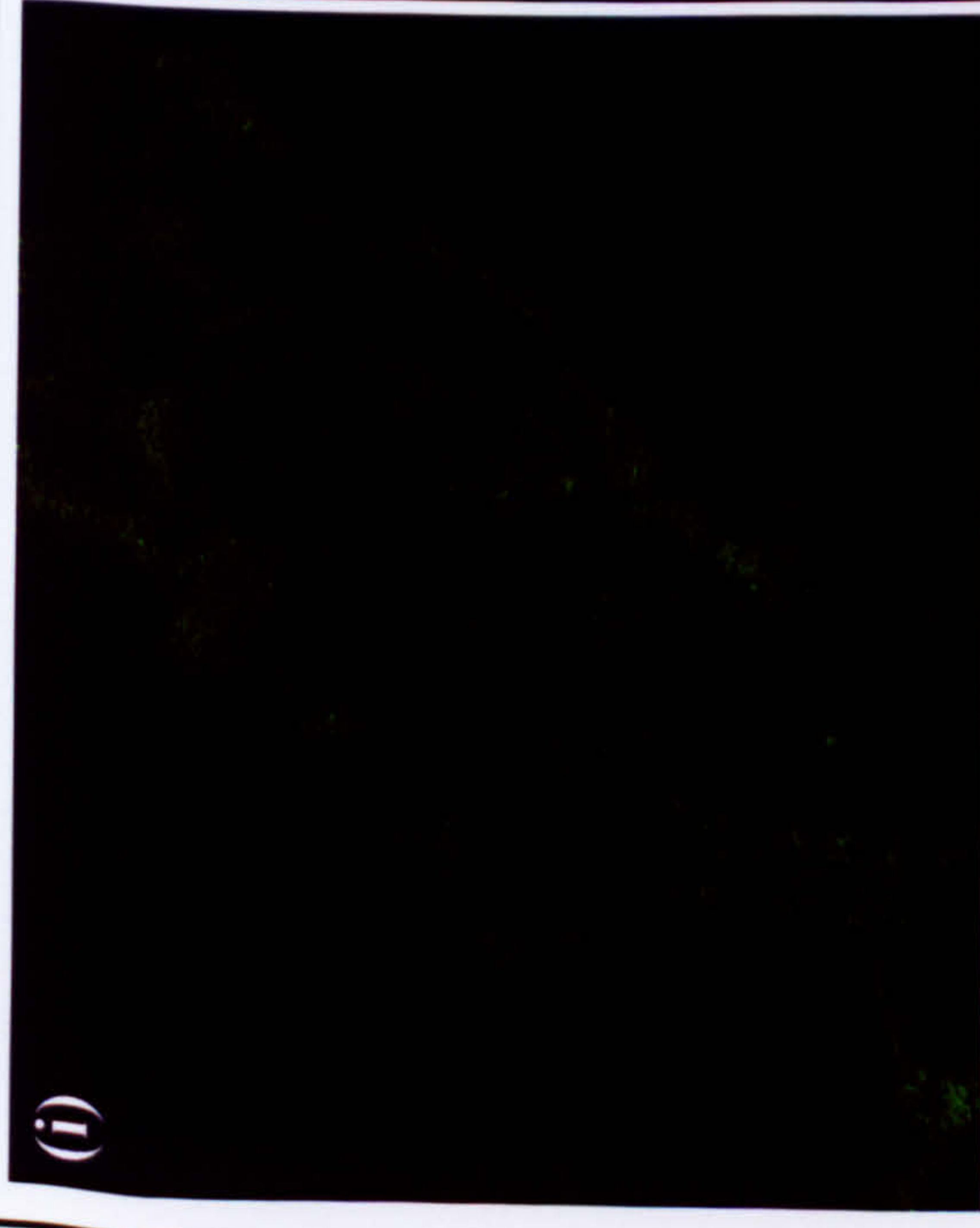
**GFP**



### **FIGURE 3.10 THE CD23B ISOFORM DOES NOT CO-LOCALISE WITH LYSOTRACKER DYE IN HEK 293 CELLS**

Coverslips bearing G418-resistant HEK 293 cells expressing CD23b or GFP-CD23b were pre-incubated with 50nM LysoTracker dye prior to confocal analysis. The wild type CD23 proteins were visualised after the addition of FITC-anti-CD23 antibody. The GFP-CD23b fusion proteins were exposed to no stimulus, 1µg NIP-specific IgE or to 1µg NIP-specific IgE followed by the addition of 1µg NIP<sub>10</sub>-BSA and examined by confocal microscopy over a 45 minute period. The pictures illustrate the results for (i) wild type CD23b and GFP-CD23b in the (ii) basal, (iii) loaded and (iv) cross-linked states respectively. Co-localisation was not observed under any of these experimental conditions.





**FITC / GFP**

**LysoTracker**

**Merged**



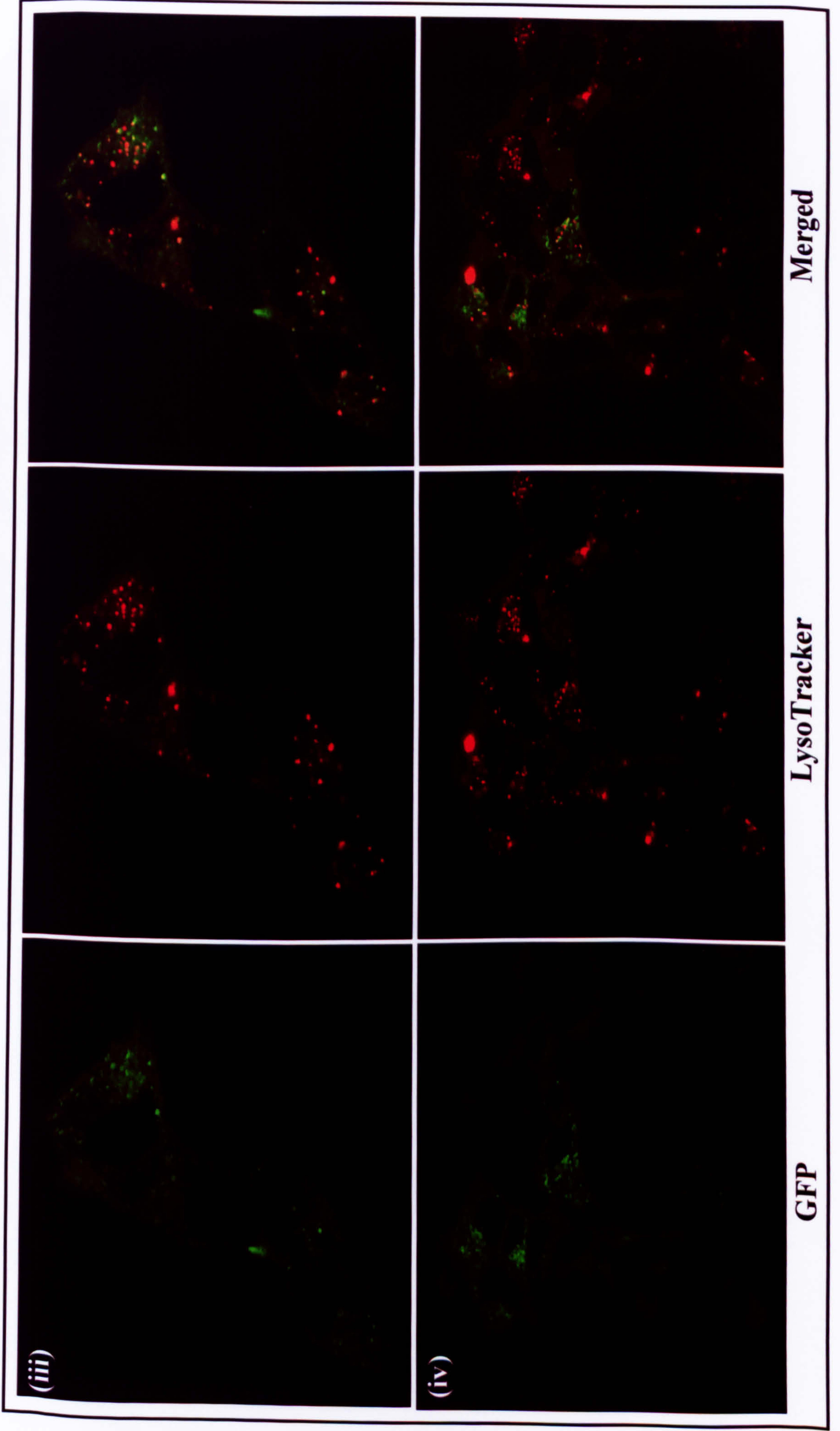
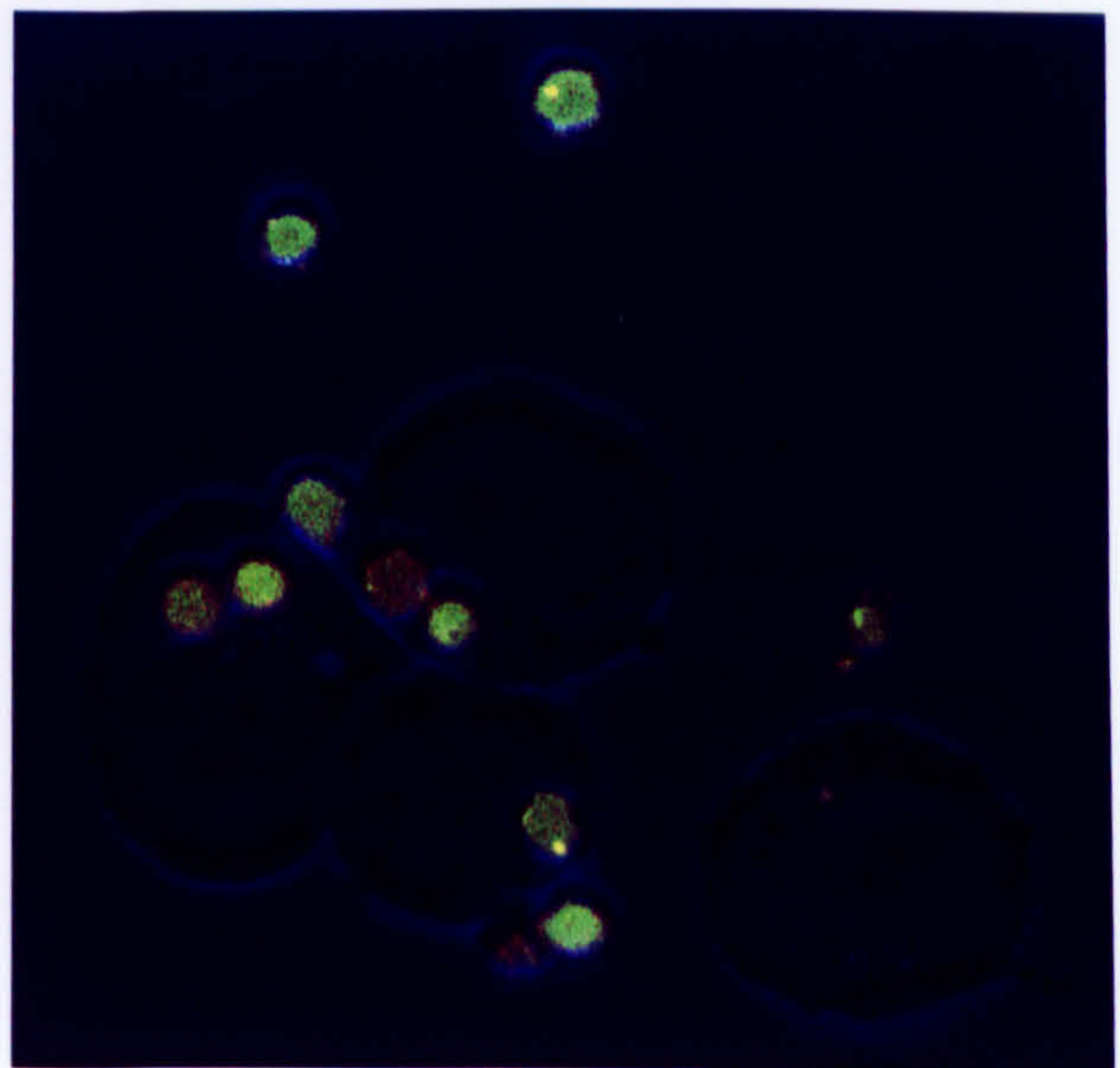
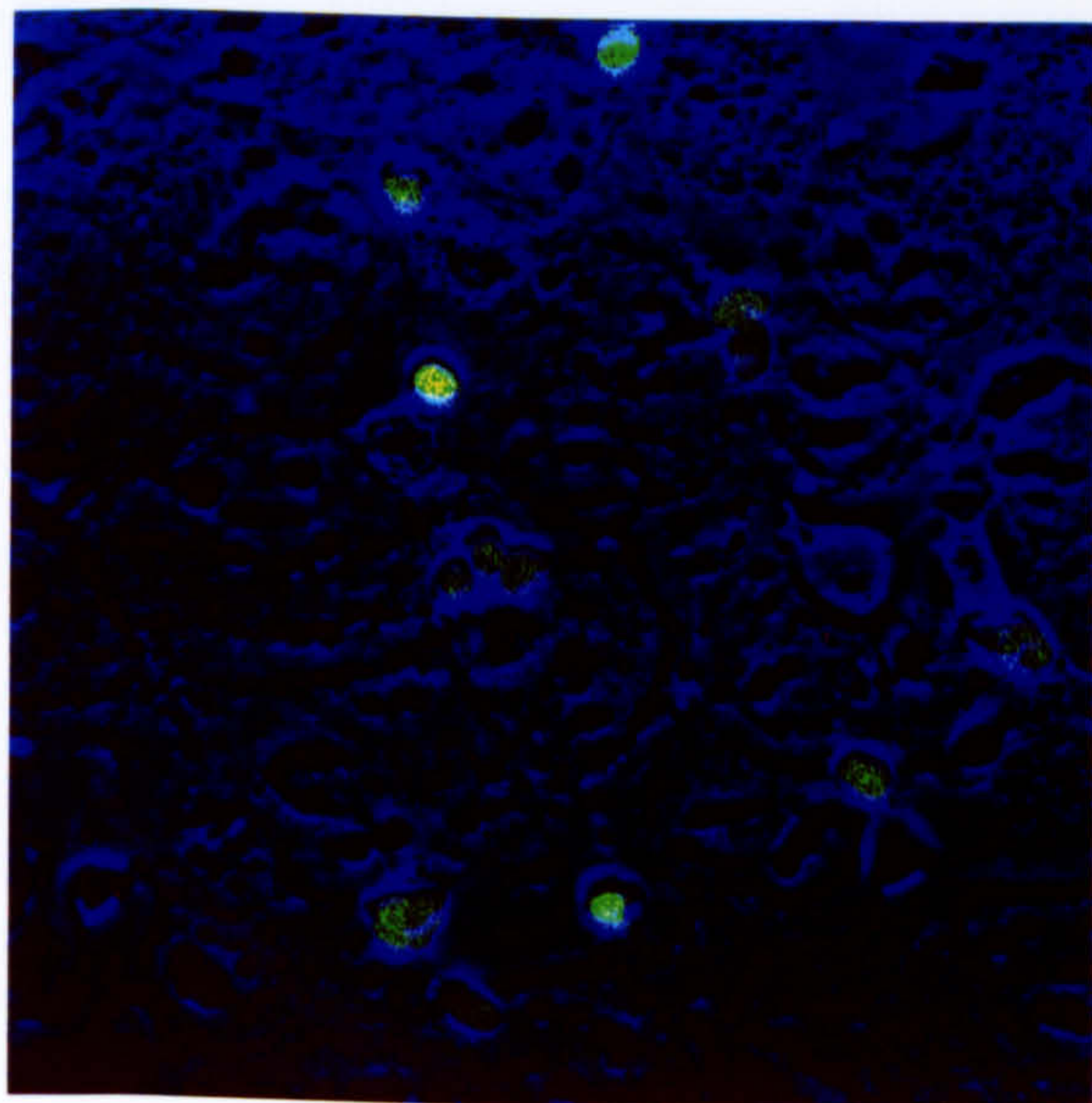
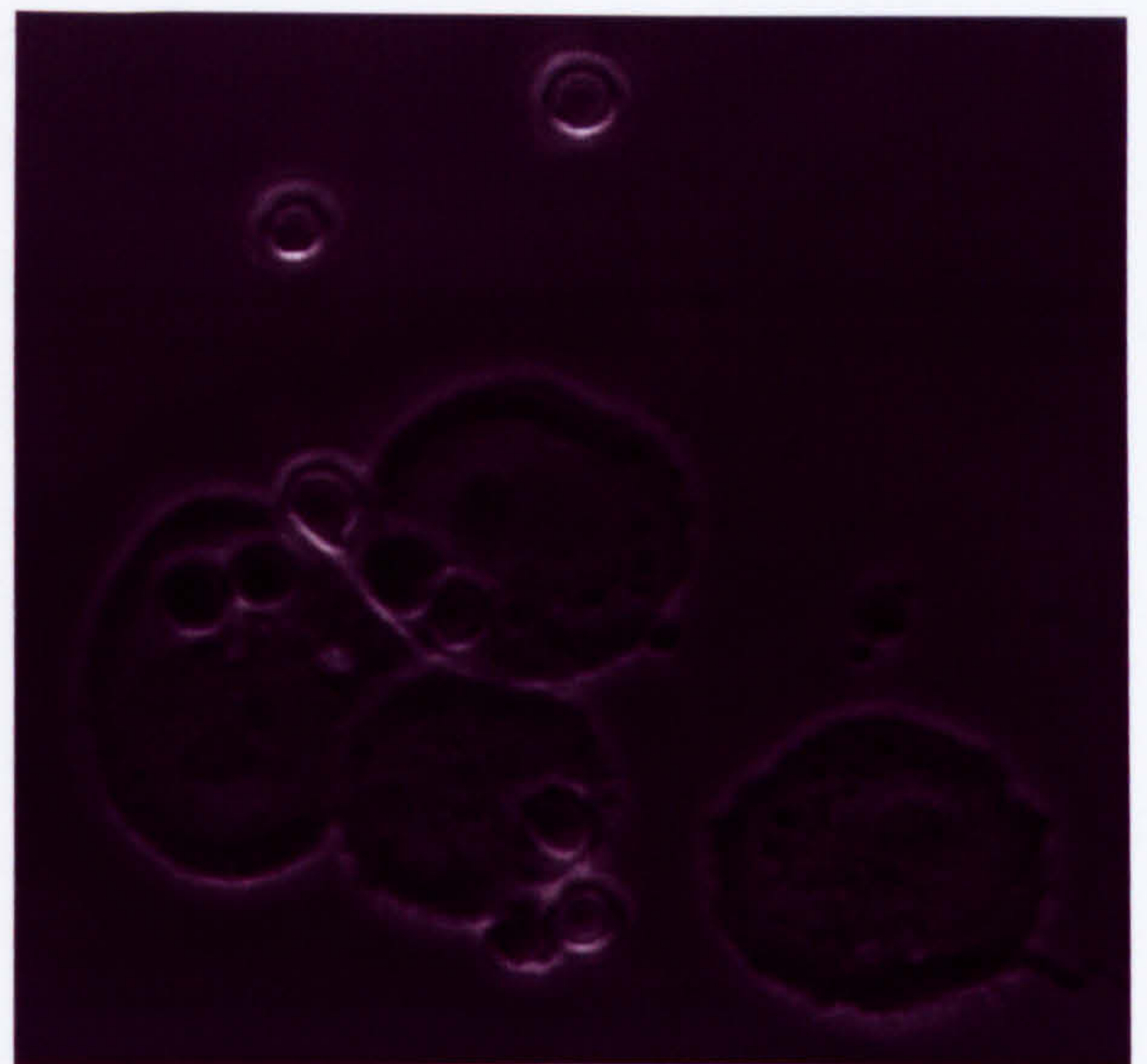
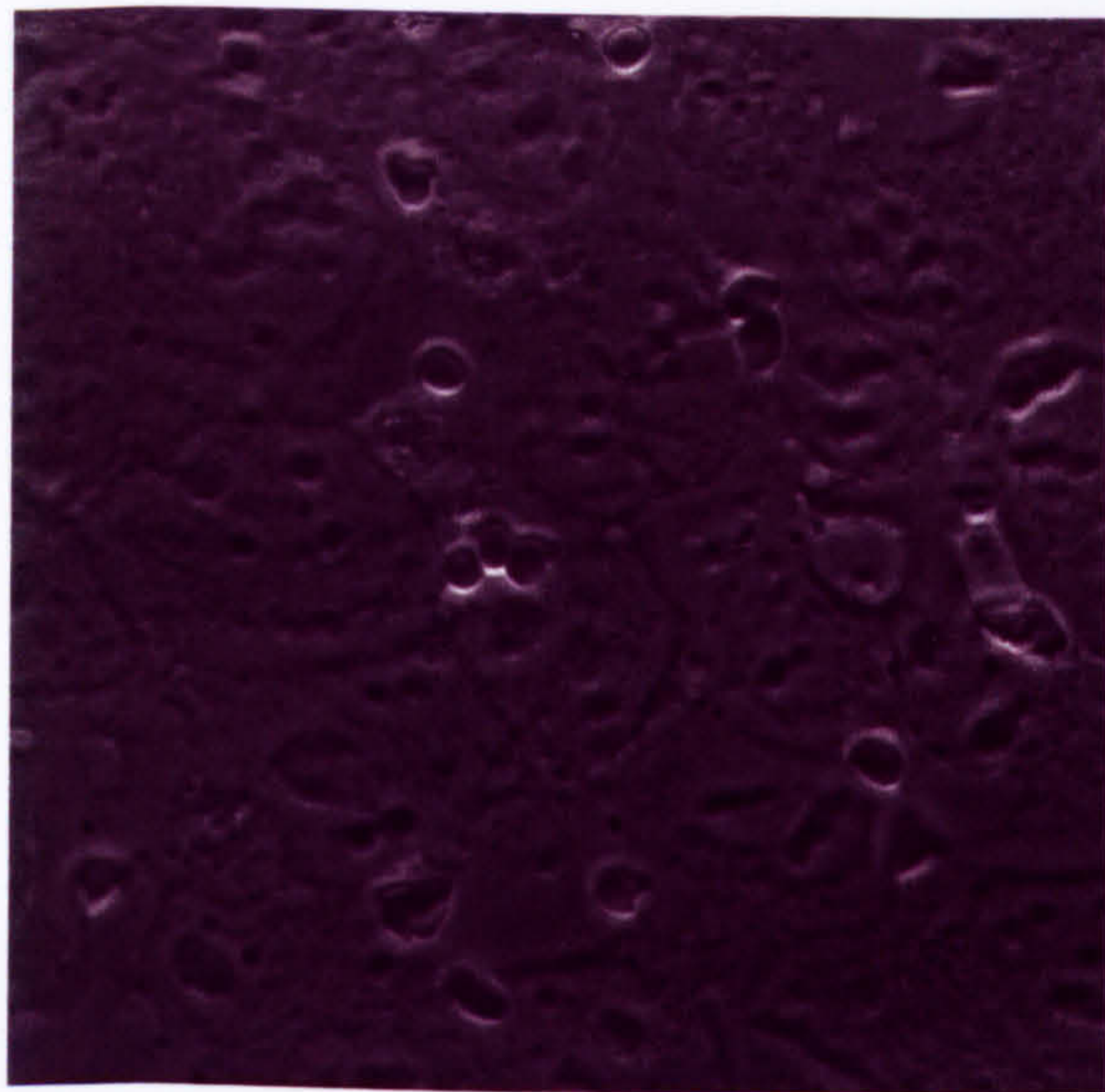




### **FIGURE 3.11 HEK 293 CELLS DO NOT UTILISE THE CLASSICAL PHAGOCYTOTIC PATHWAY**

A phagocytosis assay was performed to assess the phagocytic ability of HEK 293 cells. Sheep red blood cells (SRBC) were labelled with FITC dye, coated with anti-SRBC stromal antibody and then presented to the cells for 30 minutes at 37°C. The top panel shows the bright field images for each cell line, with the bottom panel showing an overlay of the bright field image with the confocal fluorescent image, recording the location of the green of the FITC-labelled SRBC. HEK 293 cells are unable to engulf FITC labelled sheep red blood cells (SRBC) opsonised with antibody, unlike the macrophage-like cell line U937.





HEK 293

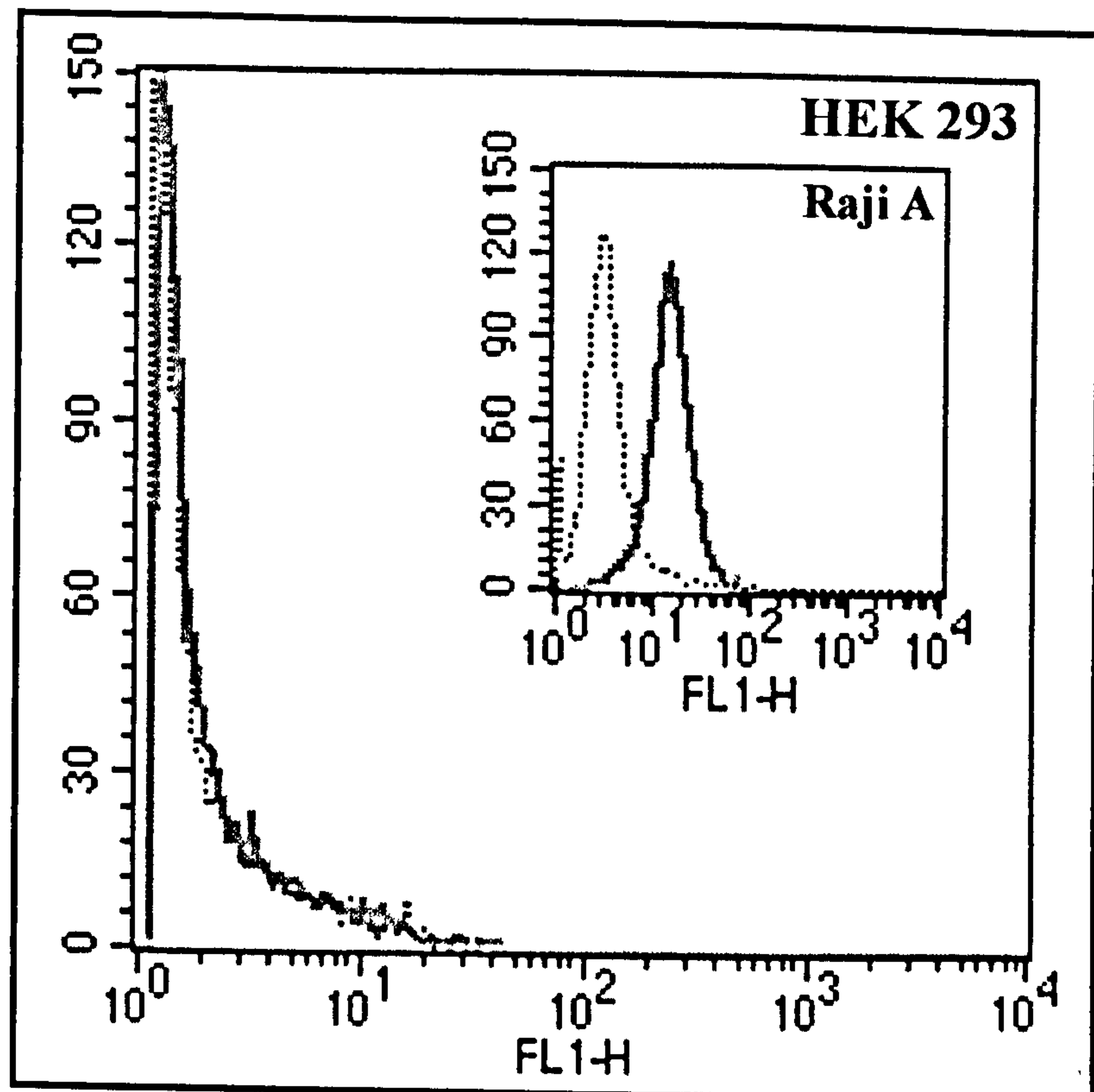
U937



### **FIGURE 3.12 HEK 293 CELLS DO NOT EXPRESS MHC CLASS II MOLECULES**

Untransfected HEK 293 were subjected to flow cytometry, analysing whether or not these cells express MHC class II molecules. The thick gray line represents the presence of MHC class II molecules, as detected by a FITC anti-HLA-DR (class II) antibody. The black dotted line represents the negative control illustrating the results for untransfected HEK 293 cells with the addition of the anti-CD23 antibody. The insert histogram illustrates the results for the Raji A cell line, indicating that these cells do express MHC class II molecules and thus serve their purpose as a positive control for this experiment.







**CHAPTER 4**

**GENERATION AND ANALYSIS OF CD23A AND CD23B**

**N-TERMINAL MUTANT PROTEINS**



## 4.1 INTRODUCTION

Human CD23, as previously discussed, has been demonstrated to exist in two isoforms [Yokota *et al.*, 1992], with these species originating from a single 11 exon gene located on chromosome 19 [Suter *et al.*, 1987; Wendel-Hansen *et al.*, 1990], differing only by a few amino acids at the very N-terminus of their short cytoplasmic domains [Yokota *et al.*, 1988]. Section 1.5 discusses the fact that the CD23a and CD23b isoforms show distinct patterns of cellular expression and are believed to have discrete functional roles. Indeed, it seems logical for these two very similar, yet distinct, proteins to have different functional roles, otherwise why would their individual production, sometimes on the very same cell, be maintained? It also stands to reason that any differences that do exist between these two molecules must be attributed to the unique amino acid sequences contained within the short N-terminal cytoplasmic tail regions, as the remainder of the molecules are identical.

The two CD23 isoforms have previously been associated with different intracellular trafficking pathways, the CD23a isoform associated with receptor-mediated endocytosis and the CD23b isoform linked more to a phagocytic route of cellular entry [Yokota *et al.*, 1988]. The amino acid sequences at the extreme N-termini of each isoform may partly explain this phenomena; for example the CD23b isoform contains an asparagine and proline at positions 2 and 3 that have been suggested to be essential for phagocytosis of the CD23b isoform and experimental evidence suggests that mutation of these residues results in a severe reduction in phagocytic uptake in J774 cells [Yokota *et al.*, 1988]. The primary aim of this research was to investigate the individual amino acid differences that exist between the two isoforms, using the same cell system to analyse both isoforms, in an attempt to identify the functionally essential amino acids involved in receptor trafficking. The phosphorylation state of the molecule is often important with respect to function. This research concentrates on the unique N-terminal tail sections of the CD23 isoforms with particular focus on the serine and tyrosine residues which might function as targets for regulatory kinases.

A small library of CD23a and CD23b N-terminal mutants have been generated and the properties of each of the resultant CD23 mutant proteins assessed using flow cytometry and live cell confocal analysis. The results discussed within this chapter do indeed



indicate that certain amino acids contained within the unique N-terminal tail region do appear to be essential for the correct trafficking and thus functioning of the individual protein isoforms.

## **4.2 RESULTS**

### **4.2.1 GENERATION OF cDNAs AND PLASMIDS EXPRESSING EACH OF THE CD23 N-TERMINAL MUTANT PROTEINS.**

A small library of ten CD23 N-terminal mutant constructs, each differing from one of the wild-type CD23 proteins by only one or two amino acids, were generated using the Stratagene QuickChange Mutagenesis kit, (section 2.2.5 and according to the manufacturers instructions). Figure 2.2 shows an overview of the strategy employed. Briefly, pairs of oligonucleotide primers, each complimentary to opposite strands of the vector, were designed to incorporate the specific base changes required to alter the target N-terminal amino acids. These primers were extended during temperature cycling by means of *PfuTurbo* DNA polymerase, generating mutagenic open plasmid strands complimentary to the original plasmid in every way except the mutated bases encoded within the oligonucleotide sequences.

The obvious residues targeted for change were those amino acids that may be potentially phosphorylated or de-phosphorylated, serving to alter the phosphorylation state of the receptor molecule at the cell surface. The NPP motif in the CD23b isoform was also mutated since these amino acids, as previously discussed, have been suggested to play a role in targeting this molecule into the phagocytic pathway in J774 cells [Yokota *et al.*, 1988]. Figures 4.1 and 4.2 show the sequences of the oligonucleotides used to generate each of the mutants, together with the resultant proteins generated and the nomenclature given to the CD23a and CD23b N-terminal mutants. The DNA and amino acid sequences of the wild-type protein isoforms are also illustrated in each case. Figure 4.3 illustrates the side chains involved in each of the amino acid changes.

Each mutant clone was subjected to automated DNA sequencing to ensure the presence of the correct sequence and incorporation of the correct mutation in each instance (data not shown). As previously described in chapter 3; section 3.2.1, PCR was used to insert



a green fluorescent protein (GFP) tag at the N-terminus of each of the CD23 mutant proteins, facilitating the generation of constructs expressing each of the CD23 mutants as GFP fusion proteins. This cloning procedure was verified with restriction digestion analysis as well as with automated DNA sequencing to ensure each construct was expressing the GFP-CD23 mutant fusion proteins correctly (data not shown).

#### **4.2.2 EXPRESSION OF GFP-CD23A AND GFP-CD23B MUTANT PROTEINS IN HEK 293 CELLS**

In order to investigate the molecular differences between the two CD23 isoforms the proteins must be studied in the same cell system, under the same experimental conditions. Having previously proven the HEK 293 cell system to be a feasible means of studying the endocytic trafficking ability of each of the wild-type CD23 proteins it was postulated that the importance of the amino acid differences between these two isoforms could also be studied using this cell system.

HEK 293 cells were transfected with pcDNA3.1<sup>+</sup> constructs encoding each of the GFP-CD23 mutant fusion proteins. After 5-6 weeks, G418-resistant cell lines emerged and these were assessed for GFP-CD23 fusion protein expression by flow cytometry. The cells were analysed directly for GFP fluorescence as well as the presence of CD23 proteins using an anti-CD23-PE conjugated antibody (Figure 4.4). These results indicate that all the GFP-CD23 mutant proteins are expressed to some extent in HEK 293 cells. The majority of the stable cell lines demonstrate good levels of protein expression and the proteins appear to remain targeted to the plasma membrane. This is demonstrated by the percentage of double positive cells, shown in the upper right-hand corner of each dot plot (Figure 4.4). The GFP-CD23bP3R mutant was not well detected with the anti-CD23 antibody although the cells did demonstrate GFP fluorescence, suggesting the bP3R protein is expressed but that it may not reach the plasma membrane, either at all or in a conformation not recognised by the anti-CD23 antibody used.

With the exception of the data collected for the GFP-CD23bP3R mutant, the FACS data suggest that the incorporation of these amino acid changes does not interfere with the expression and initial targeting of these fusion proteins to the plasma membrane. The



mutant fusion proteins must also be folding correctly once at the cell surface as they are being efficiently recognised by anti-CD23 antibodies, demonstrating that the incorporation of the amino acid changes at the N-termini does not affect the extracellular domain structure of CD23.

#### **4.2.3 REAL TIME VISUALISATION OF EACH GFP-CD23 MUTANT PROTEIN IN HEK 293 CELLS; THE GFP-CD23BP3R MUTANT PROTEIN IS NOT TARGETED TO THE PLASMA MEMBRANE**

Stably-transfected HEK 293 cells expressing the individual GFP-CD23 mutant isoforms were assessed by laser scanning confocal microscopy. In each case live cells were examined and GFP-CD23 receptor trafficking was monitored over a fixed time period. Initial experiments were performed to establish if each of the GFP-CD23 mutant proteins could be visualised at the surface of HEK 293 cells. Figure 4.5 illustrates ten representative images, detailing the typical initial staining pattern observed for each of the GFP-CD23 mutant proteins in HEK 293 cells. Images for the wild-type CD23 isoforms have previously been shown in Figure 3.4. In agreement with the flow cytometric data reported in Figure 4.4, these images illustrate that all the CD23 mutant proteins are routed to the plasma membrane, with the exception of GFP-CD23bP3R. Confocal analysis shows that the bP3R protein is expressed (as was expected from the flow cytometry data shown in Figure 4.4); however, it appears trapped within the cytoplasm of these cells, with no evidence of plasma membrane localisation ever observed.

The distribution of each of the CD23 mutant proteins (with the exception of the aY6F and bP3R proteins) was then assessed in the basal, loaded and cross-linked states using the previously described NIP system (Figure 3.5). Entry into early endosomes and thus the endocytic pathway was identified by co-localisation with transferrin-Texas Red dye (Tf-TxR).



#### **4.2.3A INTERNALISATION AND INTRACELLULAR TRAFFICKING OF GFP-CD23A MUTANTS; ROLE FOR SERINE 7**

Wild-type GFP-CD23a, as previously shown (Figure 3.4B), demonstrates a distinct pattern of expression with the majority of the protein being localised to the cell membrane in the basal and loaded states. GFP-CD23a was found to co-localise with Tf-TxR, only under cross-linked conditions after the receptor had been occupied with NIP-specific IgE and cross-linked with NIP<sub>10</sub>-BSA (Figure 3.7).

GFP-CD23aS7A was observed to have a more diffuse pattern of staining, with most of the protein demonstrating an internal location throughout the cytoplasm of the HEK 293 cells (Figure 4.6). A comparatively small amount of this protein was observed at the plasma membrane; however, the vast majority seemed to be retained within the cell cytoplasm. There was evidence of concentrated areas of fluorescence within the cytoplasm in the basal state. Cross-linking studies were performed and it was observed that the aS7A proteins located at the plasma membrane could be driven to internalise only after the addition of both IgE and NIP<sub>10</sub>-BSA, as demonstrated by the appearance of distinct foci of fluorescence along the membrane and some areas of co-localisation within the cell (Figure 4.6). It should be noted that co-localisation of this mutant with Tf-TxR was only observed after cross-linking, with the position of some of the green foci of fluorescence correlating with some of the Tf-TxR, demonstrating use of the endosomal pathway.

The initial distribution of the GFP-CD23aS7D mutant in the basal state was found to be comparable to that of wild-type CD23a in a loaded or cross-linked state, as it was observed to have a punctate pattern of expression (Figure 4.7). The extent of punctation was observed to increase on loading and then again on cross-linking. Strikingly this mutant was observed to show internalisation as well as co-localisation with Tf-TxR in all three states, as evident from the presence of yellow patches in each of the three merged images shown. Collectively the data recorded for these two mutants indicate a role for serine 7 in the routing of the CD23a isoform into the endosomal pathway.

The conclusions that may be drawn from the GFP-CD23aY6F mutant are slightly more ambiguous. The DNA encoding this CD23 mutant was used to transfect HEK 293 cells



on a number of occasions with the resultant stably-transfected cell lines always found to have low expression levels of the GFP-CD23aY6F protein. GFP-CD23aY6F was initially not thought to reach the plasma membrane, however this was demonstrated to be absolutely the case (Figure 4.8). Bright field imaging was used to record the location of the cells and confocal microscopy to image the fluorescent dye and thus the position of the GFP-CD23aY6F proteins within these cells. These images illustrate that the aY6F protein does appear to reach the plasma membrane. The protein expression levels were not sufficient to enable any further investigation of its trafficking patterns following loading and cross-linking, although this was attempted during the course of a number of experiments, as no definitive effects were observed due to the very low level of protein expression. A number of GFP-CD23aY6F transfected cell lines were produced, each of which demonstrated uniformly low expression levels. Figures 4.5 and 4.8 summarise the limited data obtained for this CD23 mutant. It appears that the aY6F mutant may have a punctate expression on the plasma membrane in the basal state; however, it is difficult to say so conclusively due to the low expression levels and the poor quality images recorded as a direct result of this.

The CD23aYS67FA mutant demonstrated targeting to the plasma membrane, and concentrated foci of fluorescence within certain areas along the plane of the membrane in the basal state (Figure 4.9). A small proportion of generalised intracellular staining was also observed with this mutant in the basal state, as well as the occasional distinct focus of fluorescence within the cell. Loading and cross-linking of the CD23aYS67FA mutant did result in an increase in the amount of punctate distribution on the plasma membrane. The aYS67FA mutant was found to co-localise with Tf-TxR and this was especially evident in the loaded state, where much of the co-localisation was found on the plasma membrane, presumably due to the receptor assembling into distinct areas along the cell surface. Directed aYS67FA internalisation from the plasma membrane after loading and cross-linking was observed, as demonstrated by the presence of distinct foci of fluorescence within the cell. In contrast to the bS5F mutant (Figure 4.12) where much of the plasma membrane protein was clearly internalised, much of the aYS67FA protein appeared to remain within the plane of the plasma membrane.



The data recorded from these two CD23a mutants collectively suggests the importance of the tyrosine residue at position 6, and suggests that the phosphorylation state of this residue may play a role in CD23 trafficking.

#### **4.2.3B INTERNALISATION AND INTRACELLULAR TRAFFICKING OF THE GFP-CD23B MUTANTS; A ROLE FOR SERINE 5**

As previously discussed, the wild-type CD23b isoform, as with wild-type CD23a, was shown to have a predominant membrane localisation in HEK 293 cells (Figure 3.4). Loading with IgE and subsequent cross-linking with NIP<sub>10</sub>-BSA did result in internalisation of the CD23b protein. However, co-localisation with Tf-TxR was not evident in any of the experiments, under any of the three basal, loaded or cross-linked conditions (Figure 3.8). Three mutations were made to the serine located at position 5, resulting in the generation of the bS5A, bS5D and bS5F CD23 proteins. Initial studies demonstrated that all three of these mutants were able to locate to the plasma membrane (Figure 4.5), although characteristic differences were observed in the basal expression patterns shown by each of these mutant proteins, both in comparison to the wild-type CD23b proteins as well as with respect to each other.

Two distinct cell populations were observed with the bS5A mutant. The first was found to demonstrate a fairly uniform expression throughout the cytoplasm of HEK 293 cells, with a limited amount of CD23bS5A protein located at the plasma membrane (Figure 4.5 & 4.10A). Loading with IgE and subsequent cross-linking with NIP<sub>10</sub>-BSA resulted in the membrane-localised staining assuming a more punctate distribution, some of which was observed to enter into the cell and co-localise with Tf-TxR (Figure 4.10A). The second cell population was observed to show a more usual pattern of staining with much of the GFP-CD23bS5A protein associated with the cell membrane, or located within distinct foci of fluorescence within the cell. This population was found to demonstrate extensive co-localisation with Tf-TxR in all three basal, loaded and cross-linked states. Collectively the confocal images suggest that the bS5A protein is able to undergo directed uptake into the cell and co-localisation with Tf-TxR, regardless of whether or not the receptor is occupied with IgE and/or cross-linked with NIP-BSA. Further transfection experiment would have to be performed in order to establish which of these two populations was the true expression pattern of the bS5A mutant.



The bS5D mutant protein demonstrated the presence of distinct foci of fluorescence along the plasma membrane in the basal state (Figure 4.11). As observed with aS7D, the bS5D mutant demonstrated co-localisation in all of the three basal, loaded and cross-linked conditions, indicating that these mutants were able to enter the endocytic pathway, regardless of whether or not the receptor is occupied with IgE and/or cross-linked with NIP<sub>10</sub>-BSA. Together these proteins indicate the importance of the serine at position 5 and suggest that the phosphorylation state of this residue may play a crucial role in the trafficking of the CD23b isoform. The findings from the third serine mutation, bS5F, support this interpretation further.

CD23 bS5F showed a similar pattern of expression to the bS5D mutant and there was evidence of co-localisation with Tf-TxR in all three, basal, loaded and cross-linked, states. In the basal state there was substantial evidence of co-localisation both at the cell surface and at distinct areas within the cell. Loading with IgE and then cross-linking with NIP<sub>10</sub>-BSA stimulated an increase in directed uptake of CD23, as evident initially by an increased punctate morphology at the cell surface and then the presence of more foci of fluorescence within the cell (Figure 4.12). The majority of the fluorescence, originally located on the cell surface, was observed to enter into the cell. The results obtained from each of these three mutants collectively suggest a role for serine 5 phosphorylation in the regulation of directed entry of CD23b into the cell, and in this cell system, co-localisation with Tf-TxR in the endosomal pathway. The wild-type GFP-CD23b protein was never observed to co-localise with Tf-TxR under any of the basal, loaded or cross-linked states studied.

#### **4.2.3C A ROLE FOR THE NPP TRI-PEPTIDE MOTIF**

The NNP tri-peptide motif in the cytoplasmic tail of CD23b is believed to regulate movement of this protein into the phago-lysosomal pathway in J774 cells, and for this reason these amino acids were also targeted in this mutagenesis study. As demonstrated in Figure 4.13 incorporation of the bP3R mutation prevents the CD23b isoform from reaching the plasma membrane in HEK 293 cells, causing this protein to remain trapped within the cell, localised in distinct regions within the cytoplasm. No co-localisation was observed with Tf-TxR indicating that this protein is located in areas or vesicles distinct from either the early endosomes or indeed the endocytic pathway. Obviously



this was the limit of the analysis that could be performed using this mutant, due to the fact that there was no surface protein to be loaded or cross-linked. These findings suggest that this residue, unlike any of the others studied, may be important in the initial targeting of the CD23b isoform to the plasma membrane, in so much that mutation of this residue actively prevents this from occurring.

Unlike bP3R, mutation of the neighbouring proline residue to arginine (bP4R) had no effect on trafficking of the CD23b isoform to the cell membrane, although there was a marked difference between this protein and the wild-type GFP-CD23b protein. In contrast to the wild-type GFP-CD23b protein the bP4R protein was found to demonstrate both concentration of fluorescence on the membrane and internalisation within the cell in the basal state, (Figure 4.14). Distinct foci of fluorescence were also observed within the cell, indicating marked internalisation in all three, basal, loaded and cross-linked conditions. Co-localisation was also observed between this protein and Tf-TxR (unlike wild-type GFP-CD23b), in all three, basal, loaded and cross-linked states. These results indicate this residue, like the serine at position 5, to be important in the internalisation and directed uptake of CD23b into the cell.

As has been previously described for the bP4R protein, the bN2K mutant was also shown to demonstrate extensive co-localisation with Tf-TxR in each of the basal, loaded and cross-linked states, with internalised distinct foci of fluorescence present in each of these conditions. Punctate staining at the plasma membrane was increased on loading with IgE and subsequent cross-linking with NIP<sub>10</sub>-BSA (Figure 4.15).

The data assembled from these three mutants collectively indicate that modification of asparagine 2 and proline 4, within the NPP putative phagocytic targeting motif, yields CD23 proteins readily able to enter a recycling, and/or endocytic pathway in HEK 293 cells. These results are in stark contrast to those collected from the wild-type CD23b isoform, as it was never observed to co-localise with Tf-TxR under any conditions in HEK 293 cells.



#### 4.2.4 MUTATION OF THE N-TERMINUS OF CD23 AFFECTS PROTEOLYTIC CLEAVAGE FROM THE CELL SURFACE

Membrane-associated or full-length CD23 can be proteolytically cleaved from the cell surface to produce a number of soluble CD23 fragments (sCD23), with the enzymatic cleavage sites located within the stalk region of full-length CD23. Binding of IgE has been shown to protect CD23 from cleavage [Lee *et al.*, 1987], as have agents that prevent CD23 glycosylation [Delespesse *et al.*, 1989]. Having generated each of the N-termini mutant CD23 proteins for the trafficking studies it was interesting to see if any of these had an effect on CD23 shedding from the cell surface. An OptEIA™ Human sCD23 ELISA kit (Pharmingen) was used to measure the amount of sCD23 present in the sera collected from each of the stably-transfected HEK 293 cells, as per the manufacturer's instructions (section 2.2.7H). The supernatants were collected from nearly confluent flasks of stably-transfected cells that had been cultured in the same media over a 4 day period. Figure 4.16 illustrates the results. Firstly, there was a marked difference in shedding patterns of the CD23 isoforms. The GFP-CD23a isoform was shown to be readily cleaved from the cell surface, whilst the GFP-CD23b isoform was observed to show minimal, if any, shedding from the cell surface. The extent of release of each of the GFP-CD23 mutants was then compared to the wild-type GFP-CD23 protein isoforms. The exact figures should not be compared directly, but rather trends drawn from the overall results.

Each of the CD23a mutants illustrated a decrease in sCD23 cleavage in comparison to the CD23a isoform. The aS7A and aS7D mutants illustrated a marked decrease in sCD23 shedding, and cannot be explained by protein expression levels as these appeared to be comparable in each case. The aY6F mutant also indicated a marked decrease in shedding, however as the expression levels of this mutant were uniformly low it is not surprising that little sCD23 was detected in the supernatant collected from these cells. The aYS67FA protein was also observed to have around a 50% decrease in sCD23 shedding. In contrast to the CD23a mutants, some of the CD23b mutants were observed to demonstrate a marked increase in CD23 shedding. The most striking result observed was for the bS5A protein, as it showed a huge increase in CD23b shedding (115 fold) from the cell surface. The bS5D mutant protein also demonstrated a noticeable increase in CD23b cleavage from the cell surface, whilst the remainder of the



mutants demonstrated low-level cleavage, very much like the wild-type CD23b isoform. The expression levels of each of these CD23b proteins appeared to be generally similar (with the exception of bP3R) and cannot therefore explain the vast differences in the amounts of sCD23 protein released from the HEK 293 cells. It should be noted that the most interesting results were recorded primarily from those mutants illustrating very different trafficking patterns in comparison to the wild-type proteins in the confocal studies.

#### **4.2.5 EXPRESSION OF GFP-CD23 FUSION PROTEINS IN B LYMPHOCYTES**

The ultimate goal of the trafficking studies discussed thus far was to analyse the movement of the CD23 protein isoforms in their native cell type, the B lymphocyte. However B cells, as is the case with most mammalian cell lines, are generally very sensitive to manipulation and thus not the easiest cells to work with when trying to generate stably transfected cells expressing a particular protein of interest. The majority of cultured B cell lines also grow as free floating cells in suspension, posing a second problem as to how these cells could be visualised using the confocal microscope should any transfection method be successful.

The Raji A cell line was chosen for this investigation for a number of reasons. Firstly, Raji A cells are an adherent, immature B cell line isolated from a suspension culture of an established Burkitt's Lymphoma cell line (Raji) [Nyormoi, *et al.*, 1972]. These cells express endogenous CD23 proteins and therefore must possess all the necessary equipment and protein intermediates to enable the GFP-CD23 trafficking to occur very much as CD23 trafficking would in the real situation. Secondly, the Raji A cell line was isolated for its adhesion properties, enabling this cell line, unlike the parent Raji line, to be routinely cultured in monolayers. These cells therefore provide all the advantages of a normal B cell line with the added bonus of their ease of use for investigation using the confocal microscope.

##### **4.2.5A GENERATION OF G418-RESISTANT RAJI A CELLS EXPRESSING EACH OF THE WILD-TYPE GFP-CD23 FUSION PROTEIN ISOFORMS**

A number of transfection protocols were initially performed in an attempt to generate stably transfected Raji A cells expressing each of the wild-type GFP-CD23 proteins.



Electroporation was found to be the only successful means of transfection, but the results obtained were by no means ideal, with the technique often inducing upwards of 95% cell death. The cells subsequently took longer to recover and resume normal growth rates.

Raji A cells were electroporated with pcDNA3.1<sup>+</sup> constructs encoding each of the wild-type GFP-CD23 protein isoforms, as per the protocol detailed in section 2.2.6B. After 7-8 weeks G418-resistant cell lines finally emerged and these were assessed for CD23 protein expression by flow cytometry. The cells were analysed for GFP fluorescence (FL-1) as well as the presence of CD23 proteins using an anti-CD23-PE conjugated antibody (FL-2). These results indicate that both the GFP-CD23 protein isoforms are expressed to some extent in Raji A cells. Figure 4.17 shows the results, illustrated as dot plots. The stable cell line expressing GFP-CD23a demonstrated lower levels of protein expression, however the results do indicate that both proteins did appear to remain targeted to the plasma membrane. This is demonstrated by the percentage of double positive cells, shown in the upper right-hand corner of each dot plot. The FL-2 levels in each instance were expected to be higher than the FL-1 levels, purely due to the endogenous CD23 expressed at the surface, which would also be detected by the anti-CD23 antibody. The cell line expressing GFP-CD23b was found to have a number of cells that were positive only for GFP. This can be explained by the fact that the flow cytometer will, to some extent, detect the presence of GFP-tagged proteins within the cell as well as those at the cell surface. These cells may have considerably greater amounts of GFP-CD23 located within the cell than CD23 on the cell surface, GFP-tagged or otherwise.

#### **4.2.5B REAL TIME VISUALISATION OF THE WILD-TYPE GFP-CD23 PROTEINS IN RAJI A CELLS**

The stably-transfected cell lines expressing the individual wild-type GFP-CD23 isoforms were assessed by laser scanning confocal microscopy. Initial experiments were performed to obtain information on the expression levels of each protein and to confirm that both these GFP-CD23 protein isoforms could be visualised at the surface of Raji A cells. Figure 4.18 shows representative images, detailing the typical initial staining patterns observed for each of the wild-type GFP-CD23 isoforms. In agreement with the



flow cytometric data (Figure 4.17), these images demonstrate the GFP-CD23b proteins were routed to the plasma membrane, whilst the expression levels of GFP-CD23a were too low to confirm plasma membrane expression. A bright field image has also been included for the CD23a isoform in order to identify the location and indeed presence of the Raji A cells, due to the fact the fluorescent signal was weak. The results clearly show that the stably-transfected cell line expressing the GFP-CD23a isoform had very low levels of GFP-tagged CD23 protein (as was predicted to be the case from the flow cytometric data), and was therefore unsuitable for further trafficking studies. However, the GFP-CD23b isoform was expressed at reasonable levels and this stably-transfected cell line was subsequently used to monitor the intracellular trafficking of GFP-CD23b in Raji A cells in a basal, loaded and cross-linked state using the previously described NIP system (Figure 3.5). Another protein conjugate was also incorporated (Figure 4.19) serving to enhance the NIP system addressing the question as to whether the extent of CD23 cross-linking/oligomerisation at the cell surface has an impact on CD23 uptake from the plasma membrane. This enhanced NIP system was used in the trafficking studies performed with GFP-CD23b in Raji A cells, as discussed below.

#### **4.2.5C GFP-CD23B UTILISES THE ENDOCYTIC PATHWAY IN RAJI A CELLS WHEN LOADED WITH IGE AND WHEN LOADED AND SUBSEQUENTLY CROSS-LINKED WITH NIP-BSA**

Figure 4.20 shows the results observed in the GFP-CD23b and Tf-TxR co-localisation studies performed in Raji A cells. Representative image sets are shown for each condition; (i) basal, (ii) loaded, (iii) cross-linked with NIP<sub>10</sub>-BSA and (iv) 'ligated' with NIP<sub>1</sub>-Insulin. In the basal state GFP-CD23b was found to be predominantly located at the plasma membrane, with some movement observed within the plane of the membrane when the images were run together as a 'movie'. After loading with NIP-specific IgE antibody, some of the GFP-CD23b proteins were found to localise towards distinct areas on the plasma membrane and illustrate directed uptake into the cell. However it was not until the receptor was cross-linked with NIP<sub>10</sub>-BSA that marked uptake of the protein was observed from the cell surface. This uptake was noted not only as an increase in the amount of distinct patches present within the cytoplasm, but also as a marked decrease in the amount of GFP-CD23b present at the cell surface. In contrast to this, cross-linking with NIP<sub>1</sub>-Insulin did not cause much receptor uptake,



with much of the CD23 protein remaining localised to the plasma membrane, however areas of concentration along the membrane were evidence.

Minimal co-localisation of the cell surface receptor with Tf-TxR was observed in the basal state, primarily within the cell. In the loaded state, there was distinct evidence of yellow patches moving into the cell, suggesting the receptor to co-localise with Tf-TxR when loaded with natural ligand. Cross-linking with NIP<sub>10</sub>-BSA appeared to cause more directed uptake of the GFP-CD23b protein into the cytoplasm and there was some evidence of yellow patching within the cell and extensive patching at the cell surface. Cross-linking with NIP<sub>1</sub>-Insulin was found to result in some uptake from the cell surface, comparable to the loaded state, with much of the CD23 protein remaining in concentrated patches on the plasma membrane.

#### **4.2.5D GFP-CD23B UTILISES THE PHAGOCYTOTIC PATHWAY IN RAJI A CELLS WHEN LOADED WITH IGE AND WHEN LOADED WITH IGE AND SUBSEQUENTLY CROSS-LINKED WITH NIP<sub>10</sub>-BSA**

Figure 4.21 shows the results observed in the GFP-CD23b and LysoTracker co-localisation studies in Raji A cells. Representative image sets are shown for each condition; (i) basal, (ii) loaded, (iii) cross-linked with NIP<sub>10</sub>-BSA and (iv) 'ligated' with NIP<sub>1</sub>-Insulin. In the basal state GFP-CD23b was found to be predominantly located at the plasma membrane, with some movement observed within the plane of the membrane when the images were run together as a 'movie'. After loading with NIP-specific IgE antibody, the GFP-CD23b proteins were found to localise towards distinct areas on the plasma membrane, showing regions of concentrated fluorescence, classical of the receptor gathering into coated pits. Some evidence of cellular uptake was also observed. However it was not until the receptor was cross-linked with NIP<sub>10</sub>-BSA that marked uptake of the protein was observed from the cell surface. This uptake was noted as not only an increase in the amount of distinct patches present within the cytoplasm, but also by a decrease in the amount of GFP-CD23b present at the cell surface. In contrast to this, cross-linking with NIP<sub>1</sub>-Insulin resulted in little receptor uptake into the cell, with the vast majority of the protein remaining localised to distinct areas on the plasma membrane.



Co-localisation of the cell surface receptor with LysoTracker Red was observed in the basal, loaded and cross-linked (NIP<sub>10</sub>-BSA) states, primarily located within the cell. The presence of yellow patches, both at the cell surface, and within the cell, was most evident in the loaded state, suggesting the receptor is able to co-localise with LysoTracker Red. Cross-linking with NIP<sub>10</sub>-BSA appeared to cause directed uptake of the GFP-CD23b protein into the cytoplasm and there was some evidence of yellow patching within the cell, although some internalised patches did appear to remain green. Cross-linking with NIP<sub>1</sub>-Insulin resulted in patching at the cell surface, but very little (if any) uptake into the cell with no co-localisation observed. Collectively, the results gathered from the two previous sections suggest that the CD23b isoform may require extensive oligomerisation at the cell surface, achieved in these experimental conditions only after cross-linking with NIP<sub>10</sub>-BSA protein conjugates, as stimulus for directed uptake into the cell. No data was available for the GFP-CD23a isoform as the expression levels were too low to work with.

#### **4.2.6 ANALYSIS OF GFP-CD23 MUTANTS IN RAJI A CELLS**

Each of the CD23 mutant protein constructs, described in section 4.2.1, were used to transfect Raji A cells in an attempt to analyse the trafficking of these proteins in B lymphocytes.

##### **4.2.6A GENERATION OF G418-RESISTANT RAJI A CELLS EXPRESSING EACH OF THE GFP-CD23 MUTANT FUSION PROTEINS**

Raji A cells were electroporated (section 2.2.6B) with pcDNA3.1<sup>+</sup> constructs encoding each of the mutated GFP-CD23 proteins (Figure 4.1 and 4.2). After 7-8 weeks G418-resistant cell lines finally emerged and were assessed for CD23 protein expression by flow cytometry. The cells were analysed for GFP fluorescence (FL-1) as well as the presence of CD23 proteins using an anti-CD23-PE conjugated antibody (FL-2). Figures 4.22 and 4.23 show the results for the GFP-CD23a and GFP-CD23b mutants respectively. The results indicate that all the wild-type GFP-CD23 and mutant proteins are expressed to some extent in Raji A cells, with the majority of the stable cell lines demonstrating low levels of protein expression. However, the proteins did appear to remain targeted to the plasma membrane in the majority of cases, as demonstrated by the percentage of double positive cells, shown in the upper right-hand corner of each dot



plot. The FL-2 levels in each instance were expected to be higher than the FL-1 levels, due to the endogenous CD23 expressed at the surface.

#### **4.2.6B REAL TIME VISUALISATION OF EACH GFP-CD23 MUTANT PROTEIN IN RAJI A CELLS**

Each of the stably-transfected cell lines expressing the individual GFP-CD23 mutant CD23 proteins were assessed by laser scanning confocal microscopy. Initial experiments were performed to obtain information on the expression levels of each of the mutant proteins and to confirm that all these GFP-CD23 proteins could be visualised at the surface of Raji A cells. Figures 4.24 and 4.25 show representative images, detailing the typical initial staining patterns observed for each of the GFP-CD23a and GFP-CD23b mutants in the basal state. In agreement with the flow cytometric data (Figures 4.22 and 4.23), these images illustrate that all the GFP-CD23 proteins shown in these figures were indeed routed to the plasma membrane. A bright field image has also been included in order to identify the location and indeed presence of the Raji A cells, due to the fact the fluorescent signal was weak in many of the stably-transfected cell lines.

The expression levels observed in Raji A cells were generally much poorer than those observed using the HEK 293 cell system, however in many cases the resultant initial basal staining patterns of each mutant protein were similar. For example the aY6F and aYS67FA mutants indicate a predominantly punctate membrane distribution, as was found to be the case in the HEK 293 cells, whilst the bS5D and bS5F mutants demonstrate the presence of distinct foci of fluorescence within both cell types in the basal state. The aS7D, bP4R and bN2K expression patterns are also similar in both cell types. The Raji A aS7A mutant shows a less diffuse cytoplasmic staining pattern than was observed in the HEK 293 cells, whilst the Raji A bS5A mutants illustrate a staining pattern more like that observed in the second cell population described in Figure 4.10, similar to that observed for the bS5D and bS5F mutants in both cell types.

Limited data were collected for the GFP-CD23bP3R mutant (Figure 4.26), again due to low expression levels. It was difficult to draw definitive conclusions concerning the location of this mutant protein as two expression patterns were observed. In most of the



cells analysed this mutant was predominantly contained within the cytoplasm (Figure 4.26A, as was found to be the case in HEK 293 cells), with a few Raji A cells shown to express the mutant protein at reasonable levels at the cell surface (Figure 4.26 B). In contrast to the results observed with the HEK 293 cell system, these results may be explained as a direct effect of the protein expression levels observed in the Raji A stably-transfected cells. Cells expressing less protein may simply have less at the cell surface and therefore demonstrate very weak fluorescence at the plasma membrane rather than none at all. This theory is supported by the flow cytometric data present in Figure 4.23 and the confocal data presented in Figure 4.26A, however, further investigation would be required to clarify these findings in order to unequivocally establish the true expression pattern of the bP3R mutant in Raji A cells.

Initial attempts were made to investigate CD23 trafficking in Raji A cells. Entry into early endosomes and thus the endocytic pathway was investigated by co-localisation studies with transferrin-Texas Red dye (Tf-TxR). Figures 5.27-5.30 summarise the results obtained. The results indicate that the aS7A, aS7D, bS5A, bS5D, and bS5F mutants are able to co-localise with Tf-TxR in Raji A cells to some extent in the basal state. The findings were less clear for the aY6F and aYS67FA mutants due to the poorer expression levels demonstrated by these proteins. Loading and cross-linking studies were not performed for these stably-transfected Raji A cells expressing the GFP-CD23 mutants as the percentage of cells expressing good levels of the GFP-CD23 proteins were generally very low. The limited timescale attached to this project did not permit either the generation of further stably-transfected cell lines, or the selection (via FACs sorting, 2.2.2B) and propagation of individual cells illustrating reasonable expression levels.

### 4.3 DISCUSSION

The studies presented here, like those already discussed in chapter 3, demonstrate the usefulness of GFP-CD23 fusion proteins, the NIP system and the HEK 293 cell line in the analysis of receptor-mediated (endocytic) trafficking. As a direct extension to this work, this chapter also details some preliminary studies of CD23 trafficking in a B cell line. The principal findings to emerge from the research described in this chapter are the



importance of the serine residues located at the unique N-terminus in each of the CD23 proteins, as well as the NPP motif in the CD23b isoform.

The trafficking pathways of the wild-type CD23 isoforms were studied in detail in chapter 3. In summary, the wild-type CD23 isoforms were found to demonstrate minimal (if any) co-localisation with Tf-TxR in either the basal or loaded state (Figure 3.7 and 3.8), and only the CD23a isoform was found to readily enter the endocytic pathway after cross-linking with IgE and polyvalent antigen. The CD23b isoform was not found to enter the endocytic pathway in HEK 293 cells in any of the basal, loaded or cross-linked states. In contrast, this chapter demonstrates that many of the N-terminal CD23 mutant proteins were found to have very different trafficking patterns, with many demonstrating both internalisation and co-localisation with Tf-TxR in the basal state.

One plausible explanation for the data observed is that the presence of the aspartate residue mimics the effect of phosphorylation of the original serine residue and stimulates directed uptake of CD23 into the endosomal pathway, via a means of receptor-mediated endocytosis. This hypothesis suggests the phosphorylation state of the CD23 molecule may be an important regulator in its sorting from the cell surface. Support for this interpretation is provided by the serine to alanine mutations. These mutant proteins were observed to demonstrate a somewhat diffuse cellular staining pattern throughout the cytoplasm of HEK 293 cells, with the bS5A mutant illustrating two different expression patterns. This mutation alters the serine residue, preventing its possible phosphorylation. This suggests that CD23 trafficking becomes random in the absence of this important serine residue at the N-terminal tail in both isoforms and poses the question of its importance in the initial targeting of these proteins to the plasma membrane. The images collected support the interpretation that the majority of the aS7A CD23 protein never reaches the membrane, but rather accumulates in the cytoplasm instead. This suggests a role for the phosphorylation of the serine residue in the initial targeting of the CD23 isoform to the cell surface. Although there are no data formally demonstrating the phosphorylation of the N-terminal serine residues in either of the two CD23 proteins, the data from the aS7D and aS5D mutants suggest that a negatively charged moiety at these points facilitates movement into the same pathway as Tf-TxR. Further support for this conclusion is available from the data collected from



the bS5F mutant protein. Traditionally this type of mutation (as is true for the Y-to-F mutation) mimics a constitutively phosphorylated receptor molecule by incorporating the large phenylalanine side chain (although the residue is not actually phosphorylated itself). This protein was demonstrated to have a very similar trafficking pathway to that observed for the bS5D mutant, only demonstrating more internalisation within the cell. These data suggest that the CD23 molecule may favour internalisation if the N-terminal serine residue remains phosphorylated. This routing is presumably targeted at low pH compartments, or in class II MHC<sup>+</sup> cells, towards vesicles containing newly synthesised or re-cycling MHC class II proteins. This conclusion assumes that both the CD23a and CD23b isoforms are able to traffic via the endosomal pathway, unless actively routed via another sorting pathway. One consideration which must be taken into account is HEK 293 cells do not possess a classical phagocytic pathway therefore the CD23b mutants may have been routed via the endosomal pathway as default. The only way to investigate this further would be to perform similar experiments in a cell line capable of phagocytosis.

Mutation of the NPP motif in the CD23b isoform provided valuable mutants (bN2K, and bP4R) able to enter into the endocytic pathway, as determined by co-localisation with Tf-TxR, in sharp contrast to the wild-type CD23b proteins. It may be that these CD23b mutants, likewise with the bS5D and bS5F proteins, only enter the endosomal pathway in this cell system as a default internalisation pathway, due to the fact that the classical phagocytic pathway is not available in HEK 293 cells. Ideally, these proteins should all be expressed and tested in a B cell line, enabling further investigation of the functional importance of these amino acid changes and the ability of these mutants to swap internalisation pathways in a natural host cell type, before this hypothesis can be tested further.

Collectively, the results point to the importance of the phosphorylation state of a number of key residues effecting CD23 protein trafficking. The question remains as to which kinase (or kinases) may be involved in the phosphorylation of these serine residues at position 7 and 5 in the CD23a and CD23b protein isoforms respectively. This also leads to the question of how the phosphorylation event, should it take place, be interpreted by the intracellular trafficking machinery. It is likely that other proteins



are recruited to facilitate the internalisation of the CD23 proteins from the cell surface. This proposed model is discussed further, in the context of known molecular sorting pathways, in the main conclusion and discussion chapter.

The Raji A cell line was a natural choice in order to take the CD23 trafficking studies into B lymphocytes due to the fact these cells are an adherent B cell line (facilitating growth on glass cover-slips and easy confocal analysis) and they also express endogenous CD23 proteins. However, obtaining stably-transfected Raji A cell lines expressing each of the GFP-CD23 fusion proteins was somewhat troublesome, often resulting in stables with either uniformly low protein expression levels or mixed populations illustrating different levels of protein expression. These findings indicate that the selection process requires revision, possibly incorporating a FACs sorting step to effectively 'handpick' cells expressing the desired level of the fusion protein of interest. These cells could then be maintained under selection and cultured as usual, serving to generate stably-transfected cell lines demonstrating useful, and uniform levels of protein expression.

The data collected from the stably-transfected Raji A cell lines generated in this work was limited as a direct result of the poor expression levels. The wild-type GFP-CD23b isoform was found to co-localise with both Tf-TxR and more so with LysoTracker Red dye, suggesting this isoform may use both the endocytic and phagocytic route of cellular entry in Raji A cells. The GFP-CD23a isoform was not studied in co-localisation experiments due to low protein expression levels. These initial studies demonstrate somewhat complicated results, suggesting the CD23b isoform to be able to utilise both the endocytic and phagocytic pathway in Raji A cells. These findings, and the rest of the results presented in this chapter, are discussed further in the main conclusion chapter.

Basal trafficking studies with Tf-TxR were also performed for each of the mutant proteins, however this incomplete data set cannot neither fully support, nor refute the information gained from the same trafficking studies performed in HEK 293 cells. However, regardless of the problems encountered, many of the results observed for the CD23 mutant proteins support those observed for basal trafficking of the same mutants



in HEK 293 cells. These findings indicate two things; firstly they provide further evidence supporting the use of HEK 293 cells as an initial model system to study receptor-mediated endocytic trafficking and secondly they indicate the Raji A cells to be a useful system, should the protocol be modified in such a way to facilitate higher protein expression levels.

The information potentially available from trafficking studies performed in Raji A cells is of great significance due to the fact that these cells possess all the necessary sorting machinery and correct protein repertoire to process GFP-tagged CD23 as they would naturally process their endogenous CD23 molecules. It is therefore a great achievement to have shown these cells to be capable of producing stably-transfected cell lines, expressing our protein of interest. Obviously this basic protocol requires some modification to address the issue of protein expression levels.

On a more negative note, one possible disadvantage of the GFP-tagged approach could be the potential over expression of the GFP-tagged protein, which may subsequently lead to the saturation of certain accessory molecules necessary for folding/targeting or signalling resulting in the presentation of false results. It should also be noted that the microscopic analysis discussed within could have been strengthened and less subjective had there been software available to quantify various properties on the recorded images, such as the extent of cross-linking etc. These two points should be addressed in the future modification of these experimental procedures.



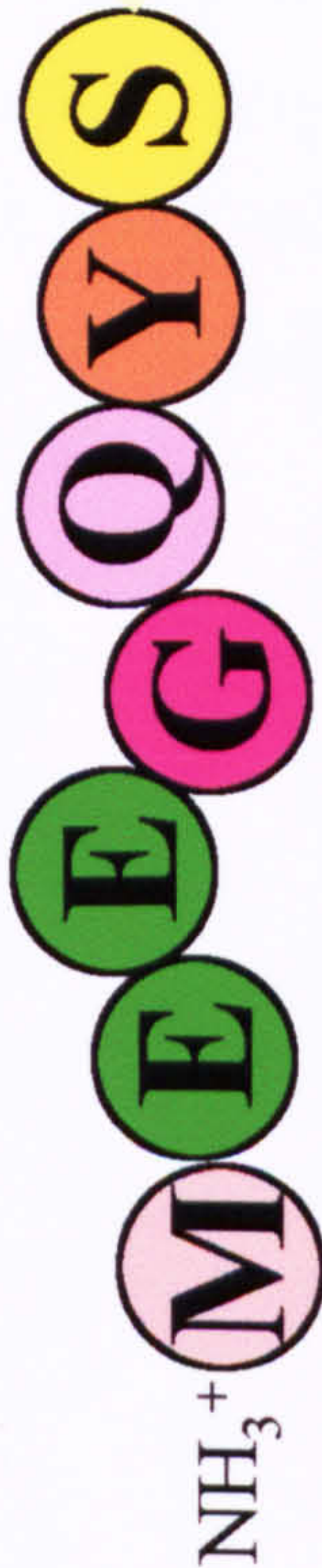
## **FIGURE 4.1 GENERATION OF MUTANT GFP-CD23A FUSION PROTEINS**

Each of the CD23 mutant constructs were generated using specifically designed oligonucleotides and the Stratagene QuikChange Mutagenesis kit, as detailed in section 2.2.5. This figure shows the sequences of the oligonucleotides used to generate each of the CD23a mutant proteins. The nucleic acids detailed in blue represent the unique tail section in each isoform and the specific base mutations have been shown in red. The resultant mutant proteins are also shown, with the altered amino acids highlighted in colour. The proteins were named according to the amino acid changes incorporated and this nomenclature is also given.



WT CD23a

ATG GAG GAA GGT CAA TAT TCA GAG ATC GAG GAG C  
TAC CTC CTT CCA GTT ATA AGT CTC TAG CTC CTC G



CD23a Y6F

5'-C ATG GAG GAA GGT CAA TTT TCA GAG ATC GAG GAG C-3'  
3'-G TAC CTC CTT CCA GTT AAA AGT CTC TAG CTC CTC G-5'



CD23a YS67FA

5'-CC ATG GAG GAA GGT CAA TTT GCA GAG ATC GAG GAG CTT CC-3'  
3'-GG TAC CTC CTT GGA GTT AAA CGT CTC TAG CTC CTC GAA GG-5'



CD23a S7A

5'-G GAG GAA GGT CAA TAT GCA GAG ATC GAG GAG C-3'  
3'-C CTC CTT CCA GTT ATA CGT CTC TAG CTC CTC C-5'



CD23a S7D

5'-CC ATG GAG GAA GGT CAA TAT GAT GAG ATC GAG GAG CTT CCC-3'  
3'-GG TAC CTC CTT CCA GTT ATA CTA CTC TAG CTC CTC GAA GGG-5'





## **FIGURE 4.2 GENERATION OF MUTANT GFP-CD23B FUSION PROTEINS**

Each of the CD23 mutant constructs were generated using specifically designed oligonucleotides and the Stratagene QuikChange Mutagenesis kit, as described in section 2.2.5. This figure shows the sequences of the oligonucleotides used to generate each of the CD23b mutant proteins. The nucleic acids detailed in blue represent the unique tail section in each isoform and the specific base mutations have been shown in red. The resultant mutant proteins are also shown, with the altered amino acids highlighted in colour. The proteins were named according to the amino acid changes incorporated and this nomenclature is also given.



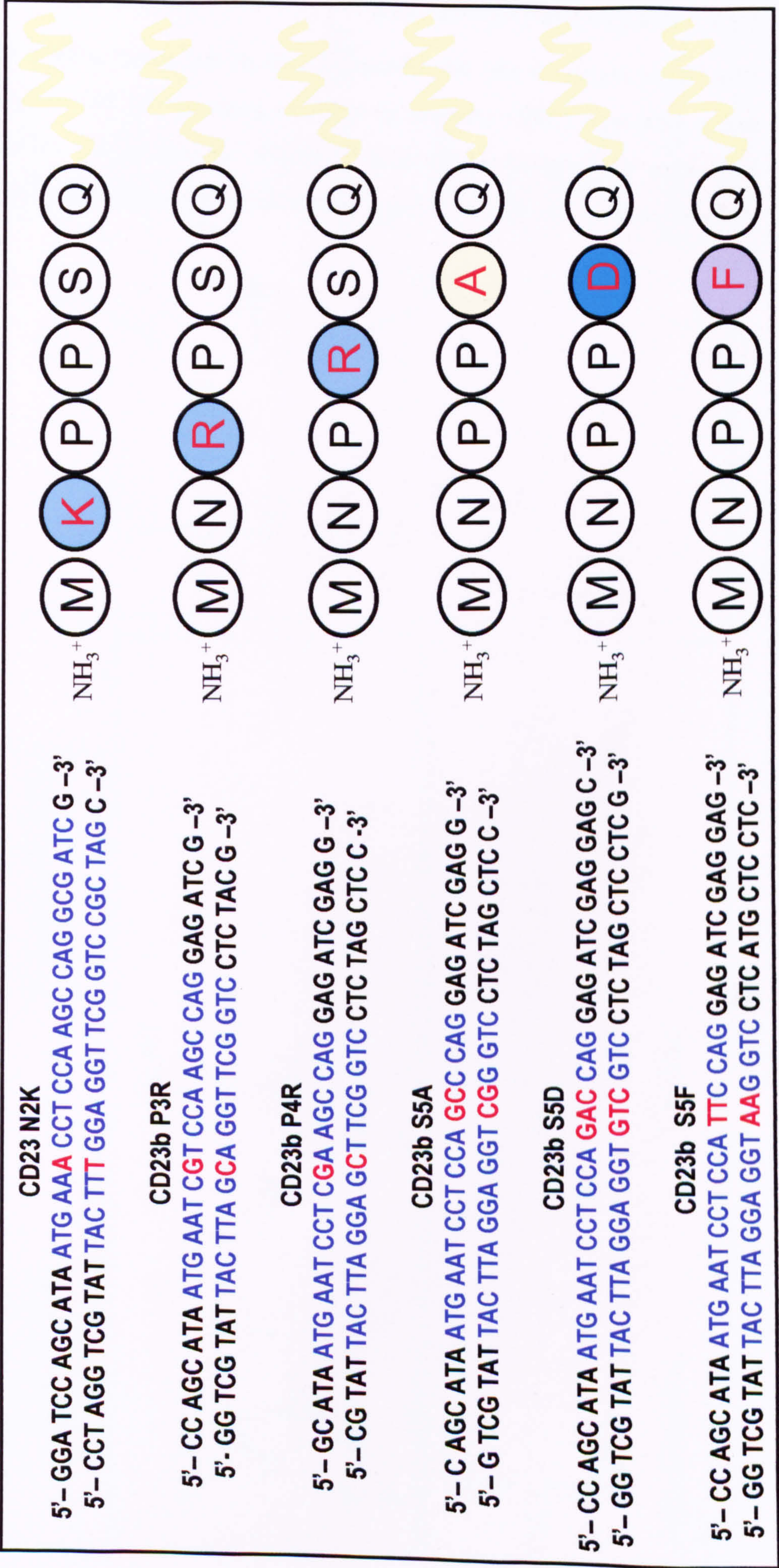




### **FIGURE 4.3 AMINO ACID SIDE CHAINS - THE RELEVANCE OF EACH OF THE MUTATIONS GENERATED**

This figure illustrates the side chains of each of the amino acids that have been altered in the wild-type CD23 proteins in order to generate the 10 mutant CD23 proteins. In each case the original amino acid is shown, as well as the amino acid it has been replaced with in the mutant. Sites of potential phosphorylation have been highlighted in blue.



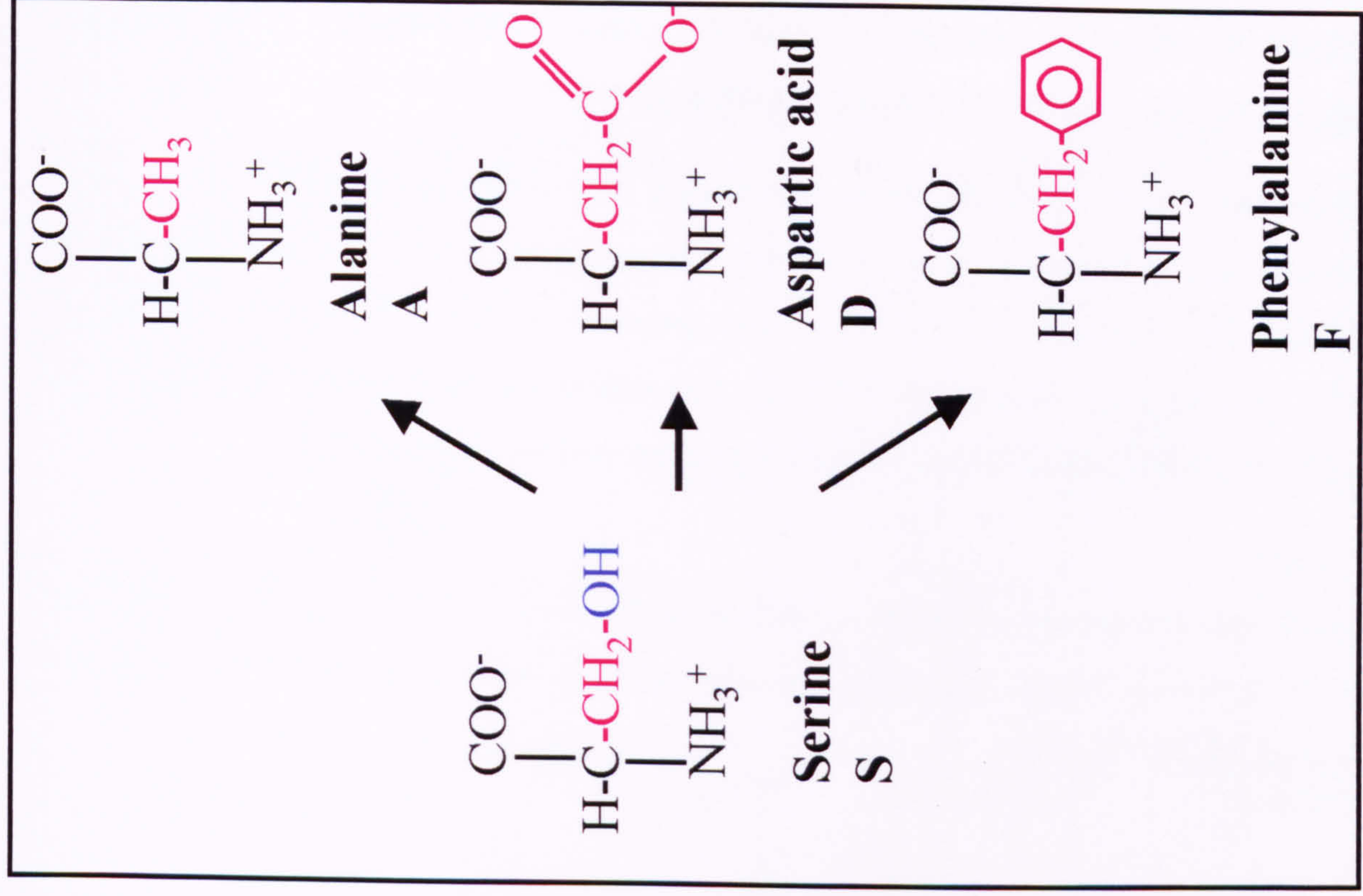
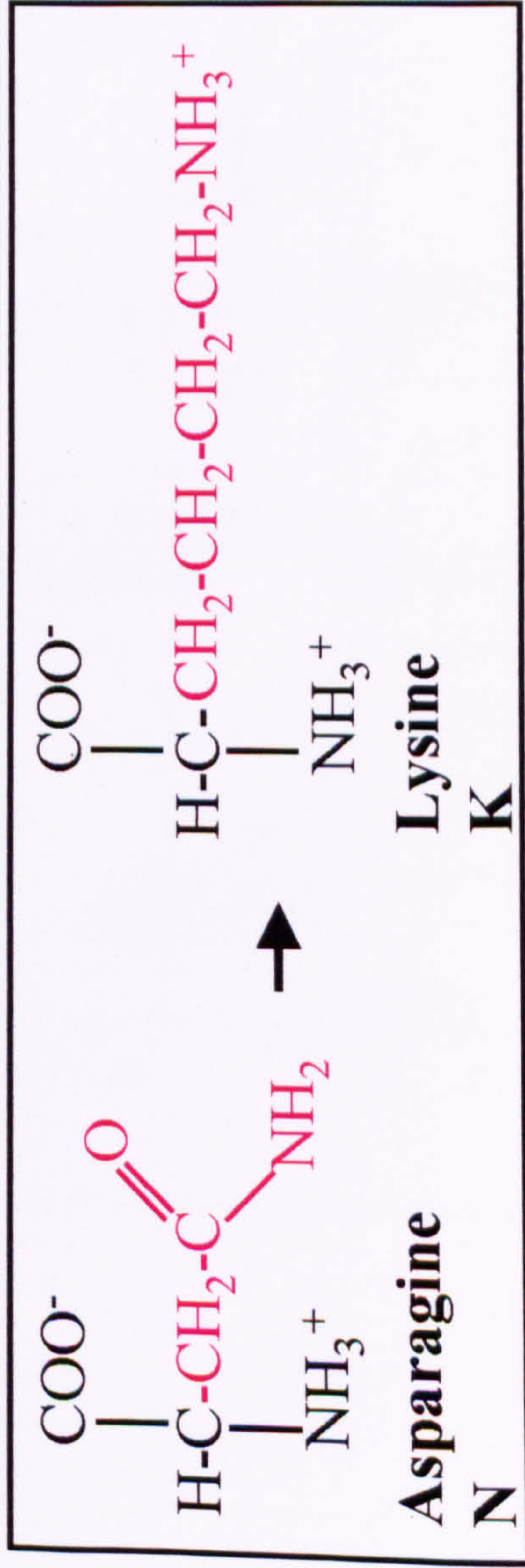
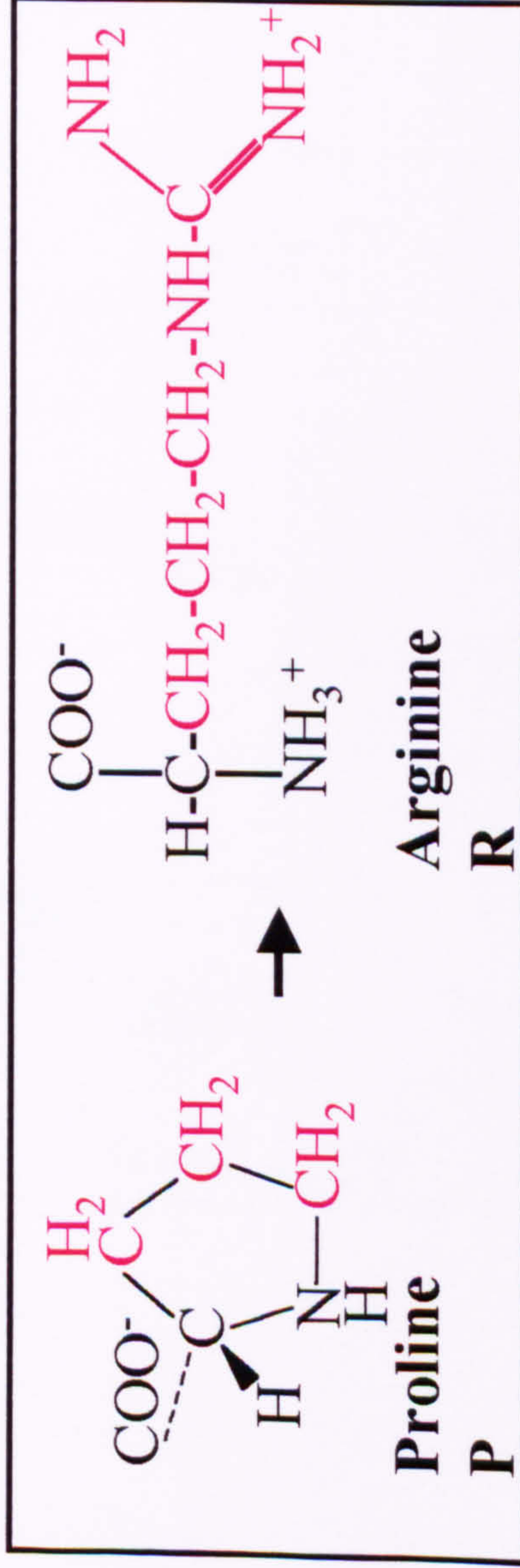
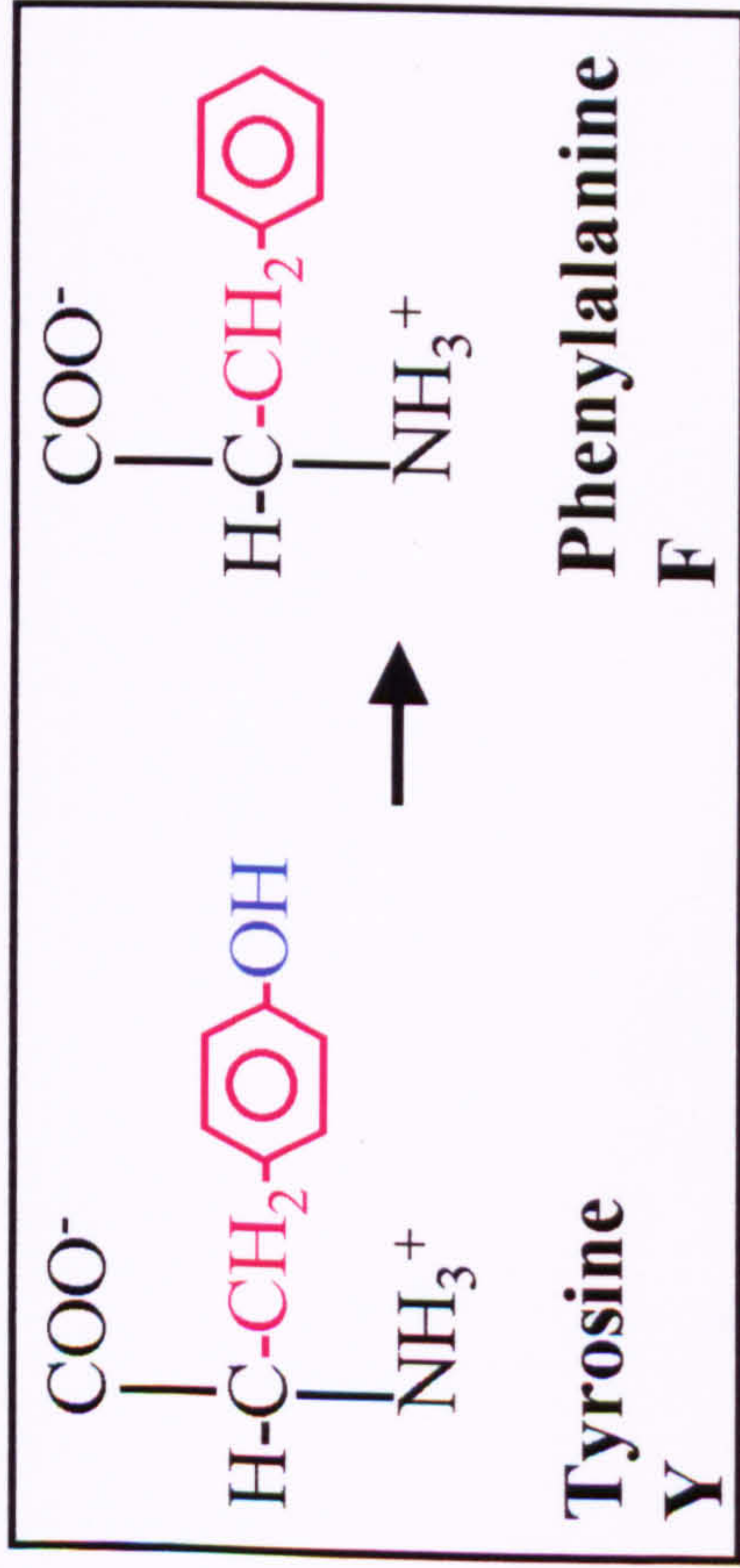


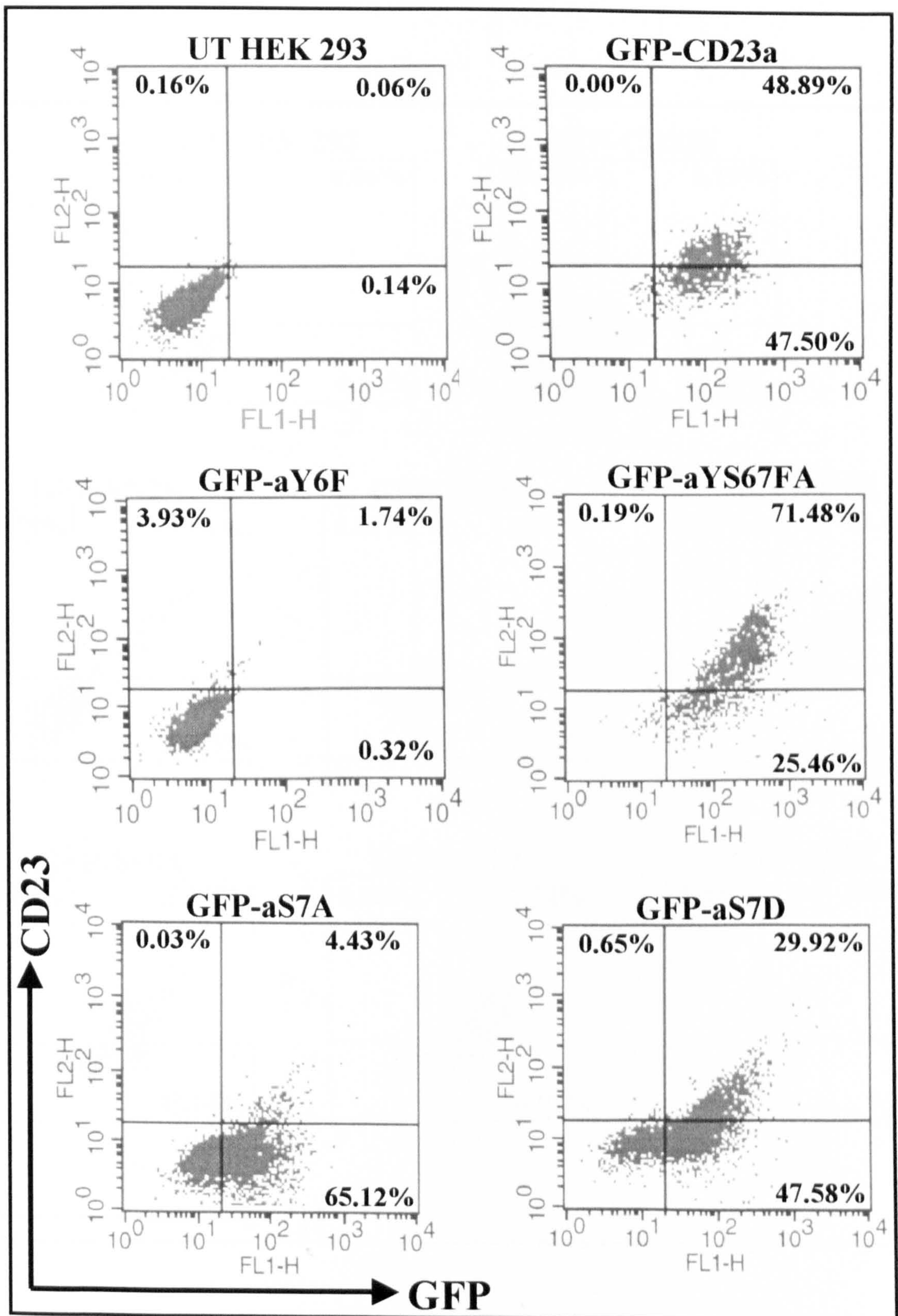


#### **FIGURE 4.4 HEK 293 CELLS STABLY EXPRESS ALL OF THE GFP-CD23 MUTANT FUSION PROTEINS AT THE PLASMA MEMBRANE - CD23BP3R APPEARS TO BE THE EXCEPTION TO THE RULE**

G418-resistant HEK 293 cells stably transfected with each of the mutant GFP-CD23 constructs were subjected to flow cytometry. The presence of CD23 was detected by an anti-CD23 PE antibody (FL-2), whilst the presence of the GFP tag was detected directly, from its green fluorescence (FL-1). The data has been presented as a number of dot-plots enabling the percentage of double positive cells to be calculated.

Although the percentage of double positives in the GFP-CD23aY6F is also relatively small the following figure illustrates that this mutant is indeed expressed at the plasma membrane.







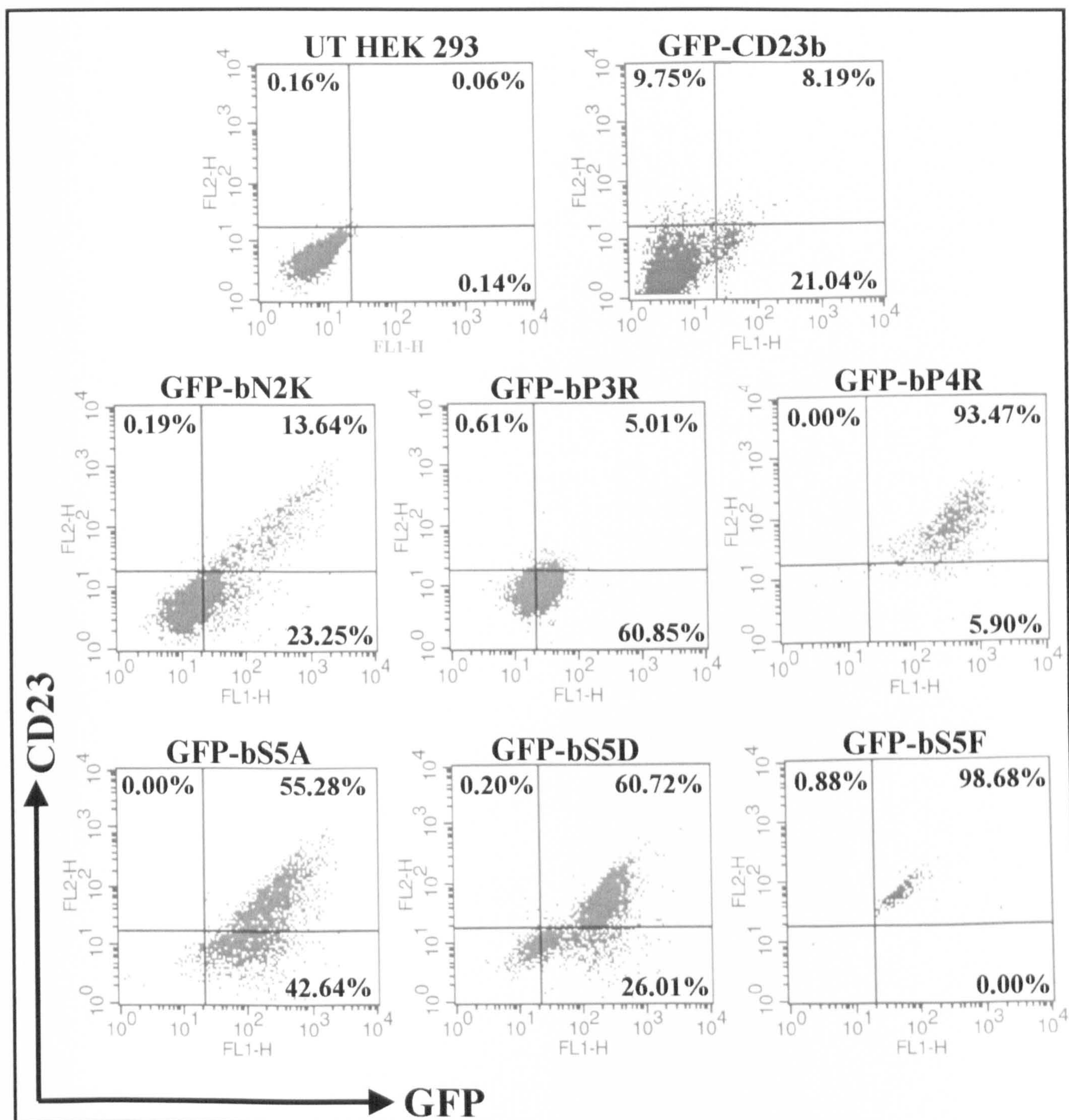


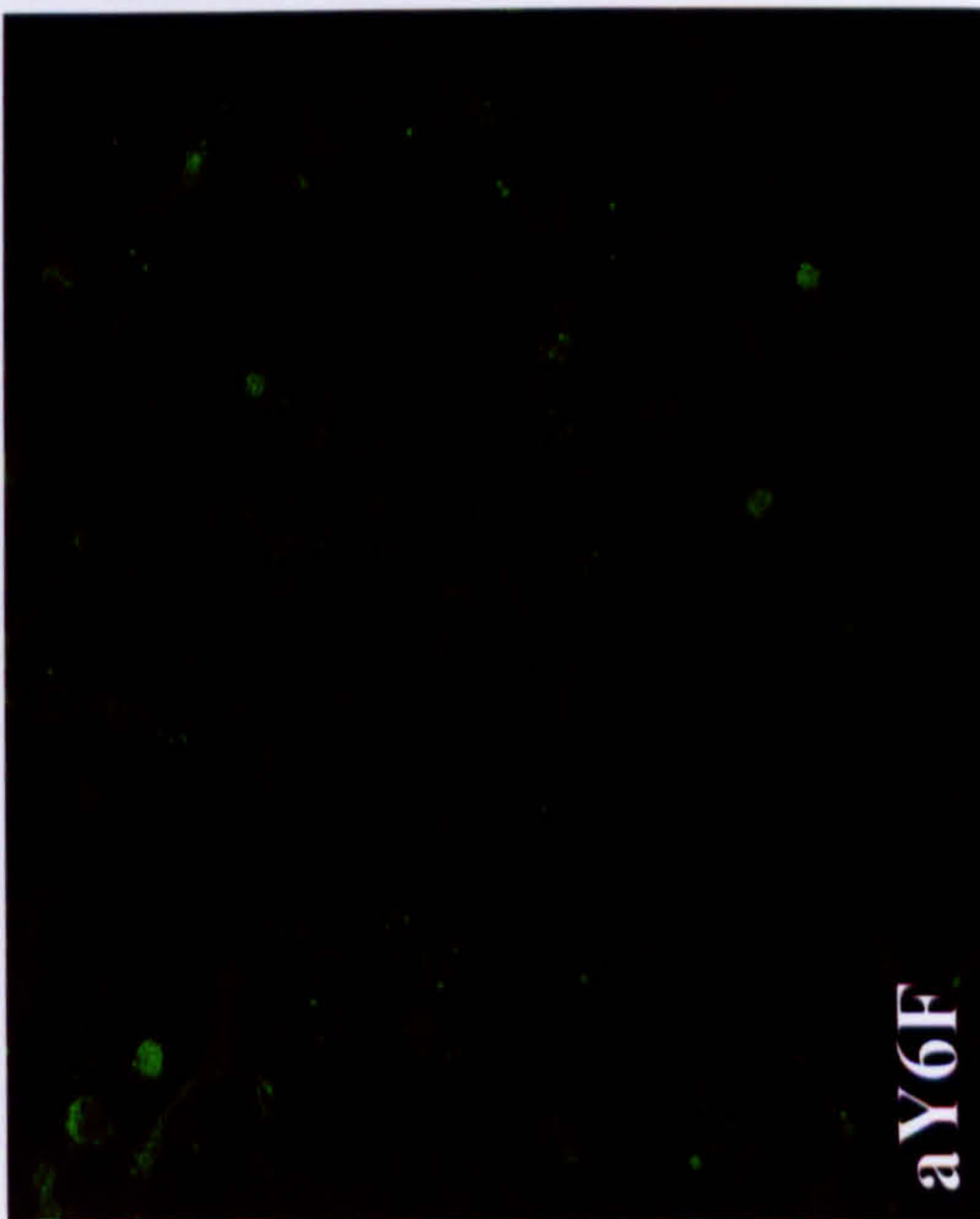
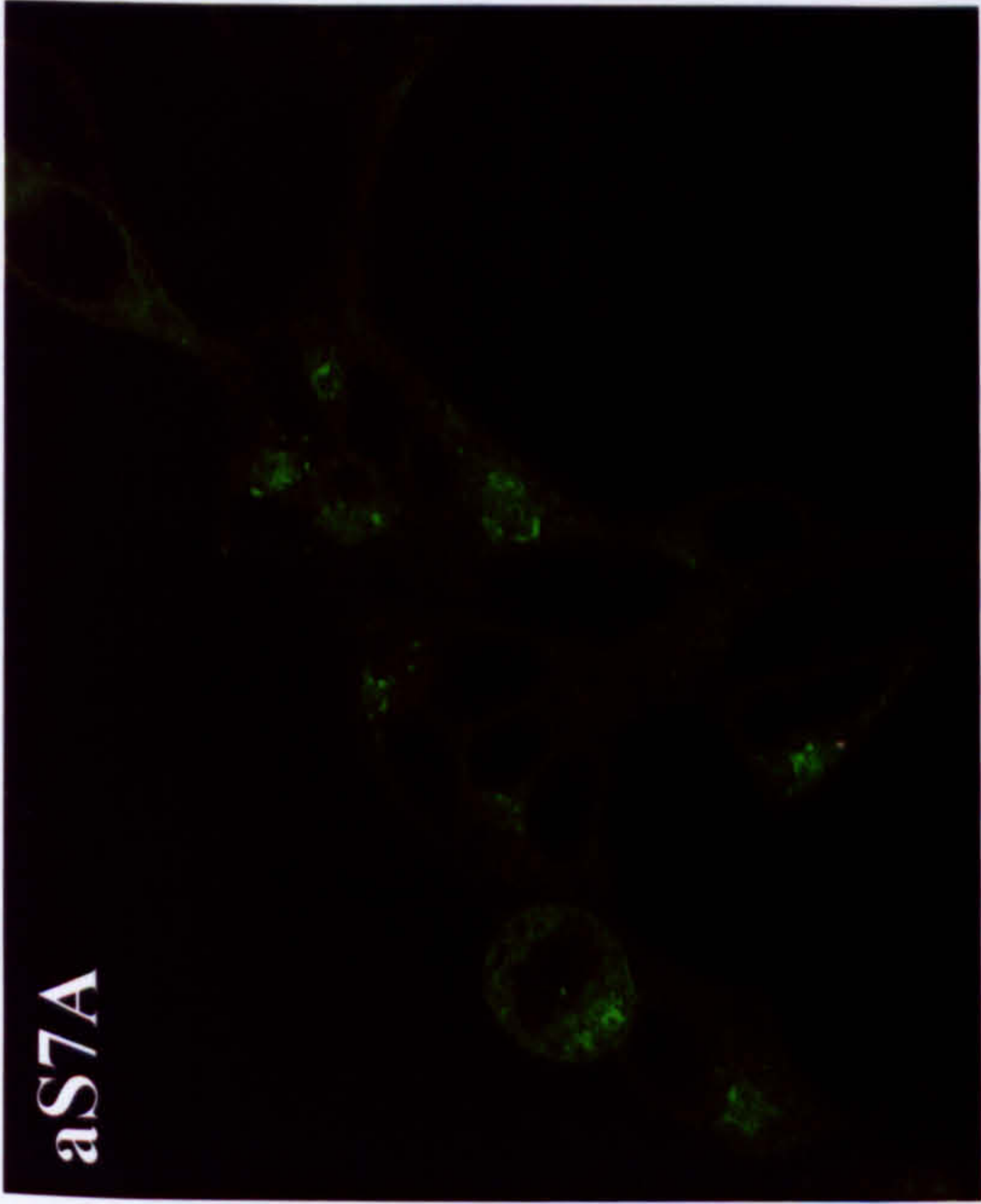
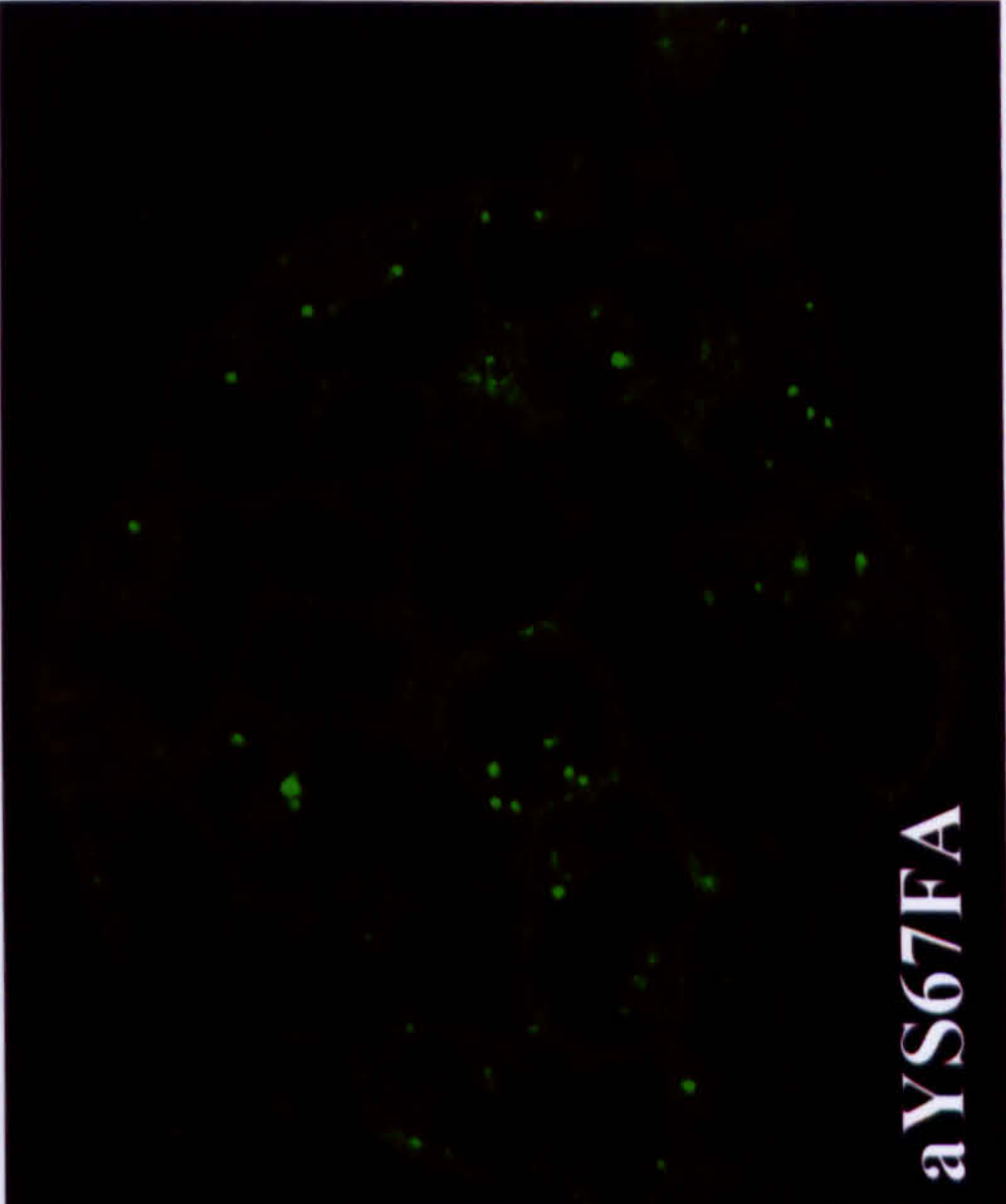
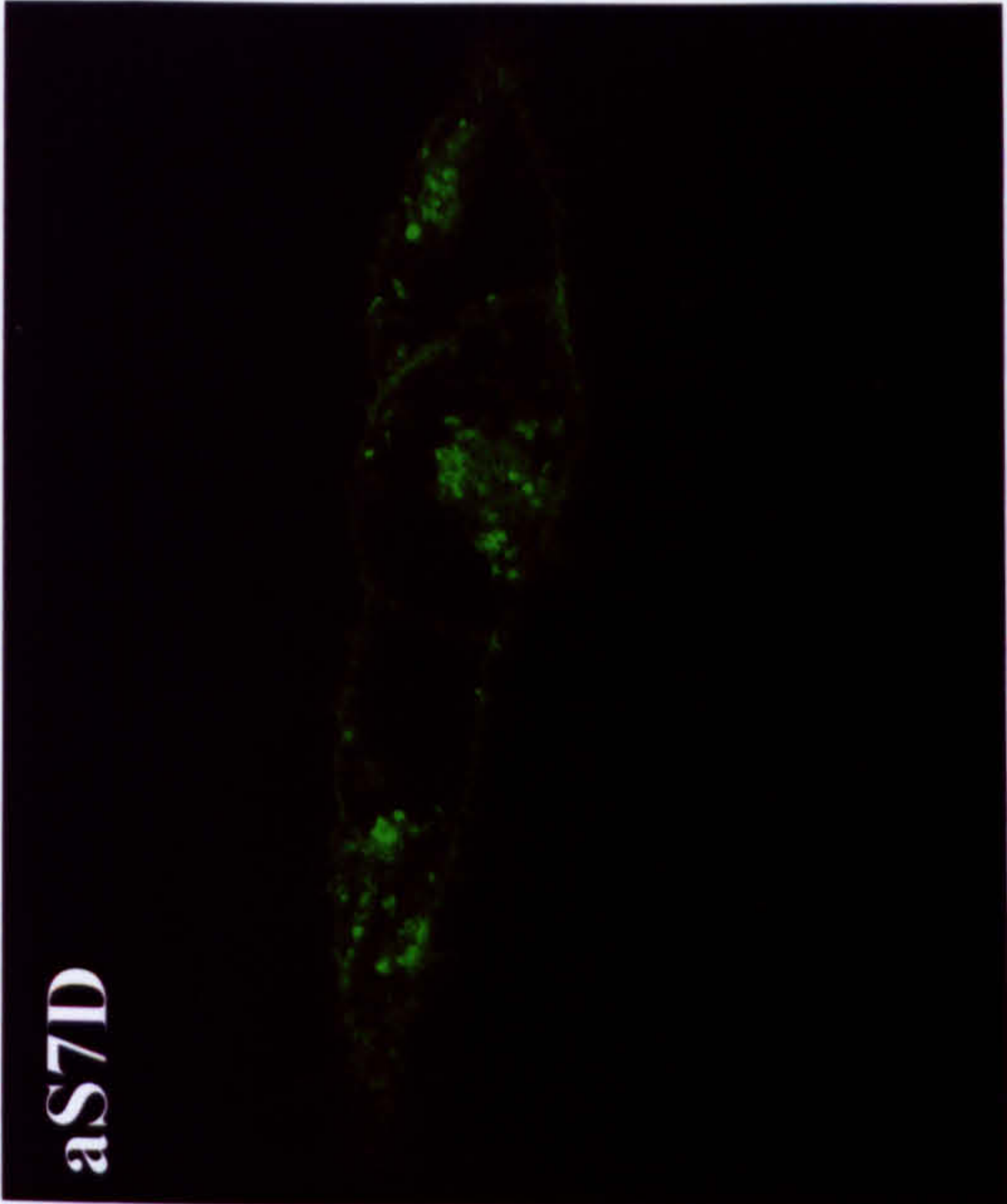


#### **FIGURE 4.5 CELLULAR LOCALISATION OF EACH OF THE GFP-CD23 MUTANT FUSION PROTEINS IN HEK 293 – GFP-CD23BP3R DOES NOT REACH THE PLASMA MEMBRANE**

G418-resistant HEK 293 cells stably transfected with each of the GFP-CD23 mutant proteins were propagated for 48 hours on poly-D-lysine (PDL) coated coverslips before being harvested, washed in KRH buffer and subjected to confocal analysis. The images demonstrate the localisation of each of the mutant proteins in the basal state, and indicate that the bP3R mutant appears to be the only CD23 protein studied that is unable to target to the plasma membrane.



GFP-CD23a Mutants





## GFP-CD23b Mutants

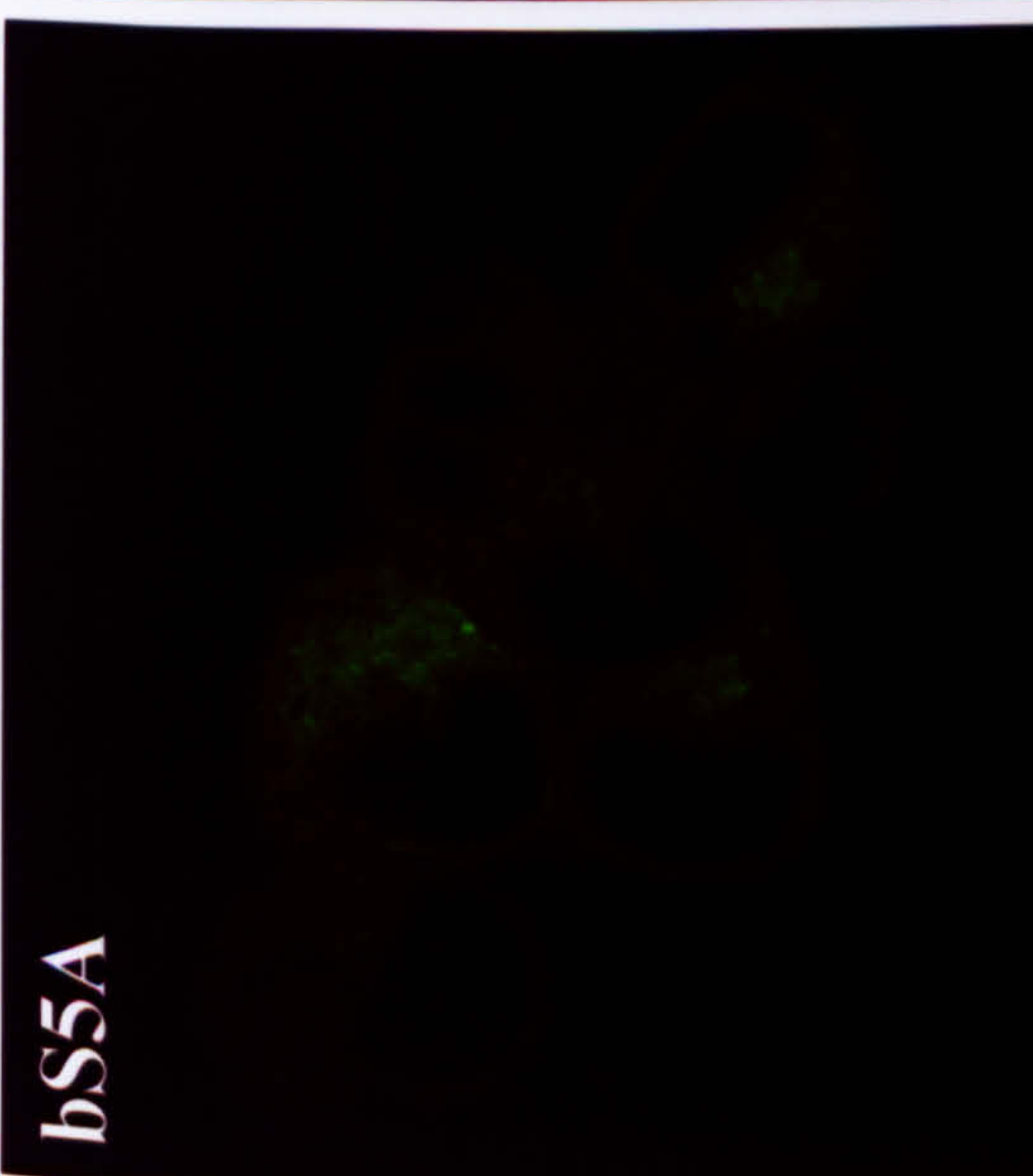
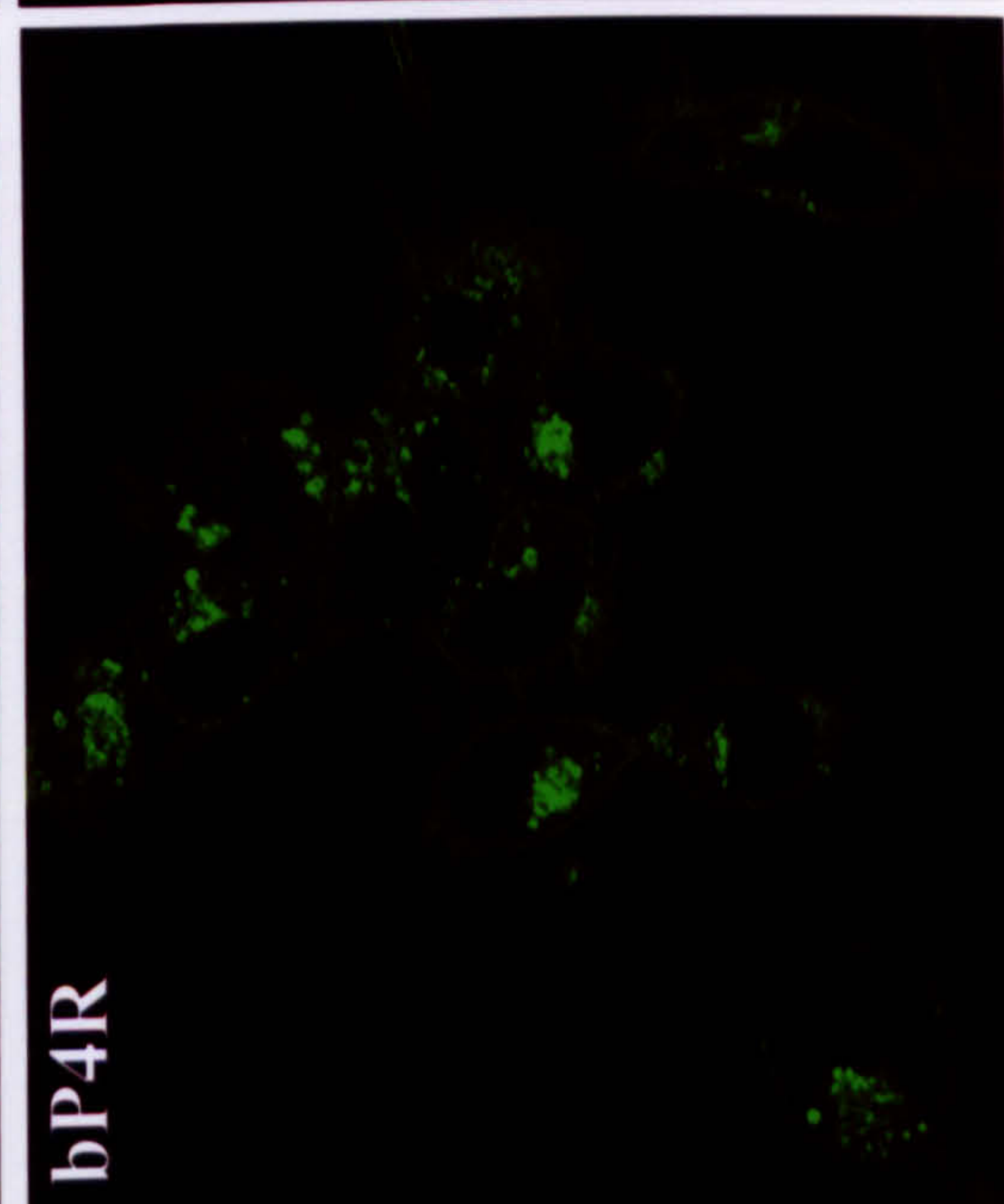
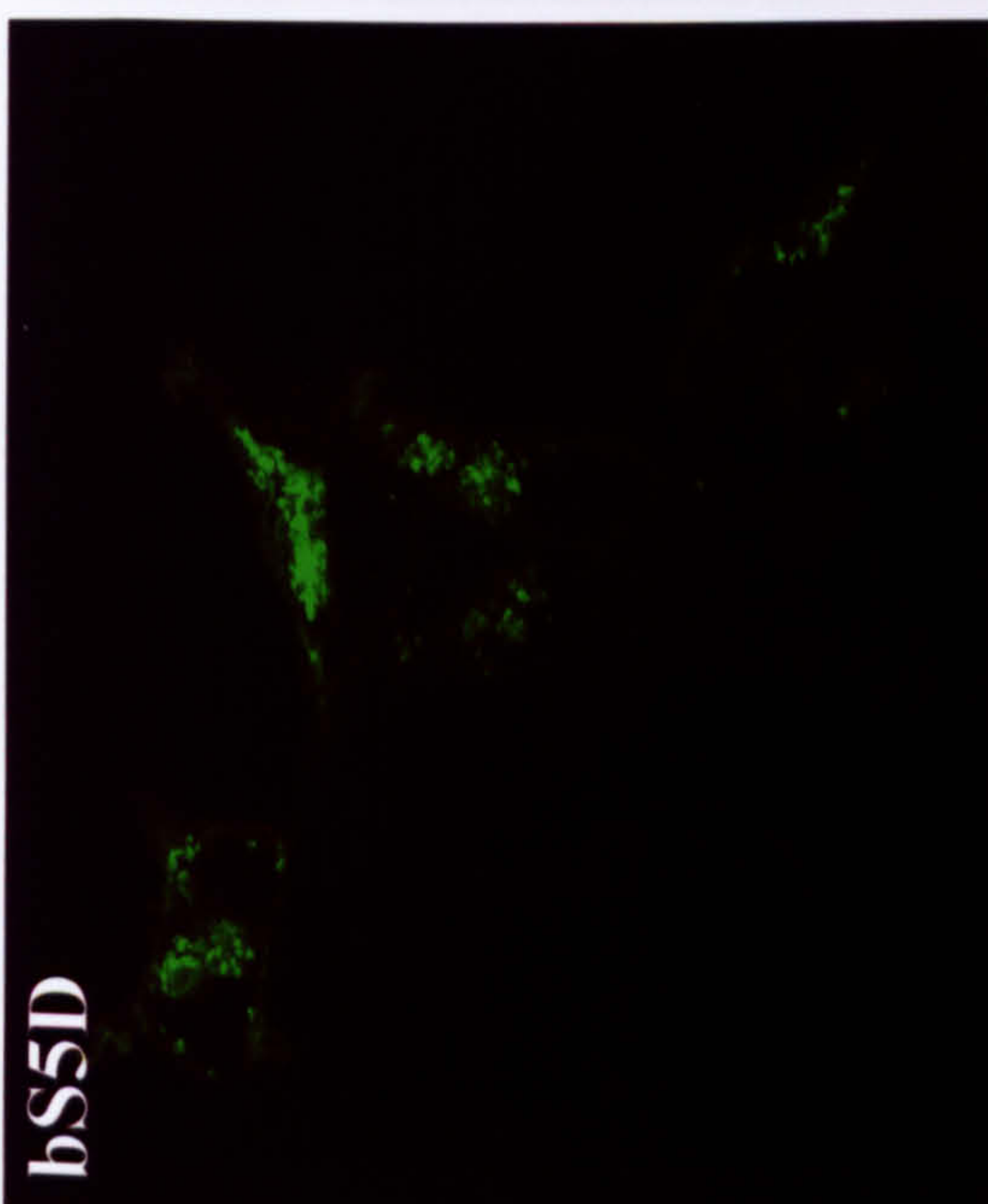
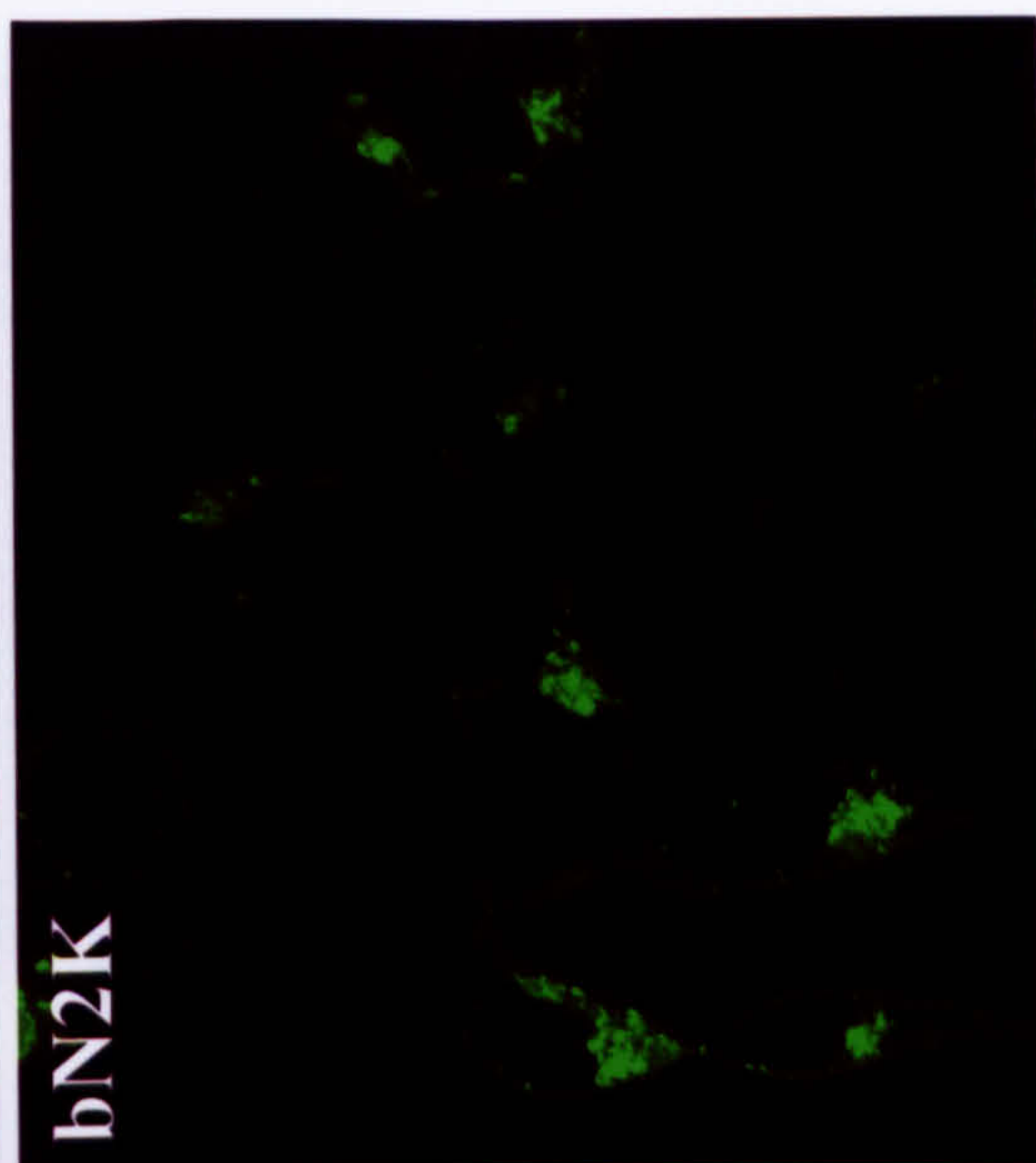
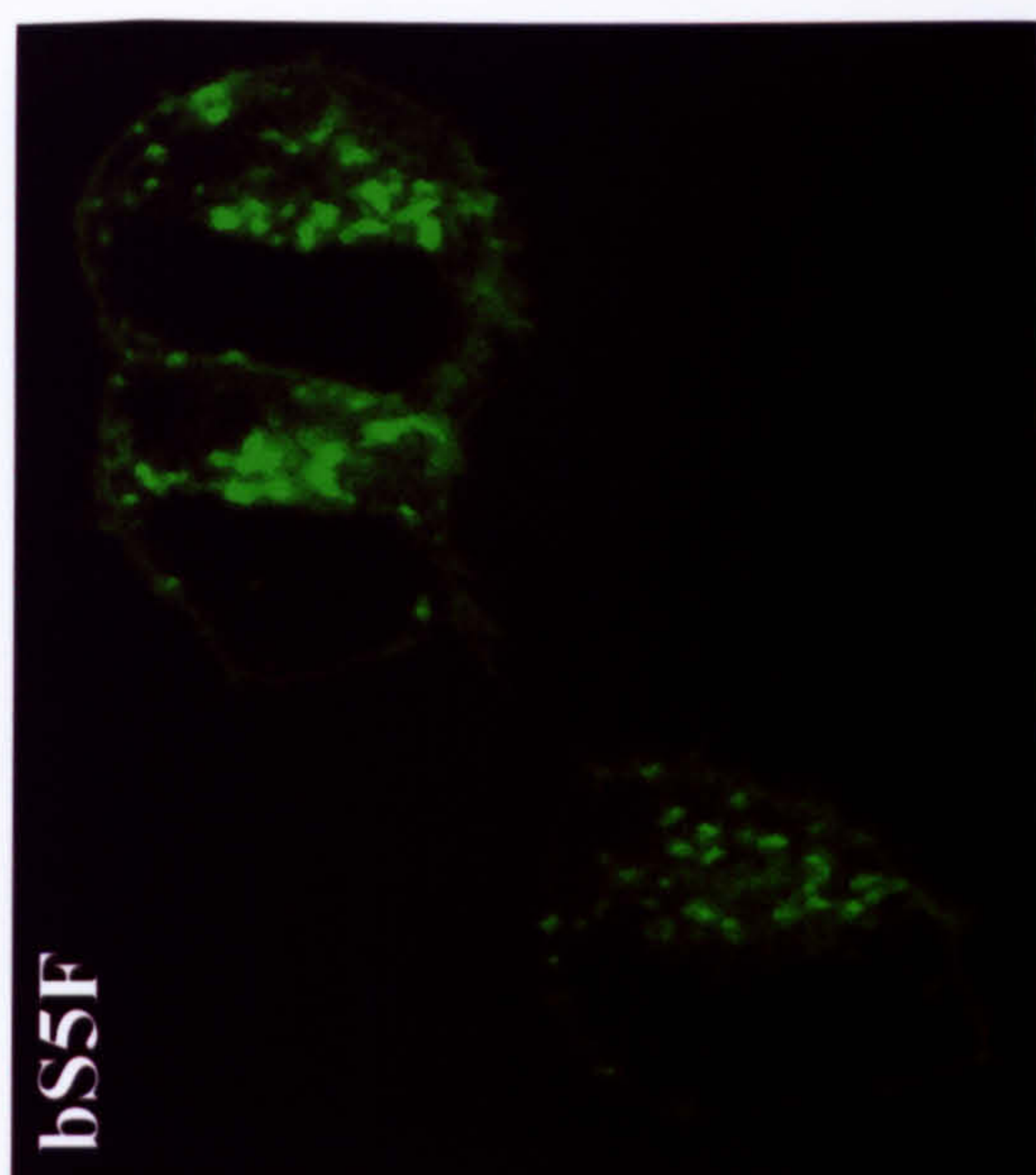




## **FIGURE 4.6 GFP-CD23aS7A PROTEIN CO-LOCALISES WITH TRANSFERRIN-MODIFIED TEXAS RED (Tf-TxR) IN HEK 293 CELLS**

Coverslips bearing G418-resistant HEK 293 cells expressing the GFP-CD23aS7A protein were pre-incubated with 20µg Tf-TxR prior to confocal analysis. The cells were exposed to (B) no stimulus, (L) 1µg NIP-specific IgE or (XL) 1µg NIP-specific IgE followed by the addition of 1µg NIP<sub>10</sub>-BSA and examined by confocal microscopy over a 45 minute period. The images shown demonstrate the typical staining patterns observed for this mutant in each of the (B) basal, (L) loaded and (XL) cross-linked states respectively.

The basal and loaded states demonstrate diffuse staining throughout the cytoplasm of the HEK 293 cells. GFP-CD23aS7A fusion proteins were found to enter the cell via directed uptake and co-localise with Tf-TxR and thus the early endosomal system, but only after being loaded with NIP-specific IgE and then cross-linked with NIP-BSA.



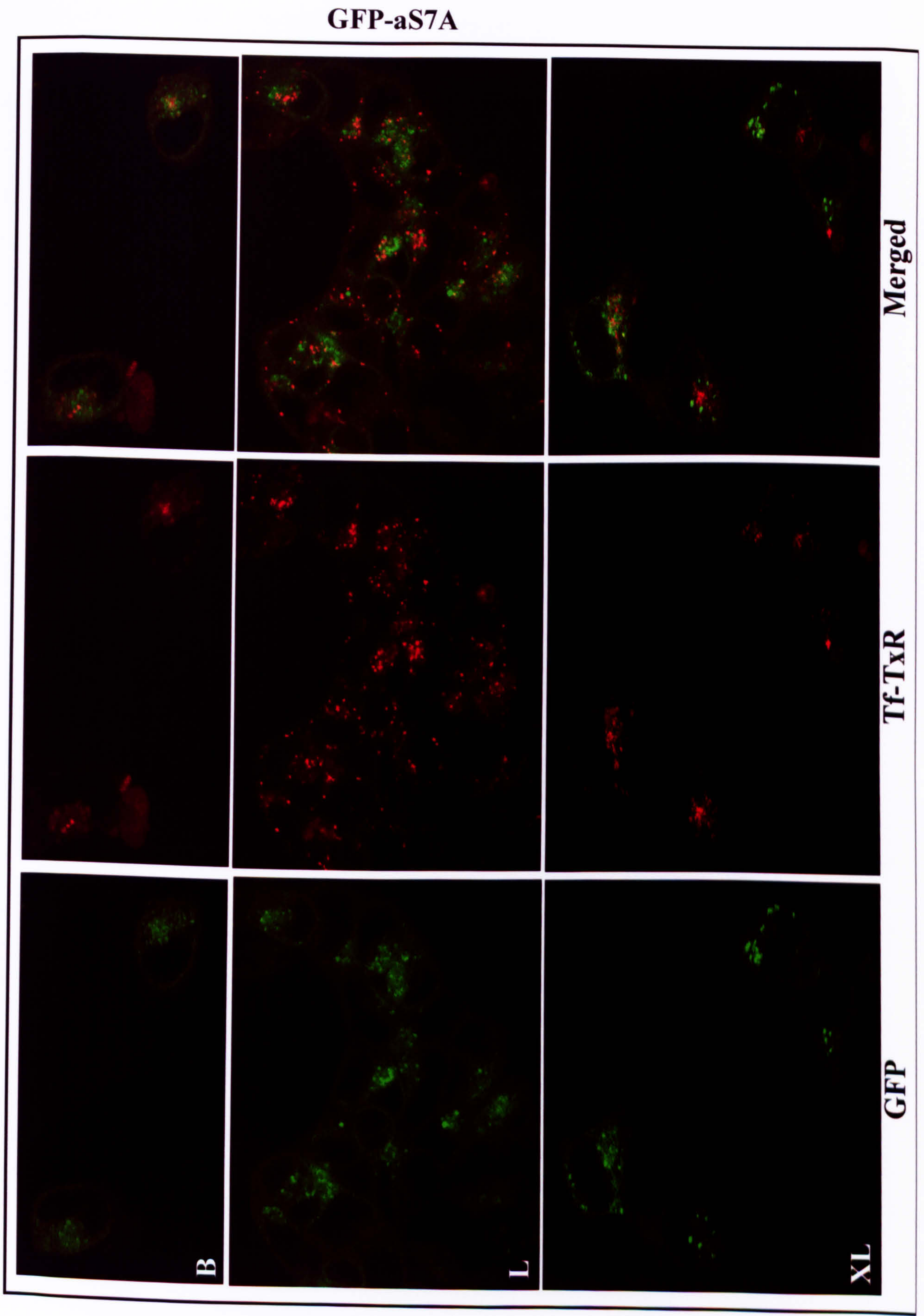




## **FIGURE 4.7 GFP-CD23aS7D PROTEIN CO-LOCALISES WITH TRANSFERRIN-MODIFIED TEXAS RED (Tf-TxR) IN HEK 293 CELLS**

Coverslips bearing G418-resistant HEK 293 cells expressing the GFP-CD23aS7D protein were pre-incubated with 20µg Tf-TxR prior to confocal analysis. The cells were exposed to (B) no stimulus, (L) 1µg NIP-specific IgE or (XL) 1µg NIP-specific IgE followed by the addition of 1µg NIP<sub>10</sub>-BSA and examined by confocal microscopy over a 45 minute period. The images shown demonstrate the typical staining patterns observed for this mutant in each of the (B) basal, (L) loaded and (XL) cross-linked states respectively.

GFP-CD23aS7D fusion proteins were found to enter the cell via directed uptake and co-localise with Tf-TxR and thus the early endosomal system in all three, basal, loaded and cross-linked states.



GFP-aS7D

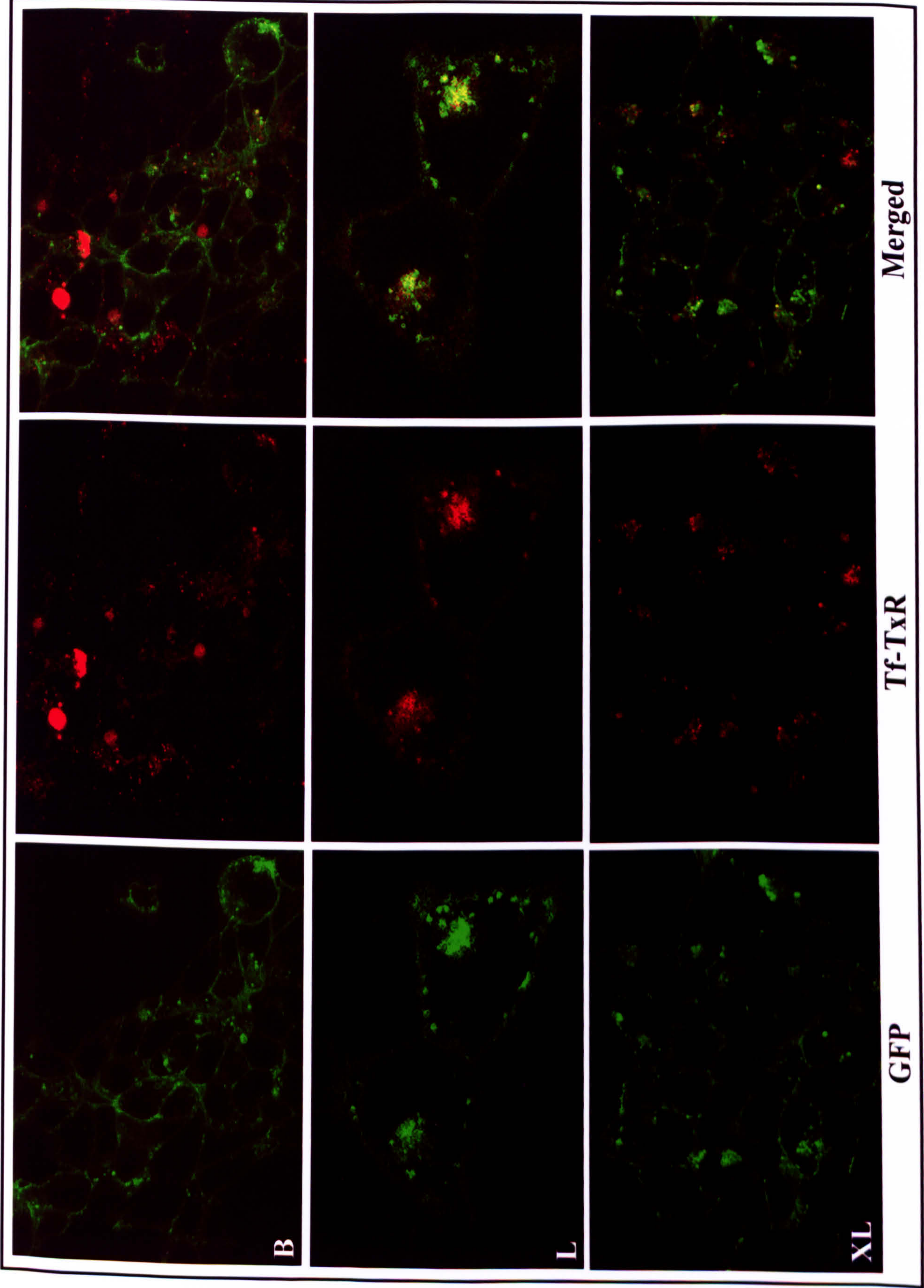




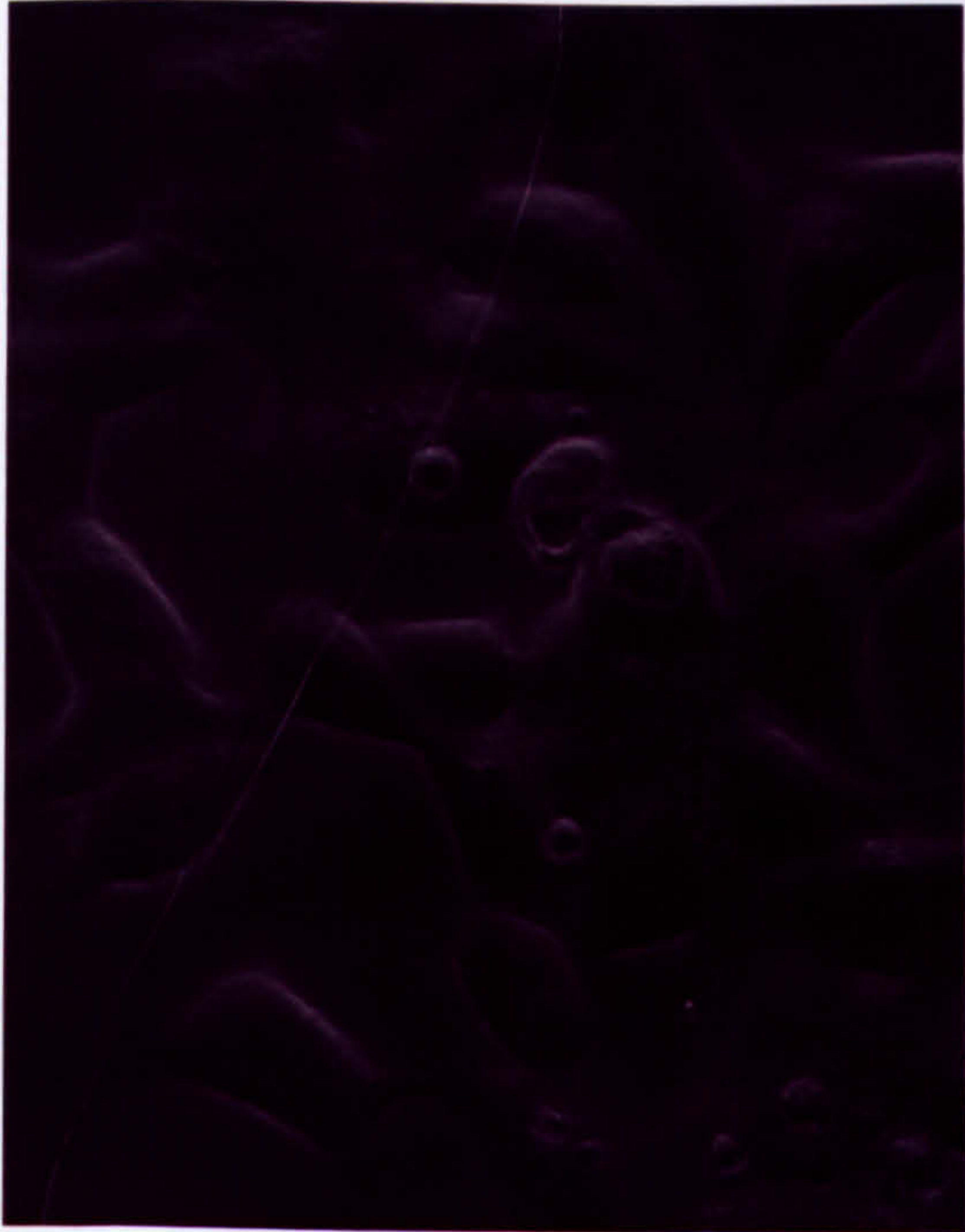
## **FIGURE 4.8 GFP-CD23AY6F PROTEIN CO-LOCALISES WITH TRANSFERRIN-MODIFIED TEXAS RED (Tf-TxR) IN HEK 293 CELLS**

Coverslips bearing G418-resistant HEK 293 cells expressing the GFP-CD23aY6F protein were pre-incubated with 20µg Tf-TxR prior to confocal analysis. The cells were examined in the basal state and it was observed that this mutant protein was expressed at very low levels in these stably transfected cells. Other GFP-CD23 aY6F-expressing cell lines were made, but with the same end result of low protein expression. The images shown are representative of the data obtained for each of the GFP-CD23aY6F cell lines. The cells were not exposed to either NIP-specific IgE or the NIP<sub>10</sub>-BSA as to the fact the CD23 receptor was present at such low levels its trafficking patterns could not be assessed as per the rest of the GFP-CD23 mutant proteins.

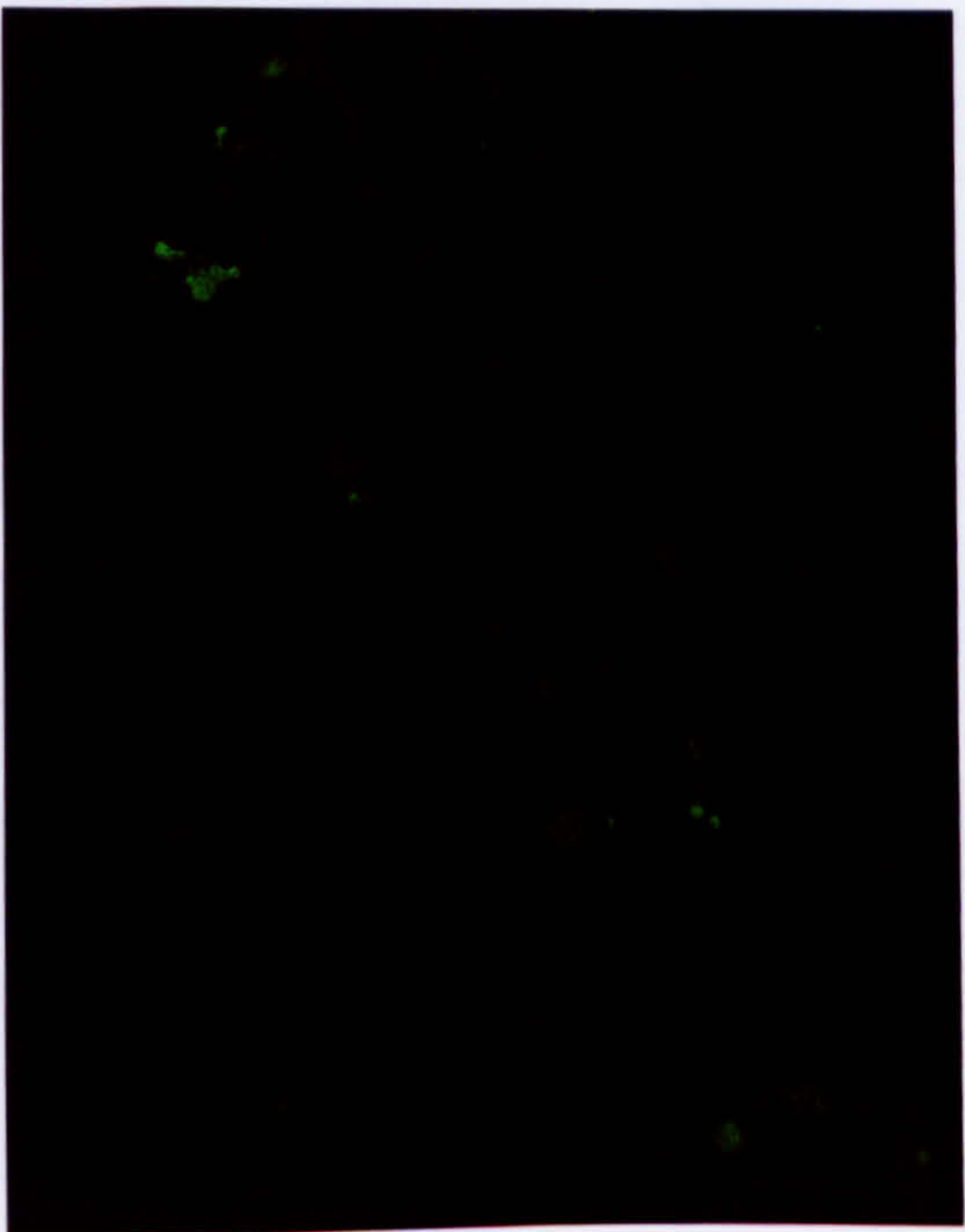
The GFP-CD23aY6F fusion proteins were found to reach the plasma membrane and there was some evidence of a punctate distribution at the cell surface in the basal state. Evidence of co-localisation was observed with Tf-TxR indicating that this protein was able to travel via the endosomal pathway within HEK 293 cells in an unoccupied state. The GFP-CD23aY6F fusion proteins were expressed in insufficient amounts to facilitate the usual trafficking studies under loaded and cross-linked conditions.



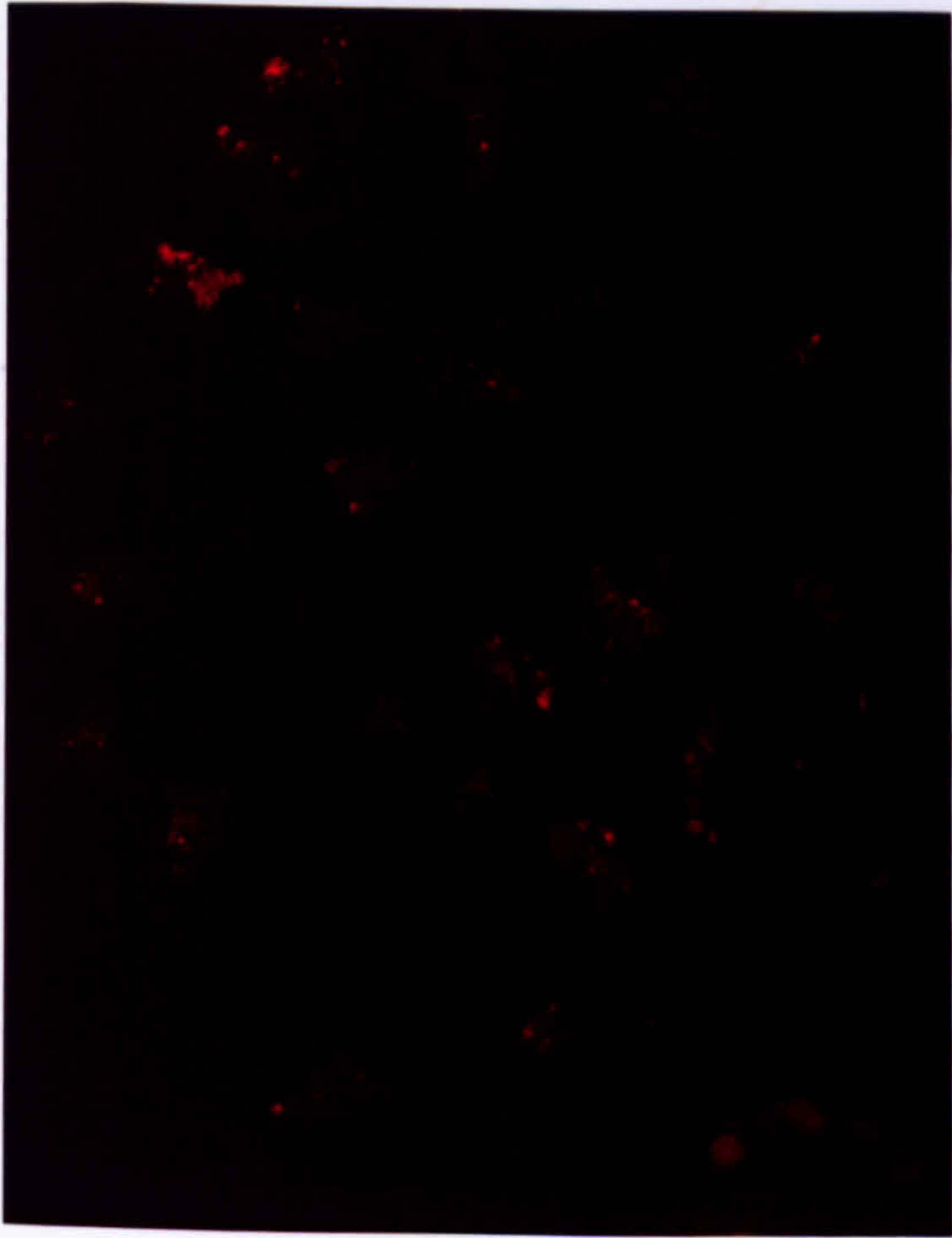
**GFP-aY6F**



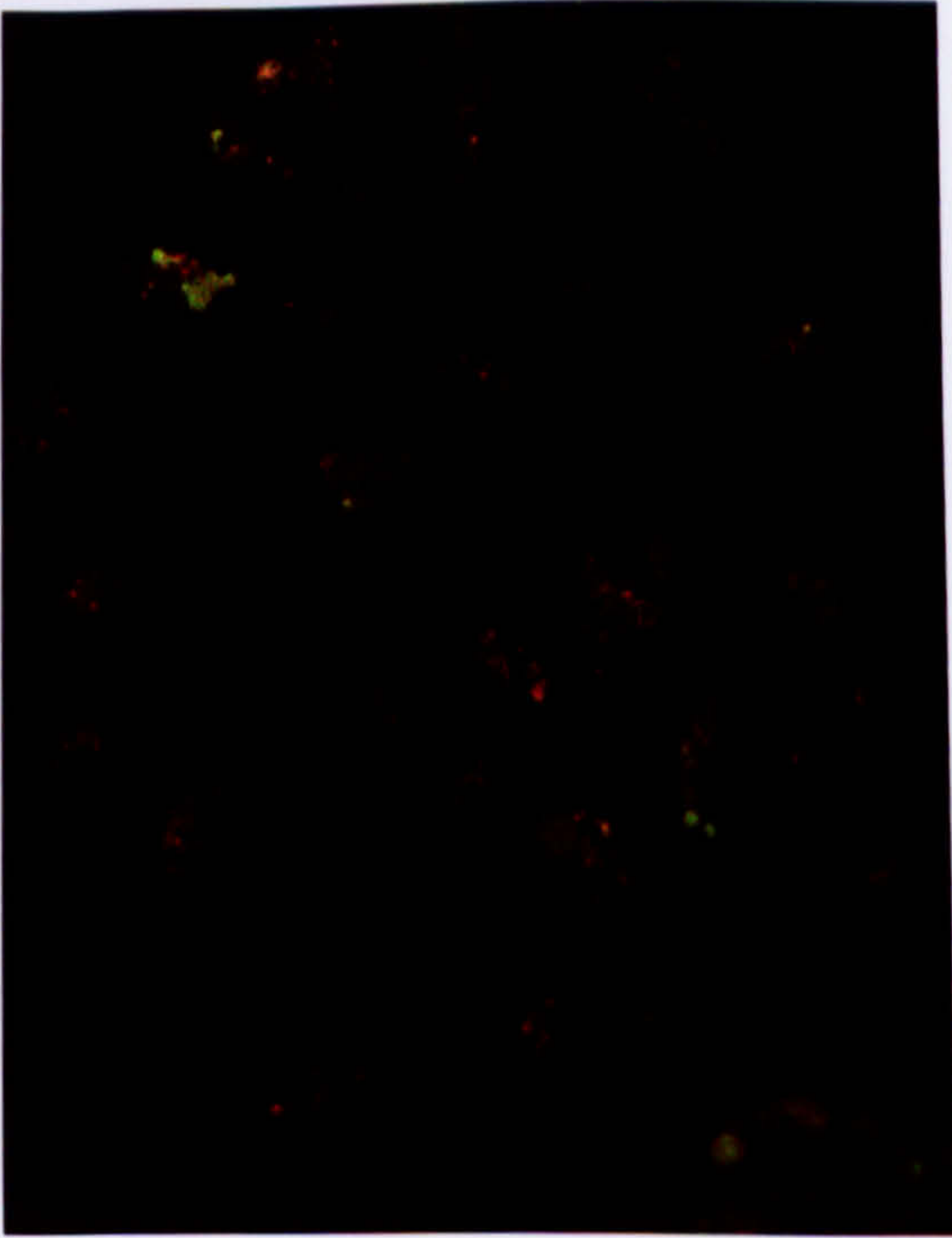
**Bright Field**



**GFP**



**Tf-TxR**



**Merged**



## **FIGURE 4.9 GFP-CD23aYS67FA PROTEIN CO-LOCALISES WITH TRANSFERRIN-MODIFIED TEXAS RED (Tf-TxR) IN HEK 293 CELLS**

Coverslips bearing G418-resistant HEK 293 cells expressing the GFP-CD23aYS67FA protein were pre-incubated with 20µg Tf-TxR prior to confocal analysis. The cells were exposed to (B) no stimulus, (L) 1µg NIP-specific IgE or (XL) 1µg NIP-specific IgE followed by the addition of 1µg NIP<sub>10</sub>-BSA and examined by confocal microscopy over a 45 minute period. The images shown demonstrate the typical staining patterns observed for this mutant in each of the (B) basal, (L) loaded and (XL) cross-linked states respectively.

GFP-CD23aYS67FA fusion proteins were found to enter the cell via directed uptake and co-localise with Tf-TxR and thus the early endosomal system in all three, basal, loaded and cross-linked states. The punctate morphology is pronounced in the loaded state where the aYS67FA mutant was also observed to co-localise extensively with the Tf-TxR probe. Co-localisation was also evident, to a far lesser extent, within the cell. In the cross-linked state, the aYS67FA mutant was found to have a very punctate morphology, so much so that practically every cell was surrounded by concentrated foci of green fluorescence, separated by patches of no fluorescence. Co-localisation was observed, but much less so than in the loaded state.



GFP-aYS67FA

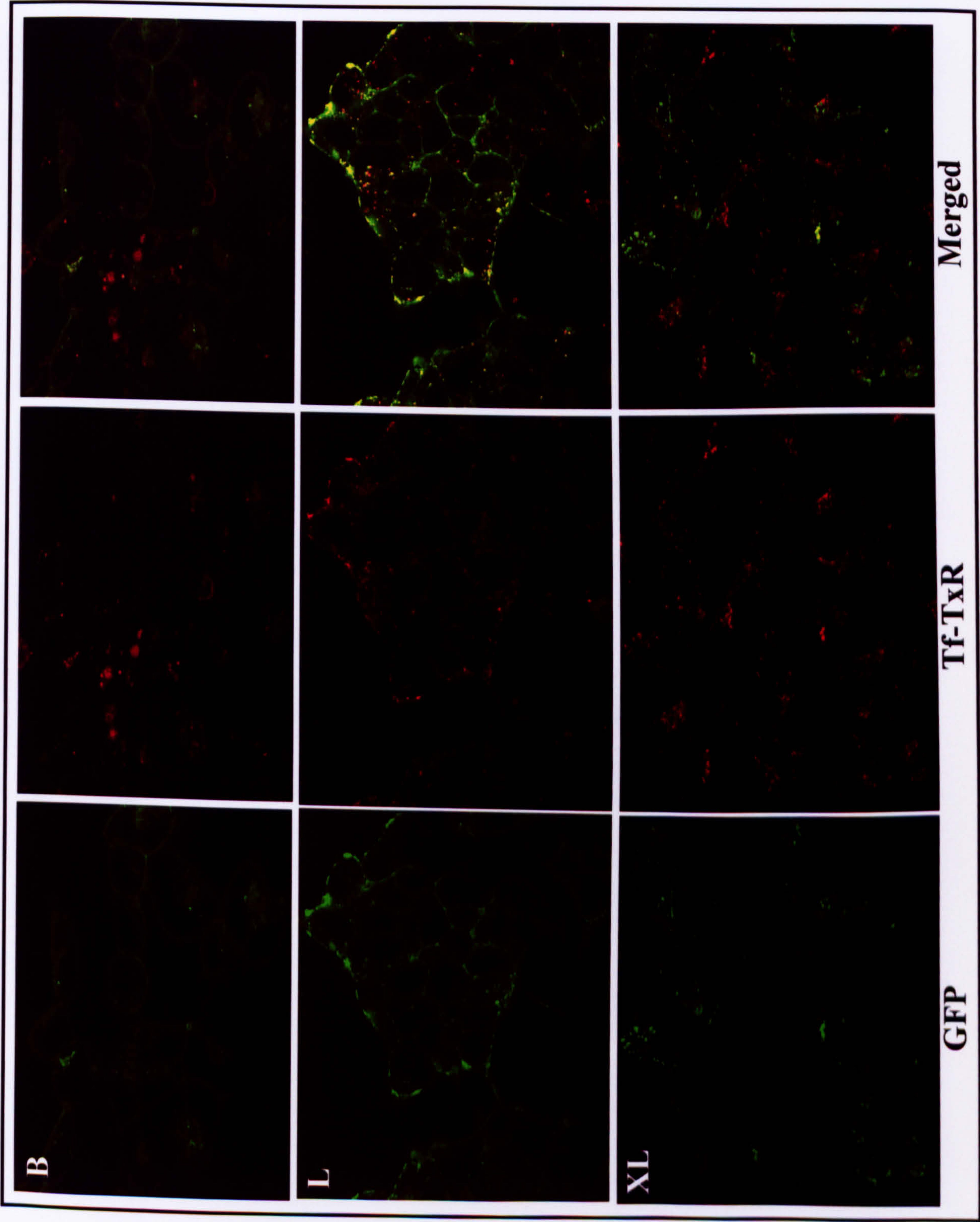




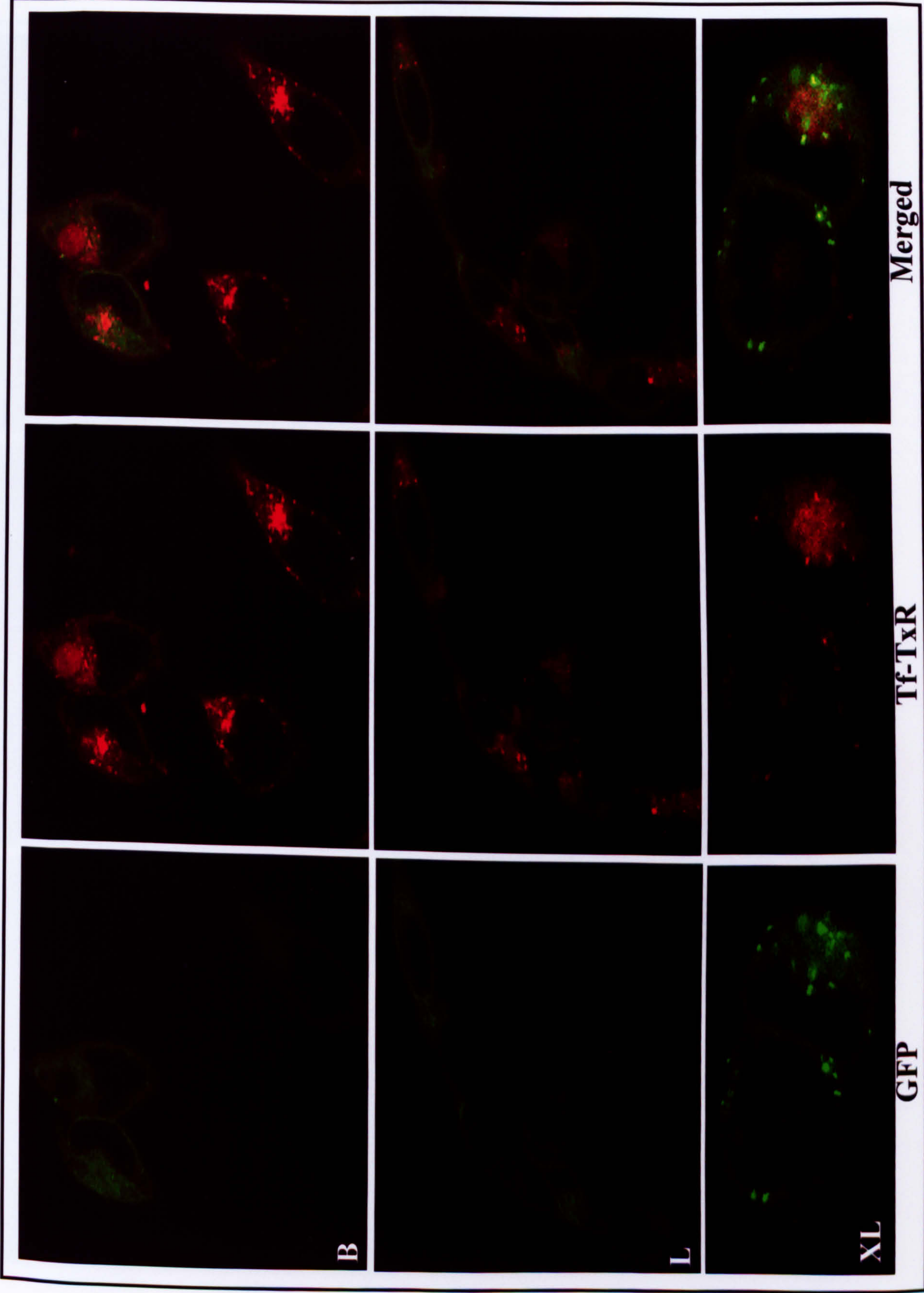
#### **FIGURE 4.10 THE GFP-CD23bS5A PROTEIN CO-LOCALISES WITH TRANSFERRIN-MODIFIED TEXAS RED (Tf-TxR) IN HEK 293 CELLS AFTER CROSS-LINKING WITH NIP-BSA**

Coverslips bearing G418-resistant HEK 293 cells expressing the GFP-CD23bS5A protein were pre-incubated with 20µg Tf-TxR prior to confocal analysis. The cells were exposed to (B) no stimulus, (L) 1µg NIP-specific IgE or (XL) 1µg NIP-specific IgE followed by the addition of 1µg NIP<sub>10</sub>-BSA and examined by confocal microscopy over a 45 minute period. The images shown demonstrate the typical staining patterns observed for this mutant in each of the (B) basal, (L) loaded and (XL) cross-linked states respectively.

Two distinct populations, as defined by their very different fluorescent staining patterns, were observed in this stably-transfected cell line. The first population (the first page of images) was found to demonstrate diffuse staining throughout the cytoplasm of the HEK 293 cells in the basal and loaded states. In this population the GFP-CD23bS5A fusion proteins were only found to enter the cell via directed uptake and co-localise with Tf-TxR and thus the early endosomal system, after being loaded with NIP-specific IgE and then cross-linked with NIP-BSA. In contrast to this, the second cell population (second set of images) was found to show co-localisation with Tf-TxR in all three basal, loaded and cross-linked states. A small amount of diffuse staining was also observed within the cytoplasm of these cells, however much of the fluorescence was contained along the plasma membrane or within distinct foci of fluorescence within the cell.



GFP-bS5A





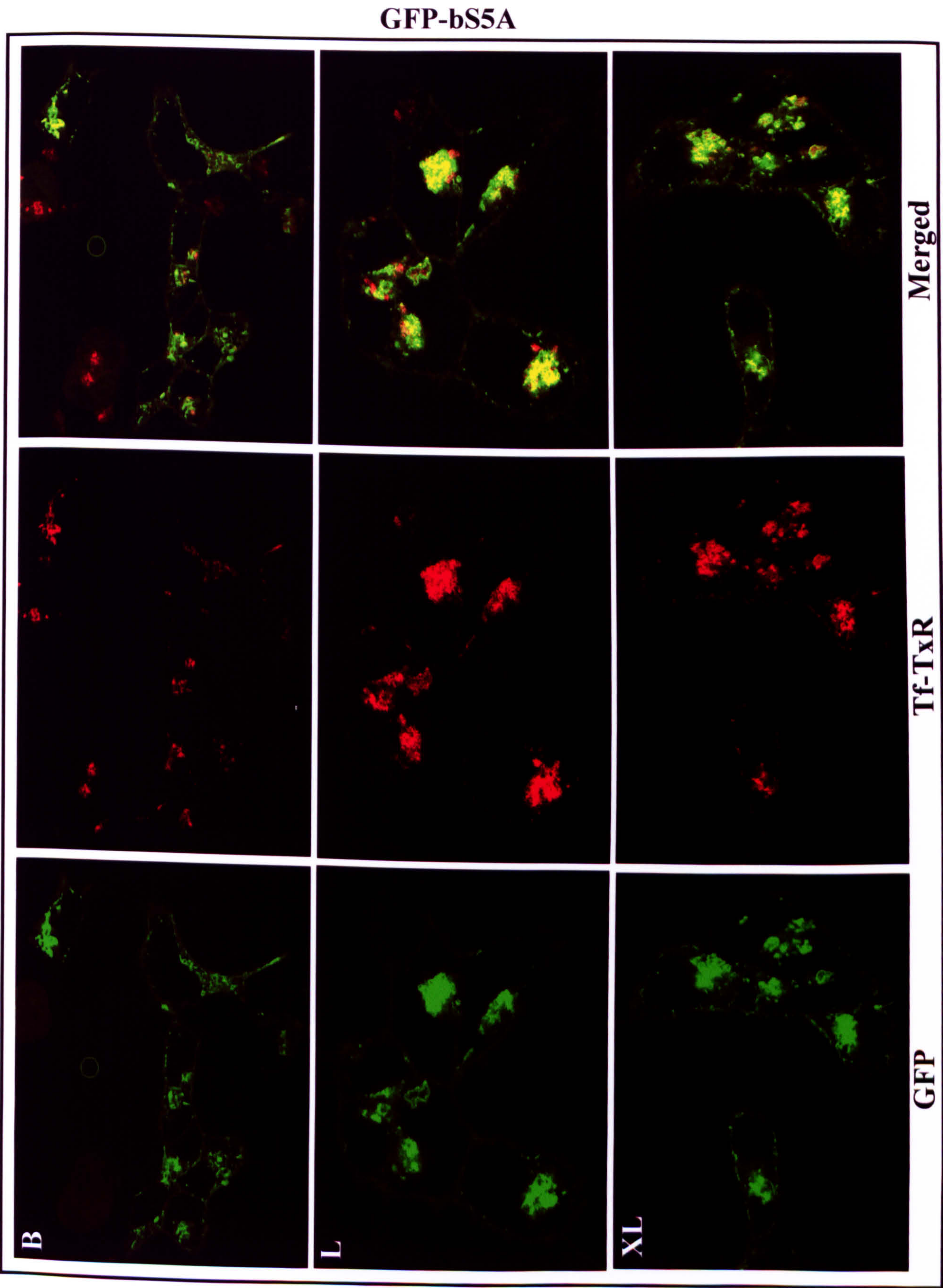




**FIGURE 4.11 THE GFP-CD23bS5D PROTEIN CO-LOCALISES WITH TRANSFERRIN-MODIFIED TEXAS RED (Tf-TxR) IN HEK 293 CELLS UNDER ALL THREE BASAL, LOADED AND CROSS-LINKED CONDITIONS**

Coverslips bearing G418-resistant HEK 293 cells expressing the GFP-CD23bS5D protein were pre-incubated with 20µg Tf-TxR prior to confocal analysis. The cells were exposed to (B) no stimulus, (L) 1µg NIP-specific IgE or (XL) 1µg NIP-specific IgE followed by the addition of 1µg NIP<sub>10</sub>-BSA and examined by confocal microscopy over a 45 minute period. The images shown demonstrate the typical staining patterns observed for this mutant in each of the (B) basal, (L) loaded and (XL) cross-linked states respectively.

GFP-CD23bS5D fusion proteins were found to enter the cell via directed uptake and co-localise with Tf-TxR and thus the early endosomal system in all three, basal, loaded and cross-linked states.



GFP-bS5D

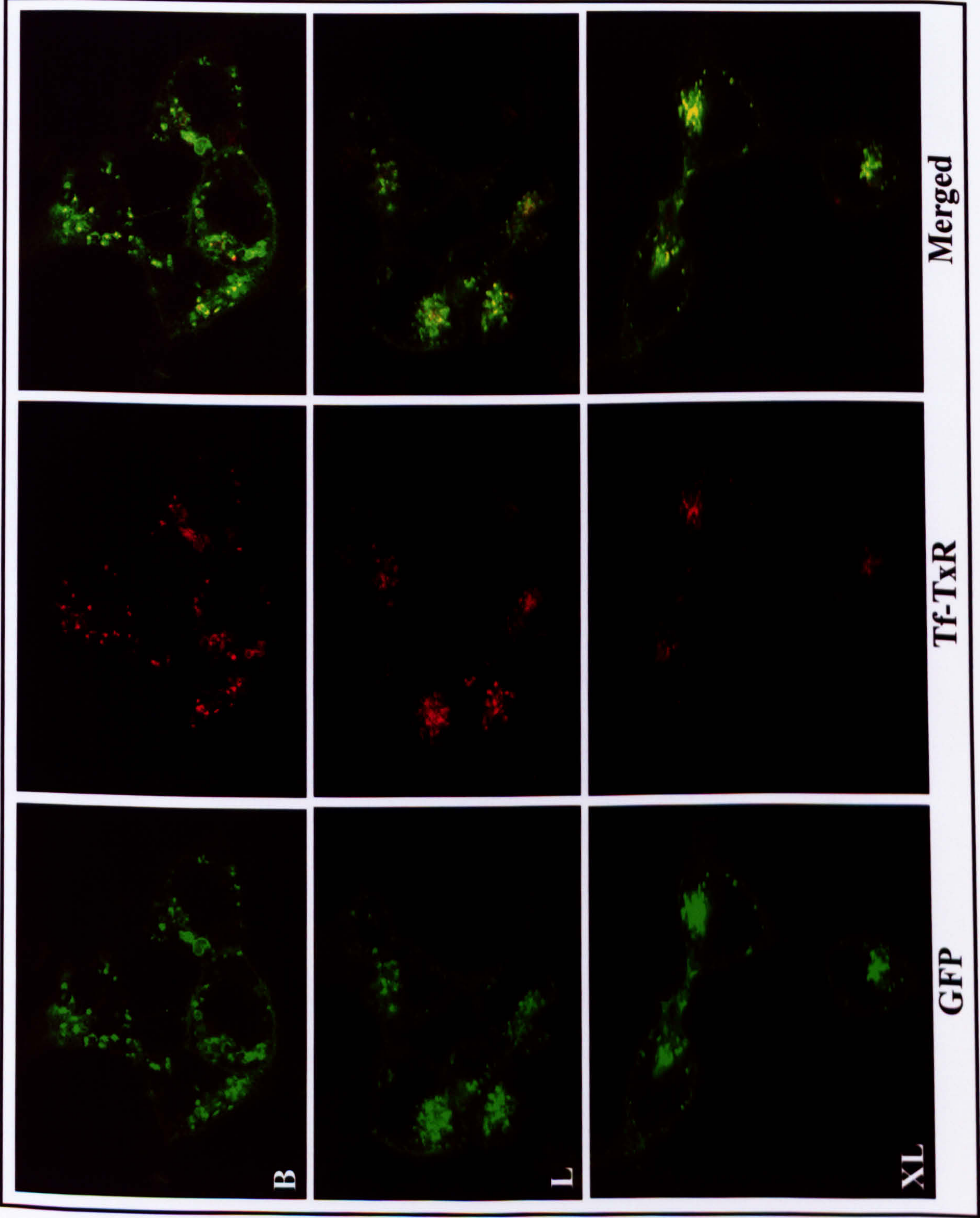




**FIGURE 4.12 THE GFP-CD23bS5F PROTEIN CO-LOCALISES WITH TRANSFERRIN-MODIFIED TEXAS RED (Tf-TxR) IN HEK 293 CELLS UNDER ALL THREE BASAL, LOADED AND CROSS-LINKED CONDITIONS**

Coverslips bearing G418-resistant HEK 293 cells expressing the GFP-CD23bS5F protein were pre-incubated with 20µg Tf-TxR prior to confocal analysis. The cells were exposed to (B) no stimulus, (L) 1µg NIP-specific IgE or (XL) 1µg NIP-specific IgE followed by the addition of 1µg NIP<sub>10</sub>-BSA and examined by confocal microscopy over a 45 minute period. The images shown demonstrate the typical staining patterns observed for this mutant in each of the (B) basal, (L) loaded and (XL) cross-linked states respectively.

GFP-CD23bS5F fusion proteins were found to enter the cell via directed uptake and co-localise with Tf-TxR and thus the early endosomal system in all three, basal, loaded and cross-linked states.



**GFP-bS5F**

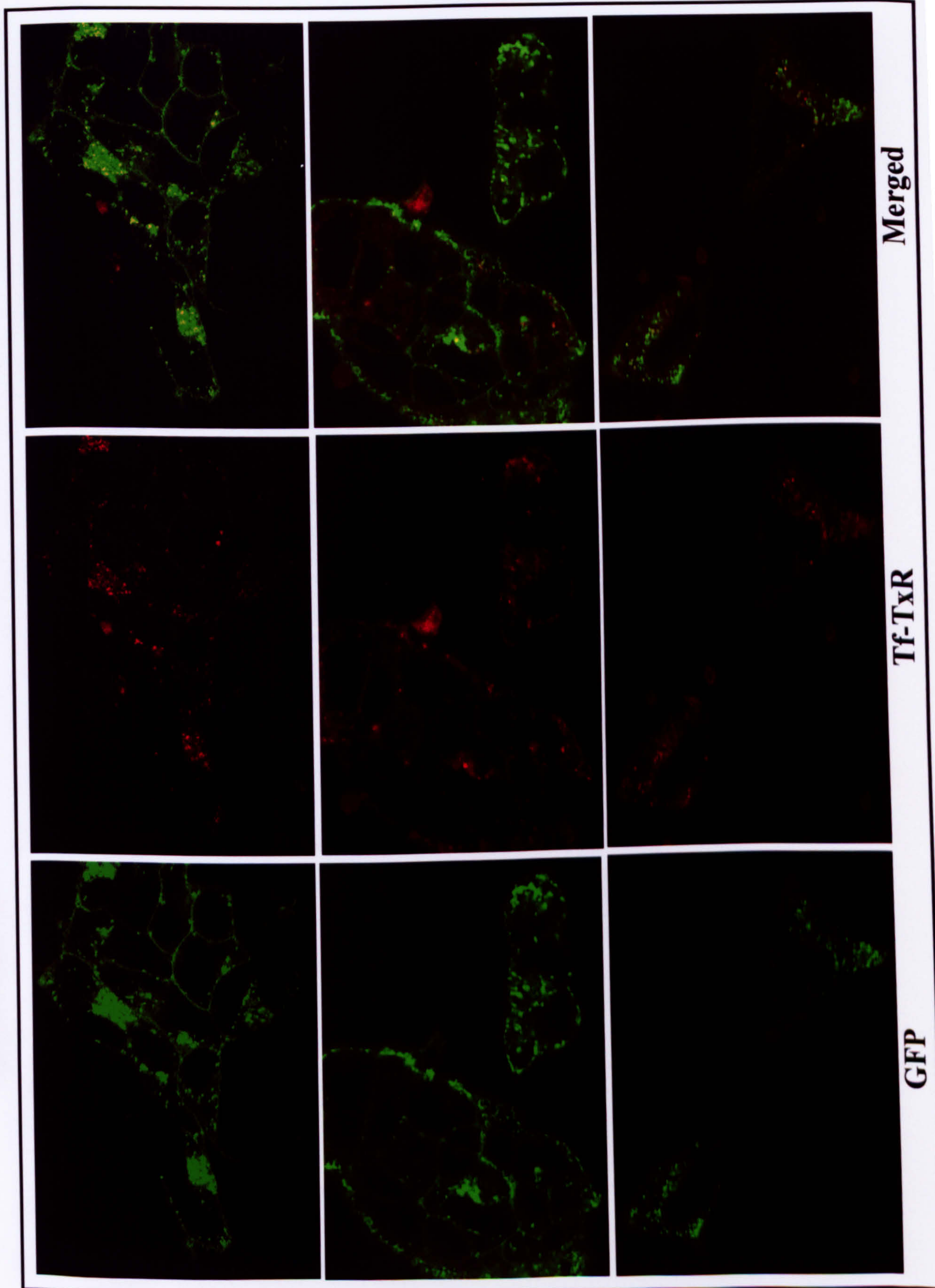




#### **FIGURE 4.13 THE GFP-CD23BP3R PROTEIN DOES NOT TARGET TO THE PLASMA MEMBRANE IN HEK 293 CELLS**

Coverslips bearing G418-resistant HEK 293 cells expressing the GFP-CD23bP3R protein were pre-incubated with 20µg Tf-TxR prior to confocal analysis. The cells were examined in the basal state and it was observed that this mutant protein was unable to target to the plasma membrane in HEK 293 cells. The cells were not exposed to either NIP-specific IgE or the NIP<sub>10</sub>-BSA as there was little point due to the fact the CD23 receptor was not at the cell surface and its trafficking patterns could not be assessed as per the rest of the GFP-CD23 mutant proteins.

GFP-CD23bP3R fusion proteins were unable to target to the plasma membrane and no co-localisation was observed with Tf-TxR indicating that this protein was trapped within the cell in compartments which were not early endosomes.



**GFP-bP3R**

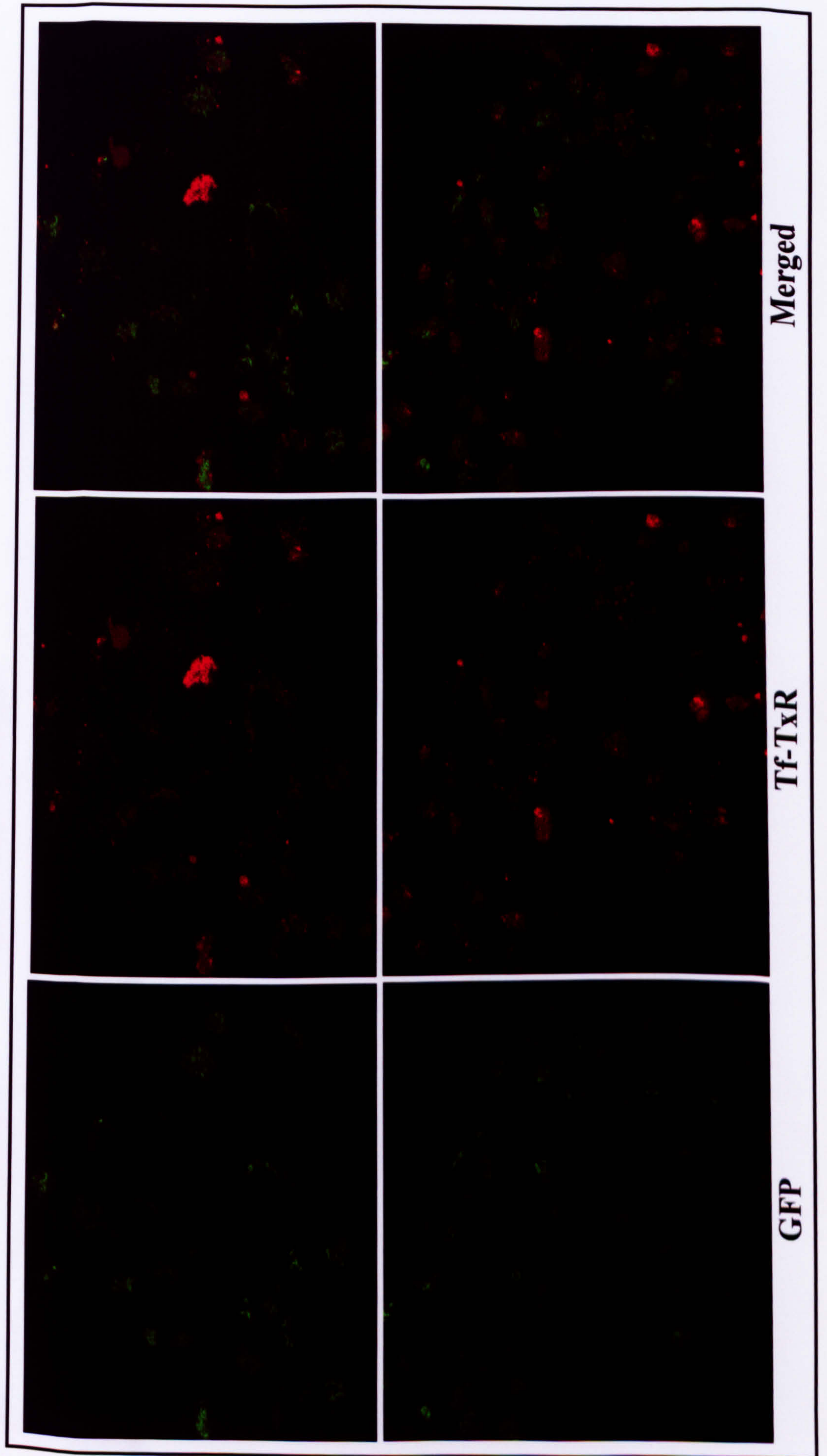




**FIGURE 4.14 THE GFP-CD23bP4R PROTEIN CO-LOCALISES WITH TRANSFERRIN-MODIFIED TEXAS RED (Tf-TxR) IN HEK 293 CELLS UNDER ALL THREE BASAL, LOADED AND CROSS-LINKED CONDITIONS**

Coverslips bearing G418-resistant HEK 293 cells expressing the GFP-CD23bP4R protein were pre-incubated with 20µg Tf-TxR prior to confocal analysis. The cells were exposed to (B) no stimulus, (L) 1µg NIP-specific IgE or (XL) 1µg NIP-specific IgE followed by the addition of 1µg NIP<sub>10</sub>-BSA and examined by confocal microscopy over a 45 minute period. The images shown demonstrate the typical staining patterns observed for this mutant in each of the (B) basal, (L) loaded and (XL) cross-linked states respectively.

GFP-CD23bP4R fusion proteins were found to enter the cell via directed uptake and co-localise with Tf-TxR and thus the early endosomal system in all three, basal, loaded and cross-linked states.



GFP-bP4R

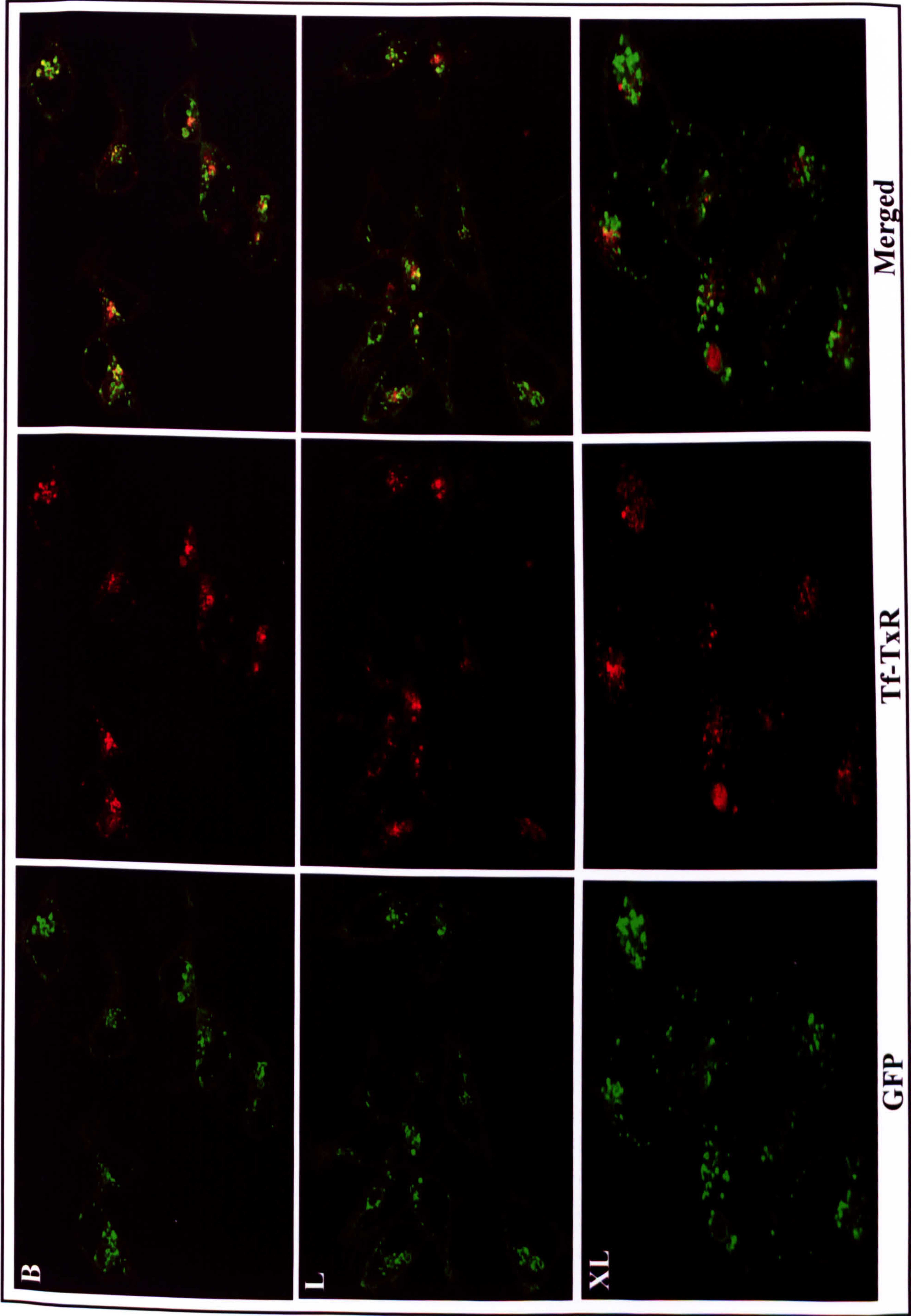




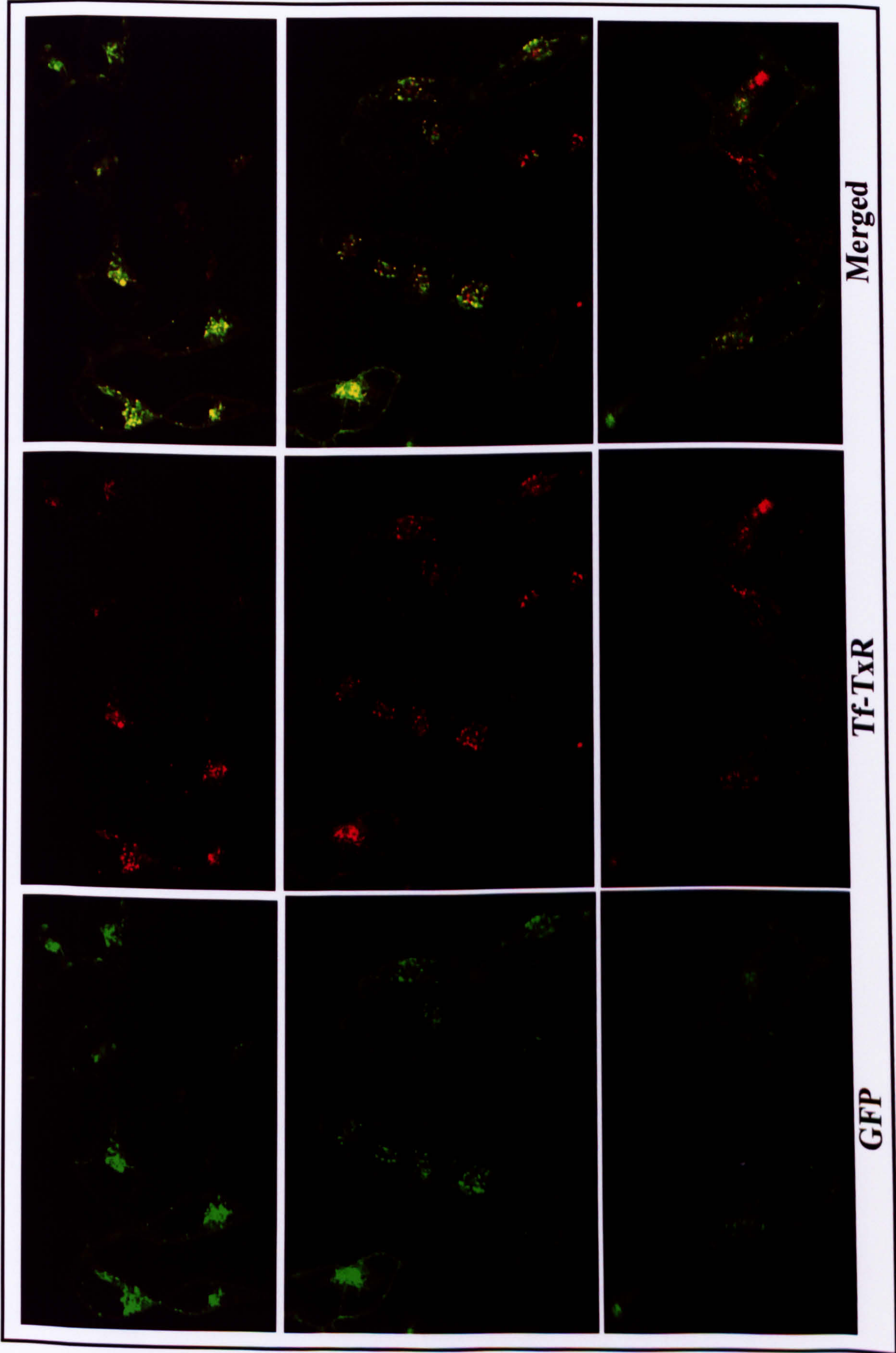
**FIGURE 4.15 THE GFP-CD23bN2K PROTEIN CO-LOCALISES WITH TRANSFERRIN-MODIFIED TEXAS RED (Tf-TxR) IN HEK 293 CELLS UNDER ALL THREE BASAL, LOADED AND CROSS-LINKED CONDITIONS**

Coverslips bearing G418-resistant HEK 293 cells expressing the GFP-CD23bN2K protein were pre-incubated with 20µg Tf-TxR prior to confocal analysis. The cells were exposed to (B) no stimulus, (L) 1µg NIP-specific IgE or (XL) 1µg NIP-specific IgE followed by the addition of 1µg NIP<sub>10</sub>-BSA and examined by confocal microscopy over a 45 minute period. The images shown demonstrate the typical staining patterns observed for this mutant in each of the (B) basal, (L) loaded and (XL) cross-linked states respectively.

GFP-CD23bN2K fusion proteins were found to enter the cell via directed uptake and co-localise with Tf-TxR and thus the early endosomal system in all three, basal, loaded and cross-linked states.



GFP-bN2K





## **FIGURES 4.16 MUTATION OF THE CYTOPLASMIC N-TERMINUS OF CD23 AFFECTS PROTEOLYTIC CLEAVAGE FROM THE CELL SURFACE**

G418-resistant HEK 293 cells expressing each of the GFP-CD23 mutant proteins were cultured for 4 days in complete DMEM media. The supernatants were collected and assayed for the presence of soluble CD23 protein using the sCD23 ELISA described in section 2.2.7H. This figure illustrates the amount of soluble CD23 detected in each of the supernatants, indicating that many of the mutations caused significant differences in the amount of CD23 shed from the cell surface in comparison to the data collected from supernatants collected from cells expressing each of the wild-type CD23 isoforms.



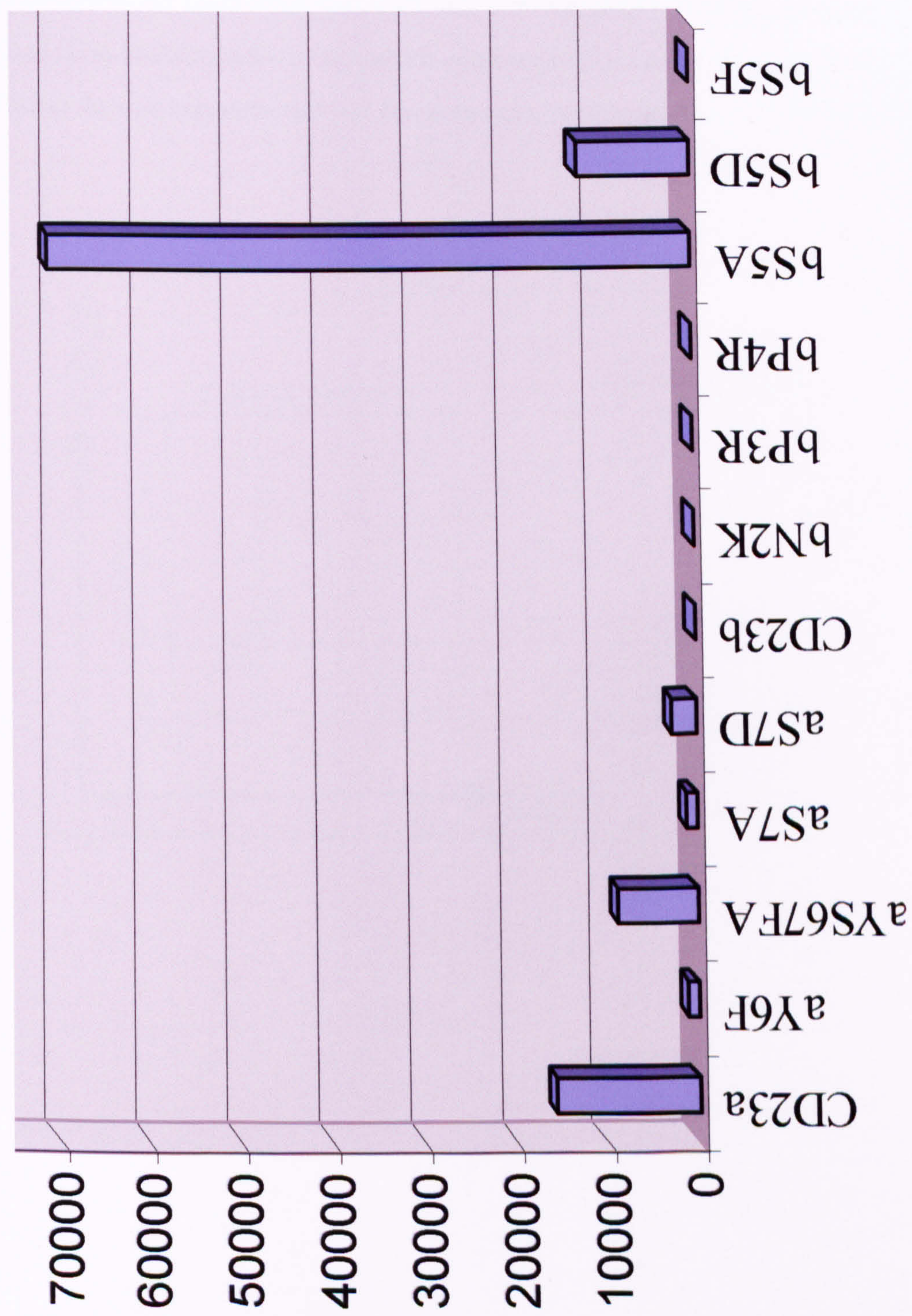




#### **FIGURE 4.17 RAJI A CELLS STABLY EXPRESS BOTH OF THE GFP-CD23 ISOFORM FUSION PROTEINS AT THE PLASMA MEMBRANE**

G418-resistant Raji A cells stably-transfected with each of the wild-type GFP-CD23 constructs were subjected to flow cytometry. The presence of CD23 was detected by an anti-CD23 PE antibody (FL-2), whilst the presence of the GFP tag was detected directly, from its green fluorescence (FL-1). The data have been presented as a number of dot-plots where the upper right quadrant shows the double positive cells in each case. Untransfected (UT) Raji cells were also assayed for the presence of endogenous CD23 protein.



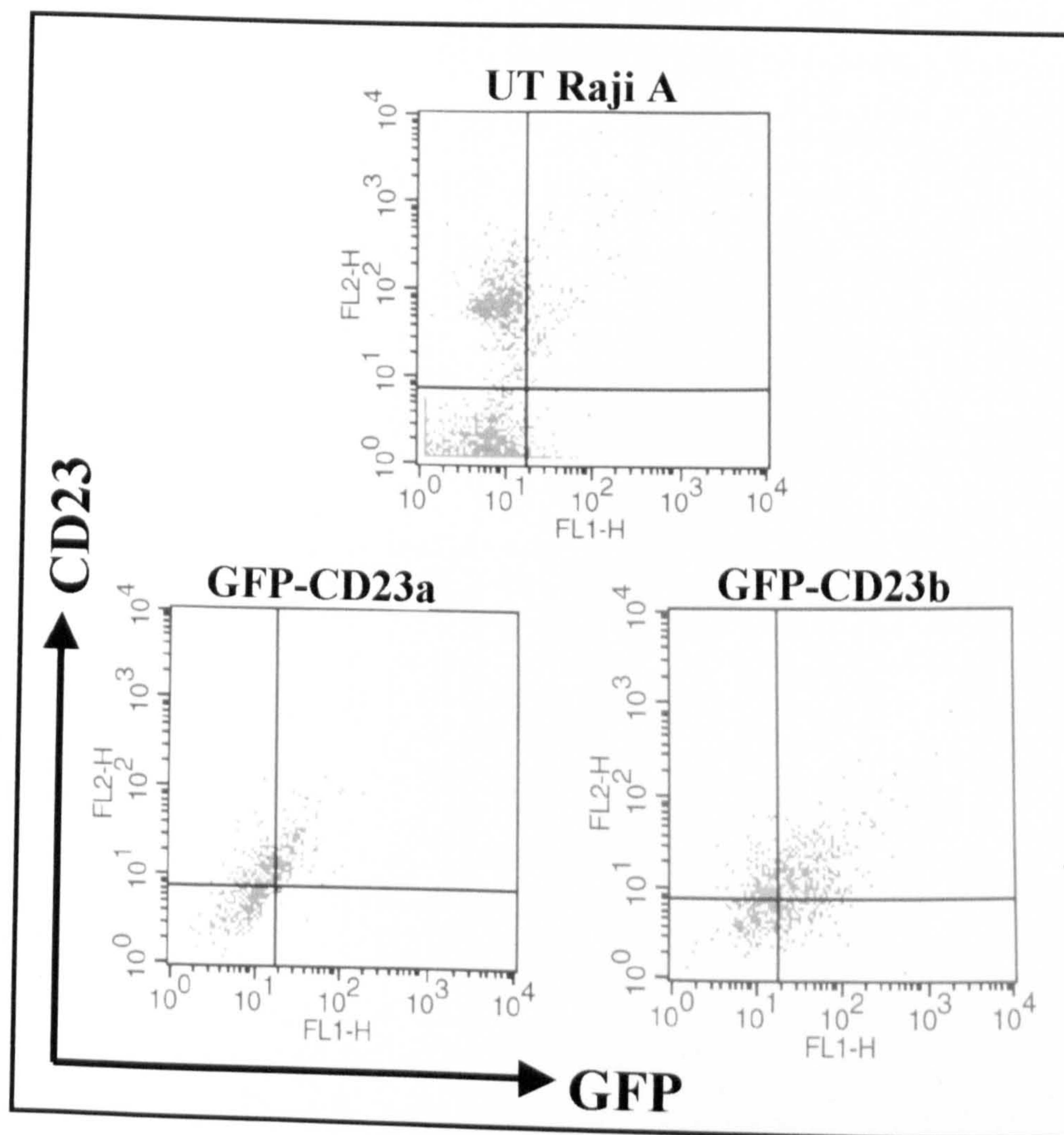




# **FIGURE 4.18 CONFOCAL ANALYSIS CONFIRMS CELL SURFACE EXPRESSION OF BOTH OF THE GFP-CD23 ISOFORM FUSION PROTEINS IN RAJI A CELLS**

G418-resistant Raji A cells stably-transfected with each of the wild-type GFP-CD23 isoforms were propagated for 48 hours on glass coverslips before being harvested, washed in KRH buffer and subjected to confocal analysis. The images demonstrate the localisation of each of the GFP-tagged isoforms in the basal state, and indicate that both CD23 isoforms appear to be targeted to the plasma membrane.



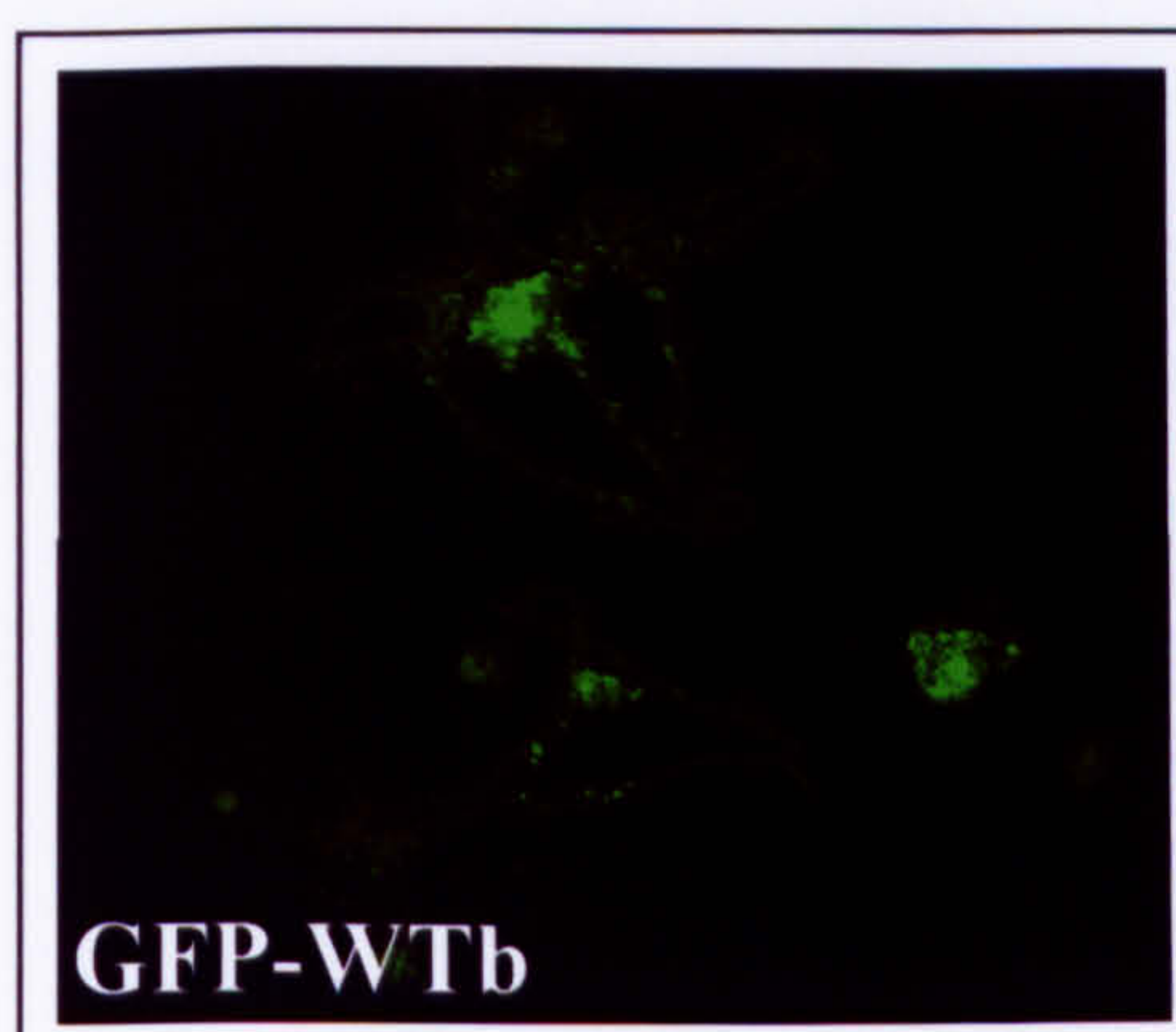
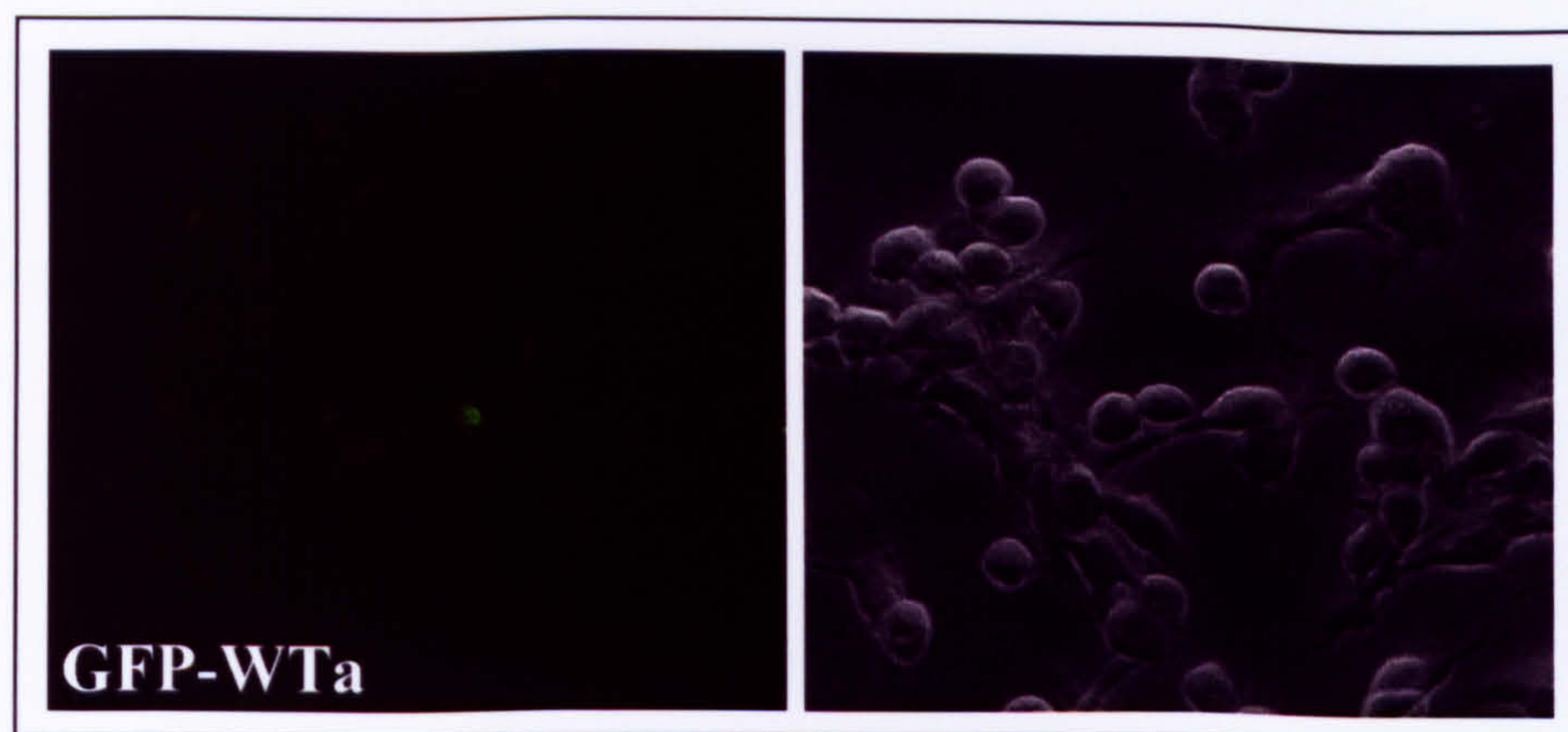




#### **FIGURE 4.19 SCHEMATIC DIAGRAM ILLUSTRATES THE ENHANCED NIP SYSTEM USING AN ADDITIONAL PROTEIN CONJUGATE – NIP-INSULIN**

Figure 3.5 is shown again in the upper diagram, illustrating how the NIP-system facilitates the study of GFP-CD23 trafficking in an unoccupied or “Basal” state, a “Loaded” state following the addition of NIP-specific chimaeric IgE antibody and a “Cross-linked” state following the addition of NIP-BSA to cell pre-loaded with NIP-specific IgE. In addition to this the lower diagram illustrates the effect of adding NIP-Insulin proteins. Like the NIP-BSA, the NIP-Insulin will serve to bind specifically to the NIP-specific IgE antibody molecules but will be unable to ‘ligate’ more than one CD23 molecule at the cell surface. The addition of this protein conjugate, and the comparison between this state and the NIP-BSA cross-linked state facilitates investigation of the importance of CD23 oligomerisation for directed uptake and internalisation. As before, the green star in each instance represents the GFP tag at the N-terminus of each CD23 fusion protein.



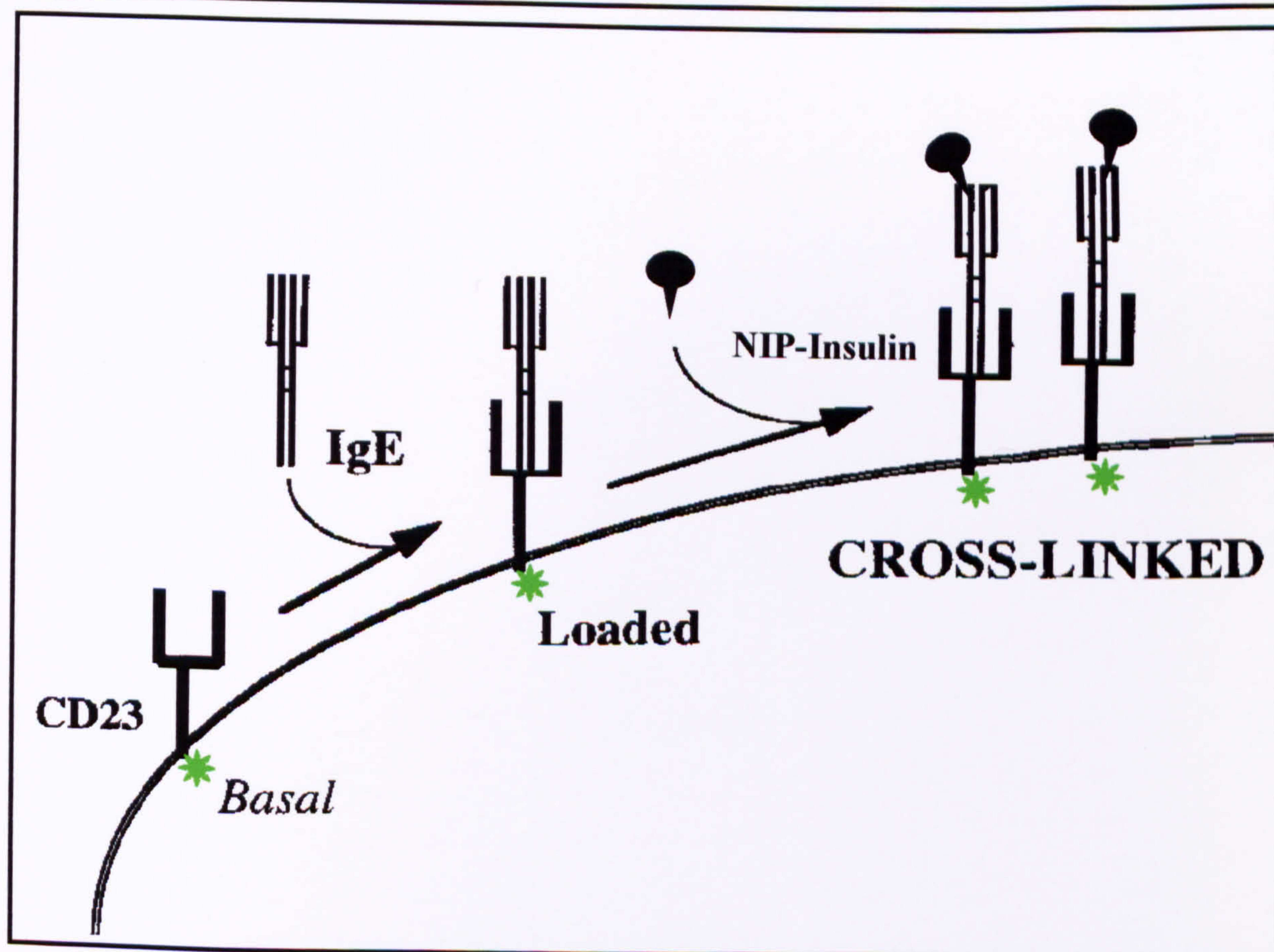
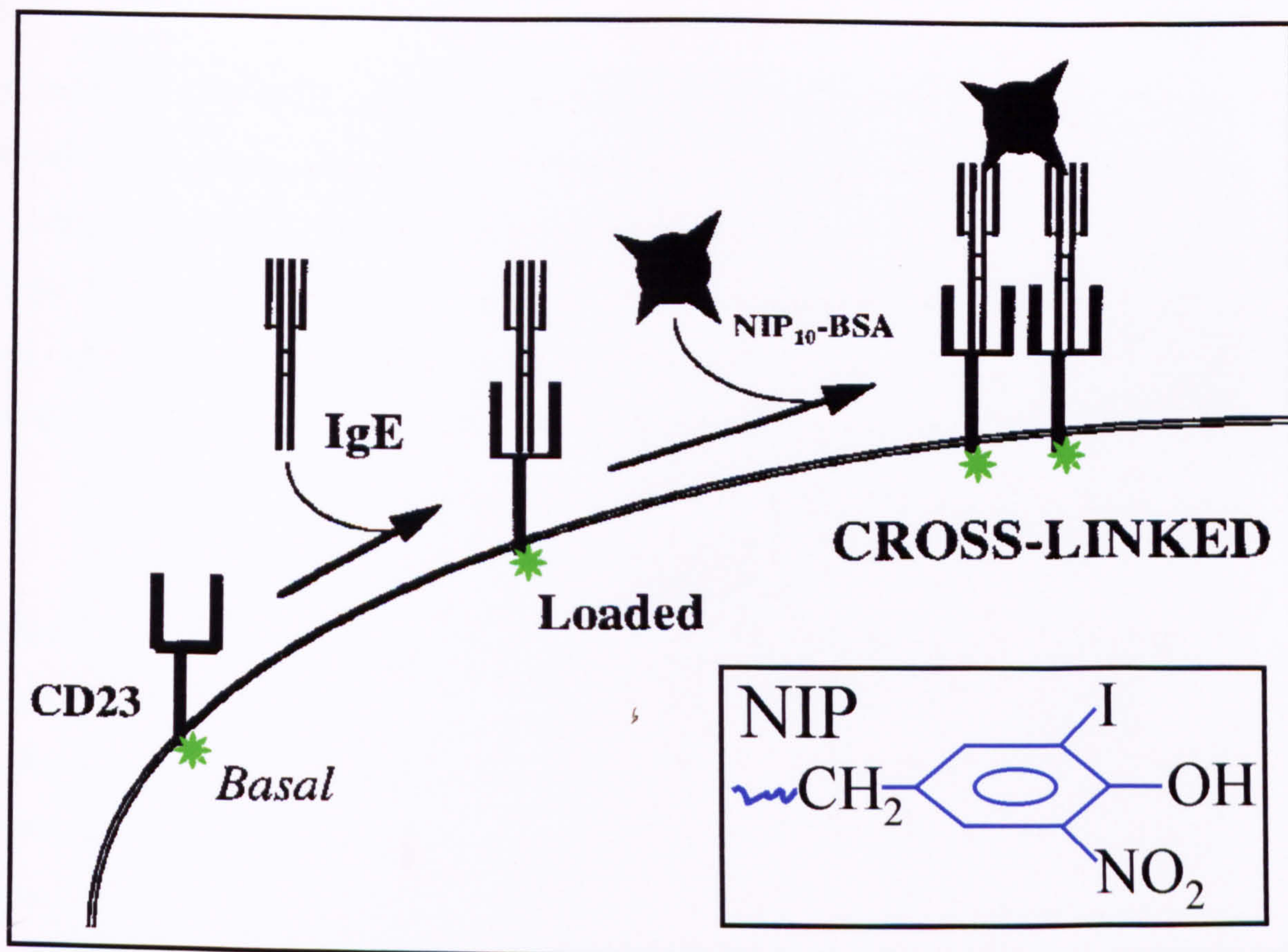


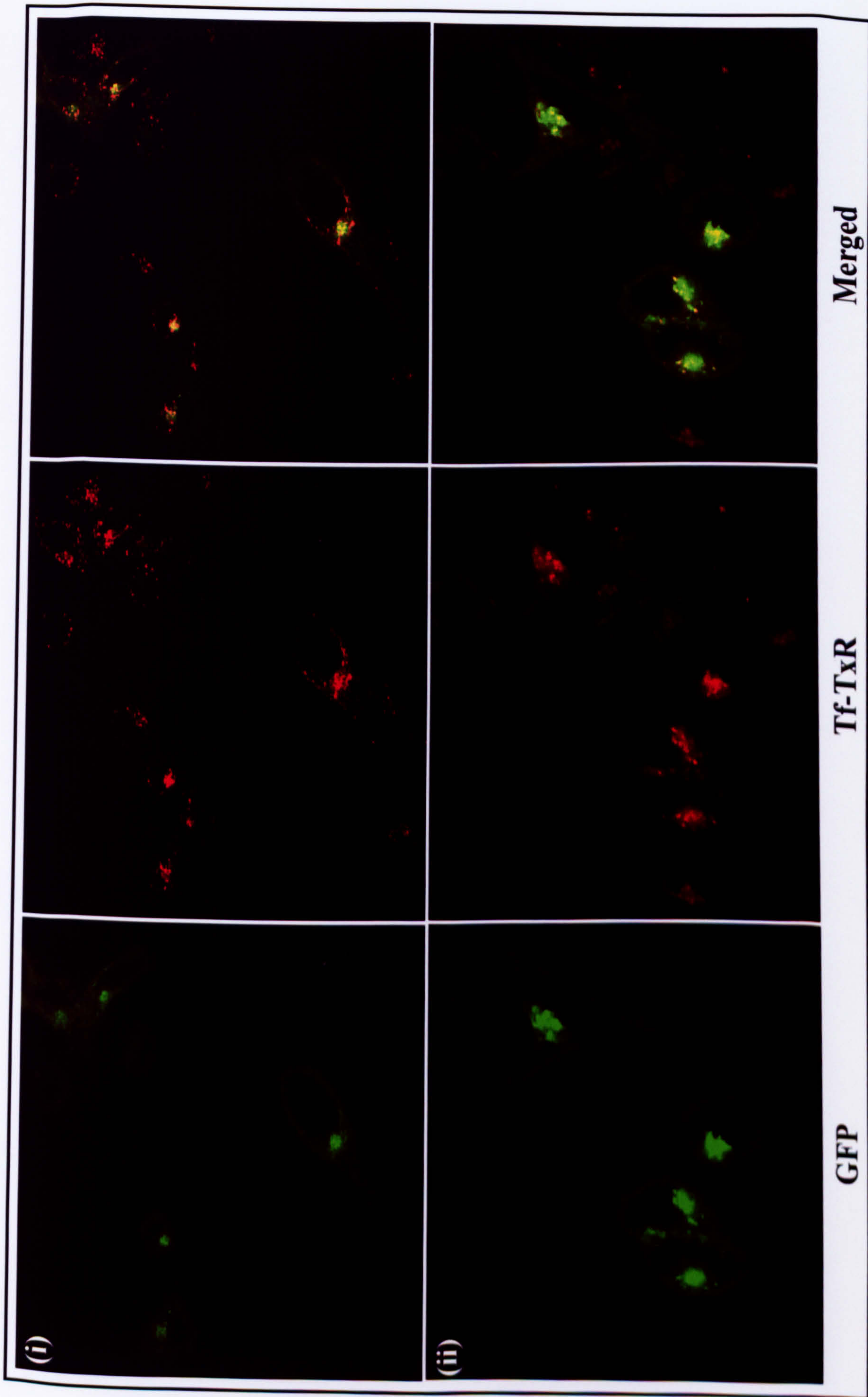


## **FIGURE 4.20 GFP-CD23B ENTERS THE ENDOCYTIC PATHWAY IN RAJI A CELLS**

Coverslips bearing G418-resistant Raji A cells expressing the GFP-CD23b protein were pre-incubated with 20µg Tf-TxR prior to confocal analysis. The cells were exposed to (i) no stimulus, (ii) 1µg NIP-specific IgE, (iii) 1µg NIP-specific IgE followed by the addition of either 1µg NIP<sub>10</sub>-BSA or (iv) NIP<sub>1</sub>-Insulin and examined by confocal microscopy over a 45 minute period. The images shown demonstrate the typical staining patterns observed for this isoform in each of the (i) basal, (ii) loaded, (iii) cross-linked and (iv) ligated states respectively.

In the basal state the majority of the CD23 protein is located at the plasma membrane, with the addition of IgE resulting in concentrated foci of fluorescence along the membrane and the initiation of uptake from the cell surface. Evidence of co-localisation with Tf-TxR is also present. Cross-linking with NIP<sub>10</sub>-BSA causes an increase in directed uptake from the cell surface and an extensive punctate distribution. In contrast to this, whilst ligating with NIP<sub>1</sub>-Insulin does results in CD23 uptake, it occurs less so than in the aforementioned cross-linked state, with the majority of the CD23 retained within the plasma membrane. Some co-localisation was noted, both on the membrane and within the cell.







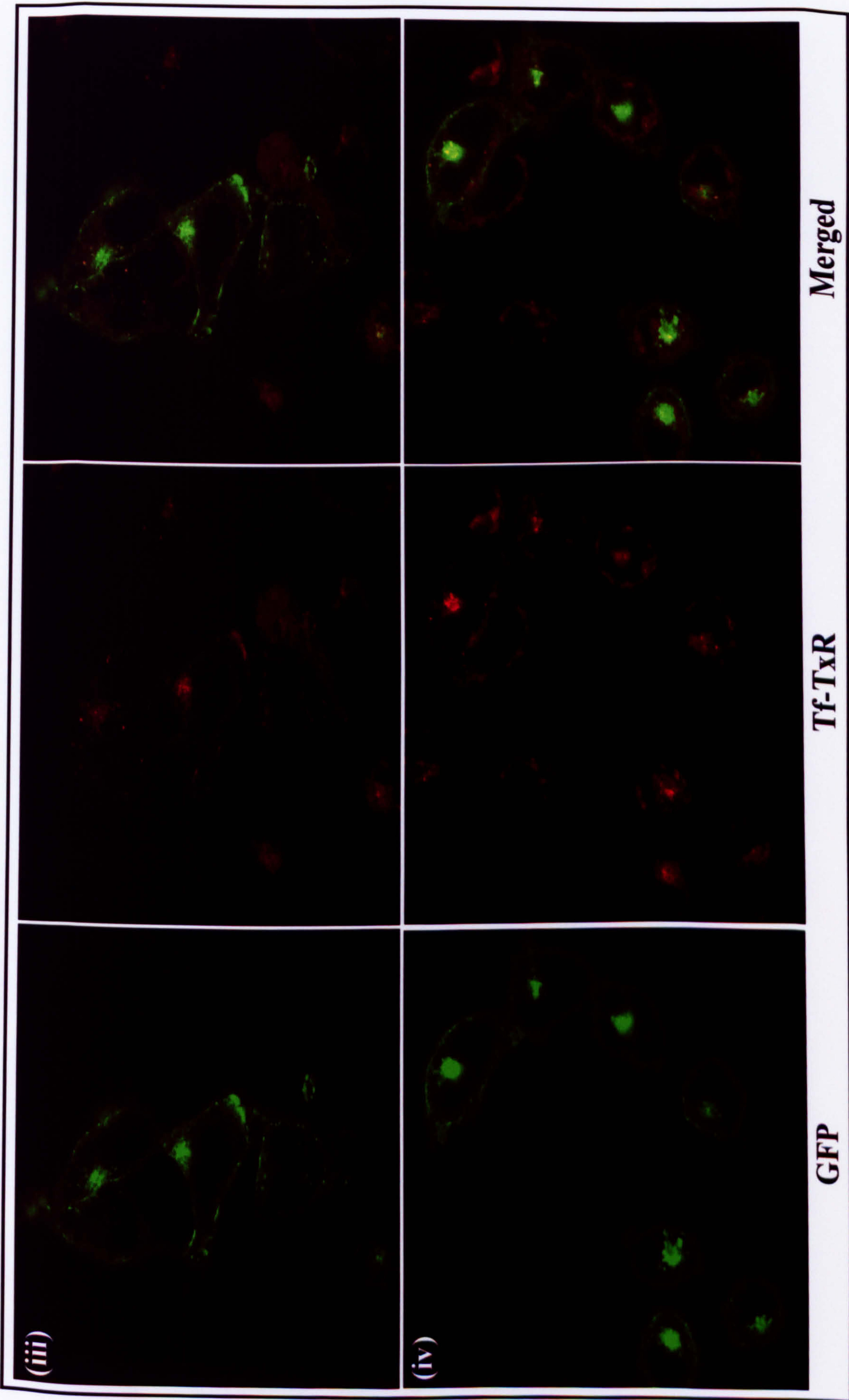


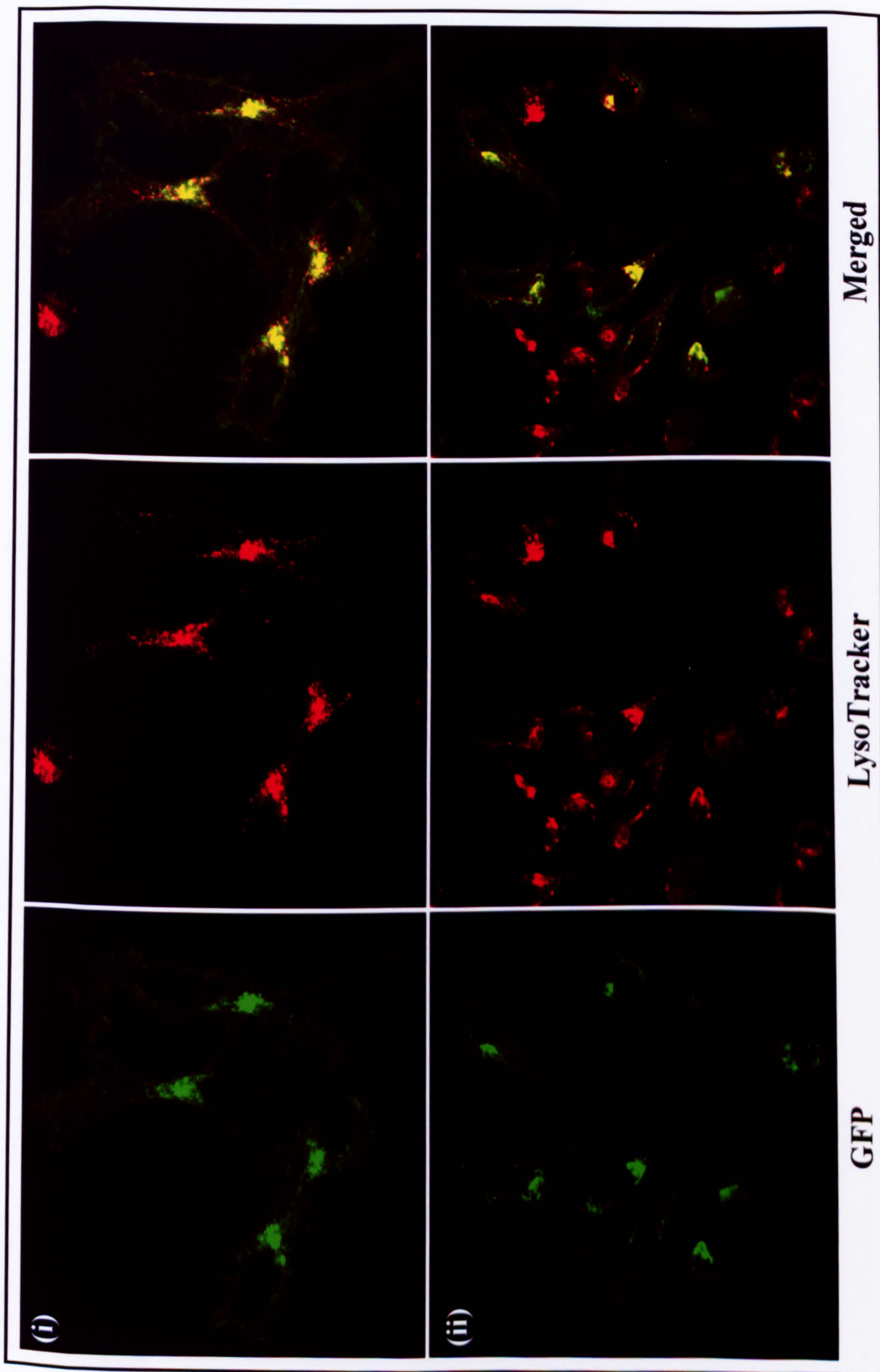


## **FIGURE 4.21 GFP-CD23B ENTERS THE PHAGOCYTOTIC PATHWAY IN RAJI A CELLS**

Coverslips bearing G418-resistant Raji A cells expressing the GFP-CD23b protein were pre-incubated with 50nM LysoTracker Red prior to confocal analysis. The cells were exposed to (i) no stimulus, (ii) 1µg NIP-specific IgE, (iii) 1µg NIP-specific IgE followed by the addition of either 1µg NIP<sub>10</sub>-BSA or (iv) NIP<sub>1</sub>-Insulin and examined by confocal microscopy over a 45 minute period. The images shown demonstrate the typical staining patterns observed for this isoform in each of the (i) basal, (ii) loaded and (iii & iv) cross-linked states respectively.

In the basal state the majority of the CD23 protein was located at the plasma membrane, with the addition of IgE resulting in concentrated foci of fluorescence along the membrane and some uptake from the cell surface demonstrating evidence of co-localisation with LysoTracker Red. Cross-linking with NIP<sub>10</sub>-BSA caused an increase in directed uptake from the cell surface and also an extensive punctate morphology. In contrast to this, cross-linking with NIP<sub>1</sub>-Insulin resulted in little uptake, with the majority of the CD23 retained within distinct patches along the plasma membrane.







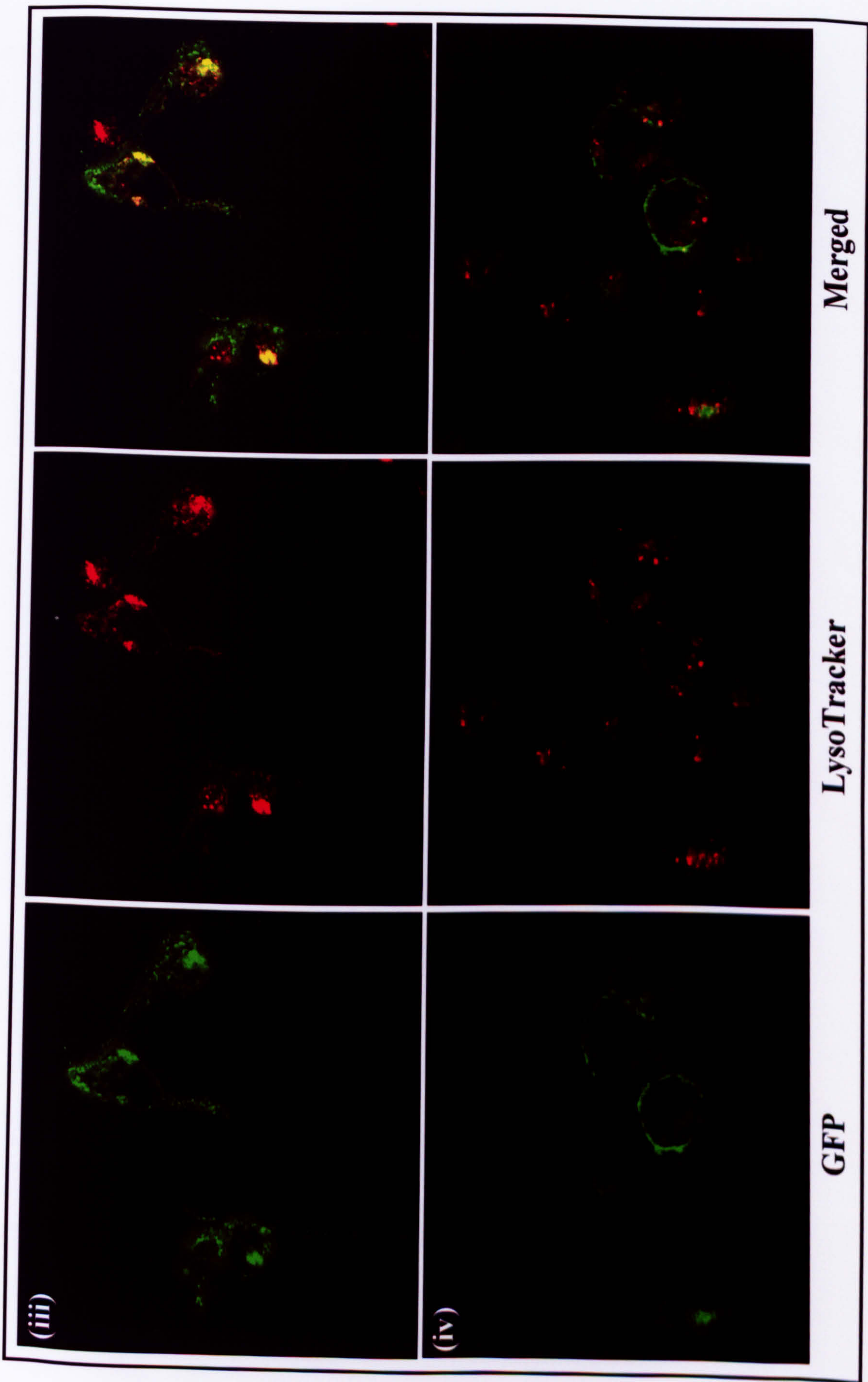




## **FIGURE 4.22 RAJI A CELLS STABLY EXPRESS EACH OF THE GFP-CD23A MUTANT FUSION PROTEINS**

G418-resistant Raji A cells stably-transfected with each of the GFP-CD23a mutant constructs were subjected to flow cytometry. The presence of CD23 was detected by an anti-CD23 PE antibody (FL-2), whilst the presence of the GFP tag was detected directly, from its green fluorescence (FL-1). The data has been presented as a number of dot-plots, with the upper right quadrant in each case illustrating cells expressing GFP-CD23a proteins on their plasma membrane.



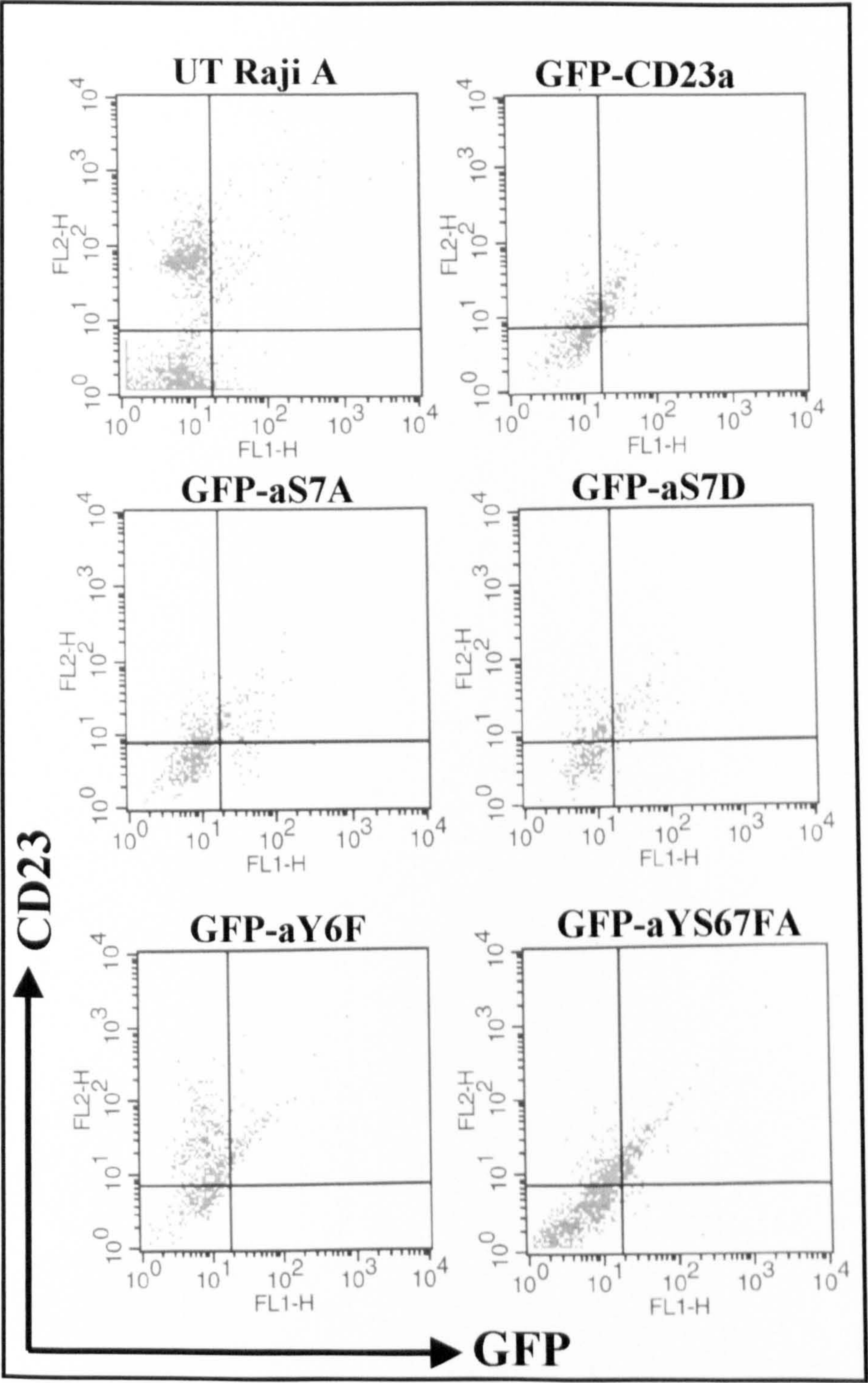




### **FIGURE 4.23 RAJI A CELLS STABLY EXPRESS EACH OF THE GFP-CD23B MUTANT FUSION PROTEINS**

G418-resistant Raji A cells stably-transfected with each of the GFP-CD23b mutant constructs were subjected to flow cytometry. The presence of CD23 was detected by an anti-CD23 PE antibody (FL-2), whilst the presence of the GFP tag was detected directly, from its green fluorescence (FL-1). The data has been presented as a number of dot-plots, with the upper right quadrant in each case illustrating cells expressing the GFP-CD23b proteins on their plasma membrane.



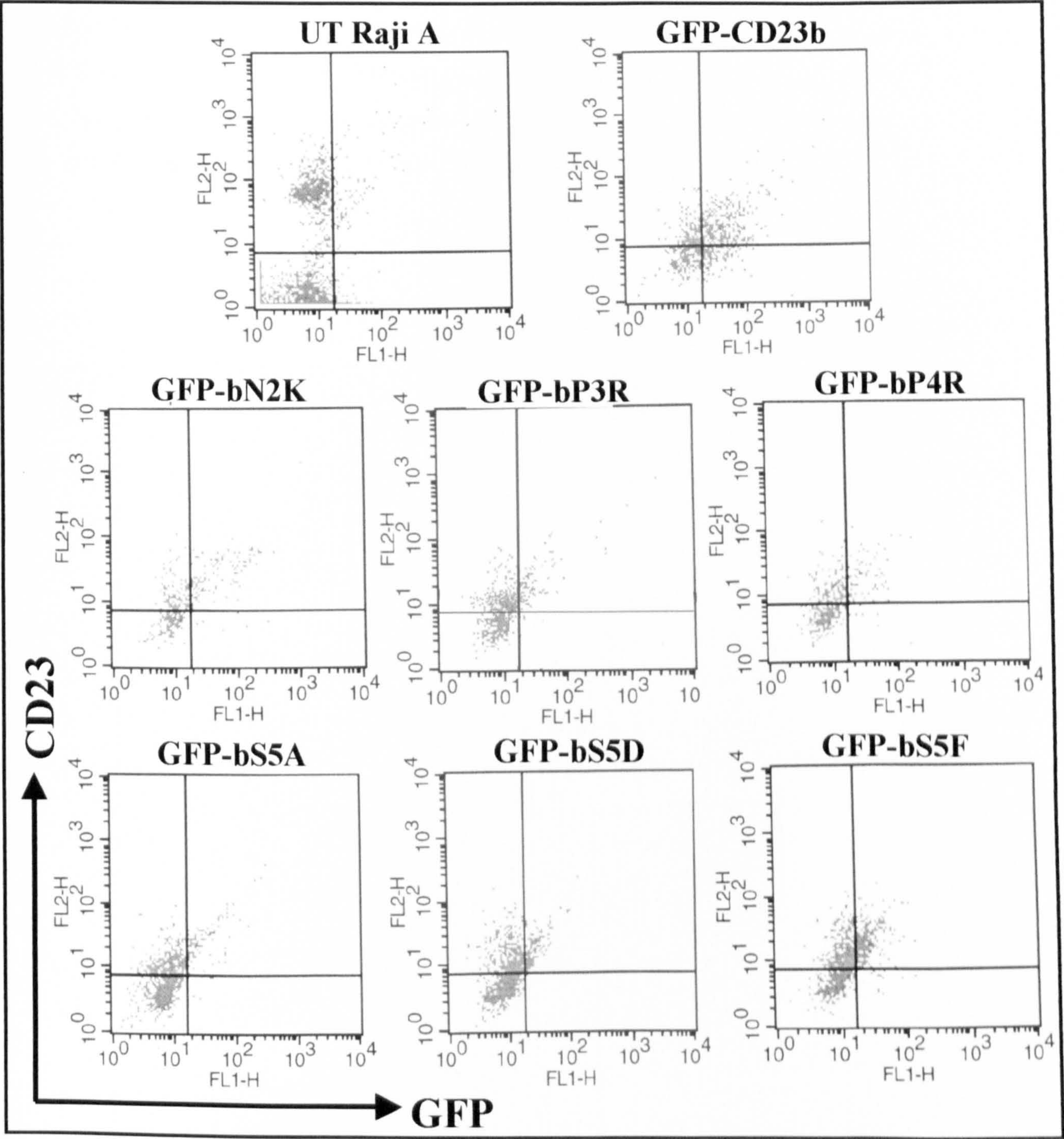




## **FIGURE 4.24 CELLULAR LOCALISATION OF EACH OF THE GFP-CD23A MUTANT FUSION PROTEINS IN RAJI A CELLS**

G418-resistant Raji A cells stably transfected with each of the GFP-CD23a mutant proteins were propagated for 48 hours on glass coverslips before being harvested, washed in KRH buffer and subjected to confocal analysis. The images demonstrate the fluorescent signal from each of the GFP-tagged mutant proteins in the basal state as well as bright field images indicating the location of each of the cells in the field of view.

The aY6F and aYS67FA proteins were observed to have a predominantly plasma membrane location, with suggestions of a punctate distribution in the basal state. The aS7A and aS7D mutant proteins were also able to target to the plasma membrane, but In contrast to the aY6F and aYS67FA mutants, there was substantially more GFP-tagged protein located within the cells, suggesting much higher expression levels of these mutant proteins.



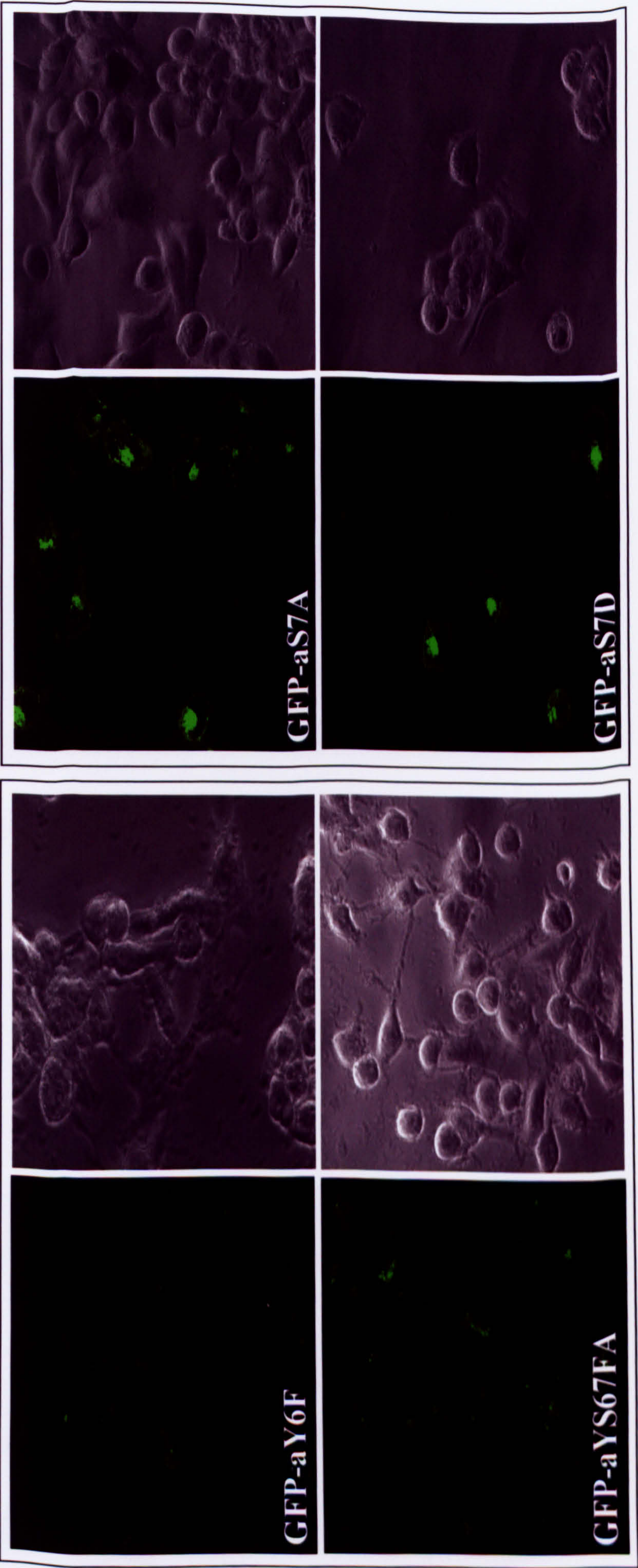
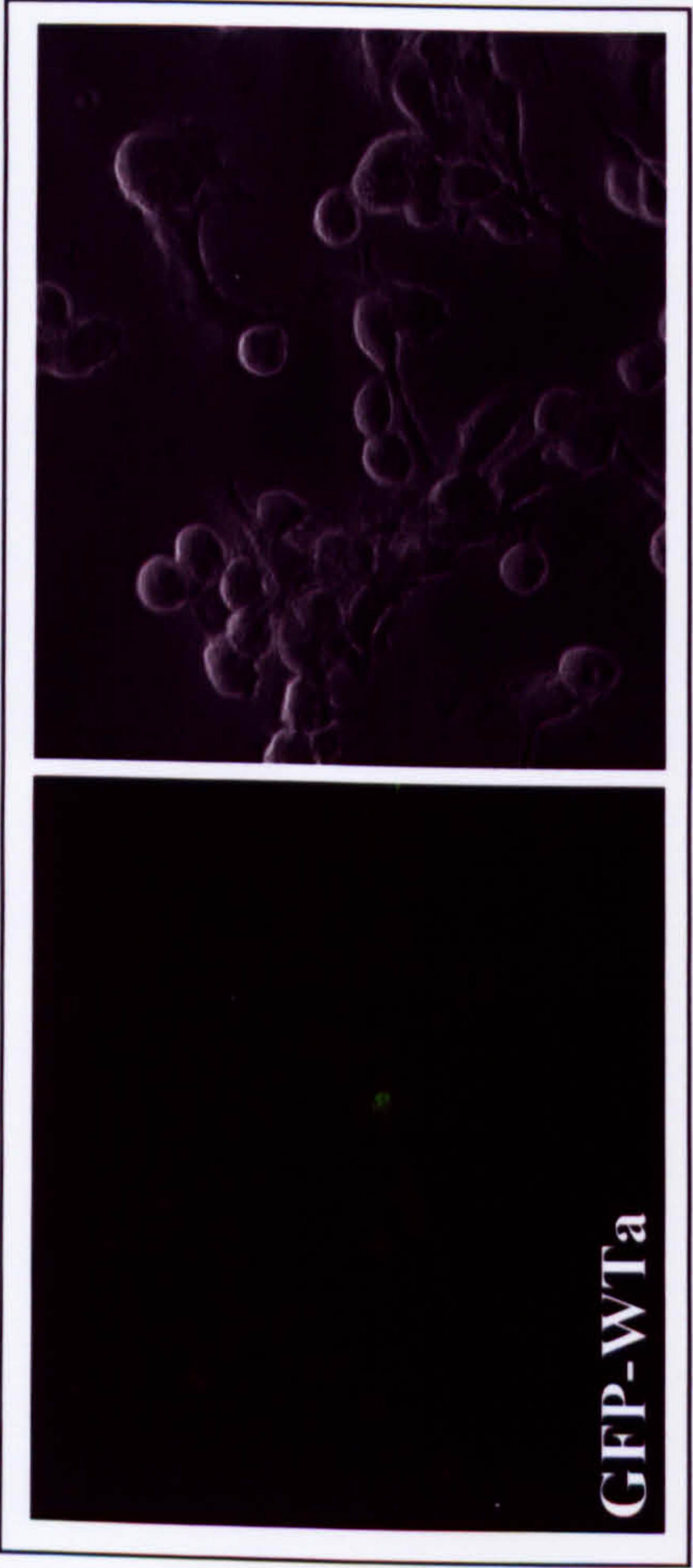




## **FIGURE 4.25 CELLULAR LOCALISATION OF EACH OF THE GFP-CD23B MUTANT FUSION PROTEINS IN RAJI A CELLS**

G418-resistant Raji A cells stably-transfected with each of the GFP-CD23b mutant proteins were propagated for 48 hours on glass coverslips before being harvested, washed in KRH buffer and subjected to confocal analysis. The images demonstrate the fluorescent signal from each of the GFP-tagged mutant proteins in the basal state as well as bright field images indicating the location of each of the cells in the field of view.

The GFP-CD23 bS5A, bS5D, bS5F, bP4R and bN2K mutants were all able to target to the plasma membrane in Raji A cells, with the majority of the stably-transfected cell lines containing few cells having reasonable protein expression levels. The bP3R mutant was expressed at lower levels than these mutants and the limited data collected for this mutant is shown in the next figure.



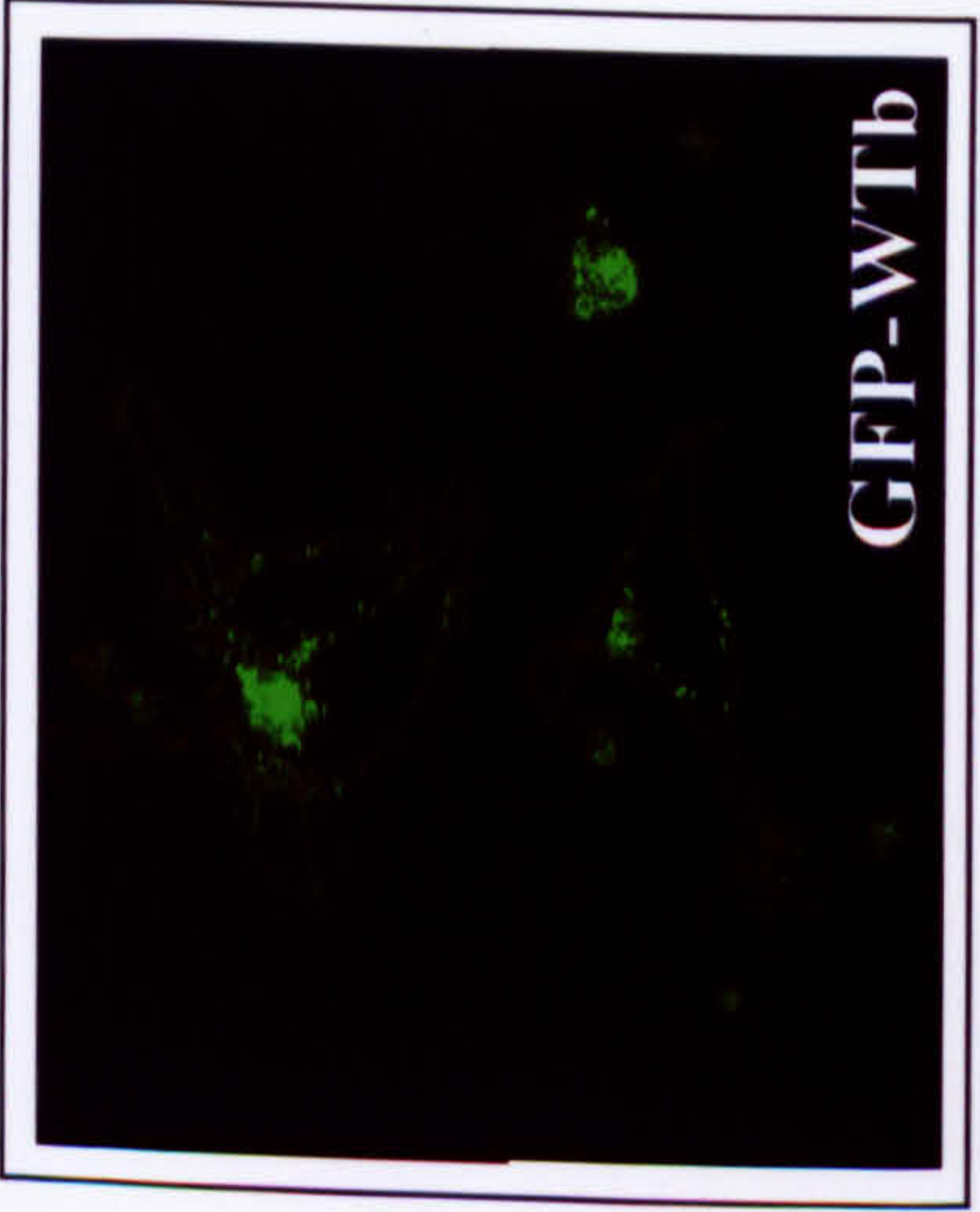
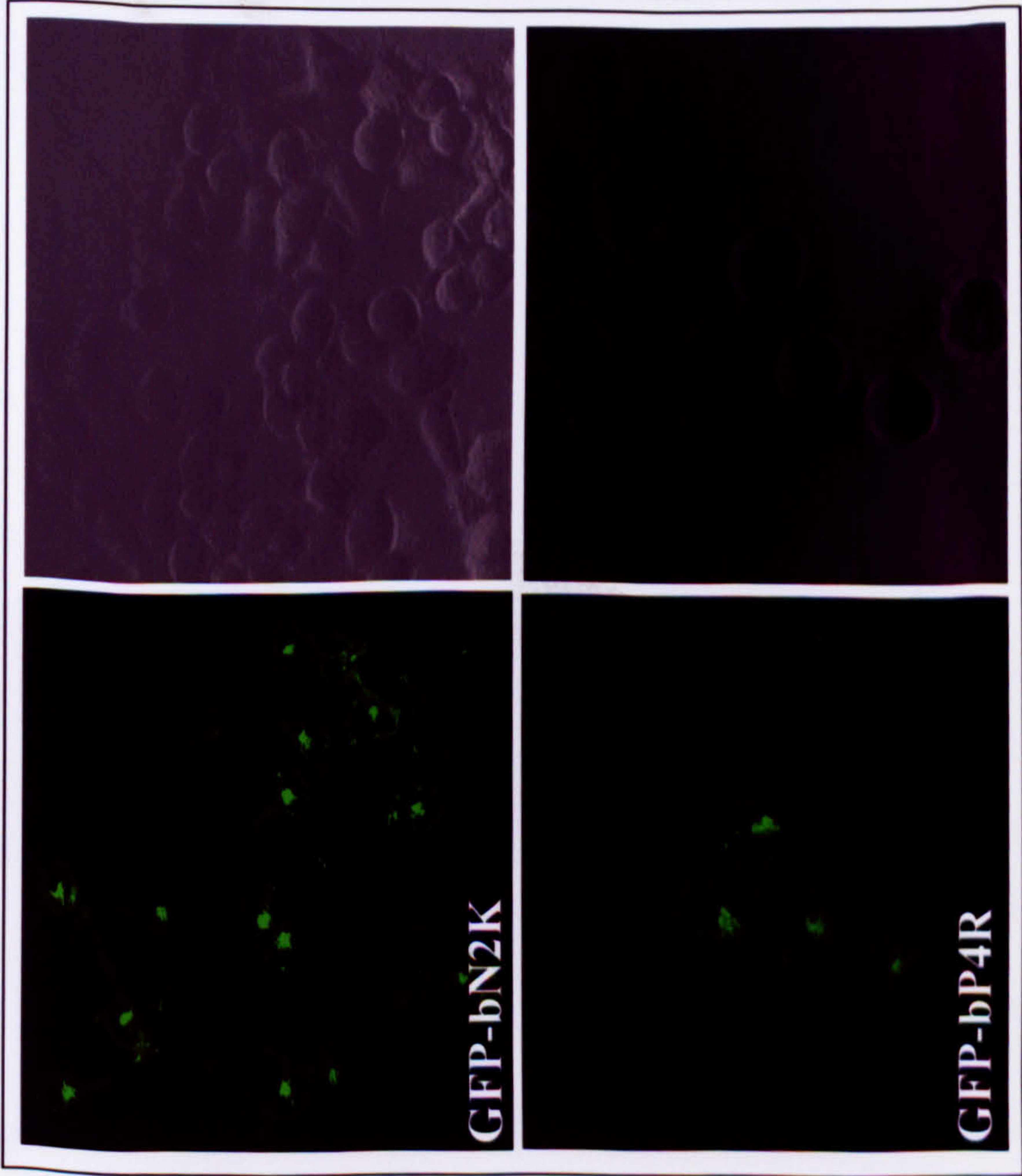
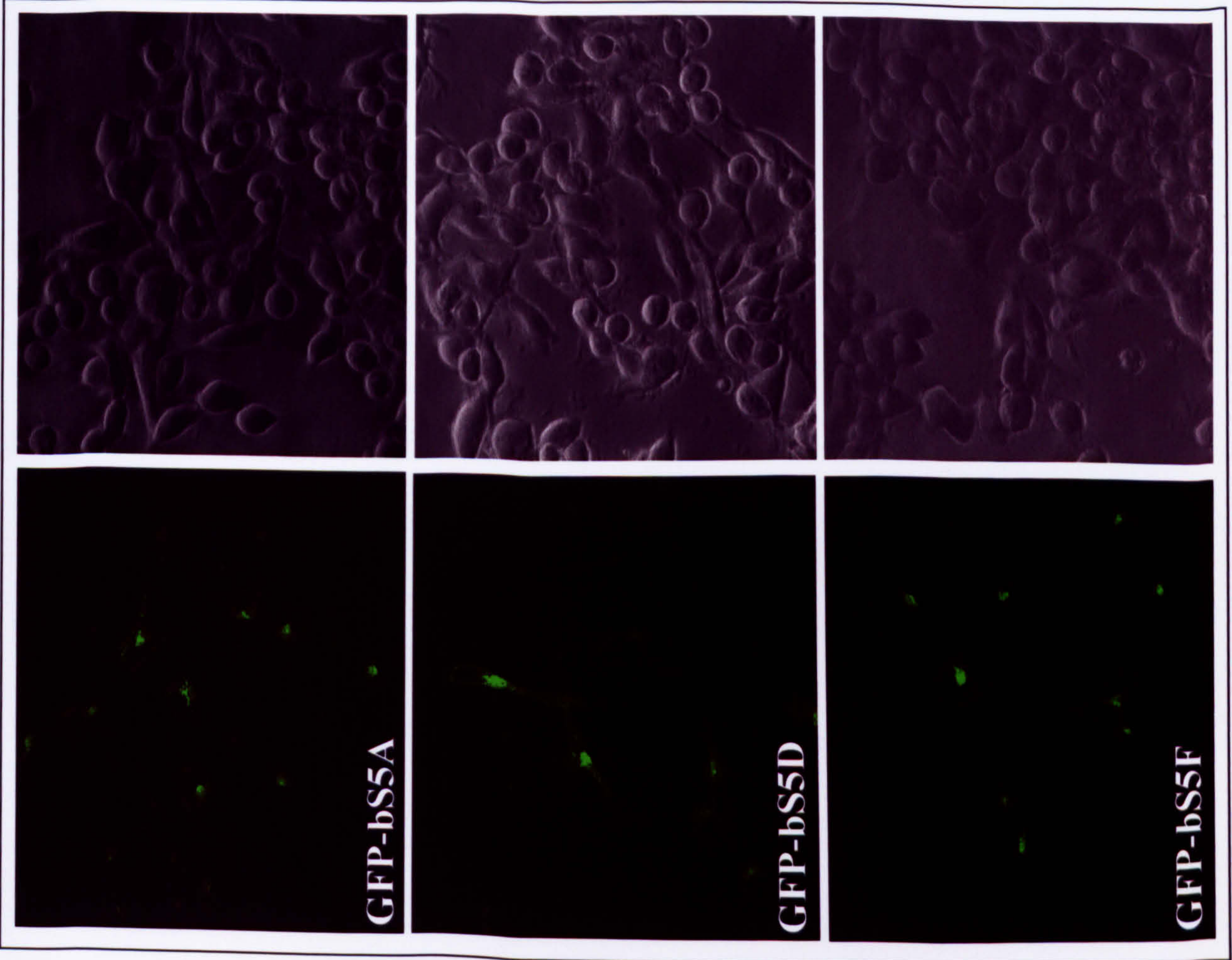




## **FIGURE 4.26 THE GFP-CD23bP3R MUTANT DEMONSTRATED TWO DISTINCT PATTERNS OF EXPRESSION**

The stably-transfected cell line expressing the GFP-CD23 bP3R mutant protein was found to result in two types of cell; those expressing little protein which in the most part seemed to be contained within the cell (A) and those expressing higher levels of the protein, and demonstrating a plasma membrane localisation. This mutant was found not to be able to target the plasma membrane in HEK 293 cells, but this appears not to be the case in this lymphocytic cell line. These findings seem to suggest that the bP3R mutant does reach the plasma membrane in Raji A cells (supported by the FACs analysis in Figure 4.23), all be it at low levels.



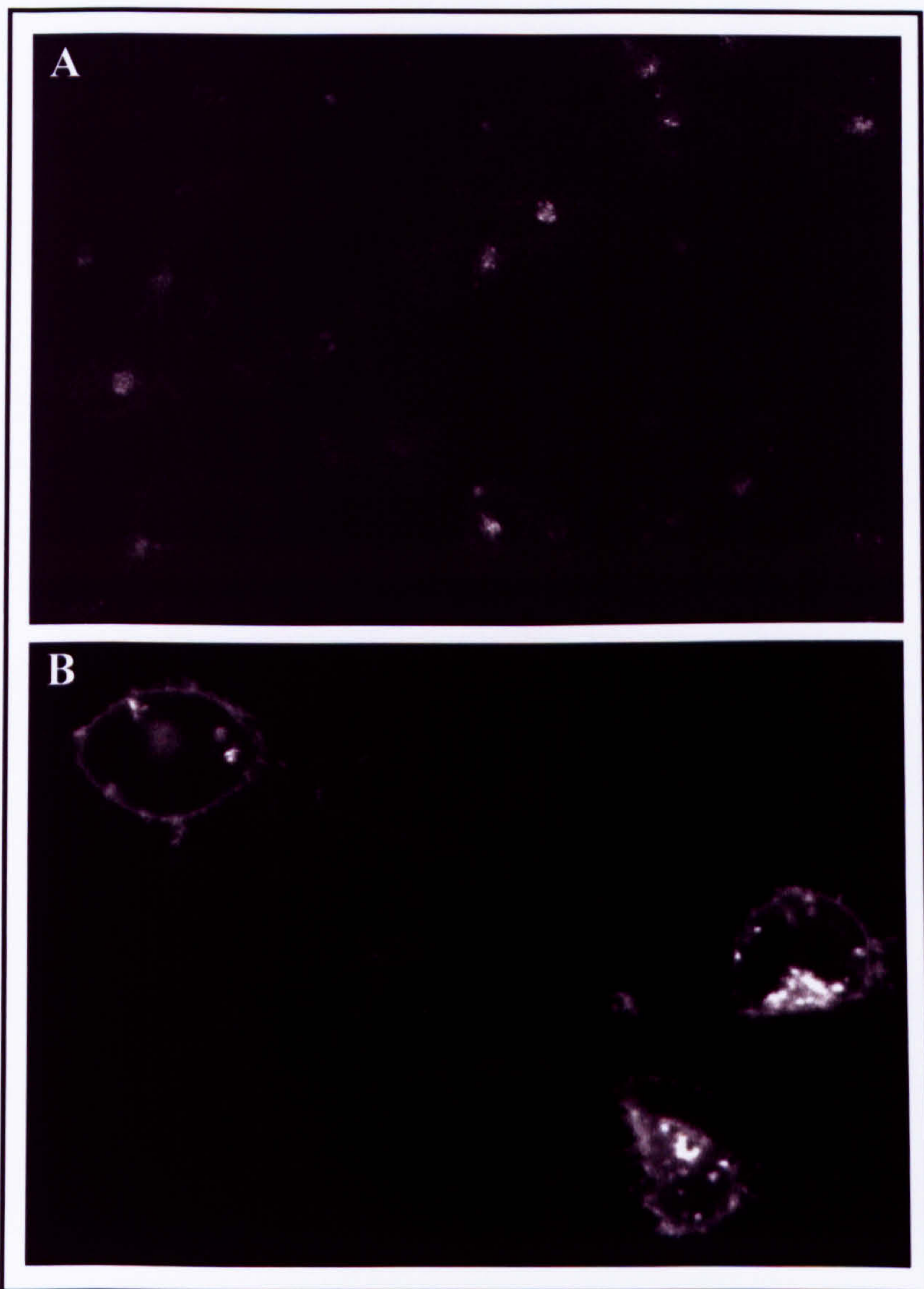


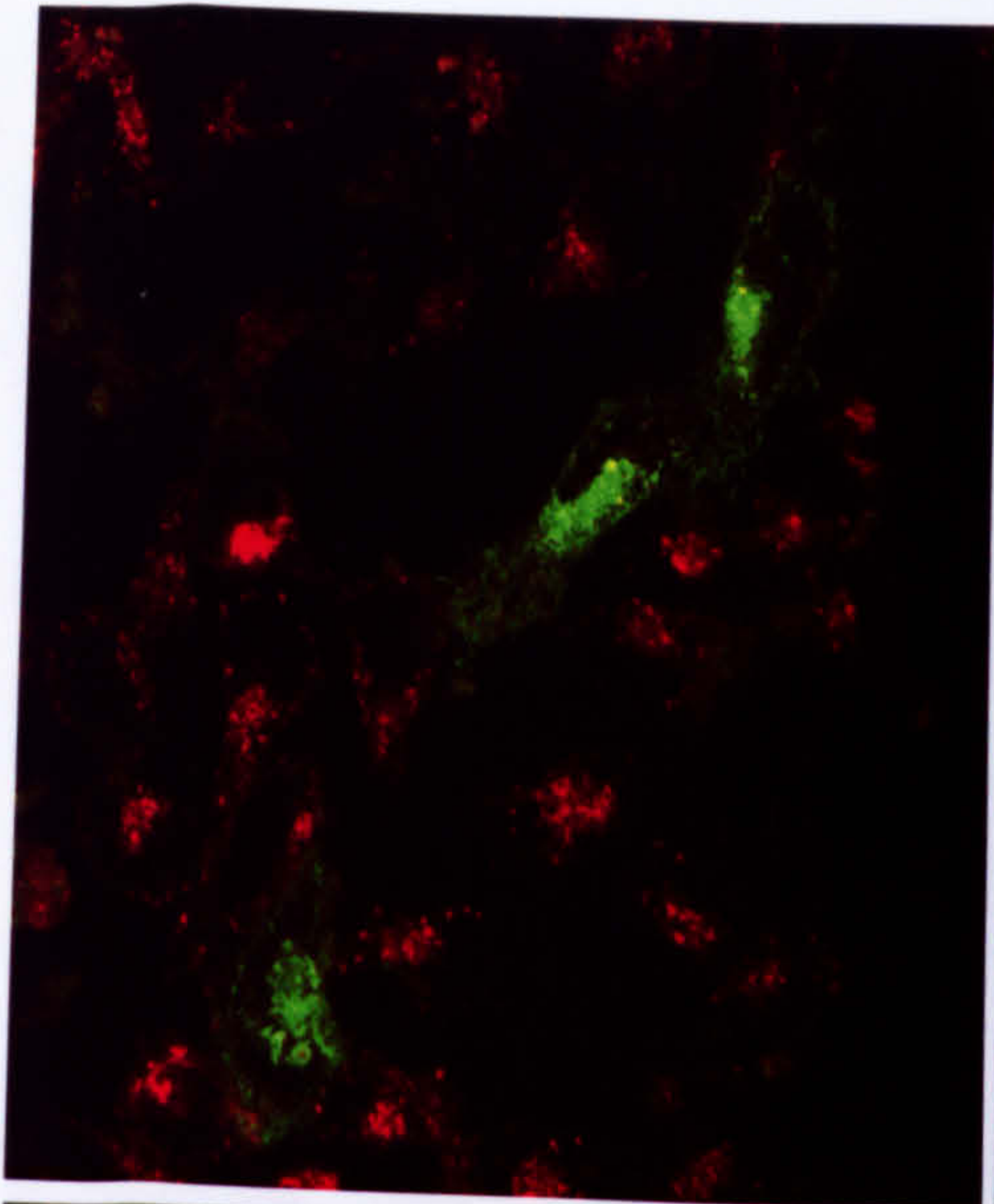
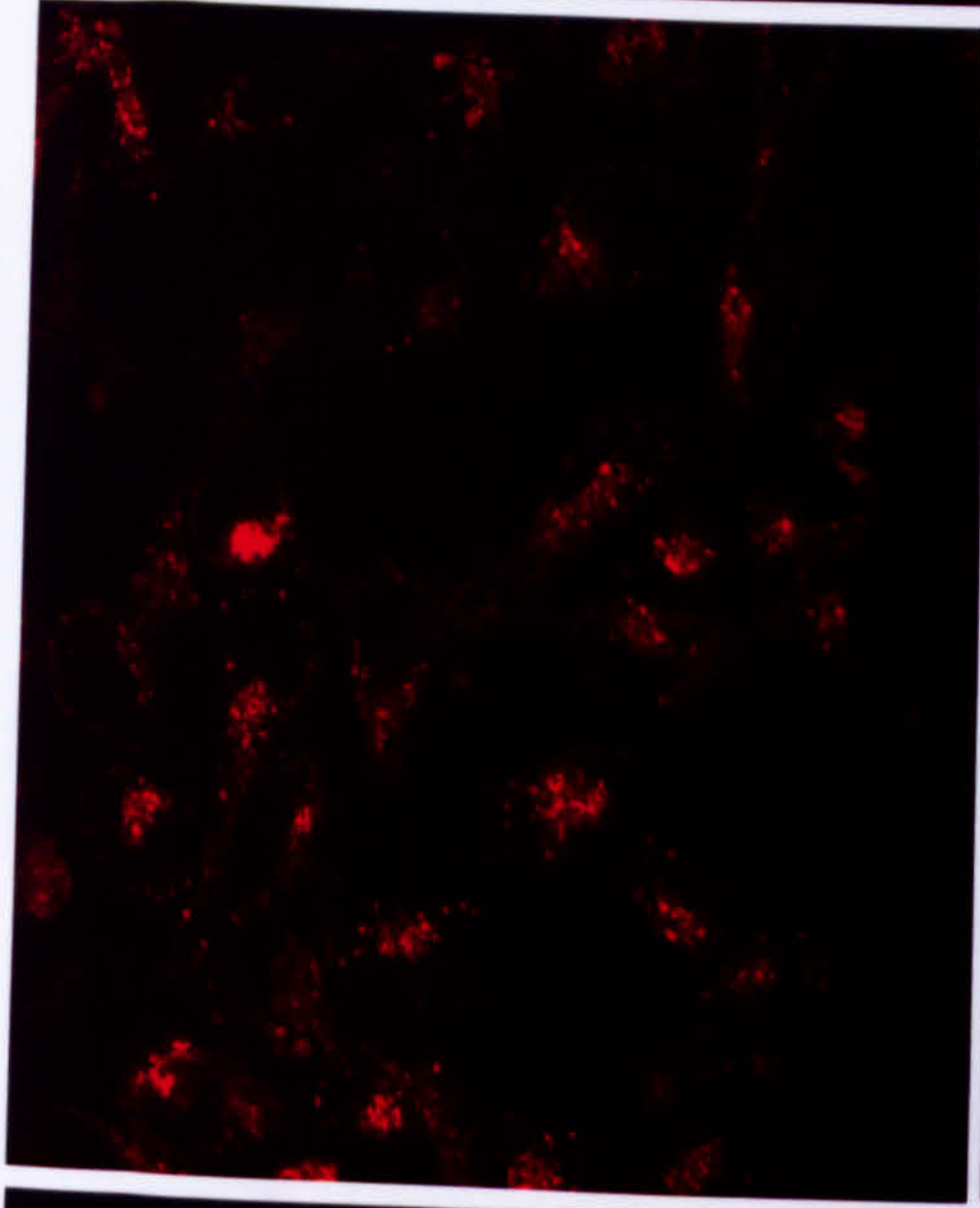
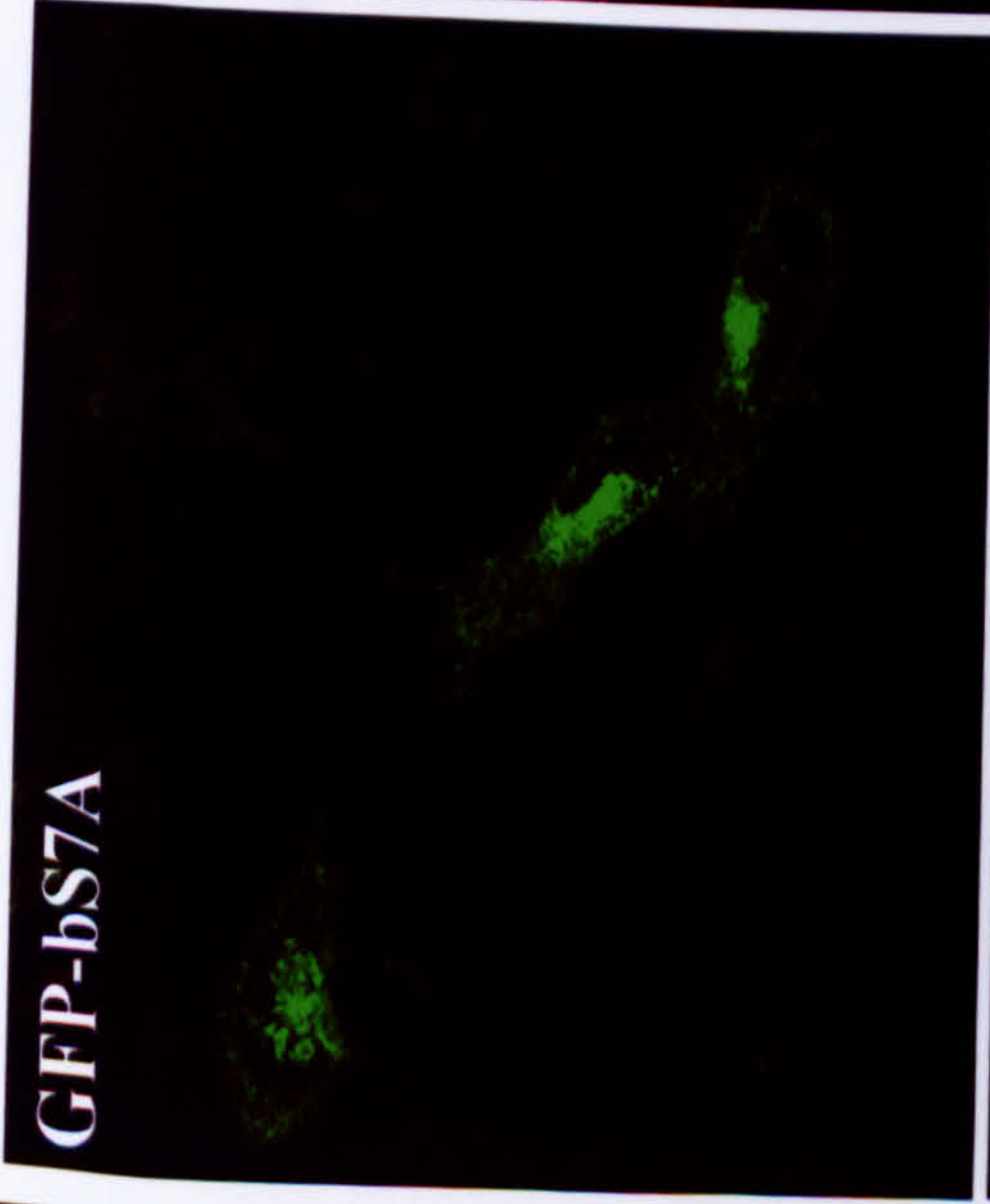


**FIGURE 4.27 BOTH GFP-CD23A S7A AND S7D MUTANTS APPEAR TO CO-LOCALISE WITH TEXAS RED-MODIFIED TRANSFERRIN (Tf-TxR) IN THE BASAL STATE IN RAJI A CELLS**

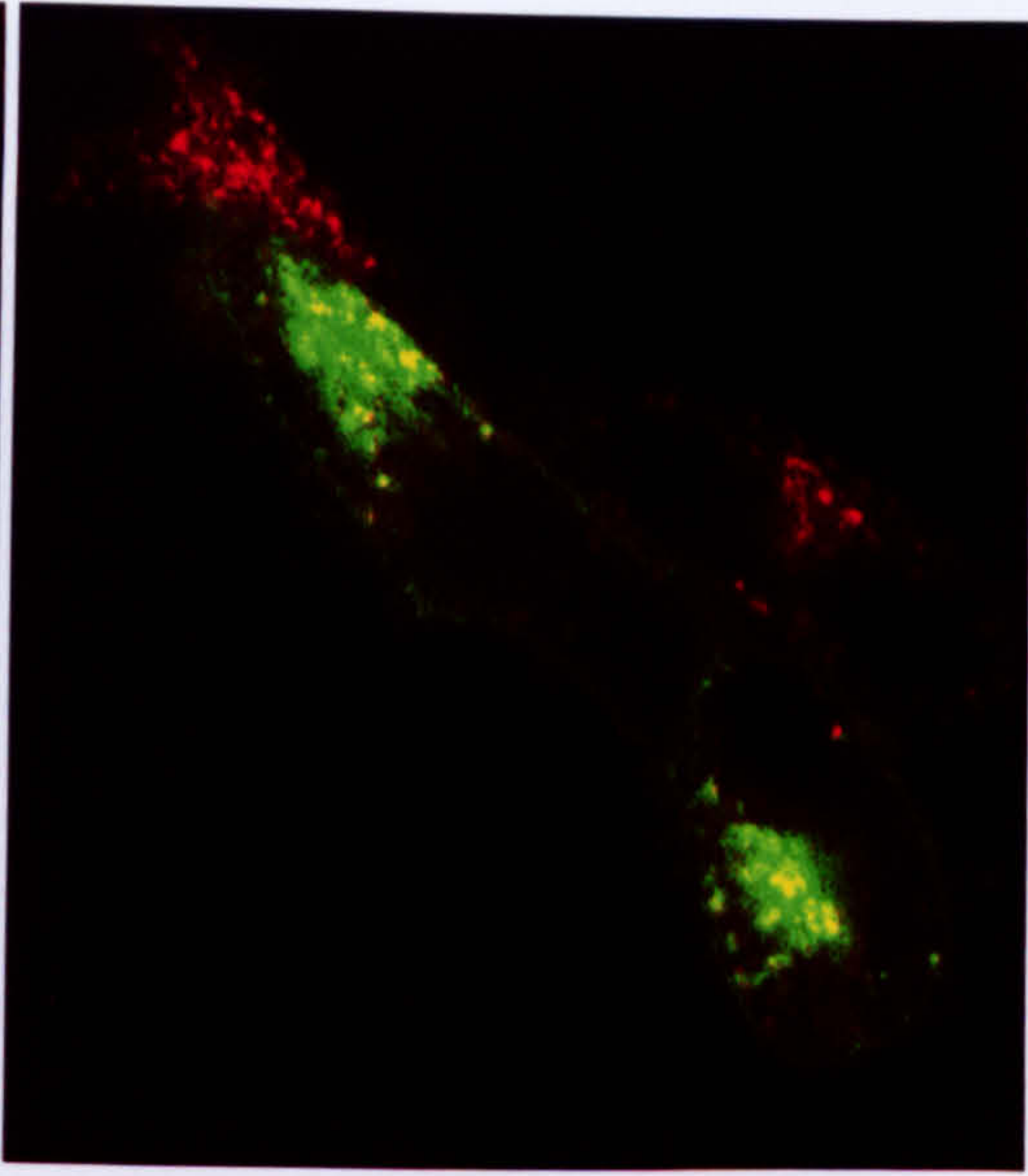
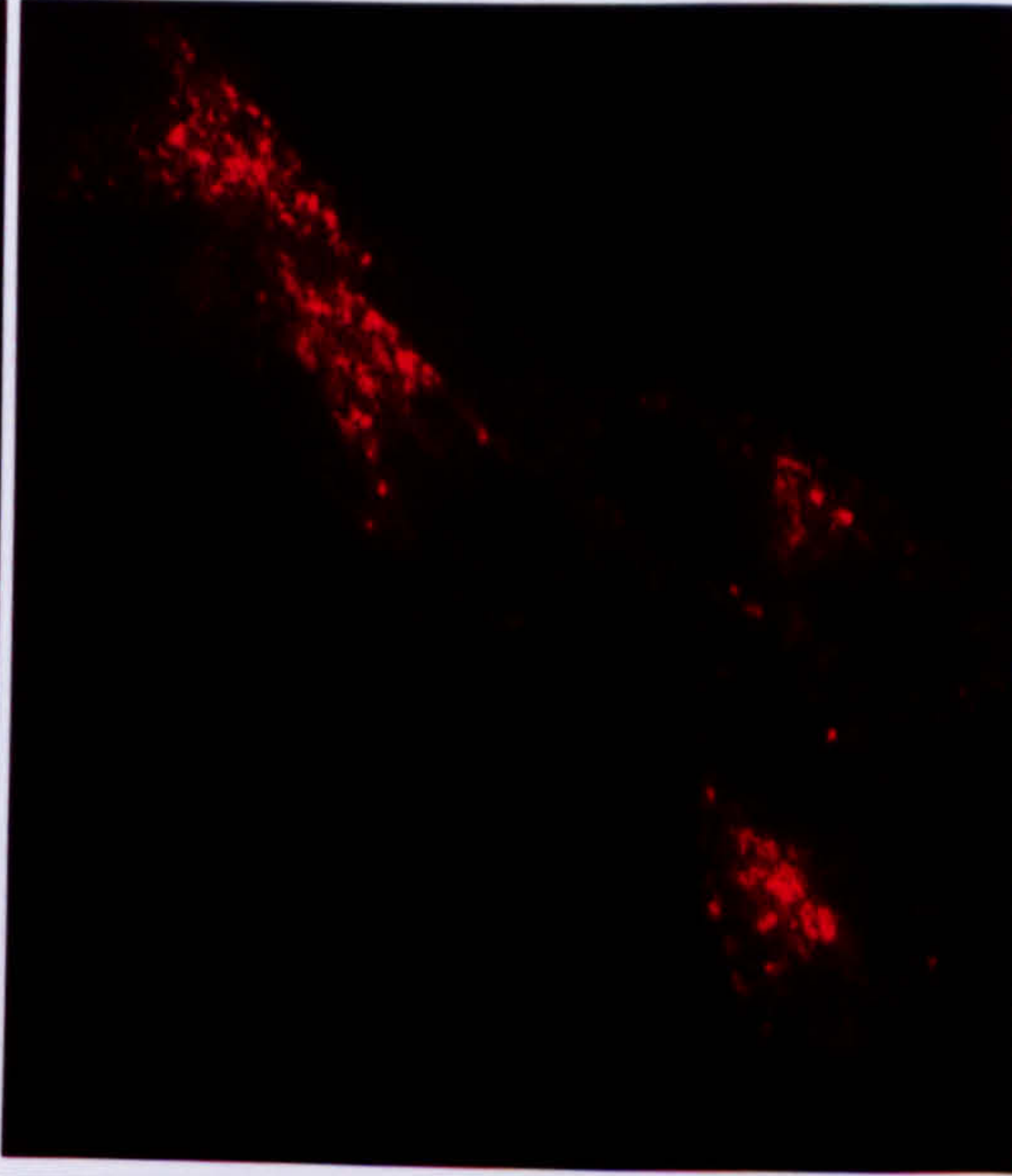
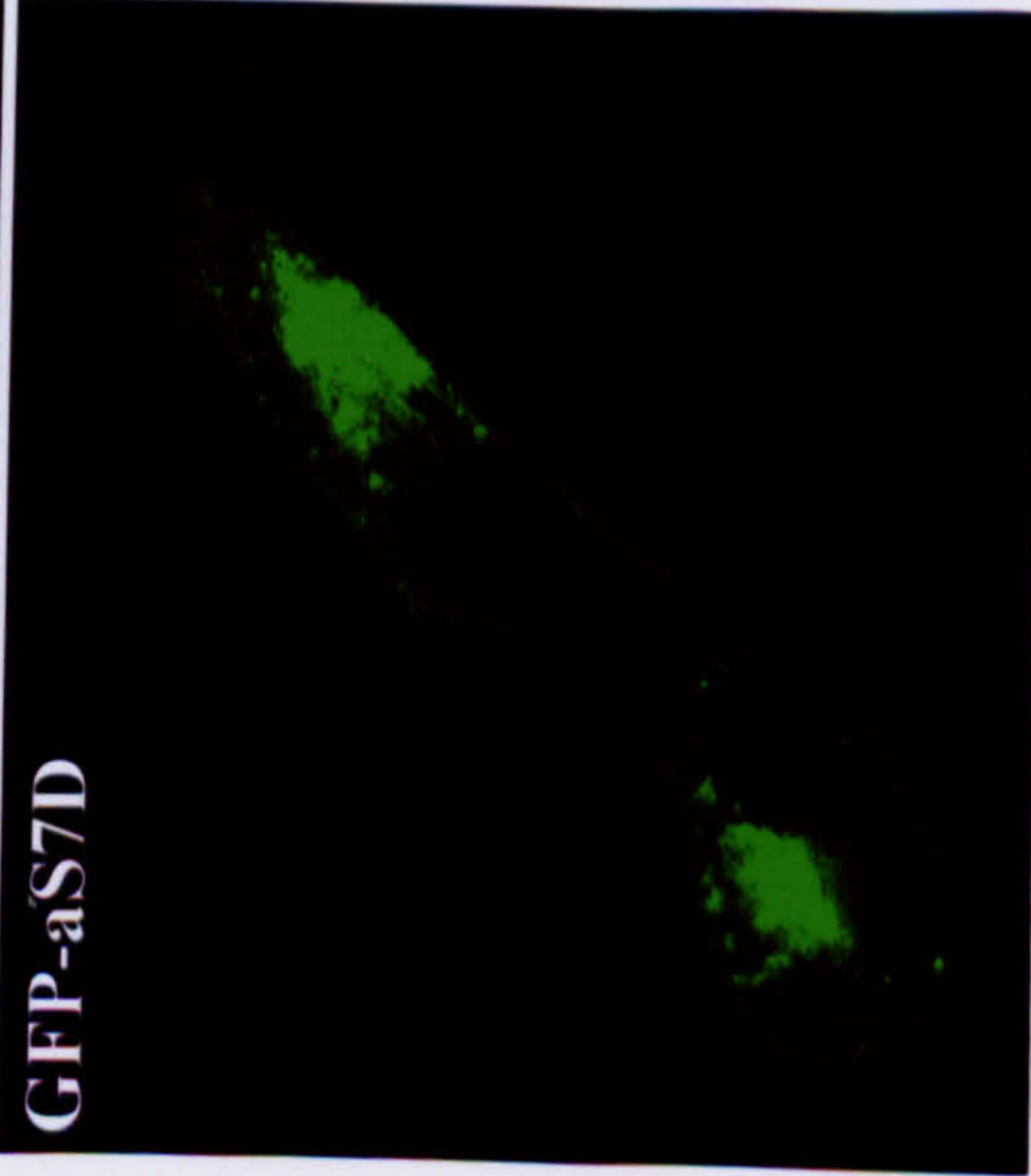
Coverslips bearing G418-resistant Raji A cells expressing either of the GFP-CD23 aS7A or aS7D mutant proteins were pre-incubated with 20µg Tf-TxR prior to confocal analysis. The cells were exposed to no stimulus and basal trafficking was monitored by confocal microscopy over a 45 minute period. The images shown demonstrate the typical basal staining patterns observed for these mutants. Much of the GFP-CD23 fluorescence was located within the plasma membrane of these cells, however there were patches of co-localisation present within the cells for both mutant proteins, as well as at the cell surface in the aS7D mutant.



GFP-bS7A



GFP-aS7D



GFP

Tf-TxR

Merged



## **FIGURE 4.28 BASAL LOCALISATION IN RAJI A – GFP-CD23<sup>aY6F</sup> AND <sup>aYS67FA</sup> MUTANTS**

Coverslips bearing G418-resistant Raji A cells expressing either of the GFP-CD23 <sup>aY6F</sup> or <sup>aYS67FA</sup> mutant proteins were pre-incubated with 20µg Tf-TxR prior to confocal analysis. The cells were exposed to no stimulus and basal trafficking was monitored by confocal microscopy over a 45 minute period. The images shown demonstrate the typical basal staining patterns observed for these mutants.

Both of these mutants were expressed at low levels in the stably-transfected Raji A cells, with much of the GFP-CD23 fluorescence located within the plasma membrane of these cells. Evidence of a punctate morphology was observed for both mutants. A couple of small patches of co-localisation were noted, in a few cells.



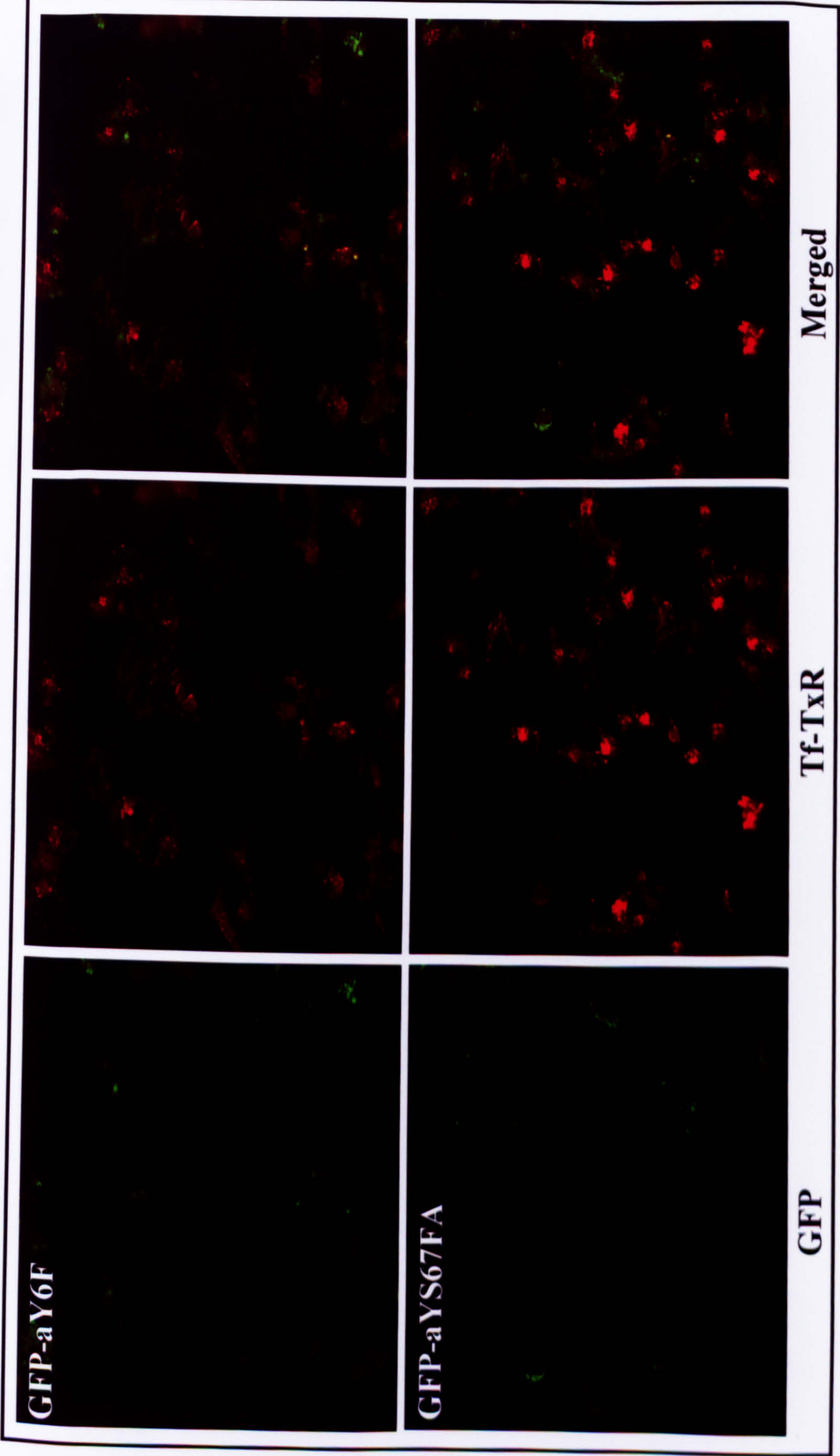




## **FIGURE 4.29 BASAL LOCALISATION IN RAJI A – GFP-CD23bS5A, S5D AND S5F MUTANTS**

Coverslips bearing G418-resistant Raji A cells expressing either of the GFP-CD23bS5A, bS5D or bS5F mutant proteins were pre-incubated with 20µg Tf-TxR prior to confocal analysis. The cells were exposed to no stimulus and basal trafficking was monitored by confocal microscopy over a 45 minute period. The images shown demonstrate the typical basal staining patterns observed for these mutants.

All of these mutants were located predominantly at the plasma membrane, and showed a punctate distribution (particularly the bS5D mutant). Patches of co-localisation with Tf-TxR were also observed in each of these stably-transfected cell lines, and was predominantly located at the cell surface.



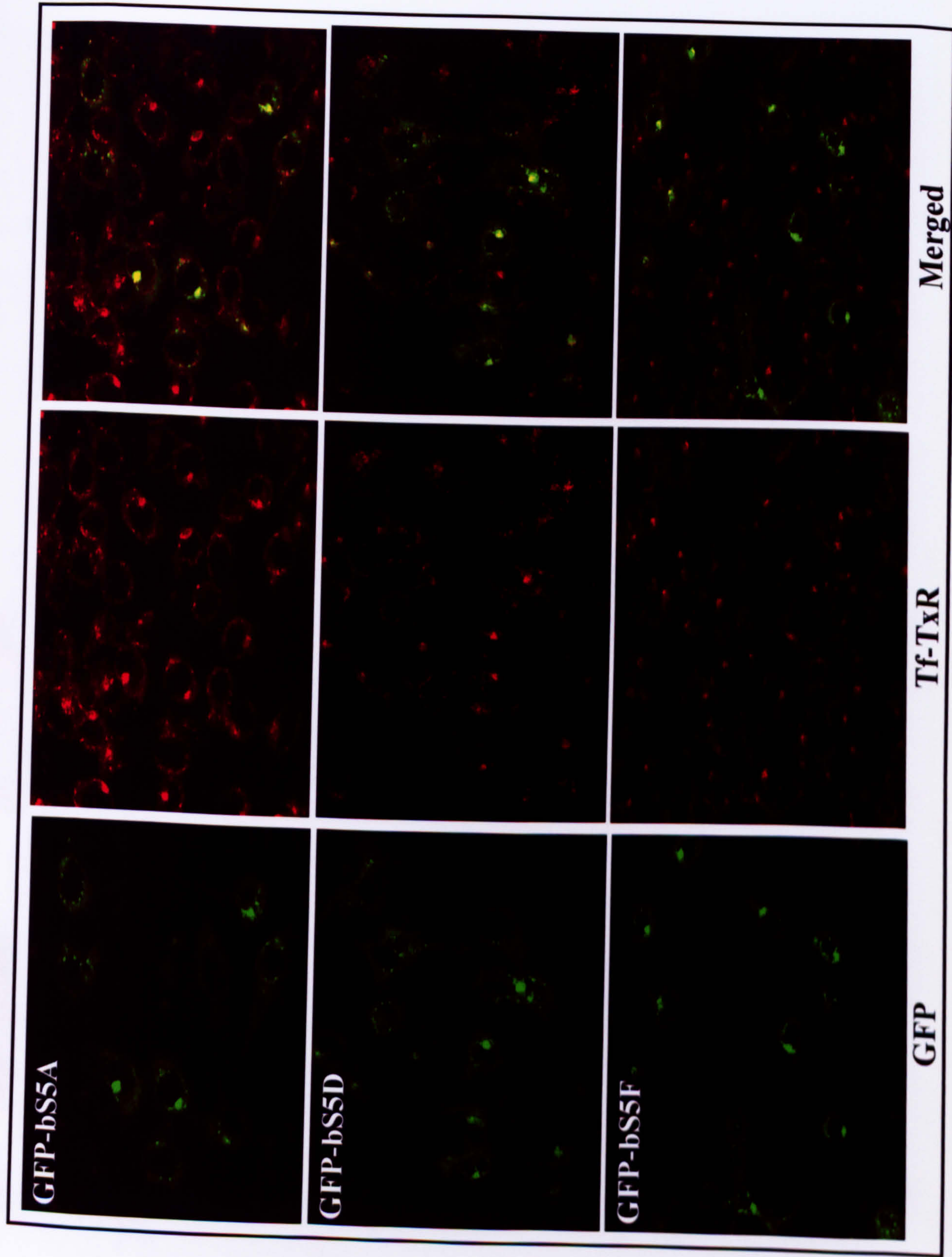


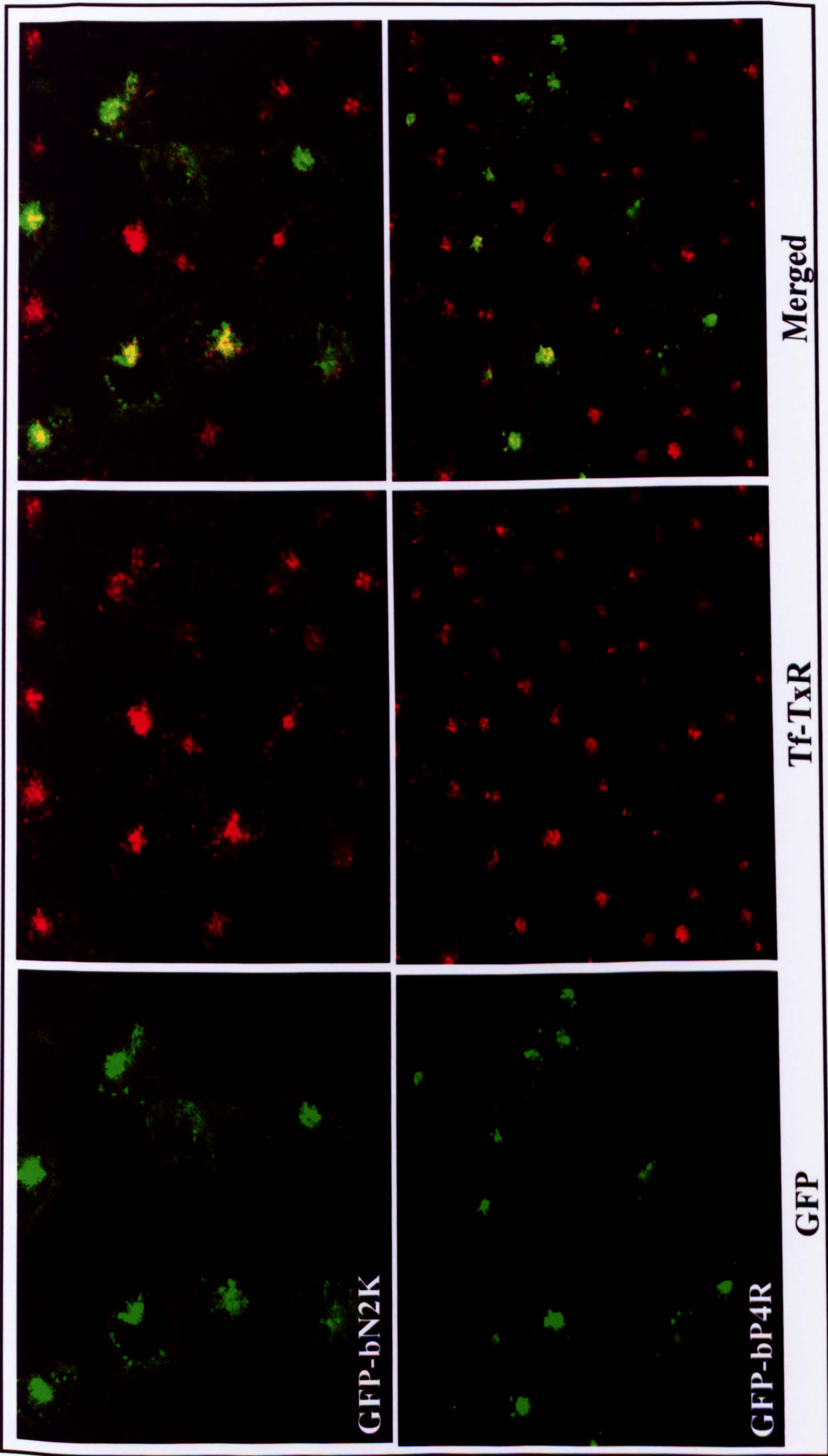


### **FIGURE 4.30 BASAL LOCALISATION IN RAJI A – GFP-CD23bN2K AND P4R MUTANTS**

Coverslips bearing G418-resistant Raji A cells expressing either of the GFP-CD23bN2K or bP4R mutant proteins were pre-incubated with 20µg Tf-TxR prior to confocal analysis. The cells were exposed to no stimulus and basal trafficking was monitored by confocal microscopy over a 45 minute period. The images shown demonstrate the typical basal staining patterns observed for these mutants.

Both of these mutants were expressed at reasonable levels in the stably-transfected Raji A cells, with much of the GFP-CD23 fluorescence located within the plasma membrane of these cells. Concentrated patches of the GFP-CD23bN2K mutant were observed at the cell surface. The GFP-CD23bP4R mutant was demonstrated to have distinct foci of green fluorescence within the cell. Patches of co-localisation with Tf-TxR were observed within the cells expressing each of these mutant proteins.







## **CHAPTER 5**

### **IDENTIFICATION OF CD23 N-TERMINAL TAIL BINDING PARTNERS USING THE YEAST TWO-HYBRID SYSTEM**



## 5.1 INTRODUCTION

Many biological processes are based upon specific interactions that occur between proteins so it is not surprising that considerable effort has been made to identify species that bind to known proteins of interest. Historically these protein-protein interactions have been detected using physical or indeed classical biochemical approaches, such as co-immunoprecipitation and cross-linking. The main disadvantage of these systems is that they result only in the identification of the apparent molecular weight of the associated interacting protein; obtaining the cloned gene is often a difficult and complex process. In one approach, this problem was circumvented by the use of purified proteins as probes against bacterial expression libraries, where a positive signal for an interacting protein is accompanied by the corresponding gene [Nelbock *et al.*, 1990].

A number of these so called 'library-based' methods have developed including protein-probing [Young & Davies, 1983] and phage display [Smith, 1985]. Protein probing utilises a labelled protein to screen an expression library, with the interactions between the immobilised protein and the labelled protein probe occurring on nitrocellulose filters. The main disadvantage of this system is that proteins encoded in the library must be capable of folding correctly in *E.coli*, generally as fusion proteins, and of maintaining their structure on nitrocellulose. Phage display utilises an *E.coli* filamentous phage, such as M13, bearing the protein of interest as a fusion to coat proteins on the cell surface. Random sequences can be inserted into the coat protein genes, enabling the generation of a library of fusion phage. Binding partners are detected by a series of affinity purifications. The main disadvantages of this system echo the previous discussion, with both systems taking place in *E.coli* cells. Phage display is primarily limited to small peptides, with larger inserts generally interfering with the function of the coat proteins. The exception to this being 25kDa ScFv antibody phage display libraries.

The yeast two-hybrid system, originally described by Fields & Song, 1989, is another library-based method by which protein-protein interactions can be identified *in vivo* through the reconstitution of the activity of a transcriptional activator. The method is based on the fact that most eukaryotic transcriptional activators are composed of two



physically separable and functionally distinct domains; a DNA binding domain (DNA-BD) which recognises and binds to a sequence upstream of the responsive genes (upstream activating sequence, UAS) and an activation domain (AD) which interacts with other components of the transcriptional machinery required to initiate transcription. Both these domains are necessary to initiate transcription of the response gene(s), and must be in close enough proximity to one another to do so, as neither domain is able to initiate transcription alone [Brent & Ptashne, 1985; Ma & Ptashne, 1987]. Figure 5.1A details a schematic representation of the general yeast two-hybrid strategy, and illustrates how it functions to detect interacting proteins.

The feasibility of the yeast two-hybrid system was originally demonstrated by using it to detect an interaction between the yeast proteins SNF1, a protein kinase, and SNF4, a protein associated with the kinase [Fields & Song, 1989]. Since then the technique has been further developed by many research groups and indeed there are now several versions of the yeast two-hybrid system commercially available. Most systems contain either the yeast GAL4 or the *E.coli* LexA protein as the DNA-BD, and the GAL4 or herpes simplex virus VP16 protein as the AD, respectively.

The yeast two-hybrid system has been used in this chapter to investigate possible interactions between the N-terminus of CD23 and proteins encoded by a human leukocyte cDNA library. The Clontech MATCHMAKER two-hybrid 3 assay based upon the GAL4 system, shown to consist of separable domains responsible for DNA-binding and transcriptional activation [Keegan *et al.*, 1986], was the system utilised for this work. Briefly, the bait gene (the N-terminal cytoplasmic domain of CD23) is expressed as a fusion to the GAL4 DNA-binding domain, while proteins encoded by the Clontech human leukocyte MATCHMAKER cDNA library are expressed as fusions to the GAL4 activation domain, Figure 5.1B.

The MATCHMAKER two-hybrid system 3 has been developed to incorporate many features serving to reduce the incidence of false positive results and enable quick identification of true protein-protein interactions. The yeast two-hybrid systems provide a sensitive method for detecting relatively weak and transient interactions, so much so



that occasionally these interactions may not be biochemically detectable, but may still be critical for correct functioning of complex biological systems [Guarente, 1993; Estojak *et al.*, 1995]. The sensitivity of the MATCHMAKER GAL4 two-hybrid system 3 is primarily attributable to the amplification of positive signals *in vivo* (i.e., transcriptional, translational and enzymatic). In addition, because the two-hybrid assay is performed *in vivo*, the proteins are more likely to be in their native conformations, which may lead to increased sensitivity and accuracy of detection.

The MATCHMAKER yeast two-hybrid system 3 also features a new yeast strain, AH109, which utilises 3 reporters – ADE2, HIS3 and MEL1 (or lacZ) – under the control of distinct GAL4 upstream activating sequences (UASs) and TATA boxes (Figure 5.2). The simultaneous use of these different reporter genes that share minimal sequence overlap in their promoters has improved the specificity of detection, thus helping to reduce the number of false positives detected. The ADE2 reporter alone provides strong nutritional selection: the option of using HIS3 selection allows the stringency of selection to be controlled and can reduce the incidence of false positives [James *et al.*, 1996]. MEL1 is an endogenous gene found in several yeast strains and encodes  $\alpha$ -galactosidase, a secreted enzyme that enables direct enzyme assay on X- $\alpha$ -Gal indicator plates, employing a blue/white, positive/negative screening. It should be noted at this stage however that some false positives will always arise due to the ability of certain target clones to activate transcription in the absence of a DNA binding domain, as well as for other unknown reasons [Bartel *et al.*, 1993]. The tight regulation of the GAL UASs by GAL4 makes it a valuable tool for manipulating expression of the reporter genes in two-hybrid systems that are dependent on the GAL4 DNA-BD. The yeast strain must also carry deletions that ensure the endogenous GAL4 gene is not expressed. In addition, GAL80 is also mutated as its product inhibits the function of GAL 4. The yeast strain must also contain auxotrophic markers for the selection of yeast transformed with target and/or bait plasmids. The genotype of the AH109 yeast strain is also detailed in Figure 5.2.

The yeast two-hybrid assay does however hold some disadvantages that largely depend upon the nature of the proteins being assayed. The assay is limited to proteins that can



be located to and stably expressed in the nucleus and therefore this may exclude some membrane and extracellular proteins. Certain post-translational modifications required for some protein-protein interactions in higher eukaryotes, such as tyrosine phosphorylation, glycosylation, disulphide bond formation and acetylation do not occur in yeast and this may also limit the proteins which can be used/detected. However it should also be noted that the yeast cell system does provide more post-translational modifications than any bacterial cell system. Since the proteins are expressed as fusion proteins, the GAL4 domains may interfere with the ability of the test proteins to interact [van Aelst *et al.*, 1993] although this is generally not found to be a common problem. It has also be noted that some proteins, including those not normally involved in transcription, are able to activate transcription when fused to the DNA-BD [Ma & Ptashne, 1987] or may be lethal or harmful when expressed in yeast [Allen *et al.*, 1995], preventing their use as bait proteins. These factors must all be considered when choosing the bait protein.

The yeast two-hybrid system identifies protein-protein interactions purely on a physical basis, therefore interactions could be detected between proteins that never come into contact with each other in a natural scenario. It is therefore paramount that all potential interactors be checked out by further biochemical analysis and cell/tissue distribution tests before the interaction can be confirmed to be true.

In summary, the yeast two-hybrid system is a very attractive tool as it is not only capable of identifying individual proteins encoded in large cDNA libraries able to interact with a known protein, but it also results in the immediate availability of the cloned gene for these interacting species. The N-terminal tail of CD23 is relatively short in comparison to most cell surface receptors and it does not contain any of the well-characterised consensus sites required for some of the more common protein-protein interactions associated with receptor signalling such as Src homology domains and the usual tyrosine-based sorting motifs. It has therefore been hypothesised that CD23 may indeed be required to bind to some sort of 'adapter-like' protein thus enabling recruitment of the necessary signalling molecules to promote its function. The work detailed in this chapter utilises the yeast two-hybrid system in an attempt to identify



proteins that bind to the cytoplasmic N-terminal tail of CD23 in order to investigate this theory.

## **5.2 RESULTS**

### **5.2.1 GENERATION OF THE GAL4 DNA-BD-CD23 FUSION CONSTRUCTS**

DNA encoding full length CD23 was amplified using PCR and the oligonucleotides detailed within Figure 5.3A, in order to generate DNA fragments containing the N-terminal tail of either the CD23a or CD23b isoform enclosed by additional endonuclease restriction sites. Both single (s) and triple (t) CD23 bait constructs were generated, containing either one or three sequential copies of the CD23 N-terminal tail, respectively. The transmembrane domain was not included as it was likely to have posed expression/sorting problems due to the nature of the amino acids involved. These PCR fragments were digested with the appropriate restriction endonuclease enzymes and directionally cloned in-frame into the multiple cloning site (MCS) of the DNA-BD vector, pGBKT7 (Figure 5.3B), to create pCD23a<sub>s</sub>, pCD23a<sub>t</sub>, pCD23b<sub>s</sub> and pCD23b<sub>t</sub> respectively. Figure 5.3C illustrates the cloning strategy involved in the generation of each of the CD23a and CD23b single and triple bait fragments and the restriction sites utilised in order to clone these baits into the pGBKT7 MCS. Figure 5.3D illustrates the resultant bait constructs, highlighting any additional amino acids incorporated as a result of the cloning strategy. Endonuclease restriction digestion was performed to check that each of the bait inserts had been cloned correctly, Figure 5.3E shows the fragment banding produced. Each construct was analysed, and the CD23 N-terminal tail fragments were confirmed to have been correctly inserted in-frame (data not shown). pGBKT7 generates a fusion of the GAL4 DNA-BD and the bait protein and facilitates the growth of yeast cells expressing this plasmid on SD/-Trp selection medium.

### **5.2.2 EXPRESSION OF THE GAL4 DNA-BD-CD23 FUSION BAIT PROTEINS IN AH109 YEAST CELLS**

The four GAL4 DNA-BD-CD23 bait constructs were individually transformed into AH109 yeast cells and tested for toxicity and autonomous activation of the MEL1 reporter gene. Toxicity was assessed by comparing the growth rate and colony number



of yeast transformed with each of the bait constructs and yeast transformed with the empty pGBKT7 plasmid, on SD/-Trp agar. The colony growth was found to be very similar in each instance, indicating that the expression of the CD23a<sub>s</sub>, CD23a<sub>t</sub>, CD23b<sub>s</sub> and CD23b<sub>t</sub> proteins was non-toxic in yeast, since no significant reduction in colony number or growth rate was observed. Figure 5.4 shows the resultant growth of AH109 yeast cells containing each of the bait vectors, on SD/-Trp agar.

Autonomous activation of the MEL1 reporter gene was assayed by growing colonies expressing each of the bait constructs +/- the empty pACT2 vector on SD/-Trp-Leu or SD/-Trp agar containing X- $\alpha$ -Gal, respectively. Had the bait plasmids been able to activate MEL1 activity, the  $\alpha$ -galactosidase enzyme produced would have been able to metabolise the X- $\alpha$ -Gal substrate resulting in the formation of blue colonies. This was found not to be the case, indicating that none of the bait plasmids are able to self activate MEL1, either alone or in the presence of the empty GAL4 AD vector, pACT2 (data not shown).

Having demonstrated each of the bait plasmids to be non-toxic and non-self activating, it was then vital to confirm each of the proteins were in fact being expressed correctly and that the negative findings discussed above were indeed real. Protein expression was analysed by direct lysis of AH109 yeast cells transformed with each of the four bait constructs using the TCA protein extraction method detailed in section 2.2.10B. The proteins were detected using antibodies specific to the c-Myc tag, resulting in the identification of a strong band at the 30 and 36kDa position in yeast cells transformed with pCD23a<sub>s</sub>/pCD23b<sub>s</sub> and pCD23a<sub>t</sub>/pCD23b<sub>t</sub> respectively (Figure 5.5). These bands correspond to the expression of each of the CD23 N-terminal tail bait proteins as fusion proteins linked to the GAL4 DNA-BD and a c-Myc tag. Collectively these results clearly demonstrate that each bait protein is not only being expressed correctly, but that each protein is also a suitable candidate for screening using this yeast two-hybrid system.



### 5.2.3 SUCCESSFUL AMPLIFICATION OF THE MATCHMAKER HUMAN LEUKOCYTE cDNA LIBRARY

A human leukocyte MATCHMAKER cDNA library, generated from normal human leukocyte mRNA pooled from 550 male/female caucasians ages 18-40, was obtained from Clontech. The cDNA had been *Xho I*-(dT)<sub>15</sub> primed and uni-directionally cloned into the *Eco RI-Xho I* sites in the multiple cloning site of pACT2, Figure 5.6A. The library had been prepared using oligo(dT) priming, used to eliminate the synthesis of lengthy poly(dT) regions and ensure that full length clones and 3' ends would be well-represented within the library [Chenchik *et al.*, 1994; Borson *et al.*, 1992; Moqadam & Siebert, 1994].

The pACT2 vector generates a fusion of the GAL4-AD (amino acids 768-881), an HA epitope tag, and the protein encoded by the cDNA in the fusion library. The expressed protein is targeted to the yeast nucleus by the nuclear localisation sequence from the simian virus 40 large T-antigen (SV40 T antigen) [Chien *et al.*, 1991] that has been cloned into the 5' end of the GAL4 AD sequence. pACT2 also contains the LEU2 nutritional gene that allows yeast auxotrophs to grow on limiting synthetic media.

The information provided along with the library demonstrated it to contain approximately  $3.5 \times 10^6$  independent clones, with insert sizes ranging from 0.4 - 4.0kb, the average size being 2.0kb. The library was re-titred in-house and found to contain  $4 \times 10^8$  colony forming units (cfu)/ml (Figure 5.6B), using the method detailed in section 2.2.8A.

The library sample had to be amplified, see section 2.2.9, in order to ensure enough DNA was available for screening purposes. The resultant DNA was used to transform JM109 bacterial cells. 10 individual colonies were randomly picked and subjected to endonuclease restriction digestion. All 10 plasmids were shown to contain inserts of varying lengths. These results indicate that the amplification step had not caused an obvious loss in library representation and indeed that the DNA sample contained plasmids expressing a variety of cDNA insert sizes, Figure 5.6C.



## 5.2.4 OPTIMISATION OF TRANSFORMATION EFFICIENCY & FIRST PILOT-SCALE SCREEN

It is vitally important to maximise plasmid uptake in order to be able to effectively screen the largest number of clones possible per  $\mu\text{g}$  of library DNA added. A number of transformation reactions were carried out in order to establish the most appropriate amount of library DNA to add, i.e. the amount of DNA producing the greatest number of colonies/ $\mu\text{g}$  DNA.

Table 5.1 shows the results for each of the CD23a bait vectors, as the number of double transformants grown on each of the SD/-Trp/-Leu agar plates. The findings indicate the addition of  $1\mu\text{g}$  of library DNA to give the best transformation efficiency with the pCD23a<sub>s</sub> vector. Addition of more DNA than this resulted in the generation of less transformants/ $\mu\text{g}$  DNA, thus demonstrating a reduction in transformation efficiency. The transformation efficiencies using the pCD23b baits were generally found to be less than those observed for the pCD23a baits in each instance (data not shown).

**Table 5.1 Optimisation of Transformation Efficiency, recorded as number of cfu per SD/-Trp/-Leu agar plate**

Library DNA ( $\mu\text{g}$ )	pCD23a <sub>s</sub>	pCD23a <sub>t</sub>
0	0	0
0.1	4	57
1.0	397	24
2.0	74	76
5.0	232	267

In the first pilot-scale yeast two-hybrid screen, the pCD23a<sub>s</sub> and pCD23a<sub>t</sub> bait constructs were employed. In each case the bait vector was initially transformed into competent AH109 cells prior to transformation of the library DNA. The resultant transformation mixes were plated onto SD/-Trp/-Leu agar in order to calculate the efficiency of the transformation reaction in each case, calculated using the formula given in section 2.2.10H. These plates were then used to replica-plate the colonies onto



triple dropout agar (SD/-Trp/-Leu/-His). In screening less than  $1 \times 10^3$  transformants this experiment was too small to identify any real positive interactors, but was rather performed as run-through/test experiment of this new technique. The pCD23a<sub>s</sub> bait was found to give higher colony growth each time and was thus chosen as the bait for all initial screening work.

### **5.2.5 FIRST SMALL-SCALE SCREEN USING THE HUMAN LEUKOCYTE CDNA LIBRARY**

Approximately  $1 \times 10^5$  yeast transformants were screened, resulting in the growth of hundreds of tiny colonies on many of the SD/-Trp/-Leu/-His agar plates. The largest, most promising of these colonies were picked and streaked onto fresh agar, identifying in excess of 40 colonies that grew on triple selection agar. Triple drop-out agar selects for yeast expressing both the DNA-BD and AD plasmids as well as activation of the HIS3 reporter gene and therefore, yeast potentially containing interacting proteins. Replica plating was used to transfer these colonies onto quadruple drop out agar (SD/-Trp/-Leu/-His/-Ade), reducing the number of colonies to 38. These 38 clones were screened for expression of the second reporter gene, MEL1 using the  $\alpha$ -galactosidase assay (section 2.2.10G). Of these, 19 were found to grow repeatedly on quadruple dropout agar and shown to express  $\alpha$ -galactosidase, as indicated by the growth of blue colonies on agar plates containing the X- $\alpha$ -Gal substrate. Figure 5.7 shows sample plates containing a number of 'positive' clones able to activate MEL 1 reporter gene activity, inducing  $\alpha$ -galactosidase enzyme activity and having the capability to metabolise the X- $\alpha$ -Gal substrate. The non-reactive (white) colonies were discarded at this stage as false positives. This library screen was found to identify 19 'positive' clones that were found to be able to activate the ADE2, HIS3 and MEL1 reporter genes.

The plasmids were isolated from each of the 'positive' yeast clones using the protocol detailed in section 2.2.10A. The resultant DNA preparations were used to transform electrocompetent KC8 *E.coli* cells (section 2.2.10C), facilitating the isolation of each of the AD plasmids. The AD plasmids were then subjected to endonuclease restriction digestion to analyse the inserts contained in each. The AD plasmids were sequenced



immediately, using the pACT2 forward and reverse insert screening primers, detailed in section 2.1.8C.

Several clones (74% of those analysed) were identified as containing cDNA inserts with strong nucleic acid sequence homology to metallothionein II (MT-II). However each of these cDNA inserts were found to contain the nucleic acid sequence for MT-II in the same, incorrect open reading frame (ORF). Figure 5.8 details one of the cDNA fragments which was identified many times. The purple box and text indicate the location and protein sequence of MT-II, incorporated in ORF 3 (Figure 5.8). The insert sequence was translated using the correct ORF utilised by the AD vector and the resultant protein sequence is shown as pink text. All of the 'positive' clones identified in this small-scale screen were deemed to be false positives (for a variety of reasons) and were not investigated further.

### **5.2.6 LARGE SCALE SCREEN WITH INCREASED SELECTION STRINGENCY**

After two unsuccessful screens identifying only false positive species, the stringency of the final screen was increased, (Figure 2.4) by plating all transformants directly onto quadruple dropout agar (SD/-Ade/-His/-Trp/-Leu). The main aim of this strategy was to reduce the number of false positives identified, as theoretically anything which could grow under these higher stringency conditions is much more likely to be a truly positive interactor. The drawback is that proteins which interact either weakly or transiently with the CD23 bait protein may not be detected under these conditions.

#### **5.2.6A IDENTIFICATION OF EIGHT POTENTIALLY POSITIVE INTERACTORS**

Approximately  $2 \times 10^6$  independent clones were screened. 50 x 150mm plates were each spread with 150µl of the transformation mix and the plates were incubated at 30°C for up to 15 days. Colonies were picked as and when they appeared. A total of 14 colonies appeared and were re-streaked twice onto quadruple drop out agar plates, the second time onto agar containing the X-α-gal substrate in order to test for MEL1 activation. Just 8 clones were found to grow consistently on the quadruple drop out agar and to have the ability to metabolise the X-α-Gal substrate (data not shown).



### 5.2.6B SEQUENCE ANALYSIS OF THE INTERACTING LIBRARY PROTEINS

The plasmids were isolated from each of the 8 'positive' yeast clones and the resultant DNA preparations used to transform electrocompetent KC8 *E.coli* cells (section 2.2.10C), facilitating the isolation of the AD plasmids in each case. The plasmids were subjected to restriction endonuclease digestion, in order to determine the size of the insert each vector contained, Figure 5.9. Each of the eight AD plasmids were then sequenced immediately, using the pACT2 forward and reverse insert screening primers, detailed in section 2.1.8C.

The sequence data was checked and manipulated using the Macintosh-based Edit View and Gene Jockey II programs, respectively. Sequence homology searches were performed by comparison of these sequences with both nucleic acid and amino acid sequences listed in the GenBank, EMBL and other databases using a number of BLAST searches on the worldwide web (<http://www.ncbi.nlm.nih.gov/BLAST>) in order to identify the interacting library cDNAs.

Figure 5.10 summarises the sequence data obtained. The nucleic acid sequences of each of the cDNA inserts have also been translated in the correct open reading frame utilised by the AD vector, thus illustrating the actual amino acid sequence of each of the expressed proteins. In the correct ORF, clone 8 contains a cDNA insert encoding a very short protein of only 4 amino acids, should the first stop codon be utilised, and is therefore likely to be a false positive. Clones 2 and 4 may also be interesting, however the sequence data obtained from these samples was not very good and contained a number of Ns or unknown bases. These samples would have to be re-sequenced before being investigated further and this could not be performed within the timescale of this project.

Clones 7 & 9 gave the most interesting leads with each of the cDNA inserts showing nucleic acid homology to a number of the human filamin proteins. Clone 7 was found to contain a relatively large cDNA insert with extensive homology to a carboxy terminal segment of human filamin A. The cDNA inserts were examined further and translated according to the open reading frame used by the pACT2 vector. The cDNA insert



contained within clone 9 was found to be inserted in the wrong open reading frame for the pACT2 vector, i.e. the actual expressed protein would not be a segment of human filamin. However the cDNA insert fragment of clone 7 was found to be in the correct open reading frame (ORF) with the translation indicating the expression of a sizable segment of human filamin A protein.

**5.2.6C CONFIRMATION OF THE INTERACTIONS IN YEAST**

The AD plasmid preparations were used to re-transform AH109 yeast cells along with either the empty GAL4 DNA-BD vector, pGBKT7 or one of the four CD23 bait vectors in order to (i) confirm the interaction with pCD23a<sub>s</sub>, (ii) identify any false interactions, highlighted by activation of reporter gene expression in the presence of the empty bait vector, and (iii) investigate whether any of the library proteins could in fact interact with any of the other CD23 bait constructs. Table 5.2 illustrates the colony growth observed.

**Table 5.2 Confirmation of Interaction in AH109 Cells**  
**Re-transformation of Isolated AD Constructs**

Clone\Plasmid	pCD23a <sub>s</sub>	PCD23b <sub>s</sub>	pCD23a <sub>t</sub>	PCD23b <sub>t</sub>	pGBKT7
2	+	+++	+	+	+++
3	+++	+	+++	+++	+++
4	+	+	+	+	-
5	-	-	-	-	+
7	++	++	++	++	-
8	+	++	+	+	+++
9	+	+	+	+	+++
10	-	-	-	-	-

Key : + = 1-25 colonies, ++ = 25-200, and +++ = >200 colonies.

These results indicate that clones 2, 3, 5, 8 and 9 contained plasmids expressing proteins able to activate reporter gene expression in the absence of bait protein (i.e. autonomously), thus demonstrating these proteins to be false positives. Clone 3 was found to contain a cDNA insert displaying homology to a number of zinc finger-like proteins and, according to the sequence data should express this protein in transformed



yeast cells. These proteins are known for their ability to bind DNA and it may indeed be the case that this protein is able to bind to the GAL4 DNA, thus stimulating reporter gene expression without any protein-protein interaction occurring with the bait vector, explaining the results observed above. Clone 10 was also demonstrated to be a false positive as re-transformation into fresh yeast was unable to facilitate any colony growth on the selection agar. The colony growth in the presence of the empty pGBKT7 bait vector is shown in Figure 5.11.

Clones 4 and 7 were demonstrated to be able to activate transcription of the reporter genes in the presence of all four bait constructs, but not when transfected with the empty bait vector, indicating that these cDNAs encode proteins able to interact with the N-terminal tail section of both the CD23 isoforms. Figure 5.12 shows the colony growth obtained with either clone 4 or clone 7 and each of the CD23 bait constructs.

Activation of the ADE2 and MEL1 reporter genes was assayed by streaking a sample of each of these newly transformed yeast cells onto SD quadruple drop out agar plates containing the X- $\alpha$ -Gal substrate. Clones 2, 3, 5, 8 and 9 were all able to activate MEL1 expression in the presence of the empty bait vector. Whilst clones 4 and 7 were found only to be able to activate MEL1 in the presence of a CD23 bait construct, (data not shown).

#### **5.2.6D ANALYSIS OF HA-TAGGED PROTEIN EXPRESSION FROM EACH OF THE ISOLATED AD CONSTRUCTS**

Protein expression was analysed by direct lysis of AH109 yeast cells transformed with the AD plasmids of clones 2, 3, 4, 5, 7, 8, 9 and 10 using the TCA protein extraction method detailed in section 2.2.10B. The pACT2 AD vector expresses proteins as fusions of the GAL4-AD with an incorporated haemagglutinin (HA) epitope tag. The proteins were therefore detected using an antibody specific for the HA-tag. Figure 5.13 shows these results. HA-tagged proteins were clearly detected in AH109 cells expressing clones 3, 7, 9 and 10. No obvious HA-tagged proteins were detected from AH109 cells expressing clones 2, 4, 5 and 8 or from the empty pACT2 vector (should have expressed



the GAL4 AD with an HA tag). For this reason it was difficult to estimate the sizes of each of the proteins detected, as it was impossible to subtract the size of the GAL4 AD segment and the HA tag.

Collectively these results suggest that clone 7 expresses a protein of real interest, due to the fact that it does not show autonomous activation, yet did activate reporter gene activity in the presence of the CD23 bait. According to the sequence homology searches it seems that this clone corresponds to a sizable section of the carboxy terminus of human filamin A, and that it is encoded in the correct open reading frame utilised by the vector, suggesting the N-terminus of CD23 may bind to filamin A. Further biochemical testing is required to prove the existence of this protein-protein interaction in native cells.

Clone 4 also gave interesting results, as it was able to activate reporter gene expression in the presence of CD23 but not autonomously. However the sequence data obtained for this clone was sub-standard, containing lots of unknowns and was therefore redundant when trying to predict the protein sequence encoded in ORF1. Further sequencing would have to be performed prior to further analysis of this clone. This was not performed during the timescale of this project.

## **5.2.7 THE CD23-FILAMIN INTERACTION**

The yeast two-hybrid system screens only for physical properties of interacting proteins, and cannot reveal anything about the biological significance of the detected partners. CD23 and filamin A must therefore be proven to interact in a natural scenario, i.e. in cells that would normally express both proteins, before this interaction can be concluded to be of biological significance.

### **5.2.7A FILAMIN A**

The positive clone isolated from the yeast two-hybrid screen encodes a large segment of the carboxy terminus of human filamin A. The first question to be asked must be one of



tissue/cellular distribution, in an attempt to address whether or not CD23 and filamin A may ever meet in a natural environment. Human filamin exists in three forms, A, B and C. Previous reports have demonstrated filamin A to be present in a wide range of different cell types encompassing a variety of cells of the human immune system, including B cells [as reviewed by Stossel *et al*, 2001]. These reports certainly suggest this may be a feasible reaction, based purely on the possibility of the two proteins being able to come into contact with one another. Table 5.3, adapted from this review paper, details the nomenclature used for the human filamin proteins as well as information on the expression patterns of each.

**Table 5.3 Proposed Nomenclature for the Human Filamin Proteins.**

Proposed name	Previous Names	No. of Repeats	Expression
hsFLNa	ABP, ABP-280, FLN1, non-muscle FLN, $\alpha$ FLN	24	Widely expressed abundantly in a variety of human tissues [Gorlin <i>et al.</i> , 1990; Gorlin <i>et al.</i> , 1993; Maestnni <i>et al.</i> , 1993]
hsFLNb	$\beta$ FLN, FH1, FLN3	24	Broad distribution [Zhang <i>et al.</i> , 1998; Takafua <i>et al.</i> , 1998; Xu <i>et al.</i> , 1998; Brocker <i>et al.</i> , 1999; Chakarova <i>et al.</i> , 2000] less abundant than FLNa
hsFLNc	$\gamma$ FLN, ABP-L, FLN2	24	Predominant in muscle

#### **5.2.7B HUMAN FILAMIN MAY IMMUNO-PRECIPITATE WITH CD23 FROM THE RPMI 8866 B CELL LINE**

Proteins expressed together in the informative, yet still artificial, yeast two-hybrid system may never in fact naturally come into contact with one another in a host cell, if for example if they were to be expressed in different sub-cellular compartments or at different stages of development. The biological significance of any identified protein-protein interaction must therefore be proven and co-immunoprecipitation or immunofluorescence assays are the usual choice, enabling the confirmation of the interaction in a relevant host cell. In an attempt to confirm the interaction between CD23 and filamin A a co-immunoprecipitation experiment was performed. The RPMI 8866 B cell line was chosen due to the fact that it is known to naturally express good



levels of CD23 protein. An initial experiment was performed in an attempt to establish whether or not filamin A is expressed in this cell line, however the results obtained were inconclusive. The co-immunoprecipitation experiment was then performed, following the protocol detailed in section 2.2.7.

RPMI 8866 cells were exposed to (i) no stimulus, (ii) 1 $\mu$ g NIP-specific IgE antibody or (iii) 1 $\mu$ g NIP-specific IgE antibody followed by 1 $\mu$ g NIP-BSA. Two experiments were performed in parallel using either anti-CD23 or anti-filamin antibodies to immunoprecipitate the proteins of interest. The samples were then separated by SDS-PAGE, transferred to nitrocellulose and immuno-blotted with anti-filamin or anti-CD23 antibodies, respectively. Figure 5.14 shows the results of the first and only CD23/filamin co-immunoprecipitation experiment performed at the end of this project. The results were promising and indicated the presence of bands of approximately the correct sizes. Filamin A is a 210kDa protein, and may be present at the top of the anti-FLN blot (Figure 5.14). The samples from the filamin immunoprecipitation were run again on a 10% SDS-PAGE gel, facilitating better separation of the proteins and thus a better estimate of the size of the resultant bands when blotted with an anti-CD23 antibody. The results suggest that the bands of interest may indeed be CD23 as they are expressed at approximately the correct 45kDa size (Figure 5.15). It should be noted that this experiment was only done once, due to the lack of time, and cannot be used to state categorically that CD23 and filamin A do not interact, but rather provide encouraging evidence to the contrary, suggesting that they might bind. Further investigation is required to unequivocally prove this interaction.

### 5.3 DISCUSSION

Binding partners for the cytoplasmic N-terminal tail of CD23 were investigated using the yeast two-hybrid assay and a human leukocyte cDNA library. The yeast two-hybrid assay has several advantages over other methods as it is performed *in vivo* (in the yeast nucleus) and therefore the proteins involved are more likely to be expressed in their natural conformation, unlike in the more biochemical methods where bait proteins are generally bound to affinity columns or nitrocellulose membranes, and therefore not necessarily displayed in their natural conformation. The conditions of the yeast two-



hybrid assay are also more likely to mimic those observed in the natural scenario in comparison to those of a typical *in vitro* biochemical assay. Finally, another advantage is that the yeast two-hybrid system is highly sensitive, with the ability to detect both weak and transient interactions that may be typical of large protein complexes [Guarente, 1993].

There are however, several disadvantages to the yeast two-hybrid system, including the completion of processes that usually require non-yeast proteins, such as protein folding. The other main disadvantage is that not all post-translational modifications occur in yeast, for example tyrosine phosphorylation rarely occurs in *S.cerevisiae* [Gartner *et al.*, 1992; Lim *et al.*, 1993]. However it has been shown that more post-translational modifications do occur in yeast than in bacterial protein expression systems [Phizichy & Fields, 1995]. The cytoplasmic tail of CD23a does theoretically have the potential to be phosphorylated, although the functional role of this modification, should it occur, is not yet known and should it occur, it may or may not affect protein binding. The mammalian two-hybrid system would offer one simple advantage over the yeast system, possibly removing all these disadvantages, in that it would allow CD23 protein interactions to occur in their native environment [Dang *et al.*, 1991; Fearson *et al.*, 1992]. However, this assay is not practical for screening large numbers of transfectants [Osborne *et al.*, 1997], a process necessary for initially identifying interacting clones from the many cDNAs encoded within a large expression library.

In summary, the results detailed within this chapter have identified human filamin A as a potential binding partner for the cytoplasmic N-terminal tail of CD23. Filamins are large actin-binding proteins that serve to stabilise delicate three-dimensional actin webs, link these to cellular membranes, and have been shown to integrate architectural and signalling functions [as reviewed by Stossel *et al.*, 2001]. Due to the fact that different members of this family were discovered using a variety of techniques and approaches there is a distinct lack of consistency in the nomenclature. A uniform naming system has since been proposed and is shown in Table 5.3 [Stossel *et al.*, 2001]. The minimal requirement for membership of the filamin family is a string of the characteristic repeated  $\beta$ -sheet units. The amino acid sequences of the human filamin members show



approximately 60-80% overall sequence homology, with the greatest variation occurring in the carboxy-terminal, self-association domains.

### 5.3.1 THE STRUCTURE OF HUMAN FILAMIN A (FLNA)

The amino-terminal actin-binding domain contains sequence motifs found in many actin-filament binding proteins [Lebart *et al.*, 1994] with the remainder of the protein consisting of 24 repeats of ~96 amino acids each, interrupted by one or two short hinge segments. Secondary structure algorithm modelling of these domains indicates the  $\beta$ -sheets to overlap in an anti-parallel manner to form a rod shape [Gorlin *et al.*, 1990], and dimerisation has been shown to occur via the 24<sup>th</sup> repeat. Figure 5.16 illustrates the structure of FLNa and indicates where CD23 is thought to bind to this molecule. Although the exact amino acids involved in the interaction between CD23 and FLNa have not yet been established, it is proposed that filamin may indeed interact with the common tail region as it was found to interact with all four of the CD23 bait species. Although the work presented in this chapter has not categorically proven the interaction between CD23 and filamin A in native cells, I firmly believe this interaction does occur in nature. A variety of information supports this theory, not least of which being that filamin A has been shown to interact with a number of other transmembrane proteins, not dissimilar to CD23, and is involved in a number of functions also relevant to the biological activity of CD23.

The biological relevance of any newly identified protein-protein interaction can be difficult to define, and certainly the function of the interaction between CD23 and filamin can only be speculated at this current time, however it seems likely that FLNa may act as an adaptor protein, linking CD23 to the necessary signalling pathways required for its function. Recent studies support this theory, having shown that FLNa can and does function as a docking protein for various cell surface receptors and intracellular proteins involved in signalling and endocytosis, these proteins include GPIIb/IIIa [Andrews & Fox, 1991, 1992], Fc $\gamma$ RI [Ohta *et al.*, 1991; Harrison *et al.*, 1994], SEK-1 [Marti *et al.*, 1997],  $\beta$ 2-integrin [Sharma *et al.*, 1995],  $\beta$ 1-integrin [Loo *et al.*, 1998], furin [Liu *et al.*, 1997], TNF receptor-associated factor 2 (TRAF-2) [Leonardi *et al.*, 2000] and the small GTPases Rac, Rho, Cdc42 and RalA [Ohta *et al.*,



1999]. Table 5.4 lists a number of proteins demonstrated to interact with filamin, and details the functional significance of these interactions. Further analysis is required to unequivocally define the biological purpose of the interaction between CD23 and FLNa.

**Table 5.4 Some of the Binding Partners Identified for the Human Filamins**

Protein	Filamin	Filamin Repeat	Reference	Functional Significance
<b>Transmembrane Proteins</b>				
GP-Ib $\alpha$ (member of Von Willebrand receptor complex)	FLN-a/b	17-19	Meyer <i>et al.</i> , 1997	Promotes cell spreading
$\beta$ 1A, $\beta$ 1D, $\beta$ 2, $\beta$ 3, and $\beta$ 7 integrins	FLN-a/b	20-24	Calderwood <i>et al.</i> , 2000	Mechanoprotection
Tissue factor	FLN-a	23-24	Ott <i>et al.</i> , 1998	Cell adhesion and migration
Fc $\gamma$ RI	FLN-a	?	Ohta <i>et al.</i> , 1991	?
Furin Receptor	FLN-a	13-14	Liu <i>et al.</i> , 1997	Directs intracellular trafficking of furin
Androgen receptor	FLN-a/c	16-19	Ozanne <i>et al.</i> , 2000	Translocation of androgen receptor to nucleus
Lnk adaptor protein	FLN-a (ABP-280)	19-23	He <i>et al.</i> , 2000	?
<b>Signalling Proteins</b>				
RhoA, Rac1, Cdc42	FLN-a	21-24	Ohta <i>et al.</i> , 1999	?
RalA	FLN-a	24	Ohta <i>et al.</i> , 1999	Promotes formation of filopodia
TRAF2	FLN-a	15-19	Leonardi <i>et al.</i> , 2000	Involved in SAPK or NF- $\kappa$ B activation

A number of false positive species were also identified during the course of these studies, (as is usually the case in a yeast two-hybrid assay), however one of these proteins was isolated several times. Although results on false positive interactions are generally not reported, it is known that some proteins are continually re-isolated using unrelated bait proteins, these include ribosomal, mitochondrial, ferritin, ubiquitin, some



proteosome subunits and certain cytoskeletal proteins [Golemis, 1995; Golemis & Brent, 1997]. The detection of some false positive clones can be due to the biological properties of the proteins, others are for as yet unknown reasons. For example, frequent isolation of ribosomal proteins could be due to the extensive hydrophobic or charged residues that can interact with corresponding regions on a bait protein [Golemis & Brent, 1997]. There may be a similar argument for the isolation of such a high number of clones expressing cDNAs with nucleic acid homology to MT-II, if the actual protein expressed contains domains/motifs recognised by the CD23 bait protein. However this information could only be obtained once it is known what proteins, and indeed the particular regions of these proteins, that CD23 binds to.

Collectively, these data have shown the yeast two-hybrid system to be a valuable tool for identifying potential binding partners of the N-terminal tail of CD23. This project has effectively opened the door for a range of future experiments, not only to further characterise the protein-protein interaction that occurs between CD23 and filamin but also to address the question of which other proteins bind to the CD23/filamin complex, should filamin be acting as an adaptor protein, facilitating the downstream signalling of or function of CD23. The yeast two-hybrid system should also be used to identify other proteins of interest, particularly as the entire cDNA library was not screened during the course of this project, and to establish if any differences do indeed exist between the signalling pathways employed by each of the CD23 isoforms, something which has been speculated many times before but has yet not been proven conclusively.



## **FIGURE 5.1A SCHEMATIC REPRESENTATION OF THE PRINCIPLE BEHIND THE YEAST TWO-HYBRID SYSTEM**

(i) In the native scenario the GAL4 protein contains both DNA-binding and activating regions and induces GAL1-lacZ transcription.

This system has been adapted to enable the identification of novel protein interactions.

(ii) Hybrids containing either the DNA-binding domain (upper) or activating region (lower) are unable to induce transcription alone.

(iii) When bait and library fusion proteins interact, the DNA-BD and AD are brought into proximity, thus activating transcription of the reporter genes.



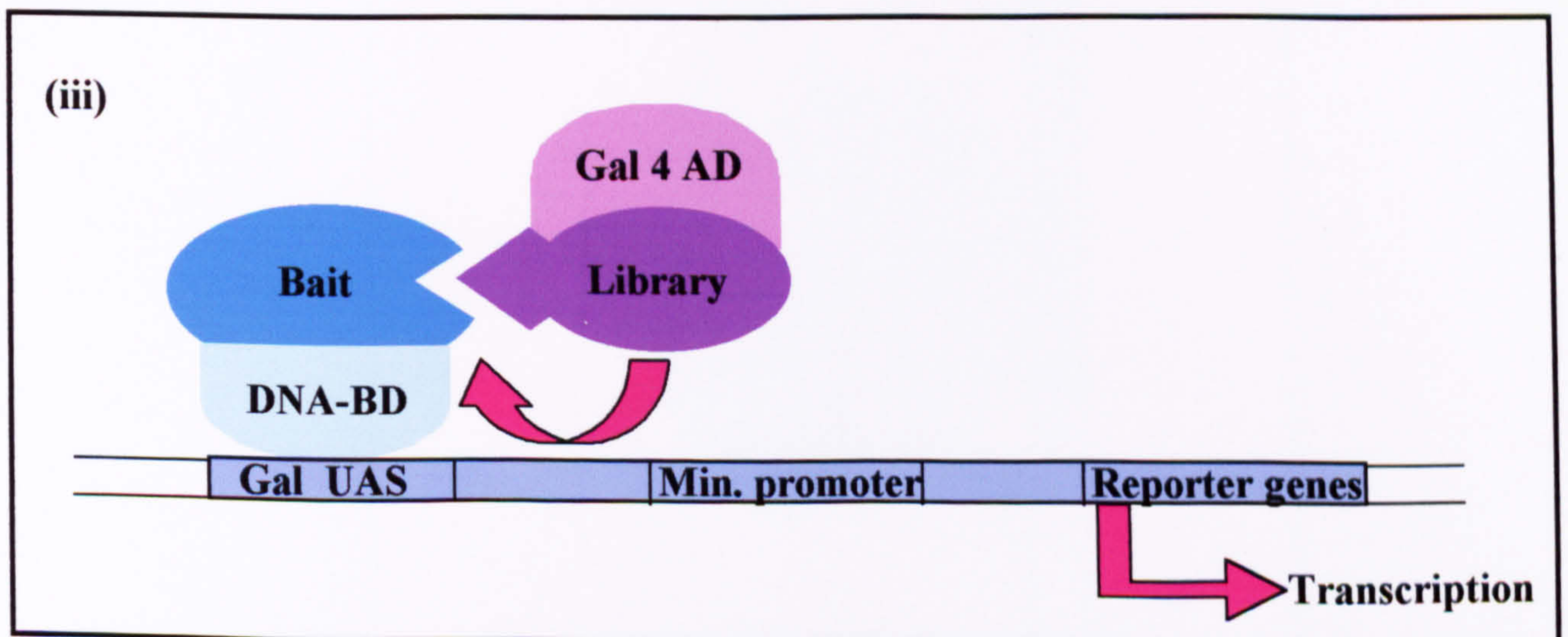
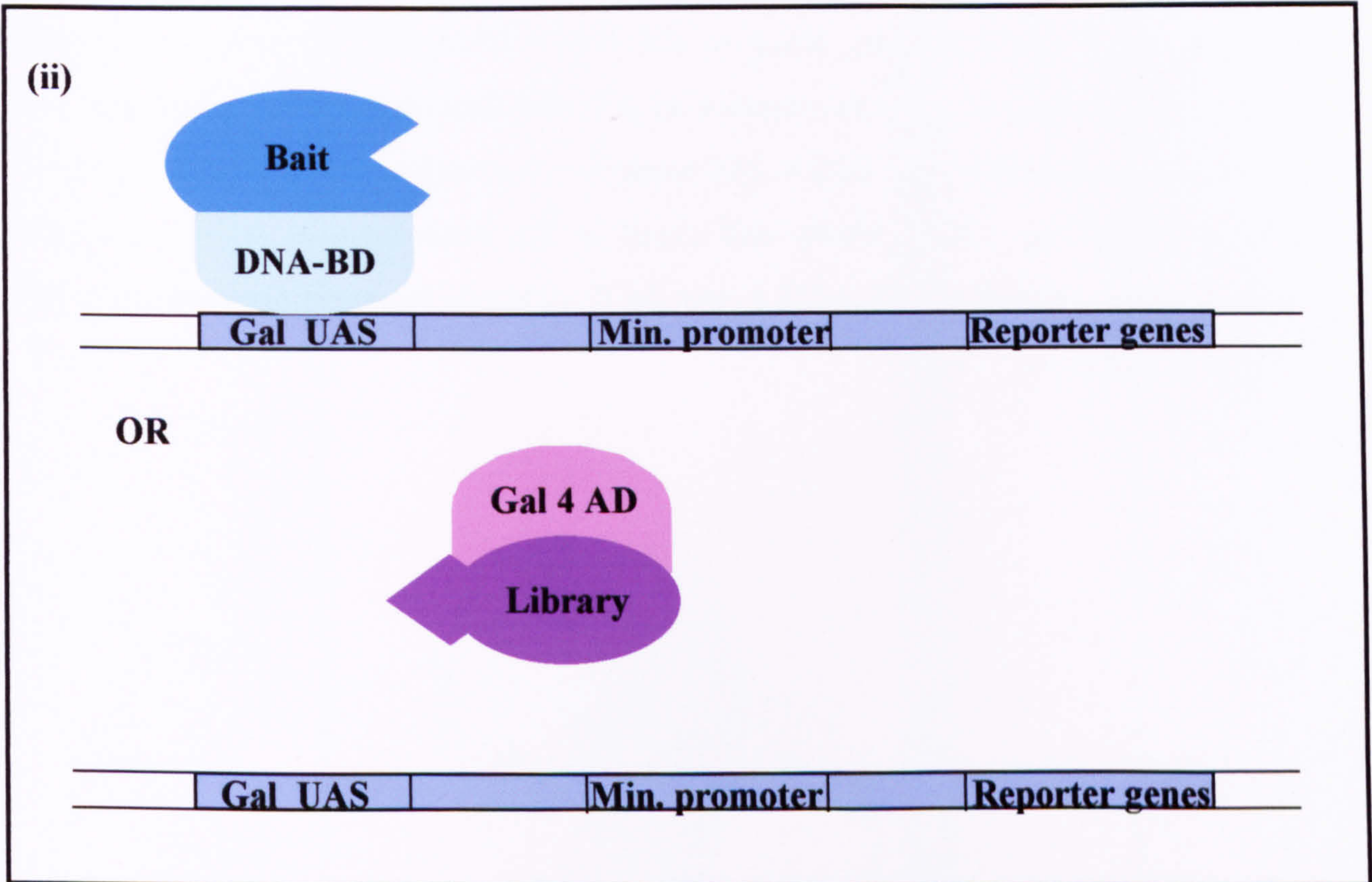
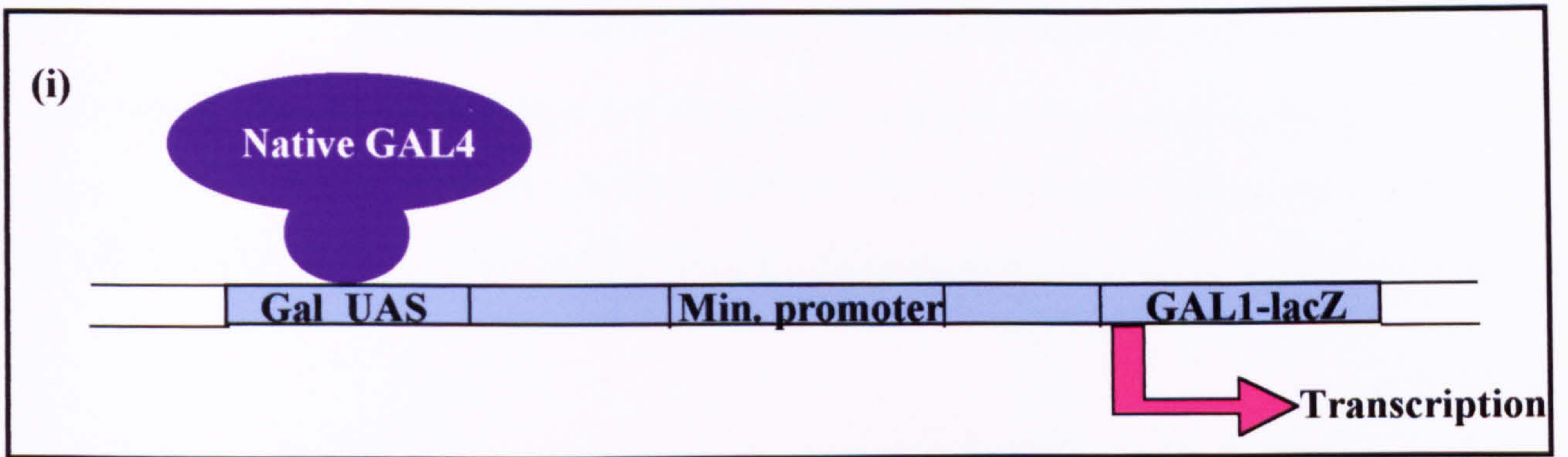




### **FIGURE 5.1B SCHEMATIC REPRESENTATION OF THE PRINCIPLE BEHIND THE MATCHMAKER 3 YEAST TWO-HYBRID SYSTEM**

The DNA-BD is amino acids 1-147 of the yeast GAL4 protein and it binds to the GAL upstream activating sequence (UAS) upstream of the reporter genes, ADE2, HIS3, MEL1 and *lacZ*. The AD is amino acids 768-881 of the GAL4 protein and it functions as the transcriptional activator.

The bait protein is the N-terminal cytoplasmic tail of human CD23, either presented as a single or triple repeat protein, fused to the GAL4 DNA-BD. Screening for binding partners will be against proteins encoded by a human leukocyte cDNA library that has been made as fusions to the GAL4 AD sequence. Interaction of CD23 with a protein encoded within the cDNA library will result in the transcriptional activation of the reporter genes, ADE2, HIS3, MEL1 and *lacZ*, detected by nutritional selection and enzymatic assay.



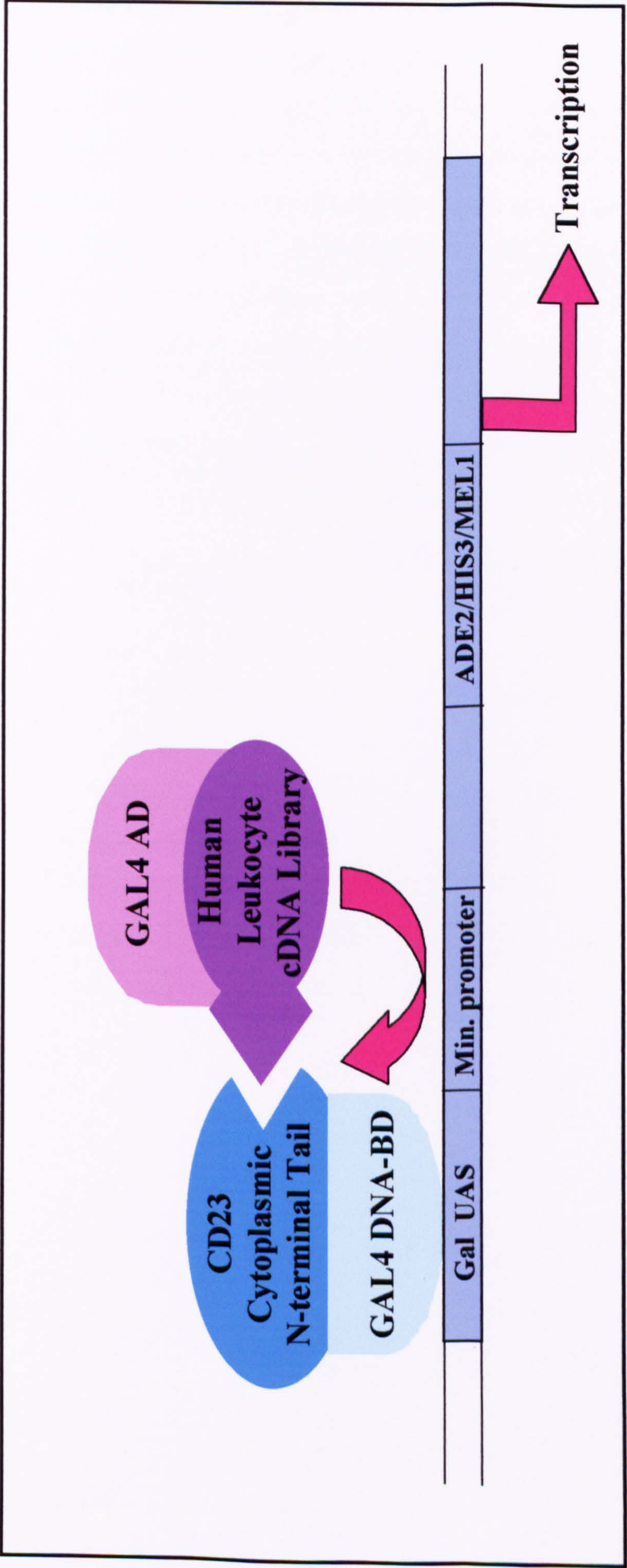


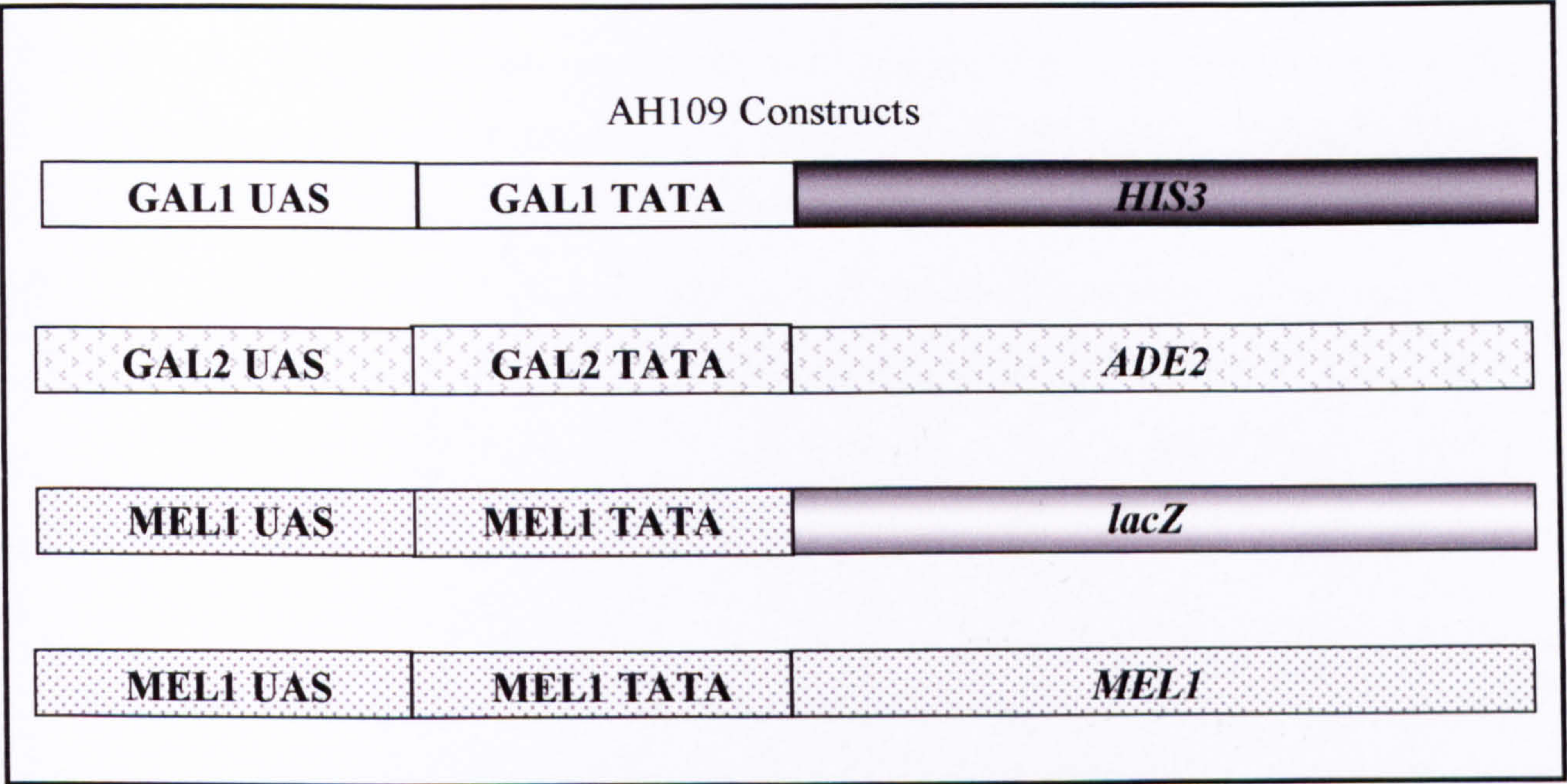


## FIGURE 5.2 THE AH109 YEAST STRAIN

The AH109 strain is a derivative of PJ69-2A yeast and includes the ADE2 and HIS3 markers [James *et al.*, 1996]. MEL1 is an endogenous GAL4-responsive gene. The *lacZ* reporter gene was introduced into PJ69-2A to create AH109 [Holtz, A. unpublished]. MEL1 and *lacZ* encode  $\alpha$ -galactosidase and  $\beta$ -galactosidase respectively, with  $\alpha$ -galactosidase being a secreted enzyme that can be assayed directly on X- $\alpha$ -Gal indicator plates which employ blue/white screening. The HIS3, ADE3 and MEL1/*lacZ* reporter genes are under the control of three completely heterologous GAL4-responsive UAS and promoter elements (TATA boxes) - GAL1, GAL2 and MEL1 respectively, serving to minimise the detection of false positives, particularly those that interact directly with the sequences flanking the GAL4 binding site and those that interact with transcription factors bound to specific TATA boxes.

The AH109 genotype is listed in the table.





AH109 Yeast Strain Genotype		
Strain	Genotype	Reference
AH109	MATa, trp1-901, leu2-3, 112, ura3-52, his3-200, gal4Δ, gal80Δ. LYS2 :: GAL1 <sub>UAS</sub> -GAL1 <sub>TATA</sub> -HIS3, GAL2 <sub>UAS</sub> -GAL2 <sub>TATA</sub> -ADE2, URA3 :: MEL1 <sub>UAS</sub> -MEL1 <sub>TATA</sub> -lacZ	James <i>et al.</i> , 1996

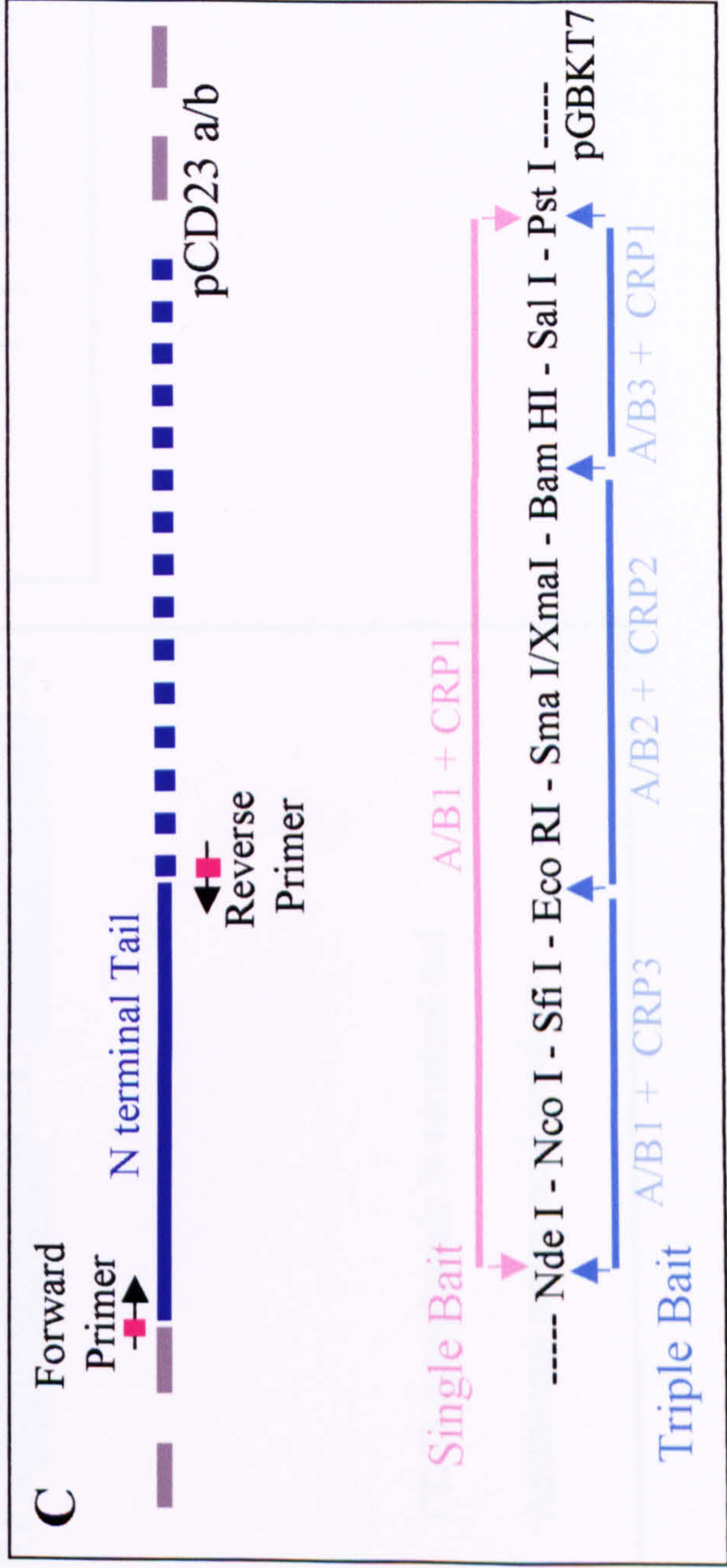
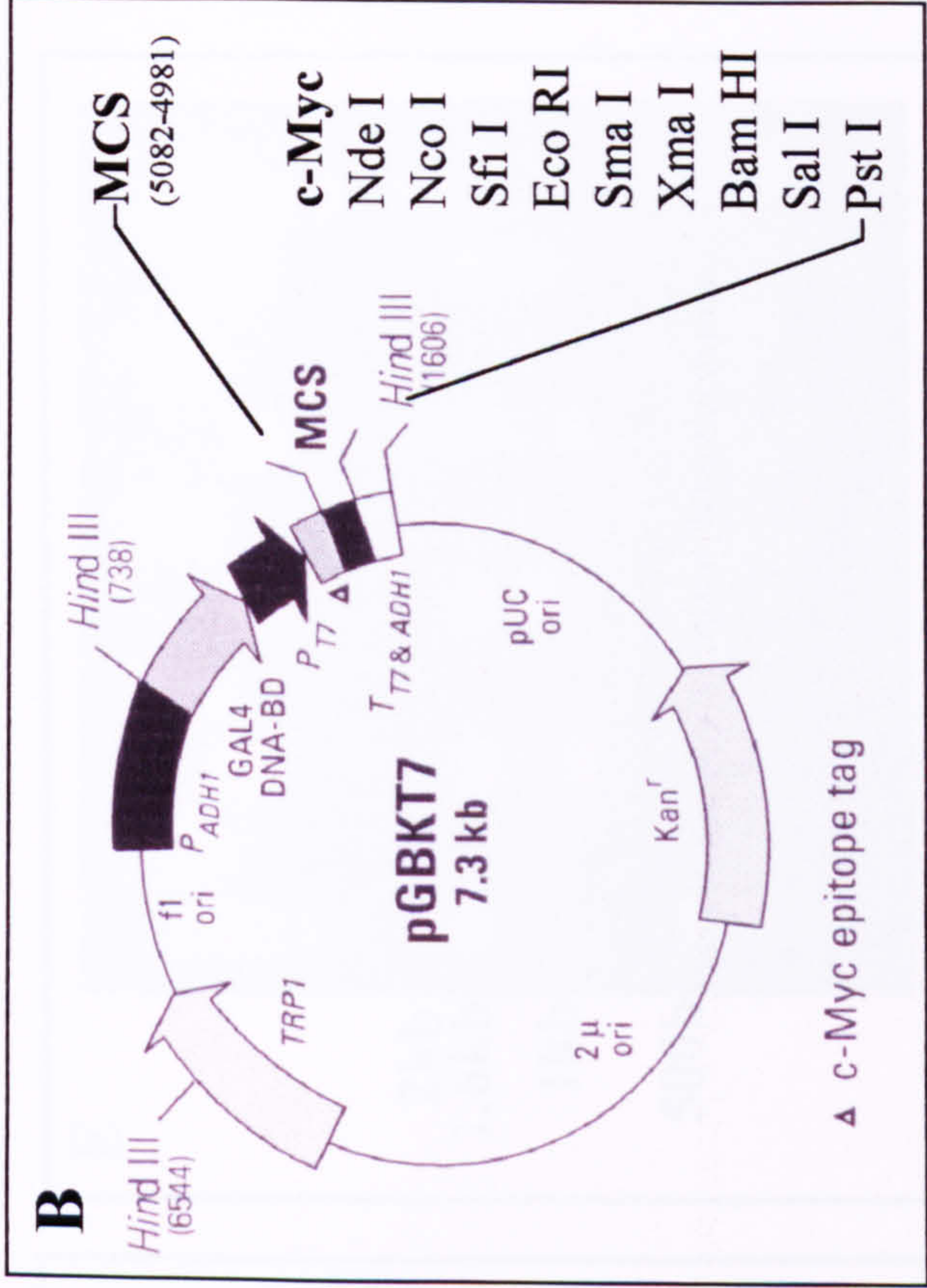


### FIGURE 5.3 GENERATION OF THE CD23 BAIT CONSTRUCTS

The oligonucleotides used to generate each of the CD23 tail fragments flanked by additional restriction sites are detailed in A, for easy insertion into the pGBKT7 multiple cloning site, plasmid map shown in B, with the cloning strategy explained in the schematic diagram C. D illustrates the resultant proteins, highlighting the additional amino acids incorporated due to the cloning strategy used. Each of the constructs were subjected to restriction digestion analysis with (i) *Nde I*–*Not I* and (ii) *Hind III* and the banding patterns produced are shown in E in lanes 2, 4, 6, & 8 and lanes 3, 5, 7, & 9 respectively. Key; CD23a<sub>s</sub> – lanes 2 & 3, CD23a<sub>t</sub> – lanes 4 & 5, CD23b<sub>s</sub> – lanes 6 & 7, CD23b<sub>t</sub> – lanes 8 & 9.



A		Primer	Primer Sequence	Restriction site
CD23a	Forward Primers	A1	CTC GGA CAT ATG GCC ATG GAG GAA GGT C	Nde I
		A2	CTC GGA GAA TCC GCC ATG GAG GAA GGT C	Eco R I
		A3	CTC GGA TGG ATC CTG ATG GAG GAA GGT C	Bam HI
CD23b	Forward Primers	B1	CTC GGA CAT ATG GCC ATG AAT CCT CCA AGC	Nde I
		B2	CTC GGA GAA TCC GCC ATG AAT CCT CCA AGC	EcoRI
		B3	CTC GGA TGG ATC CTG ATG AAT CCT CCA AGC	Bam HI
Common Reverse Primers		CRP1	CCC CAG CTG CAG GAT CTG AGT CCC ACG	Pst I
		CRP2	CCC CAG GAT CCC GAT CTG AGT CCC ACG	Bam HI
		CRP3	CCC CAG GAA TTC GAT CTG AGT CCC ACG	Eco RI





**D**

Single Bait

A [ ] LQ

Triple Bait

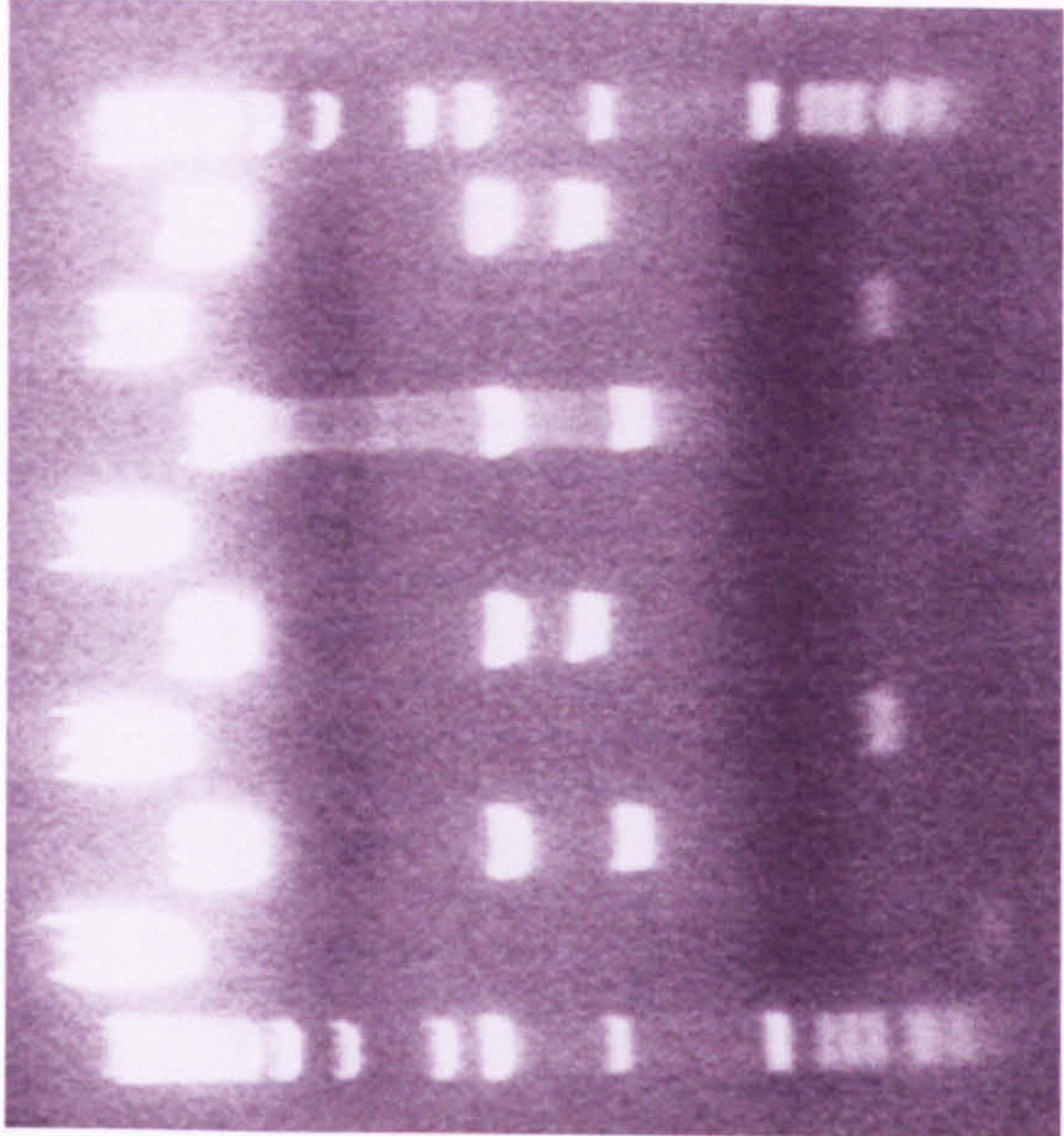
A [ ] EFA [ ] GIL [ ] LQ

Key

[ ] CD23 cytoplasmic N-terminal tail

X Additional amino acid residues

**E**



2kb  
1.6kb  
1kb  
500b

1 2 3 4 5 6 7 8 9 10



## **FIGURE 5.4 ALL FOUR OF THE CD23 N-TERMINAL BAIT CONSTRUCTS ARE NON-TOXIC IN YEAST AH109 CELLS**

Four aliquots of competent AH109 yeast were transformed with 1µl of each of the CD23 N-terminal bait plasmids. Resultant colony growth for each of these four transformants was compared with yeast transformed with the empty DNA-BD vector pGBKT7. Scans of each agar plate clearly show that colony growth is not restricted by any of the CD23 N-terminal bait proteins, indicating that these constructs are not toxic to the AH109 yeast cells.

Key to scans; A<sub>s</sub> = pCD23a<sub>s</sub>, B<sub>s</sub> = pCD23b<sub>s</sub>, A<sub>t</sub> = pCD23a<sub>t</sub>, B<sub>t</sub> = pCD23b<sub>t</sub>. Growth for yeast containing empty DNA-BD vector not shown.



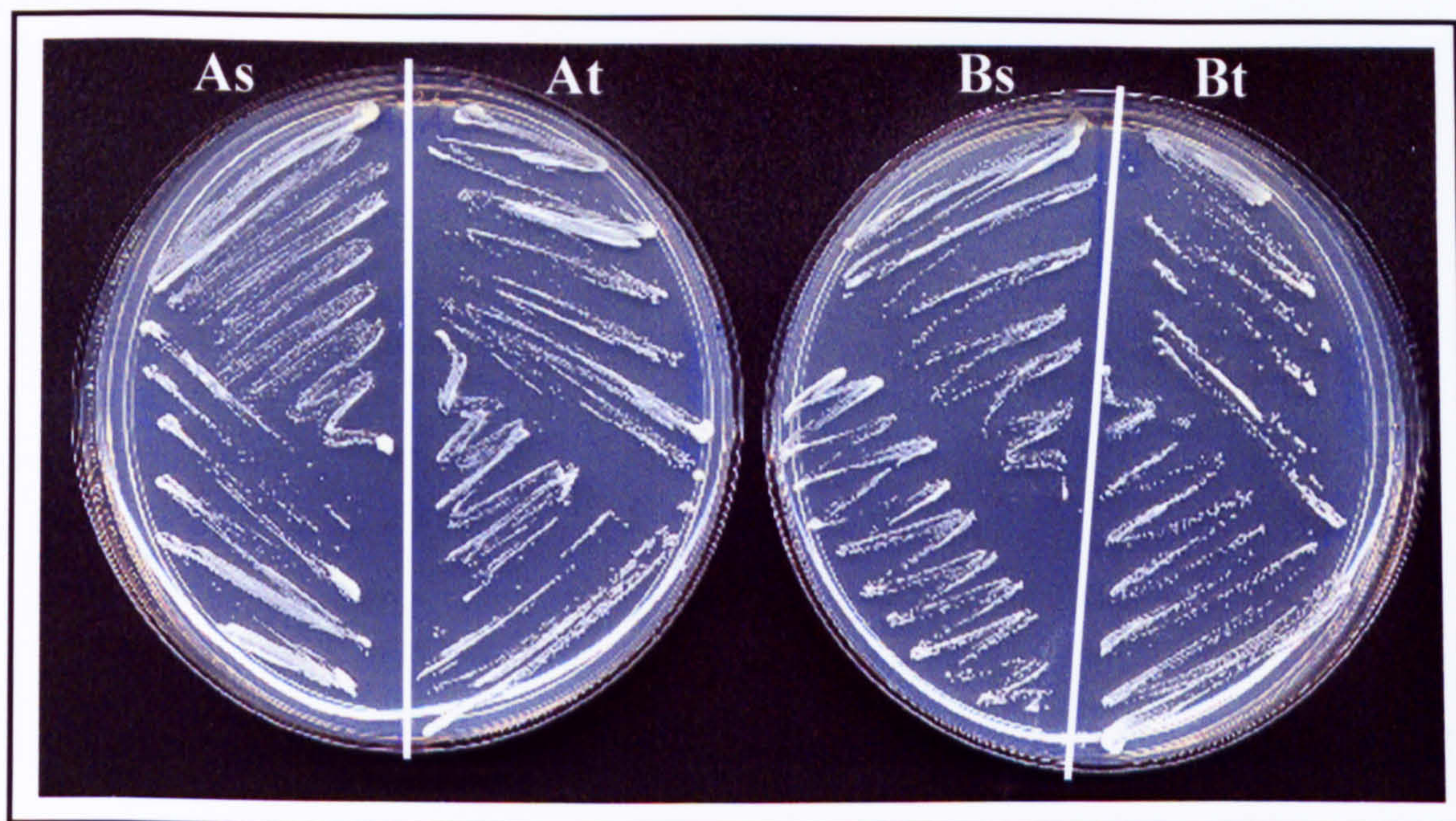




## **FIGURE 5.5 EXPRESSION OF THE CD23 N-TERMINAL TAIL AS A C-MYC FUSION PROTEIN IN AH109 YEAST**

Each of the CD23 N-terminal baits were independently transfected into AH109 yeast cells and selected on SD/-Trp agar. An overnight culture of each sample was subjected to TCA protein extraction, with 15µl of the final protein product loaded onto a 10% SDS-PAGE gel. The separated proteins were then transferred to nitrocellulose membrane and immunoblotted with anti-cMyc antibody. The blot was visualised using the BioRad ECL detection kit. The pGBKT7 vector expresses each protein as a fusion of the GAL4 DNA-BD and the c-Myc tag.

Key; Lane 1 - empty pGBKT7 vector, Lane 2 - pCD23a<sub>s</sub>, Lane 3 - pCD23a<sub>t</sub>, Lane 4 - pCD23b<sub>s</sub>, Lane 5 - pCD23b<sub>t</sub>.



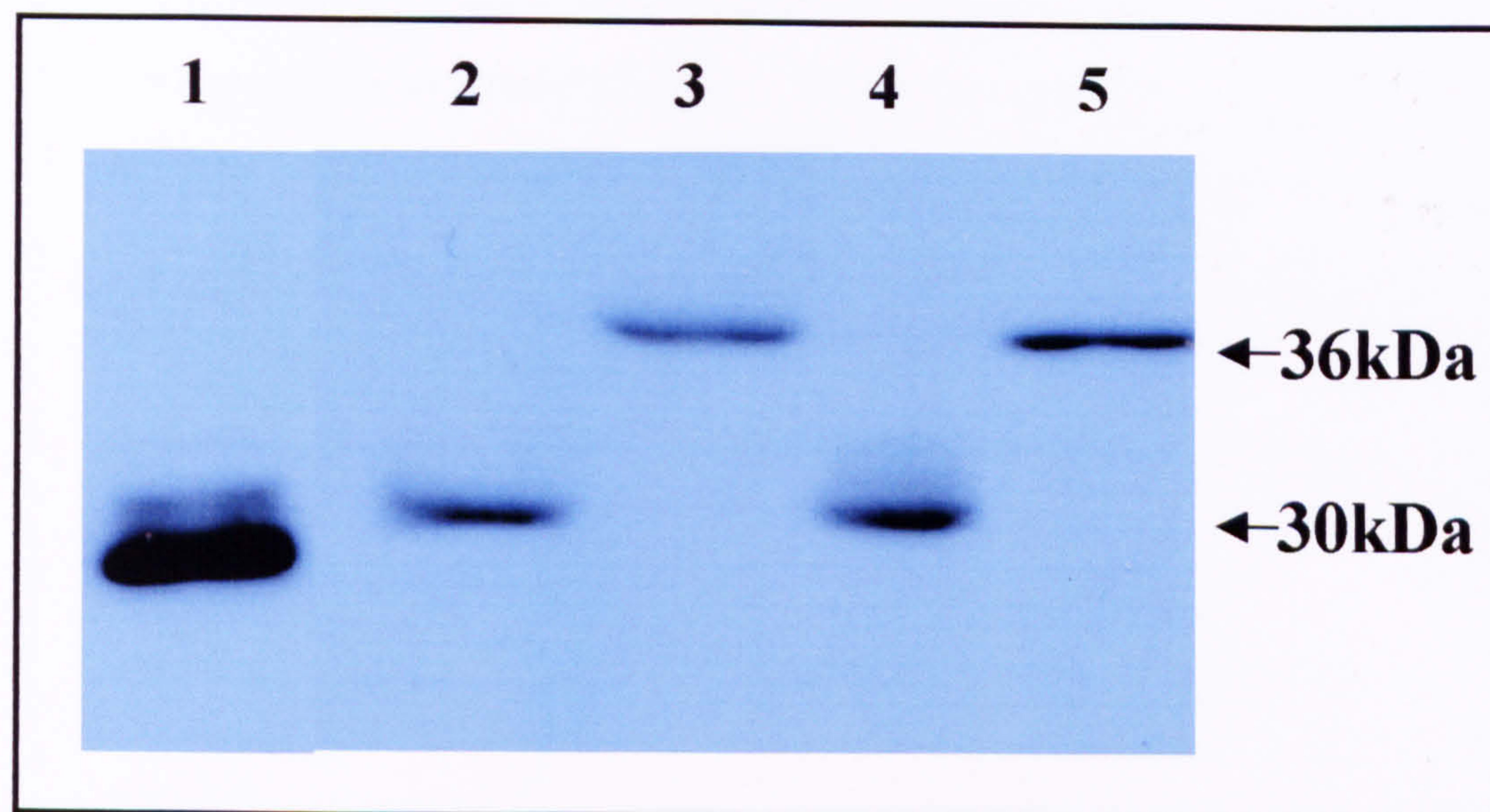




## **FIGURE 5.6 SUCCESSFUL AMPLIFICATION OF THE HUMAN LEUKOCYTE cDNA LIBRARY**

The Clontech Human Leukocyte cDNA library had been Xho I-(dT)<sub>15</sub> primed and unidirectionally cloned into the multiple cloning site (MCS) of the pACT2 vector, generating library fusion proteins with the GAL4 AD and haemagglutinin (HA) epitope tag. Figure A shows the plasmid map, and restriction sites incorporated in the MCS, for pACT2. The library sample was titred 'in-house' prior to amplification and found to contain  $4.4 \times 10^8$  colony forming units/ml, B using the method described in 2.2.8A. After amplification 10 random colonies were chosen and subjected to restriction endonuclease digestion with Bgl II, in order to analyse the cDNA insert contained within each, Figure C illustrates the results.



FIGURE 5.7 Xba I and Nde I Restriction Sites for pACT2

This figure shows the pACT2 plasmid and a cluster of restriction sites for Xba I and Nde I. The plasmid is 8.1 kb and contains several features: Amp<sup>r</sup>, Col E1 ori, 2 μ ori, LEU2, and a multiple cloning site (MCS) flanked by HA and GAL4 AD. The MCS is located between the HA and GAL4 AD regions. The restriction sites for Xba I and Nde I are indicated by arrows and their positions are given in parentheses.

restriction sites for Xba I and Nde I are indicated by arrows and their positions are given in parentheses.

number of restriction sites for Xba I and Nde I are indicated by arrows and their positions are given in parentheses.

restriction sites for Xba I and Nde I are indicated by arrows and their positions are given in parentheses.

restriction sites for Xba I and Nde I are indicated by arrows and their positions are given in parentheses.

restriction sites for Xba I and Nde I are indicated by arrows and their positions are given in parentheses.

restriction sites for Xba I and Nde I are indicated by arrows and their positions are given in parentheses.

restriction sites for Xba I and Nde I are indicated by arrows and their positions are given in parentheses.

restriction sites for Xba I and Nde I are indicated by arrows and their positions are given in parentheses.

restriction sites for Xba I and Nde I are indicated by arrows and their positions are given in parentheses.

restriction sites for Xba I and Nde I are indicated by arrows and their positions are given in parentheses.

restriction sites for Xba I and Nde I are indicated by arrows and their positions are given in parentheses.

restriction sites for Xba I and Nde I are indicated by arrows and their positions are given in parentheses.

restriction sites for Xba I and Nde I are indicated by arrows and their positions are given in parentheses.

restriction sites for Xba I and Nde I are indicated by arrows and their positions are given in parentheses.

restriction sites for Xba I and Nde I are indicated by arrows and their positions are given in parentheses.

restriction sites for Xba I and Nde I are indicated by arrows and their positions are given in parentheses.

restriction sites for Xba I and Nde I are indicated by arrows and their positions are given in parentheses.

restriction sites for Xba I and Nde I are indicated by arrows and their positions are given in parentheses.

restriction sites for Xba I and Nde I are indicated by arrows and their positions are given in parentheses.

restriction sites for Xba I and Nde I are indicated by arrows and their positions are given in parentheses.

restriction sites for Xba I and Nde I are indicated by arrows and their positions are given in parentheses.

restriction sites for Xba I and Nde I are indicated by arrows and their positions are given in parentheses.

restriction sites for Xba I and Nde I are indicated by arrows and their positions are given in parentheses.

restriction sites for Xba I and Nde I are indicated by arrows and their positions are given in parentheses.

restriction sites for Xba I and Nde I are indicated by arrows and their positions are given in parentheses.

restriction sites for Xba I and Nde I are indicated by arrows and their positions are given in parentheses.

restriction sites for Xba I and Nde I are indicated by arrows and their positions are given in parentheses.

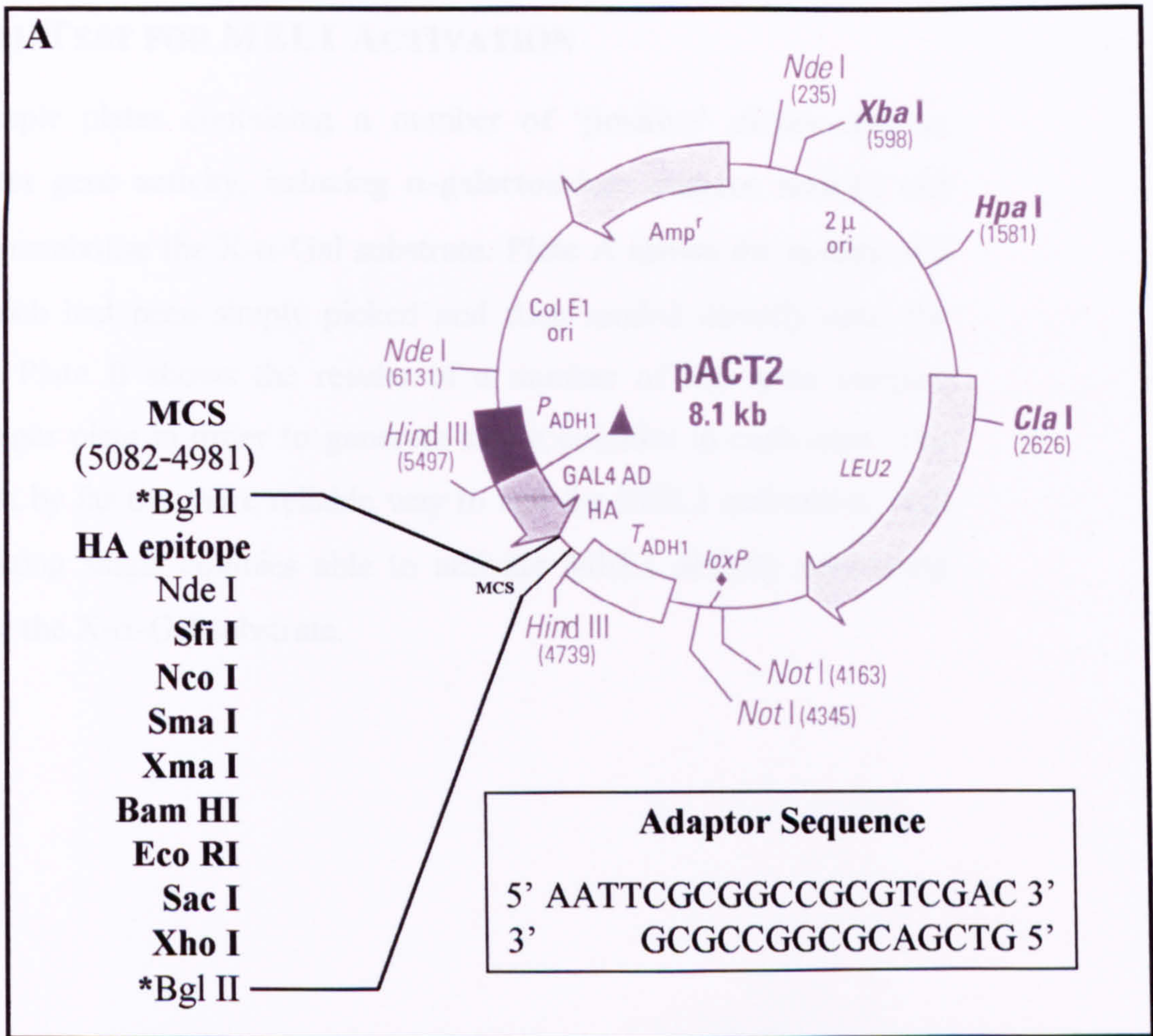
restriction sites for Xba I and Nde I are indicated by arrows and their positions are given in parentheses.

restriction sites for Xba I and Nde I are indicated by arrows and their positions are given in parentheses.

restriction sites for Xba I and Nde I are indicated by arrows and their positions are given in parentheses.

restriction sites for Xba I and Nde I are indicated by arrows and their positions are given in parentheses.

restriction sites for Xba I and Nde I are indicated by arrows and their positions are given in parentheses.



**B**

Dilution	# Colonies	Calculation (cfu/ml = )	cfu/ml
Dilution A	397	# colonies x 10 <sup>3</sup> x 10 <sup>3</sup>	3.97 x 10 <sup>8</sup>
Dilution B 50μl	22	# colonies/volume x 10 <sup>3</sup> x 10 <sup>3</sup> x 10 <sup>3</sup>	4.4 x 10 <sup>8</sup>
Dilution B 100μl	44	# colonies/volume x 10 <sup>3</sup> x 10 <sup>3</sup> x 10 <sup>3</sup>	4.4 x 10 <sup>8</sup>

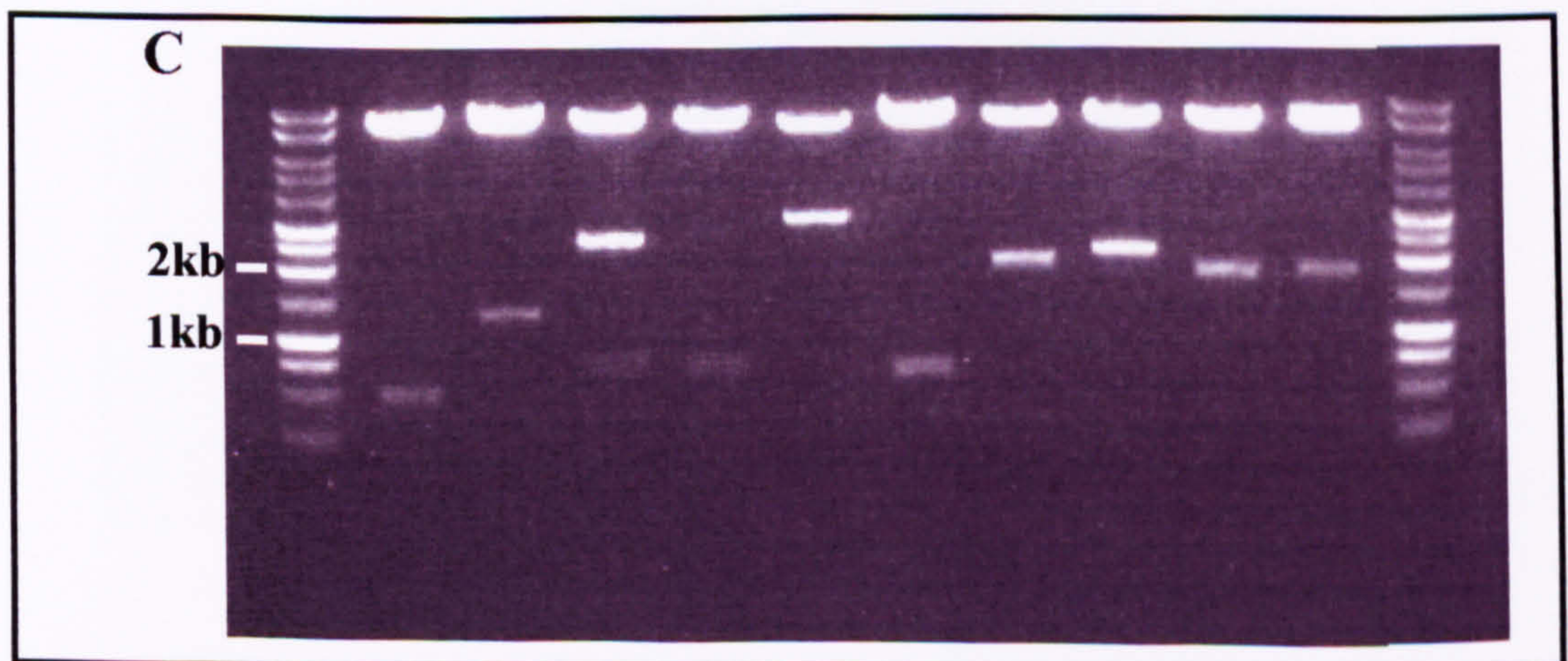




## **FIGURE 5.7 X- $\alpha$ -GAL TEST FOR MEL1 ACTIVATION**

This figure shows sample plates containing a number of 'positive' clones able to activate MEL 1 reporter gene activity, inducing  $\alpha$ -galactosidase enzyme activity and therefore the ability to metabolise the X- $\alpha$ -Gal substrate. Plate A shows the results of a number of samples which had been simply picked and then seeded directly onto the agar in a single swab. Plate B shows the results of a number of the same samples streaked out onto the agar plate in order to generate single colonies in each case. The method shown in B was by far the more reliable way to test for MEL1 activation, with those clones demonstrating single colonies able to activate MEL1 activity possessing real ability to metabolise the X- $\alpha$ -Gal substrate.



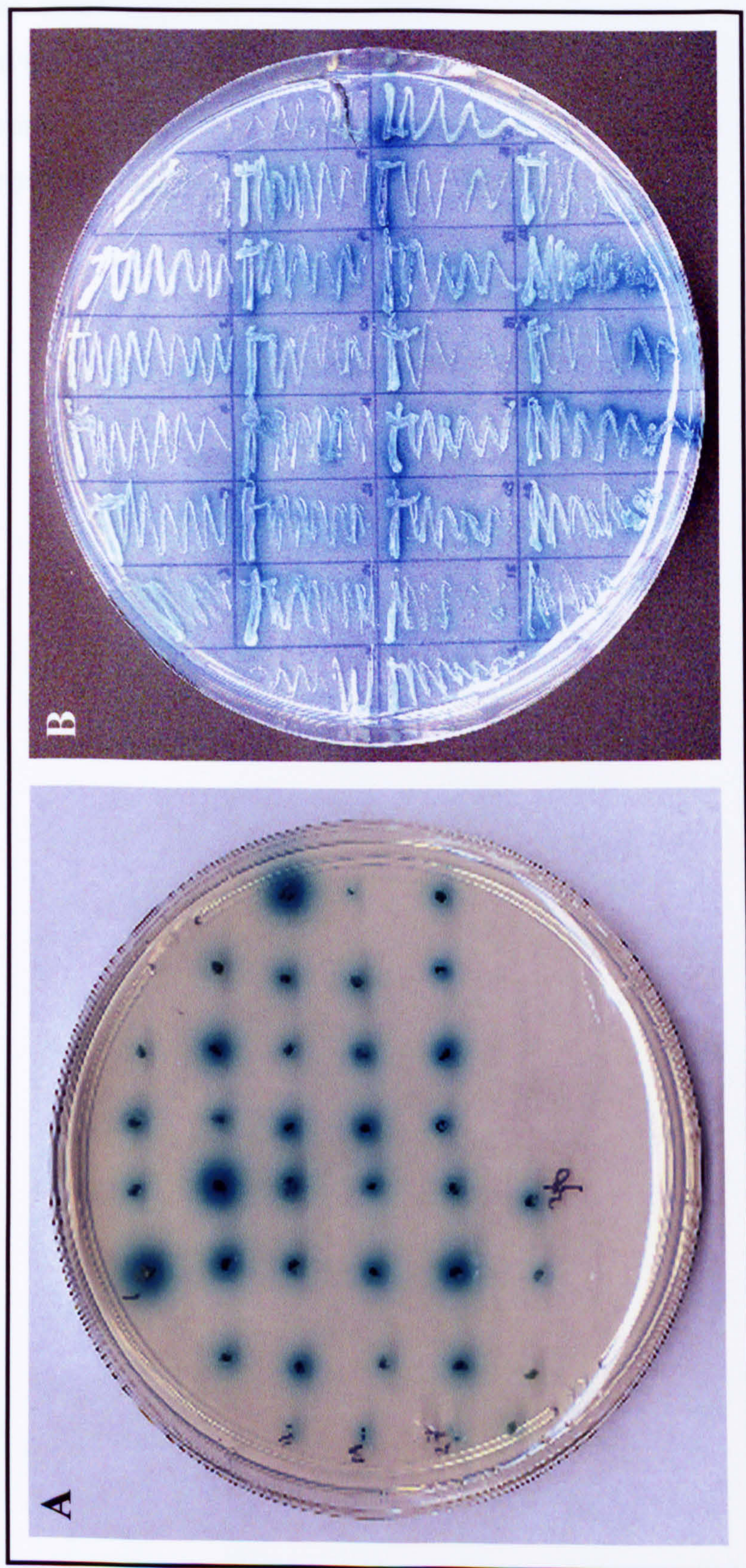




**FIGURE 5.8 THE RECURRING cDNA CLONE - IDENTIFIED TO ENCODE METALLOTHIONEIN-II (MT-II) IN OPEN READING FRAME (ORF) 3**

This figure details one of the cDNA fragments that was identified many times in the first small-scale screen. The insert sequence was translated using the correct ORF utilised by the AD vector and the resultant protein sequence is shown as **pink** text. The **purple box** indicates the location of the DNA sequence with homology to MT-II and the **purple** text indicates the protein sequence of MT-II, incorporated in ORF 3.



[illegible]



## **FIGURE 5.9 RESTRICTION ANALYSIS OF THE 8 'POSITIVES' IDENTIFIED IN THE HIGHER STRINGENCY YEAST TWO-HYBRID SCREEN**

Yeast DNA preparations were performed as per 2.2.10A and used to transform KC8 *E.coli* cells, enabling the isolation of each of the AD plasmids. The AD plasmids were subjected to restriction endonuclease digestion with *Bgl II* to clip the cDNA inserts from the MCS in the pACT2 vector. The results showed the presence of inserts of varying sizes, indicating that the same cDNA insert had not been identified 8 times.



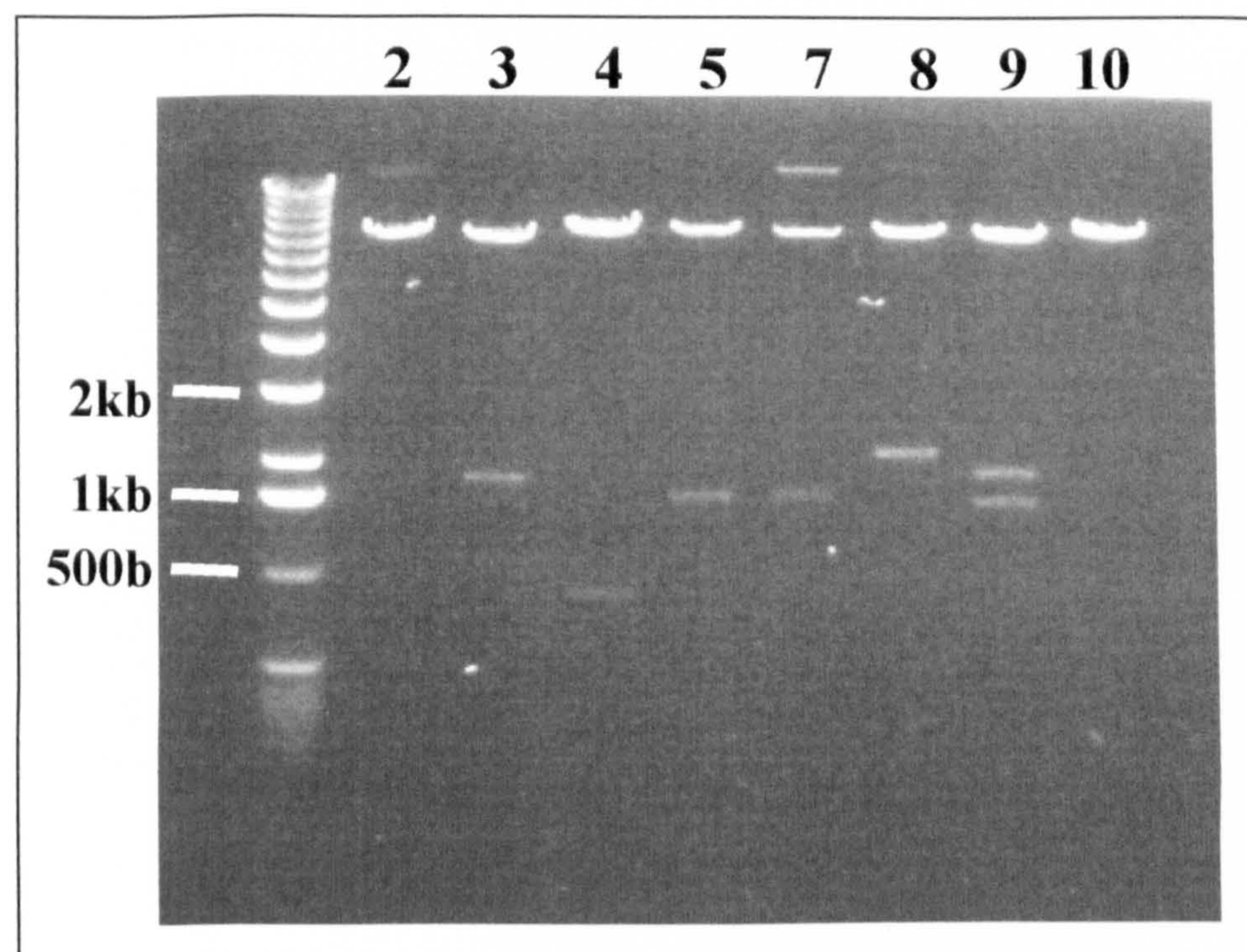




## **FIGURE 5.10 SUMMARY OF THE SEQUENCE DATA OBTAINED FOR THE EIGHT POSITIVE CLONES IDENTIFIED IN THE FINAL YEAST TWO-HYBRID SCREEN**

The DNA sequences for each of the cDNA inserts have been listed, with the identified nucleic acid homology also shown. The open reading frame (ORF) used by the pACT2 vector is ORF1, and the ORF for each of the homologies identified has also been shown. In each instance the cDNA encoded in each vector has been translated in ORF1 demonstrating the protein which would be generated by the cells expressing each of these vectors. These results indicate that clones 3, and 7 are the only clones to express a cDNA insert with homology for a given protein in the correct reading frame for the expression of that same protein. The data from clones 2, 4 and 5 are inconclusive with regards to ORF, due to the poor sequence information obtained.



Clone	Nucleic Acid Sequence Homology	Extent of Homology (Bases)	ORF	Protein Translation Used by Vector
2	Human monocyte antigen CD14 mRNA	~120	?	Poor sequencing results – impossible to say
3	Zn Finger Like Proteins	72	1	EKPYDCGDCGKAFSRRSTLIQHQQVHSGETRCKRKHGPAFVHGSSLTADG QIPTGEKHGRAFNHGANLILRWTVHTGEKSFGCNEYGKAFSPTSRTPTDQ IMHAGEKPYKCQECXNPSVXSQPLFNIR
4	?	?	?	Poor sequencing results – impossible to say
5	mRNA expressed in CD34 <sup>+</sup> haematopoietic stem/progenitor cells	210	?	Poor sequencing results – impossible to say
7	Filamin-A	>350	1	VVLAEMGTHTVSVKYKGQHVPGSPFQFTVGPLGEGGAHKVVRAGGPGLE RAEAGVPAEFSIWTRAGAGGLAIAVEGPSKAEISFEDRKDGCSCGVAY VVQEPGDYEVSVKFNEEHIPDSPFVVPVASPSGDAR.....
8	PER1	149	3	LGAP'LSVPNPQLSLWGTPDPC'
9	FLNa (b & c)	~130	3	EDGLSTSSTRPPSRANTSSVCALVASTCPTAPSK'
10	Mitochondrial genome	-	2 or 3	LTTNNXYILT'TTTQRLHRKIHLPLRVRLRPYIPRPRPFLHKILLSSYYLLII'



### **FIGURE 5.11 CLONES 2, 3, 5, 8 AND 9 ARE ABLE TO ACTIVATE HIS3 EXPRESSION IN THE PRESENCE OF THE EMPTY BAIT VECTOR**

Each of the KC8 DNA preparations were used to re-transform AH109 yeast cells along with either the empty pGBKT7 bait vector or one of the CD23 bait constructs and grown on triple selection media (SD/-Trp/-Leu/-His). The AD plasmids isolated from clones 2, 3, 5, 8 and 9 were able to activate reporter gene expression (His3) in the presence of the empty pGBKT7, bait vector and grow on triple selection agar. The AD plasmids isolated from clones 4, 7 and 10 were found to be unable to grow on triple selection medium in the presence of the empty bait vector.



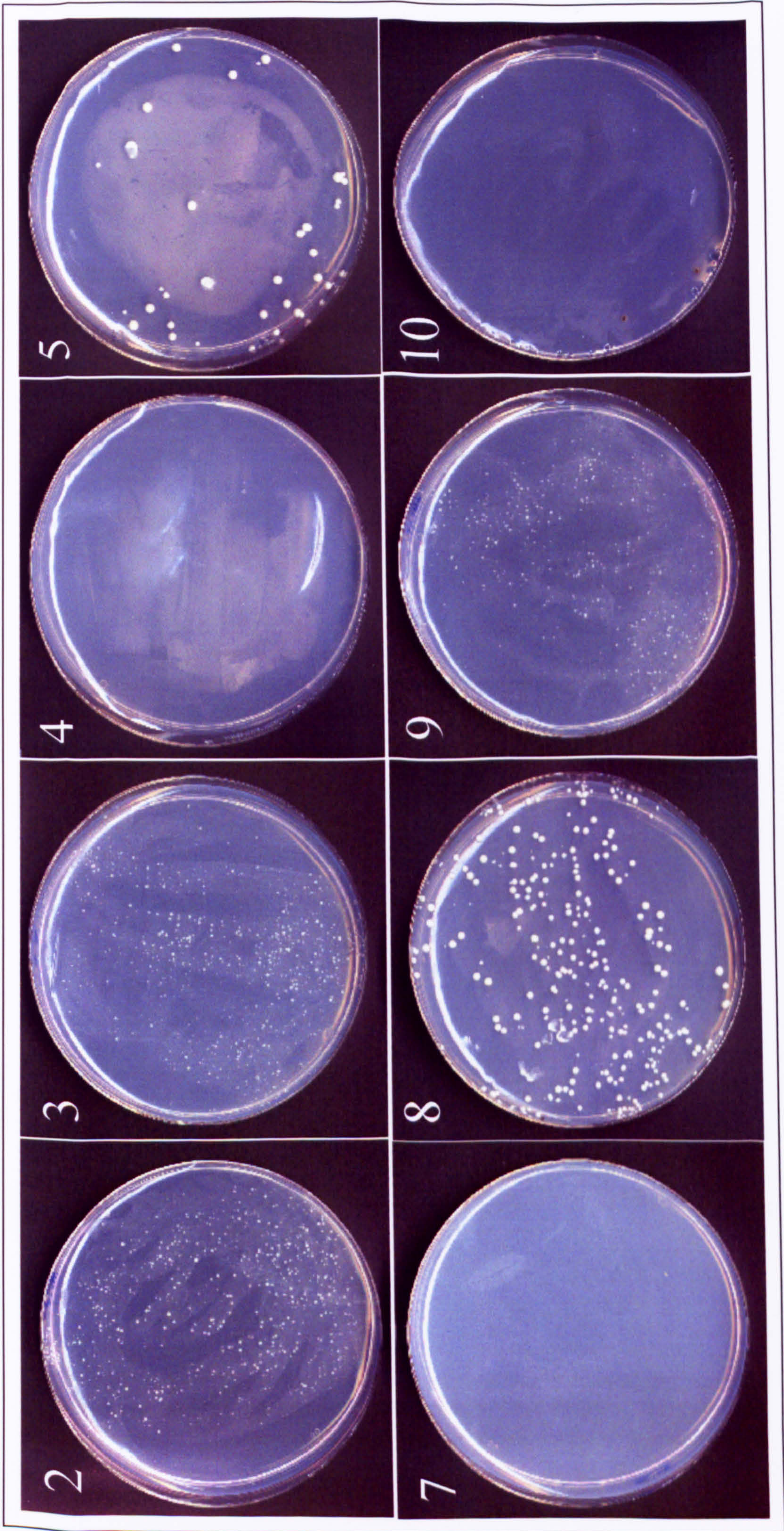




## **FIGURE 5.12 CLONES 4 AND 7 ARE ABLE TO ACTIVATE HIS3 EXPRESSION ONLY IN THE PRESENCE OF THE CD23 BAIT VECTORS**

Clone 10 was unable to grow in the presence of any of the CD23 bait constructs (data not shown), however the AD plasmids isolated from clones 4 and 7 were found to be able to activate reporter gene expression with the CD23 bait constructs but not in the presence of the empty bait vector, as shown in the previous figure. Clone 7 was found to have better growth than clone 4, demonstrating a greater number of colonies on each plate. Clone 7 also seemed to interact better with the single bait vectors, producing more transformants with these in comparison to the triple bait vectors.

Key; (i) pCD23a<sub>s</sub> (ii) pCD23b<sub>s</sub> (iii) pCD23a<sub>t</sub> (iv) pCD23b<sub>t</sub>



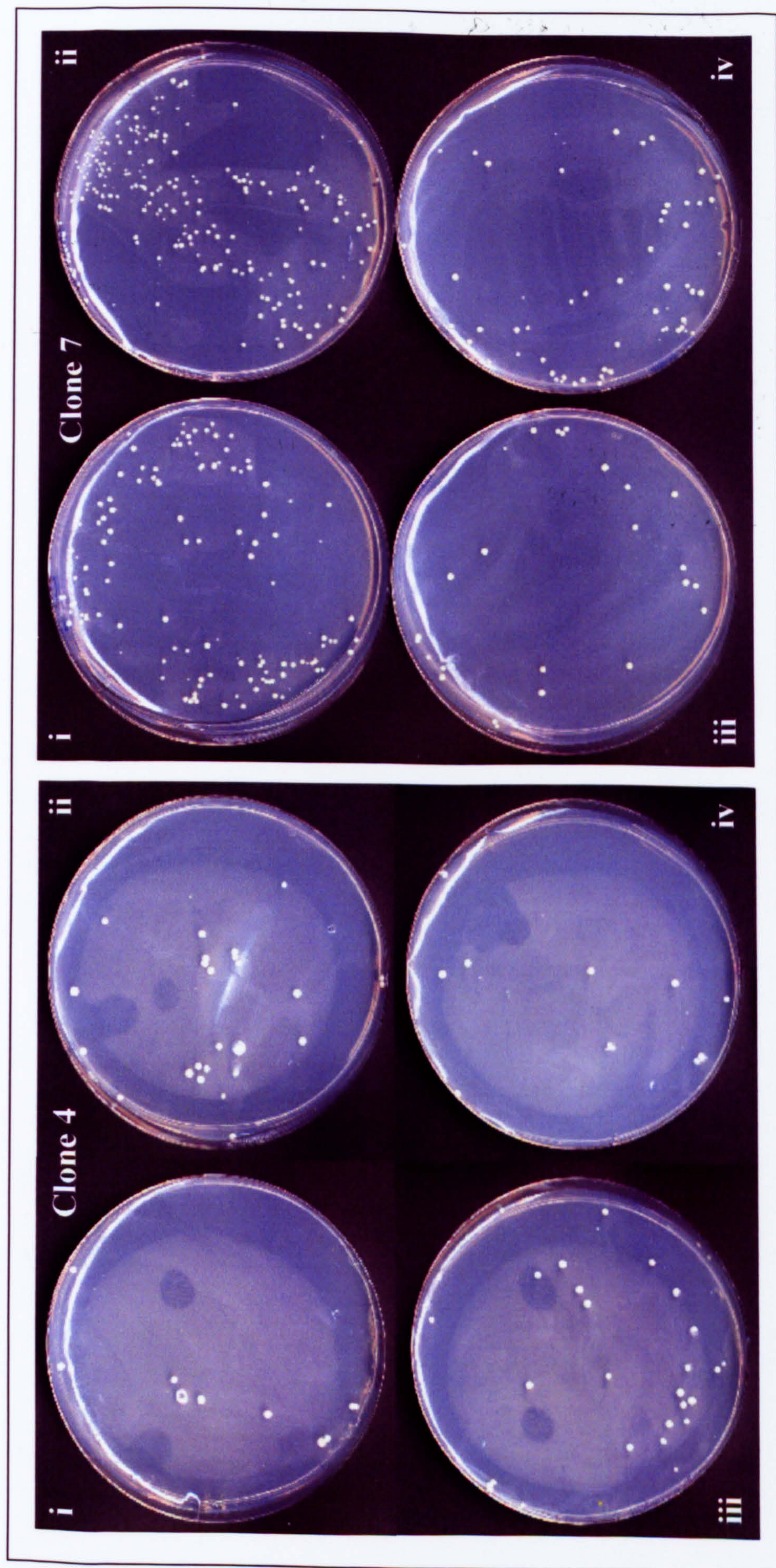




### **FIGURE 5.13 PROTEIN EXPRESSION FROM THE ISOLATED AD VECTORS**

Yeast cells were transformed with each of the AD plasmids isolated from the 8 clones, in order to assess protein expression from each vector. TCA protein extractions were performed as per 2.2.10B and 15µl of each sample was separated on a 10% SDS-PAGE electrophoresis gel. The protein samples were transferred to nitrocellulose membrane and immunoblotted with antibody specific for the HA epitope tag.

The results indicate strong protein expression of HA-fusion proteins from clones 3, 7, 9 and 10. However HA-tagged protein expression was not observed from the empty bait vector, making it impossible to estimate the sizes of each of these expressed proteins without the HA-tag and GAL4 AD protein.



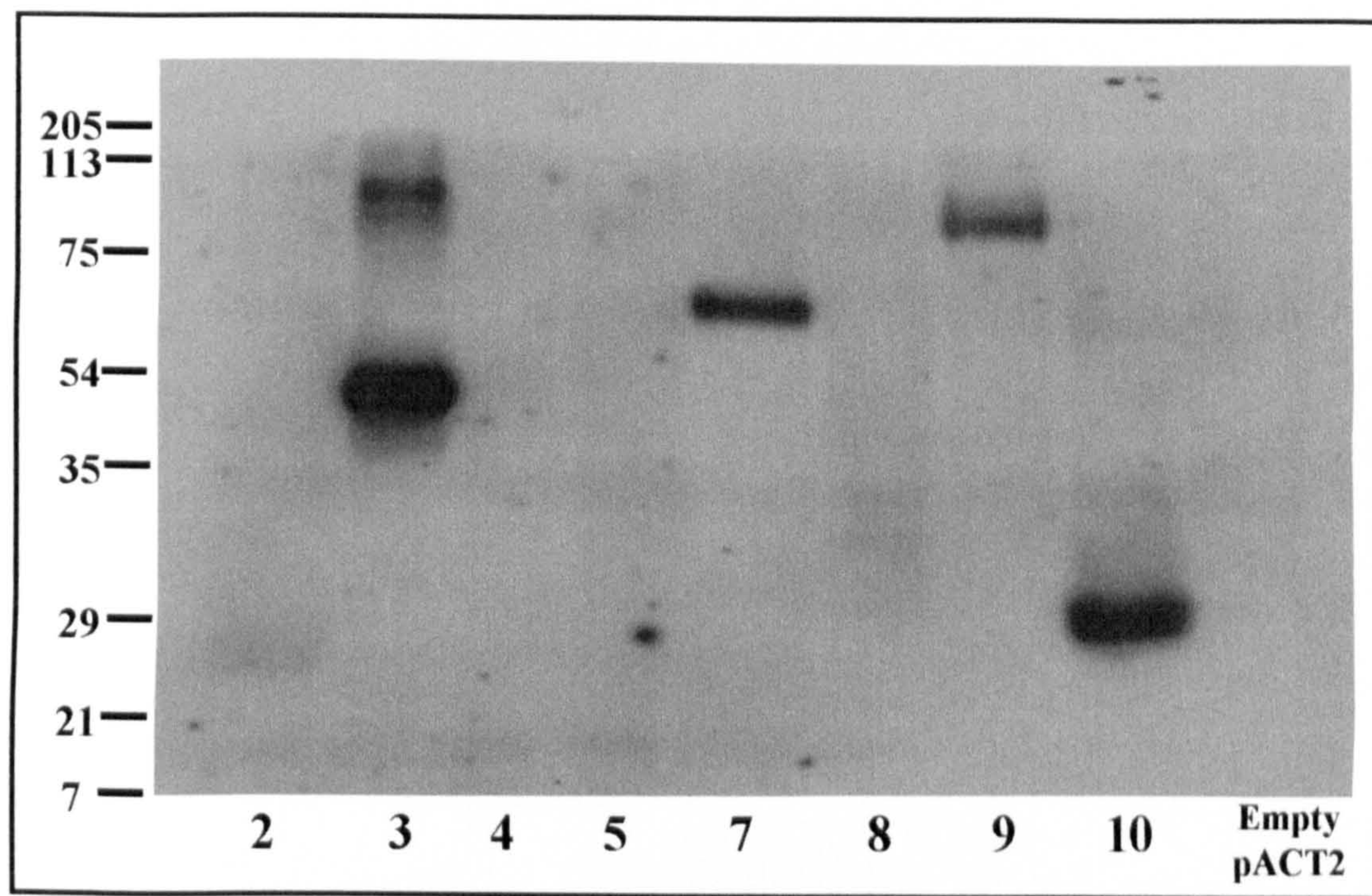
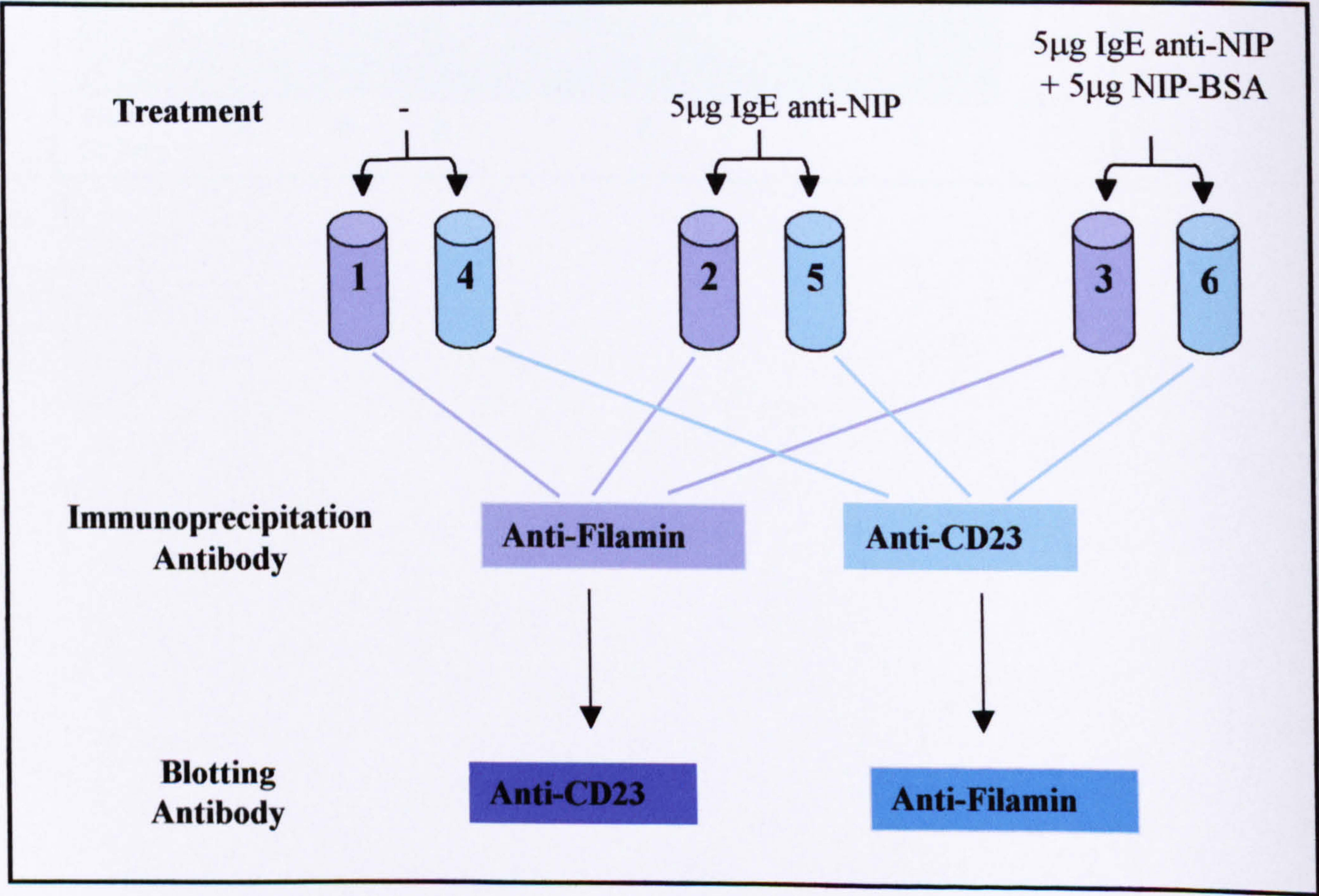




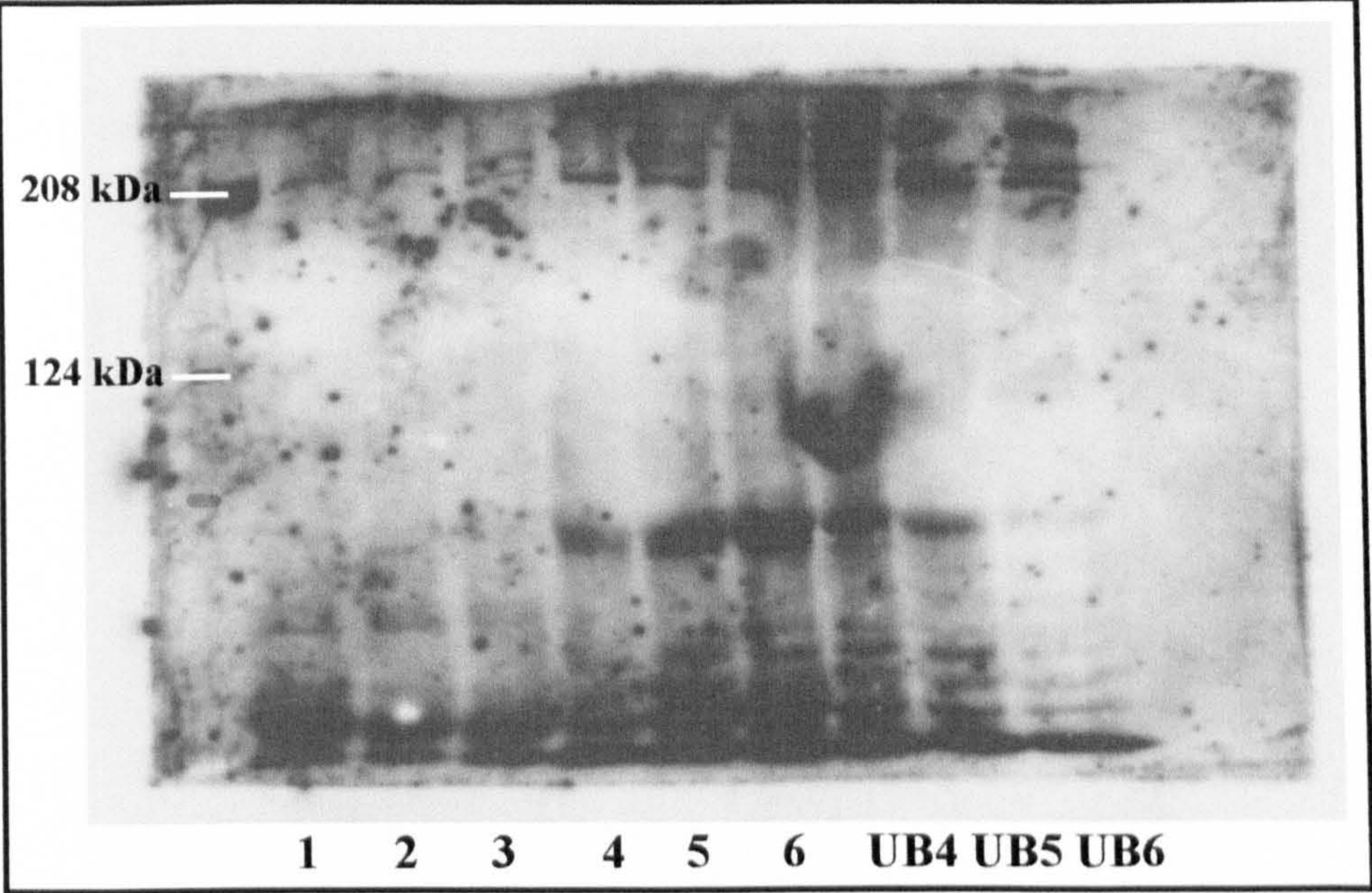
**FIGURE 5.14 CD23 MAY INTERACT WITH FLNA IN RPMI 8866 CELLS**

The B cell line RPMI 8866 were cultured in complete RPMI media and harvested on the day of experimentation. The cells were counted, resuspended in 12ml of RPMI medium at  $1.5 \times 10^7$  cells/ml and split equally amongst the wells of a 6 well plate. The three duplicate samples were treated with (i) no addition, (ii) IgE anti-NIP antibodies or (iii) IgE anti-NIP antibodies, followed by NIP<sub>10</sub>-BSA for 10 minutes at 37°C before they were subjected to lysis with OGP buffer and immunoprecipitated with either anti-CD23 or anti-filamin antibody. The proteins bound to sepharose-protein G beads were harvested, separated on 6% SDS-PAGE and immunoblotted with the opposite antibody. The blot was visualised using the BioRad ECL detection kit. The flow chart summarises this experiment and the numbers attached to each sample corresponds with the numbers labelling the ECL gel scan. UB denotes the unbound samples from the appropriately labelled tubes.





**Anti-FLN Blot**



**Anti-CD23 Blot**

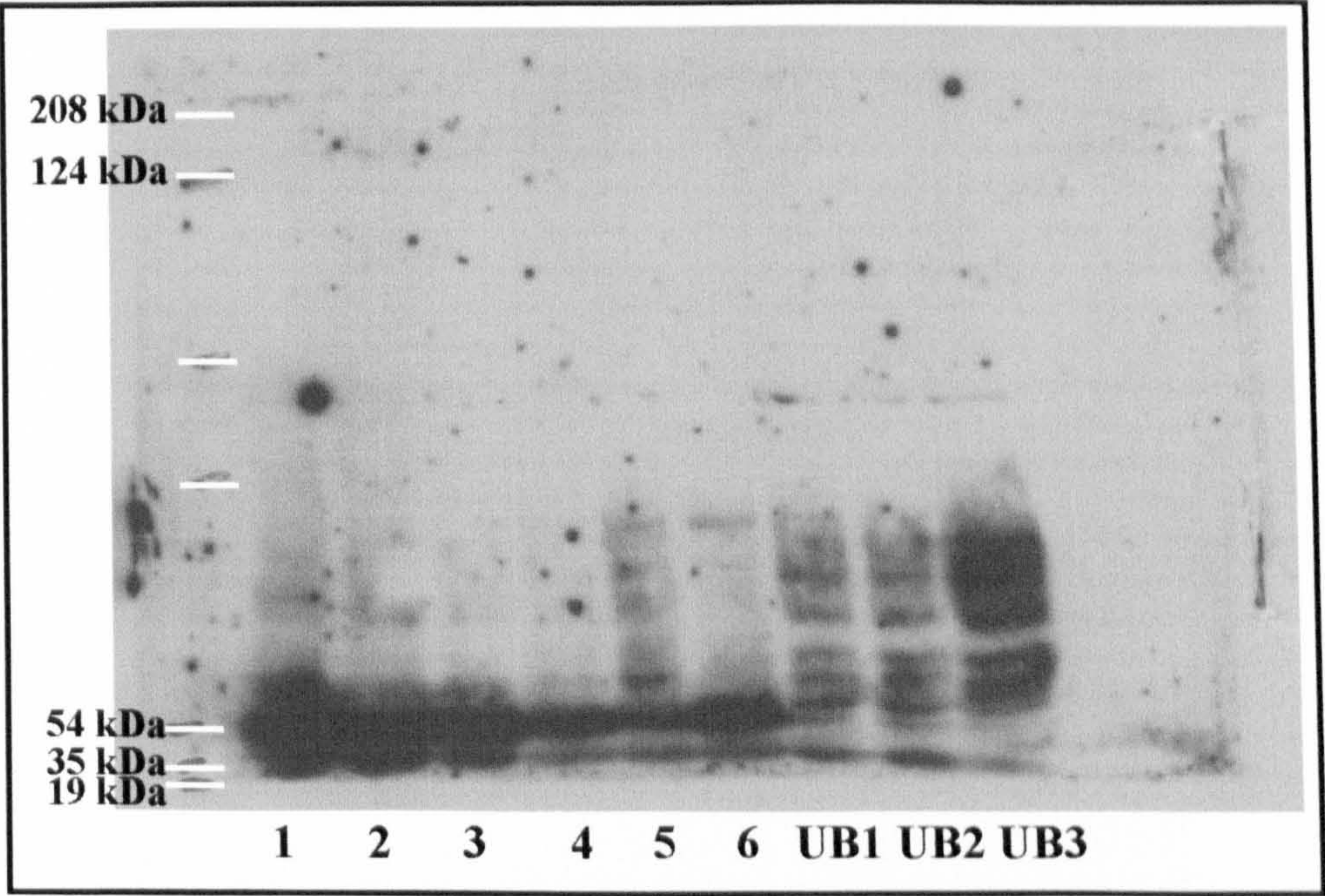




## **FIGURE 5.15 CD23 MAY INTERACT WITH FLNA IN RPMI 8866 CELLS (2)**

Those samples shown on the lower blot of the previous figure were run again on a 10% SDS PAGE gel in order to enhance protein separation, and immunoblotted with anti-CD23 antibody. The blot was visualised using the BioRad ECL detection kit. The flow chart shown on the previous figure summarises the experimental conditions, and details the contents of each lane. UB denotes the unbound samples from the appropriately labelled tubes.



**Anti-CD23 Blot**

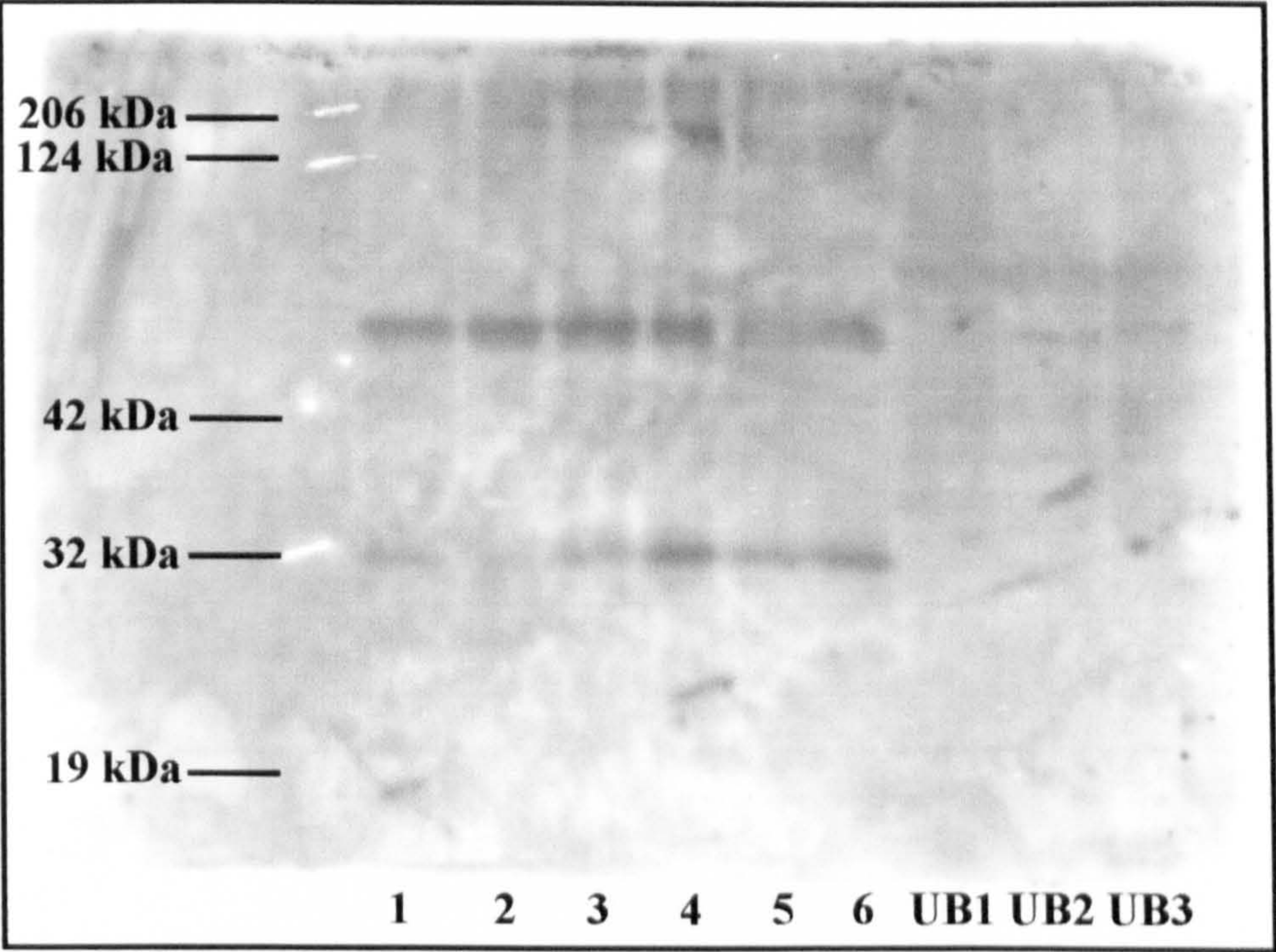




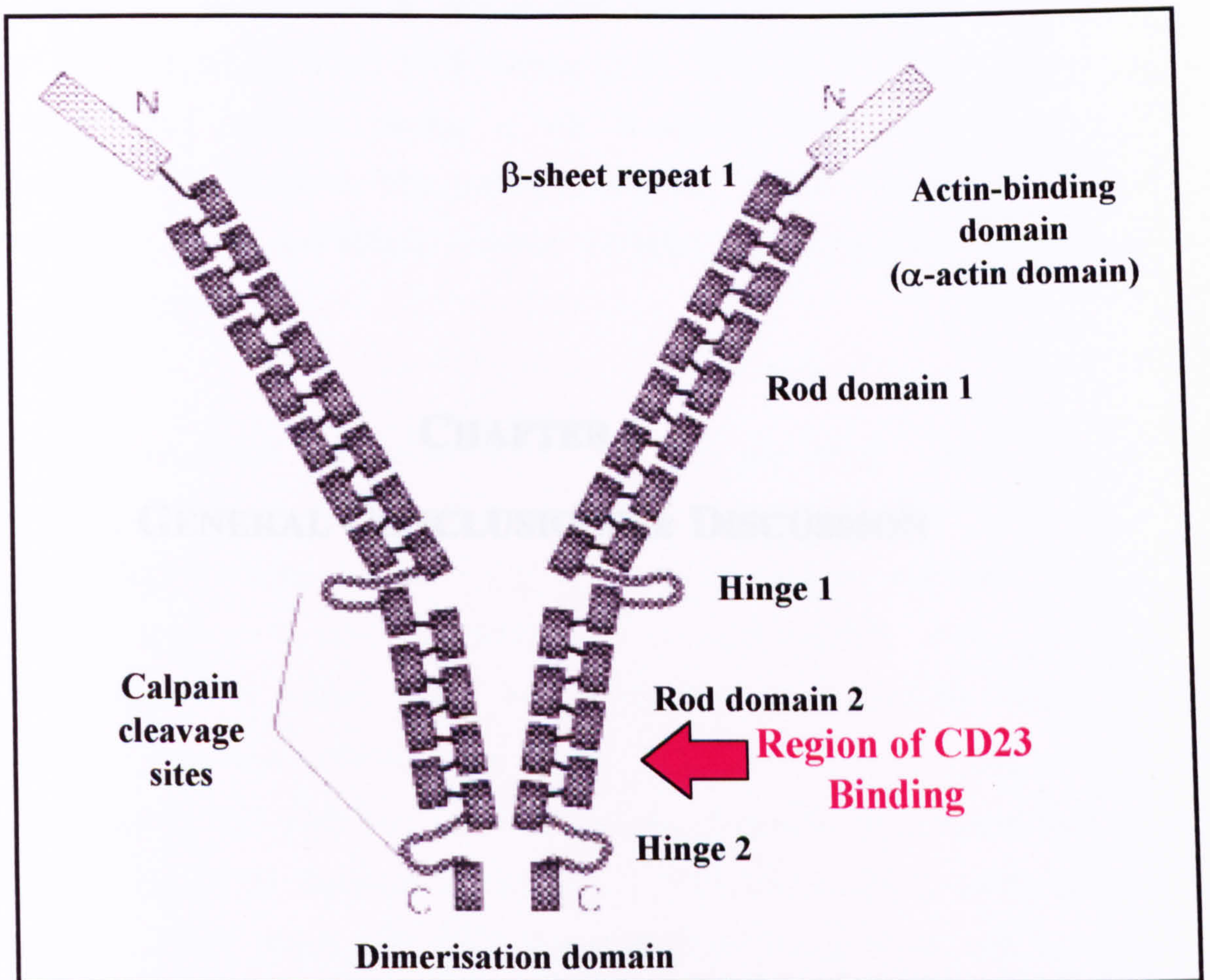
## **FIGURE 5.16 SCHEMATIC DIAGRAM ILLUSTRATING THE PROPOSED STRUCTURE OF HUMAN FLNA**

The diagram illustrates the structural model for human filamin a, (FLNa). FLNa contains 24 repeats of ~96 amino acids each. These domains are thought to fold into anti-parallel  $\beta$ -pleated sheet structures that overlap, generating the rod arrangement illustrated in the diagram. Dimerisation is thought to occur through the 24<sup>th</sup> repeat. The amino-terminal actin-binding domain contains sequence motifs common to many actin-filament-binding proteins.

The arrow demonstrates where the N-terminal tail of CD23 is thought to bind FLNa, based upon the clone purified from the yeast two-hybrid screen detailed within this chapter. Clone 7 encodes at least repeat 20, with the remainder of the insert having to be sequenced.

This diagram was adapted from Stossel *et al.*, 2001.







## **CHAPTER 6**

### **GENERAL CONCLUSIONS & DISCUSSION**



## 6.1 CURRENT UNDERSTANDING OF THE HUMAN CD23 ISOFORMS

CD23 is a 45kDa leukocyte cell surface antigen expressed on various cells of the haematopoietic lineage including B cells, T cells and monocytes [Capron *et al.*, 1986; Sarfati *et al.*, 1986; Bieber *et al.*, 1989; Billaud *et al.*, 1989]. CD23 is a multifunctional receptor/ligand and cytokine, playing a role in antigen presentation, macrophage activation and cell adhesion. The principal function of the full-length/membrane associated form is as the low affinity receptor for IgE (Fc $\epsilon$ RII) [Bonnefoy *et al.*, 1987; Yukawa, *et al.*, 1987].

Early evidence suggested two distinct roles for CD23, one being a stage-dependent involvement in B cell growth and differentiation [Gordon, *et al.*, 1987; Kolb, *et al.*, 1990], the second involving the effector phase(s) of IgE-mediated immunity, including allergy and the response to parasitic infections [Kehry & Yamashita, 1989; Luo, *et al.*, 1991]. Two species of human CD23 were originally hypothesised by Yokota and colleagues and then later identified and termed CD23a and CD23b [Yokota *et al.*, 1988]. The human CD23 gene has been mapped to an 11 exon gene on chromosome 19, encoding both the CD23 isoforms [Ludin, *et al.*, 1987; Suter, *et al.*, 1987; Wendel-Hansen, *et al.*, 1990] which arise from use of different transcription start sites and differential RNA splicing. The isoforms have been demonstrated to differ only in a short amino acid stretch in the cytoplasmic tail region where the N-terminal 7 amino acids of CD23a (MEEGQYS) are distinct from the alternative 6 amino acids of CD23b (MNPPSQ), see Figure 1.4. The presence of both cell type-specific and stimulus-specific expression of the two CD23 variants suggests that each isoform has a different cellular function, despite having identical extracellular domains.

Early studies of CD23a and CD23b indicated that the two isoforms may be internalised via distinct pathways, with CD23a shown to enter the cell via receptor-mediated endocytosis in  $\psi_2$  cells whilst CD23b was demonstrated to have a more phagocytic route of cellular entry in J774 cells [Yokota, *et al.*, 1992]. The aromatic tyrosine residue at position 6 and the Asn-Pro residues at positions 2-4 were thought to be important for CD23a endocytosis and the phagocytosis of CD23b respectively. These findings suggest endocytosis and phagocytosis to be separate functions that appear to be attributable to



distinct amino acid residues. The studies presented here employed a single model to analyse the intracellular trafficking patterns of each of the CD23 isoforms in the same cell system, with emphasis on a number of potentially key residues located in the unique cytoplasmic N-terminal tail of each protein.

With respect to downstream signalling, current understanding generally links the CD23a isoform to a cAMP pathway with the CD23b isoform thought to function generally via inositol-1,4,5-trisphosphate and  $\text{Ca}^{++}$  mobilisation [as reviewed by Mossalayi *et al.*, 1997]. Much of this understanding is speculative with no conclusive proof of protein-protein interactions physically linking CD23 to any of these signalling pathways. CD23 has however been demonstrated to associate with a src family tyrosine kinase p59<sup>lyn</sup>, as identified using co-immunoprecipitation experiments [Sugie *et al.*, 1991]. The fact that CD23 appears able to transmit a signal in a variety of cells, together with the fact that it has a very short cytoplasmic tail strongly suggest that CD23 may associate with other molecules in order to exert its function. The later part of the work presented herein addresses the gaps in this knowledge and the conclusions of these studies are discussed herewith.

### **6.1.1 MAIN CONCLUSIONS**

The main findings of the research presented in this thesis are two fold. The results firstly demonstrate that the two human CD23 isoforms do indeed traffic differently in the same cell model. The second section of research provides an insight into a potential mechanism enabling CD23 function, identifying a protein-protein interaction which may explain how CD23 and its short cytoplasmic tail facilitates signalling.

### **6.2 INTRACELLULAR TRAFFICKING OF CD23**

The research presented in this thesis demonstrates that there are indeed fundamental differences between the intracellular trafficking of each of the CD23 isoforms, something which had been suggested before [Yokota *et al.*, 1992] but never proven using the same stimulation method and cell system to analyse both protein isoforms. The HEK 293 system reported here has the obvious advantages of not expressing



endogenous CD23 in the first instance, enabling the use of fluorescent antibodies to detect and monitor the transfected CD23 proteins, by confocal microscopic analysis in a readily adherent cell line. This system facilitated the comparison of wild-type CD23 (identified using a fluorescently labelled antibody) with GFP-tagged CD23 fusion proteins. Firstly the presented results demonstrate the usefulness of GFP-fusion proteins in CD23 intracellular trafficking studies, facilitating the investigation of the unoccupied or 'basal' receptor, a phenomena uncharacterised prior to this research. There are also a number of technical advantages as GFP-fusion proteins have been found to give greater sensitivity and resolution in comparison to staining with fluorescently labelled antibodies, exhibiting low background fluorescence and greater resistance to photo bleaching [Wang & Hazelrigg, 1994]. The use of the GFP tag is also well characterised in kinetic studies of protein localisation and trafficking [Flach *et al.*, 1994, Wang & Hazelrigg, 1994], with chimeric genes encoding either N- or C-terminal GFP-fusions retaining the normal biological activity of the heterologous partner, as well as maintaining fluorescent properties similar to native GFP [Flach *et al.*, 1994; Wang & Hazelrigg, 1994; Marshall *et al.*, 1995; Sterns, 1995]. The studies presented within certainly illustrate this to be the case for CD23, with basal GFP-CD23 acting as per FITC-labelled wild-type CD23 proteins, demonstrating that the addition of the GFP tag does not affect CD23 trafficking, an important consideration in any study utilising fusion proteins.

Secondly, the results also demonstrate the usefulness of the NIP-system, a single model system facilitating the investigation of CD23 trafficking in the 'basal', 'loaded' and 'cross-linked' state, again, something which had not been investigated prior to the initiation of this research. The combination of the GFP-tag and the NIP-system generates an elegant methodology facilitating the investigation of CD23 trafficking in a situation minimally perturbed from that which would be present in the native state.

In summary the findings from the HEK 293 study demonstrate that both the CD23a and CD23b molecules show a degree of re-cycling in the basal, unligated state and that, following the cross-linking of GFP-CD23 molecules or loading of CD23 with anti-CD23 antibodies, only the CD23a isoform is able to demonstrate rapid directed uptake and co-localisation with Tf-TxR and thus sorting into the endosomal system. The



CD23b isoform was internalised, but did not enter the endosomal pathway under any conditions in HEK 293 cells. These findings demonstrate that the two isoforms appear to traffic differentially, but that each isoform requires ligation with IgE as stimulus for the receptors to collect at particular areas along the plasma membrane, prior to uptake from the cell surface. Cross-linking with NIP<sub>10</sub>-BSA stimulated a definite increase in the extent of directed uptake from the cell surface, and this was found to be true for both CD23 isoforms. Wild-type GFP-CD23b was also studied, and was demonstrated to use both the endocytic and phagocytic pathways in Raji A cells as judged by co-localisation with both Tf-TxR and LysoTracker dyes, respectively. No data were generated for the GFP-CD23a isoform as the expression levels were too low to work with. The data suggest that the CD23b isoform requires extensive oligomerisation at the cell surface, achieved in these experimental conditions only after cross-linking with NIP<sub>10</sub>-BSA protein conjugates, as stimulus for directed uptake into the endosomal system, but readily enters the phagocytic pathway on loading with IgE and antigen. These findings suggest that cross-linking of CD23 at the plasma membrane is required to drive directed movement into the endosomal system and, potentially, towards the antigen processing machinery of the cell. This requirement parallels mast cell and basophil degranulation, a process triggered by cross-linking of the high affinity IgE receptors. The requirement for cross-linking may also reflect a situation where antigens for which high levels of IgE exist are most readily internalised via a CD23-dependent mechanism for processing and presentation to T cells for negative regulation of the IgE response. Data from CD23<sup>-/-</sup> mice support a role for IgE in negative regulation of the IgE response [Yu *et al.*, 1994]. CD23 has also been shown to be spatially associated with HLA-DR molecules on the B cell surface [Bonney *et al.*, 1988] and this interaction facilitates a well characterised function of membrane bound CD23 in B cells, the enhancement of the IgE-dependent antigen presentation to T cells [Pirron *et al.*, 1990; van der Heijden *et al.*, 1993; Squire *et al.*, 1994; Gustavsson *et al.*, 1994; Fujiwara *et al.*, 1994; Mudde *et al.*, 1995; Oshiba *et al.*, 1997; Karagiannis *et al.*, 2001]. This requires the binding of antigen-IgE antibody complexes to CD23, internalisation of the complexes and transport to compartments of the endosomal network containing proteolytic enzymes and major histocompatibility (MHC) class II antigens.



The findings from the mutagenesis study suggest that there may be a number of key residues which affect the trafficking patterns of the CD23 proteins. The results suggest that the phosphorylation state of the serine residue, present in both isoforms, may play a regulatory role in CD23 uptake from the cell surface. Two expression patterns were observed for bS5A in HEK 293 cells. If the first population to be described (demonstrating a diffuse intracellular staining with a limited amount located on the plasma membrane in the basal state) was correct, then when the serine is not phosphorylated, and unable to be phosphorylated, cross-linking is required before directed uptake is observed, as was shown to be the case for serine mutations in both CD23 isoforms. Mutation of these residues to aspartate or phenylalanine resulted in proteins able to undergo directed uptake from the cell surface in all three states, regardless of receptor occupancy or oligomerisation state. The second population demonstrated a more usual staining pattern, with much of the protein associated with the plasma membrane, however this population was observed to show extensive co-localisation with Tf-TXR in all three basal, loaded and cross-linked states. If this second population was found to be the true case, the results become more complicated and harder to explain. Further investigation is required to establish which of the two expression patterns was true for the bS5A mutant protein, before any definitive conclusions as to the importance of this residue can be drawn.

The other point to consider is that a number of different residues were observed to have an effect on CD23 trafficking, therefore it seems likely that the modification of a single residue may not solely explain the requirements for sorting, but rather that a number of key residues may play a role in the vesicular transport of the receptor from the cell surface into the cell. However, collectively, the results do strongly suggest that the phosphorylation state of this residue does play an important role in CD23 trafficking. The preliminary results obtained from the mutagenesis studies performed in Raji A cells, were generally supportive of the findings observed in the HEK 293 cells. The basal staining pattern observed for the bS5A mutant protein in Raji A cells was similar to that of the second population observed in the HEK 293 cells. This observation 'muddies the water' on the simple theory of the phosphorylation state of the serine residue having a regulatory role on CD23 protein trafficking. Loaded and cross-linked states were not examined using the Raji A cells, as a direct result of the poorer



expression levels observed in this cell type, therefore comparisons can only be drawn between the basal data sets from each cell line.

The NNP tri-peptide motif located within the N-terminal tail of the CD23b isoform has previously been linked to CD23 sorting into a phagocytic route in J774 cells [Yokota, *et al.*, 1992], therefore these residues were also targeted for manipulation in this study. The bP3R mutant was found to remain trapped within distinct regions of the cytoplasm in HEK 293 cells, unable to reach the plasma membrane, as determined by both flow cytometric and confocal analysis. No co-localisation was observed with Tf-TxR indicating that this protein is located in areas or vesicles distinct from either the early endosomes or indeed the endocytic pathway. In contrast to this the bP3R protein was observed to have a different expression pattern in Raji A cells, with some of the protein recorded at the cell membrane, both by flow cytometric and confocal analysis. This situation was found to be similar for that of the bS5A protein in HEK 293 cells, as two different expression patterns were also observed for the bP3R proteins, this time in Raji A cells. The most likely explanation in this instance is that the differences were a result of protein expression levels; with cells that expressed lower amounts of the CD23 protein not clearly demonstrating its presence at the plasma membrane, however cell surface CD23 was detected in cells expressing higher amounts of the bP3R protein. Collectively these results suggest there to be a difference in expression patterns between the two cell types investigated. This observation may be explained with respect to the cell types and their abilities to utilise differential trafficking pathways. Raji A cells are capable of trafficking proteins via a phagocytic route, whereas HEK 293 cells are unable to use this pathway. This finding suggests the two cells possess different sorting machinery, therefore it is conceivable that this protein, thought to traffic by phagocytosis, may be processed differently in cells capable of this sorting route to those not able to use it. HEK 293 cells, unlike Raji A cells, do not express MHC class II proteins, therefore the CD23 trafficking observed in HEK 293 cells is intrinsic to the CD23 protein itself.

The bP4R and bN2K mutants were found to demonstrate both directed uptake and co-localisation with Tf-TxR in HEK 293 cells. It was initially proposed that these mutants may have been forced to use the endocytic route of entry as a default pathway as it was



the only one available to them in this cell type. This theory was supported by the fact that the bP4R and bN2K mutants were not observed to co-localise with Tf-TxR in Raji A cells. The wild-type GFP-CD23b proteins were observed to use the phagocytic route of entry in Raji A cells. The bN2K mutant was also observed to co-localise with LysoTracker dye, in all three states in Raji A cells, (data not shown) whilst the bP4R mutant was not studied in the presence of LysoTracker Red. Yokota and colleagues reported that altering the proline at position 4 to an arginine caused a decrease in the extent of CD23 uptake by phagocytosis in J774 cells [Yokota, *et al.*, 1992], the quantitative difference (if any) of uptake of wild-type CD23b and bN2K proteins was not determined from the confocal images recorded in this investigation. The best way to address this question would have been to use I<sup>125</sup> labelled IgE/CD23, measuring the amount internalised into the cell after a certain time point under the various conditions of interest. However, bearing in mind that the Raji A transfectants were made towards the end of the project, this experiment was not performed due to the timescale restrictions.

CD23a contains a tyrosine residue at position six, and two mutants were generated to address the potential role phosphorylation of this residue may play in CD23 intracellular trafficking. Unfortunately the expression levels of these proteins were low in each of the cell lines studied, limiting the conclusions that could be drawn. Cytoplasmic aromatic amino acid residues are known to be important for sorting of a variety of molecules, including the low density lipoprotein receptor [Davis, *et al.*, 1987], mannose-6-phosphate receptor [Lobel, *et al.*, 1989], and transferrin receptor [Jing, *et al.*, 1990]. The CD79a and CD79b molecules contain cytoplasmic tyrosine residues and function as transducers of B cell antigen receptor signals [Gold, *et al.*, 1990] via the immunoreceptor tyrosine-based activation motif (ITAM). Fc receptor-mediated phagocytosis of IgG-coated particles by macrophages is also associated with localised tyrosine phosphorylation of a variety of cytoplasmic proteins [Greenberg *et al.*, 1993; Greenberg, 1995]. ITAMs contain two conserved tyrosine residues that can become phosphorylated upon receptor aggregation [Gold, *et al.*, 1991] and bind distinct effectors via their SH2 domains. CD23 does not contain an ITAM motif, however CD23a does contain a cryptic tyrosine motif (YSEI), utilising both “unique” and “common” elements of the CD23a cytoplasmic tail sequence that is similar to the



tyrosine motif found in lamp-1 (GYSEI) which favours a phagocytic sorting pathway. The lack of the key preceding glycine residue, suggests that this motif may favour endocytic rather than lysosomal uptake of CD23a, as indeed was observed to be the case in the experiments detailed in chapter 3. Further experimentation is required to gain more information as to the potential importance of tyrosine phosphorylation, should it occur.

The cytoplasmic domain of CD23, shown in figure 1.5, does not contain any of the standard tyrosine or di-leucine-based motifs described in section 1.3.5 of the introduction. Recently, an acidic dipeptide motif (EE) has also been demonstrated to be important for intracellular sorting of HIV-1 Nef protein [Piguet *et al.*, 1999]. Mutation of the EE diacidic motif of HIV-1 Nef abrogates its ability both to target CD4 from the early to the late endosomal compartment and to interact with  $\beta$ -COP, yet it does not affect adaptor protein complexes binding or indeed Nef-induced CD4 endocytosis. Both CD23 isoforms contain an EE acidic dipeptide motif in the common section of their N-terminal cytoplasmic tails. However, this motif was not targeted in the research discussed here as the mutagenesis focused on the residues which differ between the isoforms, in the attempt to highlight differences responsible for their potential differential functionalities.

### **6.2.1 FUTURE WORK**

This research needs to be extended further, optimising the study in lymphocyte cell lines. The initial work with Raji A cells is very promising, and certainly indicates these cells to be suitable for confocal microscopic analysis of CD23 intracellular trafficking. These cells express endogenous CD23 proteins and therefore must possess all the necessary equipment and protein intermediates to enable the GFP-CD23 trafficking to occur very much as CD23 trafficking would in the real situation. Secondly, the Raji A cell line was isolated for its adhesion properties [Nyormoi, *et al.*, 1972], enabling this B cell line (unlike Raji), to be routinely cultured in monolayers. These cells therefore provide all the advantages of a B lymphocyte cell line, with the added bonus of their ease of use for investigation using the confocal microscope.



The problem of low protein expression in Raji A cells was a limiting factor and must be overcome to facilitate further analysis in this cell line. This may be resolved by using flow cytometry to separate cells expressing GFP-tagged proteins above a particular level, thus supplying uniform populations of cells demonstrating reasonable expression levels. Another way to target this problem would be to attempt to optimise the transfection and/or selection method, by altering the electroporation conditions and concentration of G418 used, in order to maximise the survival and selection of cells demonstrating good expression levels. Further to the information provided already, it would also be useful to perform experiments where the extent of internalisation could be calculated, in order to quantitatively compare each of the mutant proteins to the wild-type isoforms. Dual transfection/staining experiments could also be performed using different fluorescent tags for each of the isoforms, (or indeed the wild-type and a mutant protein), facilitating the study of both proteins in the same cell, under exactly the same experimental conditions, investigating potential co-localisation into the very same vesicle within a given pathway.

### **6.3 BINDING PARTNERS FOR THE N-TERMINAL TAIL OF CD23**

The findings presented in this study indicate that the N-terminal tail of CD23 may bind to filamin. Filamins are a family of high molecular mass actin-binding proteins serving to organise filamentous actin into networks and stress fibres. Three filamin genes have been identified in humans; FLNa, FLNb and FLNc, with the three encoded proteins, filamin-A, -B and -C, found to show strong homology (~70%) over their entire sequence, with the exception of the flexible-loop hinge regions which show only ~45% homology between sequences. Furthermore, filamin-C contains an additional 81 amino acid insertion, located in repeat 20, not present in filamin-A or -B. The genomic organisation of the three human iso-genes is highly conserved, but there is no clear correlation between the intron-exon organisation and the repeated protein domains [Patrosso *et al.*, 1994; Chakarova *et al.*, 2000]. Several studies have revealed overlapping cellular and tissue expression patterns of human filamin-A, -B and -C with the general conclusion that Filamin-A and -B are the most ubiquitously expressed filamin isoforms having been identified in a wide variety of cell types [Gorlin *et al.*, 1990; Gorlin *et al.*, 1993; Maestrini *et al.*, 1993; Zhang *et al.*, 1998; Takafua *et al.*, 1998; Xu *et al.*, 1998; Brocker *et al.*, 1999; Chakarova *et al.*, 2000], whereas filamin-C



is largely restricted to skeletal and cardiac muscle [Thompson *et al.*, 2000]. As has been previously discussed, it is the filamin-A protein which is of relevance here, as this protein was identified as a binding partner for CD23 using the yeast two-hybrid system.

The human filamins have recently been demonstrated to bind a variety of transmembrane proteins, serving to anchor these proteins to the actin cytoskeleton, as well as providing a scaffold for numerous cytoplasmic signalling proteins (as reviewed by Stossel *et al.*, 2001). As such, filamins have been shown to stabilise the delicate three-dimensional actin webs and link these to cellular membranes [Meyer *et al.*, 1998], potentially enabling them to integrate architectural and signalling functions. For example bringing together receptors such as  $\beta$ -integrins [Calderwood *et al.*, 2000], the sub-membrane actin network and intracellular signalling components, filamins can facilitate the activation of local cellular process. It seems likely that this may also be the case with CD23. CD23 has a relatively short, 22 amino acid, cytoplasmic tail devoid of the common motifs known to be required for the binding of many signalling proteins. I have therefore hypothesised that filamin-A is necessary for the downstream functionality of CD23, effectively acting as an adaptor protein enabling the recruitment of the necessary downstream signalling molecules thereby enabling CD23 function. Figure 6.1 illustrates a schematic diagram of this proposed model.

A variety of transmembrane receptors or signalling molecules have previously been shown to bind the human filamin proteins via one or more repeats in their carboxy-terminal tail (see Table 5.4). This research indeed suggests that CD23 binds to the carboxy terminal tail of filamin-A, however the exact region(s) of the filamin molecule involved in binding have not yet been identified, as the clone isolated from the yeast two-hybrid assay contained a large segment of the C-terminal sequence of filamin-A. It is interesting to note that no basic homology has been identified between the diverse binding domains (from a variety of different proteins) found to associate with the same or different filamin repeats, so theoretical predictions of binding motifs cannot yet be made. It is therefore impossible to predict which region of the carboxy-terminal tail of filamin-A is responsible for binding CD23 without further investigation at the protein level.



In many cases the regulation of these interactions, as well as the factors that control the interactions' specificity remain to be determined. Recently, receptor occupancy has been reported to influence the association of filamin with transmembrane receptors. For instance, occupancy of FcγRI by immunoglobulin decreases its interaction with filamin [Ohta *et al.*, 1991], leading to the hypothesis that FcγRI is linked by filamin to the cortical actin cytoskeleton and suggests that receptor occupancy results in the release of receptors from their anchors facilitating reorganisation of the cytoskeleton. In contrast to this, ligation of tissue factor has been shown to be necessary for filamin-A binding [Ott *et al.*, 1998]. It therefore seems likely that the interaction between filamin-A and CD23 may also be affected/regulated by the occupancy of CD23 with IgE. This question was addressed by one experiment performed near the end of this project. However, the results were inconclusive. It would have been satisfying to have been able to characterise the CD23-filamin-A interaction further, but due to the interaction having only been identified in the yeast two-hybrid system a few months prior to the compulsory completion of this research this was simply not possible.

Interestingly fyn was not identified as a binding partner for CD23 in the yeast two-hybrid screens performed within this research. There may be a number of reasons for this with the phosphorylation (or rather lack of) state of the N-terminal tail being the most likely explanation. Another, more simple explanation is that the entire cDNA library was never actually screened in any one experiment, therefore the cDNA expressing fyn may never have been available in the studies performed. Regardless, this research has subsequently opened a number of potential avenues for further investigation.

### **6.3.1 FUTURE WORK**

Firstly the CD23-filamin-A interaction should be demonstrated unequivocally in a relevant cell line, which is purely a matter of being able to perform the necessary experiment again. The primary question which should be addressed, is that of the nature of the interaction, i.e. does it occur constitutively? This should be addressed by investigation of the effects of receptor occupancy on filamin binding etc.



Filamin can be phosphorylated and this modification has also been reported to affect its interaction with several proteins including a number of GTPase proteins [Ueda, *et al.*, 1992; Yada, *et al.*, 1990] as well as actin [Zhuang, *et al.*, 1984; Ohta, *et al.*, 1995]. Several serine/threonine protein kinases phosphorylate filamins, including protein kinase A, protein kinase C, calcium/calmodulin-dependent protein kinase II and p90 ribosomal S6 kinase [Wallach, *et al.*, 1978; Chen & Stracher, 1989; Kawamoto & Hidaka, 1984; Ohta & Hartwig, 1996; Jay, *et al.*, 2000]. Interestingly, phosphorylation of the interacting proteins has also been implicated in the regulation of filamin-protein interactions. Point mutations which mimic serine phosphorylation in the cytoplasmic tails of both tissue factor (Ser<sup>253,248</sup>Asp) [Ott, *et al.*, 1998] and the dopamine D2 receptor (Ser<sup>358</sup>Asp) [Li, *et al.*, 2000] were found to increase or diminish their interaction with filamin, respectively. Collectively these reports indicate that further investigation with the N-terminal CD23 mutants may prove very useful, potentially providing insights as to how the CD23-filamin interaction might be regulated. Other mutagenesis work should also be performed, for example, construction of deletion mutants in order to identify the minimal domain required for an interaction [Chien *et al.*, 1991] and point mutations to identify the specific amino acids involved [Li & Fields, 1993], would be one of the obvious choices to further this research.

Abundant evidence links human filamins to a number of cell signalling pathways, and it may be that some of these signalling proteins facilitate CD23 function, via binding to filamin-A as an intermediate. Another means to expand this work would therefore be to analyse further the CD23-filamin-A immuno-precipitations as it is likely that these other proteins may also have co-immunoprecipitated within the sample and may indeed be detected by western blotting. For example, filamin-A has already been shown to bind to RHO family GTPases and to some regulatory co-factors that are strongly implicated in the regulation of actin assembly and myosin activation [Bishop & Hall, 2000]. Ral also binds filamin-A in a GTP-dependent manner, whereas Cdc42, RhoA and Rac1 bind filamin-A constitutively [Marti, *et al.*, 1997; Ohta, *et al.*, 1999]. Trio, a guanine nucleotide exchange factor for Rho GTPases, binds filamin-a, implying that switching on and off Rho GTPases constitutively bound to filamins might regulate the spatial positioning of actin assembly [Bellanger, *et al.*, 2000]. By interacting directly with the Rho signalling apparatus, filamins can organise actin filaments that elongate under the



influence of these GTPases into three-dimensional configurations useful to the cell. This line of investigation may highlight those proteins involved in the initial steps of the downstream signalling pathways of CD23, and may even provide conclusive proof as to whether or not the two isoforms do indeed function via different signalling pathways.

It should also be noted that a full-scale library screen was never actually attempted during the course of this project and that all the screens discussed in this chapter used either the pCD23A<sub>s</sub> or pCD23A<sub>t</sub> bait vectors to initially identify positive interactors. The plasmids containing the cDNA fragments encoding 'positive' proteins were then isolated and used to transform AH109 cells in conjunction with the CD23b bait vectors. This simple test was able to indicate whether the interaction was specific to the CD23a isoform or indeed whether the protein could also interact with CD23b. Ideally if time had not been a limiting factor it would have been informative to have performed two library scale screens using the cytoplasmic N-terminal tail of each of the CD23 isoforms as the bait protein, in order to investigate the possibility of other novel protein interactions. Again this line of investigation may provide information as to whether the two isoforms do actually bind different proteins in order to achieve their functions.

A commercially produced vector, for use in the yeast two-hybrid assay, has also now been released which facilitates the expression of phosphorylated proteins in yeast. CD23a contains tyrosine and serine residues at positions 6 and 7 whilst the CD23b isoform contains a serine at position 5. The phosphorylation state of these residues may be an extremely important factor as to whether or not certain proteins bind. It would be very interesting to complete a screen with our bait proteins in this vector, thus investigating whether or not a separate range of protein interactors would be identified.

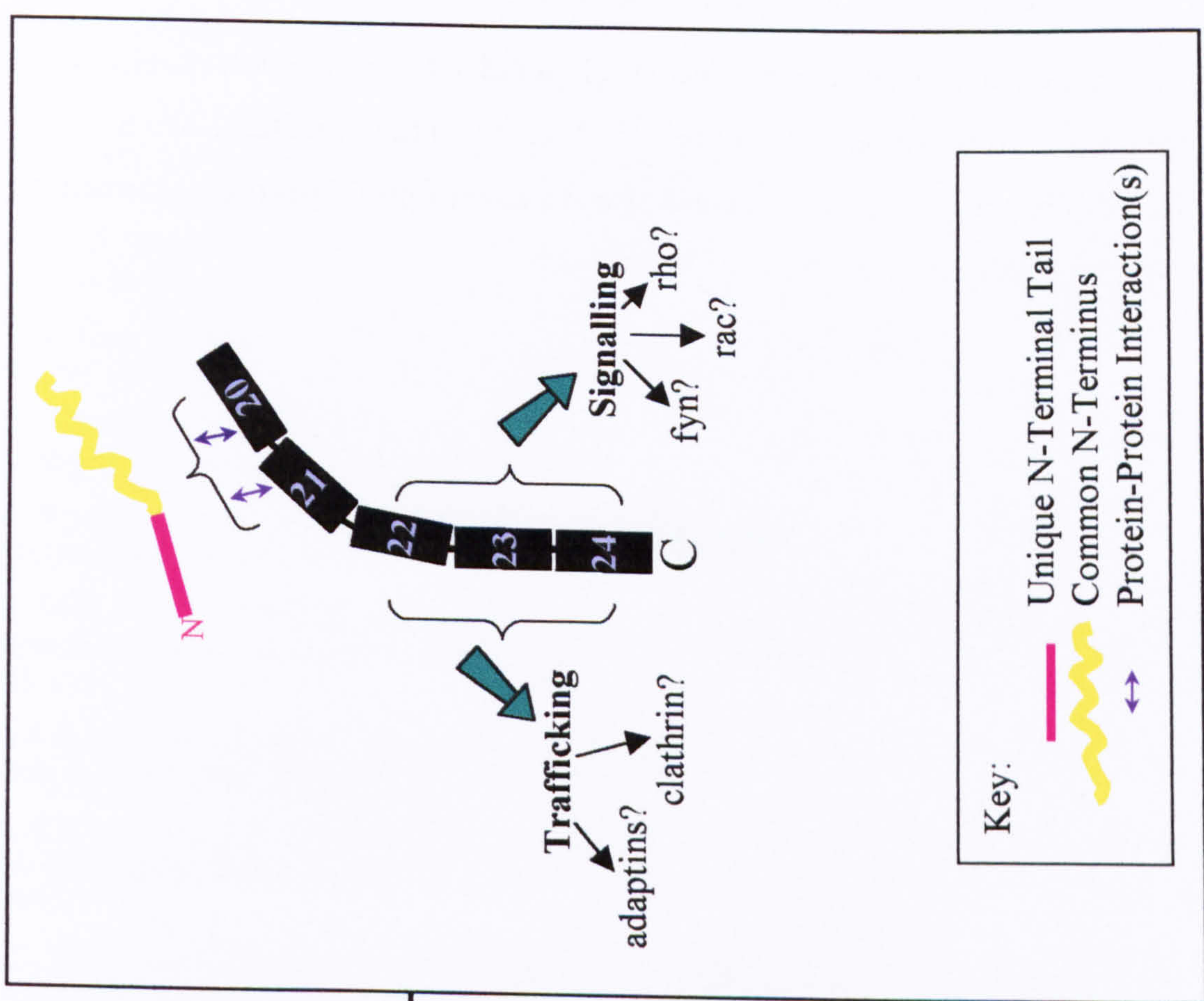
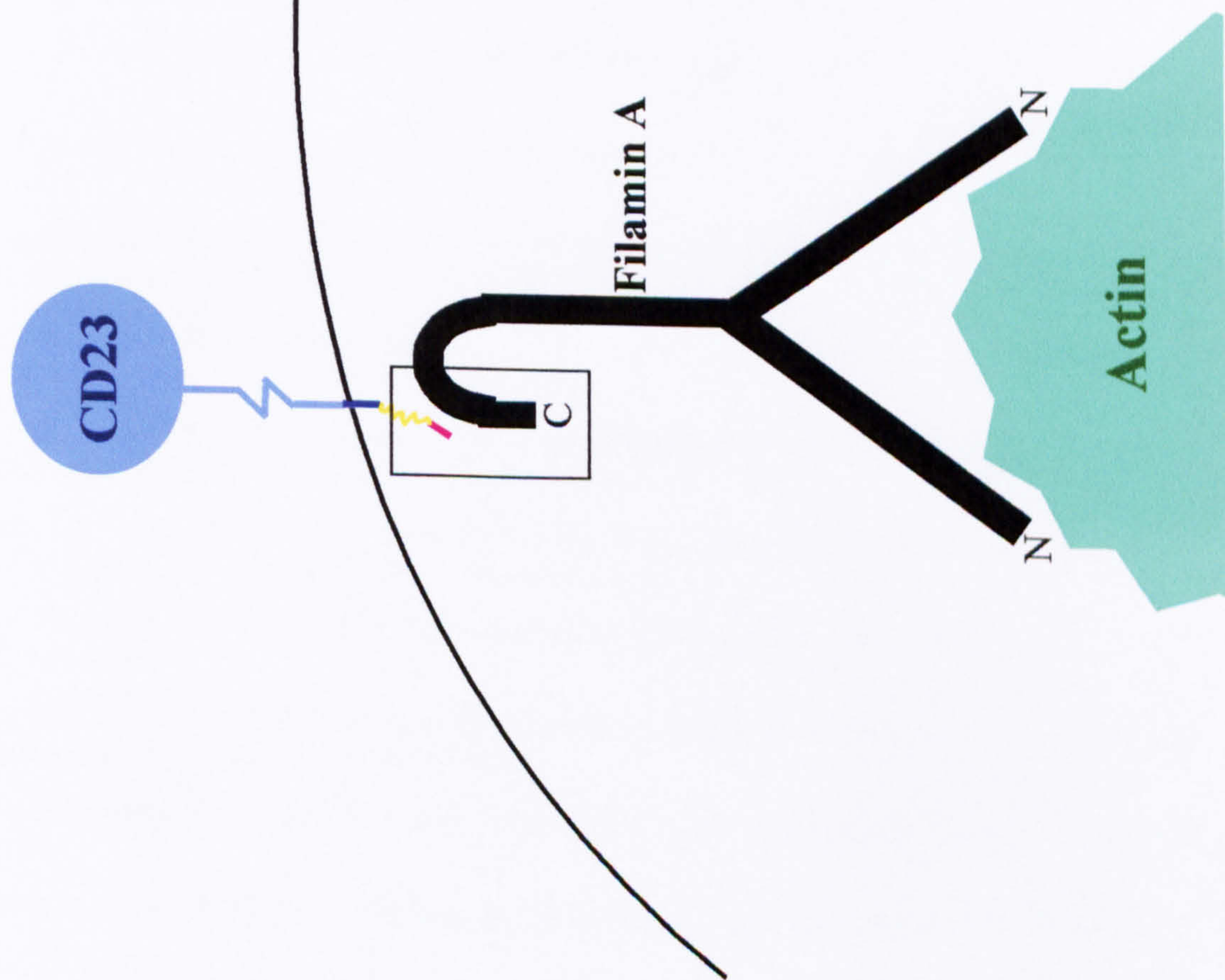
This research has effectively proven the validity of the yeast two-hybrid system for the identification of protein interactions at the N-terminal cytoplasmic tail of CD23. Whilst the results discussed provide an appetiser for what must yet remain to be discovered, the project has opened many potential avenues for investigation that should be exploited in future studies, hopefully providing more crucial information helping to elucidate how the two human CD23 isoforms function.



## **FIGURE 6.1 PROPOSED MODEL FOR THE CD23-FILAMIN INTERACTION**

This schematic diagram illustrates a proposed model showing the potential method of downstream activation after the cytoplasmic N-terminal tail of CD23 binds to the C-terminus of filamin A. The box focuses in on the area of protein-protein interaction, with the key highlighting the areas of importance.







## REFERENCE LIST



- Agatep R., Kirkpatrick R.D., *et al.* (1998) Transformation of *Saccharomyces cerevisiae* by the lithium acetate/single stranded carrier DNA/polyethylene glycol (LiAc/ss-DNA/PEG) protocol. *Technical Tips Online*
- Agematsu K., Nagumo H., *et al.* (1998) Generation of plasma cells from peripheral blood memory B cells: synergistic effect of IL-10 and CD27/CD70 interaction. *Blood* 91, 173-180.
- Aho S., Arffman A., *et al.* (1997) A novel reporter gene MEL1 for the yeast two-hybrid system. *Anal. Biochem.* 253, 270-272.
- Akiba H., Nakano H., *et al.* (1998) CD27, a member of the TNF-R superfamily, activates NF- $\kappa$ B and SAPK/JNK via TRAF2, TRAF5 and NIK. *J. Biol. Chem.* 273, 13353-13358.
- Allen J.B., Walberg M.W., *et al.* (1995) Finding prospective partners in the library - the two-hybrid system and phage display find a match. *TIBS* 20, 511-516.
- Amakawa R., Hakem A., *et al.* (1996) Impaired negative selection of T cells in Hodgkin's disease antigen CD30-deficient mice. *Cell* 84, 551-562.
- Anderson M.K., Hernandez-Hoyos G. *et al.* (1999) Precise developmental regulation of Ets family transcription factors during specification and commitment to the T cell lineage. *Genes in Development* 12, 3131-3148.
- Andrews R.K. and Fox J.E. (1991) Interaction of purified actin-binding protein with the platelet membrane glycoprotein Ib-IX complex. *J. Biol. Chem.* 266, 7144-7147.
- Andrews R.K. and Fox J.E. (1992) Identification of a region in the cytoplasmic domain of the platelet membrane glycoprotein Ib-IX complex that binds to purified actin-binding protein. *J. Biol. Chem.* 267, 18605-18611.
- Ansieau S., Scheffrahn I., Mosialos G., *et al.* (1996) TRAF-1, TRAF-2 and TRAF-3 interact in vivo with the CD30 cytoplasmic domain: TRAF-2 mediates CD30-induced NF- $\kappa$ B activation. *PNAS (USA)* 93, 14053-14058.
- Arch R.H., Gedrich R.W. and Thompson C.B. (1998) TRAFs - a family of adapter proteins that regulates life and death. *Genes in Development* 12, 2821-2830.
- Armitage R., Goff L.K. and Beverly P.C. (1989) Expression and functional role of CD23 on T cells. *Eur. J. Immunol.* 19, 31-35.
- Arpin C., Dechanet J., van Kooten C., *et al.* (1995) Generation of memory B cells and plasma cells in vitro. *Science* 268, 720-22.
- Arroyo A.G., Yang J.T., Rayburn H. and Hynes R.O. (1996) Differential requirements for  $\alpha$ 4 integrins during fetal and adult hematopoiesis. *Cell* 85, 997-1008.
- Aubry J.P., Pochon S., *et al.* (1992) CD21 is a ligand for CD23 and regulates IgE production. *Nature (Letters to)* 358, 505-507.
- Aubry J.P., Pochon S., *et al.* (1994) CD23 interacts with a new functional extracytoplasmic domain involving N-linked oligosaccharides on CD21. *J. Immunol.* 152, 5806-5813.
- Bacon K., Gauchat J.F., *et al.* (1993) CD21 expressed on basophilic cells is involved in histamine release triggered by CD23 and anti-CD21 antibody. *Eur. J. Immunol.* 23, 2721
- Baeuerle P.A. and Henkel T. (1994) Function and activation of NF-kappa B in the immune system. *Annu. Rev. Immunol.* 12, 141-179.
- Bain G., Maandag E.C., *et al.* (1994) E2A proteins are required for proper B cell development and initiation of immunoglobulin gene rearrangements. *Cell* 79, 885-892.
- Bain G., Robanus Maandag E.C., *et al.* (1997) Both E12 and E47 allow commitment to the B cell lineage. *Immunity* 6, 145-154.
- Banchereau J., Bazan F. *et al.* (1994) The CD40 antigen and its ligand. *Annu. Rev. Immunol.* 12, 881-922.



- Bansal A.S., Roberts T. and *et al.* (1992) Soluble CD23 levels are elevated in the serum of patients with primary Sjogrens syndrome and systemic lupus erythematosus. *Clin. Expt. Immunol.* 89, 452-455.
- Bansal A.S., MacGregor A.J., *et al* (1994) Increased levels of sCD23 in rheumatoid arthritis are related to disease status. *Clin. Expt. Rheu.* 12, 281-285.
- Barberis A., Windenhorn K., *et al* (1990) A novel B-cell lineage-specific transcription factor present at early but not late stages of differentiation. *Genes in Development* 4, 849-859.
- Barlowe C. (1997) Coupled ER to Golgi transport reconstituted with purified cytosolic proteins. *J. Cell Biol.* 139, 1097-1108.
- Barrett T., Shu G. and Clark E. (1991) CD40 signaling activities CD11a/CD18 (LFA1)-mediated adhesion in B cells. *J. Immunol.* 146, 1722-30.
- Bartel P.L., Chein C.T., *et al* (1993) Elimination of false positives that arise in using the two-hybrid system. *Biotechniques* 14, 920-924.
- Bartlett W.C., Kelly A.E., *et al* (1995) Analysis of murine soluble FcεRII sites of cleavage and requirements for dual-affinity interaction with IgE. *J. Immunol.* 154, 4240-4246.
- Batten M., Groom J., *et al* (2000) BAFF mediates survival of peripheral immature B lymphocytes. *J. Exp. Med* 192, 1453-1466.
- Beavil A.J., Edmeades R.L., *et al.* (1992) alpha-helical coiled-coil stalks in the low affinity receptor for IgE (FcεRII/CD23) and related C-type lectins. *PNAS (USA)* 89, 753-757.
- Beavil A.J., Graber P., *et al* (1995) CD23/FcεRII and its soluble fragments can form oligomers on the cell surface and in solution. *Immunology* 84, 202-206.
- Beck K.A. and Keen J.H. (1991) Interaction of phosphoinositide cycle intermediates with the plasma membrane-associated clathrin assembly protein AP-2. *J. Biol. Chem.* 266, 4442-4447.
- Beguin Y., Lampertz S., *et al* (1993) Soluble CD23 and other receptors (CD4, CD8, CD25, CD71) in serum of patients with chronic lymphocytic leukaemia. *Leukaemia* 7, 2019
- Behrens J. and von Kries J.P., *et al.* (1996) Functional interaction of β-catenin with the transcription factor LEF-1. *Nature* 382, 638-642.
- Bellanger J.M., Astier C., *et al.* (2000) The Rac1- and RhoG-specific GEF domain of Trio targets filamin to remodel cytoskeletal actin. *Nat. Cell Biol.* 2, 888-892.
- Berberich I., Shu G. and Clark E. (1994) Cross-linking CD40 on B cells rapidly activates nuclear factor-kappa B. *J. Immunol.* 153, 4357-66.
- Berberich I., Shu G., *et al.* (1996) Cross linking CD40 on B cells preferentially induces stress-activated protein kinases. *EMBO J.* 15, 92-101.
- Bertho J.M., Fourcade C., *et al.* (1991) Synergistic effect of interleukin 1 and soluble CD23 on the growth of human CD4+ bone marrow-derived T cells. *Eur. J. Immunol.* 21, 1073-1076.
- Bettler B., Maier R., *et al.* (1989) Molecular structure and expression of the murine lymphocyte low affinity receptor for IgE (Fc epsilon RII). *PNAS (USA)* 86, 7118-7122.
- Bieber T., Rieger A., *et al.* (1989) Induction of Fc epsilon R2/CD23 on human epidermal Langerhans cells by human recombinant interleukin 4 and gamma interferon. *J. Exp. Med* 170, 309-314.
- Billaud M., Buisson P., *et al.* (1989) Epstein-Barr virus (EBV)-containing nasopharyngeal carcinoma cells express the B-cell activator antigen blast2/CD23 and low levels of the EBV receptor CR2. *J. Virology* 63, 4121-4128.
- Billian G., Mondiere P., *et al.* (1997) Antigen receptor induced apoptosis of human germinal center B cells is targeted to a centrocytic subset. *Eur. J. Immunol.* 27, 405-17.
- Bishop A. and Hall A. (2000) Rho GT Pases and their effect on proteins. *Biochem. J.* 348, 241-255.



- Bishop G.A. and Haughton G. (1986) Induced differentiation of a transformed clone of Ly-1<sup>+</sup> B cells by clonal T cells and antigen. *PNAS(USA)* 83, 7410-7414.
- Bishop G.A. and Haughton G. (1986) Role of the LFA-1 molecule in B cell differentiation. *Curr. Top. Microbiol. Immunol.* 132, 142-147.
- Bishop G.A., Warren W.D. and Berton M.T. (1995) Signalling via MHC class II molecules and antigen receptors enhances the B cell response to gp39/CD40 ligand. *Eur. J. Immunol.* 25, 1230-1238.
- Bishop G.A. and Hostager B.S. (2001) Molecular mechanisms of CD40 signalling. *Arch. Immunol. Ther. Exp. in press*
- Blobel G. and Dobberstein B. (1975) Transfer of proteins across membranes. *J. Cell Biol.* 67, 835-851.
- Bobbitt K.R. and Justement L.B. (2000) Regulation of MHC class II signal transduction by the B cell coreceptors CD19 and CD22. *J. Immunol.* 165, 5588-5596.
- Boll W., Ohno H. and Songyang Z., *et al.* (1996) Sequence requirements for the recognition of tyrosine based endocytic signals by clathrin AP-2 complexes. *EMBO J.* 15, 5789-5795.
- Bonnefoy J.-Y., Gauchat J.F., *et al.* (1995) Regulation of IgE synthesis by CD23/CD21 interaction. *Int. Arch. Allergy. Immunol.* 107, 40-42.
- Bonnefoy J.Y., Aubry J.P., *et al.* (1987) Production and characterisation of a monoclonal antibody specific for the human lymphocyte low affinity receptor for IgE: CD23 is a low affinity receptor for IgE. *J. Immunol.* 138, 2970-2978.
- Bonnefoy J.Y., Guillot O., *et al.* (1988) The low-affinity receptor for IgE (CD23) on B lymphocytes is spatially associated with HLA-DR antigens. *J. Exp. Med* 167, 57
- Bonnefoy J.Y., Lecoanet-Hanchoz S., *et al.* (1997) Structure and Functions of CD23. *Int. Rev. Immunol.* 16, 113-128.
- Borson N.D., Sato W.L. and Drewes L.R. (1992) A lock-docking oligo(dT) primer for 5' and 3' RACE PCR. *PCR Methods Appl.* 2, 144-148.
- Bradbury L.E., Kanas G.S., *et al.* (1992) The CD19/CD21 signal transducing complex of human B lymphocytes includes the target of antiproliferative antibody-1 and Leu-13 molecules. *J. Immunol.* 149, 2841-2850.
- Brennwald P., Kearns B., *et al.* (1994) Sec9 is a SNAP-25-like component of a yeast SNARE complex that may be the effector of Sec4 function in exocytosis. *Cell* 79, 245-258.
- Brent R. and Ptashne M. (1985) A eukaryotic transcriptional activator bearing the DNA specificity of a prokaryotic repressor. *Cell* 43, 729-736.
- Brodksy F.M. (1997) New fashions in vesicle coats. *Trends Cell Biology* 7, 175-179.
- Bröcker F., Bardenheuer W., *et al.* (1999) Assignment of human filamin gene FLNB to human chromosome band 3p14.3 and identification of YACs containing the complete FLNB transcribed region, Cytogenet. *Cell Genetics* 85, 267-268.
- Burlinson E.L., Graber P., *et al.* (1996) Soluble CD40 ligand induces expression of CD25 and CD23 in resting human tonsillar B lymphocytes. *Eur. J. Immunol.* 26, 1069-1073.
- Burrows B., Martinez F.D. *et al.* (1989) Association of asthma with serum IgE levels and skin-test reactivity to allergens. *New England J. Medicine* 320, 271-277.
- Calderhead D.M., Kosaka Y., *et al.* (2000) CD40-CD154 interactions in B-cell signalling. *Curr. Top. Microbiol. Immunol.* 245, 73-99.
- Calderwood D., Shattil S. and Ginsberg M. (2000) Integrins and actin filaments: reciprocal regulation of cell adhesion and signaling. *J. Biol. Chem.* 275, 22607-22610.
- Candeias S., Muegge K. and Durum S. (1997) IL-7 receptor and VDJ recombination: tropic versus mechanistic actions. *Immunity* 6, 501-8.



- Capron A. and Dessaint J.P. (1986) From parasites to allergy: A second receptor for IgE. *Immunol. Today* 7, 15-18.
- Capron M., Jauault T., *et al* (1986) Functional study of a monoclonal antibody to IgE Fc receptor (Fc epsilon R2) of eosinophils, platelets and macrophages. *J. Exp. Med* 164, 72-89.
- Carson D.A., Kulczycki A.Jr. and Metzger H. (1975) Interaction of IgE with rat basophilic leukemia cells III Release of intact receptors on cell-free particles. *J. Immunol.* 114, 158
- Cerutti A., Schaffer A., *et al.* (1998) CD30 is a CD40-inducible molecule that negatively regulates CD40-mediated Ig class switching in non-antigen selected human B cells. *Immunity* 9, 247-256.
- Cerutti A., Schaffer A., *et al.* (2000) Engagement of CD153 by CD30<sup>+</sup> T cells inhibits class switch DNA recombination and antibody production in human IgD<sup>+</sup> IgM<sup>+</sup> B cells. *J. Immunol.* 165, 786-794.
- Chakarova C., Wehnert M.S., *et al.* (2000) Genomic structure and fine mapping of the two human filamin gene paralogues FLNB and FLNC and comparative analysis of the filamin gene family. *Hum. Genet.* 107, 597-611.
- Chen M. and Stracher A. (1989) In situ phosphorylation of platelet actin-binding protein by cAMP-dependent protein kinase stabilizes it against proteolysis by calpain. *J. Biol. Chem* 264, 14282-14289.
- Chen W.J., Goldstein J.L. and Brown M.S. (1990) NPXY, a sequence often found in cytoplasmic tails, is required for coated pit-mediated internalization of the low density lipoprotein receptor. *J. Biol. Chem* 265, 3116-3123.
- Chenchik A., Diatchenko L., *et al.* (1994) Great Lengths TM cDNA synthesis kit for high yields of full length cDNA. *CLONTECHniques* IX, 9-12.
- Cheng A.M., Rowley B., *et al.* (1995) Syk tyrosine kinase is required for mouse viability and B-cell development. *Nature* 378, 303-306.
- Chessels J.M. (2000) Recent advances in management of acute leukaemia. *Arch. Dis. Child* 82, 438-442.
- Chien C.T., Bartel P.I., *et al.* (1991) The two-hybrid system: a method to identify and clone genes for proteins that interact with a protein of interest. *PNAS (USA)* 88, 9578-9582.
- Choe J., Kim H.S., *et al.* (1996) Cellular and molecular factors that regulate the differentiation and apoptosis of germinal center B cells. Anti-Ig down-regulates Fas expression of CD40 ligand-stimulated germinal center B cells and inhibits Fas-mediated apoptosis. *J. Immunol.* 157, 1006-16.
- Choi M., Brines R., *et al.* (1994) Induction of NF-AT in normal B lymphocytes by anti-Ig or CD40 ligand in conjunction with IL-4. *Immunity* 1,
- Clevers H., Alarcon B., *et al.* (1988) The T cell receptor/CD3 complex: a dynamic protein ensemble. *Annu.Rev.Immunol.* 6, 629
- Conrad D.H. and Froese A. (1976) Characterisation of the target cell receptor IgE II Polyacrylamide gel analysis of the surface IgE receptor from normal rat mast cells and from rat basophilic leukemia cells. *J. Immunol.* 116, 319-326.
- Constant S.L. (1999) B lymphocytes as APC for CD4<sup>+</sup> T cell priming. *J. Immunol.* 162, 5695-5703.
- Corbi A.L., Kishimoto T., *et al.* (1988) The human leukocyte adhesion glycoprotein Mac-1 (Complement receptor type 3, CD11b) alpha subunit. Cloning, primary structure, and relation to integrins, von Willebrand factor and factor B. *J. Biol. Chem.* 263, 12403-12411.
- Cornall R.J., Goodnow C.C. and Cyster J.G. (2000) Regulation of B cell antigen receptor signalling by the Lyn/CD22/SHP1 pathway. *Curr. Top. Microbiol. Immunol.* 244, 57-68.
- Cowles C.R., Odorizzi G., *et al.* (1997) The AP-3 adaptor complex is essential for cargo-selective transport to the yeast vacuole. *Cell* 91, 109-118.
- Cresswell P. (1994) Assembly, transport and function of MHC class II molecules. *Annu. Rev. Immunology* 12, 259-293.



- Cutrona G., Dono M., *et al.* (1997) The propensity to apoptosis of centrocytes and centroblasts correlates with elevated levels of intracellular myc protein. *Eur. J. Immunol.* **27**, 234-38.
- Dang C.V., Barrett J., *et al.* (1991) Intracellular leucine zipper interactions suggest c-Myc hetero-oligomerization. *Mol. Cell. Biol.* **11**, 954-962.
- Dautry-Varsat A., Ciechanover A. and Lodish H. (1983) pH and the recycling of transferrin during receptor-mediated endocytosis. *PNAS (USA)* **80**, 2258-2262.
- Davis C.G., van Driel I.R., *et al.* (1987) The low density lipoprotein receptor. Identification of amino acids in the cytoplasmic domain required for rapid endocytosis. *J. Biol. Chem* **262**, 4075-4082.
- DeBenedette M.A., Wen T., *et al.* (1999) Analysis of 4-1BBL-deficient mice and of mice lacking both 4-1BBL and CD28 reveals a role for 4-1BBL in skin allograft rejection and in the cytotoxic T cell response to influenza virus. *J. Immunol.* **163**, 4833-4841.
- Declayre A.X., Salas F., *et al.* (1991) EBV/complement C3d receptor is an interferon alpha receptor. *EMBO J.* **10**, 919-926.
- Defrance T., Aubry J.P., *et al.* (1987) Human recombinant interleukin-4 induces Fc epsilon receptors (CD23) on normal human B lymphocytes. *J. Exp. Med* **165**, 1459-1467.
- DeKoter R.P. and Singh H. (2000) Regulation of B lymphocyte and macrophage development by graded expression of PU.1. *Science* **288**, 1439-1441.
- Delespesse G., Sarfati M., *et al.* (1992) The low affinity receptor for IgE. *Immunol. Rev.* **125**, 78
- Delespesse G., Sarfati M., *et al.* (1989) Human IgE binding factors. *Immunol. Today.* **10**, 159-164.
- Delespesse G., Suter U., *et al.* (1991) Expression, structure and function of the CD23 antigen. *Advan. Immunol.* **49**, 149-191.
- Dell'Angelica E.C., Ohno H., *et al.* (1997) AP-3: An adaptor-like protein complex with ubiquitous expression. *EMBO J.* **16**, 917-928.
- Desjardins M., Huber L.A., *et al.* (1994) Biogenesis of phagolysosomes proceeds through a sequential series of interactions with the endocytic apparatus. *J. Cell. Biol.* **124**, 677-688.
- Dierks S.E., Bartlett W.C., *et al.* (1993) The oligomeric nature of the murine Fc epsilon RII/CD23. Implications for function. *J. Immunol.* **150**, 2372-2382.
- Difilippantonio M.J., McMahan C.J., *et al.* (1996) RAG1 mediates signal sequence recognition and recruitment of RAG2 in V(D)J recombination. *Cell* **87**, 253-62.
- Dorshkind K. (1994) Transcriptional control points during lymphopoiesis. *Cell* **79**, 751-753.
- Drickamer K. (1988) Two distinct classes of carbohydrate-recognition domains in animal lectins. *J. Biol. Chem.* **263**, 9557-9560.
- Drickamer K. (1993) Ca<sup>2+</sup>-dependent carbohydrate-recognition domains in animal proteins. *Curr. Opin. Struct. Biol.* **3**, 393-400.
- Dugas B., Paul-Eugene N., *et al.* (1992) Possible role for CD23 in allergic diseases. *Res. Immunol.* **143**, 448-451.
- Eastman Q.M., Leu T.M. and Schatz D.G. (1996) Initiation of V(D)J recombination in vitro obeying the 12/23 rule. *Nature* **380**, 85-88.
- Elliot M.J., Maini R.N., *et al.* (1993) Arthritis Rheum. 36: 1681-1690. *Arthritis and Rheumatology* **36**, 1681-1690.
- Epstein J., Eichbaum Q., *et al.* (1996) The collectins in innate immunity. *Curr. Opin. Immunol.* **8**, 29-35.
- Ernst P. and Smale S.T. (1995) Combinatorial regulation of transcription. II. The immunoglobulin- $\mu$  heavy-chain gene. *Immunity* **2**, 427-38.
- Estojak J., Brent R. and Golemis E.A. (1995) Correlation of two-hybrid affinity data with *in vitro* measurements. *Mol. Cell. Biol.* **15**, 5820-5829.



- Ewart, M-A., Ozanne, B.W. and Cushley, W. (2002) The CD23a and CD23b Proximal Promoters Display Different Sensitivities to Exogenous B Lymphocyte Stimulation. *Genes & Immunity*, in press
- Ezekowitz R.A., Williams D.J., *et al.* (1991) Uptake of *Pneumocystis carinii* mediated by the macrophage mannose receptor. *Nature* **351**, 155-158.
- Fearon E.R., Finkel T. and Gillison M.L., *et al.* (1992) Karyoplastic interaction selection strategy: a general strategy to detect protein-protein interactions in mammalian cells. *PNAS (USA)* **89**, 7958-7962.
- Felding-Habermann B. and Cheresch D.A. (1993) Vitronectin and its receptors. *Curr. Opin. Cell. Biol.* **5**, 864-868.
- Ferguson S.E., Han S., *et al.* (1996) CD28 is required for germinal centre formation. *J. Immunol.* **156**, 4576-4581.
- Fields S. and Song O. (1989) A novel genetic system to detect protein -protein interactions. *Nature* **340**, 245-247.
- Flach J., Bossie M., *et al.* (1994) A yeast RNA-binding protein shuttles between the nucleus and the cytoplasm. *Mol. Cell. Biol.* **14**, 8399-8407.
- Flores-Romo L., Cairns J.A., *et al.* (1989) Soluble fragments of the low affinity IgE receptor (CD23) inhibit the spontaneous migration of U937 monocytic cells: neutralisation of MIF- activity by a CD23 antibody. *Immunology* **67**, 547
- Fourcade C. (1992) Expression of CD23 by human bone marrow stromal cells. *European Cytokine Network* **3**, 539-543.
- Fournier S., Delespesse G., *et al.* (1992) CD23 antigen regulation and signalling in chronic lymphocytic leukemia. *J. Clin. Invest.* **89**, 1312-1321.
- Fra A.M., Williamson E., *et al.* (1994) Detergent-insoluble glycolipid microdomains in lymphocytes in the absence of caveolae. *J. Biol. Chem.* **269**, 30745-30748.
- Fra A.M., Williamson E., *et al.* (1995) De novo formation of caveolae in lymphocytes by expression of VIP21-caveolin. *PNAS (USA)* **92**, 8655-8659.
- Fremaux-Bacchi V., Bernard I., *et al.* (1996) Human lymphocytes shed a soluble form of CD21 (the C3dg/Epstein Barr virus receptor CR2) that binds iC3b and CD23. *Eur. J. Immunol.* **26**, 1497
- Fremaux-Bacchi V., Fischer E., *et al.* (1998) Soluble CD21 (sCD21) forms biologically active complexes with CD23: CD21 is present in normal plasma as a complex with CD23 and inhibits soluble CD23-induced IgE synthesis by B cells. *Int. Immunol.* **10**, 1459-1466.
- Fujiwara H., Kikutani H., *et al.* (1994) The absence of IgE antibody-mediated augmentation of immune responses in CD23-deficient mice. *PNAS (USA)* **91**, 6835-6839.
- Galibert L., Burdin N., *et al.* (1996) Negative selection of human germinal center B cells by prolonged BCR cross linking. *J. Exp. Med* **183**, 2075-85.
- Gartner A., Nasmyth K. and Ammerer G. (1992) Signal transduction in *Saccharomyces cerevisiae* requires tyrosine and threonine phosphorylation of FUS3 and KSS1. *Gen. Dev.* **6**, 1280-1292.
- Gaullusser A. and Kirchhausen T. (1993) The beta 1 and beta 2 subunits of the AP complexes are the clathrin coat assembly components. *EMBO J.* **12**, 5237-5244.
- Gay D., Saunders T., *et al.* (1993) Receptor editing: an approach by autoreactive B cells to escape tolerance. *J. Exp. Med.* **177**, 999-1008.
- Georgopoulos K., Moore D.D. and Derfler B. (1992) Ikaros, an early lymphoid-specific transcription factor and a putative mediator for T cell commitment. *Science* **258**, 808-812.
- Georgopoulos K., Winandy S. and Avitahl N. (1997) The role of the Ikaros gene in lymphocyte development and homeostasis. *Ann. Rev. Immunol.* **15**, 155-176.
- Geuze H.J., Slot J.W., *et al.* (1983) Intracellular site of asialoglycoprotein receptor-ligand uncoupling: double-label immunoelectron microscopy during receptor-mediated endocytosis. *Cell* **32**, 277-287.



- Geuze H.J., Stoorvogel W., *et al.* (1988) Sorting of mannose 6-phosphate receptors and lysosomal membrane proteins in endocytic vesicles. *J. Cell. Biol.* 107, 2491-2501.
- Gietz R.D., Triggd-Raine B., *et al.* (1997) Identification of proteins that interact with a protein of interest: Applications of the yeast two-hybrid system. *Molecular and Cellular Biochemistry* 172, 67-79.
- Gladson C.L. and Cheresch D.A. (1994) *The alpha-v integrins*. CRC Press,
- Glickman J.A., Conibear E. and Pearse B.M.F. (1989) Specificity of binding of clathrin adaptors to signals on the mannose-6-phosphate/insulin-like growth factor II receptor. *EMBO J.* 8, 1041-1047.
- Gold M.R., Law D.A. and DeFranco A.L. (1990) Stimulation of protein tyrosine phosphorylation by the B-lymphocyte antigen receptor. *Nature* 345, 810
- Gold M.R., Matsuuchi L., *et al.* (1991) Tyrosine phosphorylation of components of the B-cell antigen receptors following receptor cross-linking. *PNAS (USA)* 88, 3436
- Goldfarb A.N. and Flores J.P., *et al.* (1996) Involvement of the E2A basic helix-loop-helix protein in immunoglobulin heavy chain class switching. *Mol. Immunol.* 33, 947-956.
- Goldstein J.L., Brown M.S., *et al.* (1995) Receptor-mediated endocytosis: concepts emerging from the LDL receptor system. *Annu. Rev. Cell Biol.* 1, 1-39.
- Golemis, E. A. False positives: a general view. 1995. (GENERIC)  
Ref Type: Internet Communication
- Golemis E.A. and Brent R. (1997) *Searching for interacting proteins with the Two-Hybrid system III. In: The Yeast Two-Hybrid system*. Oxford University Press,
- Gong S. and Nussenzweig M.C. (1996) Regulation of an early developmental checkpoint in the B cell pathway by Igb. *Science* 272, 411-414.
- Gonzalez-Monlina and Spiegelberg H.L. (1976) Binding of IgE myeloma proteins to human cultured lymphoblastoid cells. *J. Immunol.* 17, 1838-1845.
- Gonzalez-Monlina A. and Spiegelberg H.L. (1977) A subpopulation of normal human peripheral B lymphocytes that bind IgE. *J. Clin. Invest.* 59, 616-623.
- Goodman O.B., Krupnick J.G., *et al.* (1996) Beta-arrestin acts as a clathrin adaptor in endocytosis of the beta2-adrenergic receptor. *Nature* 383, 447-450.
- Gordon J., Rowe M., *et al.* (1986) Ligation of the CD23, p45 (BLAST-2, EBVCS) antigen triggers the cell cycle progression of activated B lymphocytes. *Eur. J. Immunol.* 16, 1075-1080.
- Gordon J. and Webb A.J. (1987) Triggering of B lymphocytes through CD23: epitope mapping and studies using antibody derivatives indicate an allosteric mechanism of signalling. *Immunology* 60, 517-521.
- Gorlin J.B., Yamin R., *et al.* (1990) Human endothelial actin-binding protein (ABP, non-muscle filamin): a molecular leaf spring. *J. Cell. Biol.* 111, 1089-1105.
- Gorlin J.B. and *et al.* (1993) Actin-binding protein (ABP-280) filamin gene (FLN) maps telomeric to the colour vision locus (R/CGP) and centromeric to G6PD in Xq28. *Genomics* 17, 496-498.
- Gorodinsky A. and Harris D.A. (1995) Glycolipid-anchored proteins in neuroblastoma cells form detergent-resistant complexes without caveolin. *J. Cell. Biol.* 129, 619-627.
- Gravestien L.A., Amsen D., *et al.* (1998) The TNF-R family member CD27 signals to JNK via TRAF2. *Eur. J. Immunol.* 28, 2208-2216.
- Grawunder U., Leu T.M., *et al.* (1995) Downregulation of RAG1 and RAG2 gene expression in preB cells after functional immunoglobulin heavy chain rearrangement. *Immunity* 3, 601-608.
- Greaves M. (1999) Molecular genetics, natural history and the demise of childhood leukaemia. *Eur. J. Cancer* 35, 1941-1953.
- Greenberg S., Chang P. and Silverstein S.C. (1993) Tyrosine phosphorylation is required for Fc receptor-mediated phagocytosis in mouse macrophages. *J. Exp. Med.* 177, 529-534.



- Greenberg S. (1995) Signal transduction of phagocytosis. *Trends Cell Biology* 5, 93-99.
- Greenberg S., Chang P., *et al.* (1996) Clustered syk tyrosine kinase domains trigger phagocytosis. *PNAS (USA)* 93, 1103-1107.
- Griffiths G. and Simons K. (1986) The trans Golgi network: Sorting at the exit site of the Golgi complex. *Science* 234, 438-443.
- Griffiths G., Back R. and Marsh M. (1989) A quantitative analysis of the endocytic pathway in baby hamster kidney cells. *J. Cell. Biol.* 109, 2703-2720.
- Grillot D.A., Merino R., *et al.* (1996) bcl-x exhibits regulated expression during B cell development and activation and modulates lymphocyte survival in transgenic mice. *J. Exp. Med* 183, 381-391.
- Grosjean I., Lachaux A., *et al.* (1994) CD23/CD21 interaction is required for presentation of soluble protein antigen by lymphoblastoid B cell lines to specific CD4+ T cell clones. *Eur. J. Immunol.* 24, 2982-2986.
- Grouard G., de Bouteiller O., *et al.* (1995) Human follicular dendritic cells enhance cytokine-dependent growth and differentiation of CD40 activated B cells. *J. Immunol.* 155, 3345-52.
- Guarente L. (1993) Strategies for the identification of interacting proteins. *PNAS (USA)* 90, 1639-1641.
- Gustavsson S., Hjulstrom S., *et al.* (1994) CD23 /IgE-mediated regulation of the specific antibody response in vivo. *J. Immunol.* 152, 4793-4800.
- Hagman J., Belanger C., *et al.* (1993) Cloning and functional characterisation of early B-cell factor, a regulator of lymphocyte-specific gene expression. *Genes. Dev.* 7, 760-773.
- Hahm K., Ernst P., *et al.* (1994) The lymphoid transcription factor LyF-1 is encoded by specific, alternatively spliced mRNAs derived from the Ikaros gene. *Mol. Cell. Biol.* 14, 7111-7123.
- Hahne M., Kataoka T., *et al.* (1998) APRIL, a new ligand of the TNF family, stimulates tumour cell growth. *J. Exp. Med* 188, 1185-1190.
- Han S., Hathcock K., *et al.* (1995) Cellular interaction in germinal centres. Roles of CD40 ligand and B7-2 in established germinal centres. *J. Immunol.* 155, 556-567.
- Han S., Zheng B., *et al.* (1995) In situ studies of the primary immune response to (4-hydroxy-3-nitrophenyl)acetyl. IV. Affinity-dependent, antigen-driven B cell apoptosis in germinal centers as a mechanism for maintaining self-tolerance. *J. Exp. Med.* 182, 1635-44.
- Han S., Zheng B., *et al.* (1996) Neoteny in lymphocytes: Rag1 and Rag2 expression in germinal center B cells. *Science* 274, 2094-97.
- Harding C.V. and Geuze H.J. (1992) Class II MHC molecules are present in macrophage lysosomes and phagolysosomes that function in the phagocytic processing of *Listeria monocytogenes* for presentation to T cells. *J. Cell Biol.* 119, 531-542.
- Hardy R.R., Carmack C.E., *et al.* (1991) Resolution and characterisation of pro-B and pre-pro-B cell stages in normal mouse bone marrow. *J. Exp. Med* 173, 1213-1225.
- Harlow E. and Lane D. (1988) *Antibodies: A laboratory manual*.
- Harper J.W., Adami G.R., *et al.* (1993) The p21 Cdk-interacting protein Cipl is a potent inhibitor of G1 cyclin-dependent kinases. *Cell* 75, 805-816.
- Harrison P.T., Davis W., *et al.* (1994) Binding of monomeric immunoglobulin G triggers Fc gamma RI-mediated endocytosis. *J. Biol. Chem.* 269, 24396-24402.
- Harter C. and Mellman I. (1992) Transport of the lysosomal membrane glycoprotein-Igp120 (Igp-A) to lysosomes does not require appearance on the plasma membrane. *J. Cell Biol.* 117, 311-325.
- Harton J.A., Van Hagen A.E. and Bishop G.A. (1995) The cytoplasmic and transmembrane domains of MHC class II b chains deliver distinct signals required for MHC class II-mediated B cell activation. *Immunity* 5, 349-358.
- Heilker R., Manning-Krieg U., *et al.* (1996) In-vitro binding of clathrin adaptors to sorting signals correlates with endocytosis and basolateral sorting. *EMBO J.* 15, 2893-2899.



- Heilker R., Spiess M. and Crottet P. (1999) Recognition of sorting signals by clathrin adaptors. *BioEssays* **21**, 558-567.
- Helenius A., Mellman I., *et al.* (1983) Endosomes. *TIBS* **8**, 245-250.
- Hellen E.A., Rowlands D.C., *et al.* (1991) Immunohistochemical demonstration of CD23 expression on lymphocytes in rheumatoid synovitis. *J. Clin. Path.* **44**, 293-296.
- Henderson A. and Calame K. (1998) Transcriptional regulation during B cell development. *Annu. Rev. Immunol.* **16**, 163-200.
- Henderson A.J. and Calame K.L. (1995) Lessons in transcriptional regulation learned from studies on immunoglobulin genes. *Crit. Rev. Eukaryot. Gene Exp.* **5**, 255-80.
- Hermann P., Armant M., *et al.* (1999) The vitronectin receptor and its associated Cd47 molecule mediates proinflammatory cytokine synthesis in human monocytes by interaction with soluble CD23. *J. Cell. Biol.* **144**, 767-775.
- Heyman B. and Liu T., *et al.* (1993) In vivo enhancement of the specific antibody response via the low affinity receptor for IgE. *Eur. J. Immunol.* **23**, 1739
- Hibbs M.L., Tarlinton D.M., *et al.* (1995) Multiple defects in the immune system of Lyn-deficient mice, culminating in autoimmune disease. *Cell* **83**, 301-311.
- Hintzen R.Q., de Jong R., *et al.* (1993) Regulation of CD27 expression on subsets of mature T-lymphocytes. *J. Immunol.* **151**, 2426-2435.
- Holder M.J., Wang H., *et al.* (1993) Suppression of apoptosis in normal and neoplastic human B lymphocytes by CD40 ligand is independent of Bcl-2 induction. *Eur. J. Immunol.* **23**, 2368-2371.
- Holland J. and Owens T. (1997) Signalling through ICAM-1 in a B cell lymphoma line. *J. Biol. Chem.* **272**, 9108-9112.
- Holstein S.E., Drucker M. and Robinson D.G. (1994) Identification of a beta-type adaptin in plant clathrin-coated vesicles. *J. Cell Sci.* **107**, 945-953.
- Hunziker C. and Geuze H.T. (1996) Intracellular trafficking of lysosomal membrane proteins. *BioEssays* **18**, 379-389.
- Ikeda K., Sannoh T., *et al.* (1987) Serum lectin with known structure activates complement through the classical pathway. *J. Biol. Chem.* **262**, 7451-7454.
- Ikizawa K., Yanagihara Y., *et al.* (1993) Possible role of CD5+ B cells expressing CD23 in mediating the elevation of serum-soluble CD23 in patients with Rheumatoid arthritis. *Int. Arch. of Allergy & Immunol.* **101**, 416-424.
- Indik Z.K., Pan X.Q., *et al.* (1994) Insertion of cytoplasmic tyrosine sequences into non-phagocytic receptor FcγIIb establishes phagocytic functions. *Blood* **83**, 2072-2780.
- Isberg R.R. and Tran Van Nhien G. (1994) Binding and internalization of microorganisms by integrin receptors. *Trends Microbiology* **2**, 10-14.
- Ishida T., Kobayashi N., *et al.* (1995) CD40 signaling-mediated induction of Bcl-XL, Cdk4, and Cdk6. Implication of their cooperation in selective B cell growth. *J. Immunol.* **155**, 5527-35.
- Jacquot S., Kobata T., *et al.* (1997) CD154/CD40 and CD70/CD27 interactions have different and sequential functions in T-cell-dependent B cell responses. *J. Immunol.* **159**, 2652-2657.
- James P., Halladay J. and Craig E.A. (1996) Genomic libraries and a host strain designed for highly efficient two-hybrid selection in yeast. *Genetics* **144**, 1425-1436.
- Janeway C.A. and Travers P. (1997) *Immunobiology -The immune system in health and disease*. Churchill Livingstone.
- Jay D., Garcia E.J., *et al.* (2000) Determination of a cAMP -dependant protein kinase phosphorylation site in the C-terminal region of human endothelial actin-binding protein. *Arch. Biochem. Biophys* **377**, 80-84.



- Jing S., Spencer T., *et al.* (1990) Role of human transferrin receptor cytoplasmic domain in endocytosis: localisation of a specific signal sequence for internalisation. *J. Cell Biol.* 110, 283-294.
- Kaiserlian D., Lachaux A., *et al.* (1993) Intestinal epithelial cells express the CD23/Fc epsilon RII molecule: enhanced expression in enteropathies. *Immunology* 80, 90-95.
- Kalberer C.P., Reininger L., *et al.* (1997) Priming of helper T cell-dependent antibody responses by HA-transgenic B cells. *Eur. J. Immunol.* 27, 2400-2407.
- Karagiannis S.N., Warrack J.K., *et al.* (2001) Endocytosis and recycling of the complex between CD23 and HLA-DR in human B cells. *Immunol.* 103, 319-331.
- Karasuyama H., Rolink A., *et al.* (1994) The expression of vpre-B/lambda 5 surrogate light chain in early bone marrow precursor B cells of normal and B cell-deficient mutant mice. *Cell* 77, 133-143.
- Kawamoto S. and Hidaka H. (1984)  $Ca^{2+}$  activated phospholipid-dependant protein kinase catalyzes the phosphorylation of actin-binding proteins. *Biochem. Biophys. Res. Commun.* 118, 736-742.
- Kawano M.M., Mihara K., *et al.* (1995) Differentiation of early plasma cells on bone marrow stromal cells requires interleukin-6 for escaping from apoptosis. *Blood* 85, 487-94.
- Keegan L., Gill G. and Ptashne M. (1986) Separation of DNA binding from the transcription-activating function of a eukaryotic regulatory protein. *Science* 231, 699-704.
- Kehry M.R. and Yamashita L.C. (1989) Low affinity IgE receptor (CD23) function on mouse B cells: role in IgE-dependent antigen focusing. *PNAS (USA)* 86, 7556
- Kelsoe G. (1995) *In situ* studies of the germinal center reaction. *Adv. Immunol.* 60, 267-288.
- Kelsoe G. (1996) Life and death in germinal centres (redux). *Immunity* 4, 107-111.
- Kelsoe G. (1996) The germinal center: a crucible for lymphocyte selection. *Semin, Immunol.* 8, 179-84.
- Kennedy M.K., Mohler K.M., *et al.* (1994) Induction of B cell costimulatory function by recombinant murine CD40 ligand. *Eur. J. Immunol.* 24, 116-23.
- Kielian M.C. and Cohn Z.A. (1980) Phagosome-lysosome fusion: characterization of intracellular membrane fusion in mouse macrophages. *J. Cell Biol.* 85, 754-765.
- Kijimoto-Ochiai S. and Noguchi A. (2000) Two peptides from CD23, including the inverse RGD sequence and its related peptide interact with the MHC class II molecule. *Biochem. & Biophys. Res. Comm.* 267, 686-691.
- Kikutani H., Suemura M., *et al.* (1986) Fc epsilon receptor, a specific differentiation marker transiently expressed on mature B cells before isotype switching. *J. Exp. Med.* 164, 1455
- Kintner C. and Sugden B. (1981) Identification of antigenic determinants unique to the surfaces of cells transformed by Epstein Barr virus. *Nature* 294, 458-460.
- Kirchhausen T. (1993) Coated pits and coated vesicles-sorting it all out. *Curr. Opin. Struct. Biol.* 3, 182-188.
- Kirchhausen T., Bonifacino J.S. and Riezman H. (1997) Linking cargo to vesicle formation: Receptor tail interactions with coat proteins. *Curr. Opin. Cell Biol.* 9, 495
- Kishihara K., Penninger J., *et al.* (1993) Normal B lymphocyte development but impaired T cell maturation in CD45-exon6 protein tyrosine phosphatase-deficient mice. *Cell* 74, 143-156.
- Kitamura D., Roes J., *et al.* (1991) A B-cell-deficient mouse by targeted disruption of the membrane exon of the immunoglobulin  $\mu$ -chain gene. *Nature* 350, 423-426.
- Kitamura D., Kudo A., Schaal S., Muller W., Melchers F. and Rajewsky K. (1992) A critical role of lambda 5 protein in B cell development. *Cell* 69, 823-831.
- Kitutani H., Suemura M., *et al.* (1986) Fc epsilon receptor, a specific differentiation marker transiently expressed on mature B cells before isotype switching. *J. Exp. Med.* 164, 1455-1469.
- Klausner R.D., van Renswoude J., *et al.* (1983) Receptor-mediated endocytosis of transferrin in K562 cells. *J. Biol. Chem.* 258, 4715-4724.



- Klemsz M., McKercher S.R., *et al.* (1990) The macrophage and B-cell specific transcription factor PU.1 is related to the ets oncogene. *Cell* 61, 113-124.
- Kolb J.P., Renard D., *et al.* (1990) Monoclonal anti-CD23 antibodies induce a rise in intracellular calcium and polyphosphoinositide hydrolysis in human activated B cells: involvement of a GP protein. *J. Immunol.* 145, 429-435.
- Koopman G., Keehan R.M., *et al.* (1997) Germinal center B cells rescued from apoptosis by CD40 ligation or attachment to follicular dendritic cells, but not by engagement of surface immunoglobulin or adhesion receptors, become resistant to CD95-induced apoptosis. *Eur. J. Immunol.* 27, 1-7.
- Korganow A., Ji H., Mangialaio S., *et al.* (1999) From systemic T cell self-reactivity to organ-specific autoimmune disease via immunoglobulins. *Immunity* 10, 451-461.
- Kumagais S., Ishida H., *et al.* (1989) Possible different mechanisms of B-cell activation in systemic lupus erythematosus and rheumatoid arthritis - opposite expression of low affinity receptor for IgE (CD23) on their peripheral B cells. *Clin. Exp. Immunol.* 78, 353
- Kumanogoh A., Watanabe C., *et al.* (2000) Identification of CD72 as a lymphocyte receptor for the class IV semaphorin CD100: a novel mechanism for regulating B cell signalling. *Immunity* 13, 621-631.
- Kunkel T.A. (1985) Rapid and efficient site-specific mutagenesis without phenotypic selection. *PNAS (USA)* 82, 488-492.
- Kuppers R., Hajadi M., *et al.* (1996) Molecular Ig gene analysis reveals that monocytoid B cell lymphoma is a malignancy of mature B cells carrying somatically mutated V region genes and suggests that rearrangement of the kappa-deleting element (resulting in deletion of the Ig kappa enhancers) abolishes somatic hypermutation in the human. *Eur. J. Immunol.* 26, 1794-1800.
- Kyburz D., Corr M., *et al.* (1999) Human rheumatoid factor production is dependent on CD40 signalling and autoantigen. *J. Immunol.* 163, 3116-3122.
- Laâbi Y. and Strasser A. (2000) Lymphocyte survival - ignorance is B<sub>Ly</sub>S. *Science* 289, 883-884.
- Laemmli U.K. (1970) Polyacrylamide gel electrophoresis. *Nature* 227, 680
- Lagresle C., Bella C., *et al.* (1995) Regulation of germinal center B cell differentiation. Role of the human APO-1/Fas (CD95) molecule. *J. Immunol.* 154, 5746-56.
- Laman J.D., Claassen E. and Noelle R.J. (1996) Functions of CD40 and its ligand, gp39 (CD40L). *Crit. Rev. Immunol.* 16, 59-108.
- Lang T., Hellio R., *et al.* (1994) *Leishmania donovani*-infected macrophages: characterization of the parasitophorous vacuole and potential role of this organelle in antigen presentation. *J. Cell Sci.* 107, 2137-2150.
- Lasky L.A. (1995) Selectin-carbohydrate interactions and the initiation of the inflammatory response. *Annu. Rev. Biochem.* 64, 113-139.
- Lebman D.A. and Cofman R.L. (1988) IL-4 causes isotype switching to IgE in T cell stimulated clonal B cell cultures. *J. Exp. Med.* 168, 853-862.
- Lebart M.C., Mejean C., *et al.* (1994) Characterization of the actin binding site on smooth muscle filamin. *J. Biol. Chem.* 269, 4279-4284.
- Lecoanet-Hanchoz S., Gauchat J.F., *et al.* (1995) CD23 regulates monocytes activation through a novel interaction with adhesion molecules CD11b-CD18 and CD11c-Cd18. *Immunity* 2, 1-20.
- Lee C.E., Yoon S.R. and Pyon K.H. (1993) IL-4 signals regulating CD23 gene expression in human B cells: protein kinase C independent signalling pathways. *Cell. Immunol.* 146, 171-185.
- Lee W.T., Rao M. and Conrad D.H. (1987) The murine lymphocyte receptor for IgE IV. The mechanism of ligand-specific receptor upregulation on B cells. *J. Immunol.* 139, 1191-1198.
- Leonardi A., Ellinger-Ziegelbauer H., *et al.* (2000) Physical and functional interaction of filamin (actin-binding protein-280) and tumour necrosis factor receptor associated factor 2. *J. Biol. Chem.* 275, 271-278.



- Letellier M., Nakajima T. and Delespesse G. (1988) IgE receptor on human lymphocytes IV Further analysis of its structure and of the role of N-linked carbohydrates. *J. Immunol.* **141**, 2374-2381.
- Letellier M., Sarfati M. and Delespesse G. (1989) Mechanisms of formation of IgE-binding factors (soluble CD23) - I FcεRII bearing B cells generate IgE-binding factors of different molecular weights. *Molecular Immunology* **26**, 1105-1112.
- Letellier M., Nakajima T., *et al.* (1990) Mechanisms of formation of human IgE-binding factors (soluble CD23): III- Evidence for a receptor FcεRII-associated proteolytic activity. *J. Exp. Med.* **172**, 693-700.
- Letourneur F. and Klausner R.D. (1992) A novel di-leucine motif and a tyrosine-based motif independently mediate lysosomal targeting and endocytosis of CD3 chains. *Cell* **69**, 1143-1157.
- Li B. and Fields S. (1993) Identification of mutations in p53 that affect its binding to SV40 large T antigen by using the yeast two-hybrid system. *FASEB J.* **7**, 957-963.
- Li M., Bermak J.C., *et al.* (2000) Modulation of dopamine D(2) receptor signaling by actin-binding protein (ABP-280). *Mol. Pharm.* **57**, 446-452.
- Li Y.S., Hayakawa K. and Hardy R.R. (1993) The regulated expression of B lineage associated genes during B cell differentiation in bone marrow and fetal liver. *J. Exp. Med* **178**, 951-60.
- Li Y.S., Wasserman R., *et al.* (1996) Identification of the earliest B lineage stage in mouse bone marrow. *Immunity* **5**, 527-535.
- Li Y.Y., Baccam M., *et al.* (1996) CD40 ligation results in protein kinase C-independent activation of ERK and JNK in resting murine splenic B cells. *J. Immunol.* **157**, 1440-47.
- Li Z., Dordai D.I., *et al.* (1996) A conserved degradation signal regulates RAG2 accumulation during cell division and links V(D)J recombination to the cell cycle. *Immunity* **5**, 575-589.
- Lim M.Y., Dailey D., *et al.* (1993) Yeast MCK1 protein kinase autophosphorylates at tyrosine and serine but phosphorylates exogenous substrates at serine and threonine. *J. Biol. Chem.* **268**, 21155-21164.
- Lin H. and Grosschedl R. (1995) Failure of B-cell differentiation in mice lacking the transcription factor EBF. *Nature* **376**, 263-267.
- Lin W.C. and Desiderio S. (1998) Regulation of V(D)J recombination activator protein RAG-2 by phosphorylation. *Science* **260**, 953-959.
- Liou H., Sha W.A., *et al.* (1994) Sequential induction of NF-kappa B/Rel family proteins during B-cell terminal differentiation. *Molecular and Cellular Biology* **14**, 5349-5359.
- Liu G., Thomas L., *et al.* (1997) Cytoskeletal protein ABP-280 directs the intracellular trafficking of furin and modulates pro-protein processing in the endocytic pathway. *J. Cell Biol.* **139**, 1719-1733.
- Liu Y.J., Cairns J.A., Holder M.J., Abbot S.D., Jansen K.U., Bonnefoy J.Y., Gordon J. and MacLennan I.C.M. (1991) Recombinant 25-kDa CD23 and interleukin 1α promote the survival of germinal centre B cells: Evidence for bifurcation in the development of centrocytes rescued from apoptosis. *Eur. J. Immunol.* **21**, 110-114.
- Liu Y.J., Malisan F., *et al.* (1996) Within germinal centres, isotype switching of immunoglobulin genes occurs after the onset of somatic mutation. *Immunity* **4**, 241-50.
- Liu Y.J., Arpin C., *et al.* (1996) Sequential triggering of apoptosis, somatic mutation and isotype switch during germinal center development. *Semin, Immunol.* **8**, 169-77.
- Liu Y.J., de Bouteiller O., *et al.* (1996) Normal human IgD + IgM - germinal center B cells can express up to 80 mutations in the variable region of their IgD transcripts. *Immunity* **4**, 603-13.
- Lobel P., Fujimoto K., *et al.* (1989) Mutations in the cytoplasmic domain of the 275kd mannose-6-phosphate receptor differentially alter lysosomal enzyme sorting and endocytosis. *Cell* **57**, 787-796.
- Loffert D., Eblich A., *et al.* (1996) Surrogate light chain expression is required to establish immunoglobulin heavy chain allelic exclusion during early B cell development. *Immunity* **4**, 133-144.



- Loo D.T., Kanner S.B. and Aruffo A. (1998) Filamin binds to the cytoplasmic domain of beta 1-integrin. Identification of amino acids responsible for this interaction. *J. Biol. Chem.* **273**, 23304-23312.
- Ludin C., Hofstetter H., *et al.* (1987) Cloning and expression of the cDNA coding for a human lymphocyte IgE receptor. *EMBO J.* **6**, 109-114.
- Luo H., Hofstetter H., Banchereau J. and Delespesse G. (1991) Cross-linking of CD23 antigen by its natural ligand (IgE) or by anti-CD23 antibody prevents B lymphocyte proliferation and differentiation. *J. Immunol.* **146**, 2122-2129.
- Lupashin V.V., Hamamoto S. and Schekman R.W. (1996) Biochemical requirements for targeting and fusion of ER-derived transport vesicles with purified yeast Golgi membranes. *J. Cell Biol.* **132**, 277-289.
- Ma J. and Ptashne M. (1987) A new class of transcriptional activators. *Cell* **51**, 113-119.
- Macaulay A.E., DeKruyff R.H., *et al.* (1997) Antigen-specific B cells preferentially induce CD4<sup>+</sup> T cells to produce IL-4. *J. Immunol.* **158**, 4171-4179.
- Mackarechtschian K., Hardin J.D., *et al.* (1995) Targeted disruption of the Flk2/Flt3 gene leads to deficiencies in primitive hematopoietic progenitors. *Immunity* **3**, 147-161.
- MacLennan I.C. (1994) Germinal centres. *Annu. Rev. Immunol.* **12**, 117-139.
- Maecker H.T. and Levy S. (1997) Normal lymphocyte development but delayed humoral immune response in CD81-null mice. *J. Exp. Med.* **185**, 1505-1510.
- Maecker H.T., Do M. and Levy S. (1998) CD81 on B cells promotes IL-4 secretion and antibody production during Th2 immune responses. *PNAS (USA)* **95**, 2458-2462.
- Maestrini E., Patrosso C., *et al.* (1993) Mapping of two genes encoding isoforms of the actin binding protein ABP-280, a dystrophin like protein, to Xq28 and to chromosome 7. *Human Mol. Gen.* **2**, 761-766.
- Male D., Champion B. *et al.* (1993) *Advanced Immunology*. Mosby,
- Malisan F., Briere F., *et al.* (1996) Interleukin-10 induces immunoglobulin G isotype switch recombination in human CD40-activated naive B lymphocytes. *J. Exp. Med.* **183**, 937-47.
- Maliszewski C.R., Grabstein K.H., *et al.* (1993) Recombinant CD40 ligand stimulation of murine B cell growth and differentiation: cooperative effects of cytokines. *Eur. J. Immunol.* **23**, 1044-49.
- Markowitz J.S., Rogers P.R., *et al.* (1993) B lymphocyte development and activation independent of MHC class II expression. *J. Immunol.* **150**, 1223-1233.
- Marolewski A.E., Buckle D.R., *et al.* (1998) CD23 (FcεRII) release from cell membranes is mediated by a membrane bound metalloprotease. *Biochem. J.* **333**, 573-579.
- Marshall J., Molloy R., *et al.* (1995) The jellyfish green fluorescent protein: a new tool for studying ion channel expression and function. *Neuron* **14**, 211-215.
- Marti A., Luo Z., *et al.* (1997) Actin-binding protein-280 binds the stress-activated protein kinase (SAPK) activator SEK-1 and is required for tumour necrosis factor-alpha activation of SAPK in melanoma cells. *J. Biol. Chem.* **272**, 2620-2628.
- Matheson J., Borland G., *et al.* (2001) The αvβ5 integrin is a marker of acute lymphocytic leukemia cells and a functional adenovirus receptor in human B Vitronectin receptor in human B lymphoid precursors. **In press.**
- Matsumoto M., Lo S., *et al.* (1996) Affinity maturation without germinal centres in lymphotoxin-α deficient mice. *Nature* **382**, 462-466.
- McBlane J F., Van Gent D.C., *et al.* (1995) Cleavage at V(D)J recombination signals requires only RAG-1 and RAG-2 proteins and occurs at two steps. *Cell* **83**, 387-95.
- McKercher S.R., Torbett B.E., *et al.* (1996) Targeted disruption of the PU.1 gene results in multiple hematopoietic abnormalities. *EMBO J.* **15**, 5658
- McWhirter J., Neuteboom S., *et al.* (1999) Oncogenic homeodomain transcription factor E2A-Pbx1 activates a novel WNT gene in pre-B acute lymphoblastoid leukemia. *PNAS (USA)* **96**, 391-399.



- Melchers F., Haasner D., *et al.* (1994) Roles of IgH and L chains and of surrogate H and L chains in the development of cells of the B lymphocyte lineage. *Annu. Rev. Immunol.* **12**, 209-225.
- Melchers F., Rolink A., *et al.* (1995) Positive and negative selection events during B lymphopoiesis. *Curr. Opin. Immunol.* **7**, 214-227.
- Melchers F. and Rolink A.G. (1998) *B-lymphocyte development and biology*. Lippincott-Raven., Philadelphia.
- Mellman I., Fuchs R. and Helenius A. (1986) Acidification of the endocytic and exocytic pathways. *Annu. Rev. Biochem.* **55**, 663-700.
- Mellman I. and Koch T. (1988) Structure and function of Fc receptors on macrophages and lymphocytes. *J. Cell Sci.* **9**, 45
- Mellman I. and Simons K. (1992) The Golgi complex: In vitro veritas. *Cell* **68**, 829-840.
- Mellman I.S., Plutner H., *et al.* (1983) Internalization and degradation of macrophage Fc receptors during receptor-mediated phagocytosis. *J. Cell Biol.* **96**, 887-895.
- Meyer S., *et al.* (1997) Identification of the region in actin-binding protein that binds to the cytoplasmic domain of glycoprotein Ib. *J. Biol. Chem.* **272**, 2914-2919.
- Meyer S.C., Sanan D.A. and Fox J.E. (1998) Role of actin-binding protein in insertion of adhesion receptors into the membrane. *J. Biol. Chem.* **273**, 3013-3020.
- Milligan G. (1999) Exploring the dynamics of regulation of G protei-coupled receptors using green fluorescent protein. *British J. Pharm.* **128**, 501-510.
- Mitchel M.A., Huang M.-M., *et al.* (1994) Substitution and deletion in the cytoplasmic domain of the phagocytic receptor FcγIIA: Effect on receptor tyrosine phosphorylation and phagocytosis. *Blood* **84**, 1753-1759.
- Miyamoto S., Chiao P.J. and Verma I.M. (1994) Enhanced I kappa B alpha degradation is responsible for constitutive NF-kappa B activity in mature murine B-cell lines. *Mol. Cell Biol.* **14**, 3276-3282.
- Molnar A. and Georgopoulos K. (1994) The Ikaros gene encodes a family of functionally diverse zinc finger DNA-binding proteins. *Mol. Cell Biol.* **14**, 8292-8303.
- Mombaerts P., Iacomini J., *et al.* (1992) Rag-1-deficient mice have no mature B and T lymphocytes. *Cell* **65**, 869-77.
- Moore P.A., Belvedere O., *et al.* (1999) BLyS: member of the TNF family and B lymphocyte stimulator. *Sci.* **285**, 260-263.
- Moqadam F. and Siebert P. (1994) Rapid amplification of the 3' end of cDNAs with the 3'-AmpliFINDER™ RACE kit. *CLONTECHniques IX*, 6-9.
- Morgan B., Sun L., *et al.* (1997) Aiolos, a lymphoid restricted transcription factor that interacts with Ikaros to regulate lymphocyte differentiation. *EMBO J.* **16**, 2004-2013.
- Morimoto S., Kanno Y., *et al.* (2000) CD134L engagement enhances human B cell Ig production: CD154/CD40, CD70/CD72 and CD134/CD134L interactions coordinately regulate T cell-dependent B cell responses. *J. Immunol.* **164**, 4097-4104.
- Morse L., Chen D., *et al.* (1997) Induction of cell cycle arrest and B cell terminal differentiation by CDK inhibitor p18 (INK4c) and IL-6. *Immunity* **6**, 47-56.
- Mossalayi M.D., Arock M., *et al.* (1990) Proliferation of early human myeloid precursors induced by interleukin-1 and recombinant soluble CD23. *Blood* **75**, 1924-1927.
- Mossalayi M.D., Lecron J.C., *et al.* (1990) Interleukin-1 synergistically induces early human thymocyte maturation. *J. Exp. Med.* **171**, 959-964.
- Mossalayi M.D., Arock M., *et al.* (1992) Cytokine effects of CD23 are mediated by an epitope distinct from the IgE binding site. *EMBO J.* **11**, 4323-4328.



- Mossalayi M.D., Arock M. and Debré P. (1997) CD23/FcεRII : Signalling and clinical implication. *Int. Rev. of Immunol.* 16, 129-146.
- Moy V.T. and Brian A.A. (1992) Signalling by LFA-1 in B cells : enhanced antigen presentation after stimulation through LFA-1. *J. Exp. Med.* 175, 1-7.
- Mudde G.C., van Reijssen F.C. and *et al.* (1990) Allergen presentation by epidermal Langerhans' cells from patients with atopic dermatitis is mediated by IgE. *Immunology* 69, 335-341.
- Mudde G.C., Bheekha R. and Bruijnzeel-Koomen C.A. (1995) Consequences of IgE/CD23-mediated antigen presentation in allergy. *Immunol. Today* 16, 380-383.
- Murata K., Ishii N., *et al.* (2000) Impairment of APC function in mice lacking expression of OX40 ligand. *J. Exp. Med.* 191, 365-374.
- Murre C., Bain G., *et al.* (1994) Structure and function of helix-loop-helix proteins. *Biochim. Biophys. Acta.* 1218, 129-135.
- Naclerio R., Adkinson N., *et al.* (1993) Intranasal steroids inhibit seasonal increases in ragweed-specific immunoglobulin E antibodies. *J. Allergy Clin. Immunol.* 92, 717-721.
- Nagumo H., Agematsu K., *et al.* (1998) CD27/CD70 interaction augments IgE secretion by promoting the differentiation of memory B cells into plasma cells. *J. Immunol.* 161, 6496-6502.
- Nakayama E., von Hoegen J. and Parnes J.R. (1989) Sequence of the Lyb-2-B-cell differentiation antigen defines a gene superfamily of receptors with inverted membrane orientation. *PNAS (USA)* 86, 1352-1358.
- Natkunam Y., Zhang X., *et al.* (1994) Simultaneous activation of Ig and Oct-2 synthesis and reduction of surface MHC class II expression by IL-6. *J. Immunol.* 153, 3476-3484.
- Nelbock P., Dillon P.J., *et al.* (1990) A cDNA for a protein that interacts with the human immunodeficiency virus Tat transactivator. *Science* 248, 1650-1653.
- Nemazee D. and Weigert M. (2000) Revising B cell receptors. *J. Exp. Med.* 191, 1813-1817.
- Nemazee D. (2000) Receptor selection in B and T lymphocytes. *Annu. Rev. Immunol.* 18, 19-51.
- Nishizumi H., Taffлучи I., *et al.* (1995) Impaired proliferation of peripheral B cells and induction of autoimmune disease in lyn-deficient. *Immunity* 3, 549-560.
- Nonoyama S., Penix L.A., *et al.* (1995) Diminished expression of CD40 ligand by activated neonatal T cells. *J. Clin. Invest.* 95, 66
- Nutt S.L., Urbanek P., *et al.* (1997) Essential functions of Pax-5 (BSAP) in pro-B cell development: difference between fetal and adult B lymphopoiesis and reduced V-to-DJ recombination at the IgH locus. *Genes Dev.* 11, 476-491.
- Nutt S.L., Heavey B., *et al.* (1999) Commitment to the B-lymphoid lineage depends on the transcription factor Pax5. *Nature* 401, 556-562.
- Nyormoi O., Sinclair J.H. and Klein G. (1972) Isolation and characterization of an adherent, 8-azaguanine resistant variant of the Burkitt lymphoma cell line, Raji. *Exp. Cell Res.* 82, 241-251.
- O'Brien S., Giglio A. and Keating M. (1995) Advances in the biology and treatment of B-cell chronic lymphocytic leukemia. *Blood* 85, 307
- O'Riordan M. and Grosschedl R. (1999) Coordinate regulation of B cell differentiation by the transcription factors EBF and E2A. *Immunity* 11, 21-31.
- Ohno H., Stewart J., Fournier M.C., *et al.* (1995) Interaction of tyrosine-based signals with clathrin-associated proteins. *Science* 269, 1872-1875.
- Ohno H., Fournier M.C., *et al.* (1996) Structural determinants of interaction of tyrosine-based sorting signals with the adaptor medium chains. *J. Biol. Chem.* 271, 29009-29015.
- Ohta Y., Stossel T.P. and Hartwig J.H. (1991) Ligand sensitive binding of actin-binding protein to immunoglobulin G Fc receptor I (Fc gamma RI). *Cell* 67, 257-282.



- Ohta Y. and Hartwig J.H. (1995) Actin filament cross-linking by chicken gizzard filamin is regulated by phosphorylation *in vitro*. *Biochem.* 34, 6745-6754.
- Ohta Y. and Hartwig J.H. (1996) Phosphorylation of actin-binding protein 280 by growth factors is mediated by p90 ribosomal protein S6 kinase. *J. Biol. Chem.* 271, 11858-11864.
- Ohta Y., Suzuki N., *et al.* (1999) The small GTPase RalA targets filamin to induce filopodia. *PNAS (USA)* 96, 2122-2128.
- Osborne M.A., Lubinus M. and Kochan J.P. (1997) *Detection of protein-protein interactions dependent on post-translational modifications. In: The Yeast Two-Hybrid system.* Oxford University Press,
- Oshiba A., Hamelmann E., *et al.* (1997) Early expansion of secondary B cells after primary immunisation with antigen complexed with IgE. *J. Immunol.* 159, 4056-4063.
- Ott I., Fischer E.G., *et al.* (1998) A role for tissue factor in cell adhesion and migration mediated by interaction with actin-binding protein 280. *J. Cell Biol.* 140, 1241-1253.
- Owens T. (1991) A role for adhesion molecules in contact-dependent T help for B cells. *Eur. J. Immunol.* 21, 979-983.
- Ozanne D.M., Brady M.E., *et al.* (2000) Androgen receptor nuclear translocation is facilitated by the f-actin cross-linking protein filamin. *Mol. Endocrin.* 14, 1618-1626.
- Palacios R., Maza-Martinez O. and Guy K. (1983) Monoclonal antibodies against HLA-DR antigens replace T helper cells in activation of B lymphocytes. *PNAS(USA)* 80, 3456-3460.
- Parton R.G. (1996) Caveolae and caveolins. *Curr. Opin. Cell Biol.* 8, 542-548.
- Pastan I. and Willingham M.C. (1983) Receptor-mediated endocytosis: Coated pits, receptorosomes and the Golgi. *TIBS.* 8, 250-254.
- Patrosso M.C., Repetto M., *et al.* (1994) The exon-intron organization of the human X-linked gene (FLNI) encoding actin-binding protein 280. *Genomics* 21, 71-76.
- Paulie S., Rosen A.E.H.B., *et al.* (1989) The human B lymphocyte and carcinoma antigen, CD40, is a phosphoprotein involved in growth signal transduction. *J. Immunol.* 142, 142
- Payet-Jamroz M., Helm S.L.T., *et al.* (2001) Suppression of IgE responses in CD23-transgenic animals is due to expression of CD23 on nonlyphoid cells. *J. Immunol.* 166, 4863-4869.
- Payet M.E., Woodard E.C. and Conrad D.H. (1999) Humoral response suppression observed with CD23 transgenics. *J. Immunol.* 163, 217-223.
- Pearse B.M. and Robinson M.S. (1990) Clathrin, adaptors and sorting. *Cell Biol.* 6, 151-171.
- Pfeffer S.R. (1996) Transport vesicles docking: SNAREs and associates. *Annu. Rev. Cell. Dev. Biol.* 12, 441-461.
- Phizichy E.M. and Fields S. (1995) Protein-protein interactions : Methods for detection and analysis. *Microbiol. Rev.* 59, 94-123.
- Piguet V., Feng G., *et al.* (1999) Nef-Induced CD4 degradation - A diacidic-based motif in Nef functions as a lysosomal targeting signal through the binding of  $\beta$ -COP in endosomes. *Cell* 97, 63-73.
- Pirron U., Schlunck T., *et al.* (1990) IgE-dependent antigen focusing by human B lymphocytes is mediated by the low affinity receptor for IgE. *Eur. J. Immunol.* 20, 1547-1551.
- Pitt A., Mayorga L.S., *et al.* (1992) Transport of phagosomal components to an endosomal compartment. *J. Biol. Chem.* 267, 126-132.
- Pochon S., Graber P., *et al.* (1992) Demonstration of a second ligand for the low affinity receptor for IgE (CD23) using recombinant CD23 reconstituted into fluorescent liposomes. *J. Exp. Med.* 176, 389-397.
- Polakis P. (2000) Wnt signaling and cancer. *Genes Dev.* 14, 1837-1851.
- Pollok K.E., Kim Y.J., *et al.* (1994) 4-1BB T cell antigen binds to mature B cells and macrophages, and co-stimulates anti- $\mu$ -primed splenic B cells. *Eur. J. Immunol.* 24, 367-374.



- Poudrier J. and Owens T. (1994) CD54/ICAM-1 and MHC class II signalling induces B cells to express IL-2 receptors and complements help provided through CD40 ligation. *J. Exp. Med.* 179, 1417-1427.
- Prasher D.C., Eckenrode V.K., *et al.* (1992) Primary structure of the *Aequorea victoria* green fluorescent protein. *Gene* 111, 229-233.
- Pulendran B., Kannourakis G., *et al.* (1995) Soluble antigen can cause enhanced apoptosis of germinal-centre B cells. *Nature* 375, 331-34.
- Rabinowitz S., Hortmann H., *et al.* (1992) Immunocytochemical characterization of the endocytic and phagolysosomal compartments in peritoneal macrophages. *J. Cell Biol.* 116, 95-112.
- Radic M.Z., Erikson J., *et al.* (1993) B lymphocytes may escape tolerance by revising their antigen receptors. *J. Exp. Med.* 177, 1165-1173.
- Rajewsky K. (1996) Clonal selection and learning in the antibody system. *Nature* 381, 751-758.
- Ramsden D.A., Van Gent D.C. and Gellert M. (1997) Specificity in V(D)J recombination: new lessons from biochemistry and genetics. *Curr. Opin. Immunol.* 9, 114-20.
- Ranheim E. and Kipps T. (1993) Activated T cells induce expression of B7/BB1 on normal leukemic B cells through a CD40 dependent signal. *J. Exp. Med.* 177, 925-35.
- Reinisch W., Willheim M *et al.* (1994) Soluble CD23 reliably reflects disease activity in B cell chronic lymphocytic leukaemia. *J. Clin. Oncol.* 12: 2146.
- Reth M. and Alt F.W. (1984) Novel immunoglobulin heavy chains are produced from DJH gene segment rearrangements in lymphoid cells. *Nature* 312, 418-23.
- Retter M.W. and Nemazee D. (1998) Receptor editing occurs frequently during normal B cell development. *J. Exp. Med.* 188, 1231-1238.
- Reya T., O'Riordan M., *et al.* (2000) Wnt signalling regulates B lymphocyte proliferation through a LEF-1 dependent mechanism. *Immunity* 13, 15-24.
- Richards M.L. and Katz D.H. (1990) The binding of IgE to murine Fc epsilon RII is calcium dependent but not inhibited by carbohydrate. *J. Immunol.* 144, 2638-2646.
- Robinson C, Kalsheker N.A., *et al.* (1997) On the potential significance of the enzymatic activity of mite allergens to immunogenicity. Clues to structure and function revealed by molecular characterization. *Clin. Exp. Allergy* 27, 10-21.
- Rolink A., Nutt S.L., *et al.* (1999) Long-term in vivo reconstitution of T-cell development by Pax5-deficient B-cell progenitors. *Nature* 401, 603-606.
- Rosen S.D. and Bertozzi C.R. (1996) Leukocyte adhesion: two selectins converge on sulphate. *Current Biology* 6, 261-264.
- Roth R.A., Maddux B.A., *et al.* (1981) Insulin-ricin B chain conjugate. A hybrid molecule with ricin-binding activity and insulin biological activity. *J. Biol. Chem.* 256, 5350-5354.
- Rothman J.E. and Warren G. (1994) Implications of the SNARE hypothesis for intracellular membrane topology and dynamics. *Curr. Biol.* 4, 220-233.
- Rothman J.E. and Wieland F.T. (1996) Protein sorting by transport vesicles. *Science* 272, 227-234.
- Saiki R., Scharf S., *et al.* (1985) Enzymatic amplification of beta-globulin genomic sequences and restriction site analysis for diagnosis of sickle cell anemia. *Science* 230, 1350-1354.
- Salzman N.H. and Maxfield F.R. (1988) Intracellular fusion of sequentially formed endocytic compartments. *J. Cell Biol.* 106, 1083-1091.
- Sambrook J., Fritsch E.F. and Maniatis T. (1989) *Molecular cloning - A laboratory manual*. Cold Spring Harbor Laboratory Press,
- Samelson L.E. and Klausner R.D. (1992) Tyrosine kinases and tyrosine-based activation motifs. *J. Biol. Chem.* 267, 24913-24916.



- Sandvig K. and van Deurs B. (1994) Endocytosis without clathrin. *Trends Cell Biology* 4, 275-277.
- Santamaria L.F., Bheekha R., *et al.* (1993) Antigen focusing by specific monomeric immunoglobulin E bound to CD23 on Epstein-Barr virus-transformed B cells. *Human Immunol.* 37, 23-30.
- Sarfati M., Rector E., *et al.* (1984) In vitro synthesis of IgE by human lymphocytes. III. IgE-potentiating activity of culture supernatants from Epstein-Barr virus (EBV) transformed B cells. *Immunol.* 53, 207-214.
- Sarfati M., Nutman T., *et al.* (1986) Presence of antigenic determinants common to Fc IgE receptors on human macrophages, T and B lymphocytes and IgE binding factors. *Immunol.* 59, 569-575.
- Sarfati M., Bron D., *et al.* (1988) Elevation of IgE binding factors in serum of patients with B cell-derived chronic lymphocytic leukemia. *Blood* 71, 94-98.
- Sarfati M., Bettler B., *et al.* (1992) Native and recombinant soluble CD23 fragments with IgE suppressive activity. *Immunity* 76, 622-627.
- Sarfati M., Chevret S., *et al.* (1996) Prognostic importance of serum soluble CD23 level in chronic lymphocytic leukemia. *Blood* 88, 4259-4264.
- Satterthwaite A. and Witte O. (1996) Genetic analysis of tyrosine kinase function in B cell development. *Annu. Rev. Immunol.* 14, 131-154.
- Saxon A., Krube-leamer M., *et al.* (1991) Inhibition of human IgE production via FcεRII stimulation results from a decrease in the mRNA for secreted but not membrane H chains. *J. Immunol.* 147, 4000-4006.
- Schekman R. and Orci L. (1996) Coat proteins and vesicle budding. *Science* 271, 1526-1532.
- Scherer P.E., Okamoto T., *et al.* (1996) Identification, sequence and expression of caveolin-2 defines a caveolin gene family. *PNAS (USA)* 93, 131-135.
- Schlissel M., Voronova A. and Baltimore D. (1991) Helix-loop-helix transcription factor E47 activates germ-line immunoglobulin heavy-chain gene transcription and rearrangement in a pre-T-cell line. *Genes Dev.* 5, 1367
- Schmid S.L., Fuchs R., *et al.* (1988) Two distinct subpopulations of endosomes involved in membrane recycling and transport to lysosomes. *Cell* 52, 73-83.
- Schmid S.L. (1997) Clathrin-coated vesicle formation and protein sorting: An integrated process. *Annu. Rev. Biochem* 66, 511-548.
- Schneider P., Mackay F., *et al.* (1999) BAFF, a novel ligand of the TNF family, stimulates B cell growth. *J. Exp. Med.* 189, 1747-1756.
- Scholl P.R. and Geha R.S. (1994) MHC class II signalling in B-cell activation. *Immunol. Today* 15, 418-422.
- Scott E.W., Simon M.C., *et al.* (1994) Requirement of transcription factor PU.1 in the development of multiple hematopoietic lineages. *Science* 265, 1573-1577.
- Sears M.R., Burrows B., *et al.* (1991) Relation between airway responsiveness and serum IgE in children with asthma and in apparently normal children. *New Eng. J. Med.* 325, 1067-1071.
- Sgroi D., Koretzky G.A. and Stamenkovic I. (1995) Regulation of CD45 engagement by the B-cell receptor CD22. *PNAS (USA)* 92, 4026-4030.
- Sharma C.P., Ezzell R.M. and Arnaout M.A. (1995) Direct interaction of filamin (ABP-280) with the β<sub>2</sub>-integrin subunit CD18. *J. Immunol.* 154, 3461-3470.
- Sherr E., Macy E., *et al.* (1989) Binding to the low affinity Fc epsilon receptor on B cells suppresses ongoing human IgE production. *J. Immunol.* 42, 481-489.
- Shi W., Kumanogoh A., *et al.* (2000) The class IV semaphorin CD100 plays nonredundant roles in the immune system: defective B and T cell activation in CD100-deficient mice. *Immunity* 13, 633-642.
- Shih A., Gaullusser A. and Kirchhausen T. (1995) A clathrin-binding site in the hinge of the beta 2 chain of mammalian AP-2 complexes. *J. Biol. Chem.* 270, 31083-31090.



- Shinkai Y., Rathbun G., *et al.* (1992) RAG-2-deficient mice lack mature lymphocytes owing to inability to initiate V(D)J rearrangement. *Cell* **68**, 855-67.
- Shokat K. and Goodnow C. (1995) Antigen induced B cell death and elimination during germinal-centre immune responses. *Nature* **375**, 334-38.
- Shortman K., Wu L., *et al.* (1996) Early T lymphocyte progenitors. *Annu. Rev. Immunol.* **14**, 29-47.
- Shu H.B., Hu W.H. and Johnson H. (1999) TALL-1 is a novel member of the TNF family that is down-regulated by mitogens. *J. Leukocyte Biol.* **65**, 680-683.
- Sigvardsson M., O'Riordan M., *et al.* (1997) EBF and E47 collaborate to induce expression of the endogenous immunoglobulin surrogate light chain genes. *Immunity* **7**, 25-36.
- Simpson F., Peden A.A., Christopoulou L. and Robinson M.S. (1997) Characterization of the adaptor-related protein complex, AP-3. *J. Cell Biol.* **137**, 835-845.
- Singh H. (1996) Gene targeting reveals a hierarchy of transcription factors regulating specification of lymphoid fates. *Curr. Opin. Immunol.* **8**, 160-165.
- Sleckman B.P., Gorman J.R. and Alt F.W. (1996) Accessibility control of antigen-receptor variable-region gene assembly: role of *cis*-acting elements. *Annu. Rev. Immunol.* **14**, 459-81.
- Smith G.P. (1985) Filamentous fusion phage - novel expression vectors that display cloned antigens on the virion surface. *Science* **228**, 1315-1317.
- Smith R.G. (1984) Paraosteal Lymphoblastic Lymphoma: A human counter part of Abelson virus-induced lymphosarcoma of mice. *Cancer* **54**, 471-476.
- Smythe E. and Warren G. (1991) The mechanism of receptor-mediated endocytosis. *Eur. J. Biochem.* **202**, 689-699.
- Snapper C.M., Hooley J.J., *et al.* (1991) Lack of FcεRII expression by murine B cells after in vivo immunization is directly associated with Ig secretion but not Ig isotype switching. *J. Immunol.* **146**, 2161
- Sollner T., Whitehart S.W., *et al.* (1993) SNAP receptors implicated in vesicle targeting and fusion. *Nature* **362**, 318-324.
- Spiegelberg H.L. (1984) Structure and function of Fc receptors for IgE on lymphocytes, monocytes and macrophages. *Advan. Immunol.* **35**, 61-88.
- Springer T.A. (1990) Adhesion receptors of the immune system. *Nature* **346**, 425-434.
- Squire C.M., Studer E.J., *et al.* (1994) Antigen presentation is enhanced by targeting antigen to the Fc epsilon R II by antigen-anti-FcεRII conjugates. *J. Immunol.* **152**, 4388-4396.
- Stall A.M., Wells S.M. and Lam K.P. (1996) B1 cells: unique origins and functions. *Semin, Immunology* **8**, 45-59.
- Stearns T. (1995) The green revolution. *Curr. Biol.* **5**, 262-264.
- Stief A., Texido G., *et al.* (1994) Mice deficient in CD23 reveal its modulatory role in IgE production but no role in T and B cell development. *J. Immunol.* **152**, 3378-3390.
- Stossel T.P., Condeelis J., *et al.* (2001) Filamins as integrators of cell mechanics and signalling. *Nature Rev.* **2**, 138-145.
- Stüber E., Neurath M., *et al.* (1995) Cross-linking of OX40 ligand, a member of the TNF/NGF cytokine family, induces proliferation and differentiation in murine splenic B cells. *Immunity* **2**, 507-521.
- Stüber E. and Strober W. (1996) The T cell-B cell interaction via OX40-OX40L is necessary for the T cell-dependent humoral immune response. *J. Exp. Med.* **183**, 979-989.
- Sugie K., Kawakami T., *et al.* (1991) Fyn tyrosine kinase associated with FcεRII/CD23 : Possible multiple roles in lymphocyte activation. *Immunology* **88**, 9132-9135.



- Sugimoto M., Esaki N., *et al.* (1989) A simple and efficient method for the oligonucleotide-directed mutagenesis using plasmid DNA template and phosphorothioate-modified nucleotide. *Anal. Biochem.* 179, 309-311.
- Suter U., Bastos R. and Hofstetter H. (1987) Molecular structure of the gene and the 5'-flanking region of the human lymphocyte immunoglobulin  $\epsilon$  receptor. *Nuc. Acids Res.* 15, 7295
- Swanson J.A. and Baer S.C. (1995) Phagocytosis by zippers and triggers. *Trends Cell Biology* 5, 89-93.
- Takafuta T., Wu G., *et al.* (1998) Human  $\beta$ -filamin is a new protein that interacts with the cytoplasmic tail of glycoprotein Iba. *J. Biol. Chem.* 273, 17531-17538.
- Tang Z., Scherer P.E., *et al.* (1996) Molecular cloning of caveolin-3, a novel membrane of the caveolin gene family expressed predominately in muscles. *J. Biol. Chem.* 271, 2255-2261.
- Tanner J., Weis J.J., *et al.* (1987) Epstein-Barr virus gp350/220 binding to the B lymphocyte C3d receptor mediates adsorption, capping and endocytosis. *Cell* 50, 203-213.
- Taylor J.W., Ott J. and Eckstein F. (1985) The rapid generation of oligonucleotide-directed mutations at high frequency using phosphorothioate-modified DNA. *Nuc. Acids Res.* 13, 8765-8785.
- Taylor M.E. (1997) Evolution of a family of receptors containing multiple motifs resembling carbohydrate-recognition domains. *Glycobiology* 7, R5-R8.
- Tenner A.J., Robinson S.L. and Ezekowitz R.A. (1995) Mannose binding protein (MBP) enhances mononuclear phagocyte function via a receptor that contains the 126,000M(r) component of the C1q receptor. *Immunity* 3, 485-493.
- Texido G., Eibel H., *et al.* (1994) Transgene CD23 expression on lymphoid cells modulates IgE and IgG1 responses. *J. Immunol.* 153, 3028
- Thompson T.G., Chan Y.M., *et al.* (2000) Filamin 2 (FLN2): A muscle-specific sarcoglycan interacting protein. *J. Cell Biol.* 148, 115-126.
- Thorley-Lawson D.A., Nadler L.M., *et al.* (1985) Blast-2 (EBVCS) an early cell surface marker of human B cell activation is superinduced by Epstein Barr virus. *J. Immunol.* 143, 3007-3012.
- Tiegs S.L., Russell D.M. and Nemazee D. (1993) Receptor editing in self-reactive bone marrow B cells. *J. Exp. Med.* 177, 1009-1020.
- Tjelle T.E., Saigal B., *et al.* (1998) Degradation of phagosomal components in late endocytic organelles. *J. Cell Sci.* 111, 141-148.
- Tonegawa S. (1983) Somatic generation of antibody diversity. *Nature* 302, 575-81.
- Trowbridge I.S., Collawn J.F. and Hopkins C.R. (1993) Signal-dependant membrane protein trafficking in endocytic pathway. *Annu. Rev. Cell Biol.* 9, 129-161.
- Tsiagbe V.K., Inghirami G. and Thorbecke G.J. (1996) The physiology of germinal centres. *Crit. Rev. Immunol.* 16, 381-421.
- Tsien R.Y. (1998) The green fluorescent protein. *Annu. Rev. Biochem* 67, 509-544.
- Turner C.A. Jr., Mack D.H. and Davis M.M. (1994) Blimp-1, a novel zinc finger-containing protein that can drive the maturation of B lymphocytes into immunoglobulin-secreting cells. *Cell* 77, 297-306.
- Turner M., Mee P.J., Costello P.S., *et al.* (1995) Perinatal lethality and blocked B-cell development in mice lacking the tyrosine kinase syk. *Nature* 378, 298-302.
- Ueda M., Oho C., *et al.* (1992) Interaction of the low-molecular-mass, guanine-nucleotide-binding protein with the actin-binding protein and its modulation by the cAMP-dependant protein kinase in bovine platelets. *Eur. J. Biochem.* 203, 347-352.
- Urashima M., Chauhan D., *et al.* (1996) CD40 ligand triggers interleukin-6 mediated B cell differentiation. *Leuk. Res.* 20, 507-15.



- Urbanek P., Wang Z.Q., *et al.* (1994) Complete block of early B cell differentiation and altered patterning of the posterior midbrain in mice lacking Pax5/BSAP. *Cell* 79, 901-912.
- Van Aelst L., Barr M., *et al.* (1993) Complex formation between RAS & RAF and other protein kinases. *PNAS (USA)* 90, 6213-6217.
- van der Heijden F.L., Joost van Neerven R.J., *et al.* (1993) Serum- IgE-facilitated allergen presentation in atopic disease. *J. Immunol.* 150, 3643-3650.
- van Ewijk W. (1991) T-cell differentiation is influenced by thymic microenvironments. *Annu. Rev. Immunol.* 9, 591-615.
- Van Gent D.C., Ramsden D.A. and Gellert M. (1996) The RAG-1 and RAG-2 proteins establish the 12/23 rule in V(D)J recombination. *Cell* 85, 107-13.
- van Kooten C. and Banchereau J. (2000) CD40-CD40 ligand. *J. of Leukocyte Biol.* 67, 2-17.
- Vandeyar M., Weiner M.P., *et al.* (2001) A simple and rapid method for the selection of oligodeoxynucleotide-directed mutants. *Gene* 65, 129-133.
- Vercelli D., Helm B., *et al.* (1989) The B cell binding site on human immunoglobulin E. *Nature* 338, 649-651.
- Vinay D.S. and Kwon B.S. (1994) Role of 4-1BB in immune responses. *Semin. Immunol.* 10, 481-490.
- von Bulow G.U. and Bram R.J. (1997) NF-AT activation induced by a CAML-interacting member of the tumor necrosis factor receptor superfamily. *Science* 278, 138-141.
- Wade W.F., Cambier J.C., *et al.* (1989) Altered I-A protein-mediated transmembrane signalling in B cells that express truncated I-A<sup>k</sup> protein. *PNAS (USA)* 86, 6297-6301.
- Wallach D., Davies P.J. and Pastan I. (1978) Cyclic AMP-dependant phosphorylation of filamin in mammalian smooth muscle. *J. Biol. Chem.* 253, 4739-4745.
- Wang J.H., Nichogiannopoulou A., *et al.* (1996) Selective defects in the development of the fetal and adult lymphoid system in mice with an Ikaros null mutation. *Immunity* 5, 537-549.
- Wang S. and Hazelrigg T. (1994) Implications for bcd mRNA localization from spatial distribution of exu protein in Drosophila oogenesis. *Nature* 369, 400-403.
- Weis J.J., Tedder T.F. and Fearon D.T. (1984) Identification of a 145 000 Mr membrane protein as the C3d receptor (CR2) of human B lymphocytes. *PNAS (USA)* 81, 881
- Weis J.J., Toothaker L.E., *et al.* (1988) Structure of the human B lymphocyte receptor for C3d and the Epstein-Barr virus and relatedness to other members of the family of C3/C4 binding proteins. *J. Exp. Med.* 167: 1047-1066.
- Wendel-Hansen V., Riviere M., *et al.* (1990) The gene encoding CD23 leukocyte antigen (FcεRII) is located on human chromosome 19. *Somatic Cell and Mol. Gen.* 16, 283-285.
- Westman S., Gustavsson S., *et al.* (1997) Early expansion of secondary B cells after primary immunization with antigen complexed with IgE. *Immunol.* 46, 10-15.
- White L.J., Ozanne B.W., *et al.* (1997) Inhibition of apoptosis in a human pre-B-cell line by CD23 is mediated via a novel receptor. *Blood* 90,
- Williams R.O., Feldman M., *et al.* (1992) Anti-tumor necrosis factor ameliorates joint disease in murine collagen-induced arthritis. *PNAS (USA)* 89, 9784-9788.
- Wilson P.C., Wilson K., *et al.* (2000) Receptor revision of immunoglobulin heavy chain variable region genes in normal human B lymphocytes. *J. Exp. Med.* 191, 1881-1894.
- Wright S.D. and Silverstein S.C. (1983) Receptors for C3b and iC3b promote phagocytosis but not the release of toxic oxygen from human phagocytes. *J. Exp. Med.* 158, 2016-2023.
- Xu S. and Lam K.-P. (2001) B-cell maturation protein, which binds the tumor necrosis factor family members BAFF and APRIL, is dispensable for humoral immune responses. *Mol. Cell. Biol.* 21, 4067-4074.



- Xu W., Xie Z., *et al.* (1998) A novel human actin-binding protein homologue that binds to platelet glycoprotein Ib $\alpha$ . *Blood* **92**, 1268-1276.
- Yada Y., Okano Y. and Nozawa Y. (1990) Enhancement of GTP $\gamma$ S-binding activity by cAMP-dependant phosphorylation of a filamin-like 250 kDa membrane protein in human platelets. *Biochem. Biophys. Res. Commun.* **172**, 256-261.
- Yanagihara Y., Sarfati M., *et al.* (1990) Serum levels of IgE-binding factor (soluble CD23) in diseases associated with elevated IgE. *Clin. Exp. Allergy* **20**, 395-401.
- Yokota A., Kikutani H., *et al.* (1988) Two species of human Fc $\epsilon$  receptor II (Fc $\epsilon$ RII/CD23): Tissue specific and IL-4-specific regulation of gene expression. *Cell* **55**, 611-618.
- Yokota A., Yukawa K., *et al.* (1992) Two forms of the low-affinity Fc receptors for IgE differentially mediate endocytosis and phagocytosis: Identification of the critical cytoplasmic domains. *PNAS(USA)* **89**, 5030-5034.
- Young R. and Davis R. (1983) Yeast RNA polymerase II genes - Isolation with antibody probes. *Science* **222**, 778-782.
- Yu G., Boone J., *et al.* (2000) APRIL and TALL-1 and receptors BCMA and TACI: system for regulating humoral immunity. *Nat. Immunol.* **1**, 256
- Yu P., Kosco-Vilbois M., *et al.* (1994) Negative feedback regulation of IgE synthesis by murine CD23. *Nature* **369**, 753-756.
- Yukawa K., Kikutani H., Owaki H., *et al.* (1987) A B cell specific differentiation antigen, CD23, is a receptor for IgE (Fc $\epsilon$ R) on lymphocytes. *J. Immunol.* **138**, 2576-2580.
- Zhang W., Han S.W., *et al.* (1998) Interaction of presenilins with the filamin family of actin-binding proteins. *J. Neuroscience* **18**, 914-922.
- Zhuang Q.Q., Rosenberg S., *et al.* (1984) Role of actin binding protein phosphorylation in platelet cytoskeleton assembly. *Biochem. Biophys. Res. Commun.* **118**, 508-513.
- Zhuang Y., Soriano P. and Weintraub H. (1994) The helix-loop-helix gene E2A is required for B cell formation. *Cell* **79**, 875-884.
- Zhuang Y., Cheng P. and Weintraub H. (1996) B-lymphocyte development is regulated by the combined dosage of three basic helix-loop-helix genes, E2A, E2-2 and HEB. *Mol. Cell Biol.* **16**, 2898-2905.
- Zinkernagel R.M., Bachmann M.F. *et al.* (1996) On immunological memory. *Annu. Rev. Immunol.* **14**, 333-367.



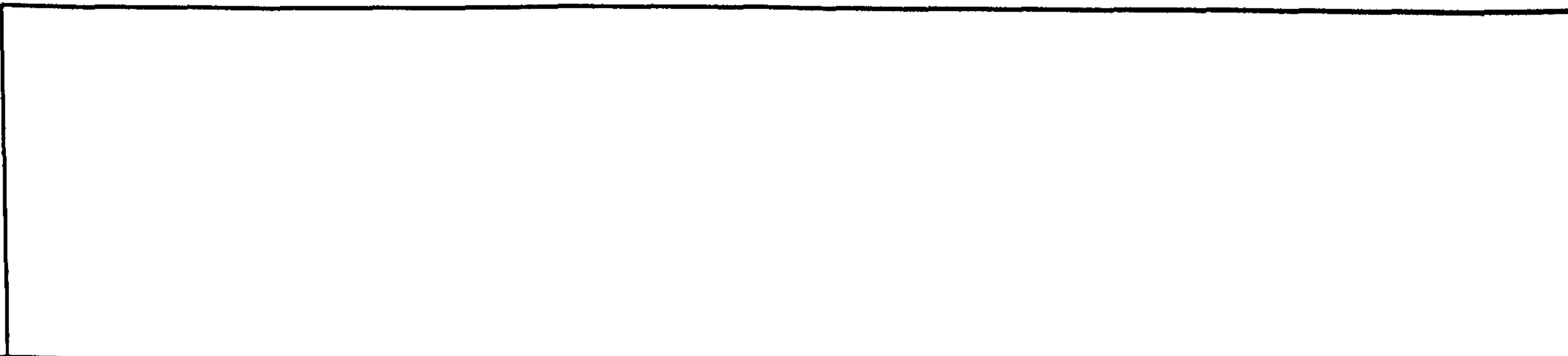
## **APPENDIX**



**SOLUTIONS AND BUFFERS**

Unless otherwise stated the quantities shown correspond to 1L stock solutions.

**E.COLI & YEAST CELL CULTURE MEDIAS & AGARS**





## **APPENDIX**



**SOLUTIONS AND BUFFERS**

Unless otherwise stated the quantities shown correspond to 1L stock solutions. . . .

**E.COLI & YEAST CELL CULTURE MEDIAS & AGARS**

Solution/Buffer	Composition
LB Broth	10g Bacto-Tryptone, 5g Bacto-Yeast extract, 10g NaCl, pH 7.5. Supplement with 0.05mg/ml Ampicillin or 0.03mg/mL Kanamycin
LB Agar	1L LB Broth, 15g Bacto-Agar. Supplement with 0.05mg/ml Ampicillin or 0.03mg/ml Kanamycin
SOC Media	2g Bacto-tryptone, 0.5g Bacto-yeast, 0.01M NaCl, 0.01M MgCl <sub>2</sub> , 0.01M MgSO <sub>4</sub> , 0.02M Glucose
YPD	20g Difco Peptone, 10g Yeast Extract. Autoclave, add Glucose (final concentration 2%) once cooled to 50°C.
YPDA	YPD made as above. Add Adenine to final concentration of 0.003 % once media cooled to 50°C.
M9 DO leu	13.5g Na <sub>2</sub> HPO <sub>4</sub> , 6g KH <sub>2</sub> PO <sub>4</sub> , 2g NH <sub>4</sub> Cl, 1g NaCl, 0.7g DO leu supplement, made up to 2L with water and autoclaved. Cooled to 50°C, added 2ml 1M MgSO <sub>4</sub> (or MgCl <sub>2</sub> ), 100µl 1M CaCl <sub>2</sub> , 1ml1M thiamine, 500µl 100µg/ml Ampicillin, 10ml 40% Glucose
M9 Agar	1L M9 Media, 9g Bacto-Agar

***E.coli* COMPETENT CELL PREPARATIONS**

Buffer/Solution	Composition
Psi Broth	5g Bacto yeast extract, 20g Bacto Tryptone, 5g Magnesium Sulphate
TfbI	30mM Potassium Acetate, 100mM Rubidium Chloride, 10mM Calcium Chloride, 50mM Magnesium Chloride, 15% v/v Glycerol
TfbII	10mM MOPS, 75mM Calcium Chloride, 10mM Rubidium Chloride, 15 % v/v Glycerol

**DNA ANALYSIS**

DNA Purification Buffers ( <i>E.coli</i> )	Composition
Solution 1	50mM Glucose, 25mM Tris-HCl, pH8.0, 10mM EDTA
Solution 2	0.2M NaOH, 1% (w/v) SDS
Solution 3	3M Potassium acetate, 3M Acetic acid



DNA Purification Buffers (Yeast)	Composition
Buffer S	10mM K <sub>2</sub> HPO <sub>4</sub> , pH7.2, 10mM EDTA, 50mM 2-mercaptoethanol, 50mg/ml zymolase
Lysis Buffer	25mM Tris-HCl, 25mM EDTA, 25% (w/v) SDS

DNA Purification Buffers (Kit)	Composition
Qiagen P1 Resuspension Buffer	50mM Tris-HCl (pH 8), 10mM EDTA, 100µg/ml RNase A
Qiagen P2 Lysis Buffer	200mM NaOH, 1% (w/v) SDS
Qiagen P3 Neutralisation Buffer	3M potassium acetate, pH 4.8
Qiagen QBT Equilibration Buffer	750mM NaCl, 50mM MOPS, pH 7.0, 15% isopropanol, 0.15% Triton <sup>®</sup> X-100
Qiagen QC Wash Buffer	1M NaCl, 50mM MOPS (pH 7), 15% (v/v) Isopropanol
Qiagen QF Elution Buffer	1.25mM NaCl, 50mM Tris-HCl (pH 8.5), 15% (v/v) Isopropanol
Promega Resuspension Buffer	50mM Tris-HCl (pH 7.5), 10mM EDTA, 100µg/ml RNase A
Promega Lysis Buffer	0.2mM NaOH, 1% SDS
Promega Neutralisation Buffer	4.09M guanidine hydrochloride, 0.759M potassium acetate, 2.12M glacial acetic acid, pH 4.2
Promega Column Wash Buffer	60mM potassium acetate, 10mM Tris-HCl (pH 7.5), 60% ethanol

Buffers/Dyes	Composition
DNA Loading Dye (5X)	0.25% (w/v) Bromophenol blue, 0.25 % (w/v) xylene cyanol FF and 15% Ficoll
50X TAE Buffer	242g Tris, 18.6g EDTA, 57ml of Glacial Acetic acid, dH <sub>2</sub> O to 1L
TE Buffer	10mM Tris-HCl (pH 8), 1mM EDTA



## PROTEIN ANALYSIS

SDS PAGE Gels	Composition
6% SDS-PAGE Separation Gel	6% (w/v) Acrylamide/Bis Acrylamide, 0.375M Tris-HCl (pH 8.8), 0.1% (w/v) SDS, 0.05% (w/v) Ammonium Persulphate, 0.0003% (v/v) TEMED
10% SDS-PAGE Separation Gel	10% (w/v) Acrylamide/Bis Acrylamide, 0.375M Tris-HCl (pH 8.8), 0.1% (w/v) SDS, 0.05% (w/v) Ammonium Persulphate, 0.0003% (v/v) TEMED
12% SDS-PAGE Separation Gel	12% (w/v) Acrylamide/Bis Acrylamide, 0.375M Tris-HCl (pH 8.8), 0.1% (w/v) SDS, 0.05% (w/v) Ammonium Persulphate, 0.0003% (v/v) TEMED
5% SDS-PAGE Stacking Gel	5% (w/v) Acrylamide/Bis Acrylamide, 0.13M Tris-HCl (pH 6.8), 0.1% (w/v) SDS, 0.1% (w/v) Ammonium Persulphate, 0.0007% (v/v) TEMED

Solutions	Composition
Protein Transfer Buffer	48mM Tris, 39mM Glycine, 1.3mM SDS, 20% (v/v) Methanol
4x Protein Loading Buffer	200mM Tris-HCl pH 8, 8% (w/v) SDS, 0.4% (w/v) Bromophenol blue, 40% (v/v) Glycerol, 20% (v/v) $\beta$ -Mercaptoethanol
2x Non Reducing Loading Buffer	25mM Tris pH 6.8, 20% glycerol, 10% SDS, 5mM EDTA, bromophenol blue
10x Phosphate Buffered Saline (PBS)	1.37M NaCl, 26.8mM KCl, 42mM $\text{Na}_2\text{HPO}_4$ , 14.7mM $\text{KH}_2\text{PO}_4$ , pH 7.2
RIPA Buffer	50mM Tris-HCl (pH 7.4), 1% (v/v) NP40, 1mM sodium deoxycholate, 150mM NaCl, 1mM EGTA, 1mM $\text{Na}_3\text{VO}_4$ , 1mM NaF, 1mM PMSF, 2 $\mu\text{g/ml}$ Leupeptin, 0.5mM DTT
OGP Buffer	50mM HEPES-KOH, pH7.4, 5mM $\text{CaCl}_2$ , 140mM NaCl, 1% octyl- $\beta$ -D-glucopyranoside, 1mM PMSF, 1mM Aprotinin, 1mM Leupeptin
SDS-PAGE Running Buffer	25mM Tris-HCl (pH 8.3), 250mM Glycine, 0.1% (w/v) SDS
Blocking Buffer for Westerns	10% Marvel, 0.05% Tween in 1x PBS
Blotto	0.5% Marvel, 0.05% Tween in 1x PBS
High Urea Buffer	8M urea, 5% (w/v) SDS, 200mM Tris-HCl pH 6.8, 0.1mM EDTA, 0.5mg/ml Bromophenol blue, 10% (v/v) $\beta$ -mercaptoethanol.



SILVER STAIN

Reagent	Composition
Fix 1	40% ethanol 10% acetic acid
Fix 2	10% ethanol 5% acetic acid
Oxidiser	0.02g sodium-thio-sulphate in 100 ml dH <sub>2</sub> O
Silver Stain	0.2g AgNO <sub>3</sub> , 75 µl formaldehyde in 100 ml dH <sub>2</sub> O
Developer	6g sodium carbonate, 4mg sodium-thio-sulphate, 50µl formaldehyde in 100ml dH <sub>2</sub> O
Stop	5% acetic acid

sCD23 ELISA

Antibody/Reagent	Details
Capture Antibody	Anti-human CD23, 1:250 dilution in coating buffer
Detection Antibody	Biotinylated anti-human CD23, 1:250 dilution in assay diluent
Enzyme Reagent	Avidin-Horseradish Peroxidase conjugate, 1:250 dilution
Standard	Recombinant Human CD23

Buffer/Solution	Composition
Coating Buffer	0.2 M Sodium Phosphate, pH 6.5.
Assay Diluent	PBS with 10% heat inactivated Fetal Bovine Serum, pH 7.0
Wash Buffer	PBS 0.05% Tween-20
Substrate Solution	Tetramethylbenzidine (TMB) and Hydrogen Peroxide
Stop Solution	2 N H <sub>2</sub> SO <sub>4</sub>

PROTEIN TRAFFICKING - CONFOCAL ANALYSIS

Buffers/Dyes	Composition
2x KRH Buffer	120mM NaCl, 5mM KCl, 1.2mM MgSO <sub>4</sub> , 1.2mM CaCl <sub>2</sub> , 20mM HEPES, 1.2mM NaHPO <sub>4</sub> , pH 7.4.
KRH Working Stock	50% volume 2x KRH with 0.1% (w/v) Glucose, 0.18% (w/v) BSA
Carbonate Buffer	39.8ml 1M NaHCO <sub>3</sub> , 3.41ml 1M Na <sub>2</sub> CO <sub>3</sub> , make up to final volume of 1L, pH 9.0